GEOLOGIJA

2019 | št.: **62/2**

GeoZS
Geološki zavod Slovenije

ISSN
Tiskana izdaja / Print edition: 0016-7789
Spletna izdaja / Online edition: 1854-620X

GEOLOGIJA

62/2 – 2019

GeoZS
Geološki zavod Slovenije

GEOLOGIJA	2019	62/2	149-321	Ljubljana

GEOLOGIJA
ISSN 0016-7789

Izdajatelj: Geološki zavod Slovenije, zanj direktor Miloš Bavec
Publisher: Geological Survey of Slovenia, represented by Director Miloš Bavec
Financirata Javna agencija za raziskovalno dejavnost Republike Slovenije in Geološki zavod Slovenije
Financed by the Slovenian Research Agency and the Geological Survey of Slovenia

Vsebina številke 62/2 je bila sprejeta na seji Uredniškega odbora, dne 19. 12. 2019.
Manuscripts of the Volume 62/2 accepted by Editorial and Scientific Advisory Board on December 19, 2019.

Naslov uredništva / Editorial Office: GEOLOGIJA Geološki zavod Slovenije / Geological Survey of Slovenia
Dimičeva ulica 14, SI-1000 Ljubljana, Slovenija
Tel.: +386 (01) 2809-700, Fax: +386 (01) 2809-753, e-mail: urednik@geologija-revija.si
URL: http://www.geologija-revija.si/

GEOLOGIJA izhaja dvakrat letno. / GEOLOGIJA is published two times a year.
GEOLOGIJA je na voljo tudi preko medknjižnične izmenjave publikacij. /
GEOLOGIJA is available also on exchange basis.

Izjava o etičnosti
Izdajatelji revije Geologija se zavedamo dejstva, da so se z naglim naraščanjem števila objav v svetovni znanstveni literaturi razmahnili tudi poskusi plagiatorstva, zlorab in prevar. Menimo, da je naša naloga, da se po svojih močeh borimo proti tem pojavom, zato v celoti sledimo etičnim smernicam in standardom, ki jih je razvil odbor COPE (Committee for Publication Ethics).

Publication Ethics Statement
As the publisher of Geologija, we are aware of the fact that with growing number of published titles also the problem of plagiarism, fraud and misconduct is becoming more severe in scientific publishing. We have, therefore, committed to support ethical publication and have fully endorsed the guidelines and standards developed by COPE (Committee on Publication Ethics).

Baze, v katerih je Geologija indeksirana / Indexation bases of Geologija: Scopus, Directory of Open Access Journals, GeoRef, Zoological Record, Geoscience e- Journals, EBSCOhost

Cena / Price

Posamezni izvod / Single Issue	Letna naročnina / Annual Subscription
Posameznik / Individual: 15 €	Posameznik / Individual: 25 €
Institucija / Institutional: 25 €	Institucija / Institutional: 40 €

Tisk / Printed by: GRAFIKA GRACER d.o.o.

Slika na naslovni strani: Flišni ostanki znotraj kraške depresije na južnem delu otoka Krk (foto: E. Šegina).
Cover page: Flysch sediments within a depression on karst, the southern part of Krk Island (photo: E. Šegina).

GEOLOGIJA *62/2*, 149-321, Ljubljana 2019

VSEBINA – CONENTS

GEOLOGIJA *62/2*, 153–173, Ljubljana 2019

https://doi.org/10.5474/geologija.2019.007

Triassic deep-water sedimentation in the Bled Basin, eastern Julian Alps, Slovenia

Triasna globljevodna sedimentacija v Blejskem bazenu, vzhodne Julijske Alpe, Slovenija

Luka GALE[1,2], Tea KOLAR-JURKOVŠEK[2], Barbara KARNIČNIK[3], Bogomir CELARC[2], Špela GORIČAN[4] & Boštjan ROŽIČ[1]

[1]Univerza v Ljubljani, Naravoslovnotehniška fakulteta, Oddelek za geologijo, Aškerčeva 12, SI-1000 Ljubljana, Slovenia; e-mail: luka.gale@geo-zs.si
[2]Geološki zavod Slovenije, Dimičeva ulica 14, SI-1000 Ljubljana, Slovenia
[3]Škalska cesta 9, 3320 Velenje, Slovenija
[4]ZRC SAZU, Paleontološki inštitut Ivana Rakovca, Novi trg 2, SI-1000 Ljubljana, Slovenia

Prejeto / Received 3. 10. 2019; Sprejeto / Accepted 7. 11. 2019; Objavljeno na spletu / Published online 24. 12. 2019

Key words: Upper Triassic, Southern Alps, paleogeography, conodonts, radiolarians
Ključne besede: zgornji trias, Južne Alpe, paleogeografija, konodonti, radiolariji

Abstract

The Bled Basin was a Middle Triassic–Early Cretaceous basin whose remnants are preserved in the eastern Southern Alps in western Slovenia. The early evolution of the basin is recorded in the Upper Ladinian to Lower Jurassic Zatrnik cherty limestone formation, which in the Pokljuka Nappe overlies Middle Triassic volcanics, volcaniclastics and hemipelagic limestones. The Zatrnik Limestone is poorly documented and biostratigraphically not well constrained. The base of the Zatrnik Limestone was logged in four sections in the eastern part of the Pokljuka plateau. An Upper Ladinian *Muelleritortis cochleata* Radiolarian Zone was recognised in the lowermost part, whereas conodont data indicate Julian to latest Tuvalian/early Norian age for the rest of the logged sections. Microfacies analysis indicates hemipelagic deposition on a basin plain and/or distal slope, which is often interrupted by distal calciturbidites.

Izvleček

Blejski bazen je bil srednjetriasni do zgodnjekredni globljemorski sedimentacijski prostor, katerega ostanki so ohranjeni v Pokljuškem pokrovu vzhodnih Južnih Alp v zahodni Sloveniji. Zgodnji razvoj bazena je zabeležen v srednjetriasnih vulkanitih, vulkanoklastitih in hemipelagičnih apnencih, ki jim sledi zgornjeladinijska do spodnjejurska formacija Zatrniškega apnenca z roženci. Zatrniški apnenec je sedimentološko in biostratigrafsko razmeroma slabo raziskan. V članku so predstavljeni štirje profili Zatrniškega apnenca z vzhodnega dela Pokljuke, ki zajemajo spodnji del formacije. V najnižjem delu formacije je bila določena zgornjeladinijska radiolarijska cona *Muelleritortis cochleata*, višji deli profilov pa vsebujejo julske, tuvalske in/ali spodnjenorijske konodontne združbe. Mikrofaciesi kažejo na hemipelagično in turbiditno sedimentacijo na bazenski ravnici in/ali na distalnem delu pobočja.

Introduction

Stratigraphically continuous successions of Upper Triassic hemipelagic, pelagic and gravity-flow deposits up to several hundred meters thick preserved in north-western Slovenia testify to the existence of at least three long-lived Mesozoic marine basins located near the western margin of the Neotethys Ocean. Continuous successions of Ladinian to Upper Cretaceous deeper-marine strata are mostly located in the Tolmin Nappe of the eastern Southern Alps (Buser, 1987). This basin is usually referred to as the Slovenian Basin s. str. (Cousin, 1970, 1973; Buser, 1989, 1996) or the Tolmin Basin (Cousin, 1981; Rožič, 2009) and is relatively well studied (e.g., Rožič et al., 2009; Gale, 2010; Gale et al., 2012; Goričan et al., 2012; Rožič et al., 2017, with references). The second basin has been identified on the basis of Upper Triassic to Lower Jurassic open-marine facies exposed in the northern Julian Alps (Lieberman, 1978; De Zanche et al., 2000; Gianolla et al., 2003; Gale et al., 2015), the Southern Kara-

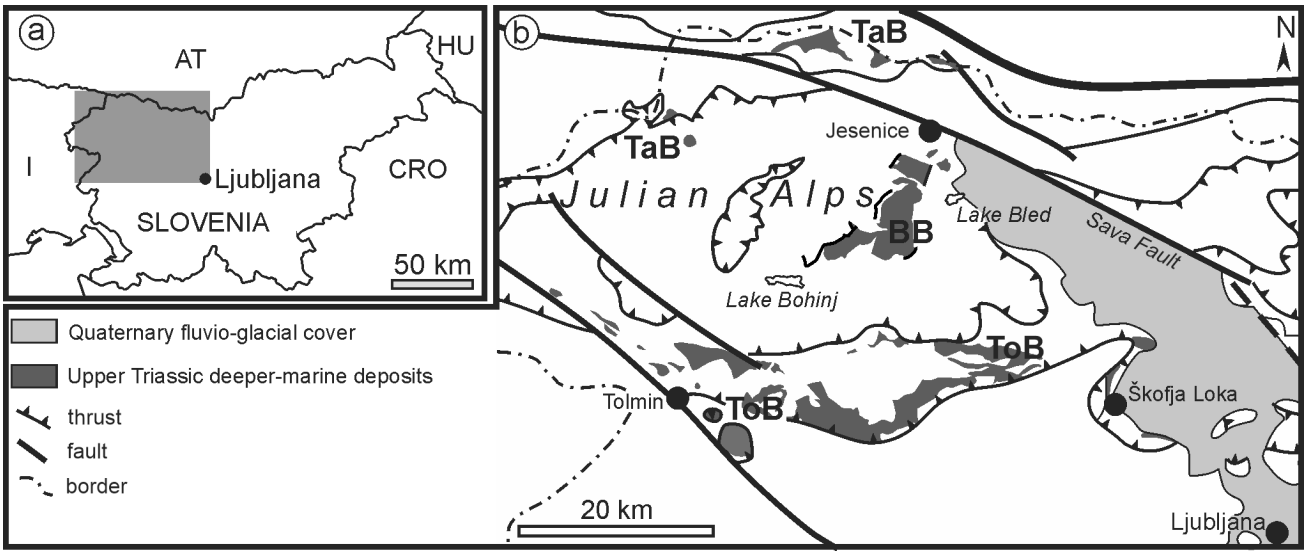

Fig. 1. Location of the studied area. (a) Geographic position of the area shown in Figure 1b. (b) Simplified tectonic map of NW Slovenia with extent of Upper Triassic deeper-marine deposits divided into distinct basins, as discussed in the paper: Bled Basin (BB), Tarvisio Basin (TaB), and Tolmin Basin (ToB). The map is modified after Placer (1999), Buser (2010), Gale et al. (2015), Goričan et al. (2018). The spatial distribution of basinal deposits is based on the map in Rožič (2016).

vanke Mountains (Krystyn et al., 1994; Lein et al., 1995; Schlaf, 1996), and in several outcrops west of this area (Geyer, 1900; Gianolla et al., 1998, 2010; Caggiati, 2014). Gianolla et al. (2010) and Gale et al. (2015) refer to this paleogeographic unit as the Tarvisio Basin. Finally, the third area with Upper Ladinian to Lower Cretaceous deeper marine successions, paleogeographically belonging to the Bled Basin, extends between the lakes Bohinj and Bled (Fig. 1).

The stratigraphic succession of the Bled Basin starts with Upper Anisian – Ladinian carbonate breccias and volcaniclastic rocks deposited on top of massive Anisian dolomite (Buser, 1980). The overlying formation, which constitutes the focus of this paper, is composed of bedded limestone with chert some hundreds of meters thick (Cousin, 1981; Buser, 1987; Goričan et al., 2018). This formation was first noted by Diener (1884), Härtel (1920), and Budkovič (1978). Cousin (1981) referred to it as the Zatrnik Limestone. He considered the upper part of the Zatrnik Limestone to be Rhaetian to Early Jurassic in age, while the base of the formation was dubiously placed in the Carnian. The name Zatrnik Limestone was later abandoned and the informal term Pokljuka Limestone or Pokljuka Formation was more commonly used instead (Dozet & Buser, 2009; Buser, 2010). Fossil bivalves (Buser, 1980) and conodonts (Kolar-Jurkovšek et al., 1983; Ramovš, 1986, 1998), confirmed ages from Late Ladinian to Late Norian, but no continuous sections have

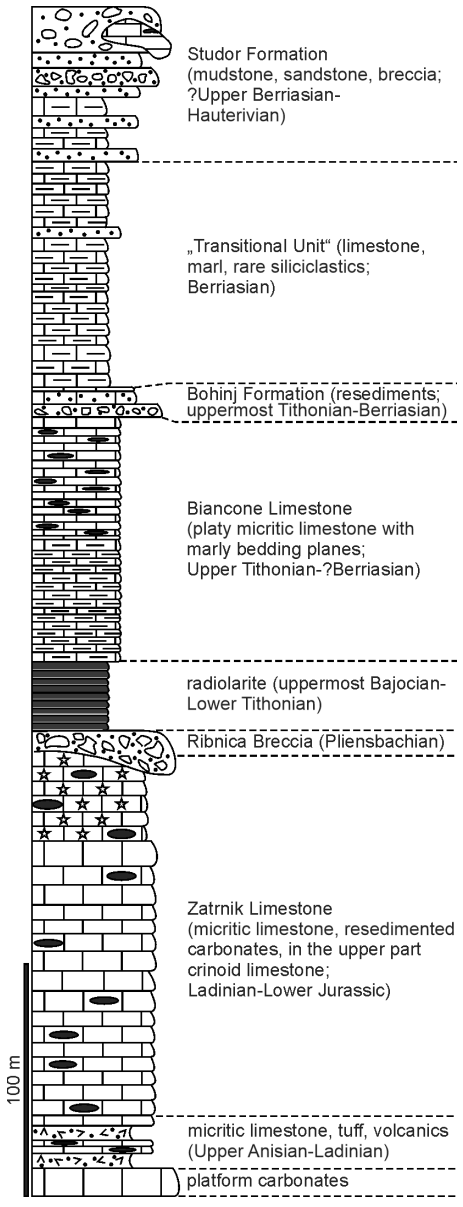

Fig. 2. Lithostratigraphy of the Bled Basin (Pokljuka Nappe). The thickness of the Zatrnik Limestone is not yet fully reconstructed. The measured sections indicate roughly 220 m covering Longobardian to Lower Norian. Modified after Goričan et al. (2018).

been logged. The recent reambulation of the area stratigraphically places the Zatrnik Limestone between the Upper Anisian to Ladinian volcanics and volcaniclastics, and the Pliensbachian carbonate Ribnica Breccia. The succession continues with various pelagic and gravity deposits (see Fig. 2 and Goričan et al., 2018).

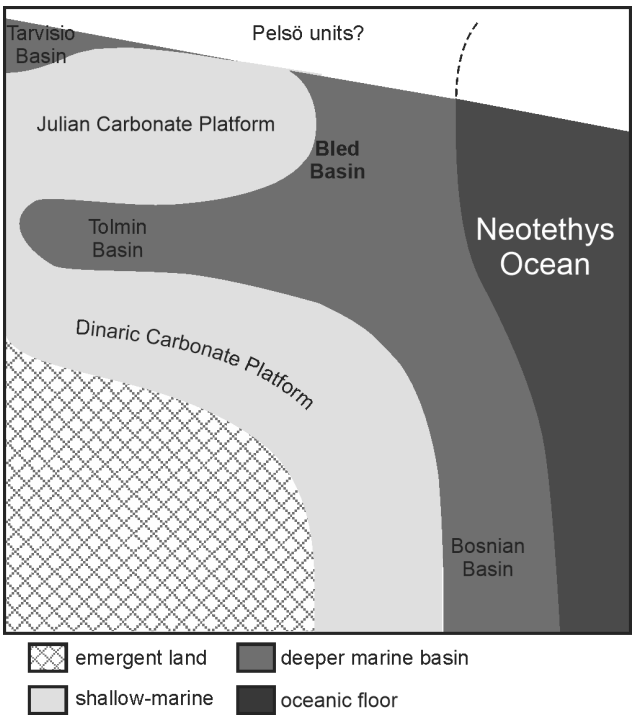

Fig. 3. Paleogeographic position of the Tolmin, Bled and Tarvisio basins at the end of the Carnian. Note that continuations of the units towards the present north are uncertain due to displacements along the Periadriatic Fault System. Modified after Goričan et al. (2018).

In this paper we present three detailed sections and one schematic section from the eastern part of the Pokljuka plateau encompassing the lower part of the Zatrnik Limestone. The sedimentological characteristics of the Zatrnik Limestone are described for the first time in order to identify the depositional environment and the type of sedimentation there. Conodonts, radiolarians, benthic foraminifera and microproblematica were determined from residues and thin sections.

Geological setting

Recent paleogeographic reconstructions place the Bled Basin on the oceanward side of the Julian Carbonate Platform (Fig. 3; Kukoč et al., 2012; Goričan et al., 2018). The sedimentary succession of the Bled Basin is situated today within the Julian Alps that belong to the eastern Southern Alps (Fig. 4; Placer, 1999). Two episodes of thrusting were recognised in the eastern Southern Alps: the latest Cretaceous–Eocene NW-SE striking and SW verging thrusts are overlapped by younger (Oligocene?–Miocene) E-W striking, S-verging thrusts (Doglioni & Siorpaes, 1990; Poli & Zanferarri, 1995; Placer & Čar, 1998). Goričan et al. (2018) called all nappes of the eastern Julian Alps the Julian Nappes. From the bottom to the top these comprise the Krn Nappe, the Slatna Klippe and the Pokljuka Nappe (Fig. 5). Primary thrust contacts are only preserved around the Slatna Klippe. Elsewhere, they were cut and displaced along NE-SW and NW-SE striking faults. Both, the Krn Nappe and the Pokljuka Nappe in

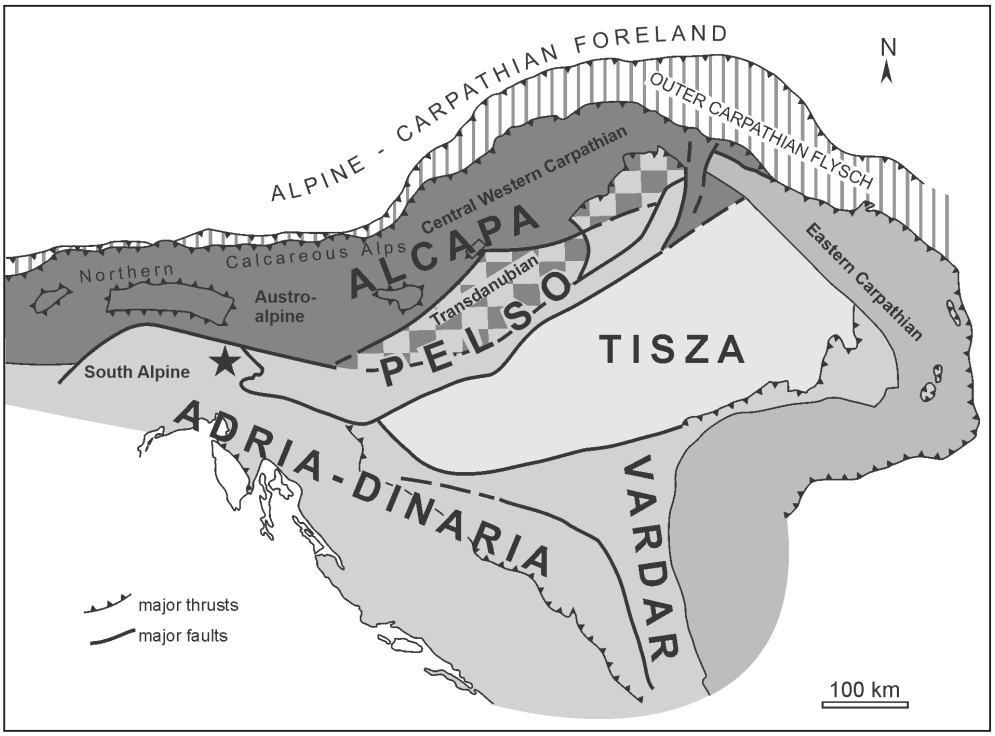

Fig. 4. Position of the studied area (star) on a regional tectonic map. Modified after Kovács et al. (2011).

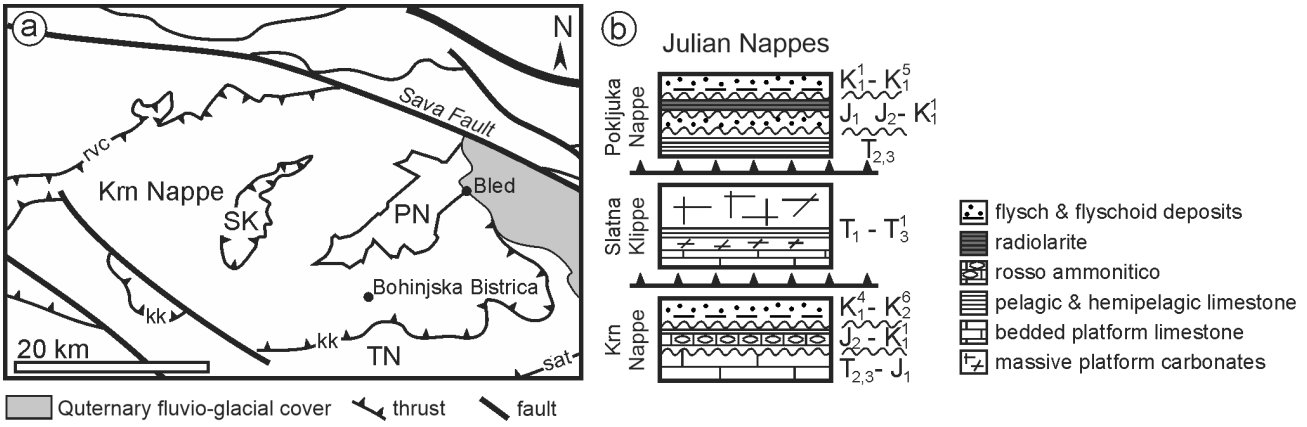

Fig. 5. Structure of the Julian Alps. (a) Schematic structural map of the Julian Alps. Abbrevations: SK – Slatna Klippe, PN – Pokljuka Nappe, TN – Tolmin Nappe, kk – Krn-Kobla Thrust, rvc – Resia-Val Coritenza Backthrust, sat – South Alpine Thrust. Simplified after Gale et al. (2015) and Goričan et al. (2018). (b) Superposition of the Julian Nappes and their simplified lithostratigraphy.

the lower part consist of Anisian shallow marine carbonates and Upper Anisian–Ladinian pelagic limestone and volcaniclastics. In the Krn Nappe and the Slatna Klippe these are followed by massive Carnian limestone and dolomite, while in the Pokljuka Nappe the succession continues with the deeper-marine Zatrnik Limestone (Goričan et al., 2018, with references). Towards the south, the Julian Nappes are in thrust or steep reverse-fault contact with the Tolmin Nappe, preserving successions of the Tolmin Basin (Placer, 1999). The investigated sections within the Zatrnik Limestone were logged in relatively tectonically undisturbed blocks of the Pokljuka Nappe with gently to moderately steep dipping strata, generally in the W and NW directions.

Material and methods

The lowermost part of the Zatrnik Limestone was logged in four sections (Fig. 6). Microfacies analysis is based on 174 thin sections 47×28 mm in size. Thin sections were studied in transmitted light with an optical microscope. Dunham's (1962) classification was used for the description of textures. Point-counting was performed on microphotographs taken from selected thin sections. We counted 300 points on a random grid using JMicroVision v1.2.7 (Copyright 2002-2008 Nicolas Roduit) software. Composite conodont samples were taken over intervals of 1.5 to 10 m, depending on the uniformity of the lithology. Carbonate rock samples were treated in acetic acid (*cca.* 8 %) followed by heavy liquid separation. The recovered faunas are kept in the micropaleontological collection at the Geological Survey of Slovenia (samples GeoZS 5793-5798, 5924-5928, 6001-6019). The SEM photos of conodont specimens were taken at the GeoZS (JEOL JSM

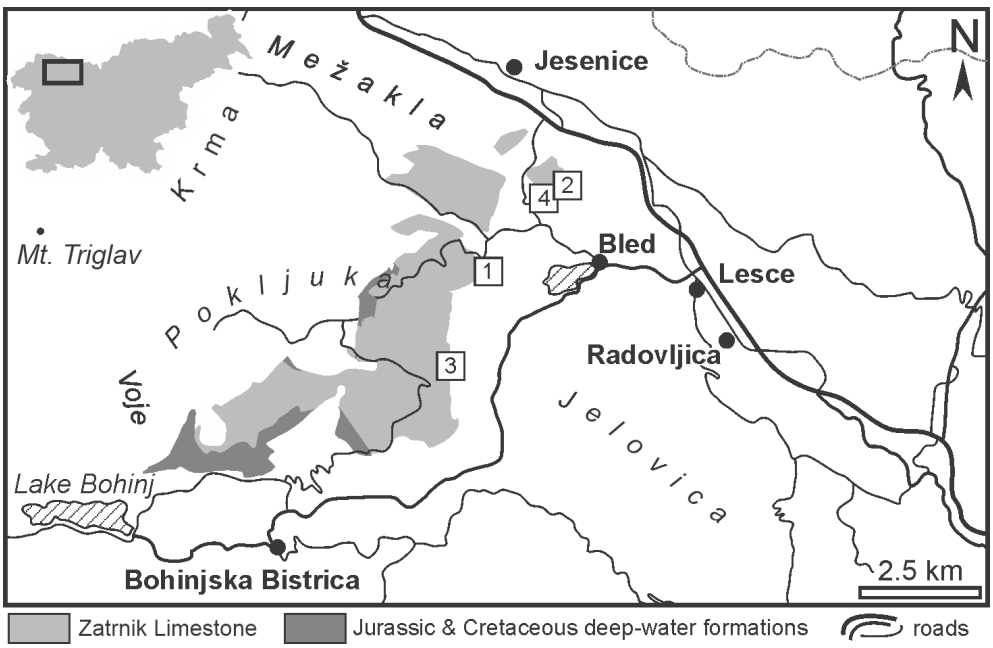

Fig. 6. Geographic position of the studied sections. The numbers indicate sections: Zatrnik (1), Blejski vintgar (2), Galetovec (3), and Poljane (4). Distribution of the basinal formations is drawn after Buser (2009), and Goričan et al. (2018).

6490LV Scanning Electron Microscope). Conodont biostratigraphy follows Rigo et al. (2018), and Kolar-Jurkovšek and Jurkovšek (2019). It should be noted, however, that Chen et al. (2015) have a slightly different view on the species and their ranges, so that stratigraphic boundaries could also be assigned somewhat differently. At the Zatrnik location, two radiolarian samples were taken after radiolarians were detected in the field with a hand lens. These samples were processed in the same manner as the conodont samples. The illustrated radiolarian specimens are stored at ZRC SAZU, Ljubljana (samples RA 5843, RA 5844).

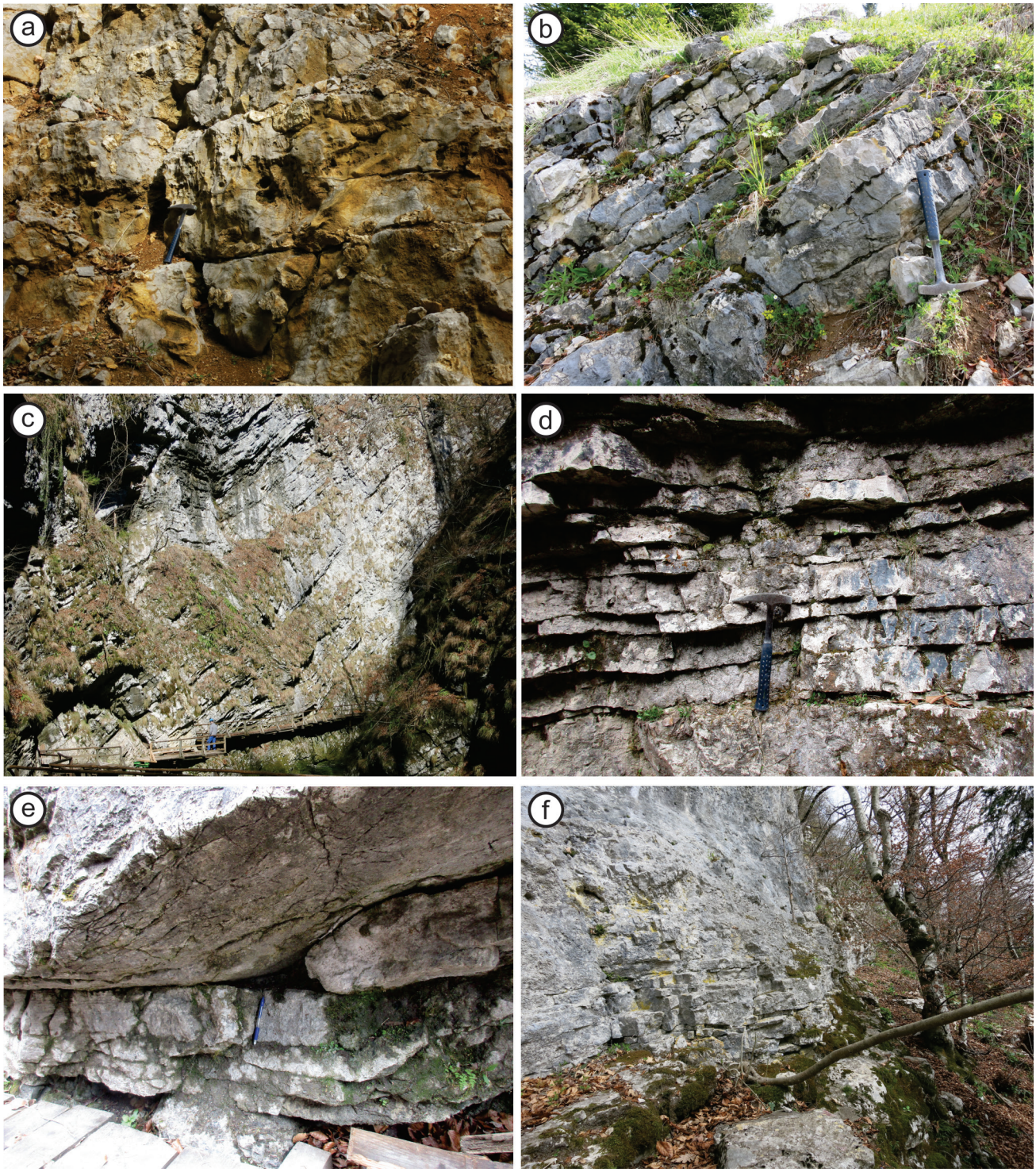

Fig. 7. Field view of the Zatrnik Limestone. **(a)** Medium-thick bedded mudstone with chert nodules, characterizing the upper (Norian and Rhaetian?) part of the formation. **(b)** Zatrnik Limestone at the top of the Zatrnik section, Carnian. **(c)** View of the Blejski vintgar gorge with exposures of the Carnian part of the formation. **(d)** Thin-bedded calcarenites (packstone, grainstone) in the Blejski vintgar section. **(e)** Slump and scour structures in the Blejski vintgar section. **(f)** Transition from bedded limestone with chert into seemingly massive limestone in the Poljane section.

Description of sections

In the lower part the Zatrnik Limestone is represented by thin- and medium-bedded cherty micritic limestone and calcarenites. Medium-thick bedded micritic limestone with chert nodules is the dominant lithofacies in the upper part of the formation (Fig. 7). The logged sections comprise only the lower, Upper Ladinian to Lower Norian part of the formation (Fig. 8), as a good exposure of the Norian and Rhaetian part of the formation has yet to be found. A detailed description of microfacies (MF) types from the logged sections (Figs. 9–12) is given in Table 1 and which are illustrated in Figures 13–14, whereas the determined fossils are listed in Table 2 and illustrated in Figures 15–17.

The Zatrnik section (bottom: 46°21'47''N, 14°2'25''E; top: 46°21'56''N, 14°2'26'' E) is stratigraphically the lowest of the logged sections. Fragments of volcanics and tuff are found in the scree, approximately 10–15 m below the section. Platy to medium-bedded loose bioclastic wackestone (MF 2 in Table 1) predominates (Fig. 9); this limestone may be silicified and locally has small chert nodules. Thin layers of dark brown marlstone intercalate with limestone in the lower 3 m of the formation. Radiolarian fauna (Fig. 16) from two samples of radiolarian packstone (MF 3), taken in this part of the section, indicates Upper Ladinian *Muelleritortis cochleata* Zone (Kozur & Mostler, 1994, 1996). Marlstone is absent in the section higher up. Filament-radiolarian-peloidal packstone (MF 8; Fig. 13c) sporadically intercalates with loose wackestone. Parallel lamination is rarely present. Moving upwards, the proportion of packstone gradually increases. Slumping and amalgamations are locally visible. Conodonts *Gladigondolella malayensis* Nogami, *Budurovignathus* cf. *diebeli* (Kozur & Mock), *B. mostleri* (Kozur) and *Paragondolella praelindae* Kozur suggest that beds above the radiolarian fauna and up to the 24th meter of the section are (middle-late) Julian in age. Between the 26th and 46th meter, the conodont assemblage comprises *P. praelindae*, *Quadralella polygnathiformis* (Budurov & Stefanov) and rare *Q.* aff. *noah* (Hayashi), indicating early-middle Tuvalian age (Rigo et al., 2018; Kolar-Jurkovšek & Jurkovšek, 2019). From the 57th meter up, peloidal packstone (MF 4), peloidal grainstone (MF 9), pebbly intraclastic grainstone (MF 10), bioclastic-intraclastic floatstone (MF 12), and closely-fitted intraclastic rudstone (MF 13) also occur among microfacies types. Normal grading is present in some beds. Approximately 60 m from the base of the section, *P. praelindae* is accompanied by *Paragondolella inclinata* (Kovacs), and later by *Paragondolella tadpole* (Hayashi). The association indicates late Julian to early Tuvalian age. When we also take into consideration the low number of specimens, which makes determination of assemblages difficult, we suggest the sequence between 11th and 24th m of the section is (undivided) Julian in age, while the upper part of the section is early Tuvalian.

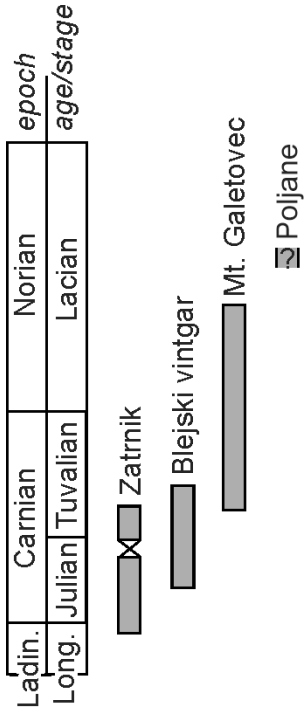

Fig. 8. Schematic position of the logged sections as indicated by biostratigraphic data. The position of the Poljane section is uncertain due to negative conodont samples.

The Blejski vintgar section (bottom: 46°23'49''N, 14°5'19''E; top: 46°23'54''N, 14°5'24''E) was logged in shorter subsections and separated by minor faults (Fig. 10). In contrast to the Zatrnik section, this part of the formation is dominated by pebbly intraclastic grainstone (MF 10). Peloidal grainstone (MF 9) and peloidal-intraclastic packstone (MF 7) are also common, while other microfacies types (MF 2 - loose bioclastic wackestone, MF 4 - peloidal packstone, MF 5 - bioclastic wackestone to packstone, MF 6 - dense mollusc wackestone, MF 8 – filament-radiolarian-peloidal packstone) are subordinate. Scour structures, normal and inverse grading are often observed in micritic limestone, but rarely parallel

Fig. 9. Sedimentary log of the Zatrnik section with ranges of conodont species. Microfacies types (see Table 1) are indicated on the right side of the logs.

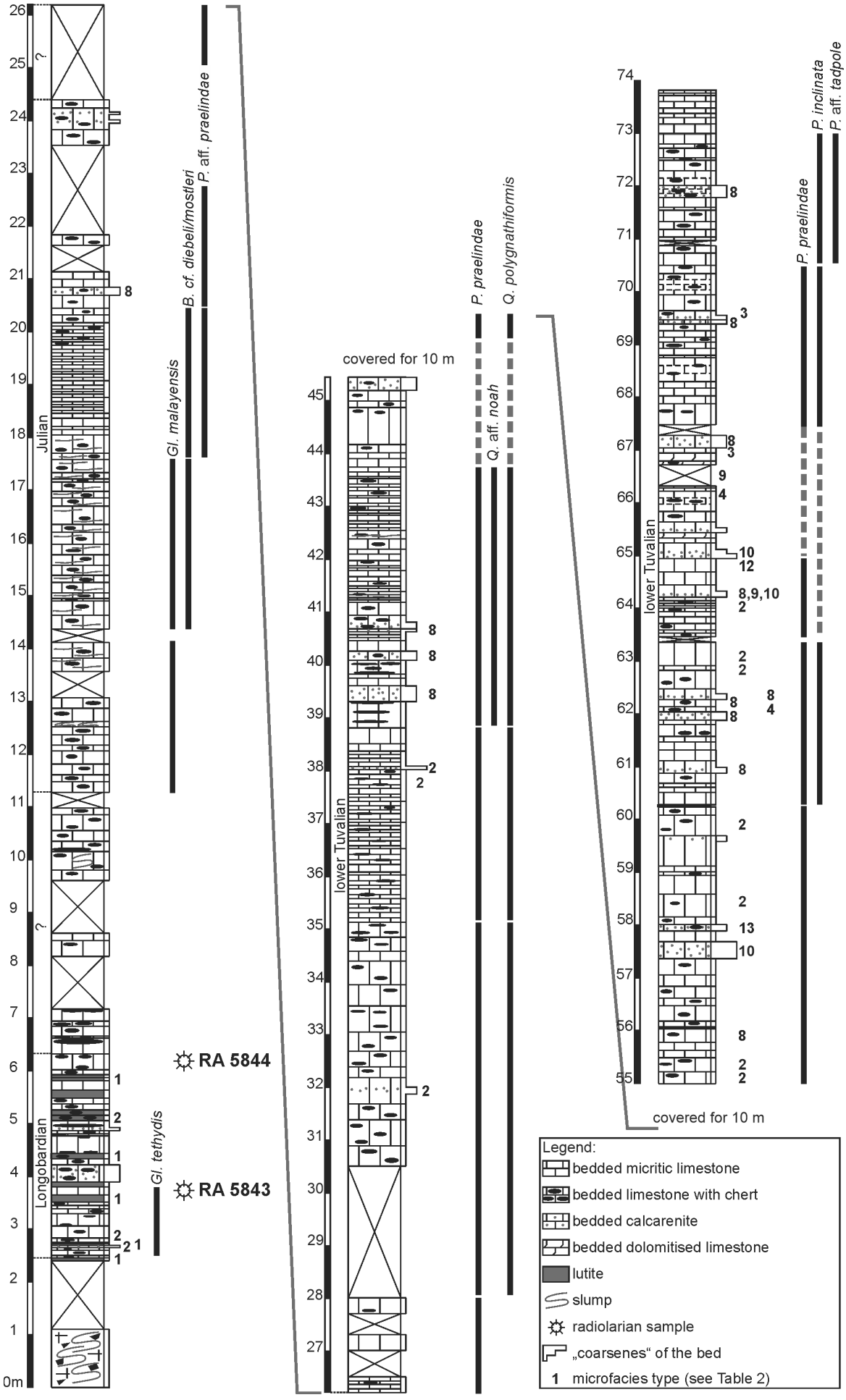
Julian
Longobardian
lower Tuvalian
lower Tuvalian
covered for 10 m
covered for 10 m
Gl. malayensis
B. cf. diebeli/mostleri
P. aff. praelindae
Gl. tethydis
P. praelindae
Q. aff. noah
Q. polygnathiformis
P. praelindae
P. inclinata
P. aff. tadpole
RA 5844
RA 5843
Legend:
bedded micritic limestone
bedded limestone with chert
bedded calcarenite
bedded dolomitised limestone
lutite
slump
radiolarian sample
„coarsenes“ of the bed
1 microfacies type (see Table 2)

Fig. 9.

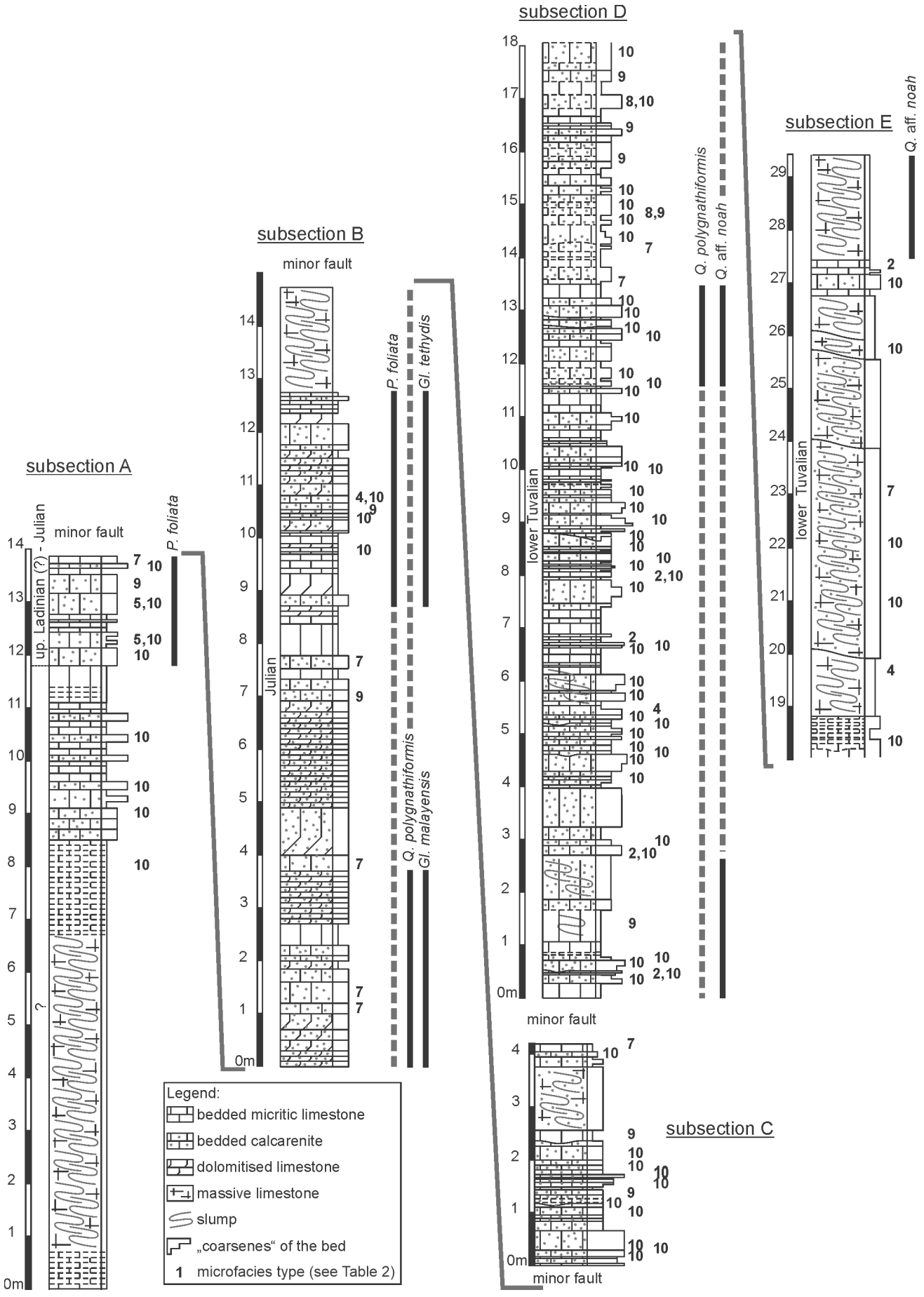

Fig. 10. Sedimentary log of the Blejski vintgar section with ranges of conodont species. Microfacies types (see Table 1) are indicated on the right side of the logs.

lamination and amalgamation. Slumps up to approx. 6 m thick are common. Conodont samples from the lower 12 m of the subsection A were negative. *Paragondolella foliata* Budurov was recovered from the upper 2 m. Subsection B comprises *Paragondolella foliata* Budurov, *Q. polygnathiformis, G. malayensis* and *G. tethydis* (Julian). Subsection D contains *Q. polygnathiformis* and *Q.* aff. *noah,* suggesting early Tuvalian age.

At Mt. Galetovec (bottom: 46°19'38''N, 14°2'28''E, top: 46°19'36''N, 14°2'23''E), the section was measured schematically along the sides of a vertical wall. Micritic limestone with chert nodules predominates (Fig. 11), and the beds tend to thicken towards the top. Amalgamation is commonly present, and some massive beds probably represent slumps. *Quadralella tuvalica* (Mazza & Rigo) was found at the base of the cliff wall, indicating early to middle Tuvalian age (Rigo et al., 2018). In the samples from higher up in the section *Epigondolella quadrata* Orchard, *Epigondolella rigoi* Noyan & Kozur and *Epigondolella vialovi* (Buryi) were collected. The stratigraphic range of all three species originates from the late Tuvalian to the Lacian (Rigo et al., 2018). The upper part of the section also contains some beds of pebbly intraclastic grainstone (MF 10), but in contrast to the same MF type in the Zatrnik and Blejski vintgar sections, the amount of microbialites, microbial-sponge boundstone clasts and microproblematica is clearly lower on account of mollusc fragments. The difference in foraminiferal assemblages is also very obvious: whereas foraminifera are rare, but diverse in the two stratigraphically lower sections, samples from the top of the Mt.Galetovec section commonly contain involutinids *Aulotortus sinuosus* Weynschenk and *Parvalamella friedli* (Kristan-Tollmann), which can be present in relative abundance.

The fourth section was logged at Poljane (46°23'46''N, 14°4›32»E; Fig. 12). Medium, and rarely thick beds of micritic limestone (MF 2 – loose bioclastic wackestone) and fine-grained bioclastic wackestone to packstone (MF 5) are present in the lower part of the section. Amalgamation and chert nodules are locally present. Just as at the top of the Mt. Galetovec section, skeletal carbonate is relatively abundant, and the foraminiferal assemblage is dominated by aulotortids. Thus, we presume these beds are late Tuvalian or younger in age. The section ends at the foot of the massive limestone unit, which is several tens of meters thick. Indistinct, slightly curved and sloping bedding planes can be seen in the lowermost part of this massive limestone

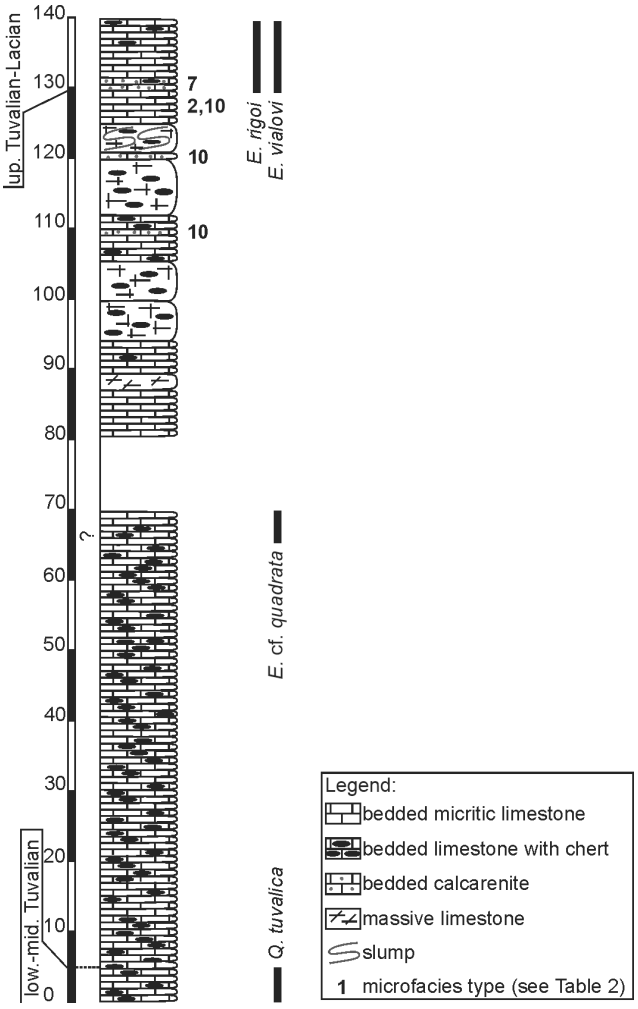

Fig. 11. Sedimentary log of the Mt. Galetovec section with ranges of conodont species. Microfacies types (see Table 1) are indicated on the right side of the logs.

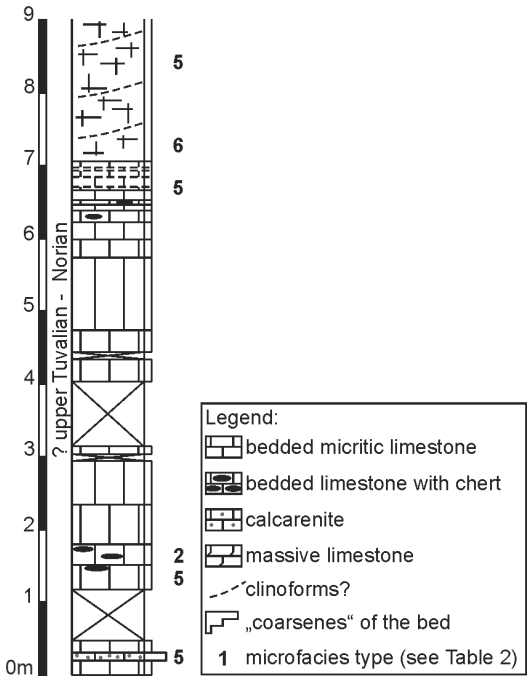

Fig. 12. Sedimentary log of the Poljane section. Microfacies types (see Table 1) are indicated on the right side of the logs.

(see Fig. 7f), texturally a bioclastic wackestone to packstone (MF 5) and a dense mollusc wackestone (MF 6). Foraminifera *Alpinophragmium perforatum* Flügel was found in this part. This species is mostly known from the Norian to Rhaetian (e.g., Flügel, 1967; Matzner, 1986; Kristan-Tollmann, 1990; Gale et al., 2012).

Table 1. Description of microfacies types of the Zatrnik Limestone.

Facies	Microfacies (MF)	Description	Figures
marlstone	marlstone (MF 1)	Dark brown marlstone is finely laminated and partly silicified. It is present only in the lowermost part of the Zatrnik section in beds up to 15 cm thick that interchange with limestone. Lamination is caused by different amounts of organic matter (as opaque bands), orientation of elongated particles and small differences in grain size. Besides very fine-grained matrix, there are a few grains large enough to be identified in thin sections: angular quartz grains and chlorite, small peloids and micritic intraclasts (the largest 0.65 mm in diameter), ostracod shells, echinoderm plates, thin-shelled bivalves and radiolarians.	13a
micritic limestone	loose bioclastic wackestone (MF 2)	Due to variations in clast composition, at least three subtypes were recognised. All have a high amount of matrix in common (77–84 %). In subtype MF 2A, 6 % of the matrix has been washed away. Clasts comprise peloids (12%), sparitic fragments (3 %) and echinoderm plates (1.5 %). Nodosariid foraminifers and radiolarians are very rare. In subtype MF 2B, peloids represent 5.5 % of the area; more common are filaments (4.5 %), and possible radiolarians (2 %), whereas sparitic fragments and undetermined bioclasts occupy 1% of the area, and microproblematica (*Plexoramea gracilis*), foraminifers and echinoderm plates each 0.5 %. In MF 2C, there are no vugs and very few peloids. Clasts are sparitic fragments (5.5–12 %), echinoderms (2.5–6 %), and filaments (3.5–5 %).	13b-d
	radiolarian packstone (MF 3)	Radiolarians are in rock-forming abundance, packed closely together. Very rare are thin-shelled bivalves ("filaments"). Radiolarian tests are filled with calcite or are silicified.	13e
	peloidal packstone (MF 4)	Sediment was bioturbated or deposited in laminae 1 cm thick. Average grain size is between 0.06 and 0.07 mm, with the largest grains 0.17 mm in size. Sediment is thus well to very well sorted. Peloids represent around 44 % of the area. Far more rare are fragmented bioclasts replaced by spar (up to 3.5 %), thin-shelled bivalves (3 %), echinoderms, foraminifers (*Agathammina austroalpina*, *Earlandia gracilis*, ?*Hoyenella* sp., *Turriglomina mesotriassica*, nodosariid lagenida), and microproblematica (*Ladinella porata*, *Thaumatoporella parvovesiculifera*, *Tubiphytes*-like form).	13f
	bioclastic wackestone to packstone (MF 5)	Micritic matrix represents 40–61 % of the area; up to 4.5 % of the surface consists of irregular vugs filled with drusy-mosaic spar, possibly representing areas where micrite had been washed away. The composition of clasts is variable, but a few types dominate: peloids (7–15 % of area), micritic intraclasts (up to 17 %; radiolarians were recognised in one), sparitic fragments (3.5–15 %), echinoderm plates (1–15 %) and thin-shelled bivalves (up to 16 %). Foraminifers (*Duotaxis*, sessile forms, and small nodosariid and miliolid species), spicules and ostracods are very rare. One sample contains larger pieces of brachiopod shells.	13g
	dense mollusc wackestone (MF 6)	Grains represent 42 % of the area, and on average measure 0.18 mm in size. Grains are well sorted. Angular sparitic fragments predominate (21 % of the area). Other grains are angular micritic intraclasts (6 %), foraminifers, echinoderm plates, ostracods and thin-shelled bivalves.	13h
calcarenite	peloidal-intraclastic packstone (MF 7)	In most samples, intergranular space is filled with micritic matrix. In fewer samples, most of the mud has been washed away and the space filled by calcitic cement. Grains represent more than 50 % of the thin section area. Average grain size is from 0.1 to 0.2 mm, with the largest grains up to 2 mm. Sorting ranges from moderately to well sorted. The majority of grains are peloids and dark intraclasts, together representing from 20 to 55 % of the thin section area. The latter may be mud chips or fragments of microbialites (distinction is rarely possible at smaller magnifications). Other grains are mostly microproblematica (2.5–4.5 %), echinoderm plates (3–8 %), locally thin-shelled bivalves (up to 11 %), very rare nodosariid foraminifers and brachiopods. Differentiation from MF 4 is by virtue of smaller grain size and better sorting of the latter. Dolomitization is locally present.	14a
	filament-radiolarian-peloidal packstone (MF 8)	Sediment may be laminated, with laminae differing in grain size, density and percentage of thin-shelled bivalves (these are oriented parallel to laminae) and radiolarians. Alternatively, it is bioturbated. Grains represent 65–70 % of the area. Peloids measure 0.07–0.09 mm (largest up to 0.24 mm), while radiolarians measure 0.18–0.20 mm in size. Intraclasts, although rare, are the largest grains with diameters of up to 6 mm. Peloids are thus very well sorted. The upper-size limit is represented by light echinoderm plates and flat thin-shelled bivalves. The most common grains are peloids (26–37 %), thin-shelled bivalves (9.5–34 %), radiolarians (2.5–25 %) and echinoderms (3.5–7.5 %). Intraclasts represent 0.5–1 % of the area, while foraminifers, sparitic clasts, ostracods, fragments of brachiopods, microproblematica and possible dasycladacean algae are very rare. Intergranular space is filled with micritic matrix, locally recrystallized into pseudosparite. Larger calcite crystals fill the space beneath bivalves. Echinoderm plates are overgrown by syntaxial calcite cement.	14b
	peloidal grainstone (MF 9)	Sediment is locally horizontally laminated (laminae differ in grain size, or exchange with laminae of other MF type). Grains represent approximately 70 % of the area; intergranular space is filled by granular or drusy-mosaic calcite spar. Grains on average measure 0.15 mm, while the largest reach 0.83 mm in size. Sediment is moderately well to well sorted. Peloids are the predominating grain type (50–60 %). Also present are sparitic fragments (6.5–9 %), echinoderm plates (1.5–2.5 %), microproblematica (up to 4.5 %). Foraminifera, gastropods, calcimicrobes and brachiopod fragments are very rare. Echinoderm plates are overgrown by syntaxial calcite. Dolomitization is locally present; dolomite crystals are euhedral, overgrowing peloids or crosscutting older cement and grains.	14c
	pebbly intraclastic grainstone (MF 10)	Grading is commonly present. The largest clasts measure up to 1 cm in size, while average grain size is 0.3 to 0.5 mm (size changes with grading). Grains are angular and in point contacts. They comprise between 45–75 % of the area (on average 67 %). The most common grains are intraclasts (49.5 %). Microproblematica is more common in Ladinian and Carnian samples (7.5 % compared to 0.5 % in the Norian samples; note that this is a very conservative estimate, as point counting was performed mainly at small magnifications, which often do not allow for differentiation from micritic intraclasts). Sparitic fragments (5.9 %), echinoderms (3.4 %), and foraminifers (1 %) appear in approximately the same abundance, irrespective of the samples' age.	14d-e

	pebbly intraclastic grainstone (MF 10)	**Within the lower – middle Carnian part** of the succession, intraclasts comprise pelletal packstone with *Bacinella floriformis*, peloidal packstone, bioclastic-peloidal packstone, bioclastic wackestone, calcimicrobes (types *Garwoodia* and *Cayeuxia*), microproblematica-sponge boundstone, microbialite (stromatolite, pelletal leiolite), *Bacinella*-like boundstone clasts and cementstone. Other clasts are peloids (small intraclasts), sparitic fragments, microproblematica, echinoderm plates, foraminifers, radial spherulites, brachiopods, rare green algae, agglutinated worm tubes, bryozoan and ammonite fragments, gastropods and ostracods. **In the upper Carnian – lower Norian samples**, mudstone, mudstone with filaments and spicules and calcimicrobes are present among intraclasts, whereas smaller grains contain peloids (small micritic intraclasts), echinoderms, foraminifers, spherulites, sparitic fragments (cortoids), agglutinated worm tubes, and brachiopod fragments. Besides fewer (or even the absence of) microbialites, microbial-sponge boundstones and microproblematica, Carnian and Norian samples differ notably in foraminiferal assemblage. Cement is represented by drusy mosaic calcite. Fibrous rim cement occurs locally. In some samples, coarse euhedral dolomite fills the intergranular space. Only one example of silicified valves was found.	14d-e
	intraclastic-mollusc packstone (MF 11)	Grains represent approximately 70 % of the area. The intergranular space is filled with micritic matrix (27 % of the area) and drusy mosaic calcite cement (4 %). Grains are mostly in point contacts. Sorting is medium to poor, with the average size of grains around 0.35 mm and the largest grains measuring 2 mm in size. The most abundant grains are sparitic fragments (31 % of the area). Most are probably mollusc fragments, but some may belong also to recrystallized involutinid foraminifers. Intraclasts (bioclastic wackestone and packstone) occupy another 23 % of the area. Other grains are echinoderm plates (11.5 %), foraminifers (3 %), small fragments of *Thaumatoporella* thalli, and ostracods. Some grains are selectively silicified.	14f
fine-grained breccia	bioclastic-intraclastic floatstone (MF 12)	Micritic matrix represents 46 % of the area, whereas clasts occupy the rest of the space. Clasts are poorly sorted, up to 4.5 mm large. Among them, intraclasts are the most common (23 % of area). They are variable, mostly angular, comprising bioclastic-peloidal wackestone, cementstone, mudstone (or structureless microbialite), stromatolite, microproblematica boundstone, and *Bacanella* boundstone. Other clasts include fragments of bivalves, oncoids, microproblematica (*Tubiphytes*, *Plexoramea*, *Ladinella*), *Dendronella* algae, sponges, echinoderm plates, foraminifers, solitary corals, gastropods and ostracods. Bivalve shells are micritized at the margins. Aragonite is replaced by drusy mosaic calcite.	14g
	closely-fitted intraclastic rudstone (MF 13)	One sample comprises closely fitted angular intraclasts (pelletal packstone, fine-grained dense bioclastic-pelletal wackestone, undetermined silicified clasts, bioclastic-intraclastic wackestone). Rare echinoid spines also occur. The matrix between clasts seems to be micritic. Bioclastic-intraclastic grainstone is locally visible among clasts, and may be infiltrated into rudstone.	14h

Table 2. List of determined fossils. Distribution of conodont taxa (from composite samples) is shown next to sedimentary logs in Figures 9–11. See Figure 9 for position of the radiolarian samples.

Fossil group	Taxa
Conodonts	*Budurovignathus* cf. *B. diebeli* (Kozur & Mock) vel *mostleri* (Kozur), *Epigondolella quadrata* Orchard, *E. rigoi* Noyan & Kozur, *E. vialovi* (Buryi), *Gladigondolella tethydis* (Huckriede), *G. malayensis* Nogami, *Paragondolella praelindae* Kozur, *P. foliata* Budurov, *P. inclinata* (Kovacs), *P.* aff. *tadpole* (Hayashi), *Quadralella polygnathiformis* (Budurov & Stefanov), *Q. noah* (Hayashi), *Q. tuvalica* (Mazza & Rigo) **(for distribution of taxa see Figs. 9-12)**
Radiolarians	**Sample 5843 (Zatrnik):** *Acanthotetrapaurinella variabilis* Kozur & Mostler, *Annulotriassocampe* cf. *eoladinica* Kozur & Mostler, *Archaeocenosphaera* sp., *Dumitricasphaera trialata* Tekin & Mostler, *Karnospongella bispinosa* Kozur & Mostler, *Muelleritortis cochleata* (Nakaseko & Nishimura), *M. expansa* Kozur & Mostler, *M.s* aff. *expansa* Kozur & Mostler, *M. longispinosa* Kozur, *M. tumidospina* Kozur, *Paurinella triangularis* Kozur & Mostler, *Pseudostylosphaera nazarovi* (Kozur & Mostler), *Ropanaella* sp., *Scutispongus latus* Kozur & Mostler, *Spinotriassocampe longobardica* Kozur & Mostler, *Spongoserrula rarauana* Dumitrica, *Spongotortilispinus tortilis* Kozur & Mostler, *Triassocampe*? sp., *Tritortis dispiralis* (Bragin) **Sample 5844 (Zatrnik):** *Acanthotetrapaurinella variabilis* Kozur & Mostler, *Archaeocenosphaera* sp., *Dumitricasphaera trialata* Tekin & Mostler, *Muelleritortis cochleata* (Nakaseko & Nishimura), *M. expansa* Kozur & Mostler, *Paurinella triangularis* Kozur & Mostler, *Pseudostylosphaera nazarovi* (Kozur & Mostler), *Ropanaella* sp., *Scutispongus latus* Kozur & Mostler, *Spongoserrula rarauana* Dumitrica, *Spongotortilispinus slovenicus* (Kolar-Jurkovšek), *Steigerispongus cristagalli* (Dumitrica), *Triassocampe*? sp., *Tritortis dispiralis* (Bragin)
Foraminifera	**Carnian (Zatrnik and Blejski vintgar sections, lower part of Galetovec sections):** *Glomospirella* cf. *pokornyi* (Salaj), *Reophax rudis* Kristan-Tollmann, *Ammobaculites* sp., *Gaudyina* sp., *Paleolituonella meridionalis* (Luperto), *Earlandia amplimuralis* (Pantić), *Earlandia tintinniformis* (Mišik), *Agathammina austroalpina* Kristan-Tollmann & Tollmann, *Arenovidalina*/*Ophthalmidium* sp., *Gsollbergella spiroloculiformis* (Oravecz-Scheffer), *Turriglomina mesotriasica* (Koehn-Zaninetti), *Hydrania dulloi* Senowbari-Daryan, *Piallina bronnimanni* Martini et al., *Cucurbita longicollum* Senowbari-Daryan, *C. infundibuliforme* Jablonský, *C.* cf. *minima* Senowbari-Daryan, *Trocholina turris* Frentzen, *Trocholina* sp., Duostominidae, *Koskinobullina socialis* Cherchi & Schroeder, *Pseudonodosaria* cf. *obconica* (Reuss), *Austrocolomia* sp., nodosariid Lagenida **Upper Tuvalian - Lower Norian (middle and upper part of the Galetovec section, Poljane section):** *Pilammina sulawesiana* Martini et al., *Reophax rudis* Kristan-Tollmann, *Ammobaculites* sp., "*Trochammina*" *almtalensis* Koehn-Zaninetti, *Duotaxis* sp., "*Tetrataxis*" *humilis* Kristan, *Alpinophragmium perforatum* Flügel, Endothyracea, *Planiinvoluta* sp., *Agathammina austroalpina* Kristan-Tollmann & Tollmann, *Miliolechina stellata* Zaninetti et al., *Aulotortus sinuosus* Weynschenk, *Parvalamella friedli* (Kristan-Tollmann), Duostominidae, *Variostoma cochlea* Kristan-Tollmann, *Lenticulina* sp., *Pseudonodosaria* sp., nodosariid Lagenida
Microproblematica	**Carnian (Zatrnik and Blejski vintgar sections, lower part of Galetovec sections):** *Tubiphytes* group (?*Tubiphytes obscurus* Maslov), *Plexoramea cerebriformis* Mello, *Ladinella porata* Ott, *Baccanella floriformis* Pantić, *Plexoramea gracilis* (Schäfer & Senowbari-Daryan), *Bacinella irregularis* Radoičić, *Radiomura cautica* Senowbari-Daryan & Schäfer **Upper Tuvalian - Lower Norian (middle and upper part of the Galetovec section, Poljane section):** *Thaumatoporella* sp., ?*Plexoramea cerebriformis* Mello, *Baccanella floriformis* Pantić

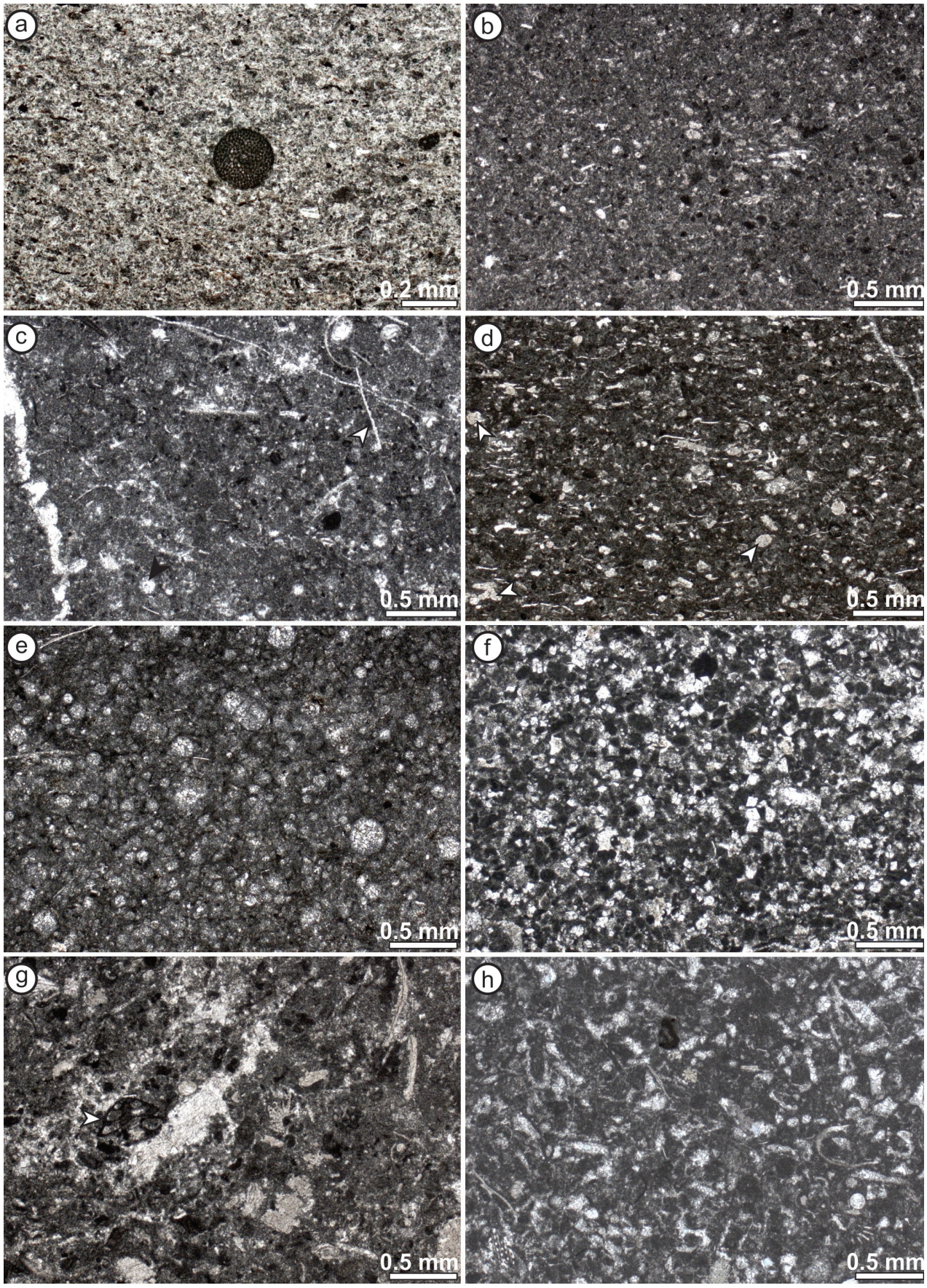

Fig. 13. Microfacies of the Zatrnik Limestone. **(a)** Pyritized (?) radiolarian test in lutite (MF 1). Section Zatrnik; 6th meter. **(b)** Loose bioclastic wackestone (MF 2A). Section Zatrnik; 55th meter. **(c)** Loose bioclastic wackestone (MF 2B). Note rare filaments (white arrowhead) and radiolarians (black arrowhead). Section Zatrnik; 32nd meter. **(d)** Loose bioclastic wackestone (MF 2C). Note slightly greater abundance of echinoderms (arrowhead). Section Zatrnik; 60th meter. **(e)** Radiolarian packstone (MF 3). Section Zatrnik; 4th meter. **(f)** Peloidal packstone (MF 4), slightly dolomitized. Blejski vintgar section, subsection D; 5.5 meters. **(g)** Bioclastic wackestone to packstone (MF 5). Note foraminifera *Duotaxis* sp. (arrowhead). Section Poljane; 1.2 meters **(h)** Dense mollusc wackestone (MF 6). Section Poljane; 6.5 meters.

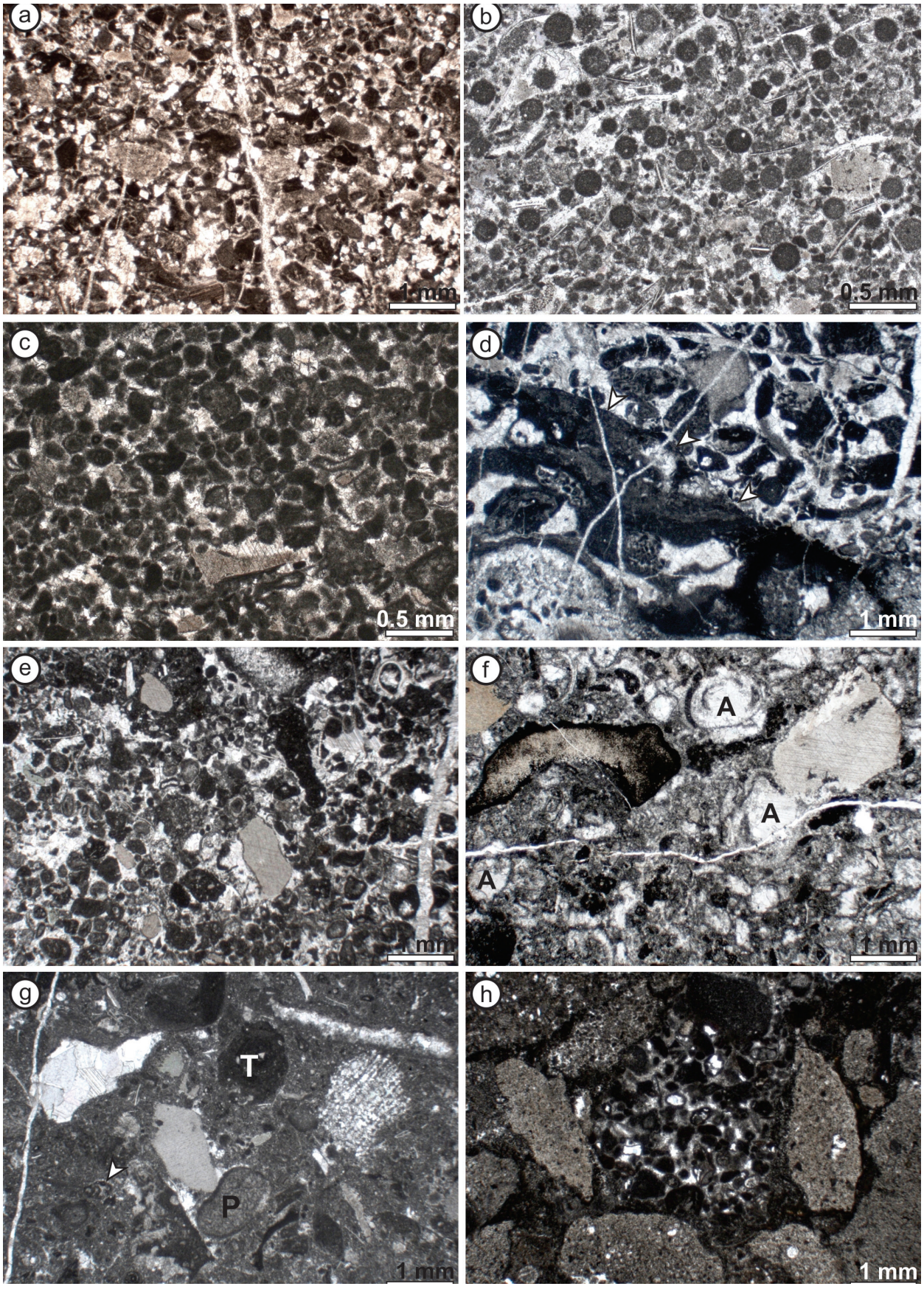

Fig. 14. Microfacies of the Zatrnik Limestone. **(a)** Peloidal-intraclastic packstone (MF 7). Section Blejski vintgar; subsection B; 1st meter. **(b)** Filament-radiolarian-peloidal packstone (MF 8). Section Zatrnik; 69.5 meters. **(c)** Peloidal grainstone (MF 9). Section Blejski vintgar, subsection D; 16.5 meters. **(d)** Pebbly intraclastic grainstone (MF 10). Arrowheads point at the margin of the microbialite boundstone. Section Blejski vintgar, subsection A; 10.5 meters. **(e)** Pebbly intraclastic grainstone (MF 10). Sample 1177. **(f)** Intraclastic-mollusc packstone (MF 11). Section Galetovec; 110th meter. Letter "A" denotes foraminifera *Parvalamella friedli* (Kristan-Tollmann). **(g)** Bioclastic-intraclastic floatstone (MF 12). Letter "T" denotes *Tubiphytes*-like clast, letter "P" a *Plexoramea*, and white arrowhead a small foraminifera *Reophax* sp. Section Zatrnik; 58.5 meters. **(h)** Closely-fitted intraclastic rudstone (MF 13). Section Zatrnik; 58th meter.

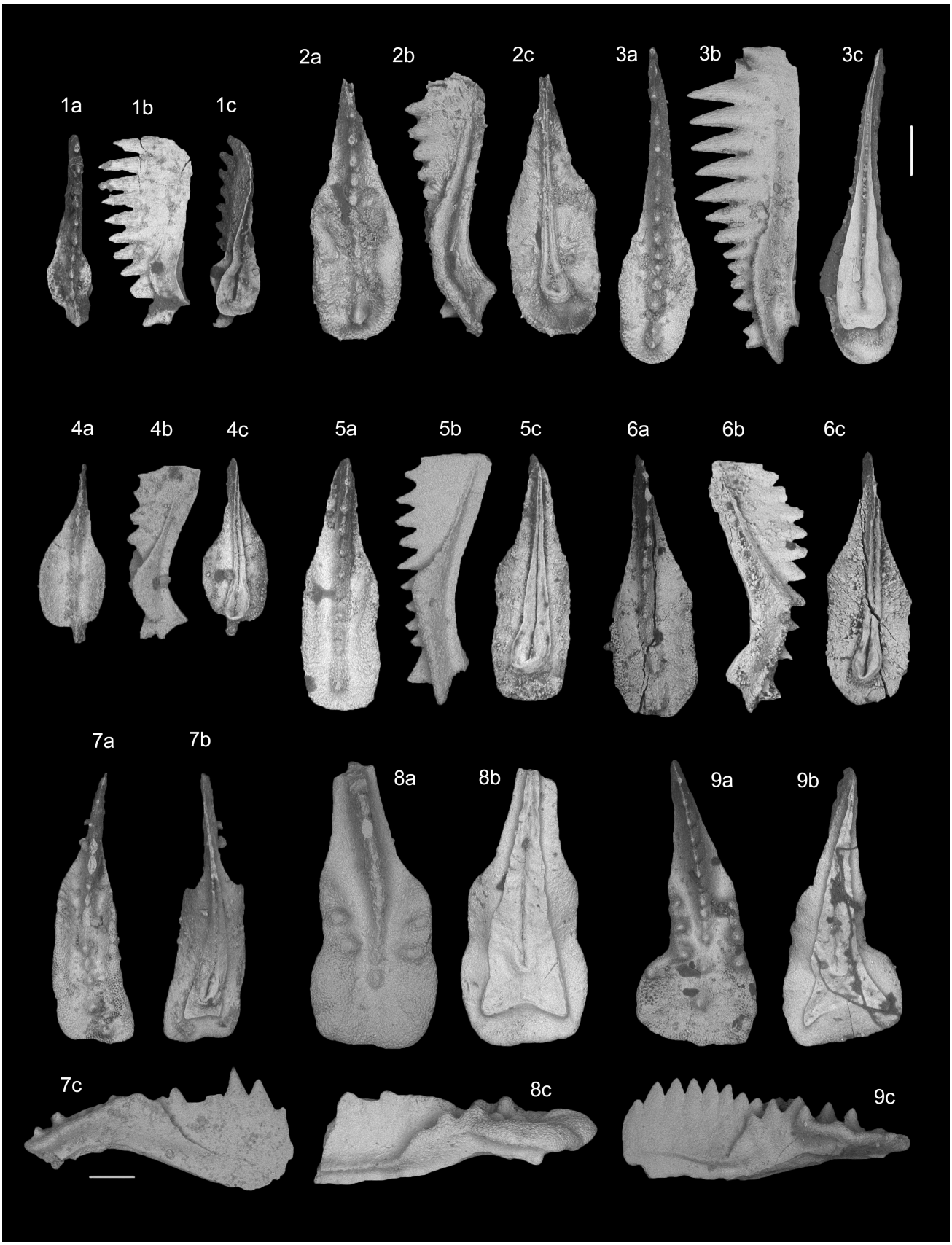

Fig. 15. Conodonts from Late Ladinian to Norian part of the Zatrnik Limestone. **1.** *Paragondolella foliata* Budurov – immature specimens with very wide basal cavity. Sample GeoZS 5793; Blejski vintgar; Julian. **2.** *Paragondolella inclinata* (Kovacs). Sample HV 6006-2; Zatrnik; Julian. **3.** *Paragondolella tadpole* (Hayashi). Sample HV 6006-1; Zatrnik; Julian. **4.** *Paragondolella praelindae* Kozur. Sample ZA 6017-2; Zatrnik; Julian. **5.** *Quadralella polygnathiformis* (Budurov and Stefanov). Sample ZA 6018-1; Zatrnik; Julian. **6.** *Quadralella polygnathiformis* (Budurov and Stefanov) – with rounded posterior and rounded keel. Sample GeoZS 5796; Blejski vintgar; Julian. **7.** *Quadralella tuvalica* (Mazza and Rigo) – primitive form with weak nodes. Sample GA 5928-1; Galetovec; Tuvalian. **8.** *Epigondolella* cf. *quadrata* Orchard. Sample GA 5927-1; Galetovec; Tuvalian-Lacian. **9.** *Epigondolella rigoi* Noyan and Kozur. Sample GA 5924-6; Galetovec; Tuvalian-Lacian.

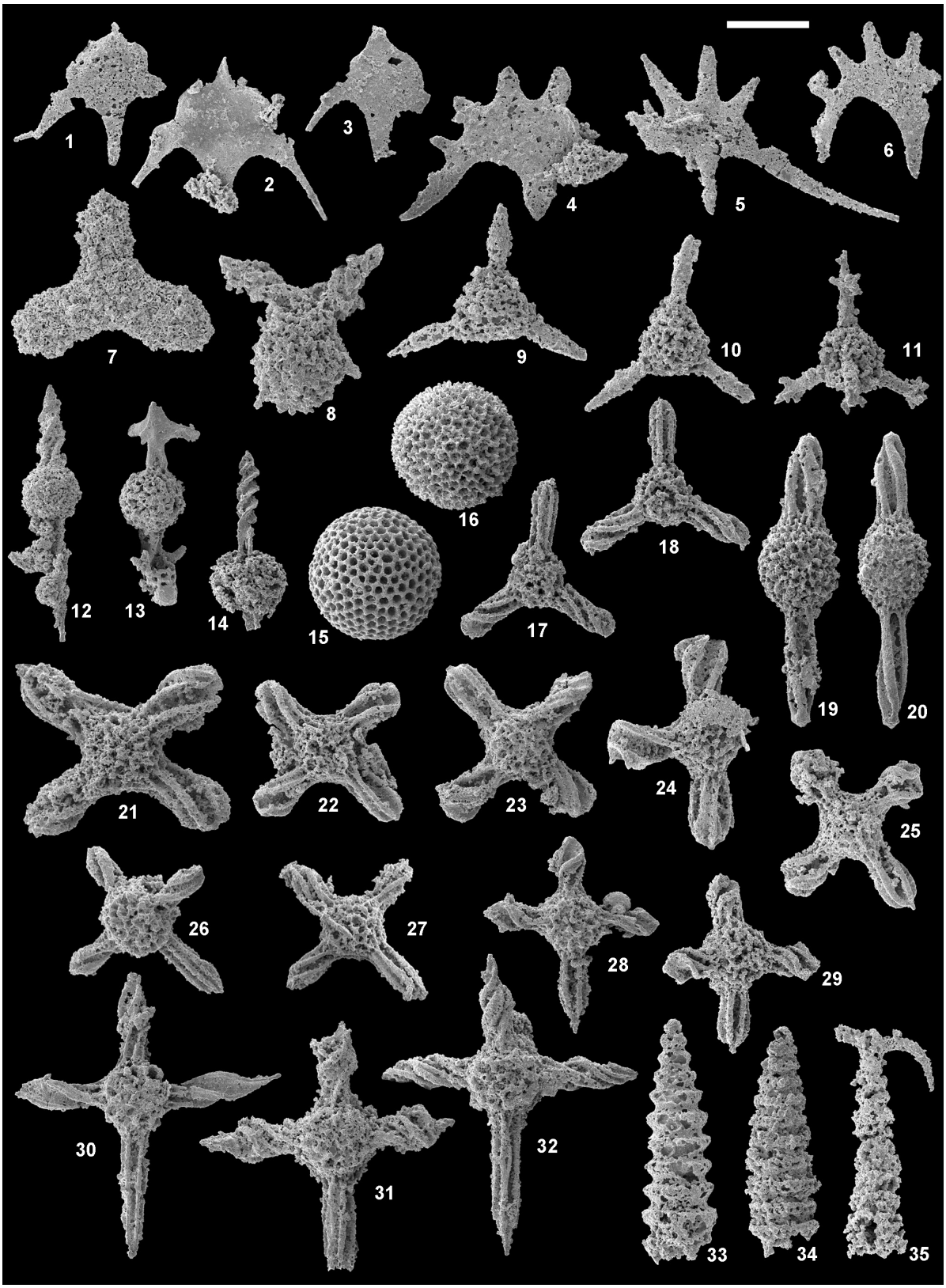

Fig. 16. Late Ladinian radiolarians from locality Zatrnik. **1–3**. *Scutispongus latus* Kozur and Mostler. **4, 6**. *Spongoserrula rarauana* Dumitrica. **5**. *Steigerispongus cristagalli* (Dumitrica). **7**. *Ropanaella* sp. **8**. *Karnospongella bispinosa* Kozur and Mostler. **9–10**. *Paurinella triangularis* Kozur and Mostler. **11**. *Acanthotetrapaurinella variabilis* Kozur and Mostler. **12**. *Spongotortilispinus slovenicus* (Kolar-Jurkovšek). **13**. *Dumitricasphaera trialata* Tekin and Mostler. **14**. *Spongotortilispinus tortilis* Kozur and Mostler. **15–16**. *Archaeocenosphaera* sp. **17–18**. *Tritortis dispiralis* (Bragin). **19–20**. *Pseudostylosphaera nazarovi* (Kozur and Mostler). **21–25, 29**. *Muelleritortis expansa* Kozur and Mostler. **26–27**. *Muelleritortis tumidospina* Kozur. **28**. *Muelleritortis* aff. *expansa* Kozur and Mostler. This species differs from typical *M. expansa* by having pyramidal (not blunt) spine tips on the three torsioned spines and by the fourth spine being slightly longer than the other three. It is also close to *Muelleritortis koeveskalensis* Kozur but typical *M. koeveskalensis* (see the holotype in Kozur, 1988) has sinistrally torsioned spines. **30**. *Muelleritortis longispinosa* Kozur. **31–32**. *Muelleritortis cochleata* (Nakaseko and Nishimura). **33**. *Triassocampe*? sp. **34**. *Annulotriassocampe* cf. *eoladinica* Kozur and Mostler. **35**. *Spinotriassocampe longobardica* Kozur and Mostler.

Sample RA 5843: figs. 2–3, 7–8, 10–11, 13–17, 19, 22–23, 25–31, 33–35. Sample RA 5844: figs. 1, 4–6, 9, 12, 18, 20–21, 24, 32. Length of scale bar 100 µm for figs. 8–11 and 33–35; 150 µm for figs. 1–6, 13–18 and 21–32; 200 µm for figs. 7, 12, 19–20.

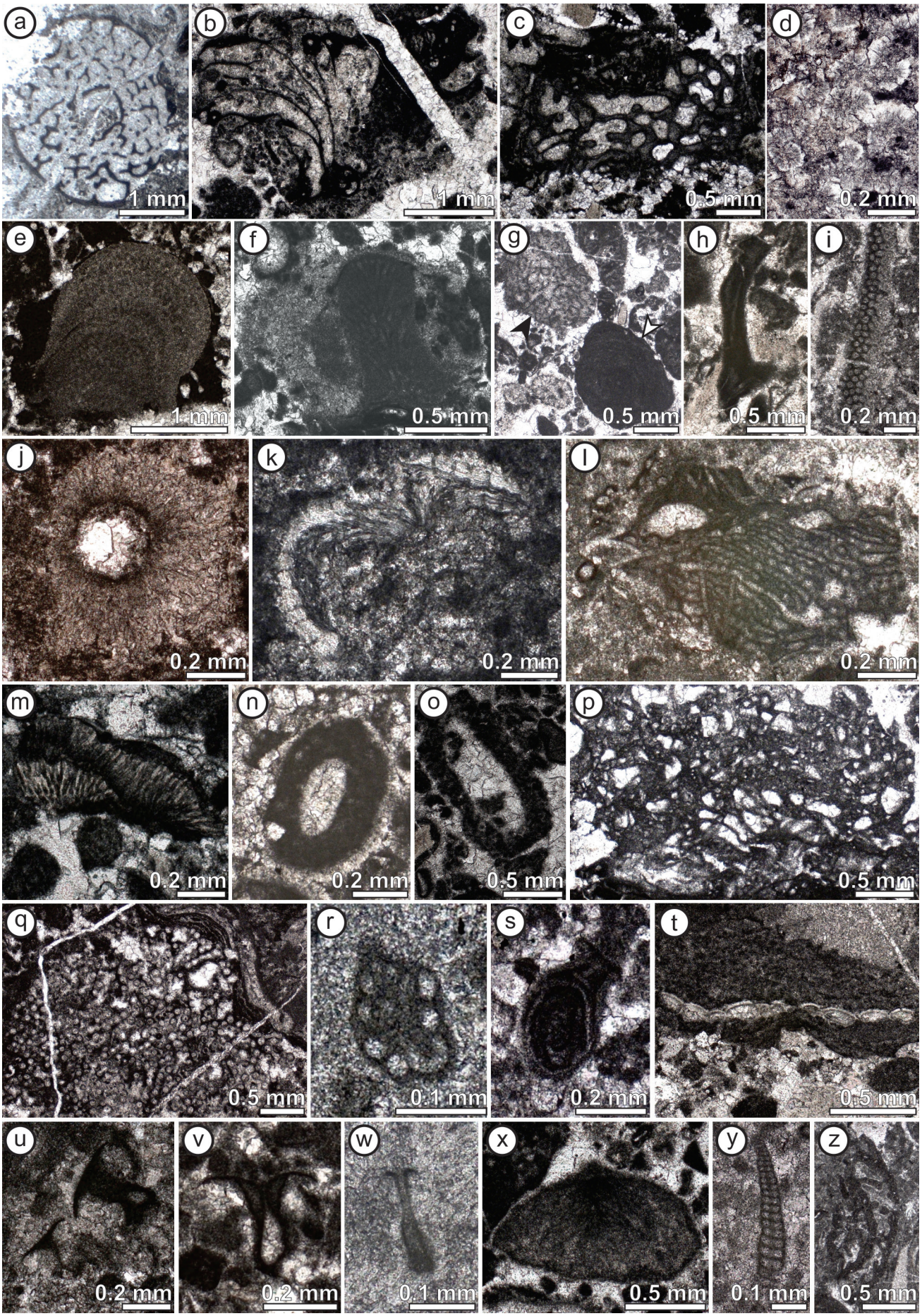
a
1 mm
b
1 mm
c
0.5 mm
d
0.2 mm
e
1 mm
f
0.5 mm
g
0.5 mm
h
0.5 mm
i
0.2 mm
j
0.2 mm
k
0.2 mm
l
0.2 mm
m
0.2 mm
n
0.2 mm
o
0.5 mm
p
0.5 mm
q
0.5 mm
r
0.1 mm
s
0.2 mm
t
0.5 mm
u
0.2 mm
v
0.2 mm
w
0.1 mm
x
0.5 mm
y
0.1 mm
z
0.5 mm

Fig. 17

Fig. 17. Sponges and various microfossils from the Carnian and Norian part of the Zatrnik Limestone. **(a-c)** Undetermined "sphinctozoan" sponges; section Blejski vintgar. (a) Julian. (b-c) Lower Tuvalian. **(d)** *Baccanella floriformis* Pantić; section Blejski vintgar; lower Tuvalian. **(e-f)** *Ladinella porata* Ott; section Blejski vintgar; Julian. **(g)** ?*Tubiphytes obscurus* Maslov (white arrowhead) and *Plexoramea cerebriformis* Mello (black arrowhead); section Blejski vintgar; Julian. **(h)** *Plexoramea gracilis* (Schäfer and Senowbari-Daryan); section Blejski vintgar; lower Tuvalian. **(i)** *Thaumatoporella* sp.; section Poljane; upper Tuvalian? - Lower Norian. **(j-k)** *Radiomura cautica* Senowbari-Daryan and Schäfer; section Blejski vintgar; lower Tuvalian. (j) Transverse section. (k) Longitudinal section. **(l)** Red algae?; section Blejski vintgar; lower Tuvalian. **(m)** Calcimicrobe?; section Blejski vintgar; lower Tuvalian. **(n)** Agglutinated worm tube; section Blejski vintgar; Carnian. **(o)** Agglutinated worm tube (*Terebella* sp.); section Blejski vintgar; lower Tuvalian. **(p)** *Bacinella irregularis* Radoičić; section Blejski vintgar; Carnian. **(q)** *Dendronella articulata* Moussavian and Senowbari-Daryan; section Blejski vintgar; Carnian. **(r)** *Piallina bronnimanni* Martini et al.; section Blejski vintgar; Julian. **(s)** *Hydrania dulloi* Senowbari-Daryan; section Blejski vintgar; Carnian. **(t)** *Koskinobullina socialis* Cherchi and Schroeder; section Blejski vintgar; lower Tuvalian. **(u-v)** *Cucurbita infundibuliforme* Jablonský. (u) Section Blejski vintgar; lower Tuvalian. (v) Section Zatrnik; lower Tuvalian. **(w)** *Cucurbita longicollum* Senowbari-Daryan; section Zatrnik; lower Tuvalian. **(x)** *Cucurbita* cf. *minima* Senowbari-Daryan; section Blejski vintgar; lower Tuvalian. **(y)** *Turriglomina mesotriasica* (Koehn-Zaninetti); section Zatrnik; lower Tuvalian. (z) *Alpinophragmium perforatum* Flügel; section Poljane; lower to middle Tuvalian.

Discussion

Conodont and radiolarian data obtained in this study confirm the Longobardian age of the base of the Zatrnik Limestone. The logged succession reaches up to the Lower Norian, but basinal sedimentation clearly continued (cf. Cousin, 1981; Goričan et al., 2018). Micritic limestone with thin-shelled bivalves and radiolarians (e.g., MF 2, 3), dominating in the Zatrnik, Mt. Galetovec and Poljane sections, indicates hemipelagic sedimentation in an open marine environment. Resedimented carbonates are subordinate in these sections, but predominate in the Blejski vintgar section. Normal grading and parallel lamination suggest deposition via turbidites. Sparite-dominated varieties (MF 9, 10) are proximal turbidites, whereas micrite-rich microfacies types (MF 2, 4-7, 8, 11) are interpreted as distal turbidites (see Maurer et al., 2003). Mud-supported bioclastic-intraclastic floatstone (MF 12) and intraclastic rudstone (MF 13) might be debris-flow deposits (Mullins & Cook, 1986; Eberli, 1991). The predomination of calcarenite in the Blejski vintgar section suggests deposition in a more proximal part of the basin. Slump structures are also more common in the Blejski vintgar section. The observed transition to massive limestone in the Poljane section remains unexplained, and is also poorly dated by fossils. One possibility is that the massive bed represents a large slump, but no internal deformations were recognised and the underlying beds do not display any deformations. In view of this last argument, we rule out the possibility that the massive bed is a large block of a platform that slid into the basin. A third explanation might suggest that the section records the transition between the basin and the slope/margin of a platform. This alternative demands further explanation as to why the Zatrnik Limestone continued to deposit until the lowermost Jurassic, after which it is followed by gravity deposits. Perhaps the extent of progradation was limited, or a relative rise in sea levels led to the retreat of the platform. The answer may lie in the younger parts of the Zatrnik Limestone, which remain to be logged.

The predominance of micritic particles in resediments is common for the Middle Triassic – Early Carnian period, when carbonate platforms from slopes to tops were dominated by microbialites (Keim & Schlager, 1999; Russo, 2005; Schlager & Reijmer, 2009). Most grains (boundstone intraclasts, microproblematica) could thus have originated from the margin, slope or top of a carbonate platform (see Marangon et al., 2011). Rare fragments of green algae on the other hand surely derive from shallower parts of the adjacent platform. An increase in resedimented skeletal material is noted in late Tuvalian and/or early Norian (Mt. Galetovec and Poljane) sections. The Latest-Carnian increase in skeletal material is consistent with the conclusions of Martindale et al. (2017), who suggests that the shift towards the skeletal boundstones of the Dachstein-type reefs was gradual rather than sudden, and that the switch in dominant reef ecologies occurred during the late Carnian through early Norian interval.

The lack of siliciclastic input into the Bled Basin during the Carnian stands in contrast to the relatively closely situated Tolmin and Tarvisio Basins. Within the Tolmin Basin, clay-rich "Amphiclina beds" several tens (probably hundreds) of meters thick deposited during the Carnian. This formation is dominated by black shale alternating with lithic sandstone and hemipelagic limestone (Čar et al., 1981; Turnšek et al., 1982, 1984; Buser, 1986), whereas the uppermost part (dated as Tuvalian) consists of hemipelagic limestone alternating with black shale (Kolar-Jurk-

ovšek, 1982). In the Tarvisio Basin, the increase in the siliciclastics is reflected in the deposition of marlstone and marly limestone of the Tor Formation (Ogorelec et al., 1984; Gianolla et al., 2003; Gale et al., 2015). This is succeeded by a shallow-marine carbonate bank (the Portella Dolomite), followed by upper Tuvalian thin-bedded hemipelagic limestone and dolomite of the Carnitza Formation (Gianolla et al., 2003; Gale et al., 2015). The absence of clay input in the Bled Basin could perhaps be related to its slightly different palaeogeographic position (e.g. a position far from some river outlet), sea currents, slope steepness, etc. Alternatively, the clay-rich part of the formation could be thin and/or covered by vegetation and has thus simply not yet been recorded.

Conclusions

The Zatrnik Limestone marks the Bled Basin as a distinct paleogeographic unit. The following conclusions can be drawn from this study:

- The base of the Zatrnik Limestone is Longobardian in age.

- The Zatrnik Limestone was deposited on a basin plain and/or distal slope of the basin. The logged succession is dominated by hemipelagic limestone and distal calciturbidites. The latter are more common in the upper Julian? to lower Tuvalian. No siliciclastic-rich interval is currently recorded for the Carnian part of the formation.

- An increase in resedimented skeletal material in calciturbidites is noted in the upper Tuvalian and/or lower Norian, marking the shift from microbe-dominated to skeletal-dominated carbonate production on the platform.

Acknowledgements

This research was financially supported by the Slovenian Research Agency (Programmes No. P1-0011 and P1-0008). We thank Camille Peybernes for discussion in determination of microproblematica, Marija Petrović and Mladen Štumergar for the technical support, and students from the University of Ljubljana who attended field work and helped with logging of the sections. Reviewers are greatly acknowledged for their time, feedbacks and suggestions which led to the final state of the paper.

References

Budkovič, T. 1978: Stratigrafija Bohinjske doline. Geologija, 21: 239-244.

Buser, S. 1980: Explanatory book to Basic Geological Map SFRY 1: 100.000, Sheet Celovec (Klagenfurt). Zvezni geološki zavod, Beograd.

Buser, S. 1986: Explanatory Book to Basic Geological Map SFRY 1: 100.000, Sheets Tolmin and Videm (Udine). Zvezni geološki zavod, Beograd:103 p.

Buser, S. 1987: Basic Geological Map SFRY 1: 100.000, Sheets Tolmin and Videm (Udine). Zvezni geološki zavod.

Buser, S. 1989: Development of the Dinaric and the Julian carbonate platforms and of the intermediate Slovenian Basin (NW Yugoslavia). Mem. Soc. Geol. It., 40: 313–320.

Buser, S. 1996: Geology of Western Slovenia and its paleogeographic evolution. In: Drobne, K., Goričan, Š. & Kotnik, B. (eds.): International workshop Postojna '96: The role of impact processes and biological evolution of planet Earth. Založba ZRC, Ljubljana: 111-123.

Buser, S. 2010: Geological map of Slovenia 1:250.000. Geološki zavod Slovenije, Ljubljana.

Caggiati, M. 2014: The depositional system of Dolomia Principale/Hauptdolomit in the eastern Southern Alps: from the flattening of palaeotopography to the emplacement of the carbonate platform (Upper Triassic, NE-Italy, NW Slovenia). PhD thesis. Università degli Studi di Ferrara, Ferrara: 256 p.

Chen, Y.L., Krystyn, L., Orchard, M.J., Ali, X.L. & Richoz, S. 2015: A review of the evolution, biostratigraphy, provincialism and diversity of Middle and early Late Triassic conodonts. Papers Palaeont., 2/6: 235-263. https://doi.org/10.1002/spp2.1038

Cousin, M. 1970: Esquisse géologique des confins italo-yougoslaves: leur place dans les Dinaride set les Alpes méridionales. Bull. Soc. Géol. France, 7/12: 1034-1047.

Cousin, M. 1973: Le sillon slovène: les formations triasiques, jurassiques et néocomiennes au Nord-Est de Tolmin (Slovénie occidentale, Alpes méridionales) et leurs affinités dinariques. Bull. Soc. Géol. France, 7/15: 326-339.

Cousin, M. 1981: Les rapports Alpes-Dinarides. Les confins de l'Italie et de la Yougoslavie. Soc. Géol. Nord, 5: vol I: 1-521, vol. II Annexe: 1-521.

Čar, J., Skaberne, D., Ogorelec, B., Turnšek, D. & Placer, L. 1981: Sedimentological

characteristics of Upper Triassic (Cordevolian) circular quiet water coral bioherms in western Slovenia, northwestern Yugoslavia. SEPM Spec. Publ., 30: 233-240. https://doi.org/10.2110/pec.81.30.0233

De Zanche, V., Gianolla, P. & Roghi, G. 2000: Carnian stratigraphy in the Raibl/Cave del Predil area (Julian Alps, Italy). Eclogae Geol. Helv., 93: 331-347.

Diener, C. 1884: Beitrag zur Geologie des Zentralstockes der julischen Alpen. Jb. Kais. König. Geol. R.-A., 34: 659-706.

Doglioni, C. & Siorpaes, C. 1990: Polyphase deformation in the Col Bechei area (Dolomites –Northern Italy). Eclogae Geol. Helv., 83: 701-710.

Dozet, S. & Buser, S. 2009: Triassic. In: Pleničar, M., Ogorelec, B. & Novak, M. (eds.): The Geology of Slovenia. Geološki zavod Slovenije, Ljubljana: 161-214.

Dunham, R.J. 1962: Classification of carbonate rocks according to depositional texture. In: Han, W.E. (ed.): Classification of carbonate rocks, A symposium. American Ass. Petrol. Geol. Mem., Tulsa: 108-121.

Eberli, G.P. 1991: Calcareous turbidites and their relationship to sea-level fluctuations and tectonism. In: Einsele, G., Ricken, W. & Seilacher, D.K. (eds.): Cycles and events in stratigraphy. Springer-Verlag, Berlin Heidelberg: 45-60.

Flügel, E. 1967: Eine neue Foraminifere aus den Riff-Kalken der nordalpinen Ober-Trias: *Alpinofragmium perforatum* n. g., n. sp. Senck. Lethaea, 48: 381-402.

Gale, L. 2010: Microfacies analysis of the Upper Triassic (Norian) "Bača Dolomite": early evolution of western Slovenian Basin (eastern Southern Alps, western Slovenia). Geol. Carpathica, 61: 293-308. https://doi.org/10.2478/v10096-010-0017-0

Gale, L., Kolar-Jurkovšek, T., Šmuc, A. & Rožič, B. 2012: Integrated Rhaetian foraminiferal and conodont biostratigraphy from the Slovenian Basin, eastern Southern Alps. Swiss J. Geosci., 105/3: 435-462. https://doi.org/10.1007/s00015-012-0117-1

Gale, L., Celarc, B., Caggiati, M., Kolar-Jurkovšek, T., Jurkovšek, B. & Gianolla, P. 2015: Paleogeographic significance of Upper Triassic basinal succession of the Tamar Valley, northern Julian Alps (Slovenia). Geol. Carpathica, 66/4: 269-283. https://doi.org/10.1515/geoca-2015-0025

Geyer, G. 1900: Ueber die Verbreitung und stratigraphische Stellung der schwarzen Tropites-Kalke bei Sau Stefano in Cadore. Verh. Kaiser. König. Geol. R.-A., 15/16: 355-370.

Gianolla, P., De Zanche, V. & Mietto, P. 1998: Triassic sequence stratigraphy in the Southern Alps (Northern Italy): definition of sequences and basin evolution. In: De Graciansky, P.C., Hardenbol, J., Jacquin, T. & Vail, P.R. (eds.): Mesozoic and Cenozoc Sequence Stratigraphy of European Basins (eds.). SEPM, Spec. Publ., 60: 719-746.

Gianolla, P., De Zanche V. & Roghi, G. 2003: An Upper Tuvalian (Triassic) platform-basin system in the Julian Alps: the start-up of the Dolomia Principale (Southern Alps, Italy). Facies, 49/1: 135-150. https://doi.org/10.1007/s10347-003-0029-7

Gianolla, P., Mietto, P., Rigo, M., Roghi, G. & De Zanche, V. 2010: Carnian-Norian paleogeography in the eastern Southern Alps. Albertiana, 39: 64-65.

Goričan, Š., Košir, A., Rožič, B., Šmuc, A., Gale, L., Kukoč, D., Celarc, B., Črne, A.E., Kolar-Jurkovšek, T., Placer, L. & Skaberne, D. 2012: Mesozoic deep-water basins of the eastern Southern Alps (NW Slovenia). J. Alp. Geol., 54: 101-143.

Goričan, Š., Žibret, L., Košir, A., Kukoč, D. & Horvat, A. 2018: Stratigraphic correlation and structural position of Lower Cretaceous flysch-type deposits in the eastern Southern Alps (NW Slovenia). Int. J. Earth Sci., 107/8: 2933-2953. https://doi.org/10.1007/s00531-018-1636-4

Härtel, F. 1920: Stratigraphische und tektonische Notizen über das Wocheiner Juragebiet. Verh. Geol. Staatsanstalt, 8-9: 134-153.

Keim, L. & Schlager, W. 1999: Automicrite on steep slopes (Triassic, Dolomites, Italy). Facies, 41: 15-26.

Kolar-Jurkovšek, T. 1982: Conodonts from Amphiclina beds and Bača dolomite. Geologija, 25: 167-188.

Kolar-Jurkovšek T. & Jurkovšek B. 2019: Conodonts of Slovenia. Geološki zavod Slovenije, Ljubljana: 260 p.

Kolar-Jurkovšek, T., Buser, S. & Jurkovšek, B. 1983: Zgornjetriasne plasti zahodnega dela Pokljuke. RMZ, 30: 151-185.

Kovács, S., Sudar, M., Grădinaru, E., Gawlick, H.J., Karamata, S., Haas, J., Péro, C., Gaetani, M., Mello, J., Polák, J., Aljinović, D., Ogorelec, B., Kolar-Jurkovšek, T., Jurkovšek, B. & Buser,

S. 2011: Triassic evolution of the tectonostratigraphic units of the Circum-Pannonian Region. Jb. Geol. B.-A., 151: 199-280.

Kozur, H. 1988: Muelleritortiidae n. fam., eine charakteristische longobardische (oberladinische) Radiolarienfamilie, Teil I. Freiberger Forschungshefte, Reihe C: Geowiss., 419: 51–61.

Kozur, H. & Mostler, H. 1994: Anisian to Middle Carnian radiolarian zonation and description of some stratigraphically important radiolarians. Geol. Paläont. Mitt. Innsbruck, Sdb. 3: 39-255.

Kozur, H.W. & Mostler, H. 1996: Longobardian (Late Ladinian) Oertlispongidae (Radiolaria) from the Republic of Bosnia-Herzegovina and the stratigraphic value of advanced Oertlispongidae. Geol. Paläont. Mitt. Innsbruck, Sdb. 4: 105-193.

Kristan-Tollmann, E. 1990: Rhät-Foraminiferen aus dem Kuta-Kalk des Gurumugl-Riffes in Zentral-Papua/Neuguinea. Mitt. Österr. Geol. Ges., 82: 211-289.

Krystyn, L., Lein, R., Schlaf, J. & Bauer, F.K. 1994: Über ein neues obertriadisch--jurassisches Intraplatformbecken in den Südkarawanken. In: Lobitzer, H., Császár, G. & Daurer, A. (eds.): Jubiläumsschrift 20 Jahre Geologische Zusammenarbeit Österreich-Ungarn. Geologische Bundesanstalt, Wien: 409-416.

Kukoč, D., Goričan, Š. & Košir, A. 2012: Lower Cretaceous carbonate gravity-flow deposits from the Bohinj area (NW Slovenia): evidence of a lost carbonate platform in the Internal Dinarides. Bull. Soc. Géol. France, 183: 383–392. https://doi.org/10.2113/gssgfbull.183.4.383

Lein, R., Schlaf, J., Müller, P.J., Krystyn, L. & Jesinger, D. 1995: Neue Daten zur Geologie des Karawanken-Strassentunnels. Geol.-Paläont. Mitt. Innsbruck, 20: 371-387.

Lieberman, H.M. 1978: Carnitza Formation. Mitt. Ges. Geol. Bergbaustud. Österr., 25: 35-60.

Marangon, A., Gattolin, G., Della Porta, G. & Preto, N. 2011: The Latemar: A flat-topped, steep fronted platform dominated by microbialites and synsedimentary cements. Sed. Geol., 240: 97-114. https://doi.org/10.1016/j.sedgeo.2011.09.001

Martindale, R.C., Foster, W. & Velledits, F. 2017: The survival, recovery, and diversification of metazoan reef ecosystems following the end--Permian mass extinction event. Palaeogeogr., Palaeoclimatol., Palaeoecol., 513: 100-115. https://doi.org/10.1016/j.palaeo.2017.08.014

Matzner, C. 1986: Die Zlambach-Schichten (Rhät) in den Nördlichen Kalkalpen: Eine Platform-Hang-Beckenentwicklung mit allochthoner Karbonatsedimentation. Facies, 14: 1-104.

Maurer, F., Reijmer, J.J.G. & Schlager, W. 2003: Quantification of input and compositional variations of calciturbidites in a Middle Triassic basinal succession (Seceda, Dolomites, Southern Alps). Int. J. Earth Sci., 92/4: 593-609. https://doi.org/10.1007/s00531-002-0301-z

Mullins, H.T. & Cook, H.E. 1986: Carbonate apron models: Alternatives to the submarine fan model for paleoenvironmental analysis and hydrocarbon exploration. Sed. Geol., 48: 37-79.

Ogorelec, B., Jurkovšek, B., Šribar, L., Jelen, B., Stojanovič, B. & Mišič, M. 1984: Carnian beds at Tamar and at Log pod Mangartom. Geologija, 27: 107-158.

Placer, L. 1999: Contribution to the macrotectonic subdivision of the border region between Southern Alps and External Dinarides. Geologija, 41: 223-255. https://doi.org/10.5474/geologija.1998.013

Placer, L. & Čar, J. 1998: Structure of Mt. Blegoš between the Inner and Outer Dinarides. Geologija, 40: 305-323.

Poli, M.E. & Zanferrari, A. 1995: Dinaric thrust tectonics in the Southern Julian Prealps (Eastern Southern Alps, NE Italy). In: Vlahović, I. (ed.): Proceedings of the first Croatian Geological Congress, Opatija 18-21-10.1995, 2. Institute of Geology & Croatian Geological Society, Zagreb: 465-468.

Ramovš, A. 1986: Paläontologisch bewiesene Karn/Nor-Grenze in den Julischen Alpen. Newslett. Strat., 16: 133-138.

Ramovš, A. 1998: Conodonten-Stratigraphie der Obertrias von Slowenien: Ergebnisse eidener Untersuchungen. Geologija, 40: 223-232. https://doi.org/10.5474/geologija.1997.009

Rigo, M., Mazza, M., Karádi, V. & Nicora, A. 2018: New Upper Triassic conodont biozonation of the Tethyan realm. In: Tanner, L.H. (ed.): Topics in Geobiology, 46: 189-235. https://doi.org/10.1007/978-3-319-68009-5_6

Rožič, B. 2009: Perbla and Tolmin formations: revised Toarcian to Tithonian stratigraphy of the Tolmin Basin (NW Slovenia) and regional correlations. Bull. Soc. Géol. France, 180: 411-430.

Rožič, B., Kolar-Jurkovšek, T. & Šmuc, A. 2009: Late Triassic sedimentary evolution of

Slovenian Basin (eastern Southern Alps): description and correlation of the Slatnik Formation. Facies, 55: 137-155.

Rožič, B., Kolar-Jurkovšek, T., Žvab Rožič, P. & Gale, L. 2017: Sedimentary record of subsidence pulse at the Triassic/Jurassic boundary interval in the Slovenian Basin (eastern Southern Alps). Geol. Carpathica, 68: 543-561. https://doi.org/10.1515/geoca-2017-0036

Russo, F. 2005: Biofacies evolution of the Triassic platforms of the Dolomites, Italy. Ann. Univ. Studi Ferrara Mus. Sci. Natur., Vol. Spec. 2005: 33-44.

Schlaf, J. 1996. Ein obertriadisches Intraplattformbecken aus den Südkarawanken (Kärnten, Östereich). Mitt. Ges. Geol. Bergbaustud. Österr., 39/40: 1-14.

Schlager, W. & Reijmer, J.J.G. 2009: Carbonate platform slopes of the Alpine Triassic and the Neogene - a comparison. Austrian J. Earth Sci., 102: 4-14.

Turnšek, D., Buser, S. & Ogorelec, B. 1982: Carnian coral-sponge reefs in the Amphiclina beds between Hudajužna and Zakriž (western Slovenia). Razprave IV razreda SAZU, 24: 51-98.

Turnšek, D., Buser, S. & Ogorelec, B. 1984: The role of corals in Ladinian-Carnian reef communities of Slovenia, Yugoslavia. Paleont. Americana, 54: 201-209.

GEOLOGIJA *62/2*, 175–187, Ljubljana 2019
https://doi.org/10.5474/geologija.2019.008

Characteristics of minerals in Slovenian marbles

Značilnosti mineralov v slovenskih marmorjih

Miloš MILER[1], Tanja MAŠERA[2], Nina ZUPANČIČ[3,4] & Simona JARC[3]

[1]Geological Survey of Slovenia, Dimičeva ulica 14, SI-1000 Ljubljana, Slovenia; e-mail: milos.miler@geo-zs.si
[2]Brezje pri Grosupljem 79, SI-1290 Grosuplje, Slovenia; e-mail: masercaa@gmail.com
[3]University of Ljubljana, Faculty of Natural Sciences and Engineering, Department of Geology, Aškerčeva 12, SI-1000 Ljubljana, Slovenia, e-mails: nina.zupancic@ntf.uni-lj.si; simona.jarc@ntf.uni-lj.si
[4]Ivan Rakovec Institute of Paleontology, ZRC SAZU, Novi trg 2, SI-1000 Ljubljana, Slovenia

Prejeto / Received 23. 7. 2019; Sprejeto / Accepted 12. 11. 2019; Objavljeno na spletu / Published online 24. 12. 2019

Key words: marbles, accessory minerals, mineral assemblages, SEM/EDS, Slovenia
Ključne besede: marmorji, akcesorni minerali, mineralne združbe, SEM/EDS, Slovenija

Abstract

Common rock-forming and accessory minerals in marbles from various localities in Slovenia were studied using scanning electron microscopy with energy dispersive spectroscopy (SEM/EDS). Minerals and their chemical composition were identified in order to verify the variability of mineral assemblages in marbles from different localities in Slovenia. The analysis showed that marbles from Košenjak are the most mineralogically diverse, followed by Pohorje and finally Strojna marbles. Common rock-forming minerals calcite and dolomite are more abundant in Pohorje marbles where calcite contains higher levels of magnesium but no strontium and iron as compared with Strojna and Košenjak marbles. Accessory minerals like quartz, mica, titanite, apatite, rutile, zircon, chlorite group minerals, kaolinite and iron oxides/hydroxides were found in marbles from all localities. Clinopyroxene, amphibole, epidote and smectite group minerals, talc, tungsten-bearing ilmenorutile, psilomelane and bismuth oxides/carbonates, were observed only in marbles from Pohorje, while tourmaline and allanite group minerals, thorite or huttonite, chalcopyrite and synchysite group minerals were detected in marbles from Košenjak and Strojna. Variations in mineral assemblages in marbles from different locations are likely a consequence of different sedimentary environment and conditions and metamorphic grade of marble. These differences indicate that marbles from Košenjak and Strojna are genetically different from those from Pohorje and probably reflect mineral composition of the protolith. Thus, they enable rough distinction between more distant locations, but not between individual sub-localities.

Izvleček

Z vrstično elektronsko mikroskopijo, z energijsko disperzijsko spektroskopijo (SEM/EDS) smo raziskali kamninotvorne in akcesorne minerale v marmorjih z različnih lokacij v Sloveniji. Opredeljeni so bili minerali in njihova kemična sestava z namenom oceniti variabilnost mineralnih združb v marmorjih. Analiza je pokazala, da so marmorji s Košenjaka mineraloško najbolj raznoliki, sledijo pohorski marmorji in marmor s Strojne. Kamninotvorna minerala kalcit in dolomit sta v največjih količinah prisotna v pohorskih marmorjih, v katerih ima kalcit višje vsebnosti magnezija kot kalcit v marmorjih s Košenjaka in Strojne, vendar ne vsebuje železa in stroncija. Akcesorni minerali, kot so kremen, sljuda, titanit, apatit, rutil, cirkon, minerali kloritne skupine, kaolinit in železovi oksidi/hidroksidi, so prisotni v marmorjih z vseh lokacij. Klinopiroksen, minerali amfibolove, epidotove in smektitne skupine, lojevec, ilmenorutil z volframom, kromit, psilomelan in bizmutovi oksidi/karbonati so bili prisotni samo v pohorskih marmorjih, medtem ko so bili minerali turmalinove in allanitove skupine, torit ali huttonit, halkopirit in minerali sinhisitove skupine prepoznani le v marmorjih s Košenjaka in Strojne. Ugotovljene so bile razlike v mineralnih združbah v marmorjih z različnih lokacij, ki so verjetno posledica različnega sedimentacijskega okolja in pogojev ter različne stopnje metamorfoze marmorjev. Te razlike kažejo, da so marmorji s Košenjaka in Strojne genetsko drugačni od tistih s Pohorja in verjetno odražajo mineralno sestavo protolita. Tako omogočajo grobo razlikovanje med bolj oddaljenimi lokacijami, vendar ne med mikrolokacijami znotraj posameznih lokacij.

Introduction

Marble is a metamorphic rock composed mostly of carbonate minerals, generally calcite prevailing over dolomite. Despite its carbonate-rich character (Blatt & Tracy, 1999), marble contains various amounts of other noncarbonate minerals, especially silicates and oxides. The variety of noncarbonate minerals is derived by abundance of the original detrital minerals in the limestone and dolostone and their reactions with carbonates during metamorphism (Blatt & Tracy, 1999). Depending on the metamorphic grade the common noncarbonate minerals are dominated by quartz, brucite, phlogopite, chlorite group minerals, tremolite, diopside, forsterite, wollastonite, grossular, Ca-rich plagioclase and vesuvianite (Blatt & Tracy, 1999; Best, 2007). Therefore, the presence of noncarbonate minerals could provide information on chemistry and mineralogy of the protolith, and even the temperature and pressure during the process of metamorphism (Blatt & Tracy, 1999; Best, 2007). Hence, they are important tracers of the source areas of marble.

In Slovenia, there are several marble outcrops on Pohorje, Strojna and Košenjak – western Kozjak (Mioč, 1978; Mioč, 1983; Mioč & Žnidarčič, 1989). In the past, much attention was given to metamorphic rocks from Pohorje Mts. (Germovšek, 1954; Hinterlechner-Ravnik, 1971, 1973; Janák et al., 2004, 2005, 2006, 2009, 2015; Jarc & Zupančič, 2009; Jarc et al., 2010; Jeršek et al., 2013; Mrvar, 2013; Vrabec et al., 2010a, b; Vrabec et al., 2018). Here, the majority of medium to high-grade marbles are located in the eastern and southern parts of the massif between Oplotnica and Dravinja brooks and in the surroundings of Šmartno, where they are placed among gneisses, mica-schists and amphibolites (Hinterlechner-Ravnik & Moine, 1977; Mioč, 1978). Calcite marbles dominate, but dolomite-containing marbles are also present. The marbles are coarse-grained to less often fine-grained with granoblastic texture (Hinterlechner-Ravnik, 1971, 1973; Hinterlechner-Ravnik & Moine, 1977). Common accessory minerals are quartz, Na-rich plagioclase, tremolite, hornblende, diospide, mica, while garnet (mostly almandine), graphite, pyrite and chlorite, epidote, clinozoisite and serpentine group minerals occur rarely (Hinterlechner-Ravnik, 1971). Besides these, titanite, ferric oxides, vesuvianite, scapolite (Jarc & Zupančič, 2009; Jeršek et al., 2013), zircon, rutile and zoisite (Mrvar, 2013) have been found. Accessory minerals occur in bands, and are more frequent on the edges of marble lenses (Mrvar, 2013). Marble outcrops are small, with the exception of Rimski kamnolom in Bistriški Vintgar which has a size of about 15m × 100m (Mrvar, 2013).

Low to medium-grade marbles from western Kozjak Mts. are bluish-greyish and laminated with the high content of accessory minerals such as quartz, plagioclases, zoisite-epidote with fragments of felsic composition and phyllite (Hinterlechner-Ravnik, 1973). Several meters thick layers and small lenses of marble in Košenjak are intercalated between gneisses and mica-schist. Marbles are granoblastic, middle to coarse grained (Mioč, 1978). On Strojna, there are small outcrops of 20 cm to 50 cm thick low-grade marbles (Mioč, 1983). They contain a lot of non-carbonate minerals (e.g. quartz; Mioč, 1983).

The SEM/EDS analysis enables detection of smaller accessory minerals, which have not been reported yet, and assessment of their chemical composition. The aim of this study was therefore to characterise the accessory minerals in the marbles from different Slovenian localities by SEM/EDS analysis and to verify the local variability of the mineral assemblages and their mineral chemistry.

Geological setting

The Pohorje Mts., Strojna and Kozjak Mts. constitute the most south-eastern part of the Eastern Alps. Eastern Alps consist of a system of large nappes named Austroalpine of Cretaceous age that formed during the Eoalpine orogeny (Frank, 1987; Schmidt et al., 2004; Fodor et al., 2008). Pohorje nappe is the deepest tectonic unit (Janák et al., 2004; 2006), mainly composed of medium- to high-grade metamorphic rocks, e.g. gneisses and mica schists with lenses of amphibolite, quartzite, marble and eclogite, and north from Slovenska Bistrica also ultramafic body (SBUC) (Janák et al., 2006).

The Pohorje nappe is overlain by the nappe of weakly metamorphosed Paleozoic rocks, mainly low-grade metamorphic slates and phyllites (Hinterlechner-Ravnik, 1971, 1973; Vrabec, 2010b). The upper-most nappe is built up of Permo-Triassic clastic sedimentary rocks, prevailingly sandstones and conglomerates (Hinterlechner-Ravnik, 1971, 1973; Janák et al., 2004; Vrabec, 2010b). The entire nappe stack is overlain by early Miocene sediments, which belong to the syn-rift basin fill of the Pannonian Basin (Fodor et al., 2003). A large granodiorite body with dacite intruded in Miocene in the central part of the Pohorje massif (Dolar Mantuani, 1935; Faninger, 1970; Zupančič, 1994a, b, Trajanova et al., 2008).

In the Pohorje Mts. area, the regional metamorphism under ultra-high pressures and temperatures took place (Hinterlechner-Ravnik, 1971; Vrabec et al., 2012; Janák et al., 2015) during the Cretaceous Eo-Alpine Orogeny (Thony, 2002; Miller et al., 2005).

The Pohorje Mts., Strojna and Kozjak Mts. have very similar lithology and structure. The Strojna is separated from Pohorje Mts. by the Labot fault and the Periadriatic fault system (Mioč, 1978; Mioč & Žnidarčič, 1989). On the southern side, the Košenjak (western Kozjak) is separated from the Pohorje Mts. by the mid-Miocene Ribnica trough (Mioč, 1978).

Materials and methods

Sampling and sample preparation

A total of 24 samples of marble were collected from larger and smaller outcrops (Fig. 1). Since marble occurrences are more frequent on Pohorje Mts. and in order to check the spatial mineralogical diversity of the marble, 13 samples were taken from five different Pohorje locations, which include Hudinja (north from Vitanje; three samples), a Roman quarry Rimski kamnolom, one of the largest marble outcrops (in Bistriški vintgar; three samples), Bojtina (two samples), a smaller outcrop in Zgornja Nova Vas (three samples), and Črešnova (north from Zreče; two samples). On Strojna, four samples were taken from two small (app. 2 × 2-3 m) outcrops, and on Kozjak (Košenjak), five samples were collected along local road in the vicinity of state border and two samples from the larger up to 20 m high outcrops near border crossing Muta. From all samples, polished thin sections were prepared for inspection with scanning electron microscopy with energy dispersive spectroscopy (SEM/EDS).

SEM/EDS analyses

SEM/EDS analysis was carried out at the Geological Survey of Slovenia using a JEOL JSM 6490LV SEM coupled with an Oxford Instruments INCA Energy 350 EDS, at an accelerating voltage of 20 kV, spot size 50 and a working distance of 10 mm. The polished thin sections were carbon-coated and analysed in backscattered electron (BSE) mode under high vacuum. The chemical composition of individual minerals was measured using EDS point analysis with acquisition time of 60 s. X-ray spectra were optimised and calibrated for quantification using pre-measured standards included in the EDS software, which is a basic standardisation procedure in fitted-standards EDS analysis (Goldstein et al., 2003), referenced to a Co optimisation standard. Based on the standard ZAF-correction

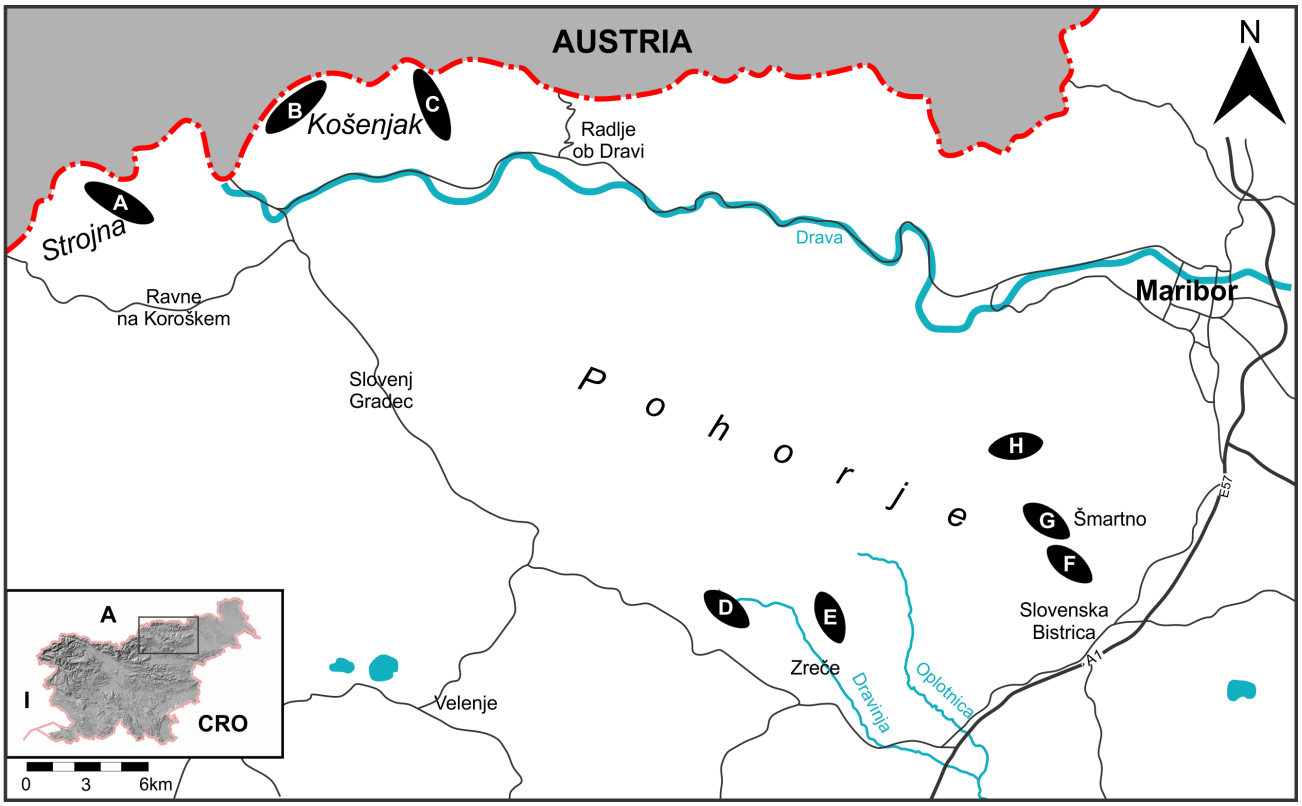

Fig. 1. Sampling locations (A – Strojna; B, C – Kozjak Mts. (Košenjak); D, E, F, G, H – Pohorje Mts. (D – Hudinja, E – Črešnova, F – Rimski kamnolom, G – Zgornja Nova Vas, H – Bojtina)).

procedure included in the INCA Energy software (Oxford Instruments, 2006), the correction of EDS data was performed. In order to assure good quality of the EDS results, only data with deviation <10 wt.% were considered for identification of minerals. Minerals were assessed by calculating stoichiometric ratios from at.% of constituent elements, acquired by the EDS analysis and comparison with atomic proportions of constituent elements in known stoichiometric minerals, obtained from mineral databases (Wünsch, 2001; Anthony et al., 2009; Barthelmy, 2010) and EDS spectra (Welton, 1984; Severin, 2004; Reed, 2005). Mineral formulae of selected minerals were obtained from mineral databases (Wünsch, 2001; Anthony et al., 2009; Barthelmy, 2010).

Results and discussion

The SEM/EDS analyses showed that calcite marbles prevail, but minor amount of dolomite is also present in samples from Pohorje. Although the focus of the study was determination of accessory minerals, the relative abundances of calcium and magnesium carbonates (calcite, dolomite) and elemental composition of calcites were also measured. The list of the identified accessory minerals or mineral groups is summarised in Table 1.

Common rock-forming minerals - calcite and dolomite

In general, marbles from Košenjak and Strojna contain between 70 to 85 % and 75 to 95 % carbonates (between 5 to 30 % noncarbonate minerals), respectively, whereas Pohorje marbles consist of 95 to 97 % of carbonates (up to 5 % of noncarbonate minerals). This indicates that Pohorje marbles are purer and appear to contain fewer accessory minerals.

Calcite in studied marbles is relatively pure, however it contains some magnesium, iron and strontium, which commonly substitute for calcium in calcite (Chang et al., 1998). Minor content of magnesium in calcite was detected in samples from all locations, with the exception of Bojtina samples. Nevertheless, calcite in Pohorje marbles contains somewhat higher levels of magnesium (mean of 0.42 at.%) compared with that in marbles from Košenjak (mean of 0.20 at.%) and Strojna (mean of 0.11 at.%). Iron in calcite was detected only in marble samples from Košenjak and Strojna. Strontium in calcite was found in all samples from Košenjak and Strojna, while it was not detected in samples from Pohorje. Presence of strontium is in agreement with marine aragonite (Fairbridge, 1967) but may also reflect different carbonate depositional environments. Since calcium/strontium ratio in calcium carbonate does not change during metamorphism (Lazzarini, 2004), and strontium is reported to be relatively immobile at high metamorphic grades (De Vos et al., 2006), and since high strontium contents have already been observed in high-grade marbles (Ofotfjorden area, Norway) whose origin was attributed to aragonitic protolith (Melezhik et al., 2003; 2013), strontium content in studied marbles probably reflects different sedimentary environment and diagenesis and metamorphic evolution. Therefore, we can assume that marbles from Košenjak and Strojna are genetically different from those from Pohorje. This finding is in agreement with findings of Jeršek et al. (2013) that Pohorje marble was metamorphosed from calcite prevailing protolith. Presence or absence of strontium could thus be used to distinguish marbles from Pohorje Mts. area from other localities.

Accessory minerals

The study showed that marbles from Pohorje, despite their higher carbonate content, seem to be mineralogically as diverse as marbles from other two localities. However, the number of different minerals or mineral groups at each specific location in Pohorje area is generally significantly smaller (Table 1). This could be explained by the higher number of analysed samples from this area, scattered sampling locations and the fact that Pohorje marbles are highly heterogeneous in isotopic and geochemical parameters as well as grain sizes (Jarc et al., 2010). Taking this into consideration, the highest number of identified minerals or mineral groups is found in marbles from Košenjak – beside calcite we identified 27 accessory minerals (Table 1). On the other hand, marble from Črešnova shows the lowest diversity in accessory minerals – only 10 of them have been observed (Table 1).

Quartz, muscovite (some grains have elevated barium content), titanite, apatite, rutile, zircon, chlorite group minerals, kaolinite and iron oxides/hydroxides are very common and have been found in samples from all localities (Table 1). SEM/EDS analyses revealed differences in chemical compositions of some very common accessory minerals, titanite and apatite. It seems that the elemental composition of titanites depends on the sampling locations, as in Košenjak and Strojna marbles they have higher contents of aluminium and fluorine incorporated in their crystal structure than those in Pohorje marbles.

Table 1. Mean number of identified accessory mineral grains in number (n) of samples from studied localities/locations

Mineral/mineral group	Sampling locality			Pohorje (PO) sampling locations				
	ST(A)	KO(B, C)	PO	HU(D)	CR(E)	RK(F)	ZNV(G)	BO(H)
	n=4	n=7	n=13	n=3	n=2	n=3	n=3	n=2
Actinolite			1.2			4.7		0.5
Alkali feldspar	0.3		0.3				1.3	
Allanite group	0.3	1.6						
Alloclasite/cobaltite		0.1						
Apatite group	3.5	2.0	2.2	1.3	3.0	2.0	2.0	3.0
Asbolane	0.3							
Ba-muscovite	3.0	0.9	0.4	1.7				
Bastnäsite	0.3							
Bismuth/bismite/bismutite			0.1			0.3		
Chalcopyrite	0.3	0.3						
Chlorite group	0.3	0.4	1.4	3.7		1.0		2.0
Diopside			0.5			0.7		2.0
Epidote			0.2					1.5
Fe-oxide/hydroxide	2.0	0.7	0.2	0.3		0.3	0.3	
Fluorite		0.4						
Galena		0.4						
Hornblende			0.2			1.0		
Ilmenorutile (W)			0.1			0.3		
Kaolinite	2.8	0.9	0.3		2.0			
Molybdenite		0.6						
Monazite group	0.3							
Muscovite	2.8	3.0	0.6	0.3			1.0	2.0
Phlogopite		0.4	1.5	1.7		3.0	1.7	
Plagioclase		2.4	0.8	1.3		0.3		2.5
Psilomelane			0.2				0.7	
Pyrite		2.4	0.7	0.7	0.5	1.7		0.5
Pyrrhotite		2.1	0.5		1.0	1.0		1.0
Quartz	3.8	3.1	2.2	3.7	1.5	0.3	1.3	5
Rutile	1.5	1.0	0.6	0.3	0.5	1.3	0.3	0.5
Smectite group			0.5				2.3	
Sphalerite		0.1	0.2		0.5	0.3		
Synchysite group/petersenite	0.3	0.3						
Talc			0.7	1.0	1.5	1.0		
Thorite/huttonite	0.8	0.1						
Titanite	0.5	3.7	1.5	1.7	1.0	1.3	1.0	2.5
Tourmaline group	1.0	0.3						
Ullmannite		0.1						
Uraninite		0.3	0.2			0.7		
Zircon	1.0	1.9	0.5	0.3		0.3	0.3	1.5
Zoisite		1.3	0.5	0.7	0.5			1.5
∑ mean number of grains	24.6	31.0	18.1	18.7	12.0	21.7	12.3	26.0
Number of mineral species	18	27	27	14	10	19	11	14

ST-Strojna, KO-Košenjak, PO-Pohorje (HU-Hudinja, CR-Črešnova, RK-Rimski kamnolom, ZNV-Zgornja Nova Vas, BO-Bojtina)

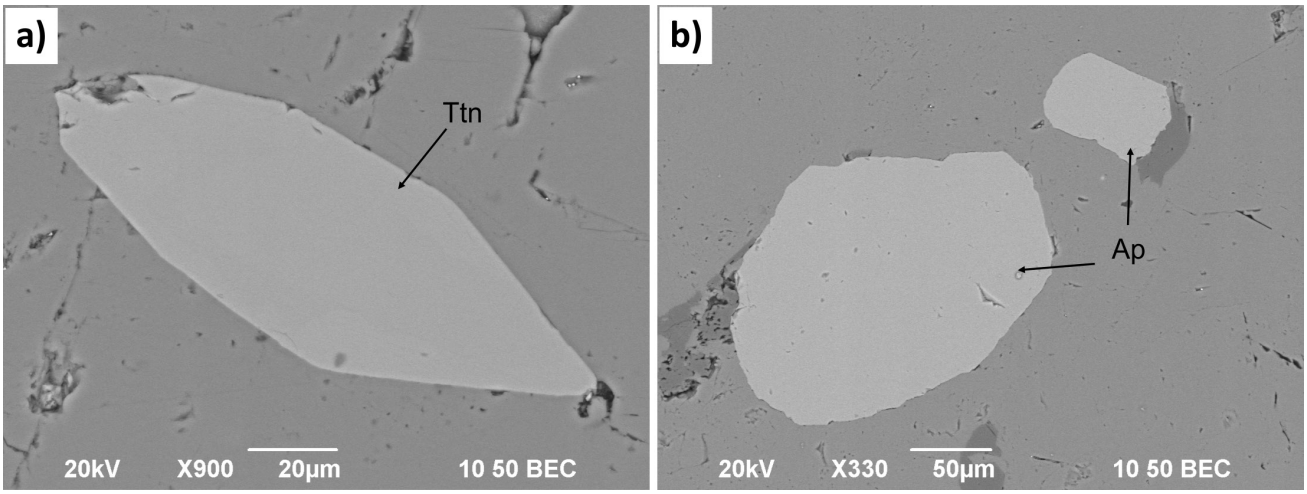

Fig. 2. SEM (BSE) images of: a) titanite (Ttn) grain in marble from Hudinja; b) apatite (Ap) grains in marble from Hudinja.

In all samples, titanite occurs mostly as euhedral individual grains (Fig. 2a) in calcite or is associated with other minerals. In samples from Košenjak, titanite is associated with plagioclase, muscovite, Ba-muscovite, zoisite, fluorapatite, uraninite and also zircon, which occurs as an inclusion in some titanite grains. In samples from Strojna, titanite was found associated with muscovite. Titanites in samples from Hudinja, Rimski kamnolom and Zgornja Nova Vas are associated with zoisite and anorthite, phlogopite and actinolite, and quartz, respectively. The mean sizes of titanite grains are 100 µm in Košenjak samples and 62 µm in Strojna samples, while in the samples from Pohorje they range from 71 µm in Črešnova to 116 µm in Rimski kamnolom samples.

Rutile, which was found in all samples (Table 1), is mostly associated with titanite. Individual euhedral grains in calcite are rarely found. By its chemical composition, rutile is mostly pure, however in samples from Košenjak and Strojna rutile grains have minor contents of vanadium and iron. It can be assumed that rutile is mostly a secondary mineral formed during metamorphism, however individual grains in calcite could also originate from the protolith. The sizes of rutile grains are up to 25 µm in Košenjak samples, up to 68 µm in Strojna samples. In the Pohorje samples they range from 5 µm in Črešnova to 35 µm in Bojtina samples.

Apatite is also found in samples from all localities (Table 1). All measured apatite grains contain fluorine, whose content depends on the location. Apatite in marble samples from Košenjak and Strojna has higher fluorine contents than those in Pohorje marbles, while those in Pohorje marbles has also minor content of chlorine. Apatite mainly forms euhedral rounded to elongated grains with isometric cross-sections (Fig. 2b) as individual grains in calcite or in association with other minerals. In samples from Košenjak, it is associated with phlogopite, plagioclase (albite and oligoclase), muscovite and quartz. Apatite in samples from Strojna is associated with iron oxides/hydroxides. In samples from Hudinja and Rimski kamnolom, it is accompanied by dolomite, while in Zgornja Nova Vas and Bojtina samples apatite is associated with muscovite and plagioclase, respectively. The mean sizes of apatite grains are 106 µm in Košenjak samples and 85 µm in Strojna samples, while in the samples from Pohorje they range from 76 µm in Zgornja Nova Vas to 231 µm in Hudinja samples.

Tourmaline and allanite group minerals, thorite or huttonite, chalcopyrite and minerals of synchysite group ($Ca(Ce,La)(CO_3)_2F$), or pseudomorphs of synchysite after petersenite ($(Na,Ca)_4(Ce,La,Nd,Sr)_2(CO_3)_5$), were detected in samples from Košenjak and Strojna, but not in Pohorje marbles. Tourmaline grains with composition of uvite or dravite are euhedral, zoned and up to 200 µm in size. They are associated with rutile and illite. Grains of allanite group minerals are zoned, anhedral and up to 70 µm large. They occur individually in calcite or accompany quartz and pyrite. Anhedral chalcopyrite grains of 50 µm in size form assemblages with pyrite and muscovite in Košenjak marbles and with kaolinite and rutile in Strojna marbles. Plagioclase, phlogopite, zoisite, pyrite, pyrrhotite, sphalerite and uraninite were observed in marbles from Košenjak and Pohorje. Compositions of plagioclase vary from albite to anorthite. Anorthite was present particularly in Košenjak and Hudinja samples. In some samples (Strojna and Pohorje), alkali feldspar (e.g. anorthoclase) is present (Table 1). Phlogopite occurs as subhedral (in Košenjak) to anhedral (in Pohorje samples)

flakes with elongated cross-sections with size of up to 550 µm. Phlogopite forms assemblages with apatite and titanite in Košenjak and with talc, dolomite, chlorite group minerals and illite in Pohorje marbles. Zoisite is up to 200 µm large in all marbles. In Košenjak marbles it is elongated and subhedral and associated with quartz, titanite and pyrite, while in Pohorje marbles it is anhedral and found as inclusions in plagioclase or kaolinite grains. In some grains of zoisite in Košenjak samples, minor content of strontium was detected. Some pyrite grains in Košenjak samples contain minor level of nickel, while some pyrites from Pohorje (Rimski kamnolom) samples contain either minor level of cobalt or arsenic. Also, some pyrrhotite grains in Košenjak and Pohorje (Rimski kamnolom, Bojtina) samples contain minor level of nickel. Pyrite and pyrrhotite commonly form assemblages with other sulphides. Sphalerite is subhedral with isometric cross-sections and up to 34 µm large and forms assemblages with pyrrhotite, pyrite with molybdenite inclusion and quartz.

Some minerals were found only in marbles of a specific metamorphic grade and from a specific location, which could be a consequence of different sedimentary environment and conditions and/or degree of metamorphism. Thus, anhedral void-filling fluorite, galena (subhedral inclusions in pyrite and pyrrhotite), molybdenite (also with minor content of tungsten), ullmannite (NiSbS) and ((Co,Fe)AsS) or cobaltite (CoAsS) were found only in marbles from Košenjak, while monazite group minerals (subhedral grains in calcite), bastnäsite ($(Ce,La)(CO_3)F$) and asbolane ($(Ni,Co)_xMn(O,OH)_4 \cdot nH_2O$) are present only in Strojna marbles. Clinopyroxene (e.g. diopside, augite) (anhedral and associated with actinolite), amphibole (hornblende, actinolite) (subhedral to anhedral and associated with pyrite, apatite, titanite, dolomite) and epidote group minerals (euhedral in assemblage with chlorite group minerals and quartz), talc (elongated anhedral and associated with phlogopite, chlorite group minerals and dolomite), smectite group minerals, tungsten-bearing ilmenorutile ($(Ti,Nb,Fe)O_2$), psilomelane (anhedral fillings in chlorite group minerals and quartz or euhedral needle-like crystals along cleavage planes in dolomite) and bismuth oxides or carbonates were observed only in Pohorje marbles. This could also result from highly variable mineral composition of marbles and the relatively small number of inspected samples. For example, epidote was observed only in samples from Bojtina, but other researchers detected it also in marbles from other localities on Pohorje (Jarc & Zupančič, 2009; Jarc et al., 2010; Jeršek et al., 2013) and Košenjak (Komar, 2006). Diopside was also previously found in Bojtina (Jeršek et al., 2013), in the surroundings of Črešnova (Hinterlechner-Ravnik, 1971) and Slovenska Bistrica (Mrvar, 2013). This shows that the marbles are very heterogeneous, also regarding content and type of accessory minerals.

The mineral assemblages of index minerals, which indicate the degree of metamorphism according to Blatt & Tracy (1999), are similar in all studied marbles and show similar metamorphic grades (Table 1). However, the greatest amount of minerals typical of low metamorphic grades (e.g. muscovite, chlorite group, rutile, albite) was found in Košenjak and Strojna marbles. Minerals of medium metamorphic grades (e.g. titanite, epidote, hornblende, diopside) are most abundant in Košenjak marbles, while minerals indicating high metamorphic grades (e.g. zoisite, alkali feldspar, phlogopite) prevail in Pohorje marbles. This is consistent with high-grade metamorphic rocks of Pohorje Mts. (Hinterlechner-Ravnik, 1971; Vrabec et al., 2012; Janák et al., 2015) and with low metamorphic grades reported for Strojna marbles (Mioč, 1983).

Some minerals described in this study have been observed for the first time in Slovenian marbles. These minerals are synchysite group minerals or pseudomorphs of synchysite after petersenite, bastnäsite, tungsten-bearing ilmenorutile, ullmannite, asbolane, alloclasite or cobaltite, bismuth/bismuth oxides or carbonates, thorite or huttonite, uraninite and molybdenite. Synchysite group minerals, or pseudomorphs of synchysite after petersenite, occur as up to 40 µm large anhedral aggregates of fibrous crystals in kaolinite (Fig. 3a), which are in Strojna samples associated with 29 µm large anhedral grains possibly of mineral bastnäsite. Synchysite fibrous crystals can also be found along cracks in grains of allanite group minerals or along the calcite-mica boundaries. Both synchysite and bastnäsite are possibly secondary minerals that could have formed due to local hydrothermal activity. Synchysite has already been found in low-grade high REE-marbles within biotite phyllites of Horní Dunajovice in Western Moravia, where REE enrichment was ascribed to protolith composition and formation of synchysite to early metamorphosis (Houzar et al., 2004). Others reported synchysite in high-grade marbles, e.g. in Otter Lake area (Quebec), occurring as inclusions within fluorapatite together with some other rare accessory minerals, such

as allanite and thorite (Martin et al., 2017). Bastnäsite was observed also in carbonatite related, altered dolomite marble in Bayan Obo (Mongolia) (Smith et al., 1999). Uraninite is mostly chemically pure, but some grains may also contain minor level of thorium. It forms euhedral to subhedral subrounded grains with sizes ranging between 3 µm and 16 µm and mostly isometric cross-sections. They are associated with about 6 µm large anhedral grain of tungsten-bearing ilmenorutile, pyrite (Fig. 3b) and titanite and only few grains are found individually in dolomite and calcite. Ullmannite occurs as euhedral to subhedral grain with size of about 5 µm associated with pyrrhotite (Fig. 3c). Ullmannite has been reported in medium to high-grade metamorphic metasedimentary rocks from hydrothermal solutions (Dobbe, 1991), but was also found in low-grade dolomite marbles in Watten valley (Austria) (Haditsch & Mostler, 1983). Asbolane is up to 12 µm large anhedral and plumose aggregates of fibrous crystals filling voids and cracks at the contact between mica and calcite (Fig. 3d). Its morphology and form of occurrence indicate that it is a secondary mineral. Alloclasite or cobaltite (Fig. 4a) forms a 4 µm large euhedral inclusion in pyrrhotite, which is associated with a grain of biotite group mineral. About 1 µm large elongated and subhedral inclusion of bismuth/bismuth oxide or carbonate (Fig. 4b) was found in pyrrhotite at the boundary with calcite. No reports on asbolane, alloclasite or cobaltite and bismuth/bismuth oxide or carbonate occurrences in marbles have been found. Thorite or huttonite occurs as euhedral to subhedral grains of 30 µm in size (Fig. 4c), mostly as inclusions in Ba-muscovite or in association with quartz, zircon and pyrite. Some grains appear to be intergrown with yttrialite. Ditz et al. (1990) reported thorite in metasomatised impure marbles near contacts of granitic and pegmatitic intrusions of Grenville subprovince (Canada), while Drábek et al. (2017) found thorite together with molybdenite, pyrite, pyrrhotite, galena and chalcopyrite also in regionally metamorphosed medium to high-grade carbonatite-like marble at Bližná. Molybdenite forms laths or tabular crystals with grain sizes ranging between 13 µm and 38 µm. They are mostly enclosed in pyrite or in mica (Fig. 4d) and quartz. Some molybdenite grains contain minor levels of tungsten. No reports on molybdenite in marbles have been found, however, lath-like tungsten rich molybdenite was found in granite rocks within orthogneiss at Vítkov (Bohemian Massif, Czech Republic) (Pašava et al., 2015).

Since these rare minerals occur in many different metamorphic rocks (including marbles) varying in metamorphic grade, they could not be considered as definite indicators of metamorphic grade.

Some minerals that were reported in the literature, such as garnet, graphite, serpentine group minerals (Hinterlechner-Ravnik, 1971), tremolite (Jarc & Zupančič, 2009; Mrvar, 2013), vesuvianite (Jeršek et al., 2013) and scapolite (Jeršek et al., 2013; Mrvar, 2013), were not observed in our study. This indicates the highly heterogeneous mineral assemblages in marbles from studied sites.

Conclusions

Marbles from Pohorje Mts. are relatively pure, composed mostly of carbonate and containing only up to 5 % of noncarbonate minerals, while marbles from Košenjak and Strojna localities contain from 5 % to 30 % of noncarbonate minerals.

Marbles from Košenjak are mineralogically the most diverse. Beside calcite, we recognized 27 minerals or mineral groups, while in marbles from Črešnova only 10 minerals or mineral groups besides calcite and dolomite were detected. Some minerals like quartz, mica, titanite, apatite, rutile, zircon, chlorite group minerals, kaolinite and iron oxides/hydroxides are very common and were found in marbles from all localities. Other minerals, such as clinopyroxene, amphibole, epidote, and smectite group minerals, talc, tungsten-bearing ilmenorutile, psilomelane and bismuth oxides or carbonates, were observed only in samples from Pohorje Mts., while tourmaline and allanite group minerals, thorite or huttonite, chalcopyrite and minerals of synchysite group, or pseudomorphs of synchysite after petersenite, were detected in marbles from Košenjak and Strojna.

Further, SEM/EDS analysis showed the differences in chemical composition of calcite, titanite and apatite in marbles from different localities. Namely, calcites in samples from Košenjak and Strojna contain detectable amounts of strontium, which is not detected in Pohorje samples. Titanites from Košenjak and Strojna contain higher level of aluminium and fluorine than those from Pohorje marbles. Apatite in marbles from Košenjak and Strojna has also higher content of fluorine than those from Pohorje marbles, however it does not contain chlorine, which is present in apatite from Pohorje.

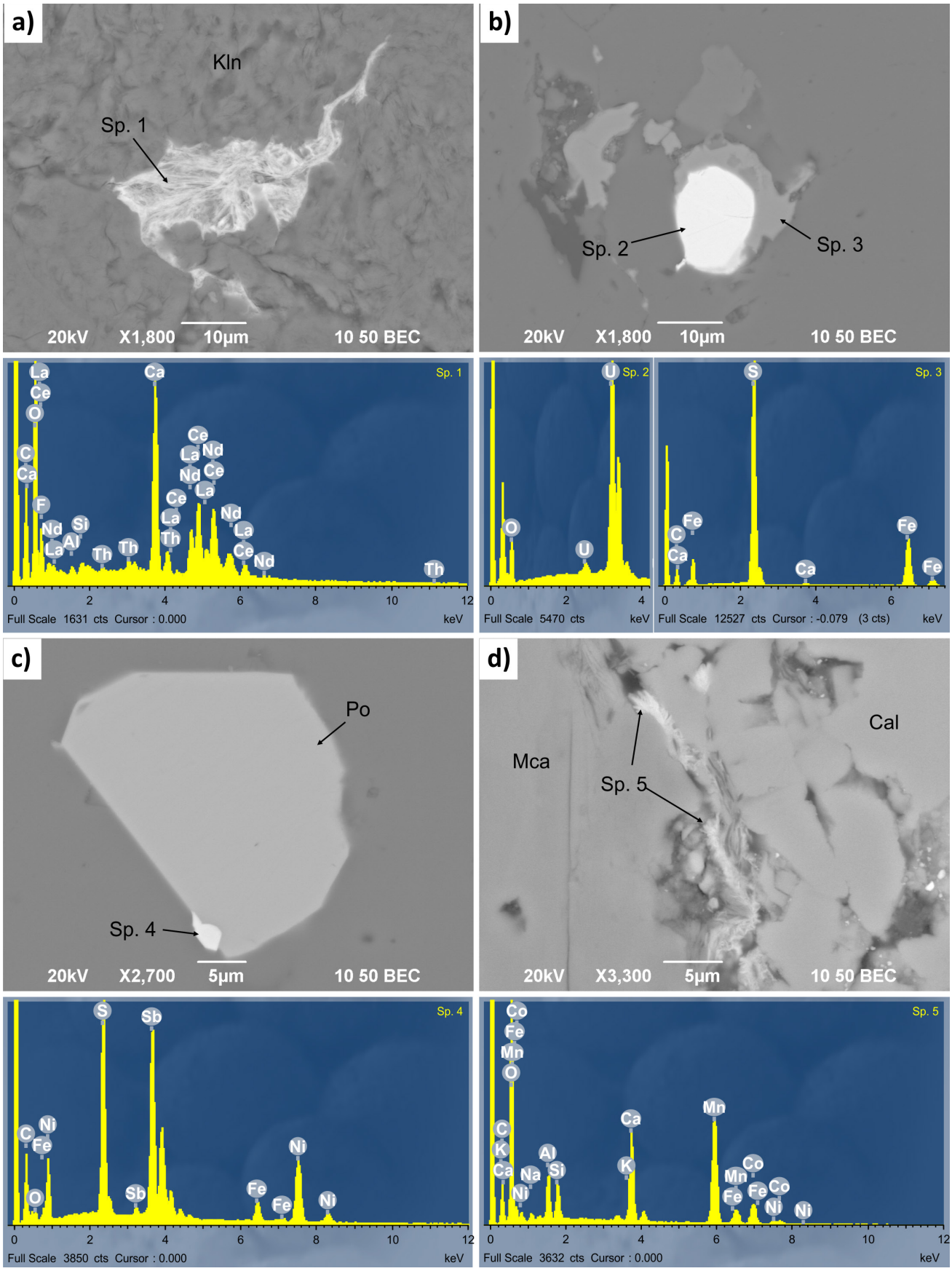

Fig. 3. SEM (BSE) images and EDS spectra of: a) grain of synchysite group mineral (Sp. 1), or pseudomorph of synchysite after petersenite in kaolinite (Kln) (marble from Košenjak); b) uraninite (Sp. 2) associated with pyrite (Sp. 3) (marble from Košenjak); c) ullmannite (Sp. 4) grain associated with pyrrhotite (Po) (marble from Košenjak) and d) asbolane (Sp. 5) aggregates at the contact between mica (Mca) and calcite (Cal) (marble from Strojna).

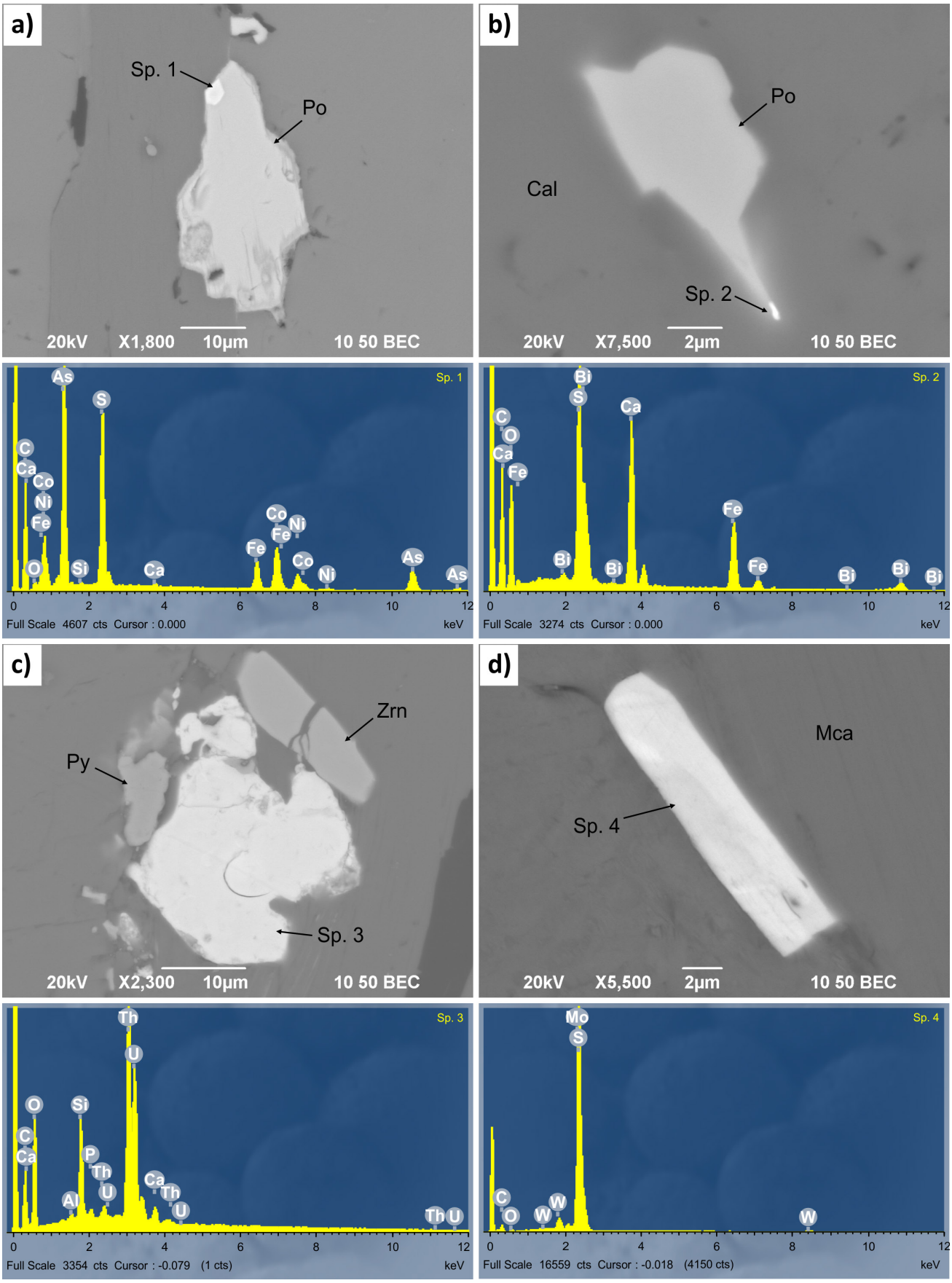

Fig. 4. SEM (BSE) images and EDS spectra of: a) inclusion of alloclasite or cobaltite (Sp. 1) in pyrrhotite (Po) (marble from Košenjak); b) inclusion of bismuth/bismuth oxide or carbonate (Sp. 2) in pyrrhotite (Po) at the boundary with calcite (Cal) (marble from Rimski kamnolom); c) thorite or huttonite (Sp. 3) associated with zircon (Zrn) and pyrite (Py) (marble from Košenjak) and d) molybdenite (Sp. 4) crystal enclosed in mica (Mca) (marble from Košenjak).

In all investigated marbles, 39 minerals or mineral groups were identified besides calcite and dolomite. For the first time in Slovenian marbles, minerals of synchysite group, or pseudomorphs of synchysite after petersenite, bastnäsite, tungsten-bearing ilmenorutile, ullmannite, asbolane, alloclasite or cobaltite, bismuth/bismuth oxides or carbonates, thorite or huttonite, uraninite and molybdenite were observed.

Although there are some differences in mineral assemblages between marbles from different locations, which are likely a consequence of different sedimentary environment and conditions and degree of metamorphism, they could also reflect heterogeneous nature of investigated marble sites and limited number of inspected samples. Based merely on mineral assemblages, we cannot argue to distinguish between marble localities of the three different massifs.

However, the differences in composition of very common minerals, such as calcite, titanite and apatite that are widespread in marbles from all three massifs, should enable rough distinction between more distant locations and marbles of different metamorphic grades, but not between individual sub-localities.

Established differences in mineral assemblages and chemical composition of common minerals could be useful for identification of sources of marbles.

Acknowledgements

The authors acknowledge the financial support from the state budget of the Slovenian Research Agency obtained through the research programs "Geochemical and structural processes" (No. P1-0195) and "Paleontology and Sedimentary Geology" (No. P1-0008) and post-doc research project "Source identification of solid pollutants in the environment on the basis of mineralogical, morphological and geochemical properties of particles" (Z1-7187). The study was partly supported by UNESCO and IUGS project IGCP 637: Heritage Stone Designation. We are also grateful to technical co-worker Ema Hrovatin for help with the preparation of samples.

References

Anthony, J.W., Bideaux, R.A., Bladh, K.W. & Nichols, M.C. 2009: The Handbook of Mineralogy. Mineralogical Society of America. Internet: http://www.handbookofmineralogy.org/

Barthelmy, D. 2010: The Mineralogy Database. Internet: http://webmineral.com/

Best, M.G. 2007: Igneous and metamorphic petrology. Second Edition, Blackwell Publishing: 729 p.

Blatt, H. & Tracy, R.J. 1999: Petrology Igneous, Sedimentary, and Metamorphic. Second Edition, W.H. Freeman and Company: 529 p.

Chang, L.L.Y., Howie, R.A. & Zussman, J. 1998: Non-silicates: Sulphates, Carbonates, Phosphates, Halides. Rock-forming minerals, Volume 5B, Second Edition. The Geological society, London: 383 p.

De Vos, W., Demetriades, A., Marsina, K., Ottesen, R.T., Reeder, S., Pirc, S., Salminen, R. & Tarvainen, T. 2006: Comparison of elements in all sample media, general comments and conclusions. In: De Vos, W. & Tarvainen, T. (eds.): Geochemical Atlas of Europe. Part 2 - Interpretation of Geochemical Maps, Additional tables, Figures, Maps, and Related Publications. Espoo: Geological Survey of Finland, Otamedia Oy: 45–432.

Ditz, R., Sarbas, B., Schubert, P. & Töpper, W. 1990: Gmelin Handbook of Inorganic Chemistry, 8th edition, Th Thorium, Supplement Volume A1a, Natural Occurrence, Minerals (excluding silicates). Springer-Verlag, Berlin-Heidelberg: 392 p.

Dobbe, R.T.M. 1991: Ullmannite, cobaltian ullmannite and willyamite from Tunaberg, Bergslagen, central Sweden. Can. Mineral., 29: 199–205.

Dolar Mantuani, L. 1935: Tonalite and aplite ratio of Pohorje massiv. Geološki Anali Balkanskog Poluostrova, 12: 1–165 (in Slovenian, with German abstract).

Drábek, M., Frýda, J., Šarbach, M. & Skála, R. 2017: Hydroxycalciopyrochlore from a regionally metamorphic marble at Bližná, Southwestern Czech Republic. N. Jb. Miner. Abh. (J. Min. Geochem.), 194/1: 49–59.

Drábek, M. & Stein, H. 2015: Molybdenite Re-Os dating of Mo-Th-Nb-REE rich marbles: pre-Variscan processes in Moldanubian Variegated Group (Czech Republic). Geol. Carpath., 66/3: 173–179.

Fairbridge, R.W. 1967: Carbonate rocks and paleoclimatology in the biogeochemical history of the planet. In: Chilingar, G.V., Bissel, H.J. & Fairbridge, R.W. (eds.): Developments in sedimentology 9a, Carbonate Rocks: origin, occurrence and classification. Amsterdam: Elsevier Publishing Company: 399–432.

Faninger, E. 1970: The tonalite of Pohorje and its differentiates. Geologija, 13: 35–104 (in Slovenian and in German).

Fodor, L., Gerdes, A., Dunkl, I., Koroknai, B., Pécskay, Z., Trajanova, M., Horváth, P., Vrabec, M., Jelen, B., Balogh, K. & Frisch, W. 2008: Miocene emplacement and rapid cooling of the Pohorje pluton at the Alpine-Pannonian-Dinaric juction, Slovenia. Swiss Journal of Geoscience, 101: 255–271. https://doi.org/10.1007/s00015-008-1286-9

Frank, W. 1987: Evolution of the Austroalpine elements in the Cretaceous. In: Flügel, H.W. & Faupel, P. (eds.): Geodynamics of the Eastern Alps. Vienna: Deuticke: 379–406.

Germovšek, C. 1954: Petrographic research of Pohorje in 1952. Geologija, 2: 191–210 (in Slovenian and in English).

Haditsch, J.G. & Mostler, H. 1983: The succession of ore mineralization of the Lower Austroalpine Innsbruck Quartzphyllite. In: Schneider, H.J. (ed.): Mineral deposits of the Alps and of the Alpine epoch in Europe. Berlin, Heidelberg: Springer-Verlag: 51–60.

Hinterlechner-Ravnik, A. 1971: Metamorphic rocks of Pohorje mountains. Geologija, 14: 187–226 (in Slovenian with English summary).

Hinterlechner-Ravnik, A. 1973: Metamorphic rocks of the Pohorje mountains II. Geologija, 16: 245–269 (in Slovenian with English abstract).

Hinterlechner-Ravnik, A. & Moine, B. 1977: Geochemical characteristics of the metamorphic rocks of the Pohorje Mountains. Geologija, 20: 107–140.

Houzar, S., Leichmann, J., Kapinus, A. & Vávra V. 2004: REE-bearing marble from Horní Dunajovice (Lukov unit, Moravicum) in Western Moravia. Acta Musei Moraviae, Sci. geol., 89: 139–148 (in Czech with English summary).

Janák, M., Froitzheim, N., Vrabec, M. & Krogh Ravna, E.J. 2004: First evidence for ultrahigh-pressure metamorphism of eclogites in Pohorje, Slovenia: Tracing deep continental subduction in the Eastern Alps. Tectonics, 23, TC5014.

Janák, M., Froitzheim, N., Vrabec, M. & Krogh Ravna, E.J. 2005: Reply to comment by R. and J. Konzett on »First evidence for ultrahigh – pressure metamorphism of eclogites in Pohorje, Slovenia: Tracing deep continental subduction in the Eastern Alps«. Tectonics, 24, TC6011.

Janák, M., Froitzheim, N., Vrabec, M., Krogh Ravna, E.J. & De Hoog, J.C.M. 2006: Ultrahigh-pressure metamorphism and exhumation of garnet peridotite in Pohorje, Eastern Alps. Journal of Metamorphic Geology, 24: 19–31. https://doi.org/10.1111/j.1525-1314.2005.00619.x

Janák, M., Cornell, D., Froitzheim, N., De Hoog, J.C.M., Broska, I., Vrabec, M. & Hurai, V. 2009: Eclogite-hosting metapelites from the Pohorje Mountains (Eastern Alps): PT evolution, zircon geochronology and tectonic implications. European Journal of Mineralogy, 21: 1191–1212.

Janák, M., Frotzhein, N., Yoshida, K., Sasinkova, V., Nosko, M., Kobayashi, T., Hirajima, T. & Vrabec, M. 2015: Diamond in metasedimentary crustal rocks from Pohorje, Eastern Alps: a window to deep continental subduction. Journal of Metamorphic Geology, 33: 495–512.

Jarc, S. & Zupančič, N. 2009: A cathodoluminescence and petrographical study of marbles from the Pohorje area in Slovenia. Chemie der Erde, 69: 75–80. https://doi.org/10.1016/j.chemer.2008.01.001

Jarc, S., Maniatis, Y., Dotsika, E., Tambakopoulos, D., & Zupančič, N. 2010: Scientific characterization of the Pohorje marbles, Slovenia. Archaeometry, 52/2: 177–190.

Jeršek, M., Kramar, S., Skobe, S., Zupančič, N. & Podgoršek, V. 2013: Minerals of Pohorje marbles. Geologija, 56/1: 49–56. https://doi.org/10.5474/geologija.2013.004

Komar, D. 2006: Marmorji iz Košenjaka, seminar work. Faculty of Natural Sciences and Engineering: 20 p.

Lazzarini, L. 2004: Archaeometric aspects of white and coloured marbles used in antiquity: the state of the art. Periodico di Mineralogia, 73: 113–125.

Martin, R.F., Schumann, D. & de Fourestier, J. 2017: The clusters of accessory minerals in Grenville marble crystallized from globules of melt. In: Book of abstracts, CAM-2017, Conference on accessory minerals, 13-17 September 2017, Vienna: Institut für Mineralogie und Kristallographie, Universität Wien, 79–80.

Melezhik, V.A., Zwaan, B.K, Motuza, G., Roberts, D., Solli, A., Fallick, A.E., Gorokhov, I.M. & Kusnetzov, A.B. 2003: New insights into the geology of high-grade Caledonian marbles based on isotope chemostratigraphy. Norw. J. Geol., 83: 209–242.

Melezhik, V.A., Roberts, D., Gjelle, S., Solli, A., Fallick, A.E., Kusnetzov, A.B. &. Gorokhov, I.M. 2013: Isotope chemostratigraphy of high--grade marbles in the Rognan area, North-Central Norwegian Caledonides: a new geological map, and tectonostratigraphic and palaeogeographic implications. Norw. J. Geol., 93: 107–139.

Miller, C., Mundil, R., Thöni, M. & Konzett, J. 2005: Refining the timing of eclogite metamorphism: a geochemical, petrological, Sm-Nd and U-Pb case study from the Pohorje Mountains, Slovenia (Eastern Alps). Contrib. Mineral. Petrol., 150: 70–84.

Mioč, P. 1978: Osnovna geološka karta SFRJ 1:100.000. Tolmač za list Slovenj Gradec (L 33–55). Zvezni geološki zavod, Beograd: 74 p (in Slovenian with English summary).

Mioč, P. 1983: Osnovna geološka karta SFRJ 1:100,000. Tolmač za list Ravne na Koroškem (L 33–54). Zvezni geološki zavod, Beograd: 69 p (in Slovenian with English summary).

Mioč, P. & Žnidarčič, M. 1989: Osnovna geološka karta SFRJ 1:100,000. Tolmač za list Maribor in Leibnitz. Zvezni geološki zavod, Beograd: 60 p (in Slovenian with English summary).

Mrvar, L. 2013: Petrological and microstructural characteristics of the eastern part of Pohorje mountains, diploma thesis. Faculty of Natural Sciences and Engineering: 61 p.

Oxford Instruments 2006: INCA Energy Operator Manual. Oxford Instrumental Analytical Ltd.: 84 p.

Pašava, J., Veselovský, F., Drábek, M., Svojtka, M., Pour, O., Klomínský, J., Škoda, R., Ďurišová, J., Ackerman, L., Halodová, P. & Haluzová, E. 2015: Molybdenite–tungstenite association in the tungsten-bearing topaz greisen at Vítkov (Krkonoše–Jizera Crystalline Complex, Bohemian Massif): indication of changes in physico-chemical conditions in mineralizing system. J. Geosci. Czech, 60, 149–161.

Reed, S.J.B. 2005: Electron Microprobe Analysis and Scanning Electron Microscopy in Geology. Second Edition. Cambridge University Press: 189 p.

Schmid, S.M., Fügenschuh, E., Kissling, E. & Schuster, R. 2004: Tectonic map and overall architecture of the Alpine orogen. Eclogae Geol. Helv., 97/1: 93–117. https://doi.org/10.1007/s00015-004-1113-x

Severin, P.K. 2004: Energy Dispersive Spectrometry of Common Rock Forming Minerals. Springer: 225 p.

Smith, M.P., Henderson, P. & Peishan, Z. 1999: Reaction relationships in the Bayan Obo Fe-REE-Nb deposit Inner Mongolia, China: implications for the relative stability of rare-earth element phosphates and fluorocarbonates. Contrib. Mineral. Petrol., 134: 294–310.

Thöni, M. 2002: Sm-Nd isotope systematics in garnet from different lithologies (Eastern Alps): age results, and an evaluation of potential problems for garnet Sm-Nd chronometry. Chem. Geol., 185: 255–281.

Trajanova, M., Pécskay, Z., Itaya, T. 2008: K-Ar geochronology and petrography of the Miocene Pohorje mountains balholith (Slovenia). Geol. Carpath., 59/3: 247–260.

Vrabec, M. 2010a: Pohorje eclogites revisited: Evidence for ultrahigh-pressure metamorphic conditions. Geologija, 53/1: 5–20. https://doi.org/10.5474/geologija.2010.001

Vrabec, M. 2010b: Garnet peridotites from Pohorje: petrography, geothermobarometry and metamorphic evolution. Geologija, 53/1: 21–36. https://doi.org/10.5474/geologija.2010.002

Vrabec, M., Janák, M., Froitzheim, N. & De Hoog, J.C.M. 2012: Phase relations during peak metamorphism and decompression of the UHP kyanite eclogites, Pohorje Mountains (Eastern Alps, Slovenia). Lithos, 144-145: 40–55.

Vrabec, M., Rogan Šmuc, N. & Vrabec, M. 2018: Deformacijski dvojčki v kalcitu pohorskega marmorja. Geologija, 61/1: 73–84. https://doi.org/10.5474/geologija.2018.005

Welton, J.E. 1984: SEM Petrology Atlas: Methods in Exploration Series No. 4. The American Association of Petroleum Geologists: 240 p.

Wünsch, K.G. 2001: Lithos 2000 (Lithos Mineraliendatenbank) (Version 2.3) [computer software]. Internet: http://www.lithos-mineralien.de

Zupančič, N. 1994a: Petrographical characteristics and classification of magmatic rocks of Pohorje. Rudarsko-metalurški zbornik, 41: 101–112 (in Slovenian with English summary).

Zupančič, N. 1994b: Geochemical characteristics and origin of magmatic rocks of Pohorje. Rudarsko-metalurški zbornik, 41: 113–128 (in Slovenian with English summary).

GEOLOGIJA *62/2*, 189–218, Ljubljana 2019
https://doi.org/10.5474/geologija.2019.009

Provenance and morphostratigraphy of the Pliocene-Quaternary sediments in the Celje and Drava-Ptuj Basins (eastern Slovenia)

Provenienca in morfostratigrafija pliocensko-kvartarnih sedimentov v Celjskem in Dravsko-Ptujskem bazenu (vzhodna Slovenija)

Eva MENCIN GALE[a, b, d], Petra JAMŠEK RUPNIK[a], Mirka TRAJANOVA[a], Luka GALE[a, c], Miloš BAVEC[a], Flavio S. ANSELMETTI[b] & Andrej ŠMUC[c]

[a]Geološki zavod Slovenije, Dimičeva ulica 14, SI-1000 Ljubljana, Slovenija
[b]Univerza v Bernu, Institute of Geological Sciences and Oeschger Centre for Climate Change Research, Baltzerstrasse 1+3, 3012 Bern, Švica
[c]Univerza v Ljubljani, Naravoslovnotehniška fakulteta, Oddelek za geologijo, Aškerčeva c. 12, SI-1000 Ljubljana, Slovenija
[d]Univerza v Ljubljani, Fakulteta za gradbeništvo in geodezijo, Jamova c. 2, SI-1000 Ljubljana, Slovenija
e-mails: eva.mencin-gale@geo-zs.si, petra.jamsek@geo-zs.si, mirka.trajanova@geo-zs.si, milos.bavec@geo-zs.si, flavio.anselmetti@geo.unibe.ch, andrej.smuc@geo.ntf.uni-lj.si

Prejeto / Received 19. 9. 2019; Sprejeto / Accepted 19. 11. 2019; Objavljeno na spletu / Published online 24. 12. 2019

Key words: Quaternary sedimentology, intramountane, geomorphology, river terrace, clast lithological analysis
Ključne besede: sedimentologija kvartarja, medgorski bazen, geomorfologija, rečna terasa, litološka analiza klastov

Abstract

This study presents the results of the first systematic morphostratigraphic and provenance analyses of the Pliocene-Quaternary fluvial sediments in the Celje and Drava-Ptuj intramontane basins. Based on the degree of terrace preservation, the dip of the terrace surfaces and fans, and the composition and degree of weathering of the sediments, low-, middle- and high-level terrace groups were constrained and tentatively attributed to Late Pleistocene, Middle Pleistocene and Plio-Early Pleistocene, respectively. The provenance analysis focused on the sediments from the high-level terrace (Plio-Early Pleistocene) and encompassed clast lithological analysis and microfacies analysis of the clasts. The results indicate a local provenance with relatively short transport, which is consistent with the morphology of the clasts. The source rocks of the Plio-Early Pleistocene deposits in the Celje Basin are attributed to the formations outcropping in the southern Pohorje Massif and the Upper Savinja River Valley corresponding to the paleo-Savinja. The possibility of resedimentation of the clasts from Miocene clastic sedimentary rocks located north of the Celje Basin also needs to be considered. The sediments of the Drava-Ptuj Basin originate from the Pohorje Massif, the Kozjak mountain range, and the area south of the Pohorje Massif which were deposited by the paleo-Drava and paleo-Dravinja rivers. Our study indicates that the drainage systems of the paleo-Savinja, paleo-Drava and paleo-Dravinja during the Plio-Early Pleistocene roughly correspond to those of the present day.

Izvleček

Predstavljamo prve sistematične analize morfostratigrafije in provenience pliocensko-kvartarnih rečnih sedimentov na območju Celjskega in Dravsko-Ptujskega medgorskega bazena. Na podlagi stopnje ohranjenosti morfologije teras, naklona terasnih površin in sestave ter stopnje preperelosti sedimentov so bili opredeljeni trije terasni nivoji in interpretirane starosti teras in vršajev. Spodnjemu terasnemu nivoju je bila interpretativno določena poznopleistocenska starost, srednjemu terasnemu nivoju srednjepleistocenska, zgornjemu terasnemu nivoju pa plio-zgodnjepleistocenska starost. Analiza provenience je bila osredotočena na sedimente višjega terasnega nivoja (pliocen-zgodnji pleistocen) in je temeljila na litološki analizi klastov in analizi mikrofaciesov klastov. Rezultati nakazujejo, da gre za lokalno provenienco proda, kar dodatno potrjujejo sedimentološka opazovanja morfologije klastov. Izvor plio-zgodnjepleistocenskih sedimentov v Celjskem bazenu so domnevno formacije, ki izdanjajo na območju južnega Pohorja in Zgornjesavinjske doline, pri čemer pa moramo upoštevati

možnost resedimentacije nekaterih litologij iz miocenskih klastičnih sedimentnih kamnin, ki se nahajajo severno od bazena. Prod v Dravsko-Ptujskem bazenu pa verjetno prihaja z območja Pohorja, Kozjaka in območja južno od Pohorja. Ugotovljeno je bilo, da je plio-zgodnjepleistocenska rečna mreža generalno sovpadala z današnjo. Tako lahko rečemo, da so se plio-zgodnjepleistocenski sedimenti na območju Celjskega bazena odlagali s paleo-Savinjo in njenimi pritoki, sedimenti na območju Dravsko-Ptujskega bazena pa s paleo-Dravo, paleo-Dravinjo in njunimi pritoki.

Introduction

The Slovenian territory is located at the junction of the Alps, Dinarides and Pannonian Basin (Placer, 2008). The Cenozoic tectonic activity responsible for uplift of the Alps and Dinarides resulted in a morphologically diverse landscape and the formation of intramontane basins. These basins were rapidly filled due to intensive post-Neogene erosion related to the eustatic sea-level changes and Quaternary compression of the area. Plio-Early Pleistocene ("Plio-Quaternary" according to e.g. Buser, 2010 and other Slovenian authors) sediments mark the onset of the youngest terrestrial sedimentation active up to now in the area of South, East and Central Slovenia (Fig. 1A). According to current interpretations, these sediments represent informal stratigraphic unit named "Plio-Quaternary" comprised by i) the sediments that were filling the Pannonian Lake, ii) terrestrial sediments of intramontane basins and iii) sediments resulted from weathering of host rock and their subsequent resedimentation (Markič, 2009, and references within).

Plio-Early Pleistocene sediments of intramontane basins in the wider area of Maribor, Slovenj Gradec, Velenje, Nazarje, Celje, Črnomelj, Kočevje and Krško are composed of interlayered beds of gravel, sand, silt and clay (Mioč, 1978; Buser, 1979; Šikić et al., 1979; Premru, 1983; Bukovac et al., 1984; Mioč & Žnidarčič, 1989; Verbič, 2004) deposited in fluvial, swamp, and lacustrine environments. The gravel clasts are composed of igneous, metamorphic and sedimentary rocks. Rare previous provenance research points to i) local origin (Mioč, 1978), ii) non-local origin, sediments were transported by paleo-flows of current rivers (i.e. paleo-Sava; Verbič, 2004). Based on the relative and numeric data, the age of these sediments was defined only in the area of Velenje and Krško. In the Velenje Basin, a Plio-Early Pleistocene age of 2,6 to 3,5 million years (Villafranchian, mammal zone MN16: Debeljak, 2017) was determined based on the finding of fossil mastodonts (Drobne, 1967; Rakovec, 1968) and palaeontological findings in coal (Brezigar, 1987; Brezigar et al., 1987; Markič & Sachenhofer, 2010). In the Krško Basin, a Plio-Early Pleistocene age was determined

Uvod

Območje Slovenije leži na stičišču Alp, Dinaridov in Panonskega bazena (Placer, 2008). V obdobju kenozoika se je zaradi tektonskih procesov, ob katerih so se med drugim dvigale Alpe in Dinaridi, oblikovala reliefno razgibana pokrajina. Intenzivna poznoneogenska erozija, povezana tudi z evstatičnimi spremembami višine morske gladine, in kvartarna kompresija, sta znatno prispevali k povečani sedimentaciji v nastalih medgorskih bazenih. Plio-zgodnjepleistocenski (»pliokvartarni« v npr. Buser, 2010 ter v ostali dosedanji literaturi slovenskih avtorjev) sedimenti označujejo začetek najmlajše, še danes potekajoče terestrične sedimentacije na območju današnje osrednje, južne in vzhodne Slovenije (sl. 1A). Po trenutnih interpretacijah neformalno enoto »pliokvartar« tako predstavljajo: i) nanosi sedimentov, ki so zasipavali Panonski bazen, ii) terestrični sedimenti odloženi v medgorskih bazenih ter iii) sedimenti nastali s preperevanjem matične kamnine in njihovo kasnejšo resedimentacijo (Markič, 2009 z referencami).

Plio-zgodnjepleistocenske sedimente (»pliokvartar« po npr. Buser, 2010) medgorskih bazenov na širšem območju Maribora, Slovenj Gradca, Velenja, Nazarij, Celja, Črnomlja, Kočevja in Krškega predstavlja menjavanje nesprijetega proda, peska, melja in gline (Mioč, 1978; Buser, 1979; Šikić et al., 1979; Premru, 1983; Bukovac et al., 1984; Mioč & Žnidarčič, 1989; Verbič, 2004), ki so se odlagali v rečnih, močvirskih in jezerskih okoljih. Med prodniki najdemo različke magmatskih, metamorfnih in sedimentnih kamnin. Redke predhodne raziskave provenience kažejo, da so sedimenti lokalnega izvora (Mioč, 1978), oziroma prineseni s paleotokovi današnjih rek (npr. paleo-Sava; Verbič, 2004). Starost sedimentov je bila na podlagi relativnih in numeričnih metod določena le na območju Velenja in Krškega. V Velenjskem bazenu je starost plio-zgodnjepleistocenskih sedimentov določena na podlagi najdbe mastodonta (Drobne, 1967; Rakovec, 1968) in paleontoloških raziskav premoga (Brezigar, 1987; Brezigar et al., 1987; Markič & Sachenhofer, 2010) ter znaša od 2,6 do 3,5 milijona let (biokronološka enota spodnji villafranchij, sesalska cona MN 16;

based on paleontological correlations (Šikić et al., 1979), morphostratigraphy (Verbič, 2008) and numerical dating (Cline et al., 2016), indicating a minimal age of 1,79 million years.

Only few studies exsist on poorly investigated Plio-Early Pleistocene sediments in the area of Slovenia (Pleničar & Ramovš, 1954; Štern & Lapajne, 1974; Brezigar, 1987; Brezigar et al., 1987; Kralj, 2001; Markič & Rokavec, 2002; Verbič, 2004). The reasons are lack of outcrops and subsurface data, degraded and poorly preserved Plio-Early Pleistocene terraces and the fact that the sediments are usually strongly weathered. Therefore, the knowledge of Plio-Early Pleistocene sedimentary evolution represents a scientific gap not only in the area of Slovenia but also in a wider pan-Alpine realm.

This study focuses on composition and provenance of the Celje (CB) and Drava-Ptuj (DPB) basins (Fig. 1B). The study is based on systematic approach using morphostratigraphic and sedimentological methods established in the field of Quaternary geology. The aim of this research is to determine morphostratigraphy of terrace systems, to define provenance of Plio-Early Pleistocene sediments and to interpret the evolution of the fluvial system in the Plio-Early Pleistocene.

Geological Setting

Celje Basin (CB)

The CB is located north of the Sava Hills, east of the Menina planina and Dobrovlje, and south of the Vitanje-Konjice part of the Karavanke Mountains. The present-day fluvial system is governed by the river Savinja, originating in the Logarska Valley in the Kamnik-Savinja Alps, and running in a northwest–southeast direction. In addition to the river Savinja, smaller streams drain into the basin from the northern and southern rims. The northwestern rim of the CB borders the Smrekovec volcanic complex of Oligocene age (Kralj, 1996; Pamić & Balen, 2001; Premru, 1983). The wider area also comprises Carboniferous siliciclastic rocks, Permian carbonates, Triassic carbonate and volcanic rocks, Jurassic and Cretaceous carbonate rocks, as well as Neogene carbonate and siliciclastic sediments and sedimentary rocks (Buser, 2010). The mentioned Paleozoic and Mesozoic rocks structurally belong to the Southern Alps and the Dinarides, while sediments and rocks of Oligocene and Miocene age were deposited near the margins of the Pannonian Basin (Placer, 1999; 2008; Kováč et al., 2007). The Pliocene-Quaternary sediments of the CB comprise the 35 m thick "Plio–Quater-

Debeljak, 2017). V Krškem bazenu je bila starost plio-zgodnjepleistocenskih sedimentov določena na podlagi paleontoloških korelacij (Šikić et al., 1979), morfostratigrafije (Verbič, 2008) in numeričnih datacij (Cline et al. 2016). Slednje kažejo na minimalno starost 1,79 milijona let.

Plio-zgodnjepleistocenski sedimenti so na območju Slovenije sorazmerno slabo raziskani oziroma študije, ki se nanašajo nanje, tematiko opisujejo le obrobno (Pleničar & Ramovš, 1954; Štern & Lapajne, 1974; Brezigar, 1987; Brezigar et al., 1987; Kralj, 2001; Markič & Rokavec, 2002; Verbič, 2004). Temu botruje dejstvo, da so izdanki in globinski podatki redki, plio-zgodnjepleistocenske terase so pogosto slabo ohranjene in močno degradirane, sedimenti pa so pogosto močno prepereli. Slaba raziskanost zato predstavlja vrzel v kvartarni geologiji ne le na območju današnje Slovenije, temveč tudi v širšem predalpskem prostoru.

V tej študiji smo se osredotočili na sestavo in provenienco plio-zgodnjepleistocenskih sedimentov v Celjskem (CB) in Dravsko-Ptujskem bazenu (DPB) (sl. 1B). Raziskava temelji na sistematičnem pristopu z uporabo ustreznih morfostratigrafskih in sedimentoloških metod uveljavljenih v kvartarni geologiji, s katerimi smo opredelili morfostratigrafijo sistema teras, ovrednotili izvorna območja plio-zgodnjepleistocenskih sedimentov ter interpretirali razvoj rečne mreže v obdobju plio-pleistocena.

Geologija območja

Celjski bazen (CB)

CB se nahaja na severno od Posavskega hribovja, vzhodno od Menine planine in Dobrovelj ter južno od Vitanjsko-Konjiških Karavank. Današnja rečna mreža CB je pogojena z njenim glavnim vodotokom, Savinjo, ki izvira v Logarski dolini v Kamniško-Savinjskih Alpah in teče v smeri severozahod-jugovzhod. Poleg tega se v bazen drenirajo njeni manjši pritoki iz severnih in južnih obronkov kotline. Severozahodno obrobje bazena meji na Smrekovški vulkanski kompleks oligocenske starosti (Kralj, 1996; Pamić & Balen, 2001; Premru, 1983). Na širšem območju se nahajajo še karbonske klastične kamnine, permske karbonatne kamnine, triasne karbonatne in vulkanske kamnine, kredne in jurske karbonatne kamnine ter neogenske karbonatne in klastične kamnine ter sedimenti (Buser, 2010). Omenjene paleozojske in mezozojske kamnine strukturno pripadajo Južnim Alpam in Dinaridom, oligocenske in miocenske kamnine pa so se odložile v robnih delih Panonskega bazena (Placer, 1999,

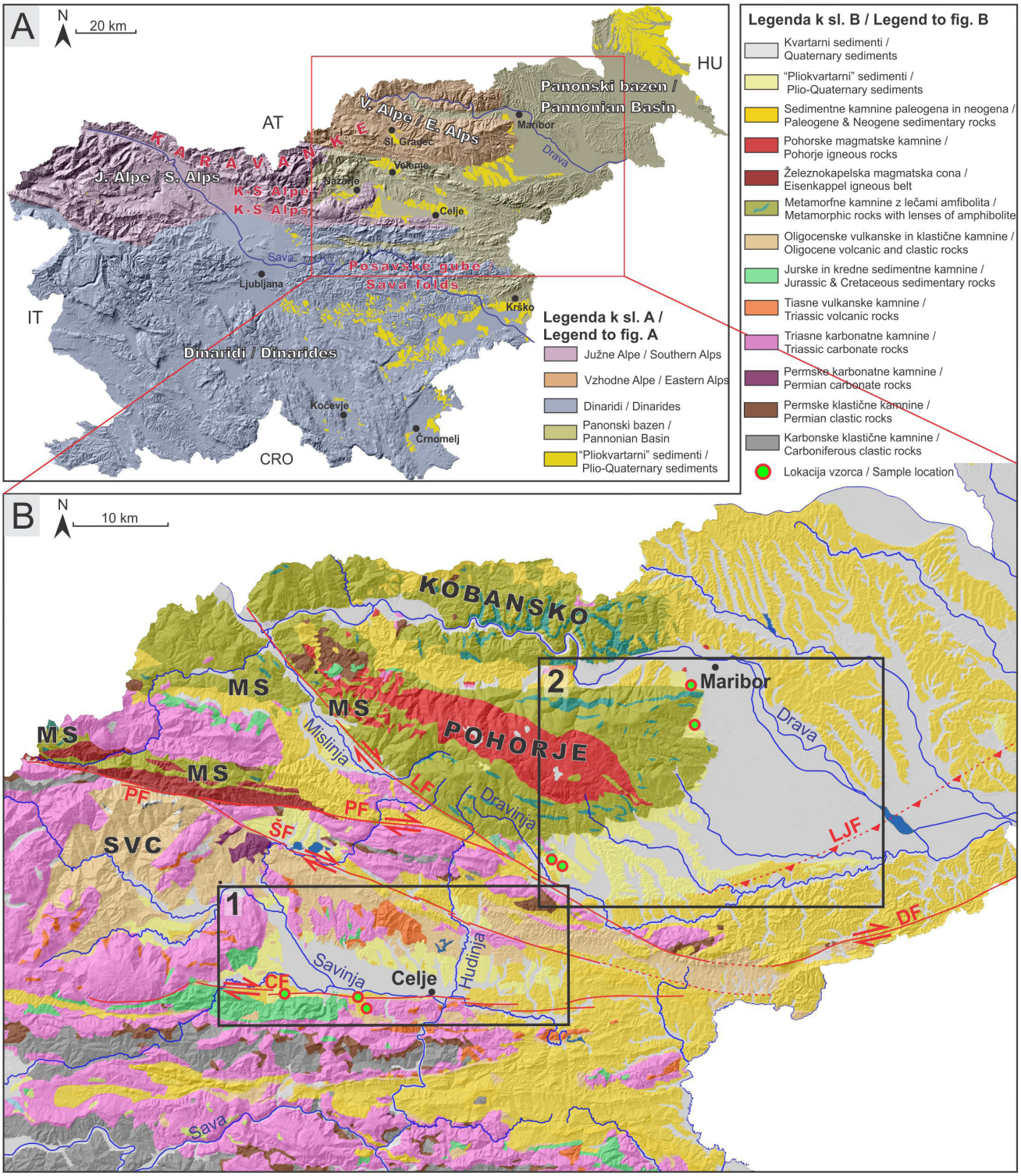

Fig. 1. Research area. (A) The area of Slovenia with geotectonic units marked (modified after Placer, 2008), and the spatial distribution of the Plio-Early Pleistocene sediments (so-called "Plioquaternary"). (B) Geological map of the Celje (1) and Drava-Ptuj (2) intramontane basins (modified after Buser, 2010). Abbreviations: MS: Magdalensberg series, SVC: Smrekovec volcanic complex, LF: Lavantall fault, ŠF: Šoštanj fault, CF: Celje fault, PF: Periadriatic fault, LJF: Ljutomer fault, DF: Donat fault.

Sl. 1. Območje raziskave. (A) Območje Slovenije z glavnimi geotektonskimi enotami (prirejeno po Placer, 2008) in pojavnostjo plio-zgodnjepleistocenskih sedimentov (t.i. »pliokvartarja«). (B) Geološka karta širšega območja Celjskega (1) in Dravsko-Ptujskega (2) medgorskega bazena (prirejeno po Buser, 2010). Na karti so označena glavna izvorna območja kamnin. Okrajšave: MS: Štalenskogorska serija, SVC: Smrekovški vulkanski kompleks, LF: Labotski prelom, ŠF: Šoštanjski prelom, CF: Celjski prelom, PF: Periadriatski prelom, LJF: Ljutomerski prelom, DF: Donački prelom.

nary" non-carbonate gravel, while the younger, Quaternary gravel deposits reach up to 25 m in thickness (Buser, 1979). The "Plio–Quaternary" deposits lie on Oligocene and Triassic basement (Fig. 1b; Buser, 1979). CB represents structurally the northernmost part of the Sava compressive wedge (Placer, 1998a, 1998b), which is reflected in the folding of its pre-Pliocene basement (the Celje syncline sensu Buser, 1977). The syncline's axis runs in an east–west direction, indicating post-Miocene compression in the north–south direction (Buser, 1977; Placer, 1998). According to Vrabec and Fodor (2006), the CB lies within the still active Periadriatic dextral transpressive fault system, experiencing local transtension between the faults running along the basin's margin.

Drava-Ptuj Basin (DPB)

The Drava-Ptuj Basin (DPB) is situated southeast of the Pohorje Massif and north of the Sava Hills. Its present-day fluvial system comprises the main river Drava, running in a north-northwest–south-southeast direction, and numerous smaller tributaries, following the direction of the Drava river, or generally flowing from the (north)west to the (south)east. The pre-Quaternary basement of the DPB belongs to several geological units (Fig. 1b). West to northwest of the DPB lies the Pohorje Massif built of low-, medium-, to (ultra) high-metamorphic rocks of the Pohorje metamorphic complex, overthrusted by very low-grade metamorphic rocks of the Magdalensberg series, unconformably overlain by Permo-Triassic, Cretaceous, and Miocene rocks and sediments (Mioč, 1978; Hinterlechner-Ravnik, 1971, 1973, 1982; Janák et al., 2004; Janák et al., 2005; Vrabec et al., 2012). The central part of the Pohorje Massif is formed of a pluton and sub-volcanic varieties of granodioritic to tonalitic composition, emplaced during the Miocene (Zupančič, 1994a, 1994b; Altherr et al., 1995; Fodor et al., 2008; Trajanova et al., 2008; Trajanova, 2013). From the structural point of view, the pre-Neogene rocks belong to the Eastern Alps. Miocene sediments and sedimentary rocks of the Maribor subbasin near the western margin of the Central Paratethys sea, filling the depression of the Pannonian Basin (Jelen & Rifelj, 2011; Trajanova, 2013). The deposition of Plio–Early Pleistocene sediments in this area started after the final regression of the Central Paratethys (Markič, 2009). According to Mioč and Žnidarčič (1989), the Plio–Early Pleistocene sediments in the DPB reach thickness up to 65 m, while the Quaternary deposits are only 30 m thick. The latter comprise four river terraces (Mioč & Žnidarčič, 2008; Kováč et al., 2007). Pliocensko-kvartarni sedimenti v CB obsegajo »pliokvartarni« nekarbonatni prod v skupni debelini 35 m, medtem ko mlajši, karbonatni kvartarni prod dosega debeline do 25 m (Buser, 1979). Podlago »pliokvartarja« v sami kotlini predstavljajo oligocenske in triasne kamnine (sl. 1b; Buser, 1979). V ožjem strukturnem smislu je po nekaterih interpretacijah kotlina še del Savskega kompresijskega klina (Placer, 1998a, 1998b), na kar kaže sinklinalna upognjenost predpliocenskih kamnin in sedimentov (Celjska sinklinala po Buser, 1977). Os sinklinale, ki poteka v smeri vzhod-zahod, kaže na post-miocensko kompresijo v smeri sever-jug (Buser, 1977; Placer, 1998). Po aktualnejših interpretacijah se kotlina nahaja znotraj aktivnega desno transpresivnega Periadriatskega sistema prelomov, kjer se odvija rotacija strižnih leč, pri čemer je območje CB verjetno podvrženo lokalni transtenziji med posameznimi prelomi, ki ga obkrožajo (Vrabec in Fodor, 2006).

Dravsko-Ptujski bazen (DPB)

DPB se nahaja jugovzhodno od Pohorja in severno od Posavskega hribovja. Rečna mreža današnjega DPB obsega glavni vodotok Dravo, ki teče v smeri sever-severozahod-jugovzhod, ter številne manjše pritoke, ki sledijo smeri glavnega toka ali tečejo generalno v smeri (severo)zahod-(jugo)vzhod. Predkvartarna podlaga DPB obsega več različnih geoloških enot (sl. 1b). Zahodno do severozahodno od DPB se nahaja Pohorje, ki je sestavljeno iz nizko, srednje do (ultra) visoko-metamorfnih kamnin Pohorskega kompleksa, na katere so narinjene zelo šibkometamorfozirane kamnine Štalenskogorske serije in diskordantno odložene permo-triasne, kredne ter miocenske kamnine in sedimenti (Mioč, 1978; Hinterlechner-Ravnik, 1971, 1973, 1982; Janák et al., 2004; Janák et al., 2005; Vrabec et al., 2012). V osrednjem delu Pohorja se nahajajo pluton in subvulkanski različki granodioritne do tonalitne sestave, ki so bili vtisnjeni v miocenu (Zupančič, 1994a, 1994b; Altherr et al., 1995; Fodor et al., 2008; Trajanova et al., 2008; Trajanova, 2013). V strukturnem smislu predneogenske kamnine uvrščamo k Vzhodnim Alpam. Miocenske kamnine in sedimenti Mariborskega podbazena so se odlagali na zahodnem robu Centralne Paratetide (sistem Panonskega bazena) (Jelen & Rifelj, 2011; Trajanova, 2013). Usedanje plio-zgodnjepleistocenski sedimentov na tem območju se je pričelo odlagati po končnem umiku Centralne Paratetide (Markič, 2009). Na snovi predhodnih podatkov so v DPB debeli do 65 m, kvartarni sedimenti pa

1989). In a structural sense, the DPB coincides with the Ptuj-Ljutomer syncline, which is bounded by the Ormož-Selnica anticline to the south (Mioč & Markovič, 1998). The later formed due to tectonic activity within the Donat fault zone. The most important faults of the latter are the dextral transpressive Donat fault and the reverse Ljutomer fault (Fodor et al., 1998, 2002).

Methods

The methodology for investigating the Plio -Early Pleistocene sediments was following guidelines from Stokes et al. (2012). Field observations were supported with geomorphological, sedimentological and microfacies analyses. Geomorphological analyses itself focused not only on Plio-Early Pleistocene sedimentary bodies, but also other younger sedimentary bodies from Pliocene-Quaternary succession.

The spatial extent of Plio-Early Pleistocene unit was constrained from Basic Geological Map, sheets Celje and Maribor (Buser, 1977; Žnidarčič & Mioč, 1988) and modified by analyzing the high -resolution digital elevation model derived from lidar data (Ministry of the Environment and Spatial Planning, Slovenian Environment Agency, 2011). Units mapped by means of remote sensing were field checked at the selected locations. Geomorphological analysis was carried out in GIS environment and encompassed analysis of topographic profiles, shaded relief map, topographic contours with 1 m equidistance, slope degree and slope aspect maps. Results of analysis are presented on two geomorphological maps, showing Plio-Early Pleistocene and other Quaternary terraces and fans in the studied basins (Figs. 2, 3). Geomorphological maps present the spatial extent of preserved surfaces of sedimentary bodies (surface forms). Therefore, oldest sediments are mostly occurring in greater spatial extent than their geomorphologically mapped present surface form (terrace or fan), i.e. the sediments at the surface occur also in the areas where their surface form is not preserved and mapped.

Seven sedimentary sections were logged: in CB these were Miklavž (MI), Šešče (SE) and Griže (GR), and in DPB Nova vas (NV), Hoče (HO), Radana vas (RA) and Škalce (SKA). Classification of lithofacies by Evans and Benn (2004) was used for logging. Sections height range from 1.5 to 5.5 m. Clasts from individual sections were sieved to 16-63 mm fraction. This fraction was chosen because it is appropriate for macroscopic identification of lithotypes of individual clasts, as well as for preparation of thin-sections.

30 m. V slednjih so vidne štiri terase (Mioč & Žnidarčič, 1989). DPB v strukturnem smislu sovpada s Ptujsko-Ljutomersko sinklinalo, na jugu pa ga omejuje Ormoško-Selniška antiklinala (Mioč & Markovič, 1998). Dviganje slednje je pogojeno z aktivnostjo Donačke prelomne cone, v kateri sta najpomembnejša potencialno aktivna desno transpresivni Donački prelom ter reverzni Ljutomerski prelom (Fodor et al., 1998, 2002).

Metode

Metodologija raziskovanja plio-zgodnjepleistocenskih sedimentov je sledila smernicam povzetih po Stokesu in sodelavcih (2012), pri čemer so bila terenska opazovanja podprta z geomorfološkimi, sedimentološkimi in mikrofaciesnimi analizami. Sama geomorfološka analiza je poleg analize plio-zgodnjepleistocenskih sedimentacijskih teles zajemala tudi mlajša sedimentacijska telesa iz pliocensko-kvartarnega zaporedja. Prostorska razširjenost enote plio-zgodnjepleistocenskih sedimentov je bila ugotovljena s pomočjo uporabe Osnovne geološke karte lista Celje in Maribor (Buser, 1977; Žnidarčič & Mioč, 1988) ter na analizi visokoločljivostnega digitalnega modela reliefa izdelanega na podlagi lidarskih podatkov (Ministrstvo za okolje in prostor, Agencija RS za okolje in prostor). Enote izdvojene z metodami daljinskega zaznavanja so bile na izbranih lokacijah preverjene s terenskim delom. Geomorfološke analize so bile izvedene v GIS okolju in so obsegale analizo topografskih profilov in kart senčenega reliefa, izohips z ekvidistanco 1 m, naklonov pobočij ter usmerjenosti pobočij. Izdelani sta bili geomorfološki karti, ki prikazujeta plio-zgodnjepleistocenske in ostale kvartarne terase in vršaje obravnavanih bazenov (sl. 2, 3). Geomorfološki karti prikazujeta razprostranjenost ohranjenih površin sedimentacijskih teles (površinske oblike). Predvsem za starejše sedimente zato velja, da je njihov obseg pojavljanja sicer večji od kartiranega obsega njihove današnje površinske oblike (terase ali vršaja), saj se sedimenti danes nahajajo tudi tam, kjer sama površinska oblika ni ohranjena.

Posnetih je bilo sedem sedimentoloških profilov, in sicer v CB Miklavž (MI), Šešče (SE) in Griže (GR) ter v DPB Nova vas (NV), Hoče (HO), Radana vas (RA) in Škalce (SKA), pri čemer je bila uporabljena klasifikacija litofaciesov po Evans in Benn (2004). Dolžina profilov znaša od 1,5 do 5,5 m. Prodniki iz posamičnih profilov so bili presejani na frakcijo od 16 do 63 mm. Ta velikost je ustrezna za makroskopsko litološko določitev klastov in za izdelavo zbruska.

Clast lithological analysis was following guidelines from Walden (2004), Lindsey et al. (2007) and Gale and Hoare (2011), adapted for the purpose of our study. 98-299 clasts were analyzed per sample from CB and 173-346 clasts per sample from DPB. 53 thin sections were prepared and examined with a polarizing microscope. Clast lithological analysis is traditionally performed on the macroscopic level (e.g. Bridgland et al., 2012), however, during our study it turned out that identification of weathered clasts is often wrong, and that microscopic analysis of the clasts significantly increases the reliability of the results. Due to lack of data on microfacies of Triassic volcanic rocks in the CB area, we additionally sampled their outcrops in the vicinity.

Results

Pliocene-Quaternary sediments of the CB and DPB are preserved in alluvial terraces and fans, following the terrace staircase model, which is typical in areas affected by relative surface uplift and erosional base lowering (e.g. Bridgland, 2000; Bridgland & Maddy, 2002; Bridgland & Westaway, 2008a; Bridgland & Westaway, 2008b; Doppler et al., 2011; van Husen & Reitner, 2011; Westaway, 2002). The oldest sediments are preserved in the highest terraces.

Pliocene-Quaternary sediments of the Celje Basin

The stratigraphy of alluvial terraces and fans in the CB is shown in the profile P1 (Fig. 2B and Table 1). Based on geomorphological mapping, five Pliocene-Quaternary terrace levels were distinguished (T0, T1, T3, T4, T5). Lithofacies and lithological analysis of gravels and clasts, respectively, were focused on Plio-Early Pleistocene sediments located on western and southern side of the basin (Fig. 2). Sediments of terrace levels T4 and T5 were analyzed in detail (Figs. 2, 4). Section MI (46,2394737°, 15,0395998°, 317 m a.s.l.) and SE (46,2307163°, 15,1398659°, 278 m a.s.l.) are located on the terrace level T4, and section GR (46,2196692°, 15,1520658°, 347 m a.s.l.) on terrace level T5.

Pliocene-Quaternary sediments of the Drava-Ptuj Basin

The stratigraphy of alluvial terraces and fans in the DPB is shown in profile P2 and P3 (Figs. 3B, 3C and Table 2). Six Pliocene-Quaternary terrace levels were distinguished (T0, T1, T2, T3, T4, T5). Lithofacies and lithological analysis of

Za litološko analizo klastov so bile upoštevane in prilagojene smernice avtorjev Walden (2004), Lindsey in sodelavcev (2007) ter Gale in Hoare (2011). V CB je bila litološka analiza izvedena na 98 do 299 klastih na vzorec, v DPB pa na 173 do 346 klastih na vzorec. Izdelanih in pregledanih je bilo 53 zbruskov klastov; 20 v CB in 33 v DPB. Tradicionalno je litološka analiza klastov izvedena makroskopsko (npr. Bridgland et al., 2012), vendar je bilo tekom študije ugotovljeno, da so napake pri identifikaciji preperelih kamnin pogoste in da mikroskopska analiza znatno pripomore k večji zanesljivosti rezultatov. Zaradi pomanjkanja podatkov o mikrofaciesu triasnih vulkanskih kamnin na območju CB, so bili dodatno vzorčeni tudi njihovi bližnji izdanki.

Rezultati

Pliocensko-kvartarni sedimenti CB in DPB so ohranjeni v terasah in vršajih, ki sledijo modelu inverzne terasne stratigrafije (ang. terrace staircase), ki je značilen za območja relativnega dvigovanja površja in zniževanja erozijske baze (npr. Bridgland, 2000; Bridgland & Maddy, 2002; Bridgland & Westaway, 2008a; Bridgland & Westaway, 2008b; Doppler et al., 2011; van Husen & Reitner, 2011; Westaway, 2002). Pri tem so najstarejši sedimenti ohranjeni na najvišje ležečih terasah.

Pliocensko-kvartarni sedimenti Celjskega bazena

Stratigrafija teras in vršajev v CB, ugotovljena s to študijo, je prikazana na profilu P1 (sl. 2B in Tabela 1). Na podlagi geomorfološkega kartiranja je bilo ugotovljenih pet pliocenski-kvartarnih terasnih nivojev (T0, T1, T3, T4, T5). Litofaciesna in litološka analiza prodov in klastov je bila osredotočena le na plio-zgodnjepleistocenske sedimente, ki se nahajajo na zahodni in južni strani bazena (sl. 2). Sedimenti so bili podrobneje analizirani na terasnem nivoju T4 in T5 (sl. 2, 4). Profila MI (46,2394737°, 15,0395998°, 317 m n.v.) in SE (46,2307163°, 15,1398659°, 278 m n.v.) se nahajata na terasnem nivoju T4, profil GR (46,2196692°, 15,1520658°, 347 m n.v.) pa na terasnem nivoju T5.

Pliocensko-kvartarni sedimenti Dravsko-Ptujskega bazena

Stratigrafija teras in vršajev v DPB, ugotovljena s to študijo, je prikazana na profilu P2 in P3 (sl. 3B, 3C in Tabela 2) pri čemer je bilo ugotovljenih šest pliocensko-kvartarnih terasnih nivojev (T0, T1, T2, T3, T4, T5). Litofaciesna in litološka ana-

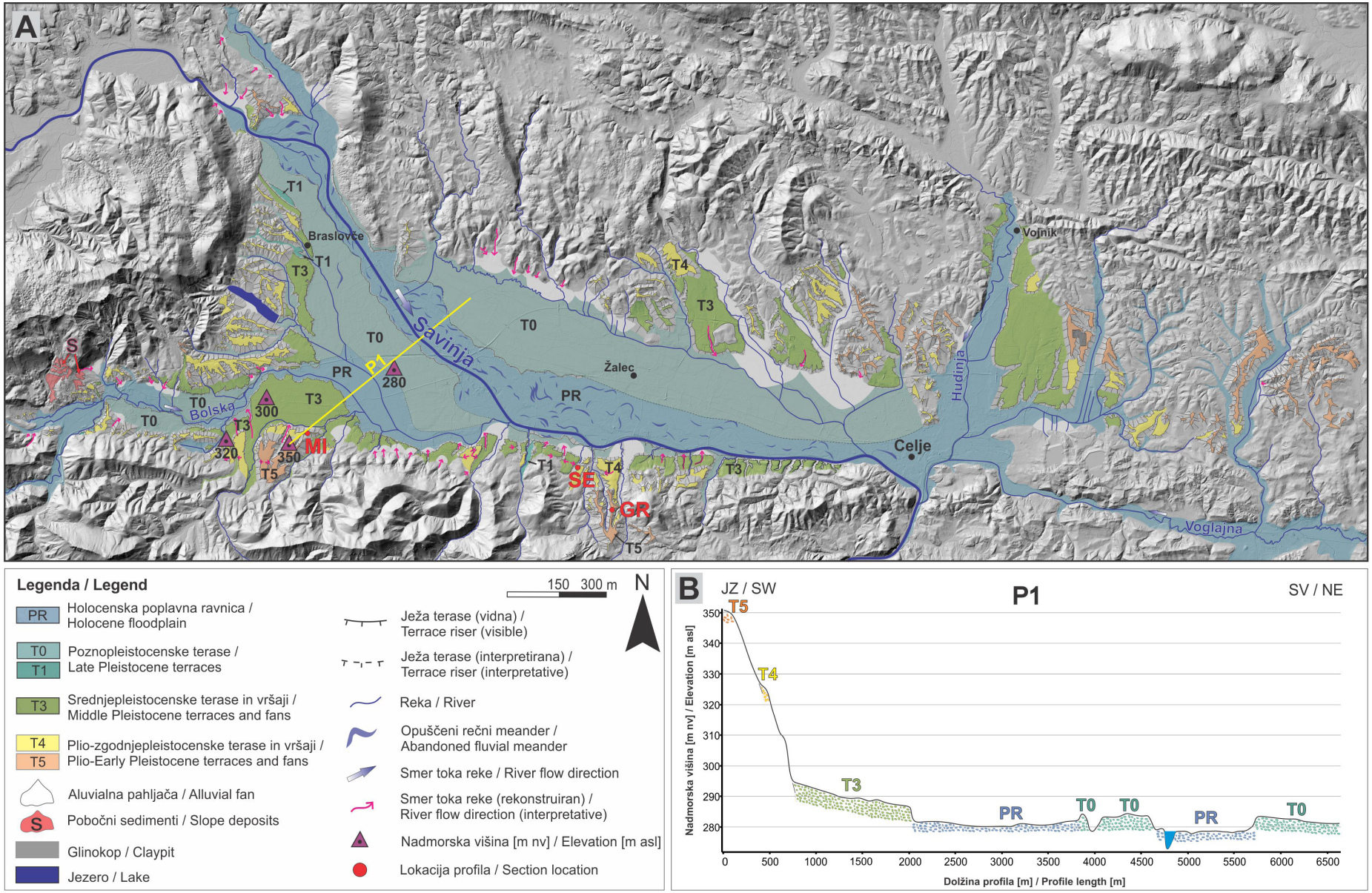

Fig. 2. Geomorphological analysis of the Pliocene-Quaternary surfaces of the Celje Basin. (A) Geomorphological map of the Plio-Early Pleistocene, Middle Pleistocene, Late Pleistocene and Holocene terraces and fans with locations of the studied sections marked (MI, SE, GR). (B) Topographic profile P1 with present-day elevations of the terraces and fans.

Sl. 2. Geomorfološka analiza pliocensko-kvartarnih površinskih oblik Celjskega bazena. (A) Geomorfološka karta plio-zgodnjepleistocenskih, srednjepleistocenskih, poznopleistocenskih in holocenskih teras in vršajev z označenimi lokacijami profilov (MI, SE, GR). (B) Topografski profil P1 z današnjimi višinami teras in vršajev.

Table 1. Basic geomorphological characteristics of the terrace system in the Celje Basin.
Tabela 1. Osnovne karakteristike sistema teras v Celjskem bazenu.

Terrace level / Terasni nivo	**Elevation [m a.s.l.] / Višina [m n.v.]**	**Height above the floodplain [m] / Relativna višina nad poplavno ravnico [m]**	**Thickness / Debelina [m] (after / po Buser, 1979)**	**Morphology of the unit / Morfologija enote**	**Composition of the sediments / Sestava sedimentov**	**Age / Starost (after / po Buser, 1979)**
Floodplain / Poplavna ravnica	236 - 304	/	25	Very well-preserved former channel pattern / Zelo dobro ohranjena morfologija rečnih meandrov	Carbonate gravel / Karbonatni prod	Quaternary / Kvartar
T0	238 - 309	2 - 5		Very well-preserved terrace morphology, rare and not well visible former channel meanders / Morfologija terase zelo dobro ohranjena, redki slabo ohranjeni rečni meandri		Quaternary / Kvartar
T1	279 - 308	7 - 8	35	Well-preserved terrace morphology, however the terrace surfaces are smaller and present only in a few places within the basin / Morfologija terase dobro ohranjena vendar terase ne zavzemajo velikih površin in so prisotne le na nekaj mestih znotraj bazena		Identified as single "Plio-Quaternary" terrace / Identificirano kot enotna »pliokvartarna« terasa
T3	245 - 324	9 - 14		Well-preserved terrace and fan morphology, present at basin boundaries / Morfologija teras in vršajev dobro ohranjena, prisotnost ob robovih bazena		
T4	258 - 338	15 - 22		Terrace and fan erosional remnants with degraded morphology incised by the drainage network / Morfologija teras in vršajev degradirana – erozijski ostanki teras, pogosto vrezovanje manjših potokov	Non-carbonate gravel / Nekarbonatni prod	
T5	262 - 366	42 - 124				

Table 2. Basic geomorphological characteristics of the terrace system in the Drava-Ptuj Basin.
Tabela 2. Osnovne značilnosti sistema teras v Dravsko-Ptujskem bazenu.

Terrace level / Terasni nivo	**Elevation [m a.s.l.] / Višina [m n.v.]**	**Height above the floodplain [m] / Relativna višina nad poplavno ravnico [m]**	**Thickness / Debelina [m] (after / po Buser, 1979)**	**Morphology of the unit / Morfologija enote**	**Composition of the sediments / Sestava sedimentov**	**Age / Starost (after / po Mioč & Žnidarčič, 1989)**
Floodplain / Poplavna ravnica	216 - 266	/	up to 30 m / do 30 m	Very well-preserved former channel pattern / Zelo dobro ohranjena morfologija rečnih meandrov	Carbonate gravel / Karbonatni prod	Quaternary / Kvartar
T0	224 - 284	7		Well-preserved former channel pattern, very well-preserved terrace morphology / Dobro ohranjena morfologija rečnih meandrov, morfologija terase zelo dobro ohranjena		Quaternary / Kvartar
T1	228 - 288	9 - 12		Moderately-preserved former channel pattern, very well-preserved terrace morphology / Srednje dobro ohranjena morfologija rečnih meandrov, morfologija terase zelo dobro ohranjena		Quaternary / Kvartar
T2	232 - 278	13 - 14		Very well-preserved terrace morphology / Morfologija terase zelo dobro ohranjena		Quaternary / Kvartar
T3	251 - 333	15 - 23	25 - 40	Well-preserved terrace and fan morphology, but the terrace surfaces are present only in a few places within the basin / Morfologija teras in vršajev dobro ohranjena, vendar terase ohranjene le na nekaj mestih znotraj bazena		Identified as single "Plio-Quaternary" terrace / Identificirano kot enotna »pliokvartarna« terasa
T4	231 - 437	15 - 50		Terrace and fan remnants with degraded morphology incised by the drainage network / Morfologija teras in vršajev degradirana – ostanki teras, pogosto vrezovanje manjših potokov		
T5	277 - 450	40 - 100				

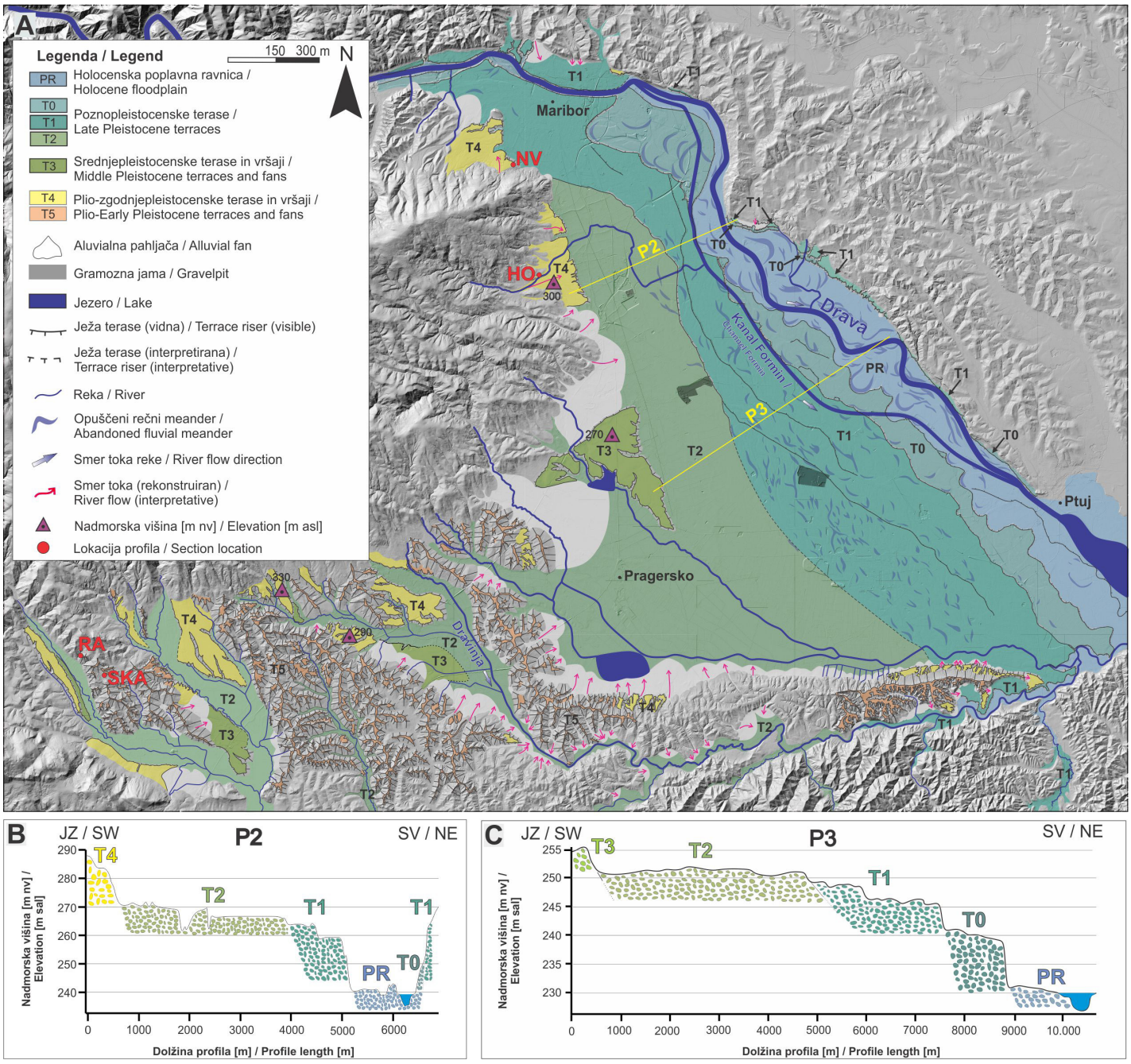

Fig. 3. Geomorphological analysis of the Pliocene-Quaternary surfaces of the Drava-Ptuj Basin. (A) Geomorphological map of the Plio-Early Pleistocene, Middle Pleistocene, Late Pleistocene and Holocene terraces and fans with locations of the studied sections marked (NV, HO, RA, SKA). (B, C) Topographic profiles P2 and P3, with present-day elevations of the terraces and fans.

Sl. 3. Geomorfološka analiza pliocensko-kvartarnih površinskih oblik Dravsko-Ptujskega bazena. (A) Geomorfološka karta plio-zgodnjepleistocenskih, srednjepleistocenskih, poznopleistocenskih in holocenskih teras in vršajev z označenimi lokacijami profilov (NV, HO, RA, SKA). (B, C) Topografska profila P2 in P3 z današnjimi višinami teras in vršajev.

gravels and clasts, respectively, were focused on Plio-Early Pleistocene sediments of terrace level T4 in sections NV (46.532506°, 15.615964°, 293 m a.s.l.) and HO (46.495161°, 15.626824°, 319 m a.s.l.), and sediments of terrace level T5 in sections SKA (46,3627381°, 15,416756°, 404 m a.s.l.) and RA (46,3691538°, 15,4047645°, 389 m a.s.l.).

liza prodov in klastov je bila osredotočena na plio-zgodnjepleistocenske sedimente na terasnem nivoju T4 v profilih NV (46.532506°, 15.615964°, 293 m n.v.) in HO (46.495161°, 15.626824°, 319 m n.v.) ter sedimente na terasnem nivoju T5 na lokacijah SKA (46,3627381°, 15,416756°, 404 m n.v.) in RA (46,3691538°, 15,4047645°, 389 m n.v.).

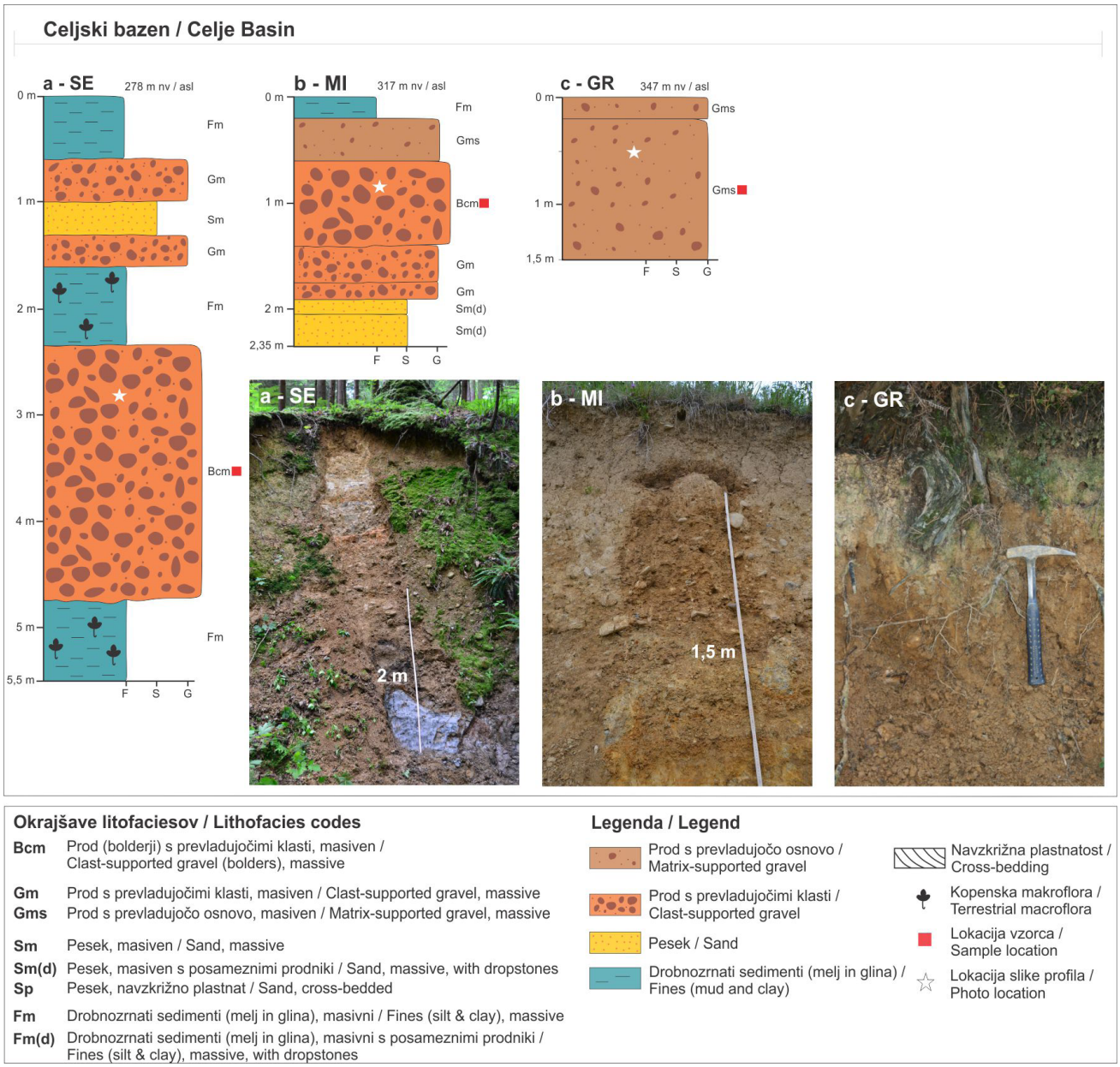

Fig. 4. Lithofacies of the Plio-Early Pleistocene sediments of the Celje Basin in sections Šešče (SE), Miklavž (MI) and Griže (GR). White stars indicate the parts of the sections presented in the photographs.

Sl. 4. Litofaciesi plio-zgodnjepleistocenskih sedimentov Celjskega bazena v profilih Šešče (SE), Miklavž (MI) in Griže (GR). Bele zvezde označujejo fotografirane dele profilov.

Lithofacies analysis of the sections and clast lithological analysis

In seven sections, eight different gravely, sandy and muddy lithofacies were recognized (Table 3). Contacts between the layers are gradual or in parts erosional. The thickness of the layers varies laterally and reach values from a few centimeters to approximately two meters. The sediments partly occur in lenses. Cross-lamination is present in some of the sandy layers and coalified plant fragments up to a few centimeters in size are present in fine-grained layers.

Litofaciesna analiza profilov in litološka analiza klastov

V skupno sedmih profilih je bilo ugotovljenih osem različnih litofaciesov (Tabela 3). Prisotni so prodnati, peščeni in muljasti sedimenti. Kontakti med posameznimi litofaciesi so postopni, mestoma tudi erozijski. Debelina plasti variira od nekaj centimetrov do približno dva metra ter se lateralno spreminja. Sedimenti se ponekod pojavljajo v lečah. Mestoma se v peščenih plasteh pojavlja navzkrižna plastnatost. Ponekod so bili v drobnozrnatih plasteh najdeni poogleneli fragmenti kopenskih rastlin veliki do nekaj centimetrov.

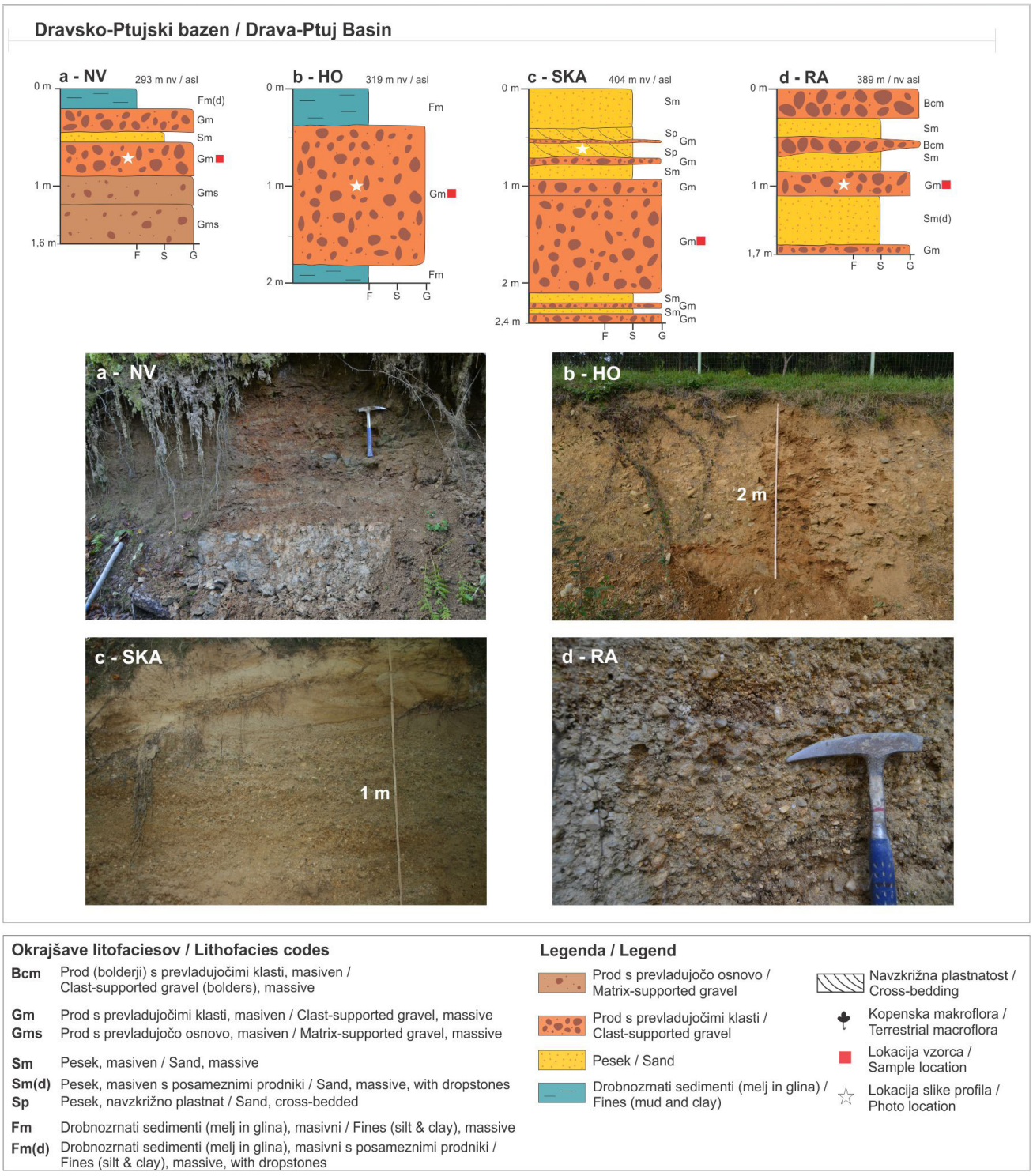

Fig. 5. Lithofacies of the Plio-Early Pleistocene sediments of the Drava-Ptuj Basin in sections Nova vas (NV), Hoče (HO), Škalce (SKA) and Radnana vas (RA). White stars indicate the parts of the sections presented in the photographs.

Sl. 5. Litofaciesi plio-zgodnjepleistocenskih sedimentov Dravsko-Ptujskega bazena v profilih Nova vas (NV), Hoče (HO), Škalce (SKA) in Radnana vas (RA). Bele zvezde označujejo fotografirane dele profilov.

The results of the clast lithological analysis are presented in tables 4 and 5 and on figures 6 and 7. In the CB, clasts of metamorphic, volcanic, volcaniclastic and clastic rocks occur, whereas in the DPB, metamorphic, volcanic, volcaniclastic and carbonate clasts are present (Fig. 8).

Rezultati litološke analize klastov so predstavljeni v tabelah 4 in 5 ter na slikah 6 in 7. Slika 8 podaja primerjavo litoloških analiz klastov obeh bazenov. V CB prevladujejo metamorfne, vulkanske in vulkanoklastčne ter klastične kamnine, v DPB pa metamorfne, vulkanske in vulkanoklastične ter karbonatne kamnine.

Table 3. Lithofacies codes and descriptions, interpretation of depositional setting and occurrences within the sections.
Tabela 3. Okrajšave in opisi litofaciesov, interpretacija sedimentacijskega okolja in pojavnost v profilih.

Litofacies code and definition / Okrajšava in definicija litofaciesa (Evans & Benn, 2004)		**Additional lithofacies description / Dodaten opis litofaciesa**	**Interpretation / Interpretacija**	**Occurrence in the sections / Pojavnost v profilih**
Bcm	Clast-supported gravel (bolders), massive / Prod (balvani) s prevladujočimi klasti, masiven	Well-sorted gravel, well-rounded clasts / Dobro sortiran prod, klasti dobro zaobljeni	Channel lag deposits and gravel (gravely-sandy) dunes; coarse-grained sediments in alluvial fans / Sedimenti korita in prodnate (prodnato-peščene) sipine; grobozrnati sedimenti v aluvialnih pahljačah	RA, SE
Gm	Clast-supported gravel, massive / Prod s prevladujočimi klasti, masiven	Sub- to well-rounded clasts, gravel locally highly weathered / Slabo do dobro zaobljeni klasti, v posameznih profilih prod močno preperel		NV, HO, SKA, RA, SE, MI
Gms	Matrix-supported gravel, massive / Prod s prevladujočo osnovo, masiven	Poorly- to moderately-sorted, angular to well-rounded clasts, locally highly weathered / Slabo do srednje sortiran prod, oglati do dobro zaobljeni klasti, mestoma močno prepereli		NV, MI, GR
Sm	Sand, massive / Pesek, masiven	In parts marmorized and pedogenized / Mestoma marmoriziran in pedogeniziran	Sand dunes / Peščene sipine	NV, SKA, RA, SE
Sm(d)	Sand, massive, with dropstones / Pesek, masiven, s posameznimi prodniki	In parts marmorized, sub-angular to well-rounded clasts / Mestoma marmoriziran, klasti pol-oglati do dobro zaobljeni		RA, MI
Sp	Sand, cross-bedded / Pesek, navzkrižno plastnat	/		SKA
Fm	Fines (silt and clay), massive / Drobnozrnati sedimenti (melj in glina), masivni	In parts marmorized and pedogenized with plant remains / Mestoma marmoriziran in pedogeniziran z rastlinskimi ostanki	Floodplain sediments and finegrained sediments in alluvial fans / Sedimenti poplavne ravnice in drobnozrnati sedimenti v aluvialnih pahljačah	HO, SE, MI
Fm(d)	Fines (silt and clay), massive with dropstones / Drobnozrnati sedimenti (melj in glina), masivni, s posameznimi prodniki	In parts marmorized and pedogenized; clasts sub- to well-rounded / Mestoma marmoriziran in pedogeniziran; klasti slabo do dobro zaobljeni		NV

Table 4. Microfacies of clasts of Plio-Early Pleistocene sediments and interpretation of the provenance in the Celje Basin. The term keratophyre was used in the Basic geological map (Buser, 1979; Premru, 1983). Although the term is outdated, we herein retain it, since the provenance analysis is based on the Basic geological map.

Tabela 4. Mikrofacies prodnikov plio-zgodnjepleistocenskih sedimentov in interpretacija provenience v Celjskem bazenu. Izraz keratofir je povzet po terminologiji Osnovne geološke karte (Buser, 1979; Premru, 1983). Ker primerjava provenience klastov temelji na Osnovni geološki karti, smo izraz obdržali kljub zastarelosti.

Lithogroup / Lito-skupina	**Lithotype / Litotip**	**General description / Splošni opis**	**Provenance interpretation / Interpretacija provenience**	**Key feature for provenance interpretation / Ključna lastnost za določitev provenience**
Metamorphic rocks / Metamorfne kamnine	Phyllitoid mica schist / Filitoidni sljudnat skrilavec	The rock consists of sparse lenticular augen of perthitic feldspar and quartz. Quartz and white mica are the main constituents. Very frequent are opaque minerals (mostly secondary) concentrated along foliation and cleavage. Tourmaline is sparsely present. / Kamnina vsebuje redka lečasta očesa perthitnega glinenca in kremena. Prevladujejo kremen in minerali sljud. Zelo pogosti so neprosojni minerali (večinoma sekundarnega izvora), ki so koncentrirani vzdolž foliacije in klivaža. Redek je turmalin.	Source rocks eroded (similar facies outcrop on the S Pohorje area (Hudinja stream drainage) / Izvorne kamnine erodirane (podobni faciesi izdanjajo na območju J Pohorja – potok Hudinja)	Metamorphic degree and facies / Stopnja metamorfoze in facies
Volcanic and volcaniclastic rocks / Vulkanske in vulkanoklastične kamnine	Keratophyre / Keratofir	The rock consists of glassy groundmass and phenocrysts of albitized plagioclases and biotite. Volcanic glass is altered to microcrystalline quartz, chlorite, sericite and locally calcite. / Kamnina vsebuje steklasto osnovo z vtrošniki albitiziranih plagioklazov, alkalnih glinencev, kremena, plagioklazov in biotita. Vulkansko steklo je spremenjeno v mikrokristalen kremen, albit, klorit, sericit in mestoma kalcit.	Triassic volcanic and volcanoclastic rocks (N, W and S slopes of the CB) / Triasne vulkanske in vulkanoklastične kamnine (S, Z in J pobočja CB)	Visible diagenesis, compact texture of the rock, typical mineral alteration / Vidni znaki diageneze, kompaktna struktura kamnine, značilne spremembe v mineralizaciji
	Fine- to coarse-grained tuff / Drobno do debelo-zrnati tuf	The rock consists of tuffaceous matrix altered to microcrystalline quartz, chlorite, sericite, muscovite, epidote and albite(?). It contains crystal grains of quartz, feldspars, oxidized mafic minerals, volcanic rock fragments and rare lapilli. / Kamnina je sestavljena iz tufske osnove, ki je spremenjena v mikrokristalen kremen, klorit, sericit, muskovit, epidot in albit(?). Vsebuje kristaloklaste kremena, glinencev in oksidiranih mafičnih mineralov ter vulkanske litične drobce in redke lapile. Kamnina je pogosto močno preperela.		
	Fine-grained vitric tuff / Drobno zrnati vitrični tuf	The rock consists of fine-grained tuffaceous matrix and glass shards of crystal grains. Volcanic glass is altered to microcrystalline quartz, phyllosilicate minerals and zeolites(?). Crystal grains belong to feldspars and subordinately quartz. Rare biotite is chloritized. / Kamnina vsebuje drobnozrnato tufsko osnovo in koščke stekla. Vulkansko steklo je spremenjeno v mikrokristalen kremen, filosilikatne minerale in zeolite(?). Kristalna zrna pripadajo glinencem in v manjši meri kremenu. Redek biotit je kloritiziran.	Oligocene Smrekovec series (wider area N and W from the CB) / Oligocenska Smrekovška serija (širše območje S in Z od CB)	Rock texture (without indicators of diagenesis), presence of glass shards / Struktura kamnine (ni znakov diageneze), dacitna sestava, vidne črepinjice stekla. (Kralj, 2016a, Kralj, 2016b)
Clastic rocks / Klastične kamnine	Siltstone to slate / Meljevec do skrilavi glinavec	The main constituents are white micas uniformly aligned along slaty cleavage. Sparse biotite is present. Sericite-chlorite aggregates are aligned transverse to slaty cleavage. The rock is strongly hydroscopic and impregnated by limonitic pigment. / Kamnina ima izrazito poudarjeno usmerjeno teksturo. Prevladuje bela sljuda, ki je orientirana vzdolž skrilave teksture. Redek je biotit. Sericitno-kloritni agregati so orientirani pravokotno na usmerjeno teksturo. Kamnina je močno higroskopična in impregnirana z limonitnim pigmentom.	Carboniferous (S slopes of the CB) / Karbon (J obronki CB)	Structure, texture, metamorphic degree and facies / Tekstura, struktura, stopnja metamorfoze in facies
	Very weakly metamorphosed quartz sandstone / Zelo nizko metamorforiziran kremenov peščenjak	The rock contains quartz, rare fragments of lithic grains (slate) and rare muscovite. Accessory minerals are opaque minerals, and rare rutile, tourmaline and zircon. Quartz-sericite matrix is recrystallized, often with directed growth and is intergrown with quartz grains on the rims. Anastomosing slaty cleavage developed with concentrations of opaque non-migrative component. / Kamnino sestavljajo kremen, redki odlomki litičnih zrn (glinastega skrilavca) in redek muskovit. Akcesorni so neprosojni minerali ter redek rutil, turmalin in cirkon. Kremenovo-sericitno vezivo je rekristalizirano, pogosto usmerjeno raščeno in se obodno prerašča s kremenovimi klasti. Med klasti je nastal povijajoč klivaž, v katerem je koncentrirana nemigrativna neprosojna komponenta.	Carboniferous (S slopes of the CB) / Karbon (J obronki CB)	Metamorphic degree and facies / Stopnja metamorfoze in facies

Table 5. Microfacies of clasts of Plio-Early Pleistocene sediments and interpretation of the provenance in the Drava-Ptuj Basin. The term keratophyre was used in the Basic geological map (Buser, 1979; Premru, 1983) and is for this reason retained, despite being outdated.

Tabela 5. Mikrofacies prodnikov plio-zgodnjepleistocenskih sedimentov in interpretacija provenience v Dravsko-Ptujskem bazenu. Izraz keratofir je povzet po terminologiji Osnovne geološke karte (Buser, 1979; Premru, 1983). Ker primerjava provenience klastov temelji na Osnovni geološki karti, smo izraz kljub zastarelosti obdržali.

Lithogroup / Lito-skupina	**Lithotype / Litotip**	**General description / Splošni opis**	**Provenance interpretation / Interpretacija provenience**	**Key feature for provenance interpretation / Ključna lastnost za določitev provenience**
Metamorphic rocks / Metamorfne kamnine	Amfibolitna skupina (epidotno amfibolski skrilavci do amfiboliti) / Amphibolitic group (epidote amphibole schists to amphibolites)	The rock consists of hornblend, epidote, clinozoisite, chlorite, feldspar and quartz (in some of the samples). Accessory minerals are rutile, titanite and opaque minerals. Some of the samples have pronounced foliation, others pronounced porphyroclastic texture. / Kamnina je sestavljena iz rogovače, epidota, klinozoisita, kloria, redko glinenca in kremena (v nekaterih vzorcih). Akcesorni so rutil, titanit in neprosojni minerali. Nekateri vzorci imajo izraženo foliacijo, drugi pa izrazito porfiroklastično strukturo.	Pohorje and Kozjak (W and N from the DPB) / Vzhodne Alpe - Pohorje in Kozjak (Z in S od DPB)	Typical facies of the Pohorje metamorphic complex / Značilen facies pohorskega metamorfnega kompleksa (Hinterlechner Ravnik 1971, 1973)
	Mica schists / Blestniki in muskovitni skrilavci	The rock consists of muscovite, quartz, garnet (mostly its relicts), chlorite, rare biotite (in parts chloritized), zoisite/clinozoisite, traces of accessory zircon, titanite, rutile, and opaque minerals). Schistose structure with pronounced foliation is present. / Kamnino sestavljajo muskovit, kremen, granati (večinoma njihovi relikti), klorit, redek biotit (mestoma kloritiziran), zoisit/klinozoisit, sledovi akcesornih mineralov cirkona, titanita, rutila in neprosojnih mineralov. Tekstura je skrilava z izrazito foliacijo. Nekateri vzorci so močno prepereli.	Eastern Alps (Pohorje and Kozjak area, also the surroundings of Ravne na Koroškem) (most probably eastern Pohorje and north of Maribor) / Vzhodne Alpe (najverjetneje vzhodno Pohorje in severno od Maribora)	Typical facies / Značilen facies
	Slate / Glinast skrilavec	Macroscopic texture seems massive. Microscopically, the rock has pronounced cleavage, expressed as preferred orientated sericite and chlorite. In-between them are grains of clastic quartz, feldspar, infrequent opaque minerals of primary and secondary origin, tourmaline, traces of zircon, apatite and epidote(?). Some sericite-chlorite aggregates and larger white mica flakes are oriented transverse to foliation. / Makroskopsko je kamnina videti masivna. Mikroskopsko je močno izražen klivaž poudarjen z usmerjenimi listki sericita in klorita. Vmes so zrna kremena, glinencev, redkih neprosojnih mineralov (primarnega in sekundarnega izvora), turmalina, sledovi cirkona, apatita in epidota(?). Posamezni sericitno-kloritni agregati in večji listki sljud so usmerjeni prečno na foliacijo.	Štalenskogorska serija (Z Kozjak in/ali SZ del Pohorja)/ Magdalensberg series (W Kozjak and/or NW part of the Pohorje area)	Typical facies / Značilen facies
	Quartzite of very low-grade metamorphism / Kvarcit zelo nizke stopnje metamorfoze	The rock contains of mineral clasts of quartz, tourmaline, opaque minerals rutile, titanite and zircon. It contains infrequent lithic grains of slate and phylite. Quartz grains have undulose extinction and serrated grain boundaries with small quantity of recrystallized matrix in between. The source rock of the quartzite represents "dirty" quartz sandstone presumably formed from Carboniferous clastic rocks from the zone of stronger dynamometamorphism. / Kamnina je sestavljena iz mineralnih klastov kremena, turmalina, neprosojnih mineralov, rutila, titanita in cirkona. Redka so litična zrna glinastega skrilavca in filita. Zrna kremena valovito potemnijo in se pogosto zobčasto preraščajo med seboj in z vmesnim vezivom. Kvarcit nastal iz nečistega kremenovega peščenjaka v coni močnejših dinamometamorfnih sprememb, predvidoma nastal iz karbonskih klastitov.	Carboniferous (Dravinja drainage, S from Slovenske Konjice) / Karbon (drenaža Dravinje, J od Slovenskih Konjic)	Typical facies / Značilen facies
Volcanic and volcaniclastic rocks / Vulkanske in vulkanoklastične kamnine	Keratophyre / Keratofir	The rock is extensively altered. The former glassy groundmass is altered to microcrystalline quartz and phyllosilicate minerals. Phenocrysts of feldspars and mafic minerals can only be anticipated by shape remains. The rock is impregnated with Fe-oxides and hydroxides. / Kamnina je močno spremenjena. Nekdanja steklena osnova je spremenjena v mikrokristalen kremen in filosilikate. Oblika popolnoma preperelih vtrošnikov nakazuje na glinence in mafične minerale. Kamnina je popolnoma oksidirana, impregnirana z železovimi oksidi in hidroksidi.	The rock does not outcrops in the today's drainage area of the sampling locality SKA (lack of detail geological map or eroded outcrops?) / Triasne vulkanske in vulkanoklastične kamnine. Kamnina ne izdanja v današnjem drenažnem območju vzorčne lokacije SKA (manjka natančna geološka karta ali pa so izdanki popolnoma erodirani)	Visible diagenesis, compact texture of the rock, typical mineral alteration / Vidni znaki diageneze, kompaktna struktura kamnine, značilne spremembe v mineralizaciji.
	Keratophyre tuff / Keratofirski tuf	The rock consists of fragments of altered feldspars, biotite and volcanic lithic fragments. The matrix is altered to microcrystalline quartz, Fe-oxides and kaolinite. Some of the samples contain welded glass shards. / Kamnino sestavljajo fragmenti spremenjenih glinencev, biotita in vulkanskih litičnih drobcev. Osnova je spremenjena v mikrokristalen kremen, železove okside in kaolinit. Nekateri vzorci vsebujejo nataljene črepinjice stekla.		

Carbonate rocks / Karbonatne kamnine	Limestone breccia / Apnenčeva breča	Polimiktna apnenčeva breča (*Tubiphytes obscurus* Maslov, *Calcitornella/Tuberitina,* Schwagerinidae, *Epimastopora* sp., *Anthracoporella spectabilis* Pia); klasti apnenca in peščenjaka, v vezivu tudi fuzulinide / Polymict limestone breccia (*Tubiphytes obscurus* Maslov, *Calcitornella/Tuberitina,* Schwagerinidae, *Epimastopora* sp. , *Anthracoporella spectabilis* Pia); limestone and sandstone clasts, isolated fusulinid foraminifera	Lower Permian breccia: Dovžanova soteska and Trogkofel Formations (west of the DPB; the area of Slovenske Konjice) / Spodnjepermska breča: Dovžanosoteška in Trogkofelska formacija (zahodno od DPB; okolica Slovenskih Konjic)	*Tubiphytes*-like microproblematica / Tubifitna mikroproblematika (*Tubiphytes obscurus* Maslov), foraminifera / foraminifere (*Calcitornella/Tuberitina,* Schwagerinidae), algae /alge (*Epimastopora* sp. in *Anthracoporella spectabilis* Pia)
	Marly limestone / Laporast apnenec	Bioclastic wackstone with terregenous admixture / Bioklastični wackstone s terigeno primesjo	Upper Permian or Lower Triassic limestone / Zgornjepermski ali spodnjetriasni apnenec	/
	Micritic limestone / Mikritni apnenci	Mudstone with dessication voids, intraclastic wackstone and calcimicrobial boundstone (with foraminifera *Endotriadella* or *Ammobaculites*, *"Trochammina"* sp.), bioclastic wackstone and packstone (*Agathammina* sp., *Aulotortus* ex gr. *sinuosus* Weynschenk, ?*Aulotortus friedli* (Kristan-Tollmann)). / Mudstone z izsušitvenimi porami, intraklastični wackstone in kalcimikrobni boundstone (s foraminiferami *Endotriadella* ali *Ammobaculites*, »Trochammina« sp.,), bioklastični wackstone in packstone (s foraminiferami *Agathammina* sp., *Aulotortus* ex gr. *sinuosus* Weynschenk, ?*Aulotortus friedli* (Kristan-Tollmann))	Ladinian to lower Carnian shallow marine facies / Ladinijski do spodnjekarnijski plitvomorski faciesi	foraminifera / foraminifere »Trochammina« sp., ?*Variostoma pralongense* Kristan-Tollmann, *Aulotortus* ex gr. *sinuosus* Weynschenk, ?*Aulotortus friedli* (Kristan-Tollmann); microproblematica / mikroproblematika (*Tubiphytes obscurus* Maslov)
	Calcarenite / Kalkarenit	Bioclastic-intraclastic grainstone (foraminifera *Glomospira* sp., *Reophax* sp., ?*Variostoma pralongense* Kristan-Tollmann, microproblematica *Tubiphytes obscurus* Maslov) / Bioklastični-intraklastični grainstone (foraminifere *Glomospira* sp., *Reophax* sp., ?*Variostoma pralongense* Kristan-Tollmann, mikroproblematika *Tubiphytes obscurus* Maslov)		
	Partly recrystallized limestone / Delno rekristaliziran apnenec	Bioclastic packstone or wackstone / Bioklastični packstone ali wackstone		
	Dolomite / Dolomit	Crystalline dolomite / Kristalinični dolomit		
	Micritic limestone / Mikritni apnenec	Radiolarian wackstone, radiolarian-filament wackstone / Radiolarijski wackstone, radiolarijski-filamentni wackstone	Middle to Upper Triassic (alternatively Jurassic or Cretaceous?) open marine facies / Srednje- do zgornjetriasni (ali jurski in kredni?) odprtomorski faciesi	Radiolarians and/ or thin-shelled bivalves / Radiolariji in/ali tankolupinaste školjke
	Calcarenite / Kalkarenit	Intraclastic grainstone (resediment?) / Intraklastični grainstone (resediment?)		
	Partly recrystallized limestone / Delno rekristaliziran apnenec	Peloid filament grainstone / Peloidni filamentni packstone		
	Limestone breccia / Apnenčeva breča	Intraclastic rudstone / Intraklastični rudstone		
	Calcarenite / Kalkarenit	Oolithic grainstone / Ooidni grainstone	Mesozoic oolithic limestones / Mezozojski ooidni apnenci	/
	Calcarenite / Kalkarenit	Rudist packstone and bioclastic packstone (*Cuneolina*?, *Moncharmontia*) / Rudistni packstone in bioklastični packstone (*Cuneolina*?, *Moncharmontia*)	Upper Cretaceous shallow water rudist limestone from Gossau group (W of the PB; the area of Zreče) / Zgornjekredni plitvomorski rudistni apnenec Gossauske grupe (Z od DPB; okolica Zreč)	rudist fragments, foraminifera / Fragmenti rudistnih školjk, foraminifere (*Cuneolina*?, *Moncharmontia*)

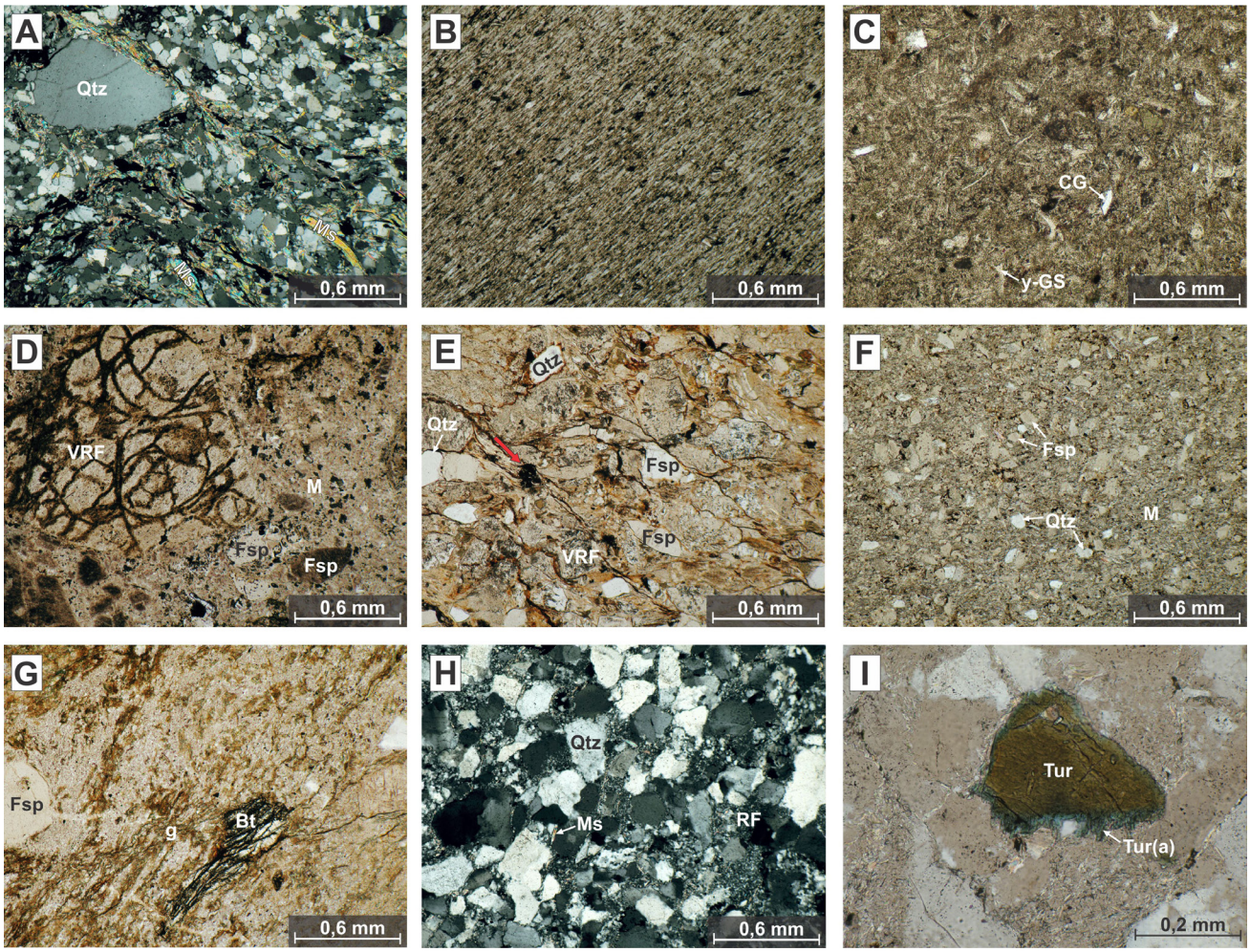

Fig. 6. Microfacies of the clasts in the Plio-Early Pleistocene sediments in the Celje Basin. (A) Slate with quartz and white mica as the main constituents. Rare quartz porphyroblasts are characteristic. (B) Foliated siltstone to shale with uniform preferred orientation of white mica forming continuous cleavage. (C) Fine-grained vitric (dacitic) tuff from the Oligocene Smrekovec series. (D) Glassy volcanic lithic fragment with perlitic texture in the sample of keratophyre lapilli tuff (Triassic). Some of the feldspars are extremely altered. (E) Coarse-grained (meta)tuff with incipient clevage marked with red arrow (Triassic). (F) Fine-grained tuff (Triassic). (G) Weathered (oxidized) biotite phenocryst in glassy groundmass altered to chlorite and microcrystalline quartz in keratophyre (Triassic). (H) Low-grade metamorphic heterogranular quartz sandstone. (I) Authigenic growth of tourmaline in the sample of slightly metamorphosed quartz sandstone. Abbreviations: Qtz – quartz, Ms - muscovite, CG – crystal grains, y-GS – y-shaped glass shards, VRF – volcanic lithic fragment, Fsp – feldspar, M – tuffaceous matrix, Bt – biotite, g – glassy groundmass, RF – rock fragment, Tur – tourmaline, Tur(a) -authigenic tourmaline.

Sl. 6. Mikrofaciesi klastov plio-zgodnjepleistocenskih sedimentov v Celjskem bazenu. (A) Filitoidni sljudnat skrilavec (peščeni metameljevec); v sestavi prevladujetakremen in muskovit. Značilni so redki porfiroklasti kremena. (B) Skrilav meljevec do glinavec s prednostno orientacijo mineralov belih sljud, ki oblikujejo kontinuiran klivaž – predvidena starost: karbon. (C) Drobnozrnat vitrični (dacitni) tuf iz Smrekovške serije oligocenske starosti. (D) Steklen vulkanski litični drobec s perlitno strukturo v vzorcu keratofirskega lapilnega tufa (trias). Nekateri K-glinenci so popolnoma prepereli. (E) Debelozrnati (meta) tuf z neizrazitim klivažem označenim z rdečo puščico (trias). (F) Drobnozrnati tuf (trias). (G) Preperel (oksidiran) vtrošnik biotita v steklasti osnovi, ki je spremenjena po kloritu in mikrokristalnem kremenu v keratofirju (trias). (H) Šibko metamorfoziran heterozrnat kremenov peščenjak. (I) Avtigena rast turmalina v neznatno metamorfoziranem heterozrnatem kremenovem peščenjaku. Okrajšave: Qtz – kremen, Ms - muskovit, CG – kristalna zrna, y-GS – črepinjice vulkanskega stekla y oblike, VRF – vulkanski litični drobec, Fsp – K-glinenec, M – tufska osnova, Bt – biotit, g – steklena osnova, RF – litični drobec, Tur - turmalin, Tur(a) -avtigeni turmalin.

Discussion

Sedimentary environment and morphostratigraphy

Pliocene-Quaternary sediments of the CB and DPB were deposited in alluvial environment, as indicated by lithofacies analysis of sections (Figs. 4, 5 and Table 3) and geomorphological analysis of sedimentary bodies (Figs. 2 , 3). Based on the results of sedimentological and geomor-

Diskusija

Okolje sedimentacije in morfostratigrafija

Pliocensko-kvartarni sedimenti so se na območju CB in DPB odlagali v aluvialnemokolju, kar je razvidno iz facielne analize profilov (sl. 4, 5 in Tabela 3) in geomorfološke analize sedimentacijskih teles (sl. 2, 3). Na podlagi rezultatov sedimentološke in geomorfološke analize interpretiramo, da so bili na območju CB vzorčeni rečni

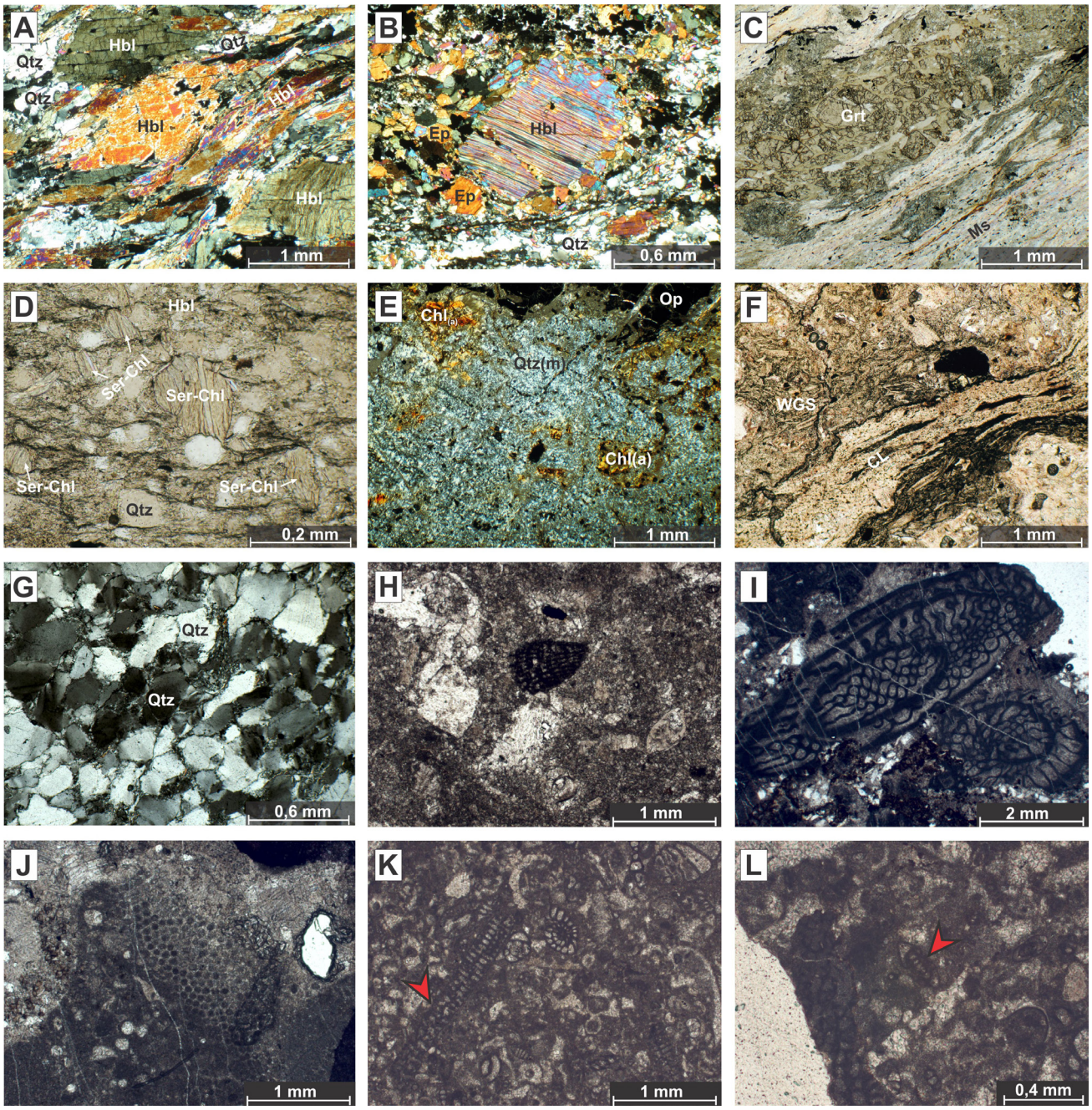

Fig. 7. Microfacies of the clasts in the Plio-Early Pleistocene sediments in the Drava-Ptuj Basin. (A) Lenticular and streched blasts of hornblende oriented along foliation plains in medium- to coarse-grained amphibolite. (B) Deformational lamellae in porphyroclast of hornblende embedded in fine-grained hornblende, plagioclase, epidote, quartz and opaque minerals in epidote amphibole schist. (C) Disintegrated and chloritized garnet surrounded by muscovite and some quartz in retrograde altered (mylonitized) mica schist. (D) Sericite-chlorite aggregates oriented transverselyl to anastomosing cleavage in slate. (E) Altered glassy keratophyre (Triassic). (F) Elongated collapsed lapilli in the sample of welded keratophyre tuff (Triassic). (G) Undulose extinction of quartz in the sample of low-grade metamorphic quartz sandstone. (H) Fragment of foraminifera Cuneolina sp. in rudist packstone (Upper Cretaceous). (I) Foraminifera of the family Schwagerinidae (Paraschwagerina? sp.) in the intergranular space in breccia (lower Permian). (J) Alga Anthracoporella spectabilis Pia in a breccia clast (lower Permian). (K) Foraminifera Cuneolina (marked with the arrowhead) and undetermined foraminifera in bioclastic packstone (Upper Cretaceous). (L) Foraminifera Moncharmontia sp. in bioclastic packstone (Upper Cretaceous). Abbreviations: Qtz – quartz, Qtz(m) – microcrystalline quartz, Hbl – hornblende, Ep – epidote, Grt – garnet, Ms – muscovite, Ser – sericite, Chl – chlorite, Chl(a) – altered chlorite, Op – opaque mineral, WGS – welded glass shards, CL – collapsed lapilli.

Sl. 7. Mikrofaciesi klastov plio-zgodnjepleistocenskih sedimentov v Dravsko-Ptujskem bazenu. (A) Lečasti blasti rogovače in vlaknata rogovača vzdolž foliacije v srednje do debelozrnatem amfibolitu. (B) Deformacijske lamele v porfiroklastu rogovače obdane z drobno rogovačo, plagioklazom, epidotom, kremenom in neprosojnimi minerali v vzorcu epidotno amfibolskega skrilavca. (C) Zdrobljen in kloritiziran granat obdan z muskovitom in malo kremena v vzorcu retrogradno spremenjenega (milonitiziranega) blestnika. (D) Sericitno-kloritni agregati orientirani pravokotno na povijajoči klivaž v vzorcu glinastega skrilavca. (E) Preperel steklast keratofir (trias). (F) Močno razpotegnjen lapil s porušeno strukturo v vzorcu nataljenega keratofirskega tufa (trias). (G) Valovita potemnitev kremena v šibko metamorfoziranemu kremenovemu peščenjaku (H) Fragment foraminifere Cuneolina sp. v rudistnem packstone-u (zgornja kreda). (I) Foraminifere družine Schwagerinidae (Paraschwagerina? sp.) v vezivu breče (spodnji perm). (J) Alga Anthracoporella spectabilis Pia v klastu znotraj apnenčeve breče (spodnji perm). (K) Foraminifera Cuneolina (označena velika hišica na levi) in številne druge nedoločene vrste v bioklastičnem packstone-u (zgornja kreda). (L) Foraminifera rodu Moncharmontia v bioklastičnem packstone-u (zgornja kreda). Okrajšave: Qtz – kremen, Qtz(m) – mikrokristalen kremen, Hbl – rogovača, Ep – epidot, Grt – granat, Ms – muskovit, Ser – sericit, Chl – klorit, Chl(a) – preperel klorit, Op – neprosojni mineral, WGS – nataljene črepinjice stekla, CL – lapil s porušeno strukturo.

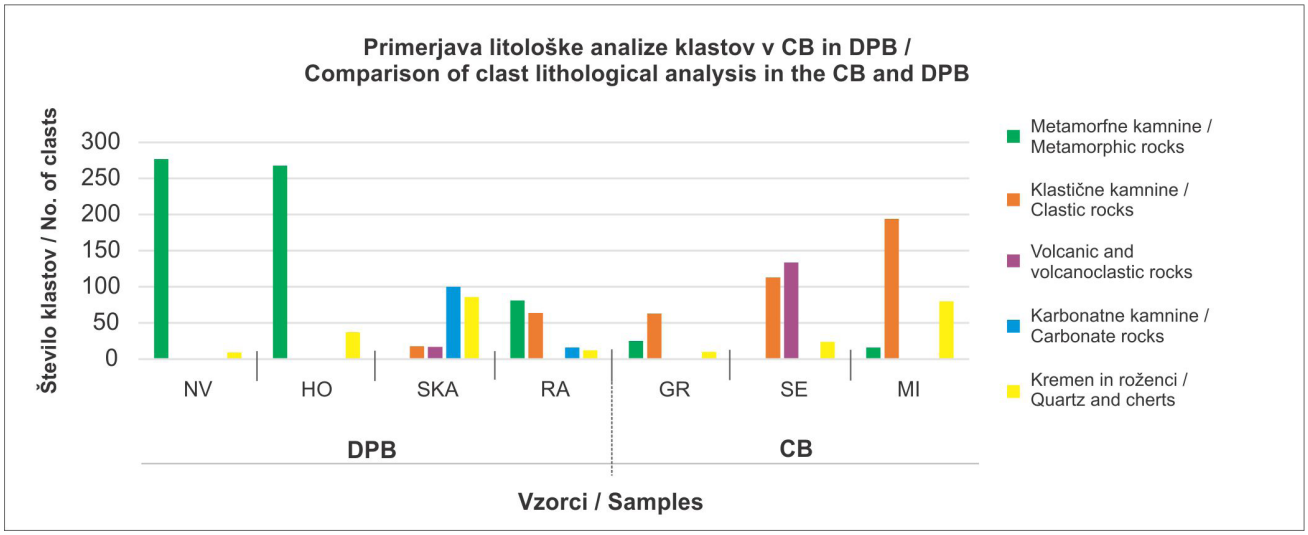

Fig. 8. Comparison of the clast lithological analysis of the Plio-Early Pleistocene sediments in the Celje (CB) and Drava-Ptuj Basin (DPB). Lithogroups correspond to those in tables 4 and 5.

Sl. 8. Primerjava litološke analize klastov plio-zgodnjepleistocenskih sedimentov v Celjskem (CB) in Dravsko-Ptujskem bazenu (DPB) pri čemer lito-skupine kamnin ustrezajo skupinam v tabelah 4 in 5.

phological analyses, we interpret sediments from CB (sections GR, SE, MI) as river sediments and from DPB as river sediments (sections RA and SKA) and alluvial fan sediments (sections NV and HO). Lithofacies Bcm, Gm and Gms were deposited in river channels and alluvial fans. Sandy lithofacies Sm, Sm(d) and Sp are present in sand dunes, while the finest sediments Fm and Fm(d) are floodplain sediments and fine-grained part of alluvial fans. Coarse-grained and poorly sorted facies with subangular to well-rounded clasts suggest relatively short transport, which agrees with the results of clast provenance analysis (see the following section of the discussion).

Alluvial sediments in CB and DPB were depositing simultaneously with the erosional base lowering and relative surface uplifting, as suggested by the inverse terrace staircase (Fig. 9). The floodplain surface (PR) in CB and DPB has well visible morphology with abandoned river meanders that are very well preserved indicating braided river system active prior to regulation of Savinja and Drava river channels. The estimated age of this floodplain deposits is Holocene. The age of higher terrace levels was interpreted based on traditional morphostratigraphy (Buser, 1979; Mioč & Žnidarčič, 1989), comparison with other basins in the region (e.g.: Krško Basin: Verbič, 2004; Velenje Basin: Drobne, 1967, and Rakovec, 1968; Ljubljana Basin: Pavich & Vidic, 1993) and on new observations from this study.

Low-level terrace group encompasses terraces T0 and T1 in CB and terraces T0, T1 and T2 in DPB, which are up to 8 m above the floodplain in

sedimenti (profili GR, SE, MI), na območju DPB pa rečni sedimenti (profila RA in SKA) ter sedimenti aluvialnih pahljač (profila NV in HO). Litofaciesi Bcm, Gm in Gms so se odlagali v rečnih koritih ter v nanosih aluvialnih pahljač. Peščeni litofaciesi Sm, Sm(d) in Sp predstavljajo peščene sipine, najbolj drobnozrnati sedimenti Fm in Fm(d) pa sedimente poplavnih ravnic ter drobnozrnate nanose aluvialnih pahljač. Debelozrnati in slabo sortirani prodnati faciesi s slabo do dobro zaobljenimi klasti nakazujejo relativno kratek transport, kar je v skladu z rezultati analize provenience klastov (glej nadaljevanje diskusije).

Odlaganje aluvialnih sedimentov v CB in DPB se je odvijalo sočasno z zniževanjem erozijske baze in relativnim dvigovanjem površja, kar se odraža v inverzni stratigrafiji teras (sl. 9). Površina poplavne ravnice (PR) v CB in DPB ima jasno razvidno morfologijo in zelo dobro ohranjene opuščene rečne meandre, ki nakazujejo na prepletajoč rečni sistem Savinje in Drave pred regulacijo strug. Ocenjena starost poplavne ravnice je holocen. Višje ležečim terasnim nivojem in vršajem so pripisane interpretativne starosti na podlagi tradicionalne morfostratigrafije (Buser, 1979; Mioč & Žnidarčič, 1989), primerjave z drugimi bazeni v regiji (npr.: Krški bazen: Verbič, 2004; Velenjski bazen: Drobne, 1967; Rakovec, 1968; Ljubljanski bazen: Pavich & Vidic, 1993) ter na podlagi novih opazovanj, ki so predmet te študije.

Spodnji terasni nivo obsega terasi T0 in T1 v CB ter terase T0, T1 in T2 v DPB, ki se nahajajo

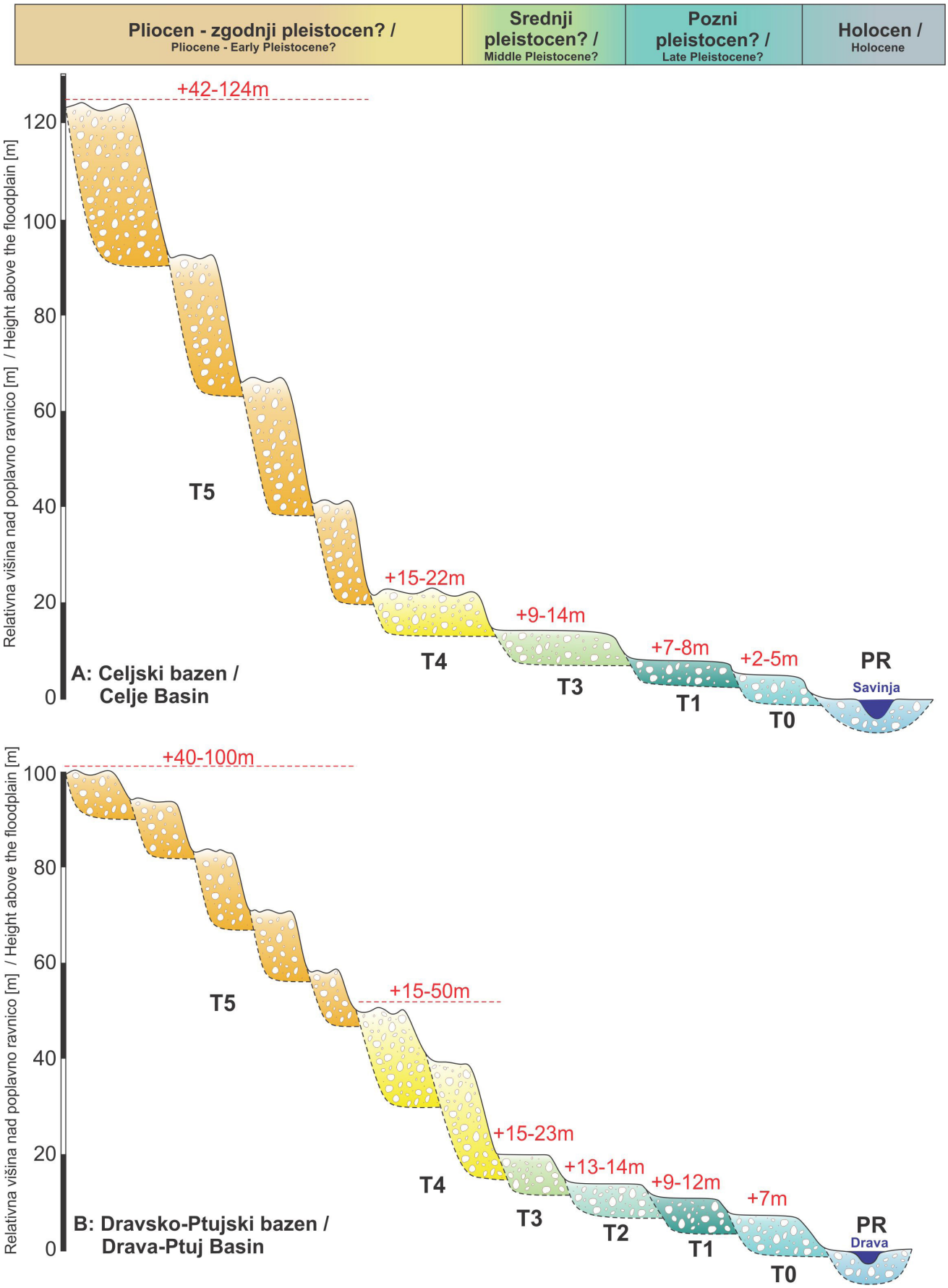

Fig. 9. Schematic profile of the terrace and fan systems in the (A) Celje Basin and (B) Drava-Ptuj Basin with levels (T0, T1, T2, T3, T4 in T5) marked, together with their relative heights above the Holocene floodplain (PR).

Sl. 9. Shematska profila sistema teras in vršajev v (A) Celjskem in (B) Dravsko-Ptujskem bazenu z označenimi nivoji (T0, T1, T2, T3, T4 in T5) ter njihovimi relativnimi višinami nad holocensko poplavno ravnico (PR).

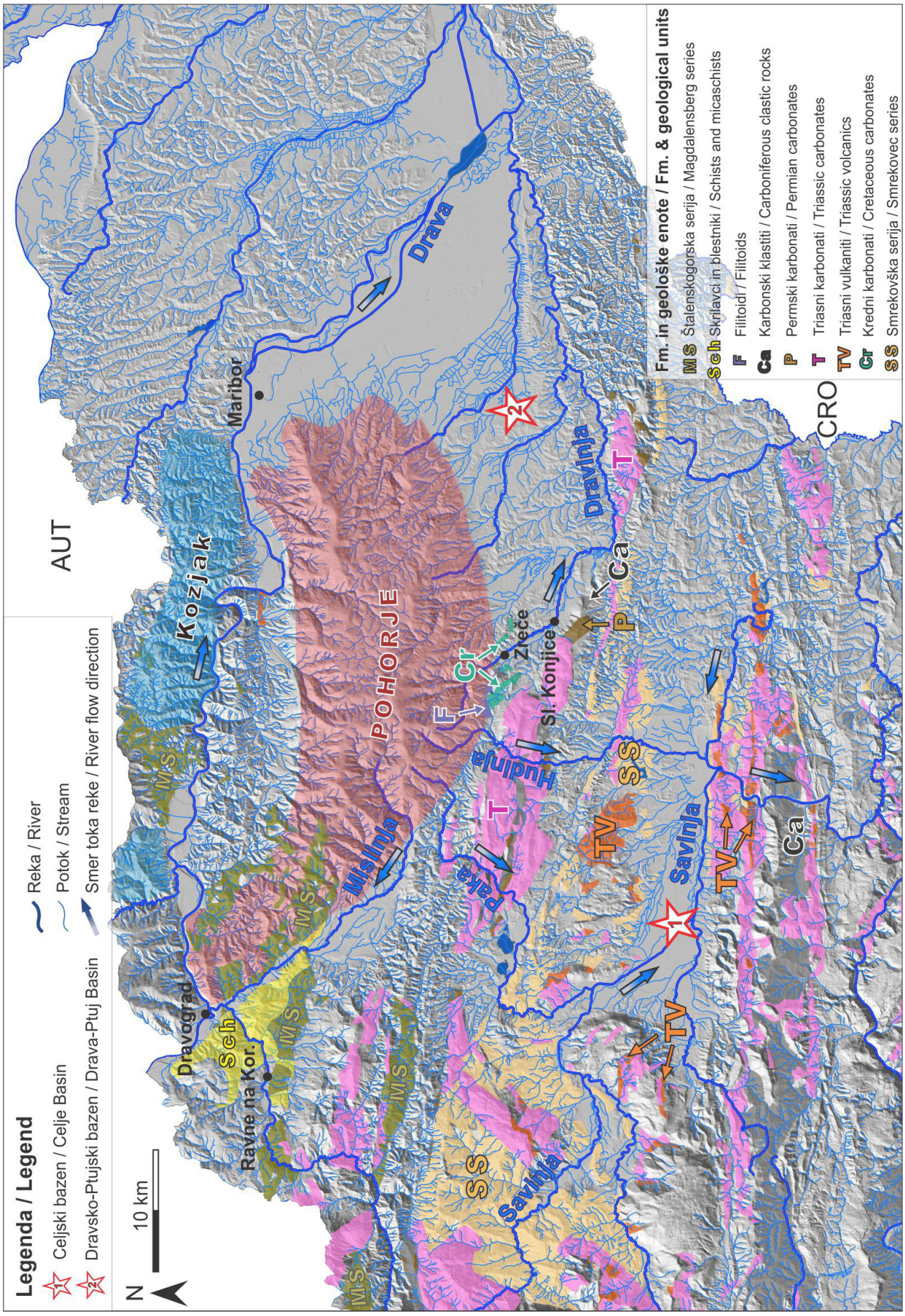

Fig. 10. Interpretation of the source areas of Plio-Early Pleistocene gravel deposits in the Celje (1) and Drava-Ptuj Basins (2).

Sl. 10. Interpretacija izvornih območij plio-zgodnjepleistocenskih prodnatih sedimentov v Celjskem (1) in Dravsko-Ptujskem bazenu (2).

CB and up to 14 m above the floodplain in DPB. Terrace treads and risers are very well preserved, terrace treads are typically wide and (almost) flat surfaces. Lidar data show that the terrace treads have preserved abandoned river meanders, which are common and moderate to well preserved in DPB, whereas rare and poorly preserved in CB. Terrace treads gently slope in direction consistent with the flow of present streams. Sediments of these terraces are composed of carbonate gravel exhibiting only low degree of weathering. Terrace riser's heights (e.g. between T0 and T1; between T1 and T2) are relatively low (2–5 m). Since the terraces T0, T1 and T2 have well preserved geomorphic traces of former river system, which is typical for youngest Quaternary periods (e.g. Blum & Törnqvist, 2000; Lewin & Macklin, 2003), and are older than the Holocene floodplain, we interpret the age of the low-level terrace group of Late Pleistocene.

Middle-level terrace group comprises terraces and fans T3 occurring at up to 14 m above the floodplain in CB and up to 23 m above the floodplain in the DPB. Similarly, as in low-level terrace group, their gravel is composed of carbonate clasts and exhibits low degree of weathering. Their terrace treads slope in direction consistent with the flow of present streams. In contrast with the low-level terrace group, the degree of terrace preservation is lower, and terrace treads occur in considerably less extensive surfaces in middle-level terrace group. Therefore, we interpret the terraces and fans T3 are of Middle Pleistocene age.

High-level terrace group encompasses terraces and fans T4 and T5. Compared to middle-level terrace group, T4 and T5 have several levels occurring at different relative height from approximately 40 to 124 m above the floodplains. Terrace, and fan surfaces are strongly degraded. Surfaces are not flat anymore but have developed a rough relief because of degradation processes. Often the surfaces are only remnants of former morphology of sedimentary bodies, preserved in narrow, flat-crest tops. Risers are clearly visible as scarps between two terrace levels but are often strongly eroded by ephemeral and perennial streams. Risers are considerably higher than risers in low- and middle-level terrace group. The degree of weathering of sediments (clasts) in CB is significantly higher than in low- and middle-level terrace group, the prominent difference is also in lithologic composition of gravel, which is here exclusively non-carbonate. In DPB, sediments of this group are as well much more

do približno 8 m nad poplavno ravnico v CB in do 14 m nad poplavno ravnico v DPB. Terase in ježe teras so zelo dobro ohranjene, pri čemer terasne ravnine zavzemajo značilno široke in ravne površine. Lidarski posnetki kažejo na površinah teras opuščene rečne meandre, ki so ponekod pogostejši in srednje dobro do dobro ohranjeni (DPB), ponekod pa redki in slabše ohranjeni (CB). Terasne površine vpadajo v smeri današnjih vodotokov. V sestavi sedimentov nastopa zgolj malo preperel karbonatni prod. Višina ježe teras med sosednje ležečimi terasami (npr. med T0 in T1; med T1 in T2) je relativno majhna (od 2 do 5 m). Glede na to, da imajo terase T0, T1 in T2 dobro ohranjene geomorfne sledove nekdanjega rečnega sistema, kar je značilno za najmlajša obdobja kvartarja (npr. Blum & Törnqvist, 2000; Lewin & Macklin, 2003), in da so starejše od holocenske PR, je interpretirana starost spodnjega terasnega nivoja pozni pleistocen.

Srednji terasni nivo obsega terase in vršaje T3, ki se nahajajo do 14 m nad poplavno ravnico v CB in do 23 metrov nad poplavno ravnico v DPB. Čeprav je prod, tako kot v spodnjem terasnem nivoju, nepreperel in karbonatne sestave, površine pa prav tako vpadajo v smeri današnjih vodotokov, so slednje za stopnjo slabše ohranjene in obsegajo znatno manjše površine kot terase spodnjega terasnega nivoja. Zato so terase in vršaji T3 interpretirani kot srednjepleistocenski.

Zgornji terasni nivo obsega terase in vršaje T4 in T5. Za razliko od srednjega terasnega nivoja je v T4 in T5 grupiranih več nivojev površin, ki se pojavljajo na različnih relativnih višinah od približno 40 do 124 m nad poplavnimi ravnicami. Površina teras in vršajev je močno degradirana. Ni več ravna, temveč je hrapava zaradi delovanja degradacijskih procesov in pogosto omejena le na ostanke nekdanjih površinskih oblik, ohranjenih v ozkih grebenih. Ježe teras so jasno razvidne kot stopnje med dvema nivojema teras, vendar so pogosto močno prečno erodirane z občasnimi ali stalnimi potoki, višine ježa pa so znatno višje kot v nižjem in srednjem terasnem nivoju. Stopnja preperelosti sedimentov (prodnikov) v CB je znatno višja kot v spodnjem in srednjem terasnem nivoju, izrazita pa je tudi razlika v litološki sestavi proda, ki je tu izključno nekarbonaten. V DPB so sedimenti prav tako znatno bolj prepereli, a razlike v litološki sestavi z nižjima sistemoma teras ni, kar je bilo ugotovljeno že v preteklih raziskavah (Mioč & Žnidarčič, 1989). Terase in vršaji zgornjega terasnega nivoja so bile tako v skladu s podatki Osnovne geološke karte (Buser, 1979;

weathered, but there is no difference in lithologic composition compared to lower terrace groups, as already pointed out by previous investigations (Mioč & Žnidarčič, 1989). Terraces and fans of high-level terrace group were thus interpreted as Plio-Early Pleistocene, which agrees with Basic geologic map (Buser, 1979; Mioč & Žnidarčič, 1989). It is important to note, however, that sediment deposition in terraces, related to strong climate changes, typical for Quaternary, as well as numerical age dating from other comparable intramountain basins in the region (Cline et al., 2016) and previous observations (e.g. Kuščer, 1993) indicate mostly Early Pleistocene and not Pliocene age.

Provenance of the Plio-Early Pleistocene sediments

The interpretation of the provenance of the Plio-Early Pleistocene sediments in the CB and the DPB is based on clast lithological analysis. We focused on the indicative lithologies; these are lithologies that can be attributed to certain formation with high reliability and that are outcropping on a relatively small area (Büchi, 2016). Interpretation of the possible source areas of Plio-Early Pleistocene gravel deposits in the CB and DPB is depicted in the figure 10.

Celje Basin

The provenance of the Plio-Early Pleistocene sediments in the CB is constrained with metamorphic, volcanic and volcaniclastic and clastic rocks (Table 4). In the group of metamorphic rocks filitoid mica schist is the main indicative lithology, which was sampled from the sediments on the southern margin of the CB. The occurrence of this type of metamorphic rocks is limited to the area of the Eastern Alps, outcropping only north of the CB (in the area of the Hudinja spring). However, the dip of the sampled terraces is indicating the sediment supply from the south. Regarding these two contradictory arguments, we propose that ether i) these metamorphic clasts are resedimented from older (possibly Miocene; Ivančič et al., 2017) deposits from the south of the CB, which were originally deposited from the north or that ii) the present day dip of the terrace surfaces is a result of post-sedimentary tectonics and does not correspond to the direction of the drainage system in the Plio-Early Pleistocene.

In the group of the volcanic and volcaniclastic rocks Triassic and Oligocene clasts were identified. The outcrops of Triassic volcanic rocks are located on the northern, western and southern

Mioč & Žnidarčič, 1989) uvrščene v plio-zgodnji pleistocen. Pri tem je potrebno poudariti, da način odlaganja sedimentov v terasah, ki je pogojen z močnejšimi podnebnimi nihanji, značilnimi za obdobje kvartarja, podatki numeričnih datacij v drugih primerljivih medgorskih bazenih v regiji (Cline et al., 2016) ter predhodna opazovanja (npr. Kuščer, 1993) nakazujejo v večji meri zgodnjepleistocensko in ne pliocensko starost.

Provenienca plio-zgodnjepleistocenskih sedimentov

Provenienca plio-zgodnjepleistocenskih sedimentov je interpretirana na osnovi litološke analize klastov. Med vsemi določenimi litotipi so za interpretacijo provenience prodnatih sedimentov CB in DPB pomembne tako imenovane indikativne litologije, t.j. litologije, ki se lahko z veliko stopnjo zanesljivosti pripišejo določeni formaciji in izdanjajo na relativno majhnem območju (Büchi, 2016). Današnja prostorska razširjenost formacij, ki bi lahko bile izvor indikativnih litologij, prepoznanih v plio-pleistocenskih prodnih sedimentih CB in DPB, je prikazana na sliki 10.

Celjski bazen

Provenienco plio-zgodnjepleistocenskih sedimentov v CB nakazujejo skupine metamorfnih, vulkanskih in vulkanoklastičnih ter klastičnih kamnin (Tabela 4).

V prvi skupini je indikativna litologija filitoidni sljudnati skrilavec, najden v sedimentih na južnem robu CB. Danes izdanja v bližini izvira potoka Hudinja, severno od CB, ne pa tudi na južnih obronkih CB. Nagib vzorčenih teras sicer nakazuje pritok iz juga CB, vendar pa se izvorne metamorfne kamnine, omejene na območje Vzhodnih Alp, pojavljajo le severno od CB. Glede na nasprotujoča si argumenta se porajajo dodatne interpretacije, in sicer i) da so prodniki omenjene litologije resedimentirani iz nanosov starejših paleopritokov, ki so prihajali s severa (miocenski sedimenti?; Ivančič et al., 2017) ali pa ii), da je današnji nagib teras rezultat post-sedimentacijske tektonike in ne ustreza smeri drenaže v plio-zgodnjempleistocenu.

V skupini vulkanskih in vulkanoklastičnih kamnin so bili ugotovljeni prodniki triasnega in oligocenskega vulkanizma. Prvi se pojavlja v manjših erozijskih ostankih na severnih, zahodnih in južnih pobočjih CB, drugi pa na širšem območju severno in zahodno od CB, kar ustreza provenienci paleo-Savinje (Buser, 2010).

hillslopes of the CB and occur as smaller erosional remnants (Buser, 2010). The outcrops of the Oligocene volcanic rocks can be found in a wider area north and west of the CB. This corresponds to the provenance of paleo-Savinja and its tributaries.

The outcrops of clastic Carboniferous rocks are located on the southern, northern and northwestern hillslopes of the CB (Buser, 2010) which corresponds to the provenance of the paleo-Paka, paleo-Savinja and their tributaries.

Source areas of Plio-Early Pleistocene sediments are therefore located in the vicinity of the deposits. Hence, we interpreted that the drainage system of the paleo-Savinja and its tributaries in Pliocene-Quaternary corresponds to the present one.

Drava-Ptuj Basin

In the DPB two indicative lithogroups were identified; metamorphic rocks are prevailing in the NV and HO samples and carbonate rocks present solely in RA and SKA samples (Table 5).

Varieties of amphibolite and epidote amphibole schists originate from Pohorje Massif and Kozjak mountain range (Buser, 2010). Mica schists and schists corresponds to the lithologies that are typical for the wider area of the Eastern Alps. The clasts likely originate from the Pohorje Massif and Kozjak mountain range, however the provenance from the area between Ravne na Koroškem and Dravograd and further away from Eastern Alps in Austria cannot be excluded. Slate varieties were interpreted to originate from Magdalensberg series located on the western part of the Pohorje Massif and in Kozjak mountain range (Buser, 2010). The group of metamorphic rocks in the NV and HO samples was therefore attributed to the provenance of paleo-Drava and its tributaries.

Carbonate rocks were identified solely in the RA and SKA samples which corresponds to the provenance of paleo-Dravinja and its tributaries. Permian carbonate rocks were attributed to Lower Permian Dovžanova soteska and Trogkofel Formations that can be found in the area around Slovenske Konjice (Buser, 2010). Varieties of Triassic carbonate rocks are located in the area west and north of the Slovenjske Konjice and Zreče. Upper Cretaceous carbonate rocks were attributed to rudist limestone from Gossau group (Pleničar, 1993; Moro et al., 2016) and occupy area east and west of Zreče (Buser, 2010).

Igneous rocks were, despite the immediate vicinity of the Pohorje Massif, not found in any of studied localities. Based on structural, radi-

Klastične kamnine karbonske starosti se danes v primarni legi pojavljajo na južnih, severnih in severozahodnih obronkih CB (Buser, 2010), kar ustreza provenienci paleo-Pake, paleo-Savinje ter njunih pritokov. Izvorna območja plio-zgodnjepleistocenskih sedimentov se torej nahajajo v relativni bližini obravnavanih rečnih nanosov, rečna mreža v pliocenu-kvartarju pa je potekala v skladu z današnjo drenažo, torej s smerjo toka Savinje in manjših potokov z obronkov CB.

Dravsko-Ptujski bazen

V DPB sta bili ugotovljeni dve indikativni skupini kamnin, in sicer metamorfne kamnine, ki močno prevladujejo v vzorcih NV in HO in karbonatne kamnine, ki se pojavljajo izključno v vzorcih RA in SKA (Tabela 5).

Različki amfibolita in epidotno amfibolskega skrilavca so bili pripisani območju Pohorja in Kozjaka (Buser, 2010). Značilnosti skupine blestnikov in skrilavcev ustrezajo različkom, ki se pojavljajo na širšem območju Vzhodnih Alp. Predvidevamo donos s Pohorja in Kozjaka, manj verjetno pa iz bolj oddaljenega območja med Ravnami na Koroškem in Dravogradom in seveda naprej iz avstrijskega dela Vzhodnih Alp. Skupino glinastih skrilavcev (ang. slate) smo povezali s Štalenskogorsko serijo, ki se nahaja na zahodnem Pohorju in na Kozjaku (Buser, 2010) ter jo danes erodirajo pritoki Drave. Skupini metamorfnih kamnin v vzorcih NV in HO je bila tako pripisana drenaža paleo-Drave in njenih pritokov.

Karbonatne kamnine so bile ugotovljene le v vzorcih RA in SKA, kar generalno ustreza drenaži paleo-Dravinje in njenih pritokov. Permske karbonatne kamnine so bile pripisane spodnjepermski Dovžanosoteški in Trogkofelski formaciji, ki izdanjata v okolici Slovenskih Konjic (Buser, 2010). Pojavnost različkov triasnih karbonatnih kamnin je omejena na območje zahodno in severno od Slovenskih Konjic in Zreč. Zgornjekredne kamnine so opredeljene kot rudistni apnenci Gossauske grupe (Pleničar, 1993; Moro et al., 2016), ki izdanjajo vzhodno in zahodno od Zreč (Buser, 2010).

Kljub pričakovanjem, magmatskih kamnin s Pohorja na vzorčenih lokacijah nismo našli. Glede na dosedanje strukturne, radiometrične in paleomagnetne raziskave (Márton et al. 2006; Trajanova et al. 2008; Fodor et al. 2008; Trajanova, 2013) se osnovna morfologija Pohorja, kljub levi (ccw) rotaciji bloka, v času kvartarja ni bistveno spremenila. Zato sklepamo, da je bil tudi drenažni sistem podoben današnjemu. Kot je razvidno s slik 1 in 3, nobeden od današnjih vodotokov,

ometric and paleomagnetic analyses (Márton et al., 2006; Trajanova et al., 2008; Fodor et al., 2008; Trajanova, 2013) the morphology of the Pohorje Massif in the Quaternary, despite its counterclockwise rotation, did not changed significantly. Therefore, the drainage system was presumably similar as today. None of the present-day streams reach up to the granodioritic pluton. (Figs. 1, 3). Besides, the relief of its eastern part in the late Miocene is modeled to be significantly higher and gravitationally disintegrated in the latest Miocene-Pliocene (Trajanova, 2013), which would yield that erosion and transport of the granodiorite to the DPB in the Quaternary was even less likely.

The results of the provenance analysis indicate two different source areas of the Plio-Early Pleistocene sediments; paleo-Drava and paleo-Dravinja. Moreover, the river system in the Plio-Early Pleistocene is similar to the present one, which corresponds to the previous studies in the area of the Eastern Alps (e.g. Keil and Neubauer, 2009).

Enigmatic carbonate clasts in the "Plio-Quaternary" sediments?

In the wider Alpine foreland area, there are several examples from Switzerland (Graf, 1993; Preusser et al., 2011), Germany (Doppler et al., 2011; Ellwanger et al., 2011) and Austria (van Husen & Reitner, 2011), where the criteria for distinguishing different terraces is the presence/absence of carbonate clasts. A similar model is currently applied in the Krško Basin, where Plio-Early Pleistocene gravel (Globoko Alloformation, Verbič, 2008) is characterized as non-carbonate gravel (e.g. Poljak, 2017). However, several authors (Verbič, 2008; Mencin Gale, unpublished data) report an exception in the Libna locality. The absence of carbonate clasts was in the previous studies explained with i) in-situ dissolution of the carbonates (Kuščer, 1993) or with ii) dissolution of the carbonate gravel during the transport and resedimentation (Verbič, 2008). Both explanations are therefore climate-related. On the contrary, carbonate clasts were reported in several "Plio-Quaternary" basins in the region; the Velenje Basin (Mioč, 1978; Kralj et al., 2018) and DPB (Mioč & Žnidarčič, 1989; this study). Therefore, we propose an alternative explanation that the presence of the carbonate clasts in these basins is not climate-related but rather dependent from the vicinity of the carbonate source rocks and the evolution of the drainage network.

ki prečijo obravnavano območje, ne sega do granodioritnega plutona. Glede na model nastanka Pohorskega tektonskega bloka (Trajanova, 2013) je bil relief njegovega vzhodnega dela v času poznega miocena celo znatno višji in je gravitacijsko razpadal koncem miocena in v pliocenu. Zaradi tega je erozija in transport granodiorita na obravnavano območje še manj verjetna.

Rezultati analize provenience nakazujejo dve glavni izvorni območji plio-zgodnjepleistocenskih sedimentov DPB, in sicer provenienci paleo-Drave in paleo-Dravinje. Nadalje, rečna mreža je v plio-zgodnjempleistocenu potekala v skladu z današnjo, kar je v skladu z drugimi opazovanji na širšem območju Vzhodnih Alp (npr. Keil and Neubauer, 2009).

Enigmatični karbonatni prodniki v »pliokvartarnih « sedimentih?

V širšem prostoru alpskega predgorja, kot na primer v Švici (Graf, 1993; Preusser et al., 2011), Nemčiji (Doppler et al., 2011; Ellwanger et al., 2011) in v Avstriji (van Husen & Reitner, 2011), terase pogosto ločujejo na podlagi vsebnosti karbonatnih prodnikov. Podoben kriterij za ločevanje različnih prodnatih zasipov je trenutno uveljavljen tudi v Krškem bazenu. Eden od kriterijev za ločevanje Plio-zgodnjepleistocenskih sedimentov Krškega bazena (Globoška aloformacija; Verbič, 2004) od mlajših sedimentov je prisotnost izključno nekarbonatnega proda (npr. Poljak, 2017), čeprav Verbič (2008) navaja izjemo prisotnosti karbonatnega proda na območju Libne (potrjeno tudi z osebnimi podatki Mencin Gale). Odsotnost karbonatnih prodnikov v plio-zgodnjepleistocenskih sedimentih Krškega bazena je možno pojasniti na dva načina: i) in-situ raztapljanje že odloženega karbonatnega proda (Kuščer, 1993), ali ii) raztapljanje karbonatnega proda med večkratno resedimentacijo rečnih nanosov (Verbič, 2008). Obe razlagi torej širše gledano pogojujeta podnebno-odvisen proces. Nasprotno so bili »pliokvartarni« karbonatni prodniki dokumentirani v nekaterih drugih medgorskih bazenih v regiji, na primer v Velenjskem bazenu (Mioč, 1978; Kralj et al., 2018) in v DPB (Mioč & Žnidarčič, 1989; pričujoča študija). Ob navedenih dejstvih se tako pojavi dodatna interpretacija, da v omenjenih bazenih ne gre pogojevati vsebnosti karbonatnih prodnikov s podnebnimi procesi, temveč z bližino izvornega območja karbonatnih kamnin in razvojem rečne mreže.

Conclusions

Investigation of Plio-Early Pleistocene sediments in the Celje and Drava-Ptuj basins bring new insights on the genesis, composition, morphostratigraphy and provenance of these sediments. Due to higher resolution obtained with detailed morphostratigraphy in this paper, we propose that the former chronostratigraphic name of the studied unit "Plio-Quaternary" is replaced with "Plio-Early Pleistocene". Plio-Early Pleistocene, Middle Pleistocene and Late Pleistocene sediments were deposited in alluvial environments and are preserved in several terrace and fan levels. Interpreted terrace and fan ages are based on several morphological and sedimentological criteria. The low-level terrace group encompasses terraces T0, T1 and T2 with an interpreted Late Pleistocene age. The middle-level terrace group represented by terraces and fans T3 is attributed to the Middle Pleistocene. The high-level terrace group comprised of terraces and fans T4 and T5 is interpreted to the Plio-Early Pleistocene.

The provenance of Plio-Early Pleistocene sediments is attributed to local source areas, which is supported by facies analysis of sediments, suggesting short transport, and provenance analysis of clasts. Metamorphic clasts in Plio-Early Pleistocene sediments of the Celje Basin originate from the southern Pohorje Massif, while clasts of volcanic, volcaniclastic and clastic rocks originate from northern, western and southern hillslopes of the Celje Basin. This is consistent with drainage of the paleo-Savinja and its tributaries. Clasts of metamorphic rocks in Plio-Early Pleistocene deposits of the Drava-Ptuj Basin probably originate mostly from Pohorje Massif and Kozjak area, and carbonate clasts are presumably from surroundings of Slovenske Konjice and Zreče. The provenance of clasts from Drava-Ptuj Basin is therefore related to the drainages of paleo-Drava, paleo-Dravinja and their tributaries. Our results thus indicate that the drainage in Plio-Early Pleistocene corresponded to present one, in agreement with other observations from the Eastern Alps.

Acknowledgements

This work was supported by the Slovenian Research Agency (ARRS) in the frame of the Young Researchers (38184), the Regional Geology (P1-0011) and Mineral Resources (P1-0025) research programmes and was carried out at the Geological Survey of Slovenia and University of Bern, Switzerland.

Zaključki

Raziskave plio-zgodnjepleistocenskih sedimentov v Celjskem in Dravsko-Ptujskem bazenu so pokazale nova spoznanja na področju geneze, sestave, morfostratigrafije in provenience sedimentov. Zaradi višje ločljivosti, ki temelji na detajlni morfostratigrafiji v tem članku opuščamo do sedaj ustaljeno kronostratigrafsko ime enote »pliokvartar« ter predlagamo ime plio-zgodnjepleistocenski sedimenti. Plio-zgodnjepleistocenski, srednjepleistocenski in poznopleistocenski sedimenti so se odlagali v rečnem okolju ter so ohranjeni v več terasnih in vršajnih nivojih. Interpretirane starosti teras in vršajev temeljijo na več morfoloških in sedimentoloških kriterijih. Spodnji terasni nivo obsega terase T0, T1 in T2 z interpretirano poznopleistocensko starostjo. Srednji terasni nivo obsega terase in vršaje T3, ki jim je bila pripisana srednjepleistocenska starost. Zgornji terasni nivo obsega terase in vršaje T4 in T5 z interpretirano plio-zgodnjepleistocensko starostjo.

Provenienca plio-zgodnjepleistocenskih sedimentov je bila pripisana lokalnim izvornim območjem, kar potrjuje facielna analiza sedimentov, ki kaže na krajši transport, kot tudi analiza provenience klastov. Metamorfni klasti v plio-zgodnjepleistocenskih sedimentih v Celjskem bazenu izvirajo iz območja južnega Pohorja, klasti vulkanskih, vulkanoklastičnih in klastičnih kamnin pa s severnih, in zahodnih in južnih obronkov Celjskega bazena. Pri tem je potrebno upoštevati možnost, da so lahko nekateri klasti resedimentirani in ne odražajo smeri transporta v plio-zgodnjempleistocenu. Generalno pojavnost izvornih kamnin ustreza drenaži paleo-Savinje in njenih pritokov. Prodniki metamorfnih kamnin v plio-zgodnjepleistocenskih nanosih Dravsko-Ptujskega bazena verjetno izvirajo predvsem z območja Pohorja in Kozjaka, karbonatni prodniki pa domnevno izvirajo iz okolice Slovenskih Konjic in Zreč. Izvorno območje klastov iz Dravsko-Ptujskega bazena je torej pogojeno z drenažo paleo-Drave in paleo-Dravinje ter njunih pritokov. Rezultati tako iz Celjskega kot iz Dravsko-Ptujskega bazena potrjujejo, da je bila drenaža v plio-zgodnjempleistocenu podobna kot danes, kar je v skladu z drugimi opazovanji na širšem območju Vzhodnih Alp.

Zahvala

Raziskava je bila izvedena v okviru projekta Mladi raziskovalec (38184) in programske skupine Regionalna Geologija (P1-0011) ter Mineralne surovine (P1-0025), ki jih financira Javna agencija za raziskovalno dejavnost Republike Slovenije (ARRS). Delo

Eva Mencin Gale was additionally supported by the Swiss Government Excellence Scholarship for Foreign Scholars and Artists. The authors would like to express gratitude to Polona Kralj for petrographic analysis of the volcanic and volcaniclastic rocks and for contribution in the discussion, Dragomir Skaberne for conducting petrographic analysis of the clastic rocks, Matevž Novak for determination of the Permian fossils and Mladen Štumergar for the preparation of the samples and thin-sections. We would also like to express our thanks to two anonymous reviewers for the constructive review that significantly improved this paper.

je bilo izvedeno na Geološkem zavodu Slovenije in na Univerzi v Bernu v Švici. Dodatno je bila raziskava financirana s štipendijo »Swiss Government Excellence Scholarship for Foreign Scholars and Artists« s strani švicarske vlade. Avtorji se zahvaljujejo Poloni Kralj za izvedene petrografske analize vulkanskih in vulkanoklastičnih kamnin ter za doprinos k diskusiji, Dragomirju Skabernetu za izvedbo petrografskih analiz klastičnih kamnin, Matevžu Novaku za določanje permskih fosilov ter Mladenu Štumergarju za pripravo vzorcev in zbruskov. Prav tako pa se zahvaljujemo dvema anonimnima recenzentoma za njune konstruktivne pripombe, ki so pripomogle k izboljšanju članka.

Literatura

Altherr, R., Lugović, B., Meyer, H. P. & Majer, V. 1995: Early Miocene post-collisional calc-alkaline magmatism along the easternmost segment of the Periadriatic fault system (Slovenia and Croatia). Mineralogy and Petrology, 54/3-4: 225-247. https://doi.org/10.1007/BF01162863

Blum, M. D. & Törnqvist, E. T. 2000: Fluvial responses to climate and sea-level change: a review and look forward. Sedimentology, 47: 2-48. https://doi.org/10.1046/j.1365-3091.2000.00008.x

Brezigar, A. 1987: Premogova plast Rudnika lignita Velenje. Geologija, 28-29: 319-336.

Brezigar, A., Kosi, G., Vrhovšek, D. & Velkovrh, F. 1987: Paleontološke raziskave pliokvartarne skladovnice velenjske udorine. Geologija, 28/29: 93-119.

Bridgland, D. R. 2000: River terrace systems in north-west Europe: An archive of environmental change, uplift and early human occupation. Quaternary Science Reviews, 19/13: 1293-1303. https://doi.org/10.1016/S0277-3791(99)00095-5

Bridgland, D. R. & Maddy, D. 2002: Global correlation of long Quaternary fluvial sequeces: A review of baseline knowledge and possible methods and criteria for establishing a database. Geologie En Mijnbouw/Netherlands Journal of Geosciences, 81/3-4: 265-281. https://doi.org/10.1017/S0016774600022605

Bridgland, D. R. & Westaway, R. 2008a: Preservation patterns of Late Cenozoic fluvial deposits and their implications: Results from IGCP 449. Quaternary International, 189/1: 5-38. https://doi.org/10.1016/j.quaint.2007.08.036

Bridgland, D. & Westaway, R. 2008b: Climatically controlled river terrace staircases: A worldwide Quaternary phenomenon. Geomorphology, 98/3-4: 285-315. https://doi.org/10.1016/j.geomorph.2006.12.032

Bridgland, D. R., Westaway, R., Romieh, M. A., Candy, I., Daoud, M., Demir, T., Galiatsatos, N., Schreve, D. C., Seyrek, A., Shaw, A. D., White, T. S. & Whittaker, J. 2012: The River Orontes in Syria and Turkey: Downstream variation of fluvial archives in different crustal blocks. Geomorphology, 165-166: 25-49. https://doi.org/10.1016/j.geomorph.2012.01.011

Bukovac, J., Poljak, M., Šušnjar, M. & Čakalo, M. 1984: Tumač za list Črnomelj: L 33-91: Osnovna geološka karta SFRJ 1: 100.000. Savezni geološki zavod, Beograd.

Buser, S. 1977: Osnovna geološka karta SFRJ. L 33-67, Celje. Zvezni geološki zavod, Beograd: 69 p.

Buser, S. 1979: Tolmač lista Celje: L 33-67: Osnovna geološka karta SFRJ 1: 100.000. Zvezni geološki zavod, Beograd.

Buser, S. 2010: Geološka karta Slovenije 1: 250.000. Geološki zavod Slovenije, Ljubljana.

Büchi, M. W. 2016: Overdeepened glacial basins as archives for the Quaternary landscape evolution of the Alps. Doktorska disertacije, Univerza v Bernu, Švica. https://doi.org/10.13140/RG.2.2.17415.80802

Cline, M. L., Cline, K. M., Jamšek Rupnik, P., Atanackov, J., Bavec, M. & Lowick, S. E. 2016: Tectonic geomorphology and geochronology supporting a probabilistic seismic hazard analysis in the Krško Basin, Slovenia: implications for a critical infrastructure. Program and short abstracts of the 7th international INQUA meeting on Paleoseizmology, Active

tectonics and Archeoseismology (PATA), Crestone, Colorado, USA, 23-26 p.

Debeljak, I. 2017: Fosilni trobčarji iz Šaleške doline. Zbirka Šaleški razgledi, Zbornik (2016-2017): 427 p.

Doppler, G., Kroemer, E., Rögner, K., Wallner, J., Jerz, H. & Grottenthaler, W. 2011: Quaternary stratigraphy of southern Bavaria. Quaternary Science Journal, 60/23: 329-365. https://doi.org/10.3285/eg.60.2-3.08

Drobne, K. 1967: Izkopavanje mastodonta v Škalah pri Velenju. Geologija, 10: 305-312.

Ellwanger D., Wielandt-Schuster U., Franz M. & Simon, T. 2011: The Quaternary of the southeast German Alpine Foreland. Quaternary Science Journal, 2-3: 306-328.

Evans, D. J. A. & Benn, D. I. 2004: A practical guide to the study of glacial sediments. Hodder Education, London: 266 p.

Fodor, L., Jelen, B., Marton, E., Skaberne, D., Čar, J. & Vrabec, M. 1998: Miocene-Pliocene tectonic evolution of the Slovenian Periadriatic fault: Implications for Alpine-Carpathian extrusion models. Tectonics, 17/5: 690-709. https://doi.org/10.1029/98TC01605

Fodor, L., Jelen, B., Marton, E., Rifelj, H., Kraljić, M., Kevrić, R., Marton, P., Koroknai, B. & Baldi-Beke, M. 2002: Miocene to Quaternary deformation, stratigraphy and paleogeography in Northeastern Slovenia and Southwestern Hungary = Deformacije, stratigrafija in paleogeografija severovzhodne Slovenije in jugozahodne Madžarske od miocena do kvartarja. Geologija, 45/1: 103-114. https://doi.org/10.5474/geologija.2002.009

Fodor, L. I., Gerdes, A., Dunkl, I., Koroknai, B., Pécskay, Z., Trajanova, M., Horvath, P., Vrabec, M., Jelen, B., Balogh, K. & Frisch, W. 2008: Miocene emplacement and rapid cooling of the Pohorje pluton at the Alpine-Pannonian-Dinaridic junction, Slovenia. Swiss Journal of Geosciences, 101: 255-271. https://doi.org/10.1007/s00015-008-1286-9

Gale, S. J., Hoare, P. G. 2011: Quaternary sediments. Petrographic Methods for the Study of Unlithified Rocks. Second Edition. The Blackburn Press, Caldwell: 325 p.

Graf, H. R. 1993: Die Deckenschotter der zentralen Nordschweiz. Doktorska disertacija. Eidgenössischen Technischen Hochschule Zürich, Švica.

Hinterlechner-Ravnik, A. 1971: Pohorske metamorfne kamenine. Geologija, 14: 187-226.

Hinterlechner-Ravnik, A. 1973: Pohorske metamorfne kamenine II. Geologija, 16: 245-270.

Hinterlechner-Ravnik, A. 1982: Pohorski eklogit. Geologija, 25/2: 251-288.

Ivančič K., Trajanova M., Skaberne D. & Šmuc A. 2017: Provenance of the Miocene Slovenj Gradec Basin sedimentary fill, Western Central Paratethys. Sedimentary Geology 375: 256-267. https://doi.org/10.1016/j.sedgeo.2017.11.002

Janák, M., Froitzheim, N., Lupták, B., Vrabec, M. & Ravna, E. J. K. 2004: First evidence for ultrahigh-pressure metamorphism of eclogites in Pohorje, Slovenia: Tracing deep continental subduction in the Eastern Alps. Tectonics, 23/5: TC5014. https://doi.org/10.1029/2004TC001641

Janák, M., Froitzheim, N., Vrabec, M., Krogh Ravna, E. J. & De Hoog, J. C. M. 2005: Ultrahigh-pressure metamorphism and exhumation of garnet peridotite in Pohorje, Eastern Alps. Journal of Metamorphic Geology, 24/1: 19-31. https://doi.org/10.1111/j.1525-1314.2005.00619.x

Jelen, B. & Rifelj, H. 2011: Površinska litostratigrafska in tektonska strukturna karta območja T-JAM projekta, severovzhodna Slovenija 1:100.000. Geološki zavod Slovenije: Ljubljana.

Keil, M. & Neubauer, F. 2009: Initiation and development of a fault-controlled, orogen-parallel overdeepened valley: The Upper Enns Valley, Austria. Austrian Journal of Earth Sciences, 102/1: 80-90.

Kováč, M., Andreyeva-Grigorovich, A., Bajraktarević, Z., Brzobohatý, R., Filipescu, S., Fodor, L., Harzhauser, M., Nagymarosy, A., Oszczypko, N., Pavelić, D., Rögl, F., Saftić, B., Sliva, L. & Studencka, B. 2007: Badenian evolution of the Central Paratethys Sea: paleogeography, climate and eustatic sea-level changes. Geologica Carpathica, 58/6: 579-606.

Kralj, P. 1996: Litofacialne značilnosti smrekovških vulkanoklastitov (severna Slovenija). Geologija, 39: 159–191. https://doi.org/10.5474/geologija.1996.007

Kralj, P. 2001: Pliocenski klastični sedimenti zahodnega dela Goričkega. Geologija, 44/1: 73–79. https://doi.org/10.5474/geologija.2001.004

Kralj, P. 2016a: Hydrothermal alteration of chlorite to randomly interstratified corrensite-chlorite: geological evidence from the Oligocene Smrekovec Volcanic Complex, Slovenia. Applied clay science, 134: 235-245. https://doi.org/10.1016/j.clay.2016.10.025

Kralj, P. 2016b: Hydrothermal zeolitisation controlled by host-rock lithofacies in the

Periadriatic (Oligocene) Smrekovec submarine composite stratovolcano, Slovenia. Journal of volcanology and geothermal research, 317: 53-65. https://doi.org/10.1016/j.jvolgeores.2016.02.009

Kralj, P., Vrabec, M., Trajanova, M., Ivančič, K. & Mencin Gale, E. 2018: Geološki razvoj kenozojskih sedimentacijskih bazenov v širši okolici Velenja. Vodič ekskurzij: Slovenski geološki kongres. Geološki zavod Slovenije. Ljubljana:

Kuščer, D. 1993: Neotektonika Krške kotline. Predhodno poročilo. Republika Slovenija, Ministrstvo za okolje in prostor, Republiška uprava za jedrsko varnost: 28 p.

Lewin, J. & Macklin. G. 2003: Preservation potential for Late Quaternary river alluvium. Journal of Quaternary Science, 18/2: 107-120. https://doi.org/10.1002/jqs.738

Lindsey, D. A., Langer, W. H. & van Gosen, B. S. 2007: Using pebble lithology and roundness to interpret gravel provenance in piedmont fluvial systems of the Rocky Mountains, USA. Sedimentary Geology, 199/3-4: 223-232. https://doi.org/10.1016/j.sedgeo.2007.02.006

Markič, M. 2009: Pliocen in pliokvartar. In: Pleničar, M., Ogorelec, B. & Novak, M. (eds.): Geologija Slovenije. Geološki zavod Slovenije, Ljubljana: 427-464.

Markič, M. & Rokavec, D. 2002: Geološka zgradba, nekovinske mineralne surovine in lignit okolice Globokega (Krška kotlina). RMZ - Materiali in geookolje: revija za rudarstvo, metalurgijo in geologijo, 49/2: 229-266.

Markič, M. & Sachenhofer, R. F. 2010: The Velenje lignite - Its petrology and genesis. Geološki zavod Slovenije, Ljubljana: 218 p.

Marton, E., Jelen, B., Tomljenivić, B., Pavelić, D., Poljak, M., Marton, P., Avanić, R. & Pamić, J. 2006: Late Neogene counterclockwise rotation in the SW part of the Pannonian Basin. Geologica Carpathica, 57/1: 41-46.

Miall, A. 2014: Fluvial depositional system. Springer, New York: 322 p.

Mioč, P. 1978: Tolmač za list Slovenj Gradec: L 33-55 SFRJ, osnovna geološka karta, 1: 100.000. Zvezni geološki zavod, Beograd.

Mioč, P. 1983: Tolmač za list Ravne na Koroškem: L 33-54 SFRJ, osnovna geološka karta, 1: 100.000. Zvezni geološki zavod, Beograd.

Mioč, P. & Žnidarčič, M. 1989: Tolmač za lista Maribor in Leibnitz: L 33-56, L 33-44 SFRJ 1: 100.000. Zvezni geološki zavod, Beograd.

Mioč, P. & Marković, S. 1998: Osnovna geološka karta republike Slovenije in Republike Hrvaške, list Čakovec, 1: 100.000. Inštitut za geologijo, geotehniko in geofiziko, Ljubljana in Inštitut za geološka istraživanja, Zagreb, Ljubljana.

Moro, A., Horvat, A., Tomić, V., Sremac, J. & Bermanec, V. 2016: Facies development and paleoecology of rudists and corals: an example of Campanian transgressive sediments from northern Croatia, northeastern Slovenia, and northwestern Bosnia. Facies, 62/3: 1-25. https://doi.org/10.1007/s10347-016-0471-y

Pamić, J. & Balen, D. 2001: Tertiary shoshonite volcanic associations from the adjoining area of the South Pannonian Basin and Dinarides. Acta vulcanologica: Journal of the National Volcanic Group of Italy, 13/1-2: 117-125. https://doi.org/10.1400/19069

Pavich, M. J. & Vidic, N. 1993: Application of Paleomagnetic and 10Be Analyses to chronostratigraphy of alpine glacio-fluvial terraces, Sava River valley, Slovenia. In: Swart, P. K., Lohmann, K. C., McKenzie, J., Savin, S. (eds.): Climate change in continental isotopic records (Geophysical monograph 78). American Geophysical Union, Washington: 263-275 p.

Placer, L. 1998: Strukturni pomen Posavskih gub. Geologija, 41: 191-221. https://doi.org/10.5474/geologija.1998.012

Placer, L. 1998: Prispevek k makrotektonski rajonizaciji mejnega ozemlja med Južnimi Alpami in Zunanjimi Dinaridi. Geologija, 41: 223-255. https://doi.org/10.5474/geologija.1998.013

Placer, L. 2008: Osnove tektonske razčlenitve Slovenije. Geologija, 51/2: 205-217. https://doi.org/10.5474/geologija.2008.021

Pleničar, M. & Ramovš, A. 1954: Geološko kartiranje severovzhodno od Brežic. Geologija, 2: 242-253.

Pleničar, M. 1993: Contribution to the nowledge of the Upper Cretaceous beds in Kočevje and Gorski Kotor area (NW Dinarides). Geologija, 36: 183-194. https://doi.org/10.5474/geologija.1994.008

Poljak, M. 2017: Geološka karta vzhodnega dela Krške kotline 1:25.000, tolmač. Geološki zavod Slovenije, Ljubljana.

Premru, U. 1983: Tolmač za list Ljubljana. Osnovna geološka karta SFRJ - 1: 100.000, L 33-66. Zvezni geološki zavod, Beograd.

Preusser, F., Grad, H. R., Keller, O., Krayss, E. & Schlüster, C. 2011: Quaternary glaciation history of northern Switzerland. Quaternary Science Journal, 2-3: 282-305. https://doi.org/10.3285/eg.60.2-3.06

Rakovec, I. 1968: O mastodontih iz Šaleške doline. Razprave, 11: 299-350.

Schmid, S. M., Bernoulli, D., Fugenschuh, B., Mantenco, L., Schefer, S., Schuster, R., Tischler, M. & Ustaszewski, K. 2008: The Alpine-Carpathian-Dinaridic orogenic system: correlation and evolution of tectonic units. Swiss Journal of Geosciences, 101/1: 139-183. https://doi.org/10.1007/s00015-008-1247-3

Šikić, K., Basch, O. & Šimunić, A., 1979: Tumač za list Zagreb. Osnovna geološka karta SFRJ 1:100.000, L 33-80. Zvezni geološki zavod, Beograd.

Štern, J. & Lapajne, V. 1974: Geološke raziskave gline in kremenovega peska v Globokem. Geologija, 17: 531-533.

Stokes, M., Cunha, P. P. & Martins, A. A. 2012: Techniques for analysing Late Cenozoic river terrace sequences. Geomorphology, 165-166: 1-6. https://doi.org/10.1016/j.geomorph.2012.03.022

Trajanova, M., Pecskay, Z. & Itaya, T. 2008: K-Ar geochronology and petrography of the Miocene Pohorje Mountains batholith (Slovenia). Geologica Carpathica, 59/3: 247-260.

Trajanova, M. 2013: Starost pohorskega magmatizma; nov pogled na nastanek pohorskega tektonskega bloka = Age of the Pohorje Mountains magmatism; new view on the origin of the Pohorje tectonic block. Doktorska disertacija, Univerza v Ljubljani: 183 p.

van Husen, D. & Reitner, J. 2011: An outline of the Quaternary Stratigraphy of Austria. Quaternary Science Journal, 2-3: 366-387. https://doi.org/10.3285/eg.60.2-3.09

Verbič, T. 2004: Quaternary Stratigraphy and Neotectonics of the eastern Krško Basin. Part 1: Stratigraphy. Classis IV: Historia Naturalis, 45/3: 171-225.

Verbič, T. 2008: Kvartarni sedimenti, stratigrafija in neotektonika vzhodnega dela Krške kotline. Doktorska disertacija. Univerza v Ljubljani: 140 p.

Vrabec, M., Janák, M., Froitzheim, N. & De Hoog, J. C. M. 2012: Phase relations during peak metamorphism and decompression of the UHP kyanite eclogites, Pohorje Mountains (Eastern Alps, Slovenia). Lithos, 144-145: 40-55. https://doi.org/10.1016/j.lithos.2012.04.004

Walden J. 2004: Particle lithology (or mineral and geochemical analysis). In: Evans, D. J. A. & Benn, D. I. (eds.): A practical guide to the study of glacial sediments. Hodder Education: 145-181.

Westaway, R. 2002: Long-term river terrace sequences: Evidence for global increases in surface uplift rates in the Late Pliocene and early Middle Pleistocene caused by flow in the lower continental crust induced by surface processes. Geologie En Mijnbouw/Netherlands Journal of Geosciences, 81/3-4: 305-328.

Žnidarčič, M. & Mioč, P. 1988: Osnovna geološka karta SFRJ. L 33-56 in L 33-44, Maribor in Leibnitz. Zvezni geološki zavod, Beograd.

Zupančič, N. 1994a: Geokemične značilnosti in nastanek pohorskih magmatskih kamnin. Rudarsko-metalurški zbornik, 41/1-2:113-128

Zupančič, N. 1994b: Petrografske značilnosti in klasifikacija pohorskih magmatskih kamnin. Rudarsko-metalurški zbornik, 41: 101-112.

GEOLOGIJA *62/2*, 219–236, Ljubljana 2019
https://doi.org/10.5474/geologija.2019.010

Multielemental composition of some Slovenian coals determined with k_0-INAA method and comparison with ICP-MS method

Multielementna sestava nekaterih slovenskih premogov določena s k_0-INAA metodo in primerjava z ICP-MS metodo

Tjaša KANDUČ[1*], Timotej VERBOVŠEK[2], Rok NOVAK[1] & Radojko JAĆIMOVIĆ[1]

[1]Department of Environmental Sciences, Jožef Stefan Institute, Jamova cesta 39, SI-1000 Ljubljana, Slovenia; e-mail: tjasa.kanduc@ijs.si
[2]Department of Geology, Faculty of Natural Science and Engineering, University of Ljubljana, Aškerčeva 12, 1000 Ljubljana, Slovenia

Prejeto / Received 4. 10. 2019; Sprejeto / Accepted 4. 12. 2019; Objavljeno na spletu / Published online 24. 12. 2019

Key words: k_0-instrumental neutron activation analysis (k_0-INAA), multielemental composition, coal, PCA analysis, Slovenia

Ključne besede: k_0-instrumentalna nevtronska aktivacijska anliza (k_0-INAA), multielementna sestava, premog, PCA analiza, Slovenija

Abstract

In this multi-elemental study, 34 elements (Ag, As, Au, Ba, Br, Ca, Cd, Ce, Co, Cr, Cs, Eu, Fe, Ga, Hg, Hf, K, La, Mo, Na, Nd, Rb, Sb, Sc, Se, Sm, Sr, Ta, Tb, Th, U, Yb, Zn and Zr) were analysed in Slovenian coals from operative (Velenje) and non-operative (Kanižarica and Senovo) coal mines and an imported Indonesia coal using k_0-Instrumental Neutron Activation Analysis (k_0-INAA) and compared to inductively coupled plasma-mass spectroscopy (ICP-MS). Weaker regressions between both methods ICP-MS and k_0-INAA are obtained for following elements: Cs, Co, Eu, Se, Sm and Tb with low concentration (below 1 mg/kg). The k_0-INAA data are comparable to the ICP-MS data for the majority of elements. The levels of major elements measured with k_0-INAA are as follows: Ca>Fe>K>Na>Sr>Ba. Minor and trace elements, as well as rare earth elements (REEs), are comparable with coal values worldwide. Data of trace elements in coal are important since they are related to air emissions. According to our data obtained with both methods (ICP-MS and k_0-INAA) we can conclude that concentrations of trace elements, which impact to human health and are combusted (Indonesian and Velenje coal) in Slovenia are comparable to world averages coal.

Izvleček

V tej raziskavi smo izmerili s k_0-INAA (instrumentalno nevtronsko aktivacijsko analizo) metodo nekaj izbranih slovenskih premogov iz velenjskega premogovnika in ne operativnih premogovnikov: Kanižarica in Senovo. Prav tako smo s to metodo analizirali vzorec iz Indonezije (uvožen premog) in ga primerjali z že objavljenimi rezultati pridobljenimi z ICP – MS (masna spektrometrija z induktivno sklopljeno plazmo) metodo. S k_0-INAA metodo smo določili naslednje elemente: Ag, As, Au, Ba, Br, Ca, Cd, Ce, Co, Cr, Cs, Eu, Fe, Ga, Hg, Hf, K, La, Mo, Na, Nd, Rb, Sb , Sc, Se, Sm, Sr, Ta, Tb, Th, U, Yb, Zn in Zr. Rezultati meritev pridobljeni s k_0-INAA metodo so za večino elementov, obravnavanih v tej raziskavi, primerljivi z rezultati meritev pridobljenih z ICP-MS metodo. Slabše regresije med metodami ICP-MS in k_0-INAA dobimo le pri nekaterih elementih (Cs, Co, Eu, Se, Sm and Tb) za katere so značilne nizke koncentracije (pod 1 mg/kg). Koncentracije glavnih elementov merjenih s k_0-INAA metodo v premogu se znižujejo kot sledi: Ca> Fe> K> Na> Sr> Ba. Elementi z nizkimi koncentracijami in elementi redkih zemelj (REE) so primerljivi z vrednostmi premoga po vsem svetu. Podatki slednih elementov v premogu so pomembni, ker so povezani z emisijami v zraku. Glede na naše podatke pridobljene z obema metodama (ICP-MS, k_0-INAA) lahko zaključimo, da so koncentracije slednih elementov, ki vplivajo na človekovo zdravje in jih sežigamo (premog iz Velenja in Indonezije) v Sloveniji primerljivi s povprečnimi vrednostmi svetovnih premogov.

Introduction

The chemical analysis of coal includes, as well as, proximate (Khandelwal and Singh, 2010, Yi et al., 2017) (moisture, volatile compounds, ash content, fixed carbon) and ultimate analyses (carbon, hydrogen, sulphur, oxygen, and nitrogen), the analysis of major, minor and trace elements. Usually, these elements are measured using inductively coupled plasma-mass spectrometry (ICP-MS) (Finkelman et al., 2018) and instrumental neutron activation analysis (k_0-INAA) (Wagner and Matiane, 2018, Lin et al., 2018) methods. Other methods for determining-trace elements include inductively coupled plasma optical emission spectrometry (ICP-OES) (Finkelman et al., 2018), hydride generation atomic absorption spectrometry (HAAS) (Chen et al., 2011) and X-Ray Fluorescence spectrometry (XRF) (Chen et al., 2011). It is widely known that these trace elements can occur in a wide variety of chemical forms or modes of occurrence, which determines the environmental, economic, technological impact, which in some cases can be significant (Finkelman, 1995, 2018). Twenty-five potential harmful trace elements (PHTEs) are typically present in coal in inorganic and organic forms (Radenovič, 2006). Among them As, Be, Cd, Cr, Co, Hg, Mn, Ni, Pb, Se, Sb and U are all potential air pollutants (Gürdal, 2008). Ketris and Yudovich (2009) include rare earth elements, yttrium, and scandium (REY + Sc) in the table of coal Clarke values, which has been a highly useful tool for making geochemical comparisons of coals globally.

Indonesian coals are generally low in ash and sulphur, but have high content of volatile matter. They are classified as low rank coals with low caloric value. The sulphur content varies from 0.1 to 1 % (Internet 1). Elemental composition (wt %, dry basis) of TOT S varied for Velenje samples from this study from 1.4 to 3.9 %, Kanižarica from 1.6 to 2.2 % and Senovo 1.9 % (Burnik Šturm et al., 2009).

The geological composition of the Velenje basin is described in detail in Brezigar et al. (1987). The origin of the Velenje basin is related to the transtention between Šoštanj and Smrekovec faults. In the pre-Pliocene basement of the basin, Triassic carbonates and dolomites prevail on the northeastern side of the Velenje fault, while Oligocene to Miocene clastic strata, consisting predominantly of marls, sandstones and volcanoclastics are dominant on the south-western side of the fault. The alkaline, calcium-rich environment during formation of Velenje basin also caused a relatively high degree of gelification, which is significantly higher than the degree of gelification observed in other lignites (Markič & Sachsehofer, 1997; Šlejkovec & Kanduč, 2005; Markič & Sachsehofer, 2010) as well as coals investigated in our study. A well known relation between alkalinity and gelification was clearly ascertained in the case of the Velenje lignite. Lignite samples with the highest calcium contents were also the samples with the strongest gelification (Markič & Sachsenhofer, 1997). The macroscopic description of the lignite samples, in term of lithotypes, was determined following the lithotype classification criteria for brown coals (lignites) provided by the International Committee for Coal Petrology (ICCP, 1993) and are described by Burnik Šturm et al. (2009). All of the samples from the Velenje excavation field -50/C in this study are classified as gelified detrital lignite (Kanduč et al., 2018). The lithological columns for Senovo, Kanižarica and Trbovlje are also presented in Burnik Šturm et al. (2009) and references therein (Brezigar, 1987; Kuščer, 1967; Markič et al., 1991). The macroscopic description of the lignite samples in terms of previous petrological (Markič & Sachsenhofer, 1997), geochemical and isotopic studies of light elements C, H, O, N, S (Bechtel et al., 2003; Kanduč et al, 2005; Burnik Šturm et al., 2009; Kanduč & Šlejkovec, 2005; Kanduč et al., 2012; Kanduč et al., 2018; 2019, Liu et al., 2019) were performed in the frame of various research projects. For example, three different lithotypes (xylitic, gelified and matrix) of Pliocene lignite for the Velenje basin, Slovenia, were investigated to establish the variations of biomarker compositions in solvent extracts and stable isotope composition of carbon and nitrogen in bulk material (Liu et al., 2019). All of these studies were focused on the Velenje basin since it is currently the only actively mined basin in Slovenia and is one of the biggest underground coal mines in Europe. All three of the Velenje lithotypes reflect the composition of the original plant material in the paleomire (Markič & Sachsenhofer, 1997). Arsenic speciation studies and the different forms of calcite present in the coal suggest that bacterial activity was a significant factor during sedimentation of the basin (Kanduč & Šlejkovec, 2005; Kanduč et al., 2018; Kanduč et al., 2019a). The analysis of other geological matrixes such as coalbed gas (Kanduč & Pezdič, 2005; Kanduč et al., 2012, Sedlar et al., 2014) and groundwater (Kanduč et al., 2014; Kanduč et al., 2019b) reveal more evidence of bacterial activity during sedimentation of the basin.

In the study of Kanduč et al. (2019a) organic and inorganic coal samples from -50/C excavation field of Velenje basin were measured using ICP-MS and revealed that the concentrations of the majority of the analysed elements were either equal to or below the global average for coal. Exceptions were Mo (7.76 ± 4.76 μg/g, 3.5 times higher) and U (5.24 ± 3.23 μg/g, 1.8 times higher) in organic-rich samples. It was found that higher than normal are concentrations of U (5-15 ppm – in comparison to 0.5-10 ppm concentrations in world coals), and of Mo (5-20 ppm – in comparison to 0.1-10 ppm in in world coals). Both elements are presumed to be organically bound (Markič & Sachsenhofer, 2010).

This study aims to present results of major, minor and trace elements measured using k_0-INAA method in coal samples collected from operative (Velenje) and non-operative (Kanižarica and Senovo) Slovenia coal mines. The study also analysed an Indonesia coal supplied by the thermal power plant Moste. Additionally, one of the objectives was to compare k_0-INAA and ICP-MS methods used to analyse the same coal samples (Kanduč et al., 2019a, Supplementary material) from Velenje coal mine and perform a statistical analysis (PCA-Principal Component Analysis) of all data (Velenje, Senovo, Kanižarica, Indonesia coals) measured with k_0-INAA method.

Methods

Sampling locations were taken from a local borehole database in the local coordinate system from the Velenje coal mine. Coordinates were then transformed to Gauss-Krüger D48 Slovenian national coordinate system and indicated on a hill-shaded relief map generated using the ESRI ArcGIS mapping software (Fig. 1). Figure 1A was produced using data from the Shuttle Radar Topography Mission SRTM data at 90 m spatial resolution. A more detailed map (Fig. 1B), was created using the digital elevation model at a 1 × 1 m spatial resolution, using LiDAR data form the national scanning campaign of the Slovenian territory (ARSO, 2014). Figure 1C includes the position of excavation field (-50/C) and cross-section of Velenje basin with main geological and tectonic units.

Samples of coal were collected from the following mining areas in Slovenia (Fig. 1): Senovo (3 samples), Kanižarica (4 samples), Velenje basin (7 delivery roadway samples, and 18 samples from excavation field -50/C), Indonesia (1 sample) in years 2004, 2005 and 2013. The Moste thermal power plant provided the sample of Indonesian coal.

For k_0-INAA analysis, samples (240-290 mg) were sealed in a pure polyethylene ampoule (SPRONK system, Lexmond, The Netherlands). For the determination of long-lived radionuclides, samples and standards (Al-0.1 %Au IRMM-530R disc of 7 mm in diameter and 0.1 mm thick) were stacked together and fixed in a polyethylene ampoule in sandwich form and irradiated for 12 hours in the carousel facility (CF) of a 250 kW TRIGA Mark II reactor (Jožef Stefan Institute, JSI) at a thermal neutron flux of 1.1×E+12 cm^{-2} s^{-1}.

Each sample was measured three times after 2, 8-13 and 25-30 days cooling time on three absolutely calibrated HPGe detectors with 40 % and 45 % relative efficiency. Measurements were carried out at a distance such that the dead time remained below 10 % with negligible random coincidences. The detectors with 40 % relative efficiency were connected to a MULTIPORT II (Canberra) computerized multichannel analyser (MCA) in LT mode operating with Genie™ 2000 spectroscopy software, while the detector with 45 % relative efficiency was connected to a DSPEC PLUS (Ortec) multichannel analyser in ZDT mode operating with Maestro®-32 spectroscopy software.

The HyperLab (2002) program was used for peak area evaluation, whereas for the determination of f (thermal to epithermal flux ratio) and α (a parameter which represents the epithermal flux deviation from the ideal 1/E distribution) the "Cd-ratio" method for multi-monitor was applied (Jaćimović et al., 2003). The values obtained for f = 28.63 and α = -0.0011 were used to calculate the element concentrations. The elemental concentrations and effective solid angle calculations were performed using the KayWin® (Kayzero for Windows, 2011) software package.

Ranges of uncertainties with coverage factor k = 1 (%) for measured elements with k_0-INAA method is as follows: i) uncertainty for elements: As, Br, Ca, Ce, Cs, Fe, Na, Sc, U, and Zn ranges from 3.5 to 7.3 % and ii) uncertainty for elements: Au, Ba, Co, Cr, Eu, Ga, Hf, Hg, K, La, Mo, Nd, Rb Sb, Se, Sm, Sr, Ta, Tb, Th, Yb, ranges from 3.5 to 28 %. Measured elements with higher concentration have lower uncertainties, while elements with lower concentration have higher uncertainties.

Chemical analysis of Velenje coal samples (13-2123, 13-2125, 13-2130, 13-2134, 13-2138, 13-2141, 13-2145, 13-2157, 13-2162) were performed with ICP – MS method in ACME lab Canada (http://acmelab.com/services/). For the analysis of SiO_2, Al_2O_3, Fe_2O_3, CaO, MgO, Na_2O, K_2O, MnO, TiO_2,

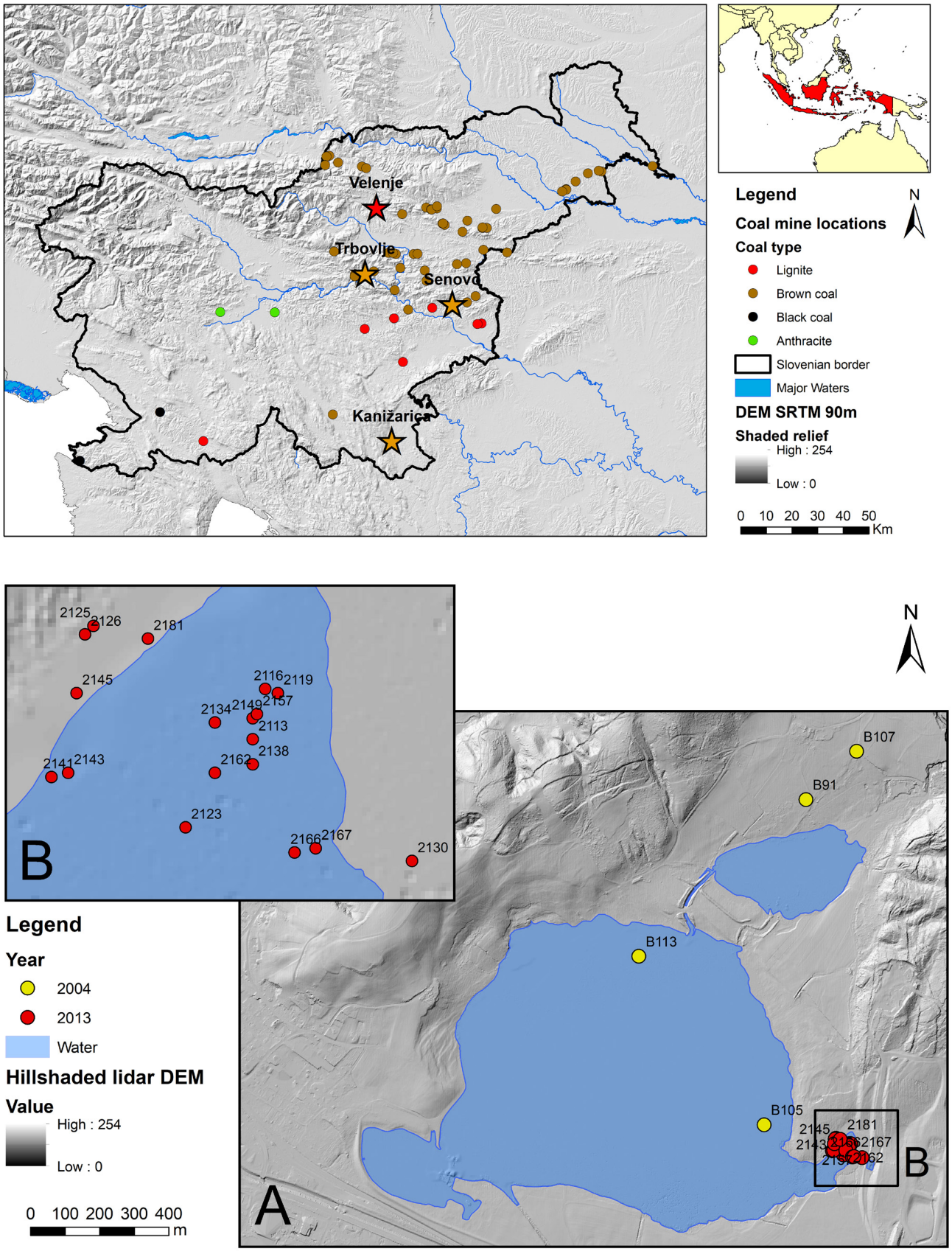

Fig. 1. General map of coals located in Slovenia showing the study area of sampled coals from Slovenia mines: Velenje Coal Basin (active coal mine, n = 25), Kanižarica (closed, n = 4), Senovo (closed, n = 3), and Indonesia (coal imported in Slovenia, n = 1). Velenje sampling locations from years 2004, n = 4 (B91, B105, B107, B113) and 2013, n = 18 (2113, 2116, 2119, 2123, 2125, 2126, 2130, 2134, 2138, 2141, 2143, 2145, 2149, 2157, 2162, 2166, 2167, 2181). B. Detailed map of Velenje sampling locations from years 2004 and 2013 are presented. C. Position of excavation field -50/C from where samples were taken and cross-section of the central part of the Velenje basin (modified from Brezigar, 1987) with main geological and tectonic units.

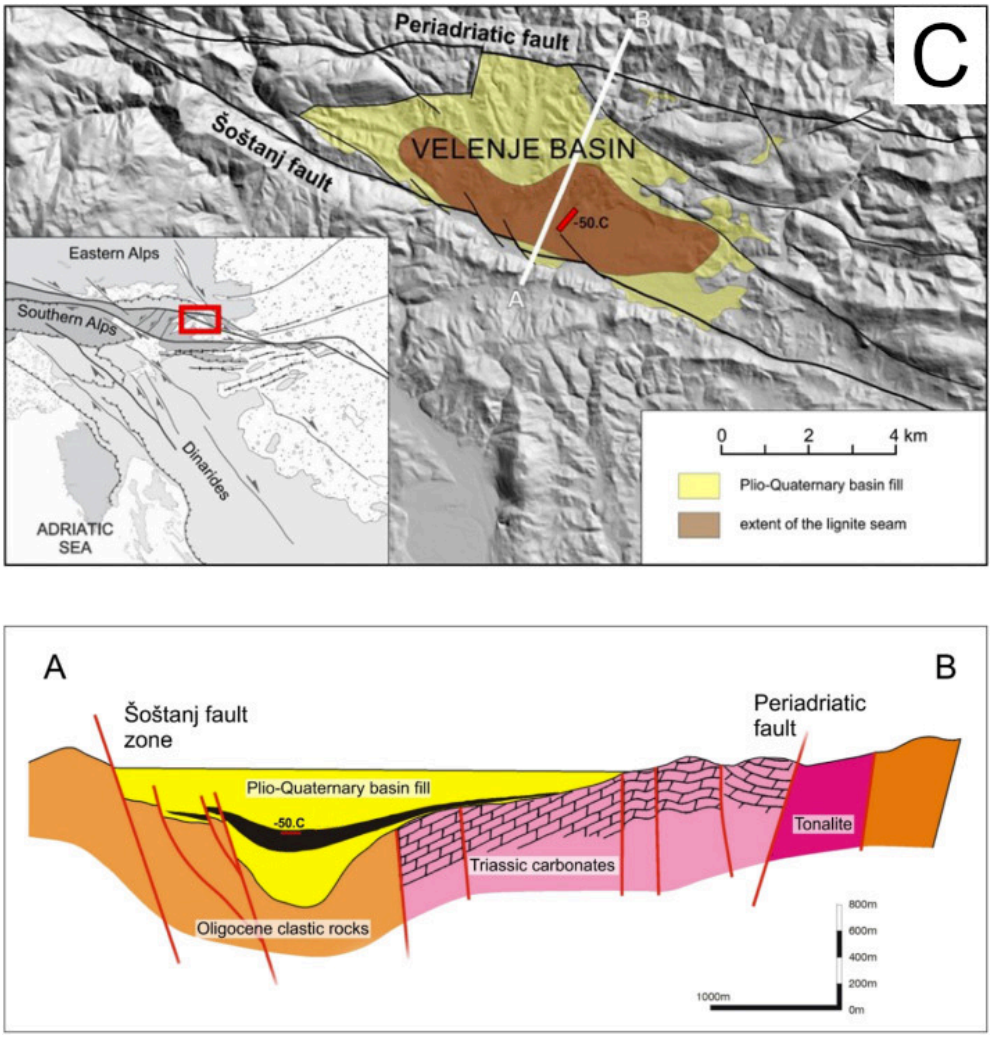

Fig. 1.

P_2O_5, Cr_2O_3, Ce, Co, Cu, and Zn samples were mixed with a $LiBO_2/Li_2B_4O_7$ flux. Crucibles were fused in a furnace. The cooled beads were dissolved in ACS grade nitric acid and analyzed by ICP and or ICP-MS.

Other elements (Ce, Co, Cs, Dy, Er, Eu, Gd, La, Ni, Nb, Nd, Pr, Rb, Sm, Sr, Tb, U, Th, V, Zr, Y) were measured with ICP-MS method. Total carbon (TOT C) and total sulphur (TOT S) were measured using LECO Carbon –Sulphur analyzer. The mean limits of detection for both elements were 0.02 %. Loss on ignition (LOI) was determined by igniting a sample split and then measuring the weight loss.

For Ag, As, Au, Bi, Cd, Hg, Mo, Ni, Pb, Sb, Se, Tl, and Zn analysis, prepared samples were digested with modified Aqua Regia solution of equal parts of concentrated HCl, HNO_3 and MiliQ H_2O for 1 h in a heating block or in a hot water bath at 95°C. Samples were made up to volume witgh diluted HCl. Sample splits of 0.5 g were analyzed optional 15 g or 30 g digestion available for AQ200. Samples were analyzed using inductively coupled-mass spectrometry (ICP-MS). The following standards were used for quality assurance: STD-SO-18, STD-GGC-02, STD-GS311-1 and STD OREAS45EA.

Statistical analysis was conducted using the R language (R Core Team, 2019), and the significance model was set at $p<0.05$. A Spearman's correlation analysis was used to identify the relationships between 27 elements (As, Ba, Br, Ca, Ce, Co, Cr, Cs, Eu, Fe, Hf, K, La, Mo, Na, Nd, Rb, Sb, Sc, Se, Sm, Sr, Tb, Th, U, Yb and Zn) with complete data sets. The crossed-out values indicate where p-values exceeded 0.05.

Principal component analysis (PCA) was used to differentiate (same as for Spearman correlation analyses) between the coal from the different mines. Due to the broad range of elemental concentrations, the dataset was central log-ratio transformed. Studied mines were grouped as "Open" and "Closed". The principle component plots were made using ggplot2 in R (Wickham, 2016).

Results and discussion

Tables 1 and 2 give the results of the k_0-INAA of 34 elements (As, Ba, Br, Ca, Ce, Co, Cr, Cs, Eu, Fe, Hf, K, La, Mo, Na, Nd, Rb, Sb, Sc, Se, Sm, Sr, Tb, Th, U, Yb, Zn) for Velenje, Senovo, and Kanižarica mines and for an imported Indonesian coal. In a previous study by Kanduč et al. (2019a), ten oxides (SiO_2, Al_2O_3, Fe_2O_3, MgO, CaO, Na_2O, K_2O, TiO_2, P_2O_5, MnO, Cr_2O_3), LOI (Loss on ignition), TOT C (Total carbon), TOT S (Total sulphur) (Kanduč et al., 2019a), along the following toxicologically and environmentally relevant elements: As, Ba, Ce, Co, Cs, Cu, Dy, Er, Eu, Gd, Hf, La, Mo, Nb, Nd, Ni, Pb, Pr, Rb, Se, Sm, Sr, Tb, Th, U, V, Y, Zn, Zr were measured in the organic-rich component of the Velenje samples. In this study, nine samples from the Velenje coal mine (13-2123, 13-2125, 13-2130, 13-2134, 13-2138, 13-2141, 13-2145, 13-2157, 13-2162), were measured using ICP-MS and k_0-INAA, while all other samples in this study were measured using only k_0-INAA. For studying elemental composition of coal with k_0-INAA method we choose only Velenje samples (from year 2013) that were organic rich, besides Kanižarica, Senovo and Indonesia coal samples that were sampled in years 2004 and 2005.

Results of ICP – MS of major elements, LOI, TOT C, TOT S in coal samples (13-2123, 13-2125, 13-2130, 13-2134, 13-2138, 13-2141, 13-2145, 13-2157, 13-2162) collected from excavation field -50/C of Velenje basin are presented in Table 3a. Results of ICP – MS of trace elements in coal samples (13-2123, 13-2125, 13-2130, 13-2134, 13-2138, 13-2141, 13-2145, 13-2157, 13-2162) collected from excavation field -50/C of Velenje basin are presented in Table 3b. Data (REEs) for coals from other locations (two power plants: Jungar (China), Tutuka (SA), Matla (SA), and the Witbank Coalfield (SA) are included for comparison purposes (Table 4).

For quality assurance and quality control (QA/QC), in the study we used the certified reference material BCR-180 Gas Coal (Fig. 2). The results obtained by k_0-INAA are in good agreement with the certified data for As, Hg, Se and Zn. It should be mentioned that expanded uncertainty (k=2) of mass fraction of Hg obtained via Hg-203 at 279.2 keV is relatively high in comparison with certified value due to correction from the mass fraction of Se via Se-75 at 279.5 keV, which was about 70 % (Fig. 2).

Among the major elements, Ca prevails. Major oxides (CaO, Na_2O, K_2O, TiO_2) and ultimate analysis (LOI, TOT C, TOT S) of the coal samples (13-2123, 13-2125, 13-2130, 13-2134, 13-2138, 13-2141, 13-2145, 13-2157, 13-2162) range as follows (Table 3 a): CaO from 1.91-5.21 %, Na_2O ranges from 0.04 to 0.13 %, K_2O ranges from 0.007-0.08 %, TiO_2 ranges from 0.07 to 0.08 %, TOT C ranges from 50.6 to 57.1 %, TOT S ranges from 1.17 to 2.46 %, and LOI (Loss on ignition) ranges from 86.7 to 97.1 % (Kanduč et al., 2019a). Figure 3 represents the major oxides (MgO+CaO, Na_2O+K_2O, $SiO_2+Al_2O_3+Fe_2O_3$) present in samples of lignite. The data were obtained from the study by Kanduč et al. (2019a) and are presented in Table 3a. The major oxides in the Velenje coal samples are CaO and MgO, suggesting that lignite was formed in a Ca-alkaline rich environment (Markič and Sachsenhofer, 1997). The most prevalent oxide is CaO (from 1.91 to 5.21 %). The concentration of oxides from the Velenje samples decrease in the following order: $CaO>Fe_2O_3>Al_2O_3>SiO_2>MgO>Na_2O>K_2O>TiO_2$. Only two Velenje coal samples (13-2134, 13-2145) have CaO + MgO concentrations less than 70 % (Fig. 3).

Figure 4 A-C shows plots of the major (Ba, Ca, Fe, K, Sr), minor (As, Br, Ce, Co, Cr, La, Mo, Nd, Rb, Sc, U, Zn) and trace element levels (Cs, Eu, Hg, Sb, Se, Sm, Ta, Tb, Th, Yb) for each of the coal mine samples (Senovo, Kanižarica, Indonesia, Velenje). From Figure 4A it can be observed that among major elements Ca prevailed for Velenje coal mine samples, while in one sample of Senovo (Senovo 3) and Kanižarica (Kanižarica 15) Fe prevails. Some samples from Velenje mine (13-2166, 13-2167, 13-2181), from excavation field -50/C have high concentrations of Ca in the range from 163700 to 307100 mg/kg (Fig. 4 A), which is in compliance with thesis of Ca-rich environment during sedimentation of Velenje basin. Among minor elements there are huge differences between coal samples between mines. The highest concentration of As, Br, Ce, Cr are observed in Kanižarica coal samples (Kanižarica 6, Kanižarica 15). Cr and Mo prevail in Velenje coal samples, while Br and Cr prevail in Senovo coal samples (Fig. 4 B). Kanižarica coal samples have also the highest concentration of rare elements (Cs, Eu, Hf, Ta, Th, Se, Sm) (Fig. 4 C). Sm and Th are enriched in three Velenje samples (B91, B105, 13-2149) (Fig. 4 C). Among all minor and trace elements Kanižarica coal samples have the highest concentrations (Figs. 4 B, C).

Figure 5 presents box-plots of the k_0-INAA data for all coal samples. From the box-plots it appears that the abundances of Ca>Fe>K>Na>Sr>Ba prevail among major elements and Mo>Zn>U>Cr>As>Br in the case of mi-

Table 1. Elements (Ag, As, Au, Ba, Br, Ca, Cd, Ce, Co, Cr, Cs, Eu, Fe, Ga, Hf, Hg, K, La, Mo, Na, Nd, Rb, Sb, Sc, Se, Sm, Sr, Ta, Tb, Th, U, Yb, Zn, Zr) measured with k_0-INAA method in following coal samples: Senovo (Sen., n = 3), Indonesia (Indon., n = 1), Kanižarica (Kan., n = 4), Velenje (Vel., n = 7), sampled in years 2004 and 2005.

Code	B91 Vel.	B105 Vel.	B106 Vel.	B106 Vel.	B113 Vel.	B113 Vel.	j.v. 3123 (1,8) Vel.	Sen.1	Sen.2	Sen.3	Indon.	Kan.6	Kan.9	Kan.19	Kan.15
Element	**mg/kg**	**mg/kg**	**mg/kg**	**mg/kg**	**mg/kg**	**mg/kg**	**mg/kg**	**mg/kg**	**mg/kg**	**mg/kg**	**mg/kg**	**mg/kg**	**mg/kg**	**mg/kg**	**mg/kg**
Ag	<LD	<LD	<LD	<LD	<LD	<LD	<LD	<LD	<LD	<LD	<LD	<LD	<LD	<LD	<LD
As	5.77	5.15	1.59	0.07	2.36	0.09	14.3	7.98	2.98	7.46	1.08	8.98	5.75	3.98	8.88
Au	<LD	<LD	0.0044	0.0002	0.0007	0.0001	<LD	0.0042	<LD	<LD	<LD	<LD	<LD	<LD	<LD
Ba	<LD	37.6	4.85	0.79	52.8	2.0	106	100	158	36.3	37.5	38.4	31.5	39.7	142
Br	8.71	5.92	1.77	0.07	5.76	0.21	4.02	1.08	1.43	0.12	1.95	1.90	2.05	7.56	2.02
Ca	16032	13401	3321	126	16854	592	10686	8812	9955	4436	1740	9576	15839	28496	8523
Cd	<LD	<LD	<LD	0.3	<LD	0.35	<LD	<LD	<LD	<LD	<LD	<LD	<LD	<LD	<LD
Ce	12.0	10.4	0.64	0.03	1.84	0.07	3.55	1.37	2.69	0.73	2.62	20.1	2.42	1.35	56.6
Co	1.28	2.05	0.24	0.01	0.21	0.01	0.71	7.82	0.54	0.22	1.88	10.7	3.02	0.54	16.1
Cr	12.3	16.3	6.81	0.39	2.54	0.19	2.75	22.6	26.3	7.26	10.1	86.0	24.5	44.9	222
Cs	1.37	2.89	0.42	0.02	0.237	0.010	0.55	0.34	0.27	<LD	0.24	3.78	0.76	0.55	13.7
Eu	0.34	0.23	<LD	0.004	0.059	0.010	0.13	0.102	0.199	0.111	0.056	0.67	0.096	0.072	1.21
Fe	9054	12501	896	32	3032	106	5199	5889	8321	119325	8631	16044	5173	6700	22968
Ga	2.70	5.64	<LD	0.07	<LD	0.05	<LD	2.05	2.25	<LD	0.78	7.33	1.67	1.79	18.3
Hf	0.24	0.44	0.038	0.003	0.075	0.005	0.099	0.102	0.196	<LD	0.133	1.28	0.178	0.154	3.08
Hg	0.39	0.17	0.27	0.02	0.064	0.009	0.104	0.22	0.08	0.11	0.03	<LD	<LD	<LD	<LD
K	1343	2874	225	23	270	27	331	244	466	65.0	216	2097	244	277	9099
La	5.58	5.94	0.31	0.02	0.89	0.05	1.41	0.75	1.66	0.43	1.27	11.8	2.46	1.60	31.2
Mo	9.53	11.1	0.53	0.05	9.11	0.33	23.7	6.78	4.05	0.19	0.06	39.0	34.2	17.1	28.8
Na	572	1625	354	12	742	26	706	282	90.6	47.0	55.9	207	104	275	533
Nd	5.59	5.27	<LD	0.20	0.73	0.18	1.83	1.77	3.46	1.17	1.60	9.79	1.46	<LD	25.5
Rb	8.98	22.5	1.64	0.15	1.57	0.14	3.11	2.00	3.37	<LD	2.10	29.6	3.76	3.51	105
Sb	0.75	1.18	0.085	0.006	0.34	0.01	1.58	0.64	0.32	0.83	0.042	1.70	0.70	0.36	1.55
Sc	1.43	3.09	0.202	0.007	0.64	0.02	0.93	1.37	2.53	0.82	0.56	8.34	1.01	0.67	15.4
Se	1.11	0.46	0.14	0.03	0.19	0.02	0.83	1.36	0.62	4.52	0.15	10.8	5.99	10.4	17.1
Sm	1.39	0.98	0.071	0.003	0.204	0.007	0.49	0.47	0.84	0.38	0.25	2.75	0.42	0.28	2.52
Sr	52.7	36.5	7.23	1.88	43.7	2.6	25.2	128	188	41.9	10.8	64.7	70.6	137	199
Ta	0.091	0.166	<LD	0.013	0.029	0.003	0.030	<LD	0.029	<LD	0.020	0.28	0.049	0.044	0.88
Tb	0.146	0.134	0.009	0.002	0.028	0.002	0.075	0.070	0.130	0.082	0.032	0.416	0.062	0.050	0.71
Th	4.46	2.40	0.15	0.01	0.356	0.014	0.49	0.85	1.17	<LD	0.35	3.79	0.58	0.51	9.79
U	63.4	7.87	0.67	0.03	2.38	0.08	8.23	4.38	4.23	0.25	0.15	65.9	43.7	50.7	36.4
Yb	0.28	0.47	0.031	0.003	0.096	0.004	0.213	0.201	0.405	0.274	0.099	1.48	0.206	0.137	2.56
Zn	72.4	18.7	5.75	0.33	3.64	0.24	21.1	26.8	7.58	4.27	13.8	46.4	11.2	5.99	126
Zr	<LD	<LD	<LD	7	<LD	27	<LD	4.41	8.59	<LD	<LD	41.0	<LD	<LD	134

<LD – values lower than detection limit

Table 2. Elements (Ag, As, Au, Ba, Br, Ca, Cd, Ce, Co, Cr, Cs, Eu, Fe, Ga, Hf, Hg, K, La, Mo, Na, Nd, Rb, Sb, Sc, Se, Sm, Sr, Ta, Tb, Th, U, Yb, Zn, and Zr) measured with k_0-INAA method in following coal samples: Velenje (n = 18), excavation field -50/C, sampled in year 2013.

Code	13-2113	13-2116	13-2119	13-2123*	13-2125*	13-2126	13-2130*	13-2134*	13-2138*	13-2141*	13-2143	13-2145*	13-2149	13-2157*	13-2162*	13-166	13-2167	13-2181
Element	**mg/kg**	**mg/kg**	**mg/kg**	**mg/kg**	**mg/kg**	**mg/kg**	**mg/kg**	**mg/kg**	**mg/kg**	**mg/kg**	**mg/kg**	**mg/kg**	**mg/kg**	**mg/kg**	**mg/kg**	**mg/kg**	**mg/kg**	**mg/kg**
Ag	<LD	<LD	<LD	<LD	<LD	0.5	<LD	<LD	<LD	<LD	<LD	<LD	<LD	<LD	<LD	<LD	<LD	<LD
As	1.26	1.88	3.17	1.88	1.69	1.87	5.26	2.43	2.66	1.55	1.48	0.72	2.88	1.29	1.83	0.21	0.81	1.11
Au	<LD	<LD	<LD	<LD	<LD	0.00051	<LD	<LD	<LD	<LD	0.00029	0.00046	<LD	0.0005	0.0005	<LD	<LD	<LD
Ba	41.7	343.0	13.1	23.7	37.7	12.7	27.1	14.5	93.9	73	28.4	2.8	15.3	95.5	48.3	147	238	127
Br	6.58	6.07	6.69	6.60	7.57	8.75	5.65	8.73	5.81	7.02	6.92	2.41	1.95	6.03	6.8	0.59	2.02	2.93
Ca	16580	41280	20790	18460	20780	12950	30110	16370	28760	17170	13930	10920	129300	15220	31320	307100	246900	163700
Cd	<LD	<LD	<LD	<LD	<LD	<LD	<LD	<LD	<LD	<LD	<LD	<LD	<LD	<LD	<LD	<LD	<LD	<LD
Ce	1.11	1.50	0.92	0.61	1.88	1.16	1.62	2.43	1.28	1.14	2.39	0.74	5.64	0.32	1.88	3.87	1.28	1.06
Co	0.26	0.23	0.49	0.29	0.35	0.36	0.411	0.554	0.287	0.301	0.321	0.022	0.407	0.242	0.186	0.016	0.12	0.082
Cr	2.32	1.13	2.26	1.74	2.95	2.52	4.76	5.94	2.39	1.54	4.1	<LD	4.09	1.32	1.54	0.26	1.26	0.7
Cs	0.11	0.04	0.08	0.07	0.22	0.17	0.21	0.626	0.161	0.046	0.54	<LD	0.26	0.045	0.121	<LD	0.122	0.046
Eu	0.02	0.04	0.03	0.02	0.05	0.029	0.051	0.049	0.035	0.043	0.059	0.028	0.787	0.014	0.047	0.093	0.093	0.039
Fe	1590	2039	2390	1438	2165	2326	5868	5035	3565	908	1279	153	4827	2216	2826	198	1474	1289
Ga	<LD	<LD	<LD	<LD	<LD	<LD	<LD	1.42	<LD	<LD	0.96	<LD	1.1	<LD	<LD	<LD	<LD	<LD
Hf	0.07	0.03	0.05	0.04	0.07	0.051	0.081	0.125	0.054	0.032	0.079	<LD	0.066	0.037	0.052	<LD	0.028	0.017
Hg	<LD	<LD	<LD	<LD	<LD	<LD	<LD	<LD	<LD	<LD	<LD	<LD	<LD	<LD	<LD	<LD	<LD	<LD
K	197	95.20	147	146	237	304	342	687	238	119	565	18.4	232	93.9	141	15.9	124	<LD
La	0.65	0.88	0.58	0.36	1.10	0.671	0.99	1.41	0.756	0.637	1.18	0.262	1.14	<LD	0.94	1.93	0.8	0.579
Mo	6.9	11.10	8.9	5.4	11.1	13.8	7.84	25.8	21.7	8.88	9.51	2.06	4.19	11.6	15.9	<LD	5.2	3.87
Na	762	675.00	1058	874	611	739	1073	798	813	688	923	364	787	712	847	232	606	398
Nd	0.52	1.09	0.34	0.36	0.62	0.49	0.8	0.94	0.52	0.59	1.45	0.45	8.07	0.31	0.88	1.96	0.58	0.59
Rb	1.28	0.41	1.11	0.85	1.80	1.85	2.31	7.15	1.86	0.9	4.52	<LD	1.96	0.59	1.03	<LD	0.95	<LD
Sb	0.19	0.22	0.21	0.23	0.31	0.365	0.394	0.614	0.37	0.221	0.253	0.01	0.87	0.228	0.259	0.009	0.096	0.083
Sc	0.34	0.21	0.28	0.26	0.39	0.341	0.522	0.97	0.31	0.313	0.682	0.029	3.98	0.28	0.279	0.036	0.205	0.418
Se	0.25	0.22	0.43	0.31	0.16	0.37	0.53	0.36	0.32	0.26	0.75	<LD	<LD	0.21	0.29	<LD	0.149	0.071
Sm	0.08	0.25	0.10	0.06	0.27	0.132	0.574	0.319	0.08	0.158	0.239	0.108	3.3	0.245	0.295	0.417	0.297	0.216
Sr	23.80	147.00	32.0	24.20	63.70	14.6	62	18.9	80.8	43.3	14.2	<LD	33.4	18.9	87.9	817	1010	540
Ta	0.01	<LD	0.02	0.02	0.02	0.016	0.031	0.036	0.017	<LD	0.033	<LD	0.04	<LD	<LD	<LD	<LD	<LD
Tb	0.02	0.02	0.01	0.01	0.02	0.017	0.026	0.036	0.018	0.026	0.03	0.013	0.509	0.012	0.021	0.038	0.042	0.02
Th	0.24	0.13	0.22	0.17	0.35	0.272	0.339	0.714	0.27	0.169	0.579	0.013	0.712	0.169	0.199	0.041	0.182	0.063
U	4.68	6.38	3.50	1.81	5.15	4.99	12.9	8.65	6.19	4.73	3.05	0.092	6.2	8.72	5.23	0.85	1.97	2.85
Yb	0.05	0.03	0.04	0.03	0.06	0.059	0.076	0.123	0.053	0.049	0.094	0.015	1.28	0.045	0.051	0.045	0.04	0.041
Zn	6.89	8.91	4.82	2.59	2.53	12.3	22.4	8.99	10.4	4.05	20.6	4.2	20.1	22	9.55	1.01	9.31	2.75
Zr	<LD	<LD	<LD	<LD	<LD	<LD	<LD	<LD	<LD	<LD	<LD	<LD	<LD	<LD	<LD	<LD	<LD	<LD

*Samples measured with ICP – MS method
<LD – values lower than detection limit

Table 3a. Results of ICP – MS of major elements, LOI, TOT C, TOT S in coal samples (Kanduč et al., 2019a, Supplementary material) for samples (13-2123, 13-2125, 13-2130, 13-2134, 13-2138, 13-2141, 13-2145, 13-2157, 13-2162) collected from excavation field -50/C from Velenje basin.

Sample ID	SiO_2 (%)	Al_2O_3 (%)	Fe_2O_3 (%)	MgO (%)	CaO (%)	Na_2O (%)	K_2O (%)	TiO_2 (%)	P_2O_5 (%)	MnO (%)	LOI (%)	TOT C (%)	TOT S (%)
13-2123	0.48	0.29	0.23	0.34	2.99	0.11	0.01	0.007	0.01	0.02	93.1	55.7	1.89
13-2125	0.52	0.43	0.29	0.46	3.19	0.08	0.01	0.01	0.01	0.01	92.7	53	1.59
13-2130	1.3	0.9	1.41	0.33	5.14	0.13	0.07	0.03	0.02	0.02	86.7	50.8	2.46
13-2134	1.22	0.99	0.83	0.45	2.32	0.1	0.08	0.08	0.02	0.02	91.6	53.1	2.28
13-2138	0.38	0.32	0.52	0.33	4.98	0.1	0.02	0.007	0.01	0.05	88.8	52.9	2.1
13-2141	0.22	0.21	0.08	0.3	3.05	0.09	0.007	0.007	0.01	0.01	93.6	57.1	1.81
13-2145	0.02	0.01	0.028	0.07	1.91	0.04	0.007	0.007	0.007	0.007	97.1	50.6	1.17
13-2157	0.23	0.2	0.34	0.37	2.36	0.09	0.007	0.007	0.02	0.02	93.5	55.2	1.86
13-2162	0.25	0.21	0.36	0.35	5.21	0.1	0.07	0.07	0.04	0.04	87.6	51.6	2.16

Table 3b. Results of ICP – MS of trace elements in coal samples (Kanduč et al., 2019a, Supplementary material) for samples (13-2123, 13-2125, 13-2130, 13-2134, 13-2138, 13-2141, 13-2145, 13-2157, 13-2162) collected from excavation field -50/C from Velenje basin.

Sample ID	As	Hg	Mo	U	Th	Zn	Ba	Co	Se	Ce	Cs	Eu	La	Nd	Rb	Sm	Sr	Tb
Units	mg/kg	mg/kg	mg/kg	mg/kg	mg/kg	mg/kg	mg/kg	mg/kg	mg/kg	mg/kg	mg/kg	mg/kg	mg/kg	mg/kg	mg/kg	mg/kg	mg/kg	mg/kg
13-2123	1.3	0.01	3.9	2	0.2	4	23	0.14	0.35	0.7	0.2	0.014	0.7	0.21	0.7	0.035	29	0.007
13-2125	1	0.03	6.7	5.7	0.3	3	43	0.5	0.35	2.1	0.2	0.03	1.4	0.8	1.3	0.2	71.8	0.02
13-2130	4.9	0.04	6.1	13.9	0.6	19	35	0.9	0.8	4.5	0.3	0.09	2.7	1.6	4.7	0.25	87.1	0.04
13-2134	2	0.06	22.6	8.1	0.6	14	19	0.4	0.7	3	0.6	0.05	1.7	1.5	6.7	0.18	20	0.04
13-2138	1.5	0.03	12.7	6.7	0.4	11	121	0.5	0.35	1.3	0.1	0.03	1.2	0.5	1.5	0.035	108.5	0.02
13-2141	1.3	0.02	6.1	4.5	0.14	13	97	0.4	0.7	1.8	0.07	0.04	1.1	0.6	0.4	0.035	60.2	0.03
13-2145	0.5	0.007	1.8	0.07	0.14	2	7	0.14	0.35	0.8	0.07	0.014	0.07	0.41	0.007	0.08	4.4	0.02
13-2157	0.8	0.04	9.2	7.8	0.3	20	99	0.14	0.35	1.1	0.07	0.014	0.7	0.021	0.4	0.035	20.4	0.02
13-2162	1.6	0.03	10.6	4.4	0.3	10	58	0.2	0.35	2.8	0.1	0.02	1.4	1.1	0.5	0.035	108.6	0.02

Table 4. Concentration of REEs (Rare Earth Elements) with Coal Clarke values and coals combusted in a thermal power plant ((Jungar power plant, Tutuka power plant (coal, ash), Matla power station)) and Witbank coalfield. Also ranges and averages of Velenje, Kanižarica, Senovo and Indonesia coal samples are presented for comparison.

	REE (mg/kg)													
	Coal Clarke valuesb		**Jungar Power Plant, Chinac**			**Tutuka Power Station SAd**		**Matla Power Station SAe**	**Witbank Coalfield, SAf**	**Velenje (range and average, n = 18) g, measured with ICP-MS method**	**Vel. k_0-INAA (n = 25, ave.)**	**Kan., k_0-INAA (n = 4)**	**Sen., k_0-INAA method (n = 3)**	**Indo., k_0-INAA method (n = 1)**
	Hard coal	**Hard coal ash**	**Coal**	**Fly ash (Economizer)**	**Fly ash (Wet)**	**Coal**	**Ash**	**Fly ash**	**Coal (No. 2 Seam)**					
La	11±1	76±3	41.2	85.4	104.3	39.9	91.4	81.55	9.72–34.16	<0.1–4.1 (1.60±0.90)	1.20	11.78	0.95	1.27
Ce	23±1	140±10	71.8	141	178	91.6	182.4	189.78		0.7–9.5 (2.73±1.99)	2.33	20.11	1.6	2.62
Pr	3.4±2	26±3	8.1	17.3	21.5	9.5	19.7	18.35		0.05–1.29 (0.30±0.29)				
Nd	12±1	75±4	27.6	58.5	72.5	30.8	81.8	63.5		<0.3–6.1 (2.21±1.34)	1.41	12.26	2.13	1.6
Sm	2.2±0.1	14±1	5.2	10.6	13.5	5.3	14.4	11.93	1.94–5.27	<0.05–1.42 (0.20±0.31)	0.41	0.56	1.49	0.25
Eu	0.43±0.02	2.6±0.1	0.9	1.8	2.4	0.9	2.7	2.35	0.26–0.77	<0.02–0.31 (0.05±0.06)	0.09	0.51	0.14	0.06
Gd	2.7±0.2	16±1	4.7	9.1	11.7	4.2	12.6	10.4		0.06–1.00 (0.22±0.20)				
Tb	0.31±0.02	2.1±0.1	0.7	1.4	1.8	0.6	1.9	1.6	0.25–0.66	<0.01–0.13 (0.03–0.03)	0.05	0.31	0.09	0.03
Dy	2.1±0.1	15±1	4.2	8.6	10.8	3.3	11.9	9.5		0.05–0.54 (0.18±0.11)				
Ho	0.57±0.04	4.8±0.2	0.8	1.7	2.1	0.7	2.4	1.97		<0.02–0.58 (<0.02)				
Er	1±0.07	6.4±0.3	2.4	4.9	6.2	1.9	6.7	5.38		<0.03–0.19 (0.08±0.05)				
Tm	0.3±0.02	2.2±0.1	0.3	0.7	0.9	0.3	1	0.77		<0.01–0.23 (<0.01)				
Yb	1.0±0.06	6.9±0.3	2.3	4.8	6	1.8	6.5	5.27		<0.05–1.60 (<0.05)	0.13	1.09	0.29	0.1
Lu	0.2±0.01	1.3±0.1	0.3	0.7	0.9	0.3	0.9	0.72		<0.01–0.23 (<0.01)				
Y	8.2±0.5	57±12	20.4	42.1	54.2	17.5	64.9	52.3		0.3–2.4 (0.91±0.51)				
Sc	3.7±0.2	24±11	-	-	-	9.7	26.5	24.94	2.72–6.79	<1–13 (<1)	0.63	6.36	1.57	0.56

[a]Taylor and McLennan (1985), [b]Ketris and Yudovich (2009), [c]Dai et al. (2010),[d]Akinyemi et al. (2012),[e]Eze et al. (2013),[f]Hart et al. (1982),[g]Kanduč et al. (2019a)

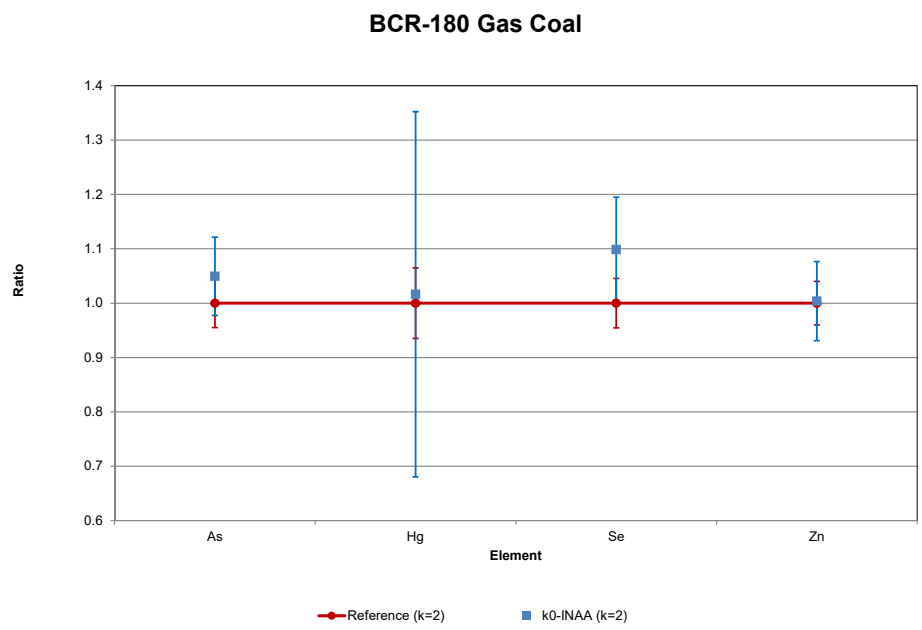

Fig. 2. QA/QC chart of measured parameters (As, Hg, Se, Zn) by k_0 – INAA, comparison with BCR-180 Coal Gas.

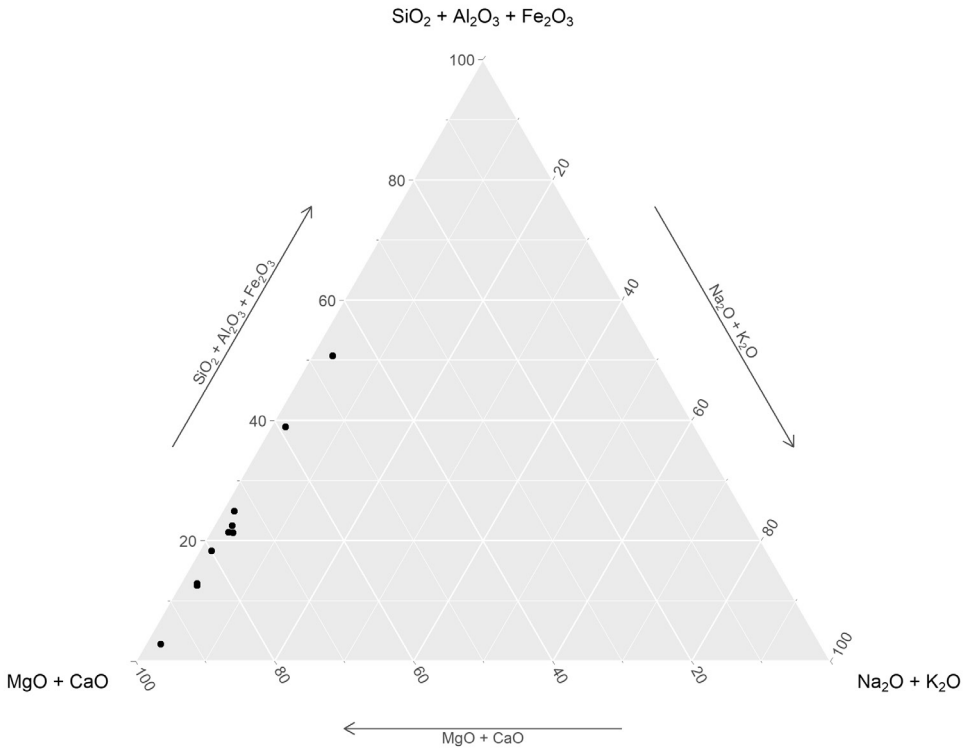

Fig. 3. Ternary plot of components: MgO+CaO/$Na_2O+K_2O/SiO_2+Al_2O_3+Fe_2O_3$ in gelified lignite samples (13-2123, 13-2125, 13-2130, 13-2134, 13-1238, 13-2141, 13-2145, 13-2157, 13-2162) determined with ICP-MS method (Kanduč et al., 2019a).

nor and trace elements. The elements: Ag, Au, Cd, Ga, Zr were excluded from plots since they were not measured in all of the coal samples, but are presented in Tables 1 and 2.

Among the 16 REEs (Table 4) recorded in coals from other locations (Taylor and McLennan, 1985, Ketris and Yudovich, 2009, Dai et al., 2010, Akineyeni et al., 2012, Eze et al., 2013, Hart et al., 1982, Kanduč et al., 2019a) only eight elements (Ce, Eu, La, Nd, Sc, Sm, Tb and Yb were determined using k_0-INAA and compared with published REEs values (mg/kg) in coal Clarke values, Jungar Power Plant (China), Tutuka Power Station (SA), Matla Power Station (SA) Witbank Coalfield (SA) (Wagner and Matiane, 2018) and the Velenje basin coal samples measured by ICP-MS. From a comparison of the data, all eight elements from this study (Velenje, Senovo, Kanižarica and Indonesia) and the data for the coal from other locations fall in the same range.

A comparison of the data for As, Ba, Ce, Co, Cs, Eu, La, Mo, Nd, Rb, Se, Sm, Sr, Tb, Th, U and Zn obtained using k_0-INAA and ICP-MS (Tables 3a and 3b) in samples 2123, 2125, 2130, 2134, 2138,

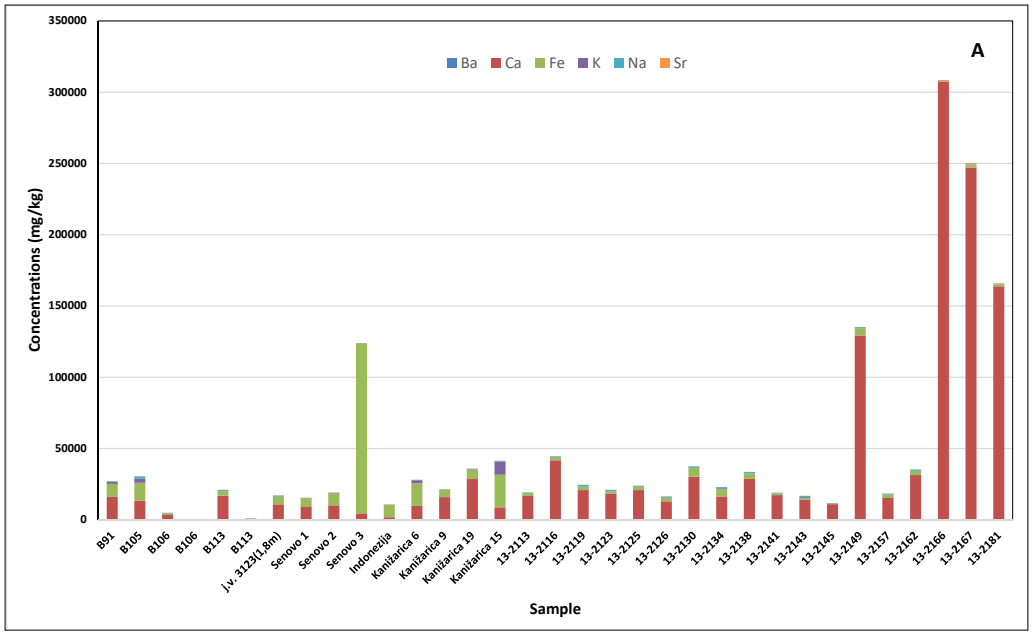

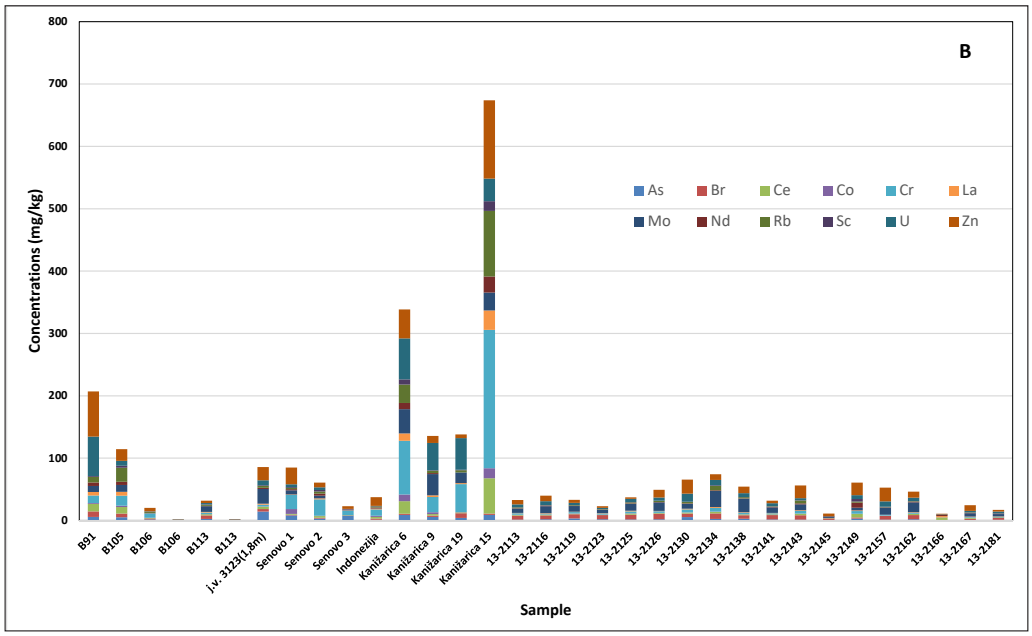

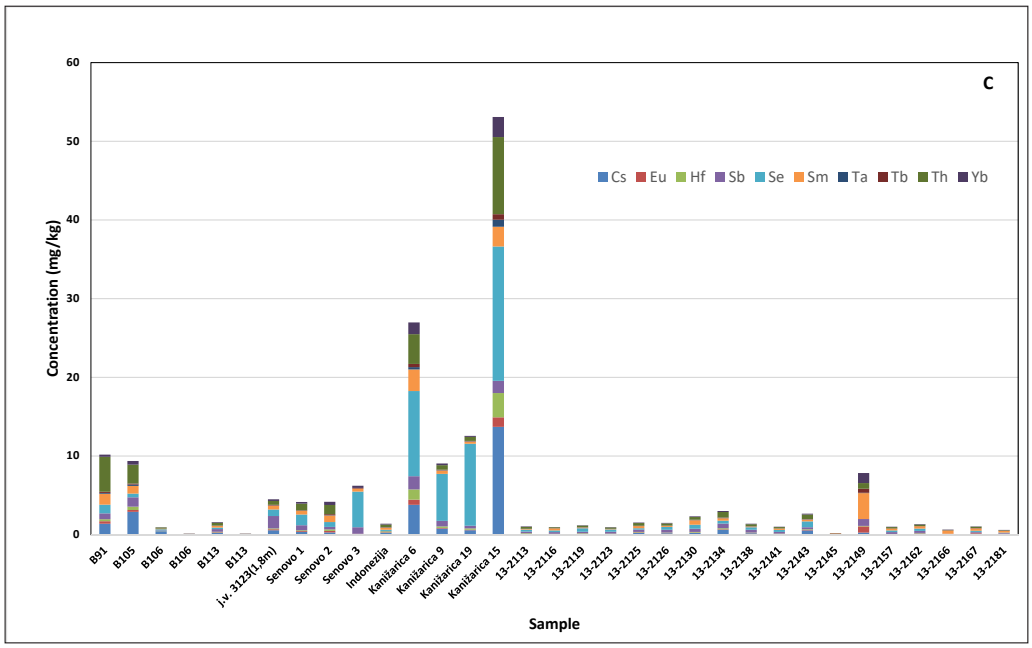

Fig. 4. Elemental composition of coals (major: Ca, Fe, K, Sr, Ba , minor: As, Br, Ce, Co, Cr, La, Mo, Nd, Rb, Sc, U, Zn and trace elements: Cs, Eu, Hg, Sb, Se, Sm, Ta, Tb, Th, Yb) from different locations (Velenje, Senovo, Kanižarica, and Indonesia) measured with k_0-INAA method.

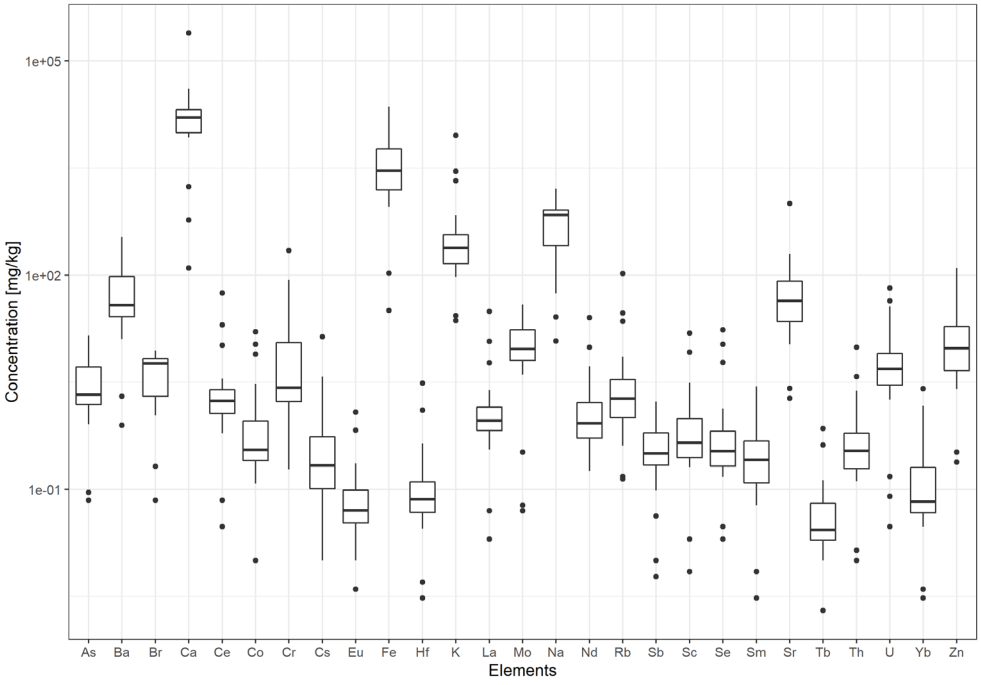

Fig. 5. Box – plot diagrams of major, minor and trace elements on "log scale" for coals from four mines (Kanižarica, Senovo, Indonesia, Velenje).

2141, 2145, 2157 and 2162 revel a strong positive correlation (R^2>0.8) in the case of As, Ba, Cs, Mo, Nd, Sr and U, (Fig. 6 A-D) and a good positive correlation (R^2 from 0.6 to 0.8) was observed for Zn and Rb (Figs 6 B-C). Though less strong, correlations (R^2 < 0.6) were found for Co, Eu, La, Se, Sm, Tb and Th (Figs. 6 C-D), which occur in low concentrations (< 1 mg/kg).

Figure 7 shows the Spearman correlations (R^2>90 %) for parameters (As, Ba, Br, Ca, Ce, Co, Cr, Cs, Eu, Fe, Hf, K, La, Mo, Na, Nd, Rb, Sb, Sc, Se, Sm, Sr, Tb, Th, U, Yb, Zn) measured with k_0-INAA method from four different mining locations (Kanižarica, Senovo, Indonesia, Velenje). Spearman's correlation analysis revealed strong positive correlations (R^2>0.95) between the following elements: Ce-La, Cs-Rb, Cs-Sc, Hf-Sc, Eu-Tb, Cs-Tb, Sc-Tb, Cs-Yb, Hf-Yb, Sc-Yb, and Th-Yb.

Principle component analysis (Fig. 8) reveals a strong gradient along the first PCA axis (49.5 %) and has the highest positive correlation with trace elements (e.g., Ce, Co, and Cs) and highest negative correlation with main elements (e.g. Ca, Na, B). These elements have the most discriminant power separating coals from open (Velenje and Indonesia) and closed (Kanižarica and Senovo) coal mines. The second axis explains an additional 16.1 % of the variance and correlates positively with Ba, Sr and negatively with U, Sb according to PCA multi-elemental grouping (Fig. 8).

Conclusion

Coal samples from Slovenia (Kanižarica, Velenje, and Senovo) and Indonesia were sampled and analysed by k_0-INAA in 2003, 2004 and 2013, while the Velenje coal mine samples (2013) was measured using both k_0-INAA and ICP-MS to compare results obtained using both methods. Based on the comparison of both methods, it can be concluded that k_0-INAA method is very accurate compared to ICP-MS method with no possibility of losses of material and contamination. A good correlation between both methods was obtained for Ba, Sr, Mo, Zn, U, As, Rb, Nd, while a weak correlation was observed for Th, Se, Cs, Eu, Sm and Tb.

The major elements determined by k_0-INAA in the Velenje lignite samples (n = 25) are Ca>Fe>Na>K>Sr>Ba while for minor and trace elements Zn>Zr>Mo>U>Br>Cr. In the coal samples from the Kanižarica mine (n=4), the levels of the main elements are Fe>Ca>K>Na>Sr>Ba, while for minor and trace elements Cr>Zr>U>Zn>Rb>Mo. In samples from Senovo mine (n = 3) the main elements are Fe>Ca>K>Na>Sr>Ba, and for trace elements Cr>Zn>As>Zr>Mo, whereas in the Indonesia coal had the following composition of main elements: Fe>Ca>K>Na>Ba>Sr and trace elements: Zn>Cr>Ce>Co. In all cases, Fe and Ca are the most abundant elements, while among trace elements; Zn and Cr are the most abundant. The levels of trace elements of samples from all investigated mines were also in the same range reported in the literature for other mining

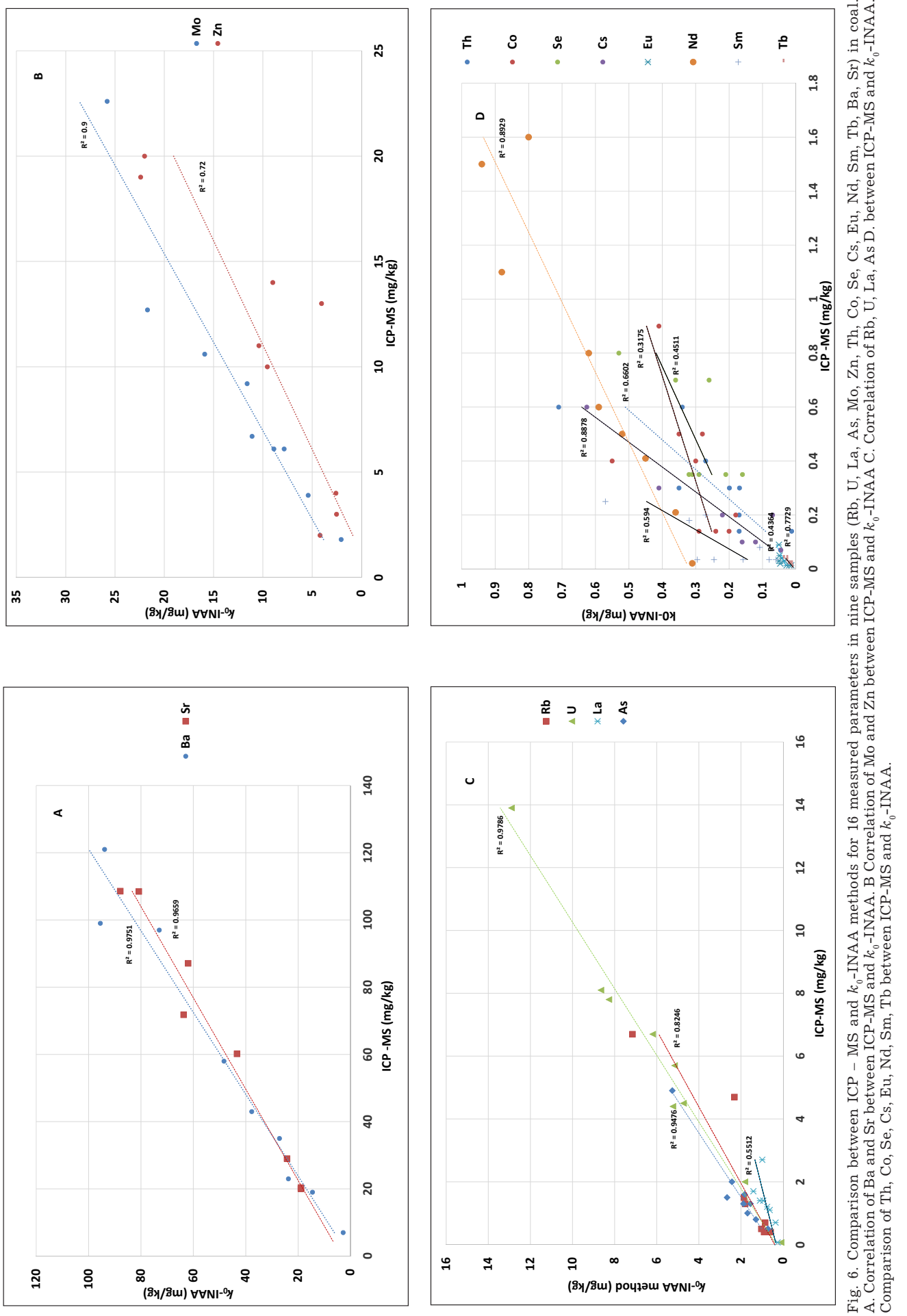

Fig. 6. Comparison between ICP – MS and k_0-INAA methods for 16 measured parameters in nine samples (Rb, U, La, As, Mo, Zn, Th, Co, Se, Cs, Eu, Nd, Sm, Tb, Ba, Sr) in coal. A. Correlation of Ba and Sr between ICP-MS and k_0-INAA. B Correlation of Mo and Zn between ICP-MS and k_0-INAA C. Correlation of Rb, U, La, As D. between ICP-MS and k_0-INAA. Comparison of Th, Co, Se, Cs, Eu, Nd, Sm, Tb between ICP-MS and k_0-INAA.

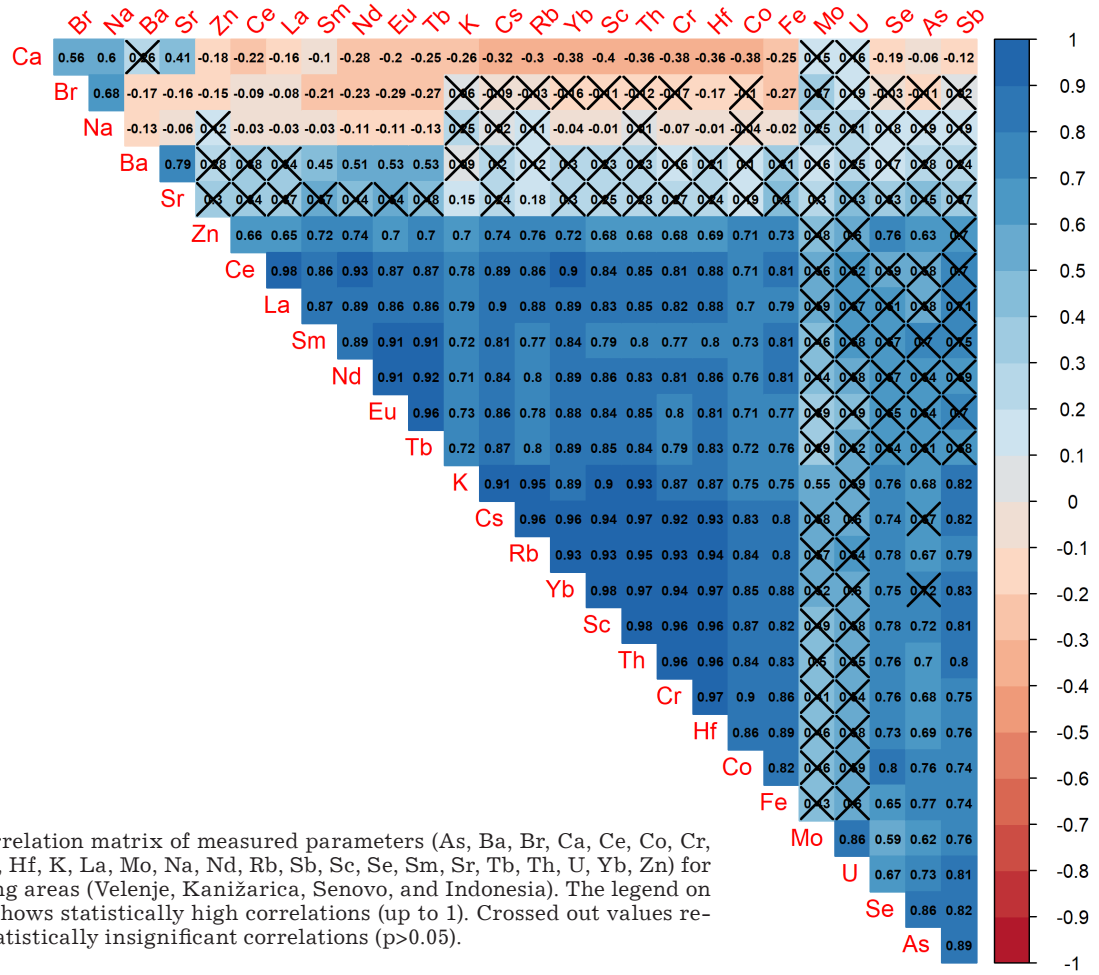

Fig. 7. Correlation matrix of measured parameters (As, Ba, Br, Ca, Ce, Co, Cr, Cs, Eu, Fe, Hf, K, La, Mo, Na, Nd, Rb, Sb, Sc, Se, Sm, Sr, Tb, Th, U, Yb, Zn) for four mining areas (Velenje, Kanižarica, Senovo, and Indonesia). The legend on the right shows statistically high correlations (up to 1). Crossed out values represent statistically insignificant correlations (p>0.05).

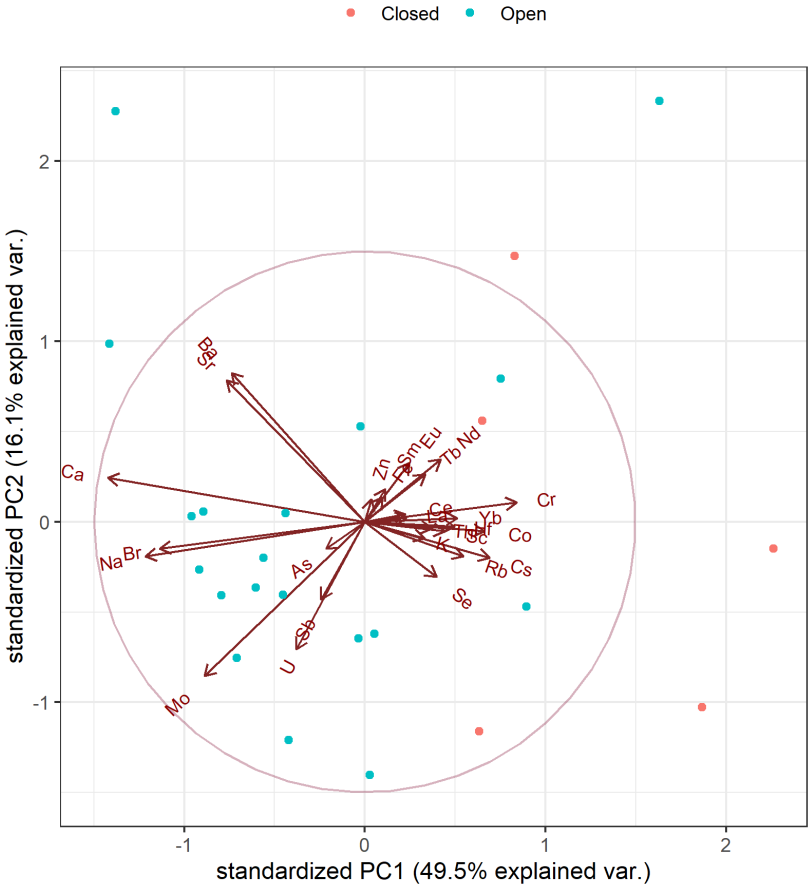

Fig. 8. PCA analysis of measured parameters (As, Ba, Br, Ca, Ce, Co, Cr, Cs, Eu, Fe, Hf, K, La, Mo, Na, Nd, Rb, Sb, Sc, Se, Sm, Sr, Tb, Th, U, Yb, Zn) from different mining areas (Velenje-open, Kanižarica-closed, Senovo-closed, and Indonesia-open).

regions (SA and China). Principal component analysis based on 27 elements (As, Ba, Br, Ca, Ce, Co, Cr, Cs, Eu, Fe, Hg, K, La, Mo, Na, Nd, Rb, Sb, Sc, Se, Sm, Sr, Tb, Th, U, Yb, Zn) revealed good discrimination between coal from the closed (Senovo, Kanižarica) and open mines (Velenje, Indonesia).

Further geochemical investigations of coal are required to investigate composition (proximate, ultimate analysis, major, minor and environmentally sensitive trace elements) of coal from active excavations in the Velenje coal mine in Slovenia, which is combusted in the Šoštanj thermal power plant and represents 30 % of energetic source in Slovenia. These analyses are essential to ensure the quality of combusted coal, which is related to atmospheric emissions.

Acknowledgement

The authors would like to thank L1-5451, P1-0143, P1-0195 and the Young researchers programme founded by Slovenian Research Agency.

References

Akinyemi, S.A., Gitari, W.M., Akinlua, A. & Petrik, I.F. 2012: Mineralogy and geochemistry of sub-bituminous coal and its combustion products from Mpumalanga Province, South Africa, Chapter 2. In: Krull, I.S. (ed.): Analytical Chemistry, inTechOpen. https://doi.org/10.5772/50692

ARSO (Agencija Republike Slovenije za okolje = Slovenian Environment Agency) 2014. http://gis.arso.gov.si/evode/profile.aspx?id=atlas_voda_Lidar@Arso

Bechtel, A., Sachsenhofer, R.F., Markič, M., Gratzer, R., Lücke, A. & Püttman, W. 2003: Paleoenvironmental implications from biomarker and stable isotope investigations on the Pliocene Velenje lignite seam (Slovenia). Organic Geochemistry, 34/9: 1277-2298. https://doi.org/10.1016/S0146-6380(03)00114-1

Brezigar, A. 1987: Premogovna plast Rudnika lignite Velenje = coal seam of the Velenje coal mine. Geologija, 28/29(1985/86): 319-336 (in Slovene with English summary).

Burnik Šturm, M., Lojen, S., Markič, M. & Pezdič, J. 2009: Speciation and isotopic composition of sulphur in low-rank coals from Slovenian coal seams. Acta Chimica Slovenica, 36: 989-996.

Chen J., Liu G., Jiang, M., Chan, C.L., Li, H., Wu, B., Zheng, L. & Jiang, D. 2011: Geochemistry of environmentally sensitive trace elements in Permian coals for the Huainan coalfield, Anhui, China. International Journal of coal geology, 88/1: 41-54. https://doi.org/10.1016/j.coal.2011.08.002

Connelly, N.G., Damhus, T., Hartshorn, R.M. & Hutton, A. T. 2005: Nomenclature of Inorganic Chemistry: IUPAC Recommendations 2005. The Red-Book. Royal Society of Chemistry, Cambridge, 340 p.

Dai S., Zhao, I., Peng, S., Chou, C. I., Wang, X., Zhang, Y., Li, D. & Sun, Y. 2010: Abundances and distribution of minerals and elements in high-alumina coal fly ash from the Jungar Power Plant, Inner Mongolia, China. International Journal of Coal geology 81: 320-332.

Eze, C.P., Fatabo, O., Madzivire, G., Ostrovnaya, T. M., Petrik, I.F., Frontasyeva, M.V. & Nechaev, A.N. 2013: Elemental composition of fly ash: a comparative study using nuclear and related analytical techiques. Chem. Didact. Ecol. Metrol. 18/1-2: 19-29. https://doi.org/10.2478/cdem-2013-0014

Finkelman, R.B. 1995: Modes of occurrence of environmentally sensitive trace elements of coal. In: Swaine, D.J. & Goodarzi, F. (eds.): Environmental aspects of trace elements of coal. Kluwer Academic Publishers, the Netherlands: 24-50.

Finkelman, R.B., Palmer, C.A. & Wang, P. 2018: Quantification of the modes of occurrence of 42 elements in coal. Int. J. Coal Geol. 185/2: 138-160. https://doi.org/10.1016/j.coal.2017.09.005

Gürdal, G. 2008: Geochemistry of trace elements in Can coal (Miocene), Canakkale, Turkey. International Journal Coal Geology 74/1: 28-40. https://doi.org/10.1016/j.coal.2007.09.004

Hart, R.J., Leahy, R., & Falcon, R. M. 1982: Geochemical investigation of the Witbank Coalfield using Instrumental Neutron Activation Analysis. J. Radioanal. Chem. 71/1-2: 285-297. https://doi.org/10.1007/BF02516156

HyperLab 2002: System, Installation and quick start guide, HyperLabs Software, Budapest, Hungary.

IRMM 2015: Joint Research Centre, Institute for reference materials and measurements, Certified Reference material BCR-180, Certificate of Analysis, 3 p.

Jaćimović, R., Smodiš, B., Bučar, T. & Stegnar, P. 2003: k_0-NAA Quality Assessment by Analysis of Different Certified Reference Materials Using the KAYZERO/SOLCOI Software. Journal of Radioanalytical and Nuclear Chemistry, 257/3: 659-663. https://doi.org/10.1023/A:1026116916580

Kanduč, T. & Pezdič, J. 2005: Origin and distribution of coalbed gases from the Velenje basin, Slovenia. Geochem. J., 39: 397-409.

Kanduč, T., Markič, M., Zavšek, S. & McIntosh, J. 2012: Carbon cycling in the Pliocene Velenje Coal Basin, Slovenia, inferred from stable carbon isotopes. International Journal of Coal Geology, 89/1: 70-83. https://doi.org/10.1016/j.coal.2011.08.008

Kanduč, T., Grassa, F., McIntosh, J., Stibilj, V., Ulrich-Supovec, M., Supovec, I. & Jamnikar, S. 2014: A geochemical and stable isotope investigation of groundwater/surface water interactions in the Velenje basin, Slovenia. Hydrogeol. J., 22/4: 971-984. https://doi.org/10.1007/s10040-014-1103-7

Kanduč, T., Vreča, P., Gregorin, Š., Vrabec, M., Vrabec, M. & Grassa, F. 2018. Authigenic mineralization in low rank coals from the Velenje basin, Slovenia. J. Sediment. Res., 88/2: 201-213. https://doi.org/10.2110/jsr.2018.7

Kanduč, T., Šlejkovec, Z., Mori, N., Vrabec, M., Verbovšek, T., Jamnikar, S. & Vrabec, Ma. 2019a: Multielemental composition and arsenic speciation in low rank coal from the Velenje Basin, Slovenia. Journal of Geochemical Exploration, 200: 284-300. https://doi.org/10.1016/j.gexplo.2018.08.001

Kanduč, T., Šlejkovec, Z., Vreča, P., Samardžija, Z., Verbovšek, T., Božič, D., Jamnikar, S., Solomon, D. K. Fernandez, D. P., Eastoe, C., McIntosh, J., Mori, N. & Grassa, F. 2019b: The effect of geochemical processes on groundwater in the Velenje coal Bain, Slovenia: insights from mineralogy, trace elements and isotopes signatures, SN Applied Sciences, 1/11: 1518-1-1518-30. https://doi.org/10.1007/s42452-019-1661-6

Kayzero for Windows (KayWin®) User's Manual, for reactor neutron activation analysis (NAA) using the k_0-standardization method, Version 2.42 (2011).

Ketris, M. & Yudovich, Y. 2009: Estimations of Clarkes for Carbonaceous Biolithes: world averages for trace element contents in black shales and coals. International Journal of Coal geology 78/2: 135-148. https://doi.org/10.1016/j.coal.2009.01.002

Khandelwal M. & Singh, T.N. 2010: Prediction of macerals contents of Indian coals from proximate and ultimate analyses using artificial neural networks. Fuel, 89/5: 1101-1109. https://doi.org/10.1016/j.fuel.2009.11.028

Kuščer, D. 1967: Zagorski terciar = Tertiary Formations of Zagorje. Geologija, 10: 5-85.

Lin R., Soong Y. & Granite E.J. 2018: Evaluation of trace elements in U.S. coals using the USGS COALQUAL database version 3.0. Part I: Rare earth elements and yttrium (REY). International Journal of Coal Geology, 192: 1-13. https://doi.org/10.1016/j.coal.2018.04.004

Liu, B., Vrabec, M. & Püttman, W. 2019: Reconstruction of paleobotanical and paleoenvironmental changes in the Pliocene Velenje Basin, Slovenia by molecular and stable isotope analyses of lignites. International Journal of Coal Geology, 206: 31-45. https://doi.org/10.1016/j.coal.2019.03.006

Markič, M. 1995: Elaborat o kategorizaciji, klasifikaciji in izračunu zalog premoga na območju Rudnika rjavega premoga Kanižarica-stanje 31.12. 1994. Elaborat, arhiv GeoZS, Ljubljana: 77 p.

Markič, M. & Sachsehofer, R.F. 1997: Petrographic composition and depositional environments of the Pliocene Velenje lignite seam (Slovenia). International Journal of coal geology, 33/3: 229-254. https://doi.org/10.1016/S0166-5162(96)00043-2

Markič, M. 2006: Anorgansko – geokemična opredelitev velenjskega lignite v reprezentativnem profile vrtine P-9k/92 = Inorganic geochemical characterization of the Velenje lignite in the representative P-9k/92 borehole profile (Slovenia). Geologija, 49/2: 311-338. https://doi.org/10.5474/geologija.2006.023

Markič, M. & Sachsenhofer R.F. 2010: The Velenje lignite- its petrology and genesis. Geološki zavod Slovenije, Ljubljana: 218 p.

R Core Team 2019: R: a language and environment for statistical computing. R Foundation for Statistical Computing, Vienna, Austria. https://www.R-project.org/.

Radenovic, A. 2006: Inorganic constituents in coal. Kem Ind. 55/2, 65-71.

Sedlar, J., Kanduč, T., Jamnikar, S., Grassa, F. & Zavšek, S. 2014: Distribution, composition and origin of coalbed gases in excavation fields from the Preloge and Pesaje mining areas, Velenje Basin, Slovenia. Int. J Coal Geol., 131: 363-377.

Shuttle Radar Topography Mission SRTM data. http://srtm.csi.cgiar.org/

Taylor, S.R. & McLennan, S. M. 1985: The Continental crust: its composition and evolution. Blackwell, Oxford: 312 p.

USGS Fact Sheet, 2014. http://pubs.usgs.gov/fs/2014/3078/pdf/fs2014 3078.pdf.

Yi, L., Feng, J., Qin, Y.H. & Li, W.Y. 2017: Prediction of elemental composition of coal using proximate analysis. Fuel, 193/1: 315-321. https://doi.org/10.1016/j.fuel.2016.12.044

Wagner, N. J. & Matiane, A. 2018: Rare aearth elements in select Main Karoo Basin (South Africa) coal and coal ash samples. International Journal of Coal Geology, 196: 82-92. https://doi.org/10.1016/j.coal.2018.06.020

Wickham, H. 201: ggplot2: Elegant Graphics for Data Analysis. Springer-Verlag New York.

Internet source:

Internet 1: http://globalenergycertification.org/indonesian-coal-quality-coal-reserves/: Indonesian Coal quality and coal reserves (cited 29.11.2019

GEOLOGIJA *62/2*, 237–249, Ljubljana 2019
https://doi.org/10.5474/geologija.2019.011

Risk assessment for open loop geothermal systems, in relation to groundwater chemical composition (Ljubljana pilot area, Slovenia)

Ocena tveganja za odprte geotermalne sisteme, glede na kemično sestavo podzemne vode (pilotno območje Ljubljana, Slovenija)

Katja KOREN & Mitja JANŽA

Geološki zavod Slovenije, Dimičeva ulica 14, SI-1000 Ljubljana, Slovenija;
e-mail: katja.koren@geo-zs.si, mitja.janza@geo-zs.si

Prejeto / Received 16. 10. 2019; Sprejeto / Accepted 5. 12. 2019; Objavljeno na spletu / Published online 24. 12. 2019

Key words: shallow geothermal energy, open loop geothermal system, groundwater, chemical composition, heat pump

Ključne besede: plitva geotermalna energija, odprti geotermalni sistemi, podzemna voda, kemična sestava, toplotna črpalka

Abstract

Shallow geothermal energy is a renewable source of energy that can be used effectively with open loop geothermal systems. Knowledge of hydrogeological conditions is a prerequisite for the successful implementation and operation of such systems. The article describes a risk assessment of open loop geothermal system operation related to the chemical composition of groundwater in the area of the City of Ljubljana. Results of the study show that in the area of the Ljubljansko polje aquifer, the geochemical characteristics of the groundwater do not represent a risk of possible operational problems for an open loop geothermal system. On the contrary, the chemical composition of the groundwater in the Ljubljansko barje aquifer indicates a risk of corrosion and/or the precipitation of minerals, which can lead to diminished efficiency of the geothermal system or even damage that can result in the interruption of operations. In order to avoid operational problems in open loop systems, wells must be a professionally designed and installed, and groundwater geochemical characteristics properly determined. In the latter, it is important to take into account the method of sampling, since the chemical composition of water in the aquifer and in the geothermal system may vary significantly.

Izvleček

Plitva geotermalna energija je obnovljivi vir energije, ki ga lahko učinkovito uporabljamo s pomočjo odprtih geotermalnih sistemov. Pogoj za njihovo uspešno namestitev in delovanje je poznavanje hidrogeoloških pogojev. Članek opisuje oceno tveganja za delovanje odprtih geotermalnih sistemov, povezanih s kemično sestavo podzemne vode na območju Mestne občine Ljubljana. Rezultati raziskav kažejo, da na območju vodonosnika Ljubljanskega polja geokemične značilnosti podzemne vode ne predstavljajo posebnega tveganja za delovanje odprtih geotermalnih sistemov. Nasprotno na območju Ljubljanskega barja kemična sestava podzemne vode nakazuje možnost korozije in obarjanja mineralov, kar lahko povzroči zmanjšanje učinkovitosti odprtega geotermalnega sistema ali celo poškodbe, ki onemogočajo njegovo delovanje. Na tem območju je v izogib težavam pri delovanju tovrstnih sistemov nujno strokovno načrtovanje in izvedba vrtine ter ugotovitev geokemičnih značilnosti podzemne vode. Pri slednjem je pomembno upoštevati način vzorčenja, saj se kemijska sestava vode v vodonosniku in geotermalnem sistemu lahko bistveno razlikuje.

Introduction

Shallow geothermal energy is a renewable source of energy with increasingly important environmental, economic and social impacts. The subsurface temperature at a depth of 10 m is practically constant throughout the year (roughly the annual average ambient temperature). Shallow geothermal systems can take advantage of the stable subsurface conditions and heat stored in the solid rocks or groundwater for heating or cooling, and for seasonal energy storage (Bonte, 2015). There are two kinds of shallow geothermal systems: closed and open loop (Fig. 1). Geothermal open loop systems, which are the focus of this study, use groundwater as a conveyor or carrier of heat. Such systems consist of extrac-

tion and injection wells and transfer withdrawn groundwater to a heat exchanger, and after exploitation it is reinjected back into the aquifer. The direct use of groundwater, which is a good carrier of thermal energy due to its high specific heat capacity, makes open loop systems more efficient in general than closed loop systems (Internet 1), which use a mixture of water and antifreeze with lower specific heat capacity and exchange heat with subsurface through a polyethylene pipe. Specific heat capacity of the water and antifreeze mixture decreases as the amount of the volume of antifreeze used in mixture increases (Roslan et al., 2017).

On the other hand, the installation and operation of open loop systems is more challenging. The first condition for the implementation of an open loop system is the availability of groundwater, whereby the hydrogeological conditions can enable the withdrawal and injection of a sufficient quantity of groundwater (or required flow rate). Furthermore, the aquifer may already be used for other priority purposes (e.g. drinking water supply) or may be protected (e.g. nature protection area). The use of shallow geothermal energy with open loop systems affects the local hydraulic regime and temperature of groundwater which can potentially mobilise contaminants and influence physical properties of groundwater, chemical reactions, microbiology and the interaction of these factors with each other (Zuurbier et al., 2013). Due to these risks and risk related to drilling of boreholes, installation of shallow geothermal systems within catchments of drinking water well is often restricted (Zuurbier et al., 2013). Böttcher et al. (2019) outlined the physical, operational and regulatory limits of such, and stressed the fact that detailed knowledge of the local hydrogeological conditions and the resulting technical potential are crucial conditions for the efficient use of open loop systems. Another important factor, which is investigated in this study, is the chemical composition of groundwater, which can introduce problems into open loop systems, namely clogging or corrosion, or both (Rafferty, 1999).

The precipitation of minerals can seriously affect the efficiency of the well and all other installations exposed to groundwater with low dissolved oxygen concentrations (Houben, 2003). When the screen section of the well is clogged with precipitated minerals, the amount of water that can flow into the well decline and thus the well's capacity decreases (Woyessa, 2011). The development of incrustation in wells can be the result of both chemical and biological processes (Park et al., 2015).

Chemical encrustation could be the secondary effect of biofouling oxidation or corrosion (Smith & Tuovinen, 1985). Changes in O_2 and CO_2 con-

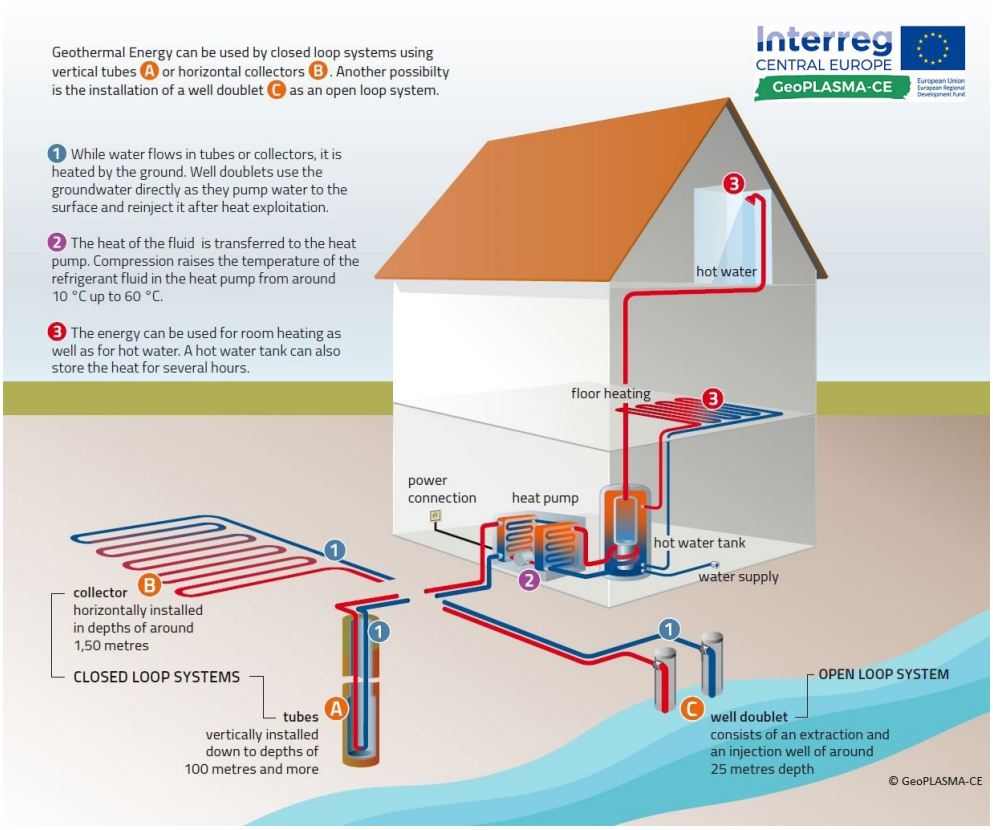

Fig. 1. Scheme of shallow geothermal energy systems, used for heating and cooling of buildings (Internet 1).

tent in groundwater, as well as in pressure and temperature, can lead to the formation of carbonate and silica minerals, as well as iron and manganese containing minerals (Abesser, 2010; Brons et al., 1991; Holm et al., 1987; Rafferty, 1999). Minerals containing iron, such as $Fe(OH)_3$, goethite (FeOOH) and hematite (Fe_2O_3) can be precipitated as scale within the open loop system (Park et al., 2015). The Langelier Saturation Index (LSI) and Ryznar Stability Index (RSI) are often used as an indication of the aggressiveness of the water and the risk of the precipitation of carbonate minerals inside the open loop system (Rafferty, 1999).

If under natural conditions the oxygen concentration in groundwater is low and the pH value ranges from 6.5 to 7.5, iron occurs primarily as dissolved ferrous iron (Fe^{2+}). Fe^{2+} is unstable in contact with oxygen, and in the presence of air it changes to insoluble ferric iron (Fe^{3+}) and precipitates as ferric oxide or oxyhydroxide. The oxidation rate of Fe^{2+} is highly dependent on pH conditions (Woyessa, 2011) and dissolved oxygen concentrations (Donald, 1997). When water is aerated, almost all the iron becomes insoluble. This condition can arise from the mixing of groundwater with low dissolved oxygen concentrations with oxygen rich groundwater during operation of the well (Donald, 1997). Ferric oxides and oxyhydroxides precipitate and coat surrounding surfaces. This process also results in rust on metal surfaces exposed to the atmosphere. If Fe^{2+} is combined with carbonate ions, iron bicarbonate is formed. Manganese resembles iron in its chemical behaviour and occurrence, but in groundwater it is less abundant than iron (Kemmer, 1977). Indicators of incrusting groundwater are high pH value (> 7.5), RSI < 7, iron content > 0.5 mg/L (precipitation of iron), carbonate hardness > 300 mg/L (precipitation of calcium carbonate), manganese content > 0.2 mg/L (precipitation of manganese) and the presence of oxygen (Driscol, 1986; Götzl et al., 2018).

Clogging can also occur due to the presence of iron bacteria, which form biological incrustations (Smith & Tuovinen, 1985). Iron bacteria's natural environment is wetlands (Pringsheim, 1949), where they mainly generate most of their energy for metabolism by oxidising soluble Fe^{2+} into insoluble Fe^{3+}, and in this way gain a small amount of energy by utilising large amounts of Fe^{2+} (Howsam, 1988).

Beside the clogging, another risk for open loop systems is corrosion, which is the result of chemical and electrochemical processes. Chemical corrosion can be expected if the water has a low pH value (< 7), elevated concentrations of dissolved oxygen (> 2 mg/L), hydrogen sulphide presence (even less than 1 mg/L), high TDS concentration (> 1000 mg/L), CO_2 concentrations > 50 mg/L and chloride content > 500 mg/L (Driscoll, 1986). Electrochemical corrosion can occur when two conditions are fulfilled: an electrical potential difference on metal surfaces, and enough dissolved solids in water to constitute a conductive fluid (electrolyte). An electrical potential difference may develop between two different kinds of metals, or between proximate yet separate areas on the surface of the same metal (Driscoll, 1986). Corrosion can cause damages (new openings) in the open loop system: the enlargement of well screen openings and increased entry of finer material into the well are particularly common, and can harm the pump and reduce the efficiency of the well (Driscoll, 1986). Due to corrosion in an ionizing solvent the metal ion initially goes into solution but may then undergo a secondary reaction, combining with other ions present in the environment to form an insoluble molecular species such as rust (Schofield, 2002).

In this study a risk assessment of the efficient operation of open loop geothermal systems, related to the chemical composition of groundwater is presented. The study follows a procedure, developed within the GeoPLASMA-CE project (Götzl et al., 2018) which was implemented in the Ljubljana pilot area. The procedure consists of three main steps. 1) Calculation of LSI and RSI indices using available archive data on chemical composition of groundwater. 2) Additional field measurements and chemical analysis of groundwater in those areas where in the previous step a risk was identified and operational problems in open loop systems were reported. Different sampling procedures (in wells and from the system) were implemented and analysed in this step. 3) Outlining areas with a risk for the efficient operation of open loop geothermal systems.

Hydogeological setting

The study area is part of the area of Municipality of Ljubljana, with aquifers potentially suitable for implementation of open loop systems: the Ljubljansko polje unconfined aquifer and the northern part of the Ljubljansko barje confined aquifer system (Fig. 2). The average annual precipitation in this area is 1383 mm (2001–2010) while the average annual ambient temperature is 11.3 °C (2001–2010) (Internet 2).

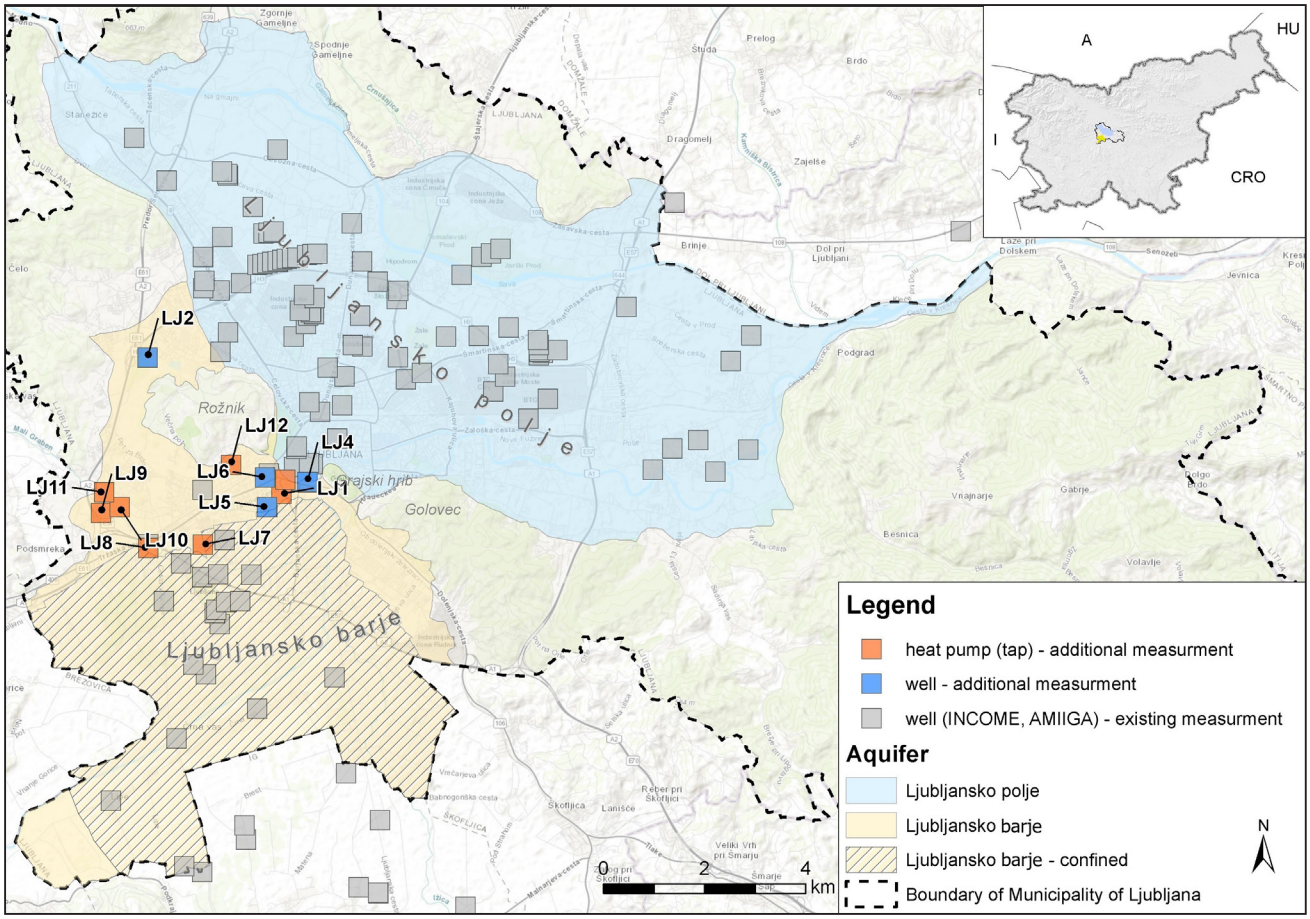

Fig. 2. Study area with locations of measurements.

The Ljubljansko polje aquifer is composed of permeable gravel and sand beds with lenses of conglomerate. Due to its great thickness (which exceeds 100 m in the deepest parts) and high permeability, this Quaternary aquifer contains significant quantities of groundwater, which is the main source of public water supply for the City of Ljubljana (Janža, 2009; Šram et al., 2012). The Ljubljansko barje aquifer is composed of alternating fluvial and lacustrine deposits with a heterogeneous composition (silt, clay, sand, gravel) (Mencej, 1988/89). The top low-permeable layer in the northern part of the Ljubljansko barje is 10–20 meters thick (Fig. 3, A).

Under this layer the heterogeneous and low permeable upper Pleistocene aquifer (Fig. 3, B) is situated. Beneath the upper Pleistocene aquifer, a thick silty and clayey layer (Fig. 3, C) is present and underneath the lower Pleistocene aquifer (Fig. 3, D), which consists of gravel and contains good quality groundwater (Prestor & Janža, 2002). It is a confined or semi-confined aquifer with artesian to sub-artesian conditions.

Research of the Barje landfill influence on groundwater has revealed a reducing environment and presence of iron, manganese, ammonium and arsenic in groundwater (Prestor & Janža, 2002). This influence of the landfill overlaps with the natural reduction environment and the consequences of reducing conditions resulting from the immission of pollution from other sources in the urbanized area (Prestor & Janža, 2002).

The Sava River, which recharges the Ljubljansko polje aquifer in its north-western part, has an electrical conductivity around 300 µS/cm (Jamnik et al., 2014). The low electrical conductivities, between 200 and 300 µS/cm, and fluctuating temperatures at the north-western part of

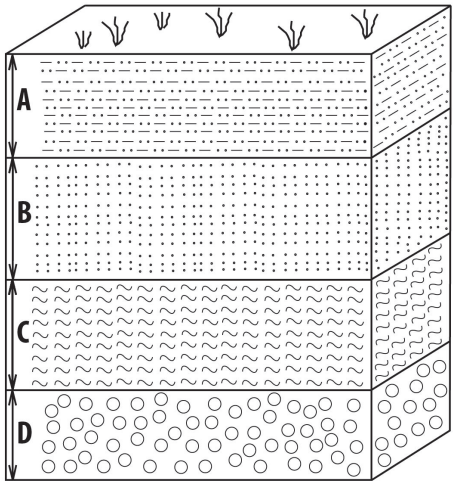

Fig. 3. Schematic representation of Ljubljansko barje aquifer (after Prestor & Janža, 2002)

Fig. 4. Iron mineral deposits on heat pump filter from northern part of Ljubljansko barje.

the Ljubljansko polje aquifer (Kleče and Jarški prod well fields) are therefore the result of a significant recharge of the Sava river (Jamnik et al., 2014). Under highly urbanized parts of the Ljubljana polje aquifer, electrical conductivity ranges between 500 and 700 µS/cm. The temperature of the groundwater at the Ljubljansko polje range between 10.6 and 14.6 °C, while in the Ljubljansko barje the temperature rises up to 15.6 °C (Janža et al., 2017).

According to the archive and publicly accessible data (Internet 3), 93 open loop geothermal systems (December 2018) are installed in the Ljubljana pilot area. Problems in the operation of open loop systems, that could be related to groundwater chemical composition, were reported from the users from northern part of the Ljubljansko barje. The most commonly reported problems consist of deposition of iron minerals on filters which requires frequent cleaning in order to maintain system efficiency (Fig. 4).

Materials and Methods

Archive data processing

The first step of the investigation involved the analysis of existing data on groundwater field parameter measurements and chemical analysis. The main body of said data was collected and organized from previous projects (AMIIGA, INCOME). Additional data from the national monitoring program, accessible through a portal (Internet 4), were used in the analysis. The datum consist of measurements for basic chemical parameters (anions and cations), which were used to determine the type of water and the ion balance (software AquaChem 2014.2.; Waterloo Hydrogeologic, 2018) for each observation point.

The LSI was calculated using readings for alkalinity, hardness, TDS, pH and temperature (Lentech, 2018a). The groundwater electrical conductivity of unpolluted groundwater is usually correlated with the concentration of dissolved carbonates in the water or the carbonate hardness of the water. If LSI < 0 the water is undersaturated with calcium carbonate and has a tendency to remove the existing protective coatings of calcium carbonate in pipelines and equipment (is corrosive); and if LSI > 0 the water is supersaturated with respect to calcium carbonate ($CaCO_3$) and the formation of scale may occur (Gonzalez et al., 2019).

Additional field measurements and groundwater sampling

Additional groundwater sampling and field measurements were focused on the northern part of the Ljubljansko barje, where operational problems of open loop systems related to the chemical composition of groundwater were reported. Since the number of locations, where the sampling could be performed from wells was limited, sampling was performed also on the surface part of the open loop systems, where water samples were taken from the heat pump system taps. A total of four observation wells and eight open loop systems were selected.

In order to assess the material resistance of open loop systems, two sampling campaigns were carried out. First sampling on all 12 sampling locations was performed in March 2018. A second sampling in May 2018 was repeated in three wells (LJ1, LJ2 & LJ6) and on one tap (LJ3) in order to analyse the comparability of results of chemical analysis of samples taken on different object types in different time periods. Groundwater sampling on wells was performed on 27th March and 14th May using a Grundfos M1 submersible pump (Eijkelkamp, 2017). Wells LJ2 (depth: 84 m), LJ4 (depth: 92 m), LJ5 (depth: 92 m) and LJ6 (depth: 72 m) are observation wells, while LJ1 (24 m) is an injection well and is part of an open loop system. In other cases, water samples from open loop systems were taken from taps. Field parameters such as pH, electrical conductivity (Cond.), temperature (T), redox potential (Eh), dissolved oxygen (DO) and oxygen saturation (O_2) were measured with a portable WTW Multimeter pH/Cond (pH value: SenTix 42, Cond. and T: TetraCon 325 (WTW GmbH, 2004) and with WTW Multi 3410/set C (redox potential: Sentix ORP (WTW GmbH, 2008), oxygen content: FDO 925 (WTW GmbH, 2010). Fe^{2+} and Fe (total)

content in water was measured with a HACH DR 2800 portable spectrophotometer (Hach Lange, 2012). Analysis of major cations (Na^+, K^+, Ca^{2+}, Mg^{2+}; SIST EN ISO 14911:2000), anions (Cl^-, SO_4^{2-}, NO_3^-; SIST EN ISO 10304-1:2009; and $HCO3^-$; ASTM D 1067-B mod.), and Fe total (SM.3500-Fe-B) (if the value in the field was above 3 mg/L) were performed by the accredited Vodovod-Kanalizacija d.o.o. laboratory. Additional samples for analysis of Mn (ISO 17294-2:2016(E), NM) and dissolved sulphide (as H_2S – SIST ISO 10530: 1996, NM) content were also taken and analysed in Vodovod-Kanalizacija d.o.o. laboratory. Uncertainties of measured contents are in following ranges: for HCO_3^- ±0.02 mg/L, Fe total (measured in laboratory) ±0.14 mg/L, Mn ±0.016 mg/L and for dissolved sulphide ±0.014 mg/L (Auersperger & Železnik Bračič, 2018).

Results and discussion

Archive data processing

Data from 126 locations, 91 from the area of the Ljubljansko polje aquifer and 35 from the area of the Ljubljansko barje aquifer, were analysed. The data consist of total 2227 analysis of chemical parameters, performed between the years 2008 and 2017. 28.7 % of the data included in the data processing procedure contain no data on NO_3^- content; therefore, a calculation for ion balance could not be performed. On the rest of the data, accuracy check was made using an AquaChem 2014.2, which indicated that 15.5 % of the data showed poor ion balance, 11.6 % fair and 44.2 % good ion balance. The most common water type in both aquifers is Ca-Mg-HCO_3.

Based on the calculated LSI in the study area, the risk of the formation of lime scale (where median LSI is > 0) and/or corrosion is present (where median LSI value is < 0) (Fig. 5). According to the distribution of electrical conductivity in the Ljubljansko polje and Ljubljansko barje aquifer, figure 5 shows the risk of corrosion or limescale formation, but since the expected changes in groundwater temperature in shallow, low-temperature open loop geothermal system is less than 5°C, such risk is low (VDI-Richtlinien, 2001).

The RSI is influenced by pH value, electrical conductivity, Ca^{2+}, HCO_3^- and water temperature (Lentech, 2018b). Based on calculations of RSI, very aggressive groundwater was identified in

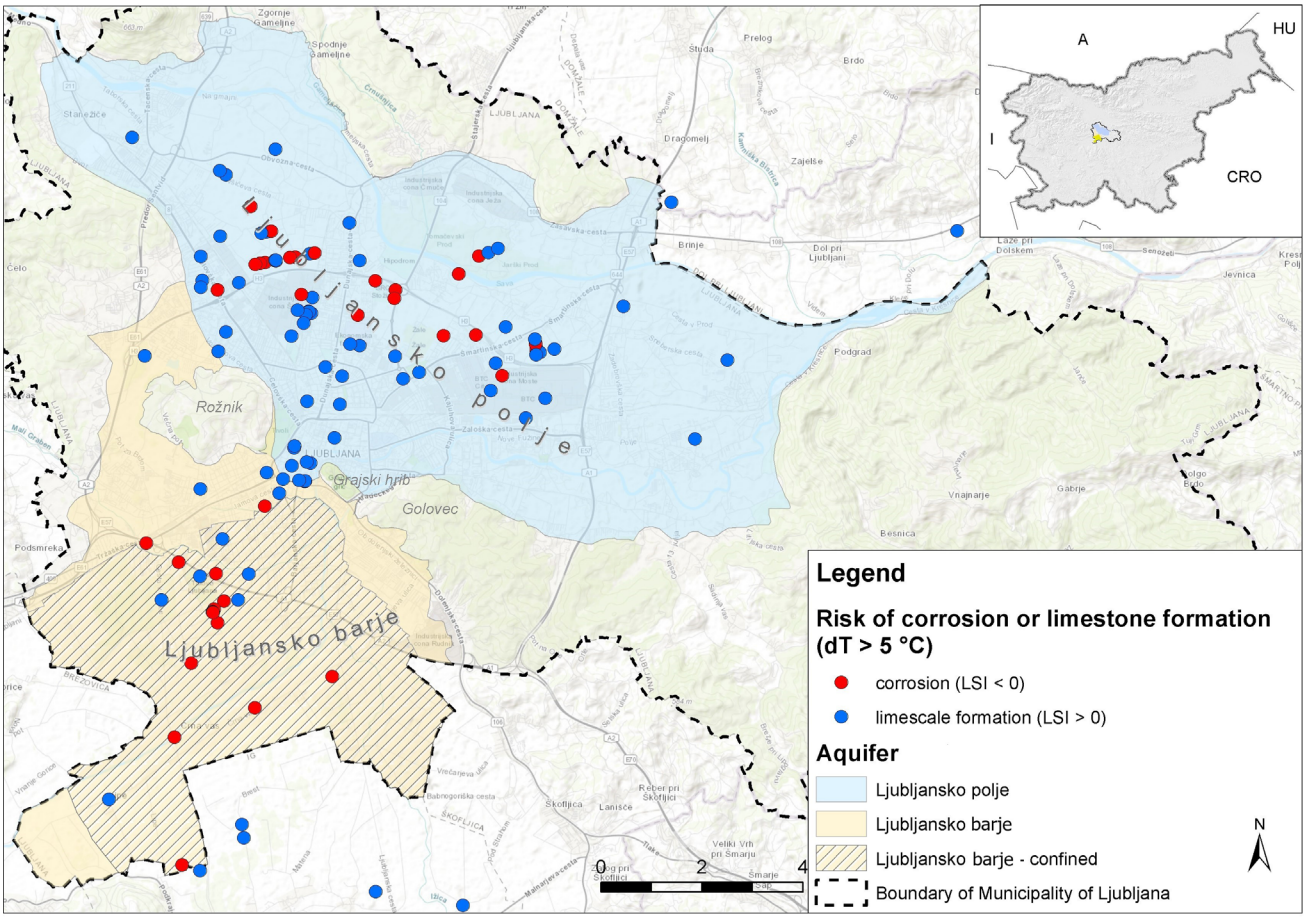

Fig. 5. Risk of corrosion or formation of limescale in the case of $_{\Delta}T$ of groundwater > 5 °C.

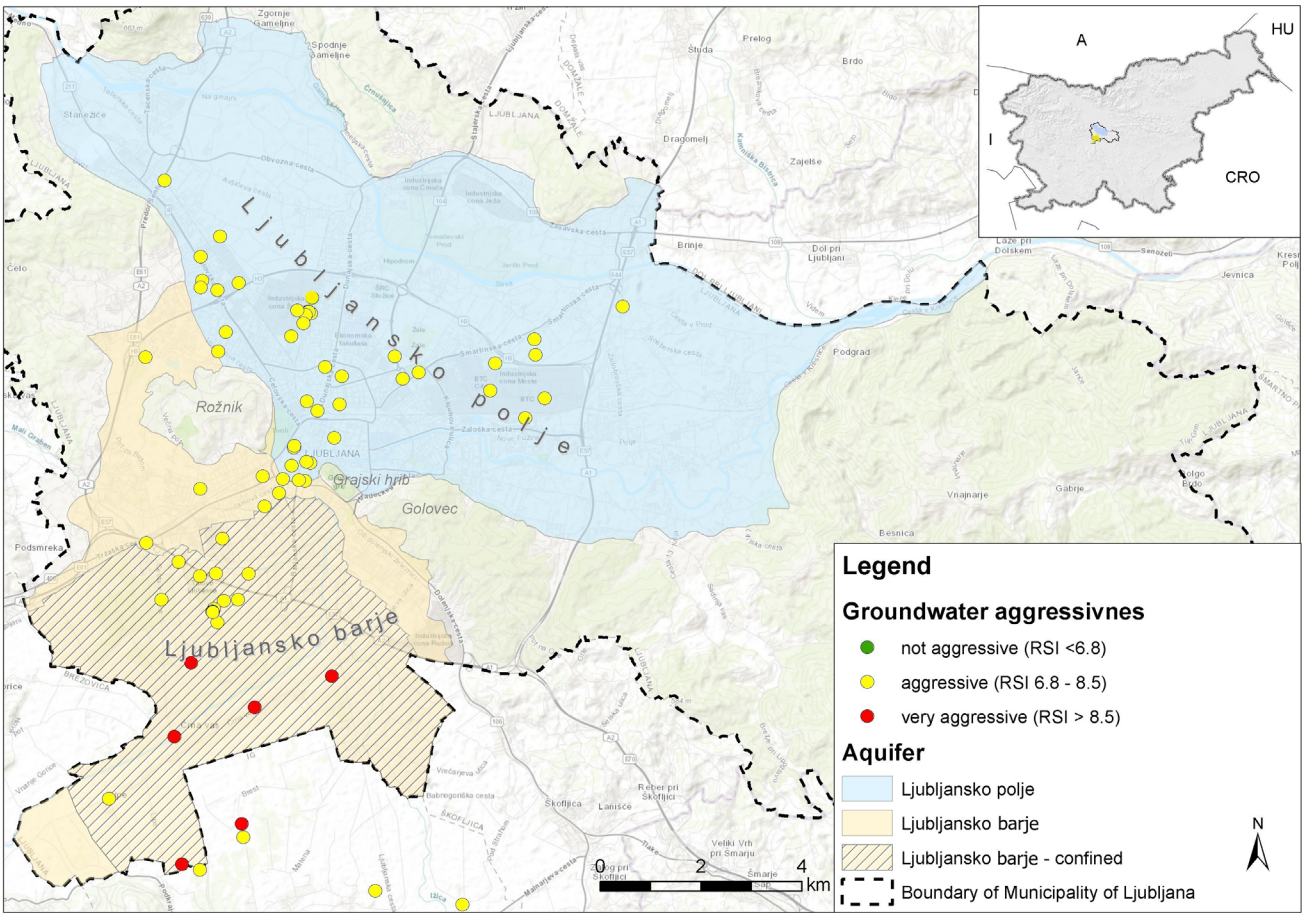

Fig. 6. Groundwater aggressiveness based on RSI.

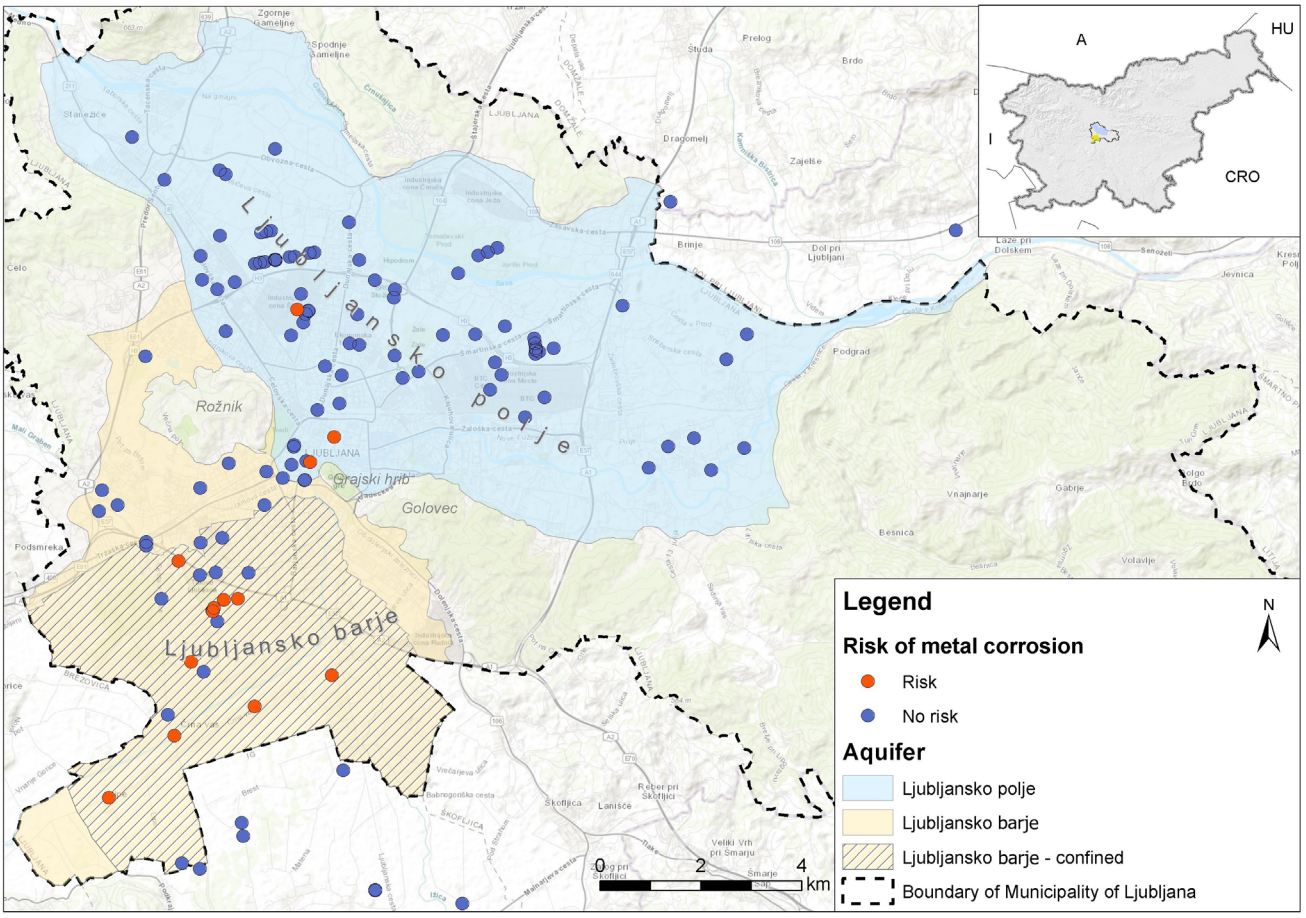

Fig. 7. Risk of metal corrosion, due to high SO_4^{2-} and DO content.

the Ljubljansko barje aquifer (Fig. 6), where the minimum pH value (6.8) is noticeable lower than in Ljubljansko polje aquifer (7.3).

RSI value higher than 7.5, pH value < 7.5 and presence of dissolved oxygen (> 2 mg/L) in groundwater indicate the risk of metal corrosion mainly in the Ljubljansko barje aquifer (Fig. 7).

Since archive data on iron and manganese content are scarce it was not possible to assess the risk of iron and manganese precipitation: therefore, additional sampling was carried out.

Additional field measurements and groundwater sampling

Results of the field measurements and chemical analyses of samples taken from wells and from taps (open loop systems) are presented in (Table 1). In order to determine the risk in relation to the chemical composition of groundwater for the operation of open loop systems, the results of field measurements and chemical analyses were compared with parameter limits. They are recommended by heat pump manufacturers Ochsner Wärmepumpen GmbH, Viessmann Ltd. and Dimplex Ltd (Kmiecik et al., 2017) and represent conditions required for the undisturbed and efficient operation of open loop systems. A conservative approach was used, and most restrictive limits of the mentioned manufacturers were considered (Table 1).

Results of the analysis (Table 1) show that manufacturers' requirements could not be met in all cases. There is no risk of corrosion at four locations (Table 1; LJ3, LJ7, LJ8 and LJ9), which can occur at eight locations (Table 1; LJ1, LJ2, LJ4, LJ5, LJ6, LJ10, LJ11 and LJ12). Due to the high iron and dissolved oxygen content at five locations a risk of iron or manganese scaling is indicated (Table 1; LJ1, LJ4, LJ5, LJ6 and LJ-12). To mitigate this kind of risk filtration after oxidation (Appelo & Postma, 2005) was reported as most cost-effective method for removal of iron or manganese scaling from the system (Power & Prasad, 2010).

The central part of the Ljubljansko barje confined aquifer is covered with a thick layer of clay, which causes lower oxygen content in groundwater. Oxygen deficiency creates hydrochemical conditions in which iron and manganese, usually present in poorly soluble chemical forms, become mobile (Jamnik et al., 2014). Based on the analyses of archive data and the results of additional measurements, including knowledge of natural hydrogeological conditions we identified metal corrosion and iron or manganese scaling as the highest risk to the efficient operation of open loop systems (Table 1) and outlined the area with the highest risk (Fig. 8).

Comparison of different sampling approaches

A comparison of the results of different sampling approaches (Table 2) shows that the values of parameters measured on different dates do not differ noticeable for the samples on locations LJ2, LJ3 and LJ6, when the samples taken from the same object type (well or heat pump tap). At location LJ-1, samples were taken one time from the well and one time from the tap, but at different times. Due to the different sampling periods, direct comparison is questionable; however, taking into account the results of measurements taken at other locations, it seems that sampling from different types of object produces the highest differences in measured parameters and reflects the different conditions in the geothermal system and in the well, or before and after heat extraction. The most noticeable differences are observed in the values of parameters dissolved oxygen (3.38 and 0.71 mg/L), electrical conductivity (676 and 483 µS/cm), and concentration of HCO_3^- (289 and 355 mg/L). Heat extraction results in lower water temperatures in the injection well (10.1 °C) than at the tap (13.0 °C). However, for more detailed comparison of two sampling approaches, more data would have to be collected. Since no data on the iron content of groundwater sampled from well are available (only at tap), no interpretation of the processes that occur during heat extraction within the system is possible.

Conclusion

Based on archive data, the calculated values of LSI and RSI indicate potential risk of lime scale formation and/or corrosion in both aquifers. But since for shallow geothermal open loop systems expected changes in groundwater temperature are smaller than 5 °C, this kind of risk is low.

Archive data on groundwater composition in the Ljubljansko polje aquifer show a high concentration of dissolved oxygen (on average 7.67 mg/L) and low iron content (on average 0.09 mg/L of Fe^{2+}), thus the risk of iron precipitation is low. In contrast, in the confined aquifer of the Ljubljansko barje the concentrations of iron are elevated (> 0.2 mg/L) and risk of iron precipitation was

Table 1. Comparison of additional field measurements and chemical analyses (different sampling dates) with limitations of the installation, as indicated by heat pump manufacturers (Kmiecik et al., 2017)

			LJ1				LJ2				LJ3				LJ4		LJ5		LJ6				LJ7		LJ8		LJ9		LJ10		LJ11		LJ12	
			Value	RISK	Value	RISK	Value	RISK	Value	RISK	Value	RISK	Value	RISK	Value	RISK	Value	RISK	Value	RISK	Value	RISK	Value	RISK	Value	RISK	Value	RISK	Value	RISK	Value	RISK	Value	RISK	Value	RISK
Parameter	Risk*	Limit value	HP tap		Well (depth: 24 m)		Well (depth: 84 m)				HP tap				Well (depth: 92 m)		Well (depth: 92 m)		Well (depth: 72 m)				HP tap		HP tap		HP tap		HP tap		HP tap		HP tap	
Sampling date			28th March 2018		14th May 2018		27th March 2018		14th May 2018		28th March 2018		14th May 2018		27th March 2018		27th March 2018		27th March 2018		14th May 2018		28th March 2018		28th March 2018		28th March 2018		28th March 2018		28th March 2018		28th March 2018	
Cond. [mg/L]	0	<10	676	–	483	+	491	+	463	+	438	+	345	+	1024	–	502	–	375	+	417	+	340	+	463	+	461	+	380	+	389	+	703	–
	+	10 - 500																																
	–	>500																																
pH value	0	<7.5	7.28	0	7.33	0	7.1	0	7.5	0	7.68	+	7.57	+	7.12	0	7.81	+	7.51	+	7.6	+	7.65	+	7.56	+	7.68	+	7.58	+	7.77	+	7.23	0
	+	7.5 - 8																																
	–	>8																																
DO [mg/L]	+	<0.2	3.38	0	0.71	0	5.7	0	5.51	0	6.81	0	6.21	0	2.51	0	0.08	+	1.64	0	3.79	0	4.87	0	7.47	0	5.88	0	5.52	0	9.91	-	7.28	0
	0	0.2 - 8																																
	–	>8																																
Fe [mg/L]	+	<0.2	2.2	-	/	/	<0.03	+	/	/	<0.03	+	/	/	2.28	-	3.11	–	0.855	–	/	/	0.13	+	<0.03	+	<0.03	+	0.025	–	0.01	+	2.14	–
	–	>0.2																																
HCO_3^- [mg/L]	0	<70	289	+	355	0	231	+	253	+	260	+	286	+	466	0	265	+	253	+	261	+	221	+	268	+	270	+	243	+	229	+	415	0
	+	70 - 300																																
	0	>300																																
SO_4^{2-} [mg/L]	+	<50	15.5	+	16.1	+	18.5	+	18.1	+	21.9	+	22.4	+	75.4	0	<1.5	+	10	+	11.9	+	5.98	+	10.5	+	8.49	+	9.03	+	7.05	+	22.1	+
	0	50 - 100																																
	–	>100																																
Cl^- [mg/L]	+	<100	53.8	+	53.4	+	28.9	+	27	+	4.59	+	4.16	+	79.3	+	50.2	+	13.5	+	12.6	+	4.95	+	21.5	+	19.6	+	8.26	+	14.3	+	30.3	+
	0	100 – 200																																
	–	>200																																
NO_3^- [mg/L]	+	<100	<2.2	+	2.26	+	7.17	+	7.17	+	<2.2	+	<2.2	+	<2.2	+	<2.2	+	5.09	+	5.98	+	<2.2	+	5.18	+	4.87	+	4.92	+	4.12	+	<2.2	+
	0	>100																																
Mn [mg/L]	+	<0.05	0.06	-	/	/	<0.0001	+	/	/	0.029	+	/	/	0.06	-	0.13	-	0.012	+	/	/	0.0006	+	0.0003	+	0.0001	+	<0.0001	+	<0.0001	+	0.23	-
	-	>0.05																																
Risk	Corrosion		May lead to corrosion and installation isn't recommended		May lead to corrosion		May lead to corrosion		May lead to corrosion		No problems expected		No problems expected		May lead to corrosion and installation isn't recommended		May lead to corrosion and installation isn't recommended		May lead to corrosion and installation isn't recommended		No problems expected		No problems expected		No problems expected		No problems expected		May lead to corrosion and installation isn't recommended		Installation isn't recommended		May lead to corrosion and installation isn't recommended	
	Scaling – iron/ manganese		Possible – high Fe, DO		/		Low risk - low Fe, Mn concentrations		/		Low risk - low Fe, Mn concentrations		/		Possible – high Fe, DO		Possible – Fe, pH – if aerated		Possible – pH, DO, Fe		/		Low risk - low Fe, Mn concentrations		Low risk - low Fe, Mn concentrations		Low risk - low Fe, Mn concentrations		Low risk - low Fe, Mn concentrations		Low risk - low Fe, Mn concentrations		Possible – Fe, Mn, DO	

- (0) may lead to corrosion, when two or more parameters are exceeded
- (-) installation isn't recommended, if one of the parameter's limit is exceeded
- (+) material is usually resistant

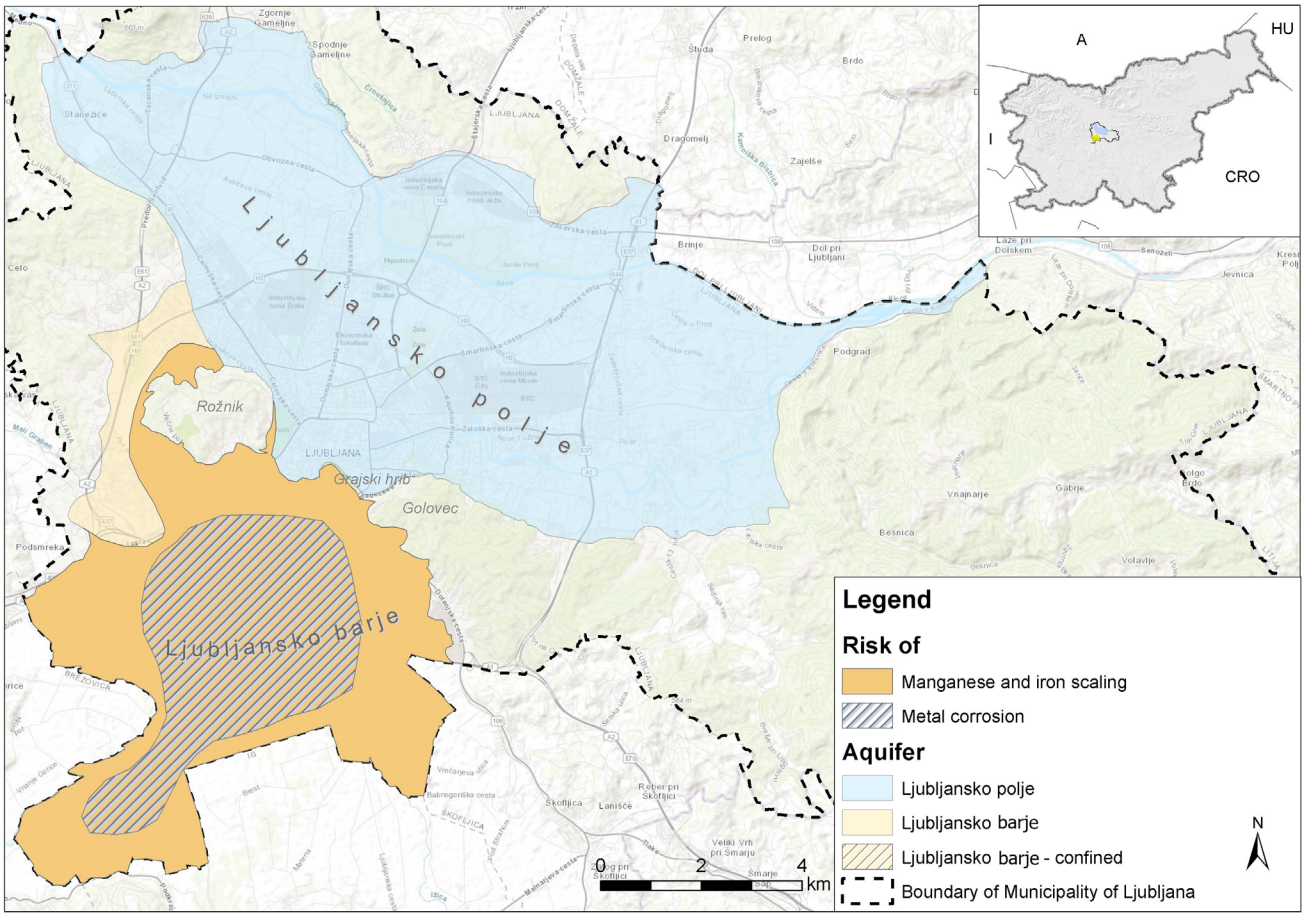

Fig. 8. Outline of area with risk of metal corrosion or iron and/or manganese scaling.

Table 2. Comparison of results of field parameter and chemical parameter measurements at tap or in well (March 27th, March 28th and May 14th, 2018).

Location	LJ1		LJ2		LJ3		LJ6	
Object type	tap	well	well	well	tap	tap	well	well
Sampling date	28th March	14th May	27th March	14th May	28th March	14th May	27th March	14th May
T [°C]	**13.0**	**10.1**	12.2	11.5	13.3	13.1	13.1	12.5
Cond [µS/cm]	**676**	**483**	491	463	438	345	375	417
pH value	*7.28*	*7.33*	7.10	7.50	*7.68*	*7.57*	7.51	7.6
Eh [mV]	*229*	*216*	*363*	*353*	400	332	96	175
DO [mg/L]	**3.38**	**0.71**	*5.7*	*5.51*	*6.81*	*6.21*	1.64	3.79
O_2 [%]	33.4		*55.0*	*52.2*	*67.5*	*60.8*	17	36.6
Fe^{2+} [mg/L]	0.27	/	<0.03	/	<0.03	/	0.186	/
Fe tot [mg/L]	2.2#	/	<0.03	/	<0.03	/	0.855	/
HCO_3^- [mg/L]	**289**	**355**	*231*	*253*	*260*	*286*	253	261
K^+ [mg/L]	*1.1*	*0.83*	*0.48*	*0.51*	*0.79*	*0.66*	1	0.97
Ca^{2+}[mg/L]	*81*	*83*	*88*	*88*	*56*	*58*	54	60
Mg^{2+}[mg/L]	*34*	*34*	*12*	*12*	*25*	*25*	22	23
SO_4^{2-}[mg/L]	*15.5*	*16.1*	*18.5*	*18.1*	*21.9*	*22.4*	10	11.9
Cl^- [mg/L]	*53.8*	*53.4*	*28.9*	*27.0*	*4.59*	*4.16*	13.5	12.6
NO3-[mg/L]	*<2.2*	*2.26*	*7.17*	*7.17*	*<2.2*	*<2.2*	5.09	5.98
Suspended solids [mg/L]	44	/	<10	/	<10	/	26	/
Mn [mg/L]	0.06	/	<0.0001	/	0.029	/	0.012	/
S diss. [mg/L]	<0.05	/	<0.05	/	<0.05	/	<0.05	/

- measured in laboratory (in-situ > 3 mg/L)
Italic – Comparable data (<10 % difference between measurements)
Bold –Noticeable difference between measurements (>40 % difference)

identified in the area of Ljubljansko barje aquifer. Taking into consideration these results and the hydrogeological conditions, the area with a high risk of threat to the efficient operation of open loop systems in the study area was outlined.

Additional measurements at the Ljubljansko barje indicate that the known operational problems of open loop systems are the consequence of manganese or/and iron precipitation. Higher sulphate and dissolved oxygen content also indicate corrosive groundwater. When compiling information on the chemical composition of groundwater in the aquifer, it must be taken into consideration that samples of water taken from the open loop system (from a tap) do not always represent the content of dissolved oxygen in groundwater of the aquifer. Due to the lack of data on the iron content of groundwater sampled from well, no interpretation of the processes that occur during heat extraction within the system was possible. This important issue should be addressed in following investigations.

Operational problems of open loop geothermal systems related to scaling or corrosion are most often the consequence of the fact that geothermal systems are installed without consideration of the chemical composition of the groundwater and hydrogeological conditions in general. In such cases mitigation measures are required in order to ensure the efficient operation of open loop systems.

The findings of this study underpin the importance of knowledge of the hydrogeological conditions and the composition of groundwater before the installation of an open loop system. Only a combination of said knowledge and proper consideration of the parameter limits recommended by heat pump manufactures can ensure the optimised, site specific selection, installation and efficient operation of geothermal systems.

Acknowledgments

The authors acknowledge the project GeoPLASMA-CE co-financed by Interreg CENTRAL EUROPE Programme, project MUSE (GeoERA) which has received funding from the European Union's Horizon 2020 research and innovation programme under grant agreement No 731166, and the financial support from the Slovenian Research Agency (research core funding No. P1-0020). The authors wish to thank Dejan Šram and Simona Adrinek for graphical work and help in cartography.

References

Abesser, C. 2010: Open-loop ground source heat pumps and the groundwater systems: A literature review of current applications, regulations and problems. British Geological Survey, Nottingham: 24 p.

AMIIGA: https://www.interreg-central.eu/Content.Node/AMIIGA.html (29. 6. 2018)

Appelo, C. A. J. & Postma, D. 2005: Geochemistry, groundwater and pollution (2nd ed.). A. A. Balkema Publishers, Leiden, London, New York, Philadelphia, Singapore: 647 p.

Auersperger, P. & Železnik Bračič, B. 2018: Poročilo o monitoringu podzemnih voda na območju odlagališča nenevarnih odpadkov Barje za leto 2017. Vodovod-Kanalizacija, d.o.o. Ljubljana: 66 p.

Bonte, M. 2015: Impacts of Shallow Geothermal Energy on Groundwater Quality. KWR Watercycle Research Institute. Iwa Publishing, London: 178 p.

Böttcher, F., Casasso, A., Götzl, G. & Zosseder, K. 2019: TAP - Thermal aquifer Potential : A quantitative method to assess the spatial potential for the thermal use of groundwater. Renew. Energ., 142: 85–95. https://doi.org/10.1016/j.renene.2019.04.086

Brons, H. J., Griffioen, J., Appelo, C. A. J. & Zehnder, A. J. B. 1991: (Bio) geochemical reactions in aquifer material from a thermal energy storage site. War. Res., 25/6: 729–736. https://doi.org/10.1016/0043-1354(91)90048-U

Donald, A. W. 1997: Geochemistry and Microbiology of Iron-Related Well-Screen Encrustation and Aquifer Biofouling in Suffolk County, Long Island, New York. Coram, New York: 42 p.

Driscoll, F. G. 1986: Groundwater and wells. Filter/Johnson Screens. St. Paul: 1089 p.

Eijkelkamp 2017: Submersible pump Grundfos MP 1 / Redi-Flo2, User manual. Giesbeek: 19 p.

Gonzalez, E., Parra, M.I. & Hernandez, M. 2019: Hardness, Alkalinity, Langelier Saturation Index, Saturation Index, Ryznar Index, Puckorius Index Calculator. http://fcca.es/en/products-and-publications/online-software/calculation-of-langelier-index-saturation-ryznar-puckorius-larson-hardness-and-alkalinity/ (25. 9. 2019)

Götzl, G., Holeček, J., Janža, M., Koren, K., Cernak, R. & Riedel, P. 2018: Identification of problematic groundwater bodies A.T2.3. GeoPLASMA-CE report: 31 p.

Hach Lange 2012: Dr 2800 TM portable spectrophotometer. Users manual. https://www.hach.

com/asset-get.download.jsa?id=7639982019 (25. 9. 2019)

Holm, T. R., Eisenreich, S.J., Rosenberg, H. L. & Holm, N.P. 1987: Groundwater geochemistry of short-term aquifer thermal energy storage test cycles. Water Resources Research, 23/6: 1005–1019. https://doi.org/10.1029/WR023i006p01005

Howsam, B. P. 1988: Biofouling in Wells and Aquifers. Water and Environment Journal, 2. 209 - 215. https://doi.org/10.1111/j.1747-6593.1988.tb01274.x

Houben, G. J. 2003: Iron oxide incrustations in wells. Part 2: Chemical dissolution and modeling. Applied Geochemistry, 18/6: 941–954. https://doi.org/10.1016/S0883-2927(02)00185-3

INCOME: http://www.life-income.si/index00a8.html?lang=2 (29. 6. 2018)

Jamnik, B., Janža, M., Smrekar, A., Breg Valjavec, M., Cerar, S., Cosma, C., Hribernik, K. Krivic, M., Meglič, P., Pestotnik, S., Piepenbrink, M., Podboj, M., Polajnar Horvat, K., Prestor, J., Schüth, C., Šinigoj, J., Šram, D., Urbanc, J. & Žibret, G. 2014: Skrb za pitno vodo. Geografija Slovenije, 31, Založba ZRC, Ljubljana: 130 p.

Janža, M. 2009: Modelling heterogeneity of Ljubljana polje aquifer using Markov chain and geostatistics. Geologija, 52/2, 233–240. https://doi.org/10.5474/geologija.2009.023

Janža, M., Lapanje, A., Šram, D., Rajver, D. & Novak, M. 2017: Research of the geological and geothermal conditions for the assessment of the shallow geothermal potential in the area of Ljubljana, Slovenia. Geologija, 60/2: 309–327. https://doi.org/10.5474/geologija.2017.022

Kemmer, F. N. 1977: Water, the universal solvent. Oak Brook, Nalco Chemical Co.: 155 p.

Kmiecik, E., Tomaszewska, B. & Mazurkiewicz, J. 2017: The Quaternary groundwater as the low temperature energy source for heat pumps in Małopolska Province. International Conference on Advance in Energy Systems and Environmental Engineering (ASEE17). E3S Web of Conferences, 22, 00082. https://doi.org/10.1051/e3sconf/20172200082

Lentech 2018a: Langelier Saturation Index calculator. https://www.lenntech.com/calculators/langelier/index/langelier.htm (7. 8. 2018)

Lentech. 2018b: Ryznar Stability Index calculator. https://www.lenntech.com/calculators/ryznar/index/ryznar.htm (7. 8. 2018)

Mencej, Z. 1990: The gravel fill beneathe the lacustrine sediments of the Ljubljansko barje. Geologija, 31/32 (1988/89): 517–53.

Park, Y., Kim, N. & Lee, J. Y. 2015: Geochemical properties of groundwater affected by open loop geothermal heat pump systems in Korea. Geosciences Journal, 19/3: 515–526. https://doi.org/10.1007/s12303-014-0059-x

Power, J. & Prasad, R. 2010: Iron and Manganese. Soil Fertility Management for Sustainable Agriculture, 255–268. https://doi.org/10.1201/9781439821985.ch13

Prestor, J. & Janža, M. 2002: The Impact of Ljubljana' s Waste Deposit Barje on Groundwater. Geologija, 45/2: 505–512. https://doi.org/10.5474/geologija.2002.056

Pringsheim, E.G. 1949: Iron Bacteria, Botany School, University of Cambridge, 24: 200–245.

Rafferty, K. 1999: Scaling in geothermal heat pump systems. Geo-Heat Center Oregon Institute of Technology: 60 p.

Roslan, A., Arbanah, M., Tukiman, N., Ibrahim, N. N. & Juanil, A. R. 2017: The effects of ethylene glycol to ultrapure water on its specific heat capacity and freezing point. J. Appl. Environ. Biol. Sci. 7/7S: 54-60.

Schofield, M. J. 2002: Corrosion. Plant Engineer's Reference Book (Second Edition). https://www.sciencedirect.com/topics/materials-science/corrosion (13. 11. 2019)

Smith, S. A. & Tuovinen, O. H. 1985: Environmental analysis of iron-precipitation bacteria in ground water and wells. Wiley Online Library, 5: 45–52.

Šram, D., Brenčič, M., Lapanje, A. & Janža, M. 2012: Prostorski model visečih vodonosnikov na Ljubljanskem polju. Geologija, 55/1: 107–116. https://doi.org/10.5474/geologija.2012.008

VDI-Richtlinien. 2001: VDI 4640 Part 2: Thermal use of the underground Ground source heat pump systems. Dűsseldorf: 43 p.

Waterloo Hydrogeologic. 2018: AquaChem 2014.2.

Woyessa, A. O. 2011: Identification of Hydrochemical Processes in the Screen Environment in Shallow Geothermal Wells from Gardermoen Identification of Hydrochemical Processes in the Screen Environment in Shallow Geothermal Wells from Gardermoen. Master Thesis, Department of Geosciences, University of Oslo: 78 p.

WTW GmbH 2004: pH / Cond 340i. In Operating manual. 82 p. http://www.durko.com.tr/Uploads/Dokuman/ddb67ac7dd92246b02d-9cd7d4e27eb58.pdf (25. 9. 2018)

WTW GmbH 2008: SenTix® PtR SenTix® Au SenTix® Ag. In ORP electrodes. 20 p. https://static.wtw.com/fileadmin/upload/Service/Downloads/Bedienungsanleitungen/

Laboranalytik/ba75741e01_sentix_Metallelektroden.pdf (25. 9. 2018)

WTW GmbH 2010: Fdo® 925. In Operating manual. 32 p. http://www.globalw.com/downloads/WQ/FDO925.pdf (25. 9. 2018)

Zuurbier, K.G., Hartog, N., Valstar, J., Post, V.E.A. & van Breukelen, B.M. 2013: The impact of low-temperature seasonal aquifer thermal energy storage (SATES) systems on chlorinated solvent contaminated groundwater: Modeling of spreading and degradation. J. Contam. Hydrol, 147: 1–13. https://doi.org/10.1016/j.jconhyd.2013.01.002

Internet sources:

Internet 1: GeoPLASMA -CE Shallow Geothermal Energy Planning, Assessmet and Mapping Strategies in Central Europe: https://www.interreg-central.eu/Content.Node/GeoPLASMA-CE.html (29. 6. 2018); https://portal.geoplasma-ce.eu/ (25. 9. 2019)

Internet 2: Statistical Office; Republic of Slovenia: https://pxweb.stat.si/SiStat/en (11. 10. 2019)

Internet 3: Slovenian environmental agency. Environmental atlas of Slovenia: http://gis.arso.gov.si/atlasokolja/profile.aspx?id=Atlas_Okolja_AXLŽARSO&culture=en-US (16. 10. 2019)

Internet 4: GIS-ARSO portal: http://gis.arso.gov.si/apigis/podzemnevode/ (29. 6. 2018)

GEOLOGIJA *62/2*, 251–266, Ljubljana 2019
https://doi.org/10.5474/geologija.2019.012

Statistical analysis of groundwater drought on Dravsko-Ptujsko polje

Statistična analiza suše podzemne vode na primeru Dravsko-Ptujskega polja

Simona ADRINEK[1] & Mihael BRENČIČ[2,1]

[1]Geological Survey of Slovenia, Dimičeva ulica 14, SI-1000 Ljubljana, Slovenia;
e-mail: simona.adrinek@geo-zs.si
[2]University of Ljubljana, Faculty of Natural Sciences and Engineering, Department of Geology,
Aškerčeva cesta 12, SI-1000 Ljubljana, Slovenia

Prejeto / Received 8. 10. 2019; Sprejeto / Accepted 12. 12. 2019; Objavljeno na spletu / Published online 24. 12. 2019

Key words: definition of groundwater drought, Standardized Groundwater Index - SGI, intergranular porosity, unconfined aquifer

Ključne besede: definicija suše podzemne vode, standardizirani indeks podzemne vode – SGI, medzrnska poroznost, odprt vodonosnik

Abstract

Drought is a complex phenomenon and can be defined in many ways. It is a globally growing problem that occurs on a time scale ranging from months to years. There are several types of drought, but the least investigated is groundwater drought. Globally, research on it started relatively recently, in the last decade. In Slovenia, there are almost no data on groundwater drought. In this research, we focused on statistical analysis of groundwater level diagrams of individual groundwater stations, which can determine periods of groundwater drought. The first method used is based on ranking statistics defined by lower percentiles that indicate low groundwater level. Another approach was based on univariant Standardized Groundwater Index – SGI. As a case study, the unconfined Quaternary aquifer of Dravsko-Ptujsko polje was chosen. The results show that the groundwater deficits in the groundwater stations appear simultaneously but differ in intensity and duration of each drought period. The important conclusion is that the intensity of groundwater drought does not depend on the length of an event but more on thickness of the unsaturated aquifer zone. Also, groundwater stations located on the western rim below Pohorje Mountains have a higher amplitude of groundwater fluctuations than the others. The result of this are more intensive dry periods with longer duration. On the other hand, we have locations in the central and eastern part of the Dravsko-Ptujsko polje with more damped fluctuation, which leads to less intensive but more frequent groundwater drought events.

Izvleček

Suša je pojav, ki v svetovnem merilu predstavlja vedno večji problem. Poznamo več vrst suš, med katerimi je najslabše razumljena suša podzemne vode. Z raziskavami suše podzemne vode se je hidrogeologija začela intenzivneje ukvarjati šele v zadnjem desetletju. Za območje Slovenije skorajda nimamo podatkov o suši podzemne vode. V tej raziskavi smo se osredotočili na statistično analizo diagramov nihanja gladin podzemne vode v posamezni opazovalni vrtini, s katerimi lahko določimo sušna obdobja. Prva metoda temelji na vrstilni statistiki, določeni z najnižjo percentilno vrednostjo niza meritev obravnavane opazovalne vrtine. Druga metoda uporablja univariatni indeks podzemne vode – SGI. Za pilotno območje je bil izbran odprti kvartarni vodonosnik Dravsko-Ptujskega polja. Rezultati so pokazali, da se primanjkljaj podzemne vode pojavi na različnih mestih skoraj hkrati, a se razlikuje v intenziteti in trajanju posameznega sušnega pojava. Opazovalne vrtine, ki se nahajajo na zahodnem obrobju pod Pohorjem imajo višje amplitude nihanja podzemne vode kot vrtine v osrednjem delu Dravsko-Ptujskega polja, kar je pogojeno z večjo debelino nezasičene cone vodonosnika. To vpliva na bolj intenzivna sušna obdobja z daljšim trajanjem. Na drugi strani imajo opazovalne vrtine v osrednjem in vzhodnem delu Dravsko-Ptujskega polja bolj dušeno nihanje gladine podzemne vode, kar povzroči manj intenzivna, a bolj pogosta sušna obdobja.

Introduction

Even though Slovenia is a water-rich country, several drought events appeared in the recent past (in years 2003, 2012, 2013, 2017), which had substantial impact on national economy (Sušnik & Gregorič, 2017; Flis, 2017). By some climatic models, it is also predicted that in the future drought will be a more frequent event (Andjelov et al., 2016). The most important drought recognized in Slovenia is agricultural drought, which is usually explained as a meteorologically driven drought event. Not much is known about other droughts, among which groundwater drought can be very important. In everyday life, attention is usually paid to meteorological and agricultural drought, because their influence is immediate and visible to everybody. As well as in other regions around the world, in Slovenia, extensive research has been performed on drought and several results regarding drought are rising significantly, but there was not much effort put in the research of groundwater drought. Research on the latter started only recently and not so many results of it are published. Due to the role of groundwater in Slovenian economy, groundwater drought can have important consequences. From that point, the question how groundwater drought is influencing general water availability in water cycle and overall groundwater management can be raised.

In Slovenia, monitoring of groundwater quantitative status is well established (Andjelov et al., 2006). In some of the alluvial aquifers, the monitoring network is relatively dense and enables detection of local trends of decrease or increase of groundwater levels, which can be taken as indicators of groundwater storage change in the aquifer. Based on groundwater monitoring results and with the application of methodology for groundwater drought detection, it would be possible to optimize groundwater management in relation to extreme event appearance.

This paper aims to investigate available definitions of groundwater drought and possible indices from the literature. Based on the collected information, it was intended to define a drought indicator suitable for analysing the effects of drought in north-eastern Slovenia. In the second step, the intention was to compare meteorological and groundwater droughts. As a case study, the unconfined Quaternary aquifer of Dravsko-Ptujsko polje was chosen. The area was chosen due to the availability of relatively long and continuous set of groundwater measurements on 22 groundwater stations as well as due to the natural characteristics of the aquifer, which is well drained and its response to the underground water shortage is relatively rapid. The analysis performed was phenomenological; during the interpretation of the calculated indices, several questions arose in relation to groundwater level time depended trends. These questions remain to be open due to their complexity, which goes over the scope of the paper.

Methods

Groundwater drought definitions

There is no uniform and widely accepted definition of groundwater drought. Most of the available definitions rely on the fact that groundwater drought appears with a decrease of groundwater or piezometric level in the aquifer. This decline and consequent drought can be a consequence of natural or anthropogenic factors (Haas & Birk, 2017, Namdar Ghanbari & Bravo, 2011); therefore, we can have natural groundwater droughts and anthropogenically induced groundwater droughts.

One of the possible approaches to define groundwater drought is a statistical analysis of groundwater level fluctuation that is described as time series measured in individual groundwater stations, which is indicated through a decrease of groundwater or piezometric level. Two possible groups of measures can be applied; the first is based on ranking statistics of groundwater measurements, and the second is based on groundwater drought indices. Their application is similar to other indices applied in studies of meteorological and hydrological droughts (Dracup et al., 1980; Palmer, 1965; Vicente-Serrano et al., 2010; Brenčič, 2016). For both groups of measures, groundwater drought is defined when values are smaller than the critical measure.

The first method is ranking statistics, defined by percentiles when groundwater level in the aquifer falls below the critical value in a given period (Van Lanen & Peters, 2000). Critical value is defined as a selected percentile of all measurements and is usually based on socioeconomic or environmental aspects (Hisdal & Tallaksen, 2000). Studies of various drought aspects in Slovenia showed that, for a reliable drought estimate, at least 30-year series of continuous measurements are needed (Kobold et al., 2012). Three useful critical drought percentiles were defined: percentile P_{25} is a critical value when intensive monitoring of drought starts, percentile P_{10} is a critical value when the drought warning starts,

and percentile P_5 represent onset of protection measures (Kobold et al., 2012). The same percentiles were used in our study.

The second method is based on groundwater drought indices, which are based on similar definitions as meteorological drought indices. In our study, we have applied Standardized Groundwater Index - SGI (Bloomfield & Marchant, 2013), which is based on groundwater level measurements. For representation of SGI, a proper selection of the time window is necessary. Its calculation depends on the available time series of groundwater measurements. For a sufficiently long measurement period where we want to determine the regional prevalence of drought (more than 30 years), it is more appropriate to use annual data of the selected parameter; while for a shorter period of time (less than 30 years), it is more appropriate to use the monthly values of the selected parameter, which give more precise local values (Mishra & Singh, 2010; Brenčič, 2017).

In our study, results of groundwater drought calculations were also compared with meteorological drought indices. As an indicator of meteorological drought, Standardized Precipitation Index – SPI was used (McKee et al., 1993). This is a univariate index where the only input parameter is precipitation. Its application is becoming more and more established, since it can quantify drought periods with a deficit or excess of precipitation at different time scales (Gregorič & Ceglar, 2017; Ceglar & Kajfež-Bogataj, 2008; Sušnik & Pogačar, 2010; Sušnik, 2014; Brenčič, 2016; Haas & Birk, 2017). It is based on the long-term average of the rainfall amount, which is often considered as a monthly value.

Statistical methods

Statistical analyses were carried out on public domain monitoring sites operated by the Agency for the Environment of RS (ARSO, 2018). Data were taken from 4 precipitation stations and from 22 groundwater stations (Fig. 1).

The daily groundwater level data were calculated to average monthly values, for which the continuity and density at individual groundwater station were analysed. Some of them were omitted due to inadequate measurements or were corrected with linear interpolation. Since the time series of the available data sets among the groundwater stations are not the same, we have chosen four different time intervals that cover the different measuring ranges. Groundwater level data were analysed with frequency distribution parameters where we described the properties of the data with respect to shape, position, and dispersion.

With time series diagrams, we detected anomalous groundwater level trends that can influence stationarity required for frequency analysis. Such stations were omitted from further analysis. Data were also analysed on a normal prob-

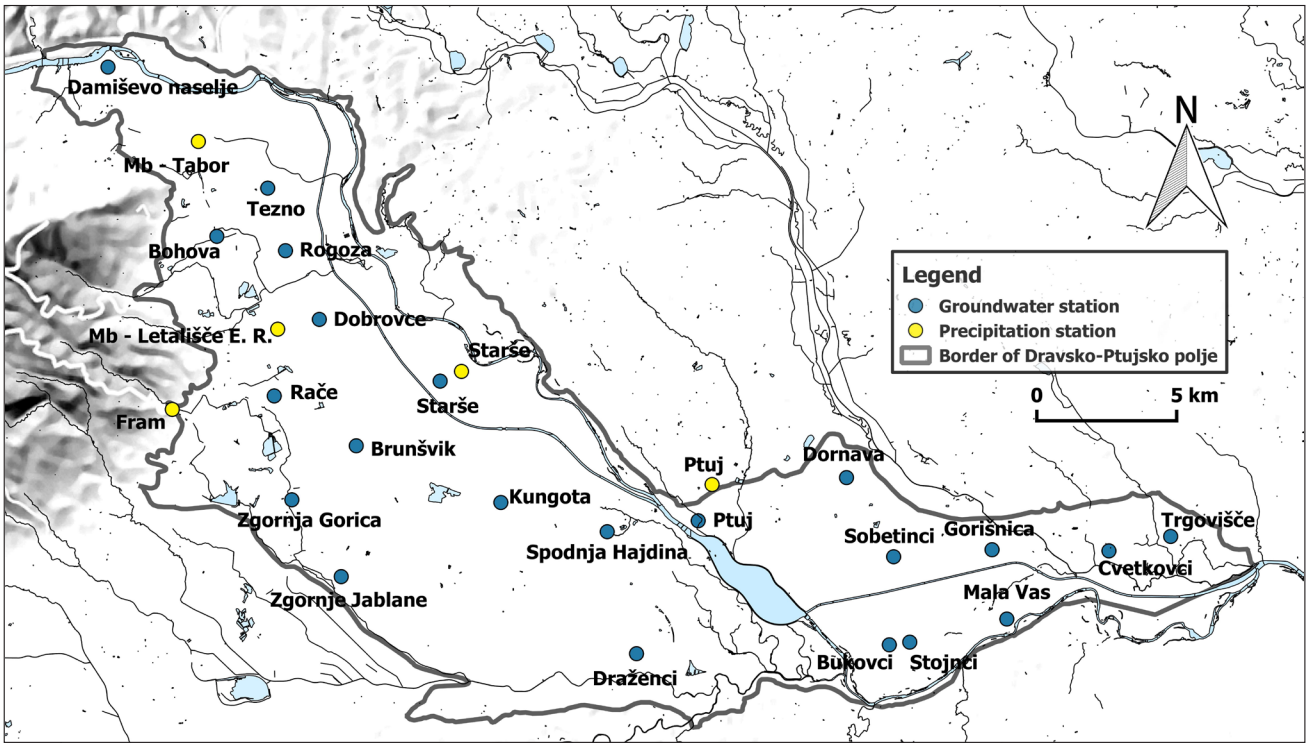

Fig. 1. Dravsko-Ptujsko polje groundwater and precipitation station locations (cartographic basis Geodetska uprava Republike Slovenije, DPK750, 2017).

ability plot where the extreme values (i.e. floods, droughts) are clearly visible, since the deviations of the lowest and highest values of the actual measurement curve are clearly separated from the theoretical curve.

For further calculations, we checked the probability distribution of groundwater levels. We used the Kolmogorov-Smirnov test, which is a non-parametric test for continuous probability distributions. It is based on the deviation of the distance between the distribution function and the comparative distribution function, which is then compared with the tabulated critical value (McKillup & Darby Dvar, 2010).

We also checked the measurements of the theoretical distribution with the Anderson-Darling test, which is suitable for testing continuous data and is based on a comparison of the empirical and theoretical distribution function (Stephens, 1974). It is a modification of the Kolmogorov-Smirnov test and gives more weight to the tails. The equation of Anderson-Darling test is defined as:

$$AD = -n - \frac{1}{n}\sum_{i=1}^{n}\{(2i-1)\ln F(X_i) + (2n+1-2i)\ln(1-F(X_{n-i+1})\} \quad (1)$$

n sample size

$F(X_i)$ cumulative distribution function for the specified theoretical distribution

i the ith rank when the data is sorted in ascending order

Ranking statistics of percentiles

The first method used for the analysis of groundwater drought was based on ranking statistics of percentiles, using the lowest 10 % of the measurements of an individual groundwater station – P_{10}. They were presented on a duration curve (Fig. 2), which shows the percentage of time in which the groundwater level was lower or equal to a certain limit value (Searcy, 1959). The values of the groundwater level were arranged in a descending order from 1 to n and the percentage was ascribed according to the equation:

$$P(\%) = \left(\frac{M}{n}\right) * 100 \quad (2)$$

P possibility that value exceed or is equal to a certain % of the time

M ranked value of n data

n number of all data

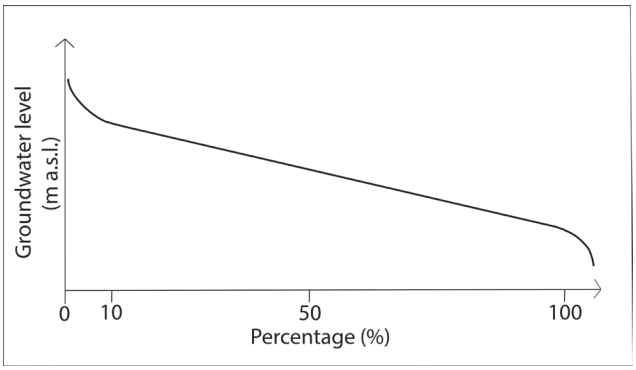

Fig. 2. Schematic representation of groundwater level duration curve.

The critical limit value P_{10} was used for the calculation of groundwater deficit D. The method for calculating D is based on the following equation (Peters et al., 2005 & 2006) (Fig. 3):

$$D = \int_{t_0}^{t_x}[P_{10} - x_i]dt \quad (3)$$

t_0 start of the drought (day)

t_x end of the drought (day)

X_i data on interval between t_0 and t_x

P_{10} threshold level value of observed data (m)

The second method used for analysis of groundwater drought was based on index calculations. We applied the concept of the SGI calculation (Bloomfield & Marchant, 2013), which has the same logic as the SPI calculation (McKee et al., 1993).

Calculation of standardized precipitation index – SPI

SPI is a univariate index where the only input is precipitation data. The index represents the number of standard deviations of precipitation from the long-term average in the observed period. This applies only to normally (Gaussian) distributed precipitation, but this is not usually their characteristic. Therefore, the appropriate theoretical distribution must be first determined. The first step is to determine the probability density that describes the past series of precipitation. This gives us a probability distribution of a continuous random variable for the selected time range of data. The range can be given for a different set of precipitation, for example, SPI1 (one month) and SPI3 (three months). The next step is to calculate the distribution function for the selected sum of precipitation that is normalized. The values obtained represent SPI (Table 1). The distribution, where the mean value is 0 and the standard deviation 1, is called the standardized Gaussian distribution (McKee et al., 1993).

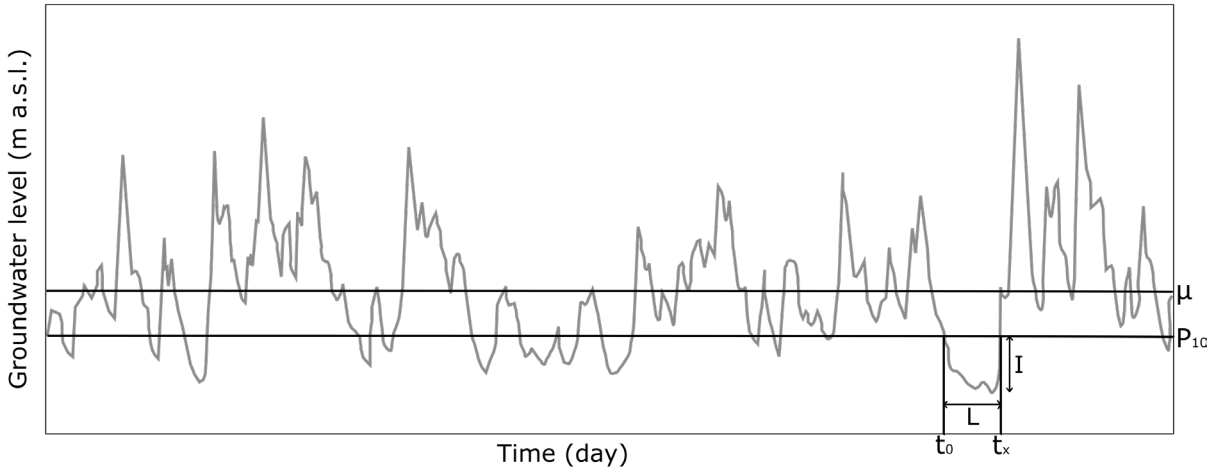

μ - arithmetric mean P10 - 10 % of lowest data t0 - start of drought tx - end of drought L - duration of drought I - intensity of drought

Fig. 3. Groundwater level fluctuations with drought parameters for groundwater station Gorišnica (1990–2016).

The most common theoretical distribution used is the gamma distribution that needs to be modified, because it is not defined at a value of 0 but occurs often due to the absence of precipitation. Then the cumulative value is transformed into a Gaussian distribution (Thom, 1966; McKee et al., 1993). The gamma distribution of a given variable is defined as follows:

$$g_x(x) = \frac{1}{\beta^{\alpha}\Gamma(\alpha)} x^{\alpha-1} e^{-\frac{x}{\beta}} \quad (4)$$

$\alpha > 0$	shape parameter
$\beta > 0$	scale parameter
$x > 0$	precipitation amount
$\Gamma(\alpha) = \int_0^{\infty} y^{\alpha-1} e^{-y} dy$	gamma function

Table 1. SPI and SGI categories (after McKee et al., 1993).

SPI values	Drought category	SGI values	Drought category
≥ 2.00	Extremely wet		
1.50 to 1.99	Very wet	Above 0	No drought
1.00 to 1.49	Moderately wet	–1.00 to 0	Minimal drought
–0.99 to 0.99	Near normal	–1.50 to –1.00	Moderate drought
–1.49 to –1.00	Moderately dry	–2.00 to –1.50	Severe drought
–1.99 to –1.50	Severely dry	< –2.00	Extreme drought
≤ –2.00	Extremely dry		

The parameters α and β should be defined so that they match the precipitation distribution for each time series and station separately. The process was described in more detail by McKee et al. (1993), who determined the calculation of the parameter estimates by the maximum probability method. The equations are as follows:

$$\hat{\alpha} = \frac{1}{4A}\left(1 + \sqrt{1 + \frac{4A}{3}}\right) \quad (5)$$

$$\hat{\beta} = \frac{\overline{x}}{\hat{\alpha}} \quad (6)$$

$$A = ln\overline{x} - \frac{\sum lnx}{n} \quad (7)$$

With the obtained parameters $\hat{\alpha}$, $\hat{\beta}$, and A, we were able to find the distribution function. Since the gamma distribution is not defined at x=0, the equation is modified and defined as the following:

$$H(x) = q + (1 - q)G(x) \quad (8)$$

q	probability with no precipitation (x=0); $q = m/n$
m	number of precipitation periods
n	number of observations

The final step is to transform the theoretical distribution into a standardized Gaussian variable with an average of 0 and a standard deviation of 1.

For a quicker calculation of SPI, a computer program was used. The program is available on the website of US National Drought Management Centre (2015).

Calculation of standardized groundwater index – SGI

Standardised Groundwater Index - SGI (Bloomfield & Marchant, 2013; Draksler et al., 2017) represents the number of standard deviations of the groundwater level deviating from the long-term average for the selected interval. SGI is based on the same principle as SPI, but there are two major differences. The first is that, for the groundwater level as an input variable, it is unnecessary to separate the parameter into predefined time periods. The second difference is in choosing the correct fit and distribution of raw data, since SGI seldom fits the gamma distribu-

tion, as is typical for SPI (Bloomfield & Marchant, 2013). If the parameter is unevenly distributed, we use non-parametric methods. In this case, each calculated monthly measurement of groundwater level gets a value that is determined on a basis of rank within the entire set of measurements. The obtained values are then determined by the inverse normal cumulative distribution. If measurements are already evenly distributed, parametric methods may be used following the procedure described for the SPI calculation. The results are SGI values within the range from +2 to –2 (Table 1).

In our case, we selected a Gaussian distribution for transformation, because we get the best fit depending on theoretical distribution. We randomly transformed the variable with the following equation (Bloomfield et al., 2015; Draksler et al., 2017; Chu, 2018):

$$z = \frac{x - \mu}{\sigma} \tag{9}$$

x random variable

μ arithmetic mean of data in observed time interval

σ standard deviation of data in observed time interval

Calculation of the probability of a continuous, normally distributed variable was performed using the following equation (Bryc, 1995):

$$p_i = \frac{1}{\sigma\sqrt{2\pi}} e^{-\frac{(x-\mu)^2}{2\sigma^2}} \tag{10}$$

To use the inverse normal cumulative distribution function, each value of the probability p_i is converted from $1/(2n)$ *to* $1 - 1/(2n)$.

The relation between SPI and SGI for groundwater stations were analysed with Pearson's correlation coefficient (Rodgers & Nicewander, 1988):

$$r = \frac{\sum_{i=1}^{n}(x_i - \overline{x})(y_i - \overline{y})}{\sqrt{\sum_{i=1}^{n}(x_i - \overline{x})^2}\sqrt{\sum_{i=1}^{n}(y_i - \overline{y})^2}} \tag{11}$$

$\overline{x}$ average value of observations for x

$\overline{y}$ average value of observations for y

n number of observations

x_i, y_i observed values with index i

Results

Groundwater stations and time intervals

After reviewing the calculated monthly groundwater measurements on 22 groundwater stations, the availability and consistency of the data were checked. At some groundwater stations, the data sets are not long enough, they do not coincide with other stations, or they do not fit to the theoretical distribution (possible reasons are indicated for each selected time interval separately). Because of that, some stations were omitted (Table 3). Where the set of missing monthly values for individual groundwater station was shorter than 6 months (station Brunšvik, Kungota, Zgornje Jablane, Spodnja Hajdina), they were replaced by linear interpolation based on the comparison with neighbouring stations. Stations used in the analysis are presented in Table 2 and Figure 4.

To compare results of calculations, the time intervals between different stations must overlap. Based on the data overlapping, four time intervals were defined (Table 2).

1. 1956–2000: The period enables to detect older dry periods, but for this period, only two stations are suitable for the analysis. During this period, boundary conditions of Dravsko-Ptujsko polje aquifer has changed, which gave a disadvantage to the analysis and caused substantial changes in time-dependent trends and groundwater level fluctuations.

2. 1982–2012: Due to a 30-year time range, this is the most suitable interval. Six stations are suitable, which allows general analysis of drought spatial distribution. Unfortunately, in this time interval, no station is available in the west and south part of the observed area. During the interval changes in the aquifer, boundary conditions were present.

3. 1991–2011: The advantage of the time interval is a relatively large number of 12 groundwater stations, distributed throughout the entire area. Fluctuations of groundwater levels at the stations do not have a distinct trend, which improves the quality of drought analysis. The disadvantage of the interval is a short period that covers only 20 years, which is not entirely appropriate for the analysis of SGI. According to the basic methodology, the calculation requires at least a 30-year dataset (Bloomfield & Marchant, 2013).

4. 1990–2016: The interval was chosen to analyse recent dry periods. The interval is not entirely appropriate, as it has a length of 26 years. The number of relevant stations is 12, which is providing reasonable spatial representation. The disadvantages of the period are bigger changes in groundwater levels that happened from 2012 at several observation stations.

Table 2. Groundwater stations used in the analysis.

Name of the borehole	Location	GKX [m]	GKY [m]	Measuring period	Selected period			
					1. 1956–2000	2. 1982–2012	3. 1991–2011	4. 1990–2016
0890	Bohova	151899	550523	1990–2016			X	X
1710, Bru-1/11	Brunšvik	144522	555551	1956–2016	X			
2401, 2411, 2412, Ku-2/09	Kungota	142561	560725	1990–2016			X	X
1250, Rač-1/11	Rače	146264	552615	1990–2016			X	X
2830, SHaj-2/14	Spodnja Hajdina	141564	564525	1981–2016		X	X	X
2120, Sta-1/11	Starše	146842	558519	1981–2016		X	X	X
1631	Zgornja Gorica	142587	553273	1990–2016			X	X
1600	Zgornje Jablane	139878	555058	1956–2016	X	X	X	X
0721	Tezno	153620	552320	1969–2016		X	X	X
0370, Do-2/09	Dornava	143579	573033	1981–2016		X	X	X
0152	Gorišnica	141084	578251	1990–2016			X	X
0283, Sob-1/14	Sobetinci	140792	574746	1990–2016			X	X
0060	Trgovišče	141641	584612	1990–2016		X	X	X

Table 3. Groundwater stations that were omitted from the analysis.

Name of the borehole	Location	GKX [m]	GKY [m]	Measuring period
0290	Damiševo naselje	157858	546607	1979–1989
1030	Dobrovce	148990	554200	1956–2016
3040, Lp-01	Draženci	137248	565618	1981–2016
Rog-1/11	Rogoza	151413	552973	2012–2016
Buk-1/14	Bukovci	137666	574631	2015–2016
0531, 0721	Ptuj	141989	567766	1982–2016
0051, 0230	Cvetkovci	141100	582420	1960–1981
0210, 0211	Mala Vas	138633	578811	1965–1984
0280	Sobetinci	140792	574746	1954–1983
0240	Stojnci	137770	575360	1981–2015

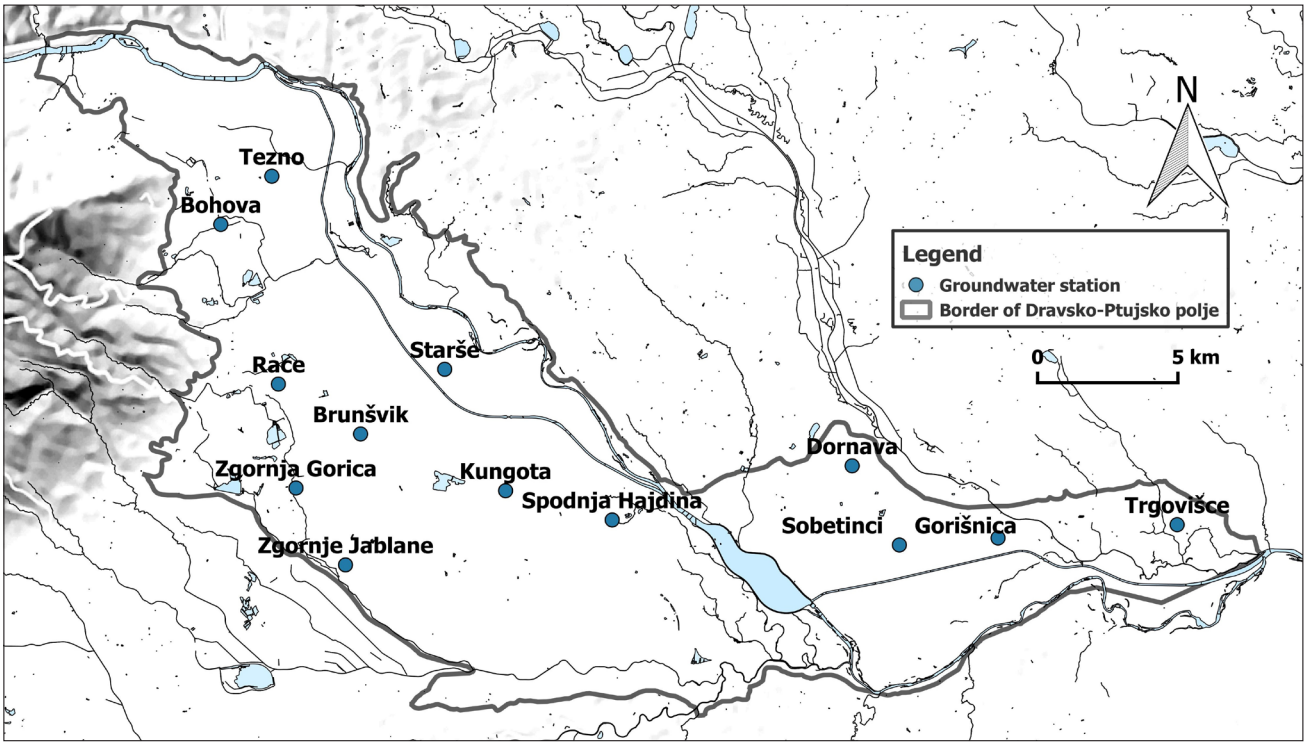

Fig. 4. Dravsko-Ptujsko polje groundwater station locations that were used in analysis (cartographic basis Geodetska uprava Republike Slovenije, DPK750, 2017).

Trend analysis

In most cases, the measurements are continuous and distributed as unimodal distributions. For groundwater stations where the data deviate from the unimodal distribution, it is typical that they have a large amplitude of fluctuations (e.g. Rače and Starše station), or the aquifer reacts rapidly to the periods of recharge, which results in high deviations from the average values of the groundwater level (e.g. the Sobetinci station). Therefore, models of unimodal distributions cannot be approved by the testing with Kolmogorov-Smirnov and Anderson-Darling tests. Such behaviour can be observed on stations Rače (Fig. 5a), Spodnja Hajdina (Fig. 5b), Zgornje Jablane, Starše, Trgovišče, and Sobetinci.

At such stations, further processing of data was not performed. Even though this is a real condition in the aquifer, it is a result of influences on the aquifer, which cannot be defined without detailed analysis. A significant linear trend in groundwater levels influences time appearance of drought events through time. For further analysis, different time intervals were selected, such that groundwater levels were not deviating from long-term average.

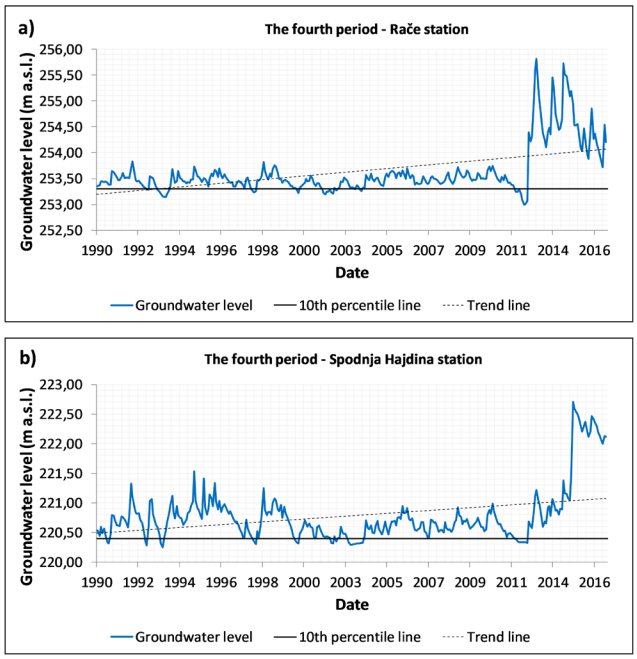

Fig. 5. a) Fluctuation of groundwater for the Rače station (fourth interval, between years 1990 and 2016). b) Fluctuation of groundwater for the Spodnja Hajdina station (fourth interval between years 1990 and 2016).

Time intervals analysis

In the continuation, each time interval is presented in detail. In the tables (Tables 4–7) are data for individual groundwater station: the range of groundwater level fluctuations, number of drought periods, trend of groundwater level fluctuations, maximum intensity *I*, maximum deficit *D* of the dry period defined as lowest 10 % percentile – P_{10}, and minimum and maximum drought duration.

The **first interval** (Table 4) represents measurements from year 1956 to year 2000. The Brunšvik station has stronger intensities *I* of the dry periods than the Zgornje Jablane station, which is probably due to a higher amplitude of groundwater level fluctuation. Same can be said for the size of the deficit *D* of drought periods, which is greater at the Brunšvik station. We assumed that this is a consequence of a thicker aquifer, which, in addition to rainfall, is also supplied by Pohorje streams. Since groundwater is located at a depth of 10 to 15 m, it takes longer to experience drought, which in turn means that it is more intense and long-lasting. The Zgornje Jablane station is in the more southwestern part of the Dravsko polje, where the aquifer is limited by the Holocene clay sediments of Pohorje streams. We can still define the fluctuation as large (depending on the range of amplitudes of other groundwater stations in the Dravsko-Ptujsko polje), but due to the low groundwater depth (1–5 m), the drought is recovered with short-term precipitation. This is confirmed by the fact that we noticed many shorter dry periods (2–3 months) in this area.

Calculation of SGI (Fig. 6) shows that the dry periods in the past did not appear as often as in the period from 1980 to 2000. Severe droughts indicated by a value of –1.5 and less have been occurring almost every year since 1975. The calculated SGI that shows periods of severe drought coincide with the drought periods defined by P_{10}.

The **second interval** (Table 5) represents measurements from year 1982 to year 2012. We can see that the intensities *I* of the dry periods of the Dornava, Tezno, and Starše stations are stronger. For the Trgovišče and Spodnja Hajdina, the

Table 4. Descriptive statistics for the first interval between years 1956 and 2000.

Station	Max. GW level fluctuation (m)	Number of drought periods	Trend of GW fluctuation	Max. *I* of dry period (m)	Max. *D* of dry period	Duration (day)	
						Min.	Max.
Brunšvik	5.93	10	decrease	0.69	151	28	275
Zg. Jablane	3.97	17	decrease	0.34	56	31	214

GW – groundwater

drought intensity values do not exceed 0.23 m. In all cases, with time we observe an increase in the intensity of dry periods. The exception is the Spodnja Hajdina station. The size of the deficit *D* of drought periods between the groundwater stations appears quite evenly, and the difference between the deficits in individual stations is noticed. Dornava, Tezno, and Starše have a larger deficit. Dornava and Tezno are located on the margins of the field where the deficit depends on the amplitude of the fluctuations of groundwater levels. The recharge is also influenced by nearby streams. At the Starše station, located in the middle of the Dravsko polje, the size of the deficit and the intensity is a consequence of greater aquifer thickness.

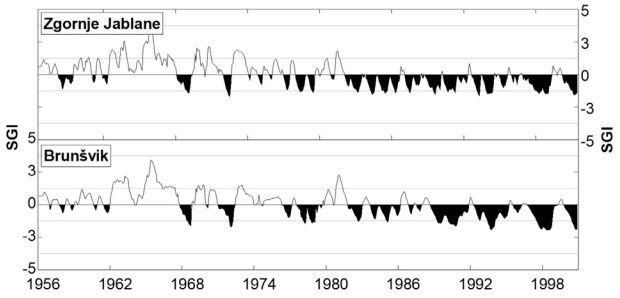

Fig. 6. SGI graph of first interval of measurements between years 1956 and 2000.

SGI was calculated (Fig. 7) at all groundwater stations except for the Zgornje Jablane, since for the second interval, the empirical distribution has not proper fit to the theoretical Gaussian distribution. For other stations, SGI showed three larger periods of severe drought when SGI values were below –1.5. For the first time, such an extreme event occurs in the year 1993 at all stations, except in the Starše station. The second larger period is between 2000 and 2003. The exceptions are the Spodnja Hajdina and Trgovišče stations, where the dry periods are shorter with the rapidly changing SGI. This reflects a thinner unsaturated area at the observed station. The third larger period occurs in December 2011 and persists to the end of 2012. It is a period that is common to all stations where the intensity rises equally. The SGI values at Trgovišče, Dornava and Starše exceed –2.0, which is characterized by extreme drought.

All stations in the Dravsko polje have common drought periods since 2000. The most likely reason for this is a permanent trend of decreasing groundwater level. Exceptions are Trgovišče and Dornava, where the trend of groundwater level is not detected.

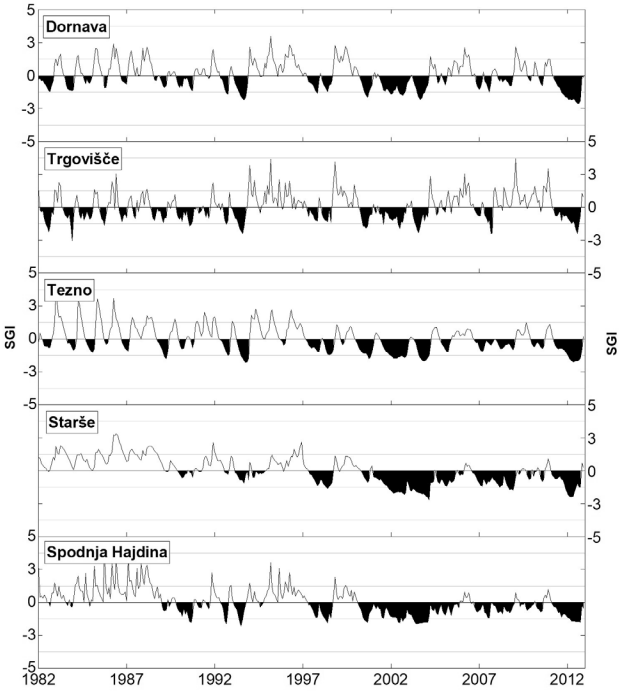

Fig. 7. SGI graph of second interval of measurements between years 1982 and 2012.

The **third interval** (Table 6) represents measurements from year 1991 to year 2011. We noticed that between the dry periods, Tezno, Bohovo, Starše, and Kungota stations have higher intensities *I*. These are areas with higher amplitudes of groundwater fluctuations, which also affects the size of the drought intensity. Rače, Zgornja Gorica, and Trgovišče stations are characterized by a small amplitude that is reflected in the lower intensity of dry periods. The size of the deficit *D* increases with time at most groundwater stations.

Table 5. Descriptive statistics for the second interval between years 1982 and 2012.

Station	Max. GW level fluctuation (m)	Number of drought periods	Trend of GW fluctuation	Max. *I* of dry period (m)	Max. *D* of dry period	Duration (day)	
						Min.	Max.
Sp. Hajdina	1.47	10	decrease	0.16	39	31	334
Starše	2.26	5	decrease	0.39	81	30	365
Tezno	3.62	7	decrease	0.34	83	31	334
Dornava	2.16	16	decrease	0.53	98	31	245
Trgovišče	1.04	15	decrease	0.23	26	28	183

GW – groundwater

Table 6. Descriptive statistics for the third interval between years 1991 and 2011.

Station	Max. GW level fluctuation (m)	Number of drought periods	Trend of GW fluctuation	Max. *I* of dry period (m)	Max. *D* of dry period	Duration (day)	
						Min.	Max.
Bohova	5.44	5	not present	0.74	135	61	273
Kungota	3.13	2	not present	0.48	336	61	702
Rače	0.69	6	not present	0.16	38	61	355
Sp. Hajdina	1.28	6	decrease	0.15	34	61	304
Starše	1.97	4	decrease	0.34	104	59	334
Zg. Gorica	1.24	12	not present	0.16	31	28	304
Zg. Jablane	1.90	9	decrease	0.15	18	31	153
Tezno	2.55	4	decrease	0.33	61	61	334
Dornava	2.07	8	not present	0.23	41	61	184
Gorišnica	1.69	8	decrease	0.23	28	31	184
Trgovišče	0.95	8	not present	0.15	23	30	153

GW – groundwater

Table 7. Descriptive statistics for the fourth interval between years 1990 and 2016.

Station	Max. GW level fluctuation (m)	Number of drought periods	Trend of GW fluctuation	Max. *I* of dry period (m)	Max. *D* of dry period	Duration (day)	
						Min.	Max.
Bohova	5.44	6	not present	0.70	128	61	304
Kungota	4.17	3	increase	0.63	479	31	758
Zg. Gorica	1.24	21	not present	0.22	47	28	304
Tezno	2.55	5	decrease	0.32	87	61	334
Dornava	2.80	9	not present	0.34	124	30	365
Gorišnica	2.28	7	not present	0.22	88	61	396

The calculation of SGI (Fig. 8) for the third interval of measurements was possible at all stations except for Sobetinci, because it has an asymmetric distribution of data; therefore, fitting it to Gaussian distribution was not possible. Otherwise, SGI shows two major periods with severe drought, meaning that SGI is lower than –1.5. First, it occurs at the end of year 1993 and lasts until spring 1994. Exceptions are the Starše and Kungota stations where drought occurs, but they were less intensive. The second period occurs between years 2001 and 2004. It starts at the end of summer 2001, but the aquifer does not recover due to lack of precipitation until spring 2003. At that time, there was a decrease in intensity at all locations, but it then starts rising until January 2004. This period is particularly persistent around Starše and Kungota stations. SGI between 2003 and 2004 at all stations exceeds –2.0, indicating extreme drought (Table 1). At Kungota station, this value persisted for two years.

The smallest fluctuations, between years 2001 and 2004, occurs in stations Zgornja Gorica, Rače, Trgovišče, and Gorišnica. This is due to the small thickness of the unsaturated area and consequentially the fast response to the recharge.

The **fourth interval** (Table 7) represents measurements from year 1990 to year 2016. The highest drought intensity *I* is noticeable at the Kungota, Bohova, Tezno, and Dornava stations. As mentioned before, this is due to the higher amplitude of the groundwater level fluctuation. The highest drought intensity was recorded at the Kungota station with 0.64 m. The low drought intensity is typical for the Zgornja Gorica station where intensity does not exceed 0.20 m. There is also a positive linear trend in the increasing intensity of dry periods. The same applies to the size of the deficit *D* of dry periods P_{10}.

In this period, empirical distributions of many stations are highly asymmetric and consequently do not fit to Gaussian distribution. We have applied transformation to transfer these distributions closer to theoretical, but again Kolmogorov-Smirnov and Anderson-Darling tests were not significant. These data were not analysed.

Three periods are typical for SGI smaller than –1.5 (Fig. 9). The first is the year 1993, visible at all stations. The smallest deficit of dry period is present at the Kungota station. The second is the period between 2000 and 2004. There is a slight increase in the groundwater level in 2001 and 2003 throughout all locations, alleviating the intensity of the dry season. The exception again is the Kungota station, this time due to SGI with

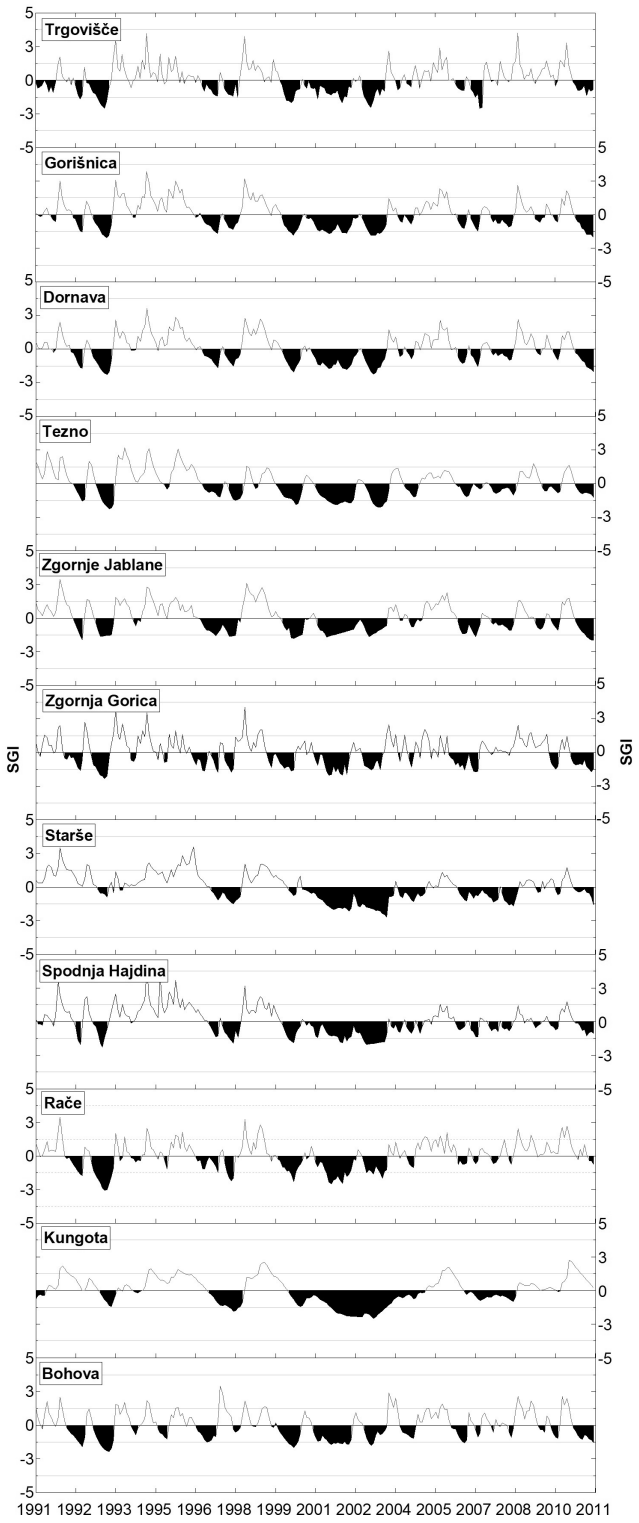

Fig. 8. SGI graph of third interval of measurements between years 1991 and 2011.

less than –2.0. Where groundwater is shallow, the curve is very irregular indicating a rapid response of the aquifer to the recharge. The third period started in summer 2011 and persisted until autumn 2013. The deficit is visible throughout all groundwater stations. The most variable in the period is index at the Zgornja Gorica station.

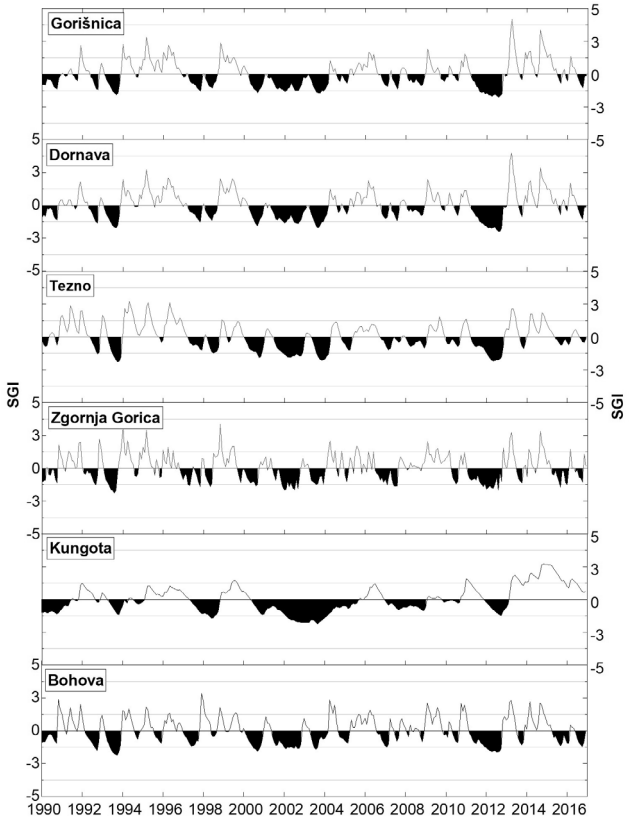

Fig. 9. SGI graph of fourth interval of measurements between years 1990 and 2016.

Comparison of meteorological drought with groundwater drought

Depending on the meteorological drought, the groundwater drought occurs with a lag, the length of which depends on the thickness of the unsaturated zone, porosity and transmissivity. Since hydrogeological systems differ one from another, the influence of the coincidence of these types of drought varies. We have chosen six different time scales for calculating SPI: SPI1, SPI2, SPI3, SPI6, SPI9 and SPI12.

To compare meteorological and groundwater drought, SPI was calculated for three meteorological stations positioned on the Dravsko-Ptujsko polje: precipitation stations Tezno, Starše and Zgornje Jablane. The time interval between year 1982 and year 2012 was chosen, despite the decreasing groundwater level trend. The results are shown in the figure (Fig. 10).

On shorter time scales, the SPI variability is greater than on longer time scales. The reason is representation of seasonal, short-term droughts. Based on the SPI and SGI graphs, we concluded that the Zgornje Jablane station does not show any delay in terms of the meteorological drought (Fig. 10c). Both droughts appear simultaneously, which is particularly noticeable in years 2002 and 2012. SPI12 for year 2002 is –1.54 in January, while in the same month the SGI value is –1.35.

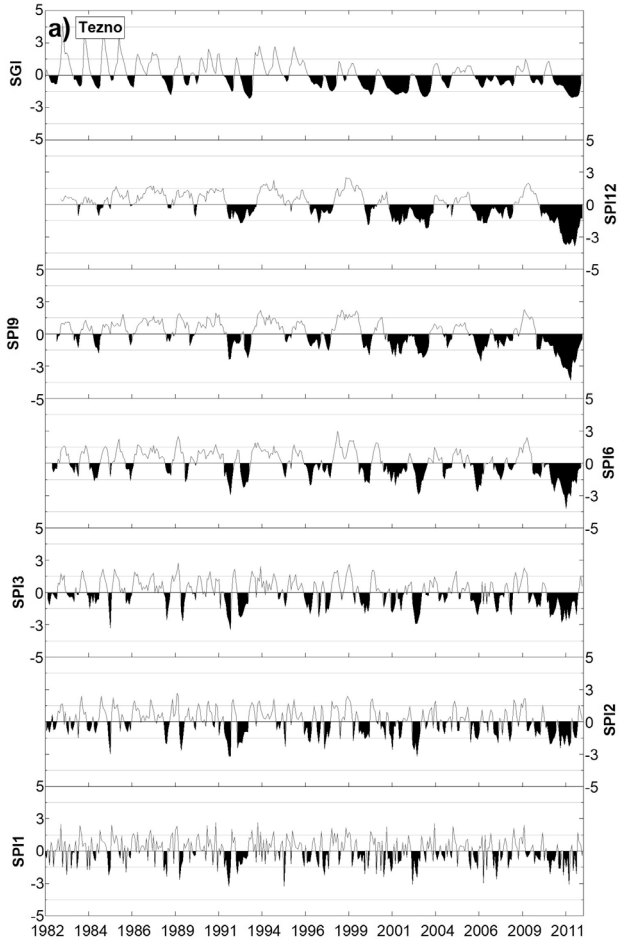

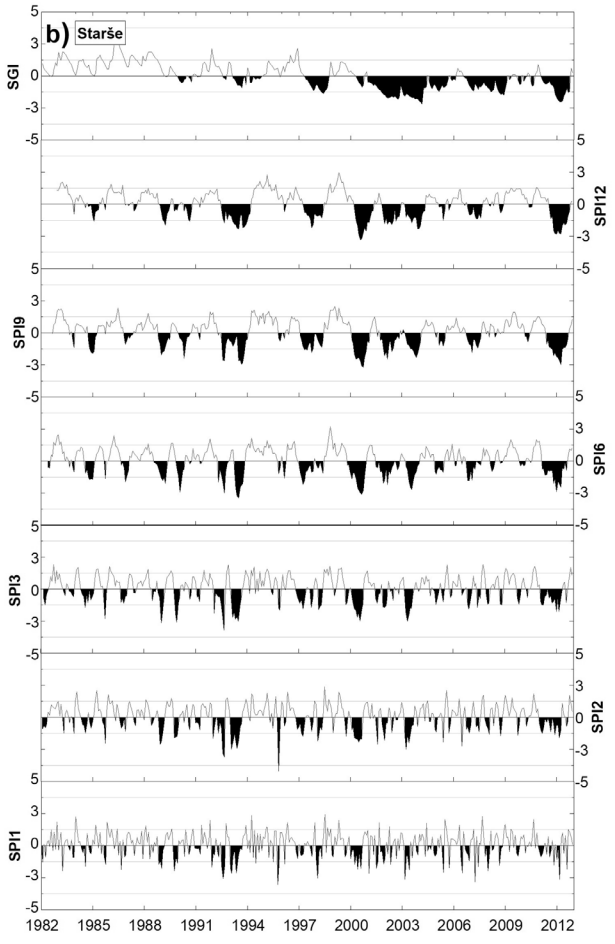

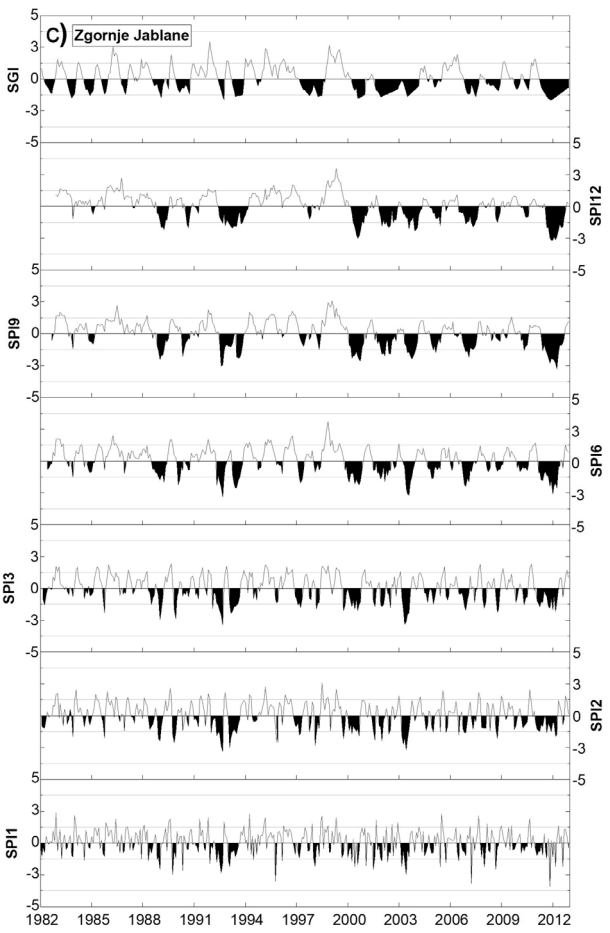

Fig. 10. Comparison of SPI and SGI between a) precipitation station Maribor Tabor and groundwater station Tezno from 1982–2012, b) precipitation station Starše and groundwater station Starše from 1982–2012 and c) between precipitation station Fram and groundwater station Zgornje Jablane from 1982–2012.

At the Tezno station, there is a delay in the appearance of groundwater drought (Fig. 10a). These differences are most noticeable in years 1993 and 2012, when groundwater drought occurs with an average half-year lag. For the year 2012, SPI12 has the lowest value in January when it exceeds –3.0, while SGI is the lowest in May with a value of –1.63. The situation is similar for the year 1993.

The meteorological drought at the precipitation station Starše (Fig. 10b) does not coincide with the groundwater drought observed at the groundwater station Starše. The shift between the lowest SPI and SGI value is greater than near Tezno. In August 2000 when the SPI12 reached the lowest value of –2.77 and when later negative values persist until the next summer, negative SGIs have started slowly but have been steadily decreasing since the end of 2000 until they reach the lowest value of –1.72 in August 2002. The amount of precipitation then increased, which led to an increase of both indices; the trend reverses again when the SPI12 persists with the negative values throughout 2003. SGI reaches the lowest

value of –2.19 only in March 2004. A delayed response of groundwater to recharge is apparent.

Drought periods occurrence map

Despite the short range of measurements, we showed the third interval of measurements (1991–2011), where the density of the stations on the western and southern parts of the Dravsko-Ptujsko polje are more dense (Fig. 11). The period from July 2002 to April 2003 is characterized by extreme drought. We can observe that the SGI values vary by month and location.

For July 2002 (Fig. 11a), drought periods with an index of –1.5 and more are present. The drought was spread over the entire Dravsko-Ptujsko polje. The lowest SGI value is in the north-western part of the area, while in the western part (near Zgornje Jablane) the values were not lower than –1.0. The reason for this is a recharge from the Pohorje streams on the western part of the area. In October 2002 (Fig. 11b), the SGI values decreased in the central part of the area (still above –1.6), and then values are diminishing towards the east. And the dry period significantly diminishes around Zgornje Jablane and Trgovišče. In January 2003 (Fig. 11c), the groundwater deficit is only present in the central part of the area (near Kungota). In the east and northwest, SGI rises above 0.0, indicating a period without groundwater drought. In April 2003 (Fig. 11d), the dry period in the central part of the area is still present. The SGI around Kungota is around –1.6, which shows a severe drought. There is no drought in the north-west of the area. Again, the reason is in the aquifer recharge from the Pohorje streams. There is a deficit to the east, where SGI is between 0.0 and –0.7.

Discussion

The presented analysis of groundwater drought can be divided into three parts. The first part consisting on the ranking statistics of groundwater fluctuations and the second part on the calculation of Standardized Groundwater Index – SGI. The third part represents a comparison between Standardized Precipitation Index – SPI and Standardized Gorunwater Index – SGI.

In the area of Dravsko-Ptujsko polje, based on the ranking statistics, we have identified one- to three-month periods of groundwater deficit, which most often occur in autumn or winter. We conclude that this is a consequence of the delayed impact of the meteorological drought that occurs in the summer. When short-term summer drought periods occur, they often have greater intensity than short-term winter drought periods.

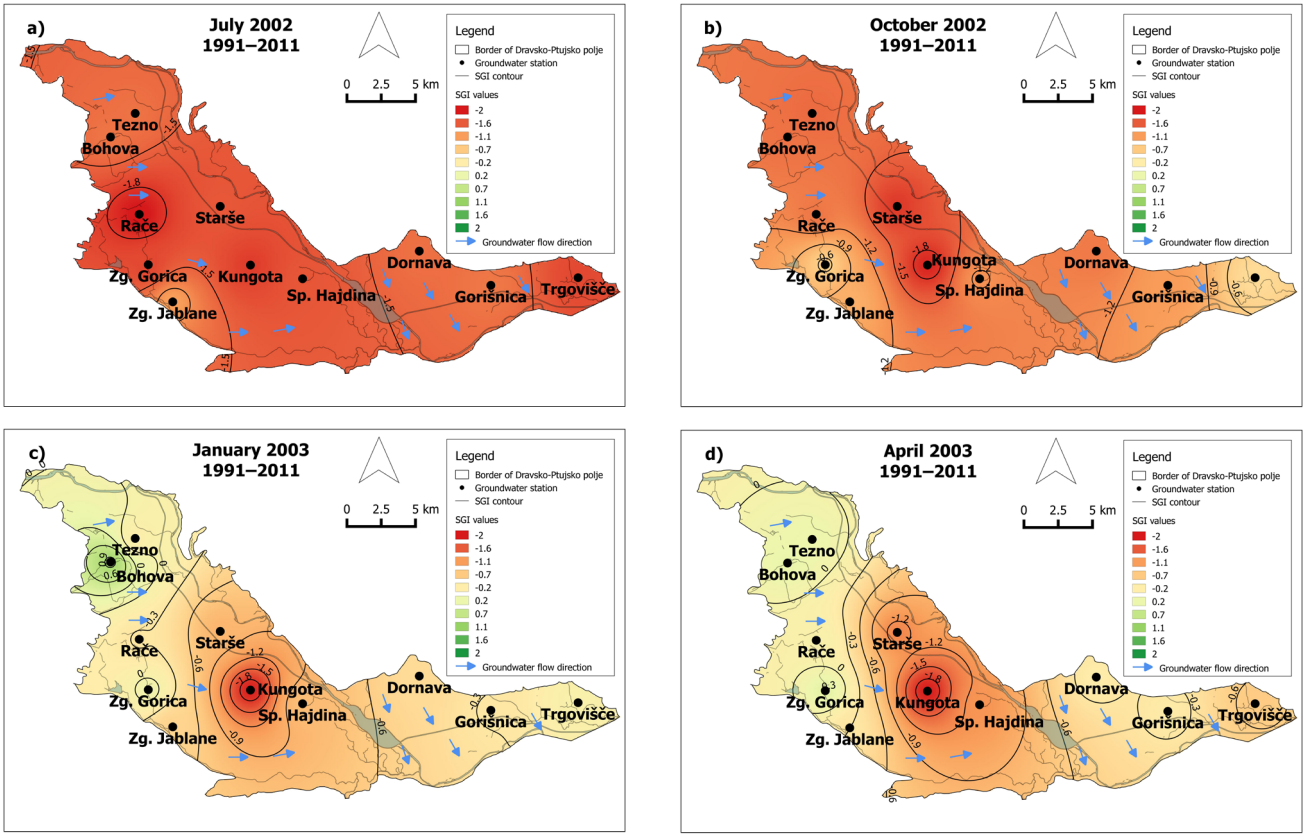

Fig. 11. Maps of dry periods for the third interval (1991–2011). SGI is shown for a) July 2002, b) October 2002, c) January 2003 and d) April 2003.

In the western part of the Dravsko-Ptujsko polje, the amplitude of groundwater level fluctuations is up to 5 m high (Brunšvik station), while in the eastern part it does not exceed 1 m (Trgovišče station). This has also effects on the duration and intensity of dry periods. In the north-western part, the Brunšvik and Tezno stations have the longest and most intense dry periods. In the southeast, the Sobetinci, Gorišnica, and Trgovišče stations have several shorter dry periods, characterized by a low intensity that does not increase with the length of the event. Many one- to three-month dry periods occur in the south-eastern part of the field in summer, as a response to the meteorological drought is almost immediate. The reason is the small thickness of the unsaturated zone. Groundwater is at the depth of 5 m; therefore, the rare longer periods of drought are not the result of the delayed impact of the aquifer but the persistence of meteorological droughts. During the analysis of different time intervals, we indicated a decreasing trend of groundwater level, which affects the variety of drought intensity and size of deficit. Due to the decreasing trend in recent time, many dry periods have occurred.

Dry periods do not occur evenly but depend on local changes in the aquifer. Sometimes, we detect very monotonous drought periods, sometimes drought periods are locally distributed. Therefore, the analysis of groundwater deficits should consider local hydrogeological and geological characteristics of individual aquifers. This is confirmed by the fact that uniform definitions of groundwater drought cannot be given. Each region under consideration has a different variation of the variables.

Based on the SGI calculations, the worst long-lasting droughts usually begin in winter, when the aquifer does not recover after the previous summer drought. Since the amount of recharge is insufficient in the springtime, along with the onset of the next summer, the intensity of drought increases and causes an even greater shortage of groundwater. An example of severe droughts in years 2003 and 2012 is seen at all stations on the Dravsko-Ptujsko polje.

A visual comparison between SGI and percentile P_{10} calculations found that the drought periods determined by both methods coincide. The comparison of the dry period's size is characteristic between the value of P_{10} and the SGI category, which indicates the occurrence of severe drought with values less than or equal to –1.5. This confirms the suitability of both methods for analysing groundwater drought.

From the comparison of SGI and SPI, we have discovered that locations with a higher groundwater level amplitude, where the duration and intensity of drought periods are higher, also have a greater lag in terms of the occurrence of meteorological droughts. At the Tezno station, the lag for the period from 2002 to 2003 is six months. Stations with a smaller amplitude that are typical for the eastern part of the Dravsko-Ptujsko polje reflect the shallow groundwater level. It also follows that relation between groundwater drought and meteorological drought is influenced by the thickness of vadose zone. Where the unsaturated zone is thicker, it takes longer time for meteorological drought to reach groundwater (e.g. Tezno and Starše). If it occurs, the intensity of the dry season is stronger, which means that it takes longer time for the aquifer to recover.

Conclusions

Groundwater drought is a phenomenon that must be investigated in more details in the future. Several theoretical improvements are needed in the future; among them is the redefinition of groundwater drought, which cannot be solely based on the groundwater level fluctuation analysis, but it must include also amount of water stored in the aquifer. Our analyses have shown that for Dravsko-Ptujsko polje, methods for groundwater drought analyses can be applied as they are already presented in the current scientific literature. Drawbacks of the methods applied are only indirectly indicated. At present, the conclusions of the case study are as follows:

- Groundwater drought develops slowly in time and space.
- The occurrence of groundwater drought depends on the thickness of the unsaturated and saturated aquifer zone.
- Where the depth to groundwater level is greater, droughts occur with a longer delay and greater intensity and where the thickness of unsaturated zone is small, the response to meteorological influences is faster.
- Standardized Groundwater Index – SGI is a more suitable index than percentile values of groundwater level; it integrates more information about groundwater fluctuations than percentile values.

As other types of drought, also groundwater drought is a complex event. From that point of view, it is important to consider different types of indices. We have illustrated applicability comparison of meteorological drought indices with

groundwater drought indices. Beside the application of indices, it is also important to consider aquifer's dynamics.

One of the drawbacks of our analysis is the lack of longer groundwater level time series and spurious spatial distribution of stations. At present, the spatial distribution of groundwater monitoring stations in Dravsko-Ptujsko polje has improved, and it is recommended to repeat our calculations in due time. It is also important to focus more on the aquifer boundary conditions that have changed several time during the course of time on Dravsko-Ptujsko polje. Also, some statistical theoretical questions in relation to groundwater level data treatment remains to be opened among them are important questions connected to the fitting of theoretical distributions in relation to extreme values.

Acknowledgement

The authors acknowledge the financial support from the Slovenian Research Agency in the frame of research program »Groundwater and Geochemistry« (No. P1-0020), which is carried out by the Geological Survey of Slovenia.

References

Andjelov, M., Gale, U., Kukar, N., Trišić, N. & Uhan, J. 2006: Ocena količinskega stanja podzemnih voda v Sloveniji. Geologija, 49/2: 383–391. https://doi.org/10.5474/geologija.2006.027

Andjelov, M., Frantar, P., Mikulič, Z., Pavlič, U., Savić, V., Souvent, P. & Uhan, J. 2016: Ocena količinskega stanja podzemnih voda za Načrt upravljanja voda 2015-2021 v Sloveniji. Geologija, 59/2: 205–219. https://doi.org/10.5474/geologija.2016.012

ARSO, 2018: Arhiv–opazovani in merjeni meteorološki podatki po Sloveniji. Internet: http://meteo.arso.gov.si/met/sl/archive/ (3. 2. 2018)

Bloomfield, J. P., Marchant, B. P., Bricker, S. H. & Morgan, R. B. 2015: Regional analysis of groundwater droughts using hydrograph classification. Hydrol. Earth Syst. Sci., 19/10: 4327–4344. https://doi.org/10.5194/hess-19-4327-2015

Bloomfield, J.P. & Marchant, B. P. 2013: Analysis of groundwater drought building on the standardised precipitation index approach. Hydrol. Earth Syst. Sci., 17: 4769–4787. https://doi.org/10.5194/hess-17-4769-2013

Brenčič, M. 2016: Extreme historical droughts in Southeastern Alps - Analyses based on Standardized Precipitation Index. Acta Geophys., 64/5: 1731–1754. https://doi.org/10.1515/acgeo-2016-0017

Brenčič, M. 2017: Kaj je suša. In: Zbornik referatov, 28. Mišičev vodarski dan, Maribor, 6. december 2017. Vodnogospodarski biro, Maribor: 27–36.

Bryc, W. 1995. The normal distribution – Characterizations with Applications. Springer-Verlag New York: 139 p. https://doi.org/10.1007/978-1-4612-2560-7

Ceglar, A. & Kajfež-Bogataj, L. 2008: Obravnava meteorološke suše z različnimi indikatorji. Acta Agric. Slov., 91/2: 407–425.

Chu, H. J. 2018: Drought detection of Regional Nonparametric Standardized Groundwater Index. Water Resour. Manag., 32: 3319–3134. https://doi.org/10.1007/s11269-018-1979-4

Dracup, J. A., Lee, K. S. & Paulson, E. G. 1980: On the definition of droughts. Water resources research, 16/2: 297-302.

Draksler, A., Frantar, P. & Savić, V. 2017: Indeks SGI – kazalnik hidrološke suše podzemnih voda. In: 28. Mišičev vodarski dan: Ranljivost Slovenije zaradi suše: zbornik referatov. Vodnogospodarski biro Maribor, Maribor: 62–68.

Flis, L. 2017: Upravljanje s sušami v Sloveniji. In: Zbornik referatov, 28. Mišičev vodarski dan, Maribor, 6. december 2017. Vodnogospodarski biro Maribor: 45–53.

Geodetska uprava Republike Slovenije 2017: Javne informacije Slovenije. Pregledna karta Slovenije, 1: 750.000.

Gregorič, G. & Ceglar, A. 2017: Monitoring suše – regionalni aspekt. In: Zbornik referatov, 28. Mišičev vodarski dan, Maribor, 6. december 2017. Vodnogospodarski biro Maribor: 124–127.

Haas, J. C. & Birk, S. 2017: Characterizing the spatiotemporal variability of groundwater levels of alluvial aquifers in different settings using drought indices. Hydrol. Earth Syst. Sci., 21/5: 2421–2448. https://doi.org/10.5194/hess-21-2421-2017

Hisdal, H. & Tallaksen, L. M. 2000: Meteorological Drought. In: Hisdal. H. & Tallaksen. L. M. (eds.): Technical Report to the ARIDE project No. 6. University of Oslo, Department of Geophysics: 6–8.

Kobold, M., Petan, S., Pogačnik, N., Sušnik, M., Polajner, J., Pavlič, U., Uhan, J., Gregorič, G., Sušnik, A. & Božič, P. 2012: Razvoj suše v Sloveniji v letu 2012. In Zbornik referatov, 23. Mišičev vodarski dan, Maribor, 5. December 2012. Vodnogospodarski biro Maribor: 1–12.

Mckee, T. B., Doesken, N. J. & Kleist, J. 1993: The relationship of drought frequency and duration to time scales. Eight Conference on Applied Climatology: 179–184.

McKillup, S. & Darby Dyar, M. 2010: Geostatistics Explained: An Introductory Guide for Earth Scientists. Cambridge University Press: 396 p. https://doi.org/10.1017/CBO9780511807558

Mishra, A. K. & Singh, V. P. 2010: A review of drought concepts. J. Hydrol., 391/1–2: 204–216. https://doi.org/10.1016/j.jhydrol.2010.07.012

Namdar Ghanbari, R. & Bravo, H. R. 2011: Evaluation of correlations between precipitation, groundwater fluctuations and lake level fluctuations using spectral methods. Hydrogeol. J., 19/4: 801–810. https://doi.org/10.1007/s10040-011-0718-1

Palmer, W. C. 1965: Meteorological drought: Research paper 45. Washington, D. C.: 58 p.

Peters, E., Van Lanen, H.A.J., Torfs, P.J.J.F. & Bier, G. 2005: Drought in groundwater drought distribution and performance indicators. J. Hydrol., 306/1–4: 302–317. https://doi.org/10.1016/j.jhydrol.2004.09.014

Peters, E., Bier, G., Van Lanen, H. A. J. & Torfs, P. J. J. S. 2006: Propagation and spatial distribution of drought in a groundwater catchment. J. Hydrol., 321/1–4: 257–275. https://doi.org/10.1016/j.jhydrol.2005.08.004

Rodgers, J. L. & Nicewander, W. A. 1988. Thirteen ways to look at the correlation coefficient. Am. Stat., 42/1: 59–66. https://doi.org/10.1080/00031305.1988.10475524

Searcy, J. K. 1959: Flow-Duration curves: USGS Numbered Series. Water supply paper. Washington: USGS. 33 p.

Stephens, M. A. 1974: EDF Statistics for Goodness of Fit and Some Comparisons. J. Am. Stat. Assoc., 69/347: 730–737. https://doi.org/10.2307/2286009

Sušnik, A. 2014: Zasnove kazalcev spreminjanja suše na kmetijskih površinah: doktorska disertacija. Univ. v Ljubljani, Biotehniška fakulteta, Ljubljana: 256 p.

Sušnik, A. & Gregorič, G. 2017: Kmetijska suša v 21. stoletju v Sloveniji. In: Zbornik referatov, 28. Mišičev vodarski dan, Maribor, 6. december. Vodnogospodarski biro Maribor: 37–44.

Sušnik, A. & Pogačar, T. 2010: Motena vodna bilanca kmetijskih rastlin leta 2009 od suše do moče. Ujma, 24: 54–64.

Thom, H. C. S. 1966: Some Methods of Climatological Analysis. Technical Note No. 81. Geneva: Secretariat of the World Meteorological Organization. 56 p.

US National Drought Management Centre. Program to Calculate Standardized Precipitation Index. 2015: Internet: http://drought.unl.edu/monitoringtools/downloadablespiprogram.aspx (17. 8. 2018)

Van Lanen, H. A. J. & Peters, E. 2000: Definition. Effects and Assessment of Groundwater Droughts. In: Vogt, J.V. & Somma, R. (eds.): Drought and Drought Mitigation in Europe. Dordrecht: Kluwer Academic Publishers. 49–61. https://doi.org/10.1007/978-94-015-9472-1_4

Vicente-Serrano, S. M., Begueria, S. & Lopez-Moreno, J. I. 2010: A Multiscalar Drought Index Sensitive to Global Warming: The Standardized Precipitation Evapotranspiration Index. J. Clim., 23/7: 1696–1718. https://doi.org/10.1175/2009JCLI2909.1

GEOLOGIJA *62/2*, 267–278, Ljubljana 2019
https://doi.org/10.5474/geologija.2019.013

Ocena doseganja trajnostnih ciljev z vidika upravljanja in varovanja podzemnih voda v Sloveniji

Assessment of achieving sustainable goals from the groundwater management and protection perspective in Slovenia

Jože UHAN & Mišo ANDJELOV

Agencija Republike Slovenije za okolje, Vojkova 1b, SI-1000 Ljubljana, Slovenija
e-mail: joze.uhan@gov.si

Prejeto / Received 18. 11. 2019; Sprejeto / Accepted 12. 12. 2019; Objavljeno na spletu / Published online 24. 12. 2019

Ključne besede: podzemna voda, trajnostno upravljanje, vodni odtis, količinski stres, nitrat
Key words: groundwater, sustainable management, water footprint, quantitative stress, nitrate

Izvleček

Doseganje trajnostnih ciljev upravljanja in varovanja podzemnih vodnih virov v plitvih vodonosnikih Slovenije smo ocenili preko kazalnikov stresa za količinsko in kemijsko najbolj obremenjene aluvialne vodonosnike vodnih teles podzemne vode: Savska kotlina in Ljubljansko Barje, Savinjska kotlina, Krška kotlina, Dravska kotlina in Murska kotlina. S tem smo poglobili dosedanji pristop ocenjevanja stanja podzemne vode v Sloveniji, kot ga za območje posameznih vodnih telesih določa Okvirna direktiva o vodah. Stopnja izkoriščenosti podzemnih voda je na posameznih najbolj obremenjenih delih plitvih vodnih teles izrazito večja, kot je bila do sedaj ocenjena na celotnih vodnih telesih. V nekaterih primerih, kot je vodonosnik Ljubljanskega polja, se količina črpanja pri srednih nizkovodnih razmerah že približuje polovici vseh razpoložljivih podzemnih vodnih virov. Stopnja nitratnega onesnaženja podzemne vode pa je na nekaterih aluvialnih vodonosnikih vodnih telesih, kot so Krška, Dravska in Murska kotlina, v manj vodnatih letih že presegla mejo trajnostne rabe podzemnih vodnih virov.

Abstract

Achieving the sustainable goals for management and protection of groundwater resources in shallow aquifers in Slovenia was evaluated with stress indicators for the alluvial aquifers of groundwater bodies with the highest quantitative and qualitative pressures: Savska kotlina with Ljubljansko Barje, Savinjska kotlina, Krška kotlina, Dravska kotlina and Murska kotlina. We have deepened the approach taken so far to assess the status of groundwater in Slovenia as defined by the Water Framework Directive for the area of individual bodies of water. The level of groundwater exploitation is markedly higher in some of the most polluted parts of shallow groundwater bodies than has been estimated so far in whole groundwater bodies. In some cases, such as Ljubljansko polje aquifer, the groundwater withdrawals in mid-low-water conditions are already approaching half of all available groundwater resources. In some alluvial aquifers of groundwater bodies, such as Krška, Dravska and Murska kotlina, the level of groundwater nitrate pollution in dry years has already exceeded the limit for the sustainable protection of groundwater resources.

Uvod

Med pomembnimi splošnimi cilji trajnostnega razvoja, ki so jih Združeni narodi zapisali v agendi za trajnostni razvoj 2030, je tudi dostop do vode in trajnostno upravljanje z vodnimi viri, da bomo lahko zadovoljili potrebe današnje in prihodnjih generacij (United Nations, 2015). Trajnostno upravljanje voda bo tudi po mnenju Evropske komisije pomembno vplivalo na zmožnost človeštva, da se prilagodi spreminjajočim se okoljskim, družbenim in ekonomskim razmeram. Pregled napredka pri doseganju ciljev trajnostnega razvoja (SDG - Sustainable Development Goals) v Sloveniji (Sachs et al., 2019) izpostavlja nekaj pomembnih izzivov tudi na področju zagotavljanja čiste vode in sanitarne ureditve (SDG6) ter odgovorne porabe in proizvodnje (SDG12). Dosedanje regionalne ocene količinskega stanja podzemnih voda v Sloveniji sicer ne nakazujejo neugodnega razmerja med razpoložljivimi in črpanimi količinami podzemne vode, po posameznih plitvih vodnih telesih z medzrnsko poroznostjo pa črpane količine že presegajo 20 % obdobno razpoložljivih količin podzemne vode (Andjelov et al., 2016). Poleg omenjenega pa so kar tri vodna telesa podzemne vode

ocenjena s slabim kemijskim stanjem in več kot polovica oskrbovalnih območij pitne vode ima v Sloveniji stalno potrebo po dezinfekciji vode (Sovič, 2017). Zaradi tega vse bolj izstopa potreba po metodološki razširitvi dosedanjega ocenjevanja stanja voda in po nadaljnjih preverbah doseganja trajnostnih ciljev na področju črpanja in onesnaževanja podzemnih vodnih virov. Hipotezo o učinkovitosti uporabe konceptov vodnega odtisa (Hoekstra & Hung, 2002; Hoekstra, 2003; Gleeson & Wada, 2013; Esnault et al., 2014; McDonald et al., 2014) ter odtisa sive podzemne vode (Hoekster et al., 2011; Franke et al., 2013) pri razširitvi dosedanjega ocenjevanja stanja voda in trajnostnega upravljanja podzemnih voda v Sloveniji smo poskušali preveriti na najbolj obremenjenih in hkrati najbolj ranljivih vodnih telesih podzemne vode v Sloveniji.

Podatki in metode

Študijsko območje

Za ocenjevanje doseganja trajnostnih ciljev z vidika upravljanja in varovanja voda v Sloveniji smo za študijsko območje izbrali pet aluvialnih vodonosnikov vodnih teles podzemne vode (sl. 1), odprtih vodonosnikov z medzrnsko poroznostjo in s povprečno gladino podzemne vode od nekaj metrov do največ 25 metrov pod površjem.

Za podrobnejšo preverbo doseganja trajnostnih ciljev na področju črpanja in onesnaževanja podzemnih vodnih virov smo izbrali dva aluvialna vodonosnika z veliko količinsko in veliko kemijsko obremenitvijo:

- Ljubljansko polje (69,4 km^2) s povprečno 2,1 m^3/s črpane podzemne vode, kar predstavlja okoli 6,7 % povprečno načrpane podzemne vode v Sloveniji in
- Spodnjo Savinjsko dolino (76,7 km^2) s povprečnim vnosom 42,3 kg dušika na hektar kmetijske obdelovalne površine v letu 2014, kar za 39 % presega povprečno obremenitev z dušikom na vseh kmetijskih obdelovalnih površinah v Sloveniji.

Vodno telo podzemne vode VTPodV_1001 Savska kotlina in Ljubljansko Barje, kamor se uvršča vodonosnik Ljubljanskega polja, s 21,1 % črpane razpoložljive količine podzemne vode v Sloveniji predstavlja povečano tveganje za doseganje dobrega količinskega stanja, predvsem zaradi velikega črpanja podzemne vode iz Lju-

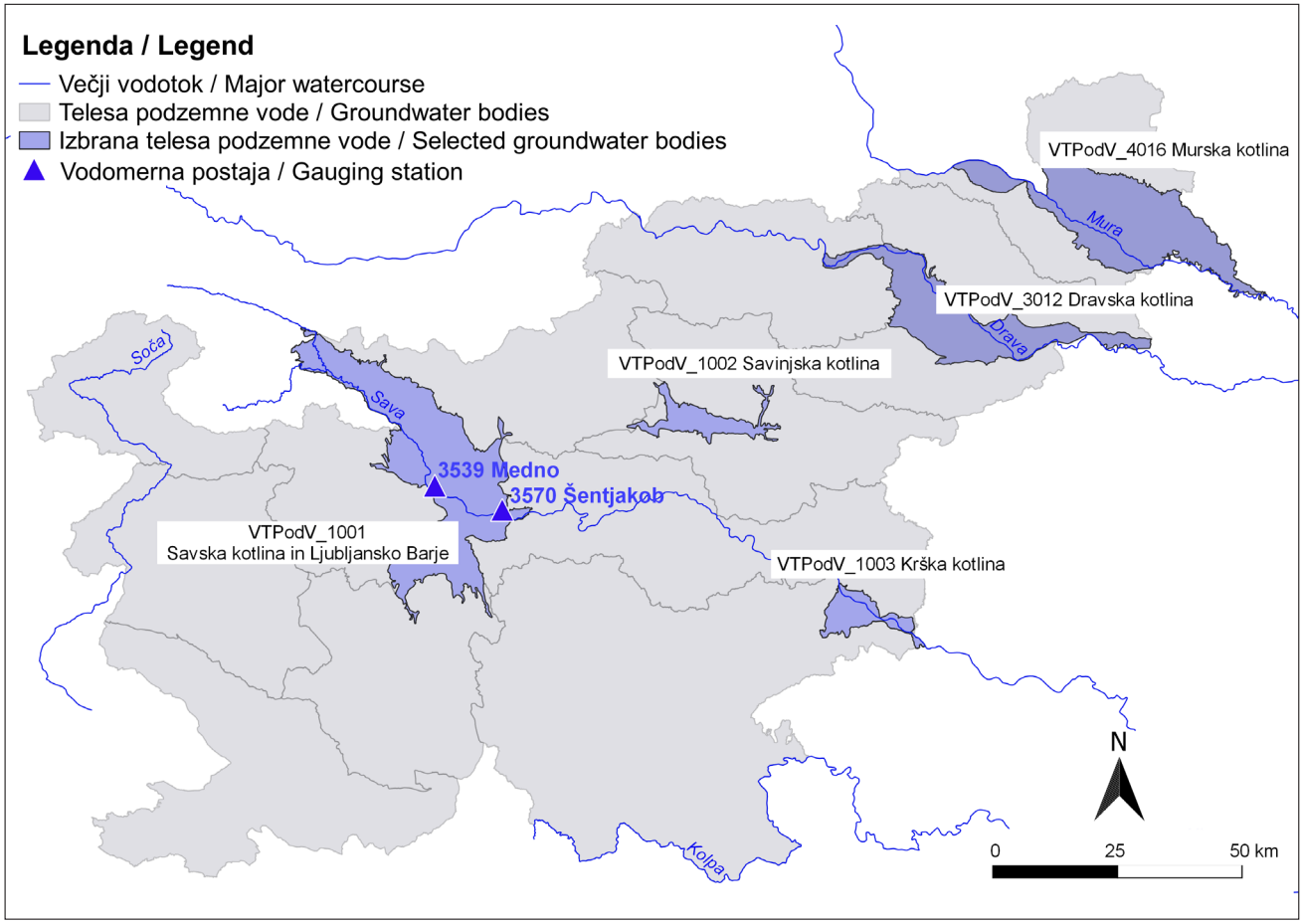

Sl. 1. Študijska območja aluvialnih vodonosnikov vodnih teles podzemne vode v Sloveniji.
Fig. 1. Study areas of alluvial aquifers of groundwater bodies in Slovenia.

bljanskega polja (MOP, 2016). Vodno telo podzemne vode VTPodV_1002 Savinjska kotlina je z aluvialnim vodonosnikom Spodnja Savinjska dolina že od prvega načrta upravljanja voda (MOP, 2009) v slabem kemijskem stanju, predvsem zaradi preseženih vsebnosti nitrata v podzemni vodi.

Koncept ocenjevanja količinskega stanja in količinskega odtisa podzemne vode

S konceptom ocenjevanja količinskega stanja podzemnih voda je okvirna vodna direktiva (Direktiva 2000/60/ES) uvedla zakonodajno obvezo po poznavanju razpoložljivih količin vode v posameznih vodnih telesih podzemnih voda za vse države članice. Primerjanje črpanih in razpoložljivih količin podzemne vode je s tem postal osnovni kazalnik količinskega pritiska na podzemne vodne vire in kazalnik vodnega stresa v različnih ocenjevalnih shemah (Vrba & Lipponen, 2007).

Ocena razpoložljivih količin podzemnih voda izhaja iz poznavanja letnega količinskega obnavljanja podzemne vode ter ocene potrebnih količin podzemnih voda za ohranjanje ekosistemov in doseganje dobrega ekološkega stanja površinskih voda. Letno količino obnavljanja podzemne vode v Sloveniji ocenjujemo z regionalnim vodnobilančnim modelom GROWA-SI (Andjelov et al., 2016), ki se na območjih količinsko močno obremenjenih vodonosnikov z medzrnsko poroznostjo za podporo upravljanja voda dopolnjuje z rezultati šestih lokalnih modelov toka podzemne vode, ki so bili izdelani s programskim orodjem MODFLOW (Souvent et al., 2016).

Letne količine podzemnih voda za ohranjanje ekosistemov in doseganje dobrega ekološkega stanja površinskih voda so bile po posameznih vodnih telesih podzemnih voda celotnega območja Slovenije podana po metodologiji Janže in sodelavcev (2016), ki ločeno obravnava potrebne količine podzemnih voda za ohranjanje:

- gozdnih habitatov na aluvialnih vodonosnikih ob pomoči ločevanja modelirane realne evapotranspiracije v izhlapele prestrežene padavine, prepuščene padavine, ki izhlapevajo iz tal, in izhlapevanje preko rastlin,
- habitatov dvoživk ter mehkužcev na kraških območjih ob uporabi ločevalnih možnosti modela z obravnavo podzemnega odtoka kot vsote modeliranega podzemnega in pripovršinskega odtoka ter
- dobrega ekološkega stanja površinskih voda ob uporabi nemškega vodnobilančnega pristopa s scenarijem petih sušnih let v zadnjem tridesetletnem obdobju (Schlüter, 2006), kar je približek vrednosti dvajsetega centila količine napajanja vodonosnikov v referenčnem vodnobilančnem obdobju in predpostavlja mejo slabih habitatnih rečnih pogojev, pogosto umeščeno v razpon od 10 do 30 % povprečnega letnega pretoka Qs (Tennant, 1976).

Omenjena regionalna ocena letnih potrebnih količin podzemnih voda za ohranjanje ekosistemov in doseganje dobrega ekološkega stanja površinskih voda je zelo posplošena. V primeru količinsko najbolj obremenjenih vodnih teles podzemne vode je priporočljiva ocena prispevka podzemne vode k ekološkemu pretoku reke (E) tudi preko razmerja med baznim (Q_{bazni}) in celotnim naravnim pretokom ($Q_{celotni}$). Ob tem pa je potrebno upoštevati ekološko sprejemljiv pretok (Q_{es}) (Charchousi et al., 2018).

$$E = \frac{Q_{bazni}}{Q_{celotni}} \cdot Q_{es}$$

Prispevek podzemne vode k ekološkemu pretoku (E) je torej mogoče oceniti ob poznavanju celotnega in baznega pretoka oz. ob poznavanju njunega razmerja, ki ga predstavlja indeks baznega odtoka (BFI). Za oceno baznega odtoka smo pri modeliranju vodne bilance Slovenije za obdobje 1981–2010 (Andjelov et al., 2016) uporabili metodologijo izračunov, znano pod oznako MoMLRr (Wundt, 1958; Kille, 1970; Demuth, 1993). Bazni odtok je po tej metodi vrednost mediane nizkih dnevnih pretokov v n mesecih obravnavanega tridesetletnega obdobja 1971–2000 na premici najboljšega prileganja, kjer enačba premice z začetno vrednostjo (y_0) in smernim koeficientom (m) izhaja iz postopne regresijske analize linearnega dela porazdelitvene S-krivulje:

$$MoMLRr = m \cdot \frac{n}{2} + y_0$$

Metodologijo izračuna vrednosti ekološko sprejemljivega pretoka (Q_{es}) v Sloveniji določa uredba o kriterijih za določitev ter načinu spremljanja in poročanja ekološko sprejemljivega pretoka (Uradni list RS, 2009):

$$Q_{es} = f \cdot sQnp$$

Po omenjeni uredbi je ekološko sprejemljiv pretok odvisen od povprečja najmanjših srednjih dnevnih pretokov posameznih let obravnavanega obdobja ($sQnp$) in faktorja (f), ki zavisi od vrste odvzema vode, dolžine odseka vodotoka s povratno rabo vode, količine odvzete vode, raz-

merja med srednjim in malim pretokom, ekološkega tipa vodotoka in od velikosti prispevnega območja.

Prispevek podzemne vode k ekološko sprejemljivemu pretoku se izkazuje kot zelo občutljiv parameter ocenjevanja količinskega stanja oz. trajnostne rabe podzemnih vodnih virov in ga je priporočljivo obravnavati po različnih pristopih, rezultate pa primerjati preko ocenjevalne sheme količinskega odtisa rabe podzemne vode (Gleeson et al., 2012).

Količinski odtis rabe podzemne vode, ki temelji na konceptu vodnega odtisa (Hoekstra & Hung, 2002), vključuje tudi princip naravnega obnavljanja in pokrivanja potreb ekoloških pretokov. Leta 2012 so pristop prvič uporabili na globalni ravni za oceno velikih regionalnih vodonosnikov, pomembnih za kmetijstvo. V naslednjih letih je ta koncept ocenjevanja prešel v široko uporabo in se izkazal za zelo primeren koncept ocenjevanja trenutne in predvidene rabe podzemne vode tudi na manjših vodonosnikih (Gleeson & Wada, 2013; Esnault et al., 2014; McDonald et al., 2014).

V izračunu količinskega odtisa rabe podzemne vode (*GF*) se črpane količine podzemne vode (*C*) primerjajo s količino letnega napajanja (*R*), zmanjšane za prispevek podzemne vode k ekološkemu pretoku (*E*). Ob upoštevanju površine obravnavanega vodonosnika (*A*) z izračunom količinskega odtisa rabe podzemne vode lahko kvantificiramo vodni stres in nakažemo velikost območja vodonosnika, ki je potreben za trajnostno rabo podzemnih vodnih virov:

$$GF = A \cdot \left[\frac{C}{R - E} \right]$$

Koncept ocenjevanja kemijskega stanja podzemne vode in odtisa sive podzemne vode

Ocena kemijskega stanja podzemnih voda v prvem koraku temelji na primerjavi povprečne letne vrednosti državnega monitoringa s standardom kakovosti oz. vrednostjo praga. V primeru preseganja mejnih vrednosti so predvideni različni preizkusi vpliva onesnaženja, opredeljeni z okoljskimi kriteriji in kriteriji rabe podzemne vode. Preizkusi se zaključijo s t.i. splošno oceno kemijskega stanja (European Communities, 2009), ki naj bi podala razmerje med delom vodnega telesa, kateremu pripadajo merilna mesta s preseženimi mejnimi vrednostmi ter celotnim telesom podzemne vode. Principom preizkusa splošne ocene kemijskega stanja sledi koncept odtisa sive vode (*ang. grey water footprint*), ki je indikator stopnje onesnaženosti vode in je opredeljen kot prostornina vode, potrebne za razredčenje bremena onesnaženja ob upoštevanju vrednosti naravnega ozadja in mejnih vrednosti (Hoekstra et al., 2011).

Ob tem se pri razpršenih virih onesnaženja podzemne vode, kot je npr. nitrat, predpostavlja, da le del bremena s pronicujočo vodo doseže vodno telo. Odtis sive podzemne vode (GWF) je tako razmerje med deležem bremena onesnaženja (*L*), ki lahko doseže vodno telo, ter razliko med mejno vsebnostjo onesnaževala (C_{max}) in mejno vrednost med naravnim ozadjem in povišanimi vrednostmi nitrata (C_{nat}):

$$GWF = \frac{L}{c_{\max} - c_{nat}}$$

Z upoštevanjem količine vode, ki doseže zasičeno območje vodonosnika (R_{inf}), lahko preko odtisa sive podzemne vode (GWF) ocenimo stopnjo onesnaženja podzemne vode WPL *(ang. water pollution level)*:

$$WPL = \frac{GWF}{R_{\inf}}$$

Za oceno povprečnega letnega napajanja smo na študijskem območju vodonosnika Spodnje Savinjske doline uporabili vodnobilančno simulacijo obdobja 1981–2010 z regionalnim modelom GROWA-SI (Andjelov et al., 2016). Za oceno deleža bremena iz bilance dušika obdobja 2007–2014 (Sušin & Verbič, 2019), ki lahko doseže vodno telo podzemne vode, je bil uporabljen regionalni model toka nitrata DENUZ-WEKU (Andjelov et al., 2014; Matoz et al., 2016). Mejno vsebnost onesnaženja podzemne vode z nitratom smo s 50 mg/l prevzeli po standardu kakovosti za oceno kemijskega stanja po uredbi o stanju podzemnih voda (Uradni list RS, 2009). Za mejno vrednost med naravnim ozadjem in povišanimi vrednostmi nitrata, ki so lahko posledica človekove dejavnosti (Panno et al., 2006), smo za izračun regionalnega odtisa sive vode prevzeli vrednost srednje točke prevoja na verjetnostnem diagramu porazdelitve modelskih vrednosti nitrata v podzemni vodi vseh rasterskih celic na aluvialnih vodonosnikih po posameznih vodnih telesih (10 mg/l). Ta vrednost je pričakovano višja od povprečja naravnega ozadja vsebnosti nitrata (3,8 mg/l) v podzemnih vodah izvirov, vodnjakov in vrtin na celotnem območju Slovenije (Mezga, 2014) in je blizu vrednosti srednje točke prevoja verjetnostne porazdelitve (8,3 mg/l) vseh rezultatov obsežnih terenskih meritev vsebnosti nitrata v aluvialnem vodonosniku Spodnje Savinjske doline (Uhan, 2011).

Rezultati

Shema kazalnikov trajnostne rabe podzemne vode (Vrba & Lipponen, 2007) vsebinsko poenoteno razširja pogled na dolgoročno vzdržnost rabe podzemnih vodnih virov od obravnave količinskega in kemijskega stanja podzemne vode, kot ga metodološko opredeljuje evropska okvirna vodna direktiva, tudi na področje ranljivosti z vidika črpanja in onesnaževanja podzemne vode. Za območje Slovenije je ocenjeno sedem kazalnikov (Tabela 1), ki nudijo prvi splošni pogled na trajnostno rabo podzemne vode na nacionalni ravni. Letna količina obnovljive podzemne vode z 2.858 m^3, oz. okoli 2.200 m^3 razpoložljive podzemne vode na prebivalca v Sloveniji, izračunana za obdobje 1981-2010, močno presega splošno prepoznano mejo 1.600 m^3, pod katero lahko nastopi vodni stres in pomanjkanje vode (Turton, 2003). V ocenjevalni shemi (Tabela 1) v Sloveniji izstopata predvsem dva kazalnika, ki govorita o:

- razmeroma majhnem deležu črpanih količin glede na razpoložljivo podzemno vodo (3,1 %) ob hkrati prevladujočem deležu podzemne vode v oskrbi prebivalstva s pitno vodo (99 %) ter
- razmeroma majhnem deležu območja Slovenije s slabim kemijskim stanjem podzemne vode (5,6 %) ob hkrati velikem deležu območja povišane ranljivosti na onesnaženje podzemne vode (70 %) in posledično velikim deležem oskrbovalnih območij pitne vode s stalno potrebo po pripravi vode (60 %).

Kazalniki količinskega stresa rabe podzemne vode

Zaradi velike prostorske in časovne spremenljivosti količinskega obnavljanja podzemne vode, ocenjenega z regionalnim vodno-bilančnim modelom, smo pogled na trajnostno upravljanje podzemnih voda na najbolj obremenjenih vodonosnikih razširili s shemo količinskega odtisa rabe podzemne vode glede na modelirane količine iz modelov toka podzemne vode in ob tem preverili različne pristope k ocenjevanju količine podzemne vode za zagotavljanje potrebnega ekološkega pretoka.

Na hidrometričnem prispevnem območju, vodozbirnem zaledju vodomerne postaje, količinsko najbolj obremenjenega aluvialnega vodonosnika vodnega telesa podzemne vode VTPodV_1001 Ljubljanska kotlina in Ljubljansko Barje je preko indeksa baznega odtoka (Charchousi et al., 2018) možno razmeroma zanesljivo oceniti prispevek podzemne vode k ekološkemu pretoku. Po metodologiji Wundta (1958), Killeja (1970) in Demutha (1993) je bazni odtok mesečna vrednost mediane nizkih dnevnih pretokov na premici najboljšega prileganja, kjer enačba premice z začetno vrednostjo (y_0) in smernim koeficientom (m) izhaja iz postopne regresijske analize linearnega dela porazdelitvene S-krivulje. Vrednosti tako določenega indeksa baznega toka ($Q_{bazni}/Q_{celotni}$) vodomernih postaj državnega hidrološkega monitoringa na reki Savi, 3530 Medno in 3570 Šen-

Tabela 1. Trajnostno upravljanje podzemne vode v Sloveniji po prirejeni shemi kazalnikov UNESCO / IAEA / IHP (prirejeno po Vrba & Lipponen, 2007).
Table 1. Groundwater sustainable management in Slovenia according to the adapted indicator scheme UNESCO / IAEA / IHP (adapted after Vrba & Lipponen, 2007).

	KAZALNIKI TRAJNOSTNEGA UPRAVLJANJA PODZEMNE VODE V SLOVENIJI / INDICATORS OF GROUNDWATER SUSTAINABLE MANAGEMENT IN SLOVENIA	VREDNOST / VALUE
K 1	Letna količina obnovljive podzemne vode na prebivalca (MOP, 2016) / Annual quantity of renewable groundwater per capita (MOP, 2016)	2.858 m3
K 2	Črpane količine podzemne vode kot delež povprečne letne obnovljive podzemne vode (MOP, 2016) / Groundwater abstraction quantities as a percentage of average annual renewable groundwater (MOP, 2016)	2,3 %
K 3	Črpane količine podzemne vode kot delež povprečne letne razpoložljive podzemne vode (MOP, 2016) / Groundwater abstraction quantities as a percentage of average annual available groundwater (MOP, 2016)	3,1 %
K 4	Podzemna voda kot delež skupne porabe pitne vode (SURS, 2017) / Groundwater as a percentage of total use of drinking water (SURS, 2017)	99 %
K 5	Delež območja z izčrpavanjem podzemne vode / Percentage of the area with groundwater depletion	ni ocenjeno / not evaluated
K 6	Črpane količine neobnovljivih podzemnih vodnih virov kot delež skupne izkoristljive neobnovljive količine podzemnih vodnih virov / Abstraction of non-renewable groundwater resources as a percentage of total exploitable non-renewable groundwater resources	ni ocenjeno / not evaluated
K 7	Delež območja povišane ranljivosti na onesnaženje podzemne vode (GeoZS, 2016) / Percentage of the area with very high vulnerability to groundwater pollution (GeoZS, 2016)	70 %
K 8	Delež območja s slabim kemijskim stanjem podzemne vode (MOP, 2016) / Percentage of the area with low groundwater chemical status (MOP, 2016)	5,6 %
K 9	Delež oskrbovalnih območij pitne vode s stalno potrebo po dezinfekciji vode (Sovič, 2017) / Percentage of the drinking water supply areas with permanent water disinfection need (Sovič, 2017)	60 %
K 10	Odvisnost kmetijskega prebivalstva od podzemne vode / Dependence of agricultural population on groundwater	ni ocenjeno / not evaluated

tjakob (sl. 1), sta 0,47 in 0,54, kar sovpada z rezultati izračunov povprečnih indeksov baznega odtoka s standardnim programom za računanje BFI (Srebovt, 2014). Po pristopu Charchousija in sodelavcev (2018) je ob srednjih gladinah podzemne vode njen prispevek k ekološkemu pretoku (*E*) 0,85 m^3/s, kar presega Tennantovo (1976) mejo dobrih habitatnih rečnih pogojev, t.j. 20 odstotkov povprečnega letnega pretoka, ki je za obdobje 1981–2010 na Savi med Mednim in Šentjakobom ocenjeno na 0,47 m^3/s (Tabela 2).

Na količinsko obremenjenih vodonosnikih se je ocena prispevka podzemne vode k ekološkemu pretoku (*E*) izkazala za zelo občutljiv parameter, ki terja podrobnejši napajalni model ob upoštevanju podatkov o celotnem, baznem in ekološko sprejemljivem pretoku. Ocena napajanja podzemne vode vodonosnika Ljubljanskega polja ob upoštevanju interakcije površinskih in podzemnih voda sloni na konceptualni shemi numeričnega modela toka podzemne vode (Souvent et al., 2016), ocena ekološkega pretoka (Janža et al., 2016) pa je povzeta iz ocene količinskega stanja podzemnih voda (Andjelov et al., 2016). Ob uporabi scenarija petih sušnih let v zadnjem tridesetletnem obdobju (Schlüter, 2006), kar je približek dvajsetemu centilu količine napajanja vodonosnikov v referenčnem vodnobilančnem obdobju po vodnobilančnem modelu GROWA-SI, je povprečni prispevek podzemne vode Ljubljanskega polja k ekološkemu pretoku 0,73 m^3/s (Tabela 2). Ob srednjih gladinah podzemne vode v vodonosniku Ljubljanskega polja s 3,11 m^3/s modeliranega napajanja vodonosnika (Petauer & Hiti, 2017, 2018) in 1,0 m^3/s črpanih količin podzemne vode je ob količinskem odtisu (*GF*) 29,2 km^2 dosežena stopnja izkoriščenosti (GF/A_A) 0,42.

Stopnja izkoriščenosti podzemne vode v izbranem časovnem obdobju med leti 2007 in 2014 z dvema hidrološkima ekstremoma zadnjih petdesetih let (2011 in 2014) je pri ocenah za celotna območja vodnih teles po pristopu Schlüterja (2006) ter Andjelova in sodelavcev (2016) največja na vodnih telesih podzemne vode VTPodV_3012 Dravska kotlina (0,28) ter VTPodV_1001 Savska kotlina in Ljubljansko Barje (0,20). Kot količinsko najbolj ranljivo vodno telo izstopa Dravska kotlina, katere stopnja izkoriščenosti podzemne vode v suhem hidrološkem letu doseže vrednost 0,60 (Tabela 3). Povprečno gre v obdobju 2007–2014 za stopnjo izkoriščenost podzemne vode v razponu od 0,08 v Krški kotlini do 0,28 v Dravski kotlini (Tabela 3, sl. 2).

Kazalniki ranljivosti in onesnaženja podzemne vode

S slabim kemijskim stanjem so v državnem načrtu upravljanja voda (MOP, 2016) opredeljena tri telesa podzemne vode: Savinjska, Dravska in Murska kotlina, ki skupaj predstavljajo 5,6 % površine države in 3,9 % obdobno razpoložljivih količin podzemne vode v Sloveniji. V nasprotju s to oceno splošni kazalniki trajnostne rabe podzemne vode (Tabela 1) prinašajo informacijo o razmeroma velikem deležu oskrbovalnih območij pitne vode s stalno potrebo po dezinfekciji vode (60 %), ki se z leti zvišuje (Sovič, 2017), visok je tudi delež območja Slovenije z najvišjo ranljivostjo na onesnaženje podzemne vode, izražene s hitrostjo toka podzemne vode (Prestor & Janža, 2016).

Tudi v primeru vodonosnika Spodnje Savinjske doline, študijskega območja enega od teles podzemne vode v slabem stanju, je delež območja

Tabela 2. Količinski odtis in stopnja izkoriščenosti podzemne vode v vodonosniku Ljubljanskega polja.
Table 2. Groundwater quantitative footprint and exploitation level in Ljubljansko polje aquifer.

VODONOSNIK LJUBLJANSKEGA POLJA / LJUBLJANSKO POLJE AQUIFER	ČRPANJE PODZEMNE VODE / GROUNDWATER ABSTRACTION	NAPAJANJE PODZEMNE VODE (Petauer & Hiti, 2017, 2018) / GROUNDWATER RECHARGE (Petauer & Hiti, 2017, 2018)	PRISPEVEK PODZEMNE VODE K EKOLOŠKEMU PRETOKU REKE / GROUNDWATER CONTRIBUTION TO ENVIRONMENTAL STREAMFLOW	KOLIČINSKI ODTIS PODZEMNE VODE / GROUNDWATER QUANTITATIVE FOOTPRINT	STOPNJA IZKORIŠČENOSTI PODZEMNE VODE / GROUNDWATER EXPLOITATION LEVEL
	C [m^3/s]	$R_{Modflow}$ [m^3/s]	E [m^3/s]	GF [km^2]	GF/A_A [-]
Povprečni hidrološki pogoji / Average hydrological conditions			0,47*		
	1,00	3,11	0,73**	29,2	0,42
			0,85***		

Opomba:
* po pristopu iz Tennant (1976) / after approach from Tennant (1976)
** po pristopih iz Schlüter (2006) in Andjelov in sod. (2016) / after approaches from Schlüter (2006) and Andjelov et al. (2016)
*** po pristopih iz Demuth (1993) in UL RS 97/09 (2009) / after approaches from Demuth (1993) and UL RS 97/09 (2009)

Tabela 3. Stopnja izkoriščenosti podzemne vode v aluvialnih vodonosnikih vodnih telesih Slovenije.
Table 3. Groundwater exploatation level in aluvial aquifers of groundwater bodies of Slovenia.

TELO PODZEMNE VODE / GROUNDWATER BODY	STOPNJA IZKORIŠČENOSTI PODZEMNE VODE / GROUNDWATER EXPLOATATION LEVEL		
	SUHO HIDROLOŠKO LETO 2011 / DRY HYDROLOGICAL YEAR 2011	MOKRO HIDROLOŠKO LETO 2014 / WET HYDROLOGICAL YEAR 2014	OBDOBJE 2007–2014 / PERIOD 2007–2014
	GF/A_A [-]		
VTPodV_1001 Savska kotlina in Ljubljansko Barje	0,31	0,13	0,20
VTPodV_1002 Savinjska kotlina	0,17	0,04	0,10
VTPodV_1003 Krška kotlina	0,19	0,05	0,08
VTPodV_3012 Dravska kotlina	0,60	0,12	0,28
VTPodV_4016 Murska kotlina	0,37	0,07	0,17

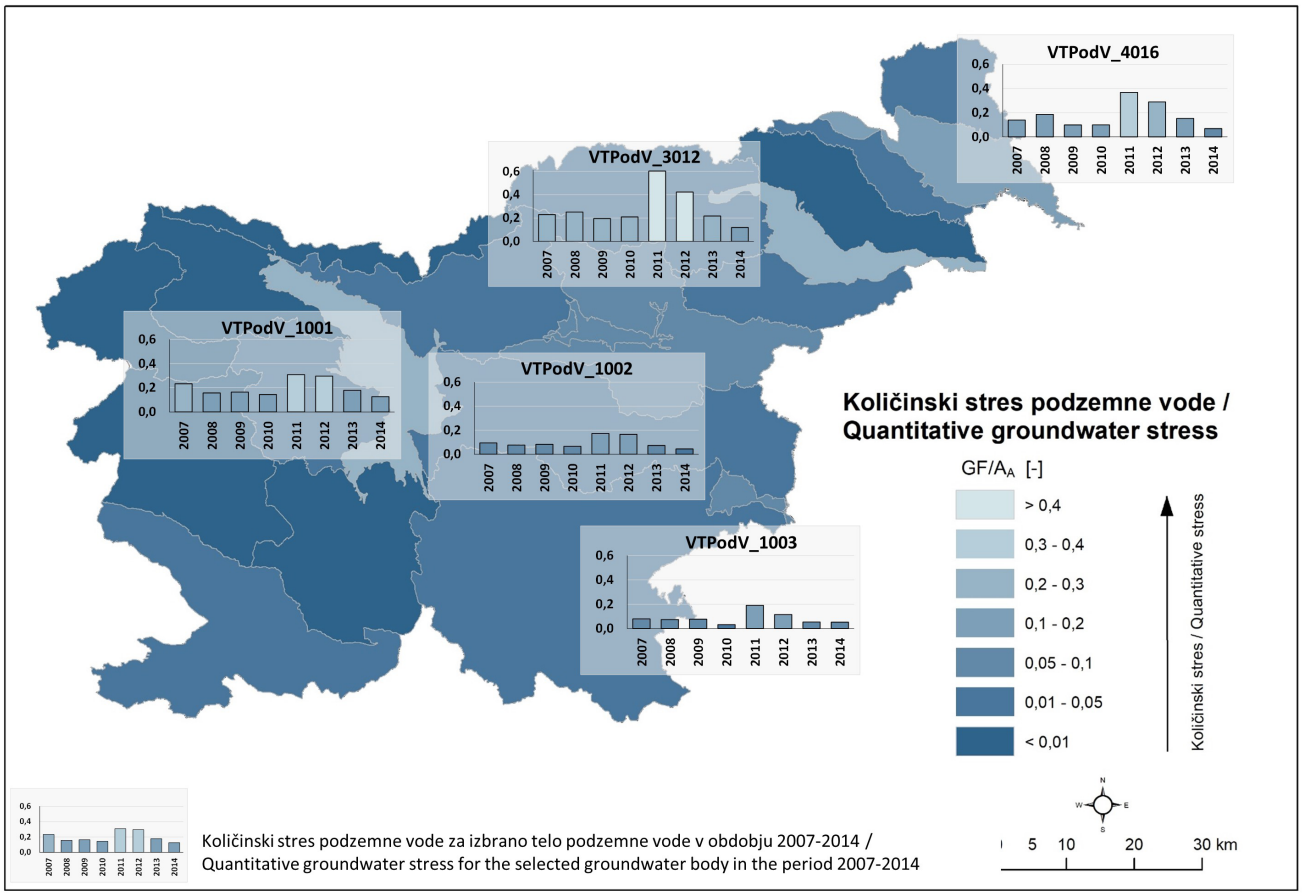

Sl. 2. Stopnja izkoriščenosti podzemne vode po izbranih telesih podzemne vode Slovenije v obdobju 2007–2014.
Fig. 2. Groundwater exploatation level for selected groundwater bodies of Slovenia in the period 2007–2014.

z največjo ranljivostjo na onesnaženje podzemne vode z omenjeno metodo razmeroma visok: 45 %. Delež površja z največjo ranljivostjo pa je nekoliko nižji pri parametrični oceni splošne ranljivosti po metodologiji SINTACS in kot posteriorna verjetnost na nitratno onesnaženje podzemne vode po metodi teže evidenc WofE: 43 in 31 % (Uhan, 2011).

Tudi odtis sive podzemne vode za onesnaženje z nitratom, razmerje med povprečnim deležem bremena onesnaženja, ki lahko doseže zasičeno območje vodonosnika, ter razliko med mejno vsebnostjo onesnaževala (50 mg/l) in vrednostjo točke prevoja nad naravnim ozadjem (10 mg/l), je za celotno telo podzemne vode VTPodV_1002 Savinjska kotlina v okviru teh vrednosti. Glede na hidrološke razmere je bil odtis sive podzemne vode za onesnaženje z nitratom v VTPodV_1002 Savinjska kotlina v razponu od 0,22 v mokrem letu 2014 do 0,79 v sušnem letu 2011. V sušnem letu 2011 so odtisi sive podzemne vode za onesnaženje z nitratom presegali vrednost 1 kar v treh

Tabela 4. Odtis sive podzemne vode v povezavi z vsebnostmi nitrata v aluvialnih vodonosnikih vodnih telesih podzemnih voda Slovenije.
Table 4. Gray groundwater footprint related to nitrate concentration for alluvial aquifers of groundwater bodies of Slovenia.

TELO PODZEMNE VODE / GROUNDWATER BODY	STOPNJA NITRATNE ONESNAŽENOSTI PODZEMNE VODE (SUHO LETO 2011) / GROUNDWATER NITRATE POLLUTION LEVEL (DRY YEAR 2011)	STOPNJA NITRATNE ONESNAŽENOSTI PODZEMNE VODE (MOKRO LETO 2014) / GROUNDWATER NITRATE POLLUTION LEVEL (WET YEAR 2014)	ODTIS SIVE PODZEMNE VODE (OBDOBJE 2007-2014) / GRAY GROUNDWATER FOOTPRINT (PERIOD 2007-2014)
	WPL [-]		
VTPodV_1001 Savska kotlina in Ljubljansko Barje	0,46	0,17	0,28
VTPodV_1002 Savinjska kotlina	0,79	0,22	0,43
VTPodV_1003 Krška kotlina	1,38	0,31	0,67
VTPodV_3012 Dravska kotlina	1,81	0,35	0,75
VTPodV_4016 Murska kotlina	3,14	0,49	0,92

vodnih telesih podzemne vode: Krška kotlina (1,38), Dravska kotlina (1,81) in Murska kotlina (3,14) (Tabela 4). Regionalna analiza je pokazala visoke vrednosti odtisa sive podzemne vode za obremenitev z dušikom v sušnem letu 2011 tudi na nekaterih drugih območjih severovzhodne Slovenije (sl. 3).

Razprava

Sheme kazalnikov trajnostne rabe podzemne vode na nacionalni ravni, kot so jih razvili v delovni skupini UNESCO / IAEA / IAH (Vrba & Lipponen, 2007) (Tabela 1), sicer nudijo prvi primerljiv vpogled v stanje podzemnih voda ter problematiko varovanja in rabe podzemnih vodnih virov, vendar lahko take ocene prekrijejo upravljavsko pomembne informacije o ključnih lokalnih preobremenitvah.

Tako lahko kljub razmeroma majhnemu deležu črpane količine razpoložljive podzemne vode za celotno Slovenijo (3,1 %), deleži v posameznih vodnih telesih podzemnih voda predvsem v sušnih letih presegajo tudi 20 % razpoložljivih količin vodnega telesa, v posameznih količinsko obremenjenih vodonosnikih, kot so npr. Ljubljansko, Dravsko in Mursko polje, pa je ta delež še nekoliko višji. Ob upoštevanju količin iz evidence vodnih pravic za rabo podzemnih voda v najbolj obremenjenih vodonosnikih v Sloveniji v posameznih obdobjih že posegamo v drugo polovico razpoložljivih količin za črpanje podzemne vode (Tabela 3). Črpane količine podzemne vode iz aluvialnih vodonosnikov petih obravnavanih vodnih teles prestavljajo 45 % podeljenih vodnih pravic (Souvent & Čenčur Curk, 2019). Ob tem pa je potrebno opozoriti na potrebo po poglobljeni analizi razpoložljivosti tudi lokalnih podzemnih vodnih virov, predvsem s poudarkom na podrobnejši oceni prispevka podzemne vode za ekološki pretok. V raziskavi smo ugotovili velika odstopanja pri izračunih prispevkov podzemne vode za ekološki pretok, ki so posledica različnih predpostavk in metodoloških pristopov, ob hkratnem neupoštevanju sezonske spremenljivosti. Zaradi tega je priporočljiva uporaba kriterija trajnostnega upravljanja podzemnih voda, da s črpanjem podzemnih vodnih virov ne zmanjšamo 10 % naravnega mesečnega baznega pretoka v površinskih vodotokih (Gleeson & Richter, 2017).

Poznavanje hidrološkega režima oz. sezonske spremenljivosti količin obnovljive podzemne vode je ključnega pomena tudi pri ocenah kemijskega stanja podzemnih voda. Kljub razmeroma stabilni dušikovi bilanci se vnosi dušika v vodonosnik v različno vodnatih hidroloških letih razlikujejo tudi za večkratnik, zato je interpretacija rezultatov monitoringa stanja podzemnih voda brez upoštevanja procesov v celotnem vodnem krogu lahko pomanjkljiva ali celo zavajajoča. Stopnja nitratnega onesnaženja podzemne vode je bila v analiziranem obdobju največja v letih 2011 in 2012, vzrokov za to pa ne najdemo v povečanem bremenu dušika, ampak v zmanjšanem napajanju, saj gre za najbolj sušno zaporedje dveh let zadnjega pol stoletja.

Za sistematično spremljanje doseganja trajnostnih ciljev pri črpanju in ohranjanju kakovosti podzemnih voda priporočamo uvedbo kazalnikov vodnega stresa in vodnega odtisa, ki zelo nazorno pokažejo človekove vplive na stanje naravnih vodnih virov (Hoekstra, 2003; Hoekstra et al., 2011). Spremljanje kazalnikov se mora opreti na rezultate vodnobilančnega modeliranje in študije pritiskov in vplivov v upravljavsko primerni prostorski in časovni skali.

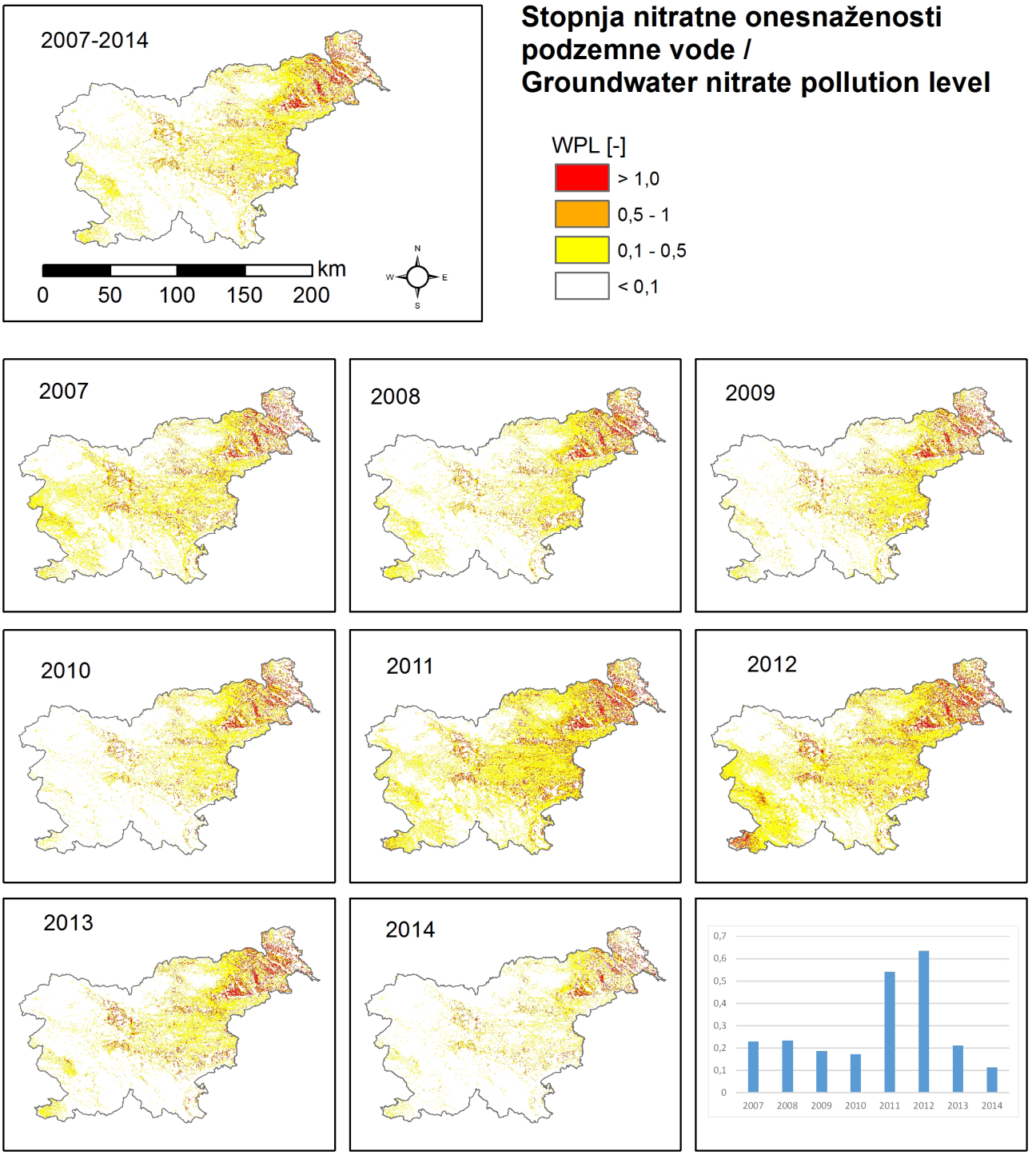

Sl. 3. Stopnja nitratne onesnaženosti podzemne vode v Slovenije v obdobju 2007–2014 po regionalnem modelu GROWA-SI / DENUZ-WEKU v prostorski skali 100 × 100 m.
Fig. 3. Groundwater nitrate pollution level in Slovenia in the period 2007–2014 after the GROWA-SI / DENUZ-WEKU regional model in the spatial resolution 100 × 100 m.

Sklep

Pri ocenjevanju doseganja trajnostnih ciljev upravljanja podzemnih voda v Sloveniji smo kot kazalnik količinskega stresa in nitratne obremenjenosti podzemnih voda prvič v Sloveniji uporabili koncept vodnega odtisa za podzemne vode, ki naj bi podpiral učinkovitejše načrtovanje upravljanja in strateški razvoj dolgoročnih okoljskih politik. V študiji je bila ob uporabi rezultatov regionalnega bilančnega modeliranja za plitve vodonosnike celotnega območja Slovenije in modeliranja toka podzemne vode na ravninskih aluvialnih vodonosnikih preizkušena metodologija količinskega odtisa podzemne vode in odtisa sive podzemne vode. Rezultati izračunanih stopenj izkoriščenosti podzemne vode na nekaterih vodonosnikih presegajo polovico razpoložljivih količin, stopnja nitratnega onesnaženja podzemne vode pa že presegajo mejo trajnostnega varovanja.

Rezultate smo primerjali z dosedanjimi ocenami stanja voda po posameznih vodnih telesih podzemnih voda in ugotovili, da uporaba koncepta količinskega stresa in količinskega odtisa podzemne vode z upoštevanjem površine napajalnega območja predstavlja koristno dopolnitev dosedanje ocene količinskega stanja podzemnih voda, odtis sive pozemne vode pa ob upoštevanju vodne bilance in hidrokemičnega ozadja prinaša možnost povsem novega vpogleda v prostorsko in časovno shemo obremenjevanja vodnih teles podzemnih voda v Sloveniji. Koncept odtisa sive vode bi bilo v prihodnje koristno uporabiti za vse parametre monitoringa, ki ogrožajo dobro stanje podzemnih voda, in preko teh kazalnikov spremljati učinke ukrepov v lokalnem in regionalnem merilu ter sprotno usmerjati prostorsko in okoljsko politiko za doseganje dobrega stanja in trajnostnega upravljanja podzemnih voda v Sloveniji.

Doseganje trajnostnih ciljev v zvezi z zagotavljanjem dostopa do vode in sanitarne ureditve ter trajnostnim gospodarjenjem z vodnimi viri do leta 2030 bo odvisno predvsem od realizacije ukrepov, ki jih bo prinesel naslednji načrt upravljanja voda. Zato naj bi načrt upravljanja voda za obdobje 2022–2027 temeljil na oceni stanja po posameznih vodnih telesih, nadgrajeni z letnimi in obdobnimi bilančnimi analizami izkoriščenosti in onesnaženosti podzemne vode na posameznih najbolj obremenjenih delih vodnih teles podzemne vode. V tem primeru bo ukrepe za doseganje ciljev okvirne direktive o vodah mogoče učinkovito usmerjati v opredeljevanje in zmanjševanje lokalnih pritiskov in vplivov, ki ogrožajo doseganje trajnostnih ciljev na področju podzemnih voda v Sloveniji.

Zahvala

Zasnova in prvi izračuni kazalnikov doseganja trajnostnih ciljev z vidika upravljanja in varovanja podzemnih voda v Sloveniji temelji na številnih simulacijah regionalnih modelskih sistemov GROWA-SI in DENUZ-WEKU, ki so rezultati nemško-slovenskega raziskovalnega projekta med Agencijo RS za okolje in Forschungszentrum Jülich. Ključno vlogo pri prenosu teh regionalnih modelskih sistemov v slovenski prostor sta imela nemška raziskovalca dr. Frank Wendland in dr. Ralf Kunkel. Avtorja članka se za njuno dolgoletno odlično sodelovanje iskreno zahvaljujeva.

Reference

Andjelov, M., Kunkel, R., Uhan, J. & Wendland, F. 2014: Determination of nitrogen reduction levels necessary to reach groundwater quality targets in Slovenia. Journal of Environmental Sciences, 26/9: 1806-1817. https://doi.org/10.1016/j.jes.2014.06.027

Andjelov, M., Frantar, P., Mikulič, Z., Pavlič, U., Savić, V., Souvent, P. & Uhan, J. 2016: Ocena količinskega stanja podzemnih voda za Načrt upravljanja voda 2015-2021 v Sloveniji. Geologija, 59/2: 205-219. https://doi.org/10.5474/geologija.2016.012

Andjelov, M., Mikulič, Z., Tetzlaff, B., Uhan, J. & Wendland, F. 2016: Groundwater recharge in Slovenia: results of a bilateral German-Slovenian research project. Schriften des Forschungszentrums Jülich, Reihe Energie & Umwelt, Bd. 339: 138 p.

Charchousi, D., Papadopoulou, M.P. & Nanou-Giannarou, A. 2018: Groundwater footprint: A tool for ecological-based groundwater resources management assessment. American Geophysical Union, Fall Meeting 2018. https://doi.org/10.1002/essoar.10500228.1

Demuth, S. 1993: Untersuchungen zum Niedrigwasser in West-Europa (European low flow study). Freiburger Schriften zur Hydrologie, Band 1, Freiburg: 205 p.

Direktiva 2000/60/ES: Direktiva Evropskega parlamenta in Sveta 2000/60/ES z dne 23. oktobra 2000 o določitvi okvira za ukrepe Skupnosti na področju vodne politike. UL L št. 327 z dne 22. 12. 2000: 1-73.

Direktiva 91/676/EGS: Direktiva Sveta 91/676/EGS z dne 12. decembra 1991 o varstvu voda pred onesnaževanjem z nitrati iz kmetijskih virov. Uradni list, št. 375 z dne 31. 12. 1991: 1-8.

European Communities 2009: Guidance on groundwater status and trend assessment. Guidance document, No. 18: 82 p.

EEA 2015: The European environment – state and outlook 2015: synthesis report, European Environmental Agency, Copenhagen: 205 p.

Esnault, L., Gleeson, T., Wada, Y., Heinke , J., Gerten, D., Flanary, E., Bierkens, M. F. P. & van Beek, L. P. H. 2014: Linking groundwater use and stress to specificcrops using the groundwater footprint in the Central Valley and High Plains aquifer systems, USA. Water Resources Research, 50/6: 4953–4973. https://doi.org/10.1002/2013WR014792

Franke, N.A., Bovaciuglu, H. & Hoekstra, A.Y. 2013: Grey Water Footprint Accounting:

Tier 1 Supporting Guidelines - Value of Water Research Report Series 65; UNESCO-IHE: Delft: 59 p.

Gleeson, T., Wada, Y., Bierkens, M. F. P. & van Beek, L. P. H. 2012: Water balance of global aquifers revealed by groundwater footprint. Nature, 488: 197-200. https://doi.org/10.1038/nature11295

Gleeson, T. & Wada, Y. 2013: Assessing regional groundwater stress fornations using multiple data sources withthe groundwater footprint. Environmental Research Letters, 8/4:1-9. https://doi.org/10.1088/1748-9326/8/4/044010

Gleeson, T. & Richter, B. 2017: How much groundwater can we pump and protect environmental flows through time? Presumptive standards for conjunctive management of aquifers and rivers. River Research and Applications, 34/1: 83-92. https://doi.org/10.1002/rra.3185

Hoekstra, A.Y. (ed.) 2003: Virtual water trade: Proceedings of the International Expert Meeting on Virtual Water Trade, Delft, The Netherlands, 12-13 December 2002, Value of Water Research Report Series No.12, UNESCO-IHE, Delft: 239 p.

Hoekstra, A.Y. & Hung, P.Q. 2002: Virtual water trade: A quantification of virtual water flows between nations in relation to international crop trade. Value of Water Research Report Series, No.11, IHE, Delft: 66 p.

Hoekstra, A.Y., Chapagain, A.K., Aldaya, M.M., Mesfin M. & Mekonnen, M.M. 2011: The Water Footprint Assessment Manual. Setting the Global Standard. Earthscan: 203 p.

Janža, M., Šram, D., Mezga, K., Andjelov, M. & Uhan, J. 2016: Ocena potrebnih količin podzemnih voda za ohranjanje ekosistemov in doseganje dobrega ekološkega stanja površinskih voda. Geologija, 59/2: 221-232. https://doi.org/10.5474/geologija.2016.013

Kille, K. 1970: Das Verfahren MoMNQ, ein Beitrag zur Berechnung der mittleren langjährigen Grundwasserneubildung mit Hilfe der monatlichen Niedrigwasserabflüsse. Zeitschrift der deutschen Geologischen Gesellschaft, Sonderheft Hydrogeologie Hydrogeochemie: 89-95

Matoz, H., Nagode, P., Mihorko, P., Cvitanič, I., Dobnikar Tehovnik, M., Remec Rekar, Š., Rotar, B., Andjelov, M., Uhan, J., Sever, M., Zajc, M., Krsnik, P., Kušar, U., Marolt, P., Hebat, I., Sušin, J., Verbič, J. & Zagorc, B. 2016: Poročilo Slovenije na podlagi 10. člena Direktive Sveta 91/676/EEC, ki se nanaša na varstvo voda pred onesnaženjem z nitrati iz kmetijskih virov za obdobje 2012 – 2015. Ministrstvo za okolje in prostor, Ljubljana: 73 p.

McDonald, R.I., Weber, K., Padowski, J., Flörke, M., Schneider, C., Green, P.A., Gleeson, T., Eckman, S., Lehner, B., Balk, D., Boucher, T., Grill, G. & Montgomery, M. 2014: Water on an urban planet: Urbanization and the reach of urban water infrastructure. Global Environmental Change. 27: 96–105. https://doi.org/10.1016/j.gloenvcha.2014.04.022

Mezga, K. 2014: Natural hydrochemical background and dynamics of groundwater in Slovenia: doktorska disertacija. Univerza v Novi Gorici, Nova Gorica: 226 p.

MOP 2009: Načrt upravljanja voda za vodni območji Donave in Jadranskega morja 2009–2015, Ministrstvo za okolje in prostor, Ljubljana: 524 p.

MOP 2016: Načrt upravljanja voda na vodnem območju Donave za obdobje 2016–2021, Ministrstvo za okolje in prostor, Ljubljana: 287 p.

Panno, S.V., Kelly, W.R., Martinsek, A.T. & Hackley, K.C. 2006: Estimating background and threshold nitrate concentrations using probability graphs. Ground Water, 44/5: 697-709. https://doi.org/10.1111/j.1745-6584.2006.00240.x

Petauer, D. & Hiti, T. 2017: Matematični model vodonosnika Ljubljanskega polja umerjen na visoke in srednje hidrogeološke razmere. Poročilo GEORAZ d.o.o., ARSO, Ljubljana: 42 p.

Petauer, D. & Hiti, T. 2018: Matematični model vodonosnika Ljubljanskega polja umerjen na visoke in srednje hidrogeološke razmere. Poročilo GEORAZ d.o.o., ARSO, Ljubljana: 34 p.

Prestor, J. & Janža, M. 2016: Karta ranljivosti podzemne vode. In: Novak, M. & Rman, N. (ur.): Geološki atlas Slovenije. Geološki zavod Slovenije, Ljubljana: 46-47.

Sachs, J., Schmidt-Traub, G., Kroll, C., Lafortune, G. & Fuller, G. 2019: Sustainable Development Report 2019. New York: Bertelsmann Stiftung and Sustainable Development Solutions Network (SDSN).

Schlüter, H. 2006: Ermittlung des nachhaltig nutzbaren Grundwasserdargebots in stark genutzten Teileinzugsgebieten – Beurteilung des mengenmäßigen Zustandes gemäß EU Rahmenrichtlinie Wasser. Ph.D. Thesis. Brandenburgischen Technischen Universität Cottbus: 193 p.

Souvent, P., Vižintin, G., Celarc, S. & Čenčur Curk, B. 2016: An expert system supporting

decision making process for sustainable groundwater use in main alluvial aquifers in Slovenia. In: European Geosciences Union, General Assembly 2016, Vienna, Austria, 17-22 April 2016, Geophysical research abstracts, 18: 4395.

Souvent, P. & Čenčur Curk, B. 2019: Uporaba numeričnih modelov toka podzemne vode pri upravljanju s podzemnimi vodami. In: Geološki zbornik, 24. posvetovanje slovenskih geologov, Ljubljana, 29. november 2019. Naravoslovnotehniška fakulteta, Ljubljana: 116-119

Sovič, N. 2017: Monitoring pitne vode 2017 – Letno poročilo o kakovosti pitne vode v letu 2017. Nacionalni laboratorij za zdravje, okolje in hrano. Maribor: 59 p.

Srebovt, A. 2014: Izračun indeksov baznega odtoka (BFI) za vodomerne postaje državnega hidrološkega monitoringa: diplomska naloga. Univerza v Ljubljani, Ljubljana: 44 p.

Sušin, J. & Verbič, J. 2019: Bilančni presežek dušika v kmetijstvu. Internet: http://kazalci.arso.gov.si/sl/content/bilancni-presezek-dusika-v-kmetijstvu-0 (14.11.2019)

Tennant, D.L. 1976: Instream flow regimens for fish,wildlife, recreation, and related environmental resources. In: Instream flow needs, Volume II: Boise, Idaho, Proceedings of the symposium and specialty conference on instream flow needs, May 3–6, American Fisheries Society: 359-373. https://trove.nla.gov.au/version/42683783

Turton, A.R. 2003: Water and state sovereignty: the hydropolitical challenge for state in aride regions. In: Wolf (ed.): 516-533

Uhan, J. 2011: Ranljivost podzemne vode na nitratno onesnaženje v aluvialnih vodonosnikih Slovenije: doktorska disertacija. Univerza v Ljubljani, Ljubljana: 163 p.

United Nations 2020: Transforming our world: the 2030 Agenda for Sustainable Development. Internet: https://www.un.org/ga/search/view_doc.asp?symbol=A/RES/70/1&Lang=E

Uradni list RS 2009: Uredba o kriterijih za določitev ter načinu spremljanja in poročanja ekološko sprejemljivega pretoka. Uradni list RS, št. 97/09.

Uradni list RS 2009: Uredba o stanju podzemnih voda. Uradni list RS, št. 25/09, 68/12 in 66/16.

Vrba, J. & Lipponen, A. 2007: Groundwater resources sustainability indicators. IHP/2007/GW-14: 123 p.

Wundt, W. 1958: Die Kleinstwasserführung der Flüsse als maß für die verfügbaren Grundwassermengen. In: Grahamm, R. (ed.): Die Grundwässer in Deutschland und ihre Nutzung. Forsch. Deut. Landeskunde, 105: 47-54.

GEOLOGIJA *62/2*, 279–300, Ljubljana 2019

https://doi.org/10.5474/geologija.2019.014

Pregled uporabe georadarja na krasu

Application of ground penetrating radar in karst environments: An overview

Teja ČERU[1] & Andrej GOSAR[2,3]

[1]Geološki zavod Slovenije, Dimičeva ul. 14, SI-1000 Ljubljana, Slovenija; e-mail: teja.ceru@geo-zs.si
[2]Agencija RS za okolje, Urad za seizmologijo, Vojkova cesta 1b, SI-1000 Ljubljana, Slovenija
[3]Univerza v Ljubljani, Naravoslovnotehniška fakulteta, Aškerčeva 12, SI-1000 Ljubljana, Slovenija

Prejeto / Received 4. 11. 2019; Sprejeto / Accepted 17. 12. 2019; Objavljeno na spletu / Published online 24. 12. 2019

Ključne besede: georadar, kras, jama, pogrezanje, epikras, kraški vodonosnik, kamnolom, brezstropa jama, jamski sedimenti

Key words: ground penetrating radar (GPR), karst, cave, subsidence, epikarst, karst aquifer, quarry, unroofed cave, cave sediments

Izvleček

Kras kot kompleksen in heterogen sistem predstavlja za georadar velik izziv. Kljub vsemu pa lahko z dobro načrtovanimi georadarskimi raziskavami pridobimo dodatne informacije o plitvem podpovršju, kjer se odvija večina kraških procesov. Zaradi specifičnosti kraškega površja so v uvodnem delu predstavljene nekatere ovire in prilagoditveni pristopi pri raziskavah na krasu. Analiza pregleda objavljene literature je pokazala, da se georadar v kraških okoljih najpogosteje uporablja za zaznavanje jam in območij pogrezanj ter pri preprečevanju nenadnih porušitev tako v urbanih območjih kot tudi pri gradbenih posegih v prostor. Georadar se uporablja tudi pri raziskavah kraških vodonosnikov, epikrasa in raziskavah v kamnolomih. Poleg uveljavljenih aplikacij so predstavljene nekatere še neuveljavljene aplikacije, kot je uporaba georadarja pri raziskavah brezstropih jam in jamskih sedimentov. Glavni namen članka je prikazati in ovrednotiti možnosti uporabe georadarja v različnih kraških okoljih in spodbuditi njegovo uporabo za nekatere nove aplikacije in opozoriti na nujnost interdisciplinarnega pristopa v takšnih študijah.

Abstract

Karst as an extremely complex and heterogeneous system, that presents a great challenge for the ground penetrating radar (GPR). However, properly planed GPR surveys can provide additional information about the shallow subsurface, where most karst processes take place. Due to the specific nature of the karst terrain, the introductory part presents some obstacles and adaptive approaches to karst research. An analysis of the published literature revealed that the GPR is most commonly used for detecting caves and subsidence areas and for preventing collapses in urban areas and for construction interventions. This is followed by exploration of karst aquifers, epikarst and quarry research. Some non-established applications are also presented, such as the use of a georadar in exploration of unroofed caves and cave sediments. The main purpose of this article is to demonstrate and evaluate the possibilities of using a georadar in different karst environments, to encourage its use in some new applications, and to emphasize the necessity of an interdisciplinary approach in such studies.

Uvod

Kraški sistem sodi med najkompleksnejša geološka okolja pri hidrogeoloških, geotehnično-inženirskih in okoljskih raziskavah. Zaradi heterogenosti in nepredvidljivosti predstavlja kraški sisitem za georadarske raziskave velik izziv, a z leti se njegova uporaba kljub vsemu veča. Z vidika zaščite podzemne vode na kraških območjih, ter zaradi ostalih nevarnosti, ki so posledica zakrasevanja (npr. nestabilnost tal), je vse večje zavedanje pomembnosti razumevanja kraških procesov vodilo v hiter porast raziskav v zadnjih dveh desetletjih (Gutiérrez et al., 2014). Ključna prednost georadarja v primerjavi s seizmično refrakcijo/refleksijo in električno upornostno tomografijo (ERT) je visoka ločljivost, ki omogoča natančen vpogled v strukturo podpovršja ter relativno hitre in enostavne meritve (Schrott & Sass, 2008). Medtem ko z geološkimi, hidrogeološkimi in geomorfološkimi metodami raziskujemo le površje krasa oz. pridobimo le točkovne informacije iz globine (vrtine), nudijo geofizikalne metode zvezen niz podatkov.

Kras pokriva 12 % vsega površja Zemlje in je zaradi svoje raznolikosti in posebnosti predmet številnih študij v okviru temeljnih ali aplikativnih raziskav na različnih znanstvenih področjih (Andreo et al., 2010). Dejstvo, da karbonatne in evaporitne kamnine pokrivajo 20 % površja in da je četrtina prebivalstva odvisna od oskrbe pitne vode v kraških vodonosnikih (Gutiérrez et al., 2014), je vodilo v vse večji interes za raziskovanje tega sistema. Zaradi občutljivosti kraškega sistema so v takšnih okoljih potrebne posebne metode raziskav za zaščito pred okoljsko-inženirskimi problemi kot so onesnaževanje kraških vodonosnikov, pogrezanje tal, nastanek udornic in jam. V zadnjem času je bilo objavljene veliko pregledne literature, ki združuje in povezuje temeljno vedenje z aplikativnimi študijami na kraškem površju (Andreo et al., 2010; 2015; Waltham et al., 2005). Še pomembnejše so raziskave krasa na urbanih območjih in pri inženirsko-geotehničnih posegih v prostor (kamnolomi, gradnja cest in predorov) za zmanjševanje geološko pogojenih nevarnosti (geohazard).

V zadnjih 30 letih se je uporaba georadarja uveljavila na številnih področjih, čemur so v zadnjih 10 letih sledile objave preglednih člankov za različne aplikacije. Eden izmed prvih celovitih preglednih člankov na področju uporabe v geologiji obravnava uporabo georadarja v sedimentologiji (Neal, 2004). Pregled uporabe geofizikalnih metod pri geomorfoloških raziskavah sta podala Schrott & Sass (2008) in poudarila pomen integracije različnih metod ter opisala njihove prednosti in omejitve. V zadnjih nekaj letih so bili objavljeni tudi pregledni članki na področju gradbeništva (Wai-Lok Lai et al., 2018). Zajícová & Chuman (2019) sta podala pregled uporabe georadarja v študijah tal, kjer obravnavata določevanje vsebnosti vode, stratigrafije tal, vsebnosti soli in strukture tal, zaznavanje drevesnih korenin in koreninske biomase. Pregled raziskav z različnimi geofizikalnimi metodami na krasu so povzeli Chalikakis et al. (2011), ki so obravnavali prednosti in omejitve za nekatere najpogostejše aplikacije. Podrobnejši pregled, ki bi obravnaval različne aplikacije georadarja na krasu, še ni bil objavljen.

Ta prispevek predstavlja krajši povzetek teorije in raziskav, ki so bile narejene v okviru doktorskega dela (Čeru, 2019). V uvodnem delu so podane osnove, ki so pomembne za razumevanje delovanja georadarja ter njegove uporabe na krasu. Sledi analiza pregleda objavljene literature v bazah Web of Science (WoS) in Scopus. Jedro članka predstavlja pregled raziskav po različnih aplikacijah s primeri radargramov. Predstavljene so nekatere najbolj uveljavljene uporabe ter tudi nekatere nove možnosti, ki so bile raziskane v okviru doktorata, kot je zaznavanje brezstropih jam in jamskih sedimentov z georadarjem.

Osnove delovanja georadarja

Georadar oddaja kratke pulze elektromagnetnega (EM) valovanja v podpovršje, kjer se del vpadnega valovanja odbije (refleksija) zaradi kontrasta dielektričnih lastnosti na meji različnih snovi (Blindow et al., 2007). Globinski doseg georadarja je poleg električnih lastnosti materiala v največji meri odvisen od frekvence oddajnih anten, zato se v praksi glede na ciljno problematiko uporabljajo georadarski sistemi različnih frekvenc. Za uporabo na krasu so najprimernejši nizkofrekvenčni georadarski sistemi (25–250 MHz), ki omogočajo večji globinski doseg ob še sprejemljivi ločljivosti. Pri plitvejših raziskavah pa je zaželeno, da se meritve dopolnjujejo tudi z višjefrekvenčnimi antenami (> 250 MHz).

Metoda georadarja je po principu delovanja podobna refleksijski seizmiki in tehnikam sonarjev (Davis & Annan, 1989). Metoda temelji na penetraciji EM valov, ki jih v kratkih impulzih pošiljamo z oddajno anteno v tla (Davis & Annan, 1989). Del vpadnega valovanja se na meji različnega materiala odbije zaradi različnih električnih lastnosti (Blindow et al., 2007), kjer ga na površju zazna sprejemna antena (sl. 1). Pri tem se meri dvojni čas potovanja valov (ang. *two-way travel time*) od oddajne antene do mejnih ploskev (reflektorji) in nazaj do sprejemne antene.

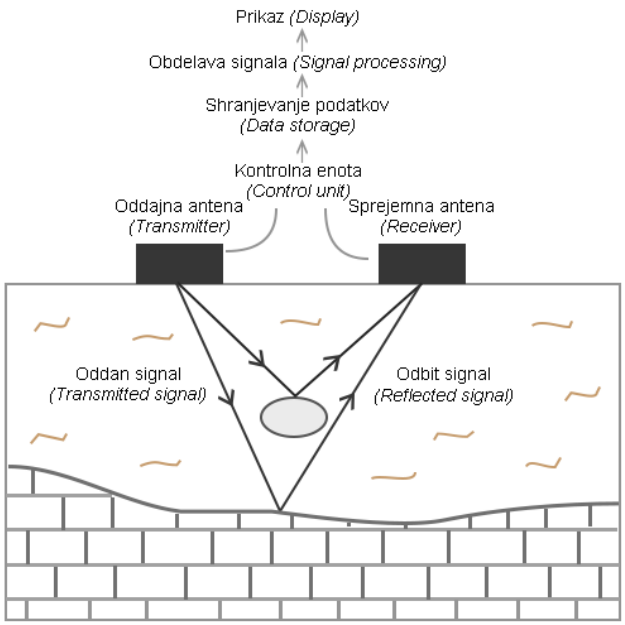

Sl. 1. Shematski prikaz delovanja georadarja.
Fig. 1. Schematic principle of GPR measurement.

Najpomembnejši lastnosti, ki vplivata na odbojnost na meji različnih plasti in na globinski doseg valovanja, sta dielektričnost (ε) in električna prevodnost (σ) snovi (Blindow, 2006). Na električne lastnosti nevezanega sedimenta v največji meri vpliva prostorninski delež vode, na spremembe električnih lastnosti kamnin pa vrsta kamnine in delež razpok zapolnjenih z vodo in/ali zrakom. Razlike v električnih lastnostih materialov vplivajo na hitrost in dušenje ter delež odbitega EM valovanja. Le dovolj velik kontrast dielektričnih lastnosti med različnimi snovmi in s tem sprememba v hitrosti EM valovanja povzroči, da pride do odboja na meji, kar omogoča razlikovanje med različnimi objekti v podpovršju (Reynolds, 2011).

Ločljivost metode ter izguba energije in dušenje signala

Ker se EM valovanje od oddajne antene širi v obliki konusnega stožca, se amplituda zaradi sferičnega razširjanja valovanja z oddaljevanjem od antene zmanjšuje (Reynolds, 2011). Zato se ločljivost in posledično velikost objekta, ki ga lahko zaznamo, z globino spreminja. Vertikalna ločljivost georadarskega sistema je funkcija predvsem frekvence in teoretično velja, da je vertikalna ločljivosti enaka ¼ valovne dolžine (λ/4). V praksi je manjša od teoretične, saj nanjo vplivajo še številni drugi dejavniki. Horizontalna ločljivost pa je odvisna od frekvence in dielektričnih lastnosti snovi. V tabeli 1 so podane vrednosti za vertikalno in horizontalno ločljivost za dva različna materiala in dve frekvenci, ki se najpogosteje uporabljata pri raziskavah na krasu. Vidimo, da se horizontalna ločljivost z globino hitro manjša.

Na izgubo energije in dušenje EM valovanja vpliva veliko dejavnikov. V prvi vrsti na zmanjšanje amplitude vpliva sama oblika oz. geometrija georadarskega signala. Ko potuje od antene v tla, se ustvari t.i. talni spoj (ang. *ground coupling*), kjer pride do prvih izgub EM valovanja. Izguba je odvisna tudi od značilnosti in kakovosti georadarskega sistema ter frekvence, saj so višje frekvence podvržene večjemu dušenju. Poleg tega pa na dušenje vplivajo predvsem dielektrične, električne in magnetne lastnosti kamnin. Na te pa vplivajo poroznost, zrnavost, mineralna sestava, prisotnost vode, prisotnost soli in ostale značilnosti materiala, zato je težko vnaprej predvideti vse dejavnike, ki imajo vpliv na razširjanje EM valovanja.

V praksi se na kraškem terenu izkaže, da ima na dušenje signala velik vpliv heterogenost sistema. Praznine, neraven in nezvezen kontakt matične podlage s tlemi z vmesnimi globokimi žepi in nehomogenosti znotraj karbonatnih kamnin povzročajo sipanje energije in vplivajo na zmanjšanje energije signala. Veliko omejitev na krasu predstavljajo tudi drobnozrnati sedimenti, ki zapolnjujejo depresije, jame in kraške žepe, saj zaradi svojih lastnosti pomembno vplivajo na izgubo signala. Sedimenti in tla na krasu vsebujejo precejšen delež glinenih mineralov, ki bistveno vplivajo na dušenje signala, še posebej ob večji prisotnosti vode. Kljub temu, da tla na karbonatnih tleh navadno niso debela, se je izkazalo, da je globinski doseg 50 MHz antene bistveno manjši (med 5–20 m, v povprečju pa med 8–15 m) v primerjavi z meritvami v kamnolomih, kjer je teren raven in na površju ni sedimentov (globinski doseg do 30 m). Na razgibanem površju prihaja do izgub energije tudi zaradi slabega stika med anteno in tlemi.

Tabela 1. Teoretična ločljivost 50 in 250 MHz antene pri različnih vrednostih dielektrične konstante na določeni globini.
Table 1. Theoretical resolution of 50 and 250 MHz antenna with different dielectric constants at certain depth.

	Globina (m) *Depth (m)*		Vertikalna ločljivost (m) *Vertical resolution (m)*		Horizontalna ločljivost (m) *Horizontal resolution (m)*	
	50 MHz	*250 MHz*	*50 MHz*	*250 MHz*	*50 MHz*	*250 MHz*
Apnenec *Limestone* ε= 7 (v= 0,11 m/ns)	5	2	1,134	0,227	2,335	0,820
	10	4	1,134	0,227	4,102	1,528
	15	6	1,134	0,227	5,870	2,235
	20	8	1,134	0,227	7,638	2,942
	30	10	1,134	0,227	11,173	3,649
*Povprečna tla *Average soil* ε= 16 (v= 0,075 m/ns)	5	2	0,750	0,15	1,588	0,560
	10	4	0,750	0,15	2,800	1,045
	15	6	0,750	0,15	4,013	1,530
	20	8	0,750	0,15	5,226	2,015
	30	10	0,750	0,15	7,651	2,500

**povprečna tla (average soil): Povprečna vrednost v razponu za različna tla (average value in the range for different soils).*

V tabeli 2 so strjene glavne prednosti in nekatere omejitve georadarja na krasu.

Tabela 2. Prednosti in pomanjkljivosti georadarske metode.
Table 2. Advantages and limitations of the GPR method.

PREDNOSTI (*Advantages*)	OMEJITVE (*Limitations*)
• Nedestruktivnost - še posebej pomembna v urbanih okoljih • *Non-destructiveness - particularly important in urban environments*	• Globinski doseg je majhen v visoko prevodnih okoljih (sedimenti z večjim deležem gline, prisotnost vode) • *The depth of penetration is limited in highly conductive environments (clayey sediments, presence of water)*
• Največja ločljivost med vsemi geofizikalnimi metodami • *The highest resolution out of all geophysical methods*	• Zaradi stika antene s tlemi mora biti teren raven in enakomeren, kar je na kraškem površju redkost • *Because the antenna must be in contact with the ground, the terrain must be level and even, which is rare in karst*
• Z mrežo vzporednih in prečnih profilov z nadaljnjo obdelavo in modeliranjem dobimo 3D modele • *A network of parallel and transverse profiles with further processing and modelling can create 3D models*	• Interpretacija radargramov je kompleksna, sploh v kraškem sistemu • *The interpretation of radargrams is complex, especially in the karst system*
• Relativno hitre in enostavne meritve v primerjavi z nekaterimi ostalimi geofizikalnimi metodami • *The measurements are relatively quick and easy compared to other geophysical methods*	• Metoda ni primerna za materiale s podobnimi dielektričnimi lastnosti • *The method has limitations if dielectric properties of materials are similar*
• Zvezen niz podatkov v primerjavi z raziskovalnim vrtanjem • *Continuous data information compared to drilling data*	• Uspešnost metode je odvisna od danih pogojev na terenu, pri čemer ima velik vpliv vsebnost vlage (padavine) • *The success of the method depends on field conditions, where moisture content (precipitation) has a high influence*
• Priročna metoda pri preliminarnih raziskavah zaradi relativno enostavnih in hitrih meritev • *A convenient method for preliminary research due to relatively simple and fast measurements*	• Pri neščitenih antenah lahko odboji od nadpovršinskih objektov onemogočijo interpretacijo radargramov • *For unshielded antennas, reflections from surface objects may prevent the interpretation of the radargrams*

Izvajanje meritev na kraškem terenu

Kraški teren je večinoma neraven in težko prehoden, kar za georadarske meritve predstavlja precejšen omejitveni dejavnik. Pred začetkom meritev zato traso profilov očistimo, kolikor je to mogoče, da omogočimo čim boljši stik antene s tlemi. Če je teren dovolj raven, se uporabljajo toge ščitene antene, s katerimi pa je premikanje po terenu polnem kamenja in škrapelj nemogoče ali pa je stik antene s tlemi preslab. Za večino raziskav v okviru doktorata je bila zato uporabljena georadarska oprema Mala ProEx (Švedska) z 50 MHz RTA (»*Rough Terrain Antenna*«) neščiteno (ang. *unshielded*) anteno. Ta se je za geološke aplikacije izkazala kot zelo uspešna tako zaradi globinskega dosega kot zaradi samega sistema, ki omogoča meritve tudi na bolj razgibanih in poraščenih območjih. Meritve smo glede na namen in terenske pogoje dopolnjevali tudi s ščiteno (ang. *shielded*) 250 MHz anteno.

Glavna prednost RTA sistema je upogljivost cevi, ki vključuje oddajno in sprejemno anteno. Takšna konfiguracija omogoča meritve na škrapljastem terenu (sl. 2a). Po drugi strani pa takšen sistem onemogoča ščitenje sevanja anten, kar pomeni, da oddajna antena EM valovanje oddaja v vse smeri in dobimo tudi nadpovršinske odboje, ki v neugodnih pogojih lahko zakrivajo reflektorje v podpovršju. Če je mogoče, zato meritve načrtujemo v mesecih, ko na drevesih ni listja in bujne podrasti ter tako zmanjšamo vpliv

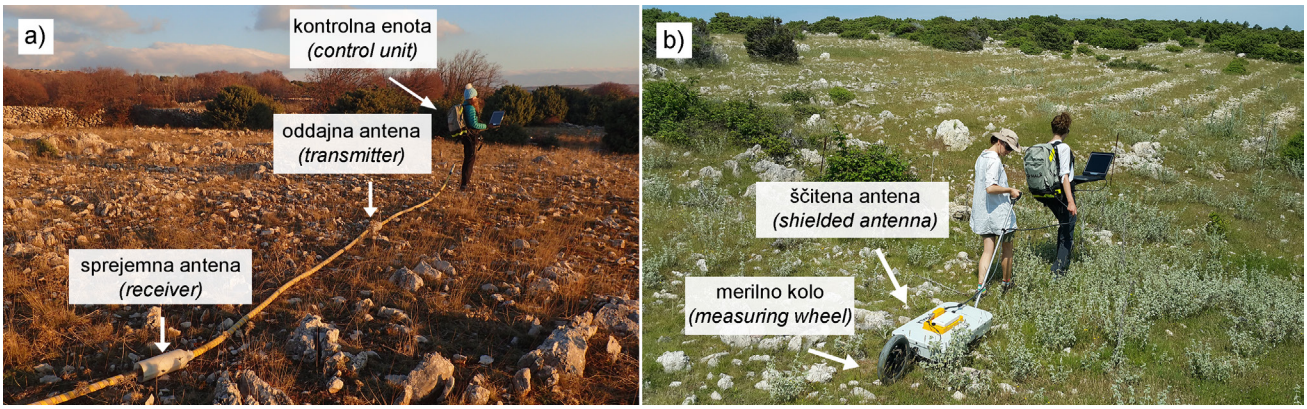

Sl. 2. Georadarski sistem Mala ProEx z a) neščiteno 50 MHz RTA (»*Rough Terrain Antenna*«) anteno; b) ščiteno 250 MHz anteno.
Fig. 2. GPR system Mala ProEx with a) an unshielded 50 MHz RTA (»*Rough Terrain Antenna*«); b) a shielded 250 MHz antenna.

nadpovršinskih odbojev. Poleg tega je takrat teren tudi bolj prehoden in posledično stik antene s tlemi boljši. Izogibamo se tudi daljnovodom, ograjam in ostalim objektom na površju, ki lahko predstavljajo izvor nadpovršinskih motenj.

Za plitvejše raziskave smo meritve dopolnjevali tudi s ščiteno 250 MHz anteno (sl. 2b). Oddajna in sprejemna antena sta ščiteni v skupnem ohišju, zato antena oddaja signal samo v smeri tal. S tem je omogočeno selektivno izboljšati želene signale in zmanjšati motnje. Poleg prednosti pa se možnost pojava večkratnega odbijanja signala (ang. *ringing*) zaradi sistema znatno poveča. Ščitenje antene nikoli ni popolno, zato včasih tudi pri ščitenih antenah dobimo nadpovršinske odboje (Annan, 2009), ki se jih lahko napačno interpretira. Zato je uporaba neščitenih anten včasih boljša izbira, če nam pogoji na terenu to omogočajo.

Izbira antene in primerjava radargramov različnih frekvenc

Ustrezna izbira frekvence antene georadarskega sistema je ključnega pomena pri načrtovanju meritev, saj frekvenca vpliva na globinski doseg in ločljivost metode. Glede na kontrast fizikalnih lastnosti ciljne strukture (jama, vrtača, cevi, prelom, geološka bariera…) v primerjavi z okolno kamnino, ciljno globino in velikostjo proučevane strukture, se odločimo za ustrezno frekvenco. Pred izbiro ustrezne antene je potrebno vedeti v kakšnih pogojih se kraške oblike pojavljajo, približno kakšnih dimenzij so, ter na kateri globini pričakujemo pojav, ki ga želimo zaznati. Če pa je le mogoče in smiselno, meritve izvedemo z več različnimi frekvencami.

Za primerjavo radargramov različnih frekvenc sem izbrala dva primera, izmerjena v različnih terenskih pogojih. Prvi profil (sl. 3) prikazuje območja povezav med segmenti brezstrope jame na otoku Krk v karbonatih (Čeru et al., 2018a). Zaradi velikega kontrasta v dielektrični konstanti med sedimenti brezstropega jamskega sistema in okoliškim kraškim terenom se ta območja jasno odražajo tako na radargramih 50 MHz kot tudi 250 MHz antene. Območja anomalij (A in B) se jasneje vidijo na radargramu 50 MHz antene, kjer je dušenje signala na območjih večje debeline sedimentov izrazitejše v primerjavi z 250 MHz anteno. Na radargramu 250 MHz antene se zaradi boljše ločljivosti antene lepo vidi skledasto obliko povezav (povečan detajl slike 3).

Drugi primer (sl. 4) prikazuje georadarski profil preko vrtače v pleistocenskem konglomeratu na Kranjskem polju (Čeru et al., 2017), kjer so lepo vidne razlike med 50 MHz neščiteno in 250 MHz ščiteno anteno. Pri 250 MHz anteni ne dobimo nadpovršinskih odbojev od dreves. Zaradi velike debeline tal je globinski doseg obeh anten manjši kot v primeru brezstropih jam v apnencih. Če primerjamo radargrama obeh fre-

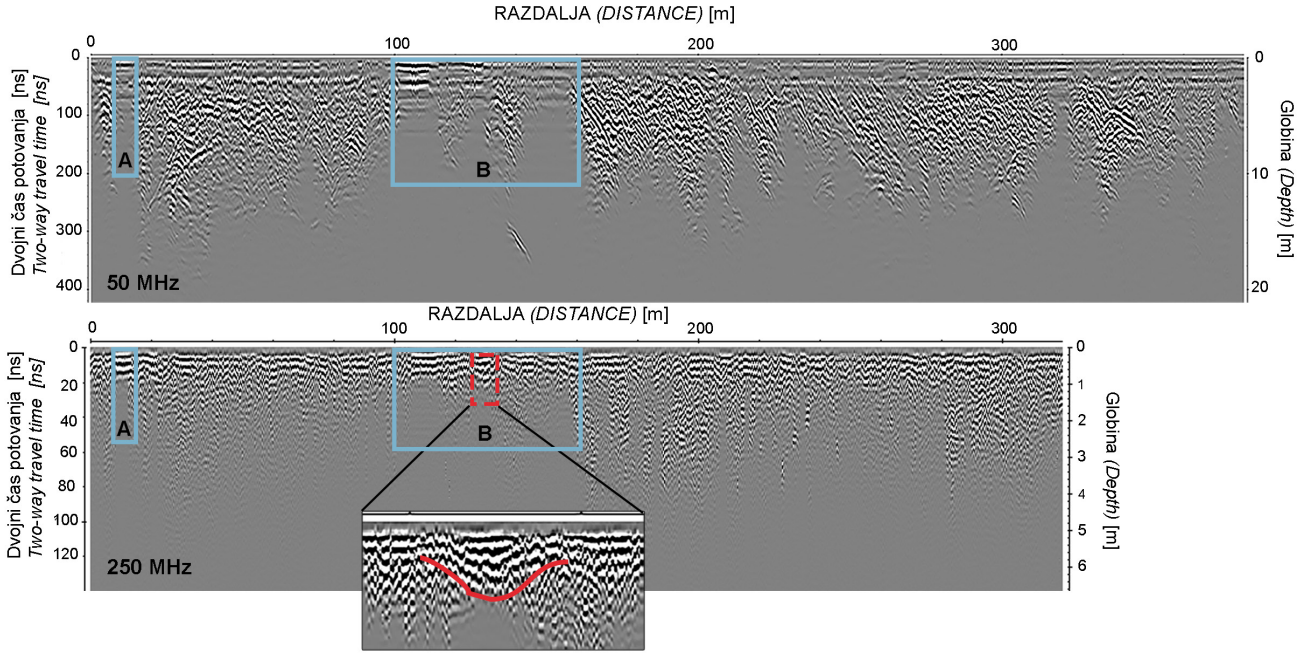

Sl. 3. Primerjava radargramov 50 in 250 MHz antene, kjer anomaliji A in B predstavljata večjo debelino sedimentov (povezava segmentov brezstrope jame). Radargram 250 MHz antene zaradi boljše ločljivosti kaže skledasto obliko na sredini anomalije B.

Fig. 3. Comparison of the 50 and 250 MHz radargrams, where interpreted anomalies A and B represent greater thickness of sediments (the connections between segments of an unroofed cave). The radargram of the 250 MHz antenna shows a bowl-shaped structure in the centre of anomaly B.

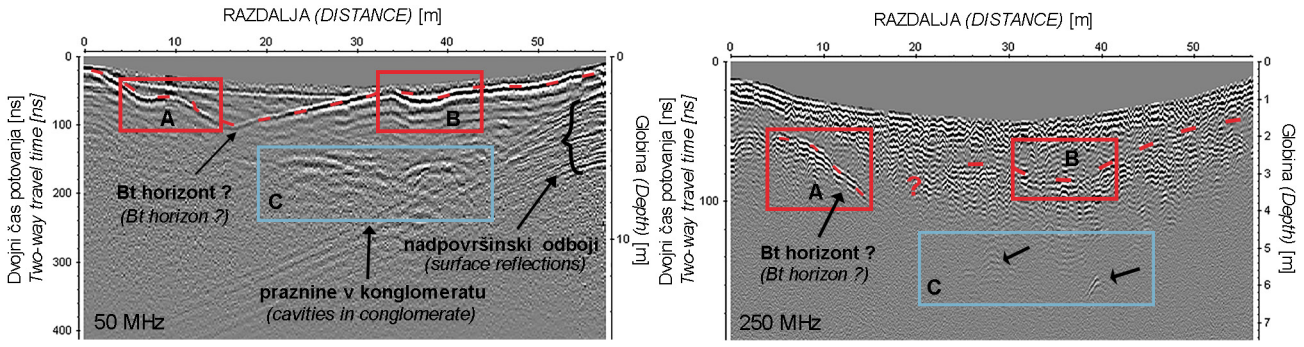

Sl. 4. Primerjava radargramov dveh frekvenc (50 in 250 MHz) na primeru profila čez vrtačo v konglomeratu (Čeru et al., 2017).
Fig. 4. Comparison of radargrams of two frequencies (50 in 250 MHz) in the case of a profile over a doline in a conglomerate (Čeru et al., 2017).

kvenc, 250 MHz antena poda bistveno manj informacij kot 50 MHz antena. Pedološki horizont Bt je na profilu 50 MHz antene zvezen, medtem ko pri 250 MHz anteni ni v celoti sledljiv. Prav tako niso jasni in izraziti odboji od praznin v dnu vrtače, kot je to vidno pri 50 MHz anteni.

Iz obeh predstavljenih primerov vidimo, da je potrebno vsak teren obravnavati ločeno, prav tako je zaželena uporaba več frekvenc. Testne meritve pri umerjanju metode so pomembne, saj nam pokažejo, katera frekvenca je primernejša za dane terenske pogoje in cilj raziskav.

Obdelava podatkov

Striktna navodila za obdelavo georadarskih podatkov ne obstajajo, razen za nekatere osnovne postopke kot je odstranitev zamika signala in določitev ničelnega časa, ki so nujni. Izbira drugih postopkov in njihovega zaporedja pa je prilagojena konkretnim podatkom. Pri izbiri postopkov je zelo pomembno dobro poznavanje lastnosti preučevanega območja. Nekateri napredni postopki obdelave lahko podajo boljše informacije, če je ciljna struktura dobro definirana, in kjer vnaprej poznamo velikost, obliko objekta in lastnosti podpovršja, da so postopki sploh smiselni, kar pa je pri raziskavah na krasu pogosto nemogoče. Zaradi slabšega globinskega dosega pri večini raziskav, sem nekoliko več časa namenila ojačenju amplitude. Vsak radargram sem obdelala z različnimi funkcijami in nastavitvami, da sem pridobila najboljši rezultat.

Vsako območje zahteva specifično obdelavo, a pri večini radargramov sem uporabila zaporedje postopkov, ki so prikazani v tabeli 3.

Postopki so prikazani na primeru radargrama obdelanem v programu ReflexW (sl. 5). Anomalija kaže na povezavo med dvema večjima depresijama (okvir na sl. 5). Območje večje debeline sedimentov dokazuje povezavo teh oblik v brezstrop jamski sistem. Nekateri naprednejši postopki kot je migracija in dekonvolucija so bili uporabljeni za posebne namene. Z vzporedno mrežo profilov lahko pridobimo 3D model podpovršja, kjer dobimo predstavo o razširjanju iskanih objektov v prostoru. Programska okolja poleg 3D modelov omogočajo tudi prikaz prerezov po globini in dolžini.

Tabela 3. Zaporedje postopkov obdelave radargramov.
Table 3. Processing sequence of radargrams.

POSTOPKI OBDELAVE (*Processing steps*)
• odstranitev zamika signala (»*subtract mean-dewow*«)
• določitev ničelnega časa pri prvem negativnem vrhu signala s postopkom korekcije maksimalne faze (»*correct max. phase*«) in prestavitvijo ničelnega časa (»*move start time*«)
• odstranitev ozadja (»*background removal*«)
• funkcija ojačenja amplitude (»*amplitude correction*«): – upadanje energije (»*energy decay*«) – avtomatsko ojačenje amplitude (»*automatic gain control–AGC*«) – ročno ojačenje amplitude (»*manual gain (y)*«)
• pasovno prepustno filtriranje (»*bandpass frequency filtering*«)
• 2D filtriranje (»*median xy filter*« in »*subtracting average*«)

Uporaba georadarja na krasu

Georadar se je v začetku uporabljal za reševanje različnih geoloških problemov, predvsem pri inženirskih in okoljskih raziskavah ter na področju glaciologije. Šele kasneje se je metoda uveljavila na številnih drugih področjih, med drugim tudi za raziskave na krasu.

Za pregled uporabe georadarja na krasu sem uporabila objavljeno literaturo v podatkovnih bazah *Scopus* in *Web of Science* (WoS). Z iskalnim vnosom (*title-abs-key (gpr) or title-abs-key (ground and penetrating and radar) and title-abs-key (karst**)) dobimo v bazi Scopus 297 zadetkov in v bazi WoS z iskalnim vnosom, ki je ekvivalenten iskanju v Scopus bazi (*topic (title, abstract, author keywors, keywords Plus): (ground*

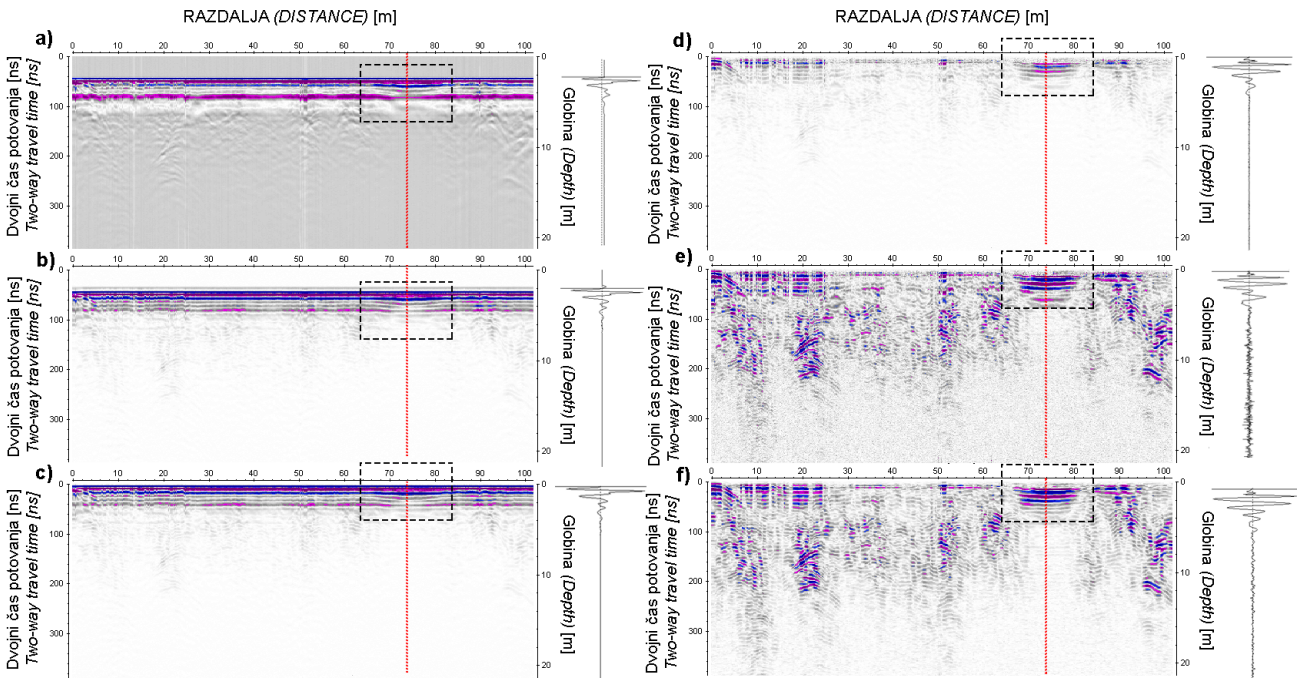

Sl. 5. Zaporedje postopkov obdelave profila 50 MHz antene, ki je bil uporabljen pri večini profilov: a) surov radargram; b) odstranitev zamika signala; c) določitev ničelnega časa; d) odstranitev ozadja; e) ročno ojačenje amplitude; f) pasovno prepustno filtriranje. Vpliv postopka na izbrano sled (označena rdeče) je prikazan desno ob profilu.

Fig. 5. Sequence of processing steps for the 50 MHz antenna that was used for most profiles: a) raw radargram; b) subtract mean-dewow; c) determination of time zero; d) background removal; e) manual amplification of amplitude; f) bandpass filtering. The impact of processing steps on the marked trace (red line) is shown to the right of the profile.

*penetrating radar or gpr) and topic: (karst**)), 244 zadetkov. Glavna razlika med zadetki v obeh bazah je delež prispevkov s konferenc. V bazi Scopus je zavedenih več prispevkov s konferenc, nabor člankov pa je podoben. Po pregledu vsebin člankov in prispevkov je očitno, da je večina prispevkov na konferencah s področja gradbeništva in geotehnike, medtem ko so vsebine člankov bolj raznolike in obravnavajo tudi nekoliko bolj temeljne krasoslovne tematike.

Največji porast objav sledimo po letu 2009, od takrat dalje je letno število prispevkov s konferenc in člankov bolj ali manj konstantno (sl. 6).

Graf slike 7 prikazuje število objav po državah, za katere pa so značilni različni interesni cilji raziskav. V ZDA prevladujejo raziskave območij pogrezanja (ang. *subsidence*) oz. nenadnih udorov (ang. *hazardous sinkhole*) in raziskave hidrogeoloških značilnosti v kraških vodonosnikih. Na Kitajskem je uporaba georadarja pove-

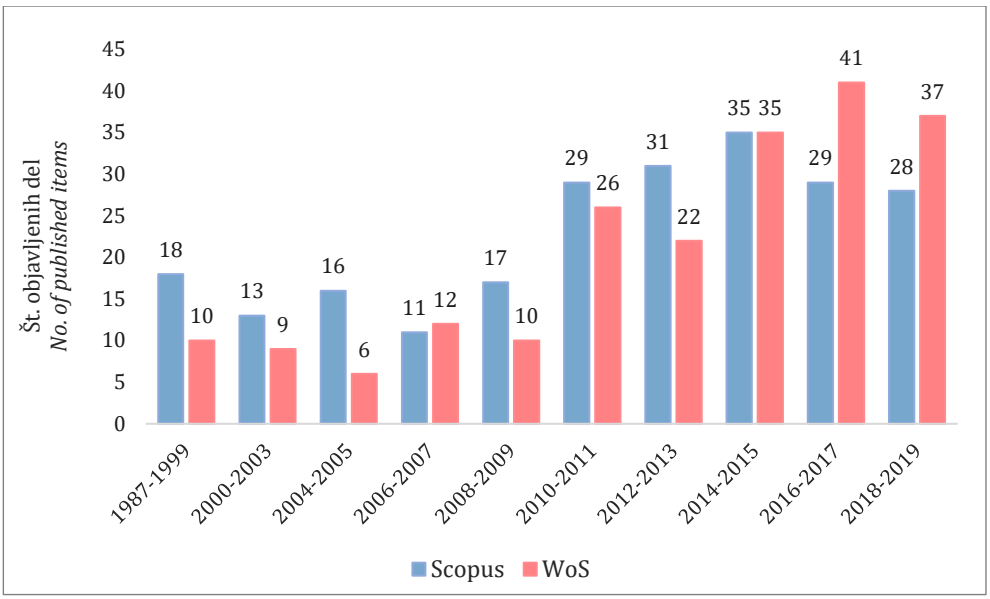

Sl. 6. Prikaz števila objavljenih del po obdobjih v bazah Scopus in WoS.

Fig. 6. Number of published items by period in Scopus and WoS databases.

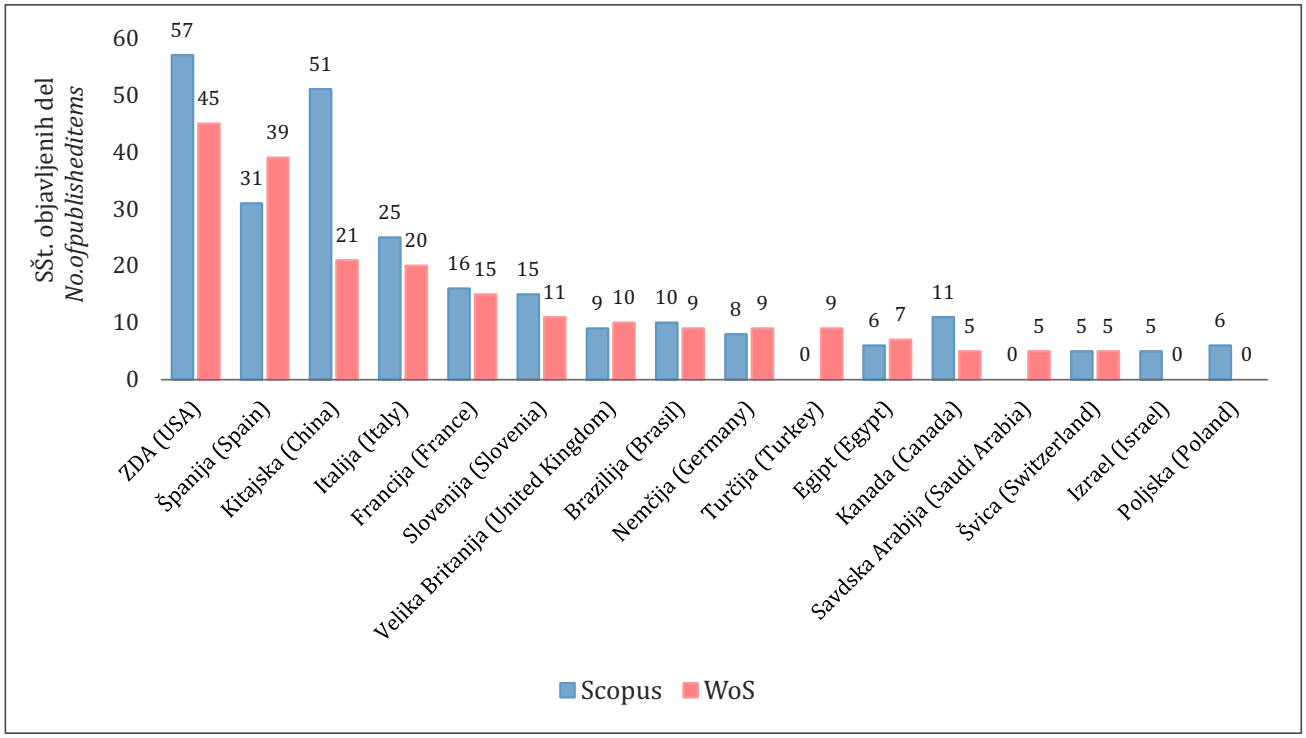

Sl. 7. Število objavljenih del po državah v obdobju med 1987–2019.
Fig. 7. The number of published items by countries in the period 1987–2019.

zana predvsem z gradbeno-inženirskimi posegi v prostor. Večina raziskav v Španiji je osredotočena na preučevanje procesov zakrasevanja v evaporitnih kamninah, kjer se georadar aplicira za zaznavanje in določevanje obsega območij pogrezanja v sadri in anhidritu. V Italiji prevladujejo arheološke raziskave v zakraselih apnencih in študije zaznavanja plitvih jam in območij nestabilnosti. Tudi v Sloveniji je bilo do sedaj uspešno izvedenih že nekaj študij z nizkofrekvenčnim georadarjem za detekcijo kraških pojavov v apnencih.

Za analizo uporabe georadarja na krasu sem v bazi Scopus posamično pregledala in izbrala 227 relevantnih člankov in prispevkov z različnih konferenc. V nabor objavljenih del sem vključila vse raziskave, ki obravnavajo vsebine povezane s krasom, in jih uvrstila v kategorije glede na glavni

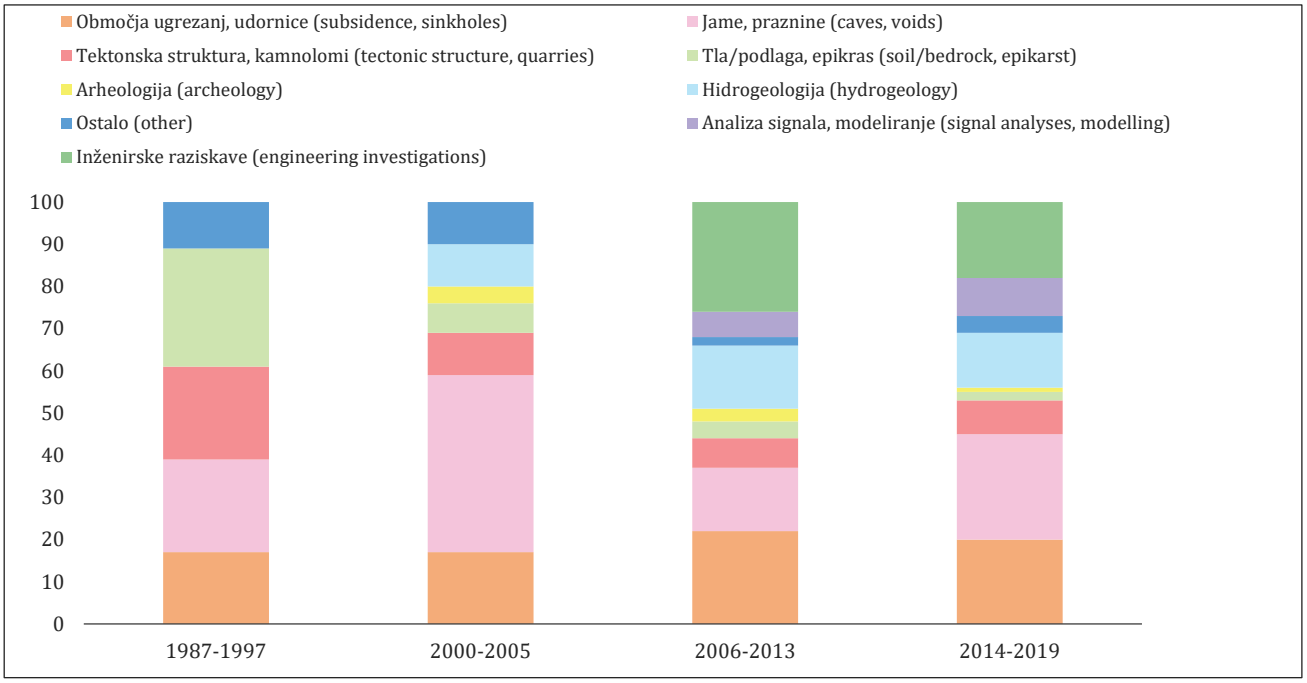

Sl. 8. Pregled objavljenih del po obdobjih glede na glavni cilj oz. področje raziskave.
Fig. 8. Review of published items by period according to the main objective of the research problem.

Wcilj raziskave (sl. 8). Iz grafa je razvidno, da se je georadar sprva uporabljal predvsem za zaznavanje praznin in jam, strukturno tektonskih značilnosti kamnin in pri raziskavah v kamnolomih ter za raziskave epikraške cone oz. za določanje meje tla/podlaga. Precejšen delež raziskav je bil že v začetku uporabe georadarja na krasu usmerjen na zaznavanje območij ugrezanj. Z leti je število aplikacij naraslo in pričele so se raziskave kraških vodonosnikov in študije v okviru arheoloških raziskav, ki pa so najmanj povezane s kraškimi vsebinami. Po letu 2006 do danes prevladujejo georadarske raziskave pri inženirsko-geotehničnih posegih v prostor, tovrstne študije večinoma obsegajo zaznavanje praznin in strukturno-tektonske značilnosti kamnin. Poleg tega je vse več raziskav, ki se ukvarjajo z analizo signala in z modeliranjem EM valovanja.

Pregled po različnih aplikacijah

Večina raziskav povezanih s kraškimi pojavi je aplikativnega značaja. Georadar se uporablja za zaznavanje praznin, strukturnih značilnosti kamnin v kamnolomih, kraških vodonosnikih, pri gradbenih posegih v prostor in tudi v arheologiji. Temeljne raziskave, ki bi obravnavale kraška vprašanja, ki niso povezana z oceno tveganj in napovedovanj nevarnosti (ang. *risk assessment, hazard*), so redka. Večina študij posredno obravnava kraški sistem, kjer so glavni cilj raziskav posledice zakrasevanja kamnin, ki lahko povzročijo škodo oz. tveganje za nevarnost (pogrezanje, udiranje) oz. ranljivost kraškega sistema (kraški vodonosniki).

V nadaljevanju so po različnih aplikacijah predstavljene objavljene ali lastne raziskave ter podane prednosti in omejitve georadarske metode.

Jame in praznine

Najbolj pogosta uporaba georadarja na kraškem površju je zaznavanje jam in praznin v povezavi z inženirsko-geotehničnimi posegi v prostor in na območjih posedanj in ugrezanj. Prazen jamski prostor se navadno dobro odraža na radargramih zaradi velikega kontrasta v dielektrični konstanti med kamnino in zrakom. Seveda je treba upoštevati, da so lahko praznine deloma ali popolnoma zapolnjene s sedimentom, kar nakazuje hitrost razširjanja EM valovanja, ki jo dobimo s prileganjem hiperbole.

Georadar je primeren za zaznavanje jam do globine 30 m, seveda v odvisnosti od izbrane frekvence in terenskih pogojev. Pomembno je, da poznamo oz. predvidevamo globinski doseg pri določeni frekvenci v danih pogojih na terenu ter vertikalno in horizontalno ločljivost metode (tabela 1). Pri tem je pomembna predvsem horizontalna ločljivost georadarja, ki se z globino manjša, kar pomeni, da na večjih globinah lahko zaznamo le večje jame. Martínez-Moreno et al. (2013, 2014) so podali pregled raziskav z različnimi geofizikalnimi metodami ter približno globino, kjer so zaznali jame. Globina detekcije podpovršinskih praznin v študijah, ki so vključevale metodo georadarja, je znašala med 4–28 metri. Za raziskave globljih jam (40–80 m) se je izkazalo, da je primernejša uporaba različnih električnih metod v kombinaciji z magnetnimi in/ali gravimetričnimi metodami (Martínez-Moreno et al., 2013). Metoda georadarja za zaznavanje jam in manjših praznin je primerna večinoma največ do globine 30 m. Georadarske raziskave zaznavanja jam in manjših praznin ter določanje geometrije in razširjanje praznih prostorov v podpovršju se največkrat dopolnjujejo z ostalimi elektromagnetnimi in električnimi metodami (Brown et al., 2011; Carrière et al., 2013; El-Qady et al., 2005; Gómez-Ortiz & Martín-Crespo, 2012; Lazzari et al., 2010), redkeje z gravimetričnimi (Beres et al., 2001; Mochales et al., 2008; Leucci & De Giorgi, 2010) in seizmičnimi metodami (Cardarelli et al., 2010). V večini naštetih raziskav je bil cilj zaznati jame in praznine, v nekaterih pa se je georadar uporabil tudi kot komplementarno metodo pri preučevanju nastanka jam in njihovih zapolnitev (Murphy et al., 2008). V arheoloških študijah so georadar uporabili tudi za zaznavanje in lociranje jam v apnencih, znotraj katerih se lahko nahajajo sedimenti primerni za izkopavanje (Chamberlain et al., 2000).

V teoriji se jamski prostor na radargramih odraža kot hiperbolični odboj. Takšen odboj dobimo, če je profil usmerjen prečno na razširjanje jame in je ta v preseku polkrožne oblike. V praksi se velikokrat izkaže, da so ti odboji kompleksnejši, in zaradi nehomogenosti, kot so različne geološke plasti, strukturne značilnosti (razpoke, prelomi), ne vedno tako očitni. Na obliko in značaj anomalije vpliva tudi velikost, oblika in globina jame, zapolnitev ter tudi terenski pogoji na površju. Poleg tega je potrebno upoštevati vse možne dejavnike, ki bi lahko na radargramih predstavljali motnjo oz. šum, npr. odboji od dreves, ograj in električnih napeljav.

Lep primer anomalije nad jamo predstavlja radargram na sliki 9 posnet nad jamo Biserujko na otoku Krku. Vhodni del jame predstavlja velika dvorana polkrožne oblike, kar se na radargramu jasno odraža z odbojem hiperbolične oblike. V praksi je takšnih primerov malo, navadno so

odboji od jam in praznin kompleksnejši. To prikazuje slika 10, kjer sta prikazana dva profila nad vhodno dvorano Najdene jame pri Lazah na Planinskem polju. Na profilu 1, kjer smo meritev izvajali prečno nad vhodno dvorano, se ta odraža z eno večjo hiperbolo na globini 10 m (sl. 10a). Povsem drugačen radargram kaže profil 2, kjer smo merili v vzdolžni smeri nad vhodno dvorano (sl. 10b). Celotna dolžina profila se nahaja nad jamsko dvorano, ki se odraža z manjšimi difrakcijskimi hiperbolami po celotni dolžini. Te se nahajajo na različnih globinah med 5 in 14 metri (rdeče puščice). Vhodna dvorana je zelo razgibane oblike z jamskim stropom na različnih globinah, zato dobimo tako kompleksen radargram.

Kljub temu, da je zaznavanje jam najbolj razširjenja in relativno enostavna uporaba georadarja, je dobljen radargram lahko zelo kompleksen. Izdelava sintetičnih modelov in modeliranje je zato bistvenega pomena pri interpretaciji in inverziji georadarskih podatkov (Beres et al., 2001; Leucci & De Giorgi, 2010).

Območja udorov in pogrezanj

Na krasu zaradi procesov zakrasevanja v podpovršju prihaja do nenadnih porušitev, kar je lahko nevarno, še posebej v urbanih okoljih. Procesi, ki vodijo do nastanka udorov in pogrezanj, so različni. Obstajajo številne genetske klasifikacije, kar pa presega namen tega prispevka.

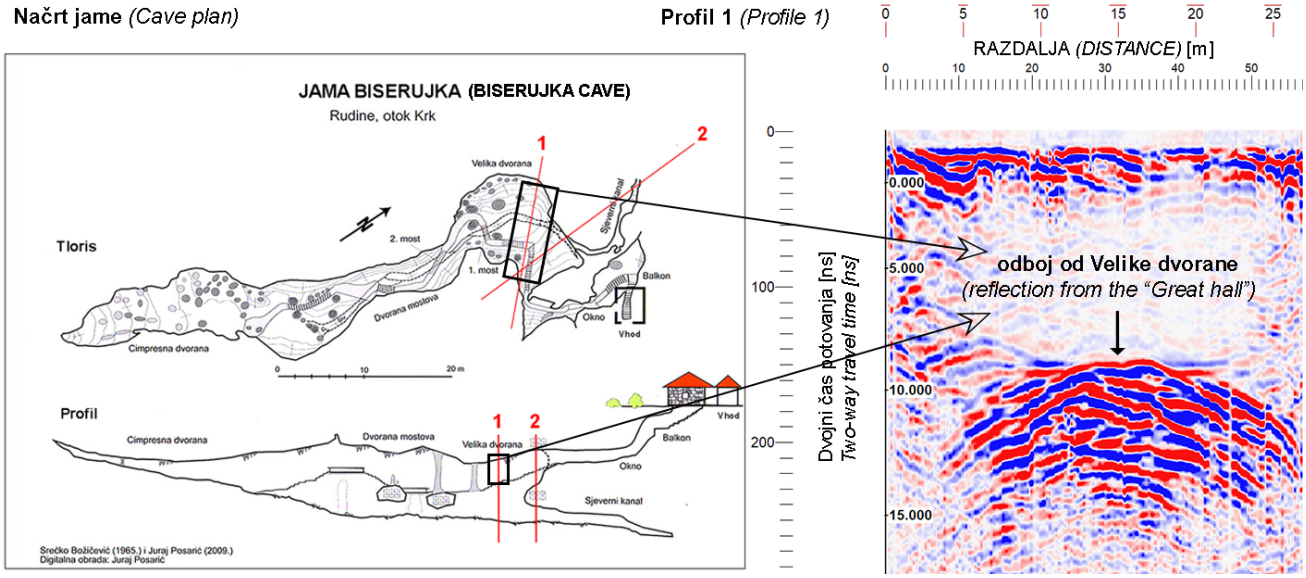

Sl. 9. Primer radargrama nad jamo Biserujko na Krku. Dvorana je velika in polkrožne oblike, zato izmerjeni prečni profil nad jamo povzroči jasno hiperbolično anomalijo.

Fig. 9. Example of a radargram above the Biserujka cave on Krk. The hall is large and of a semi-circular shape, so the measured transverse profile above the cave causes a clear hyperbolic anomaly.

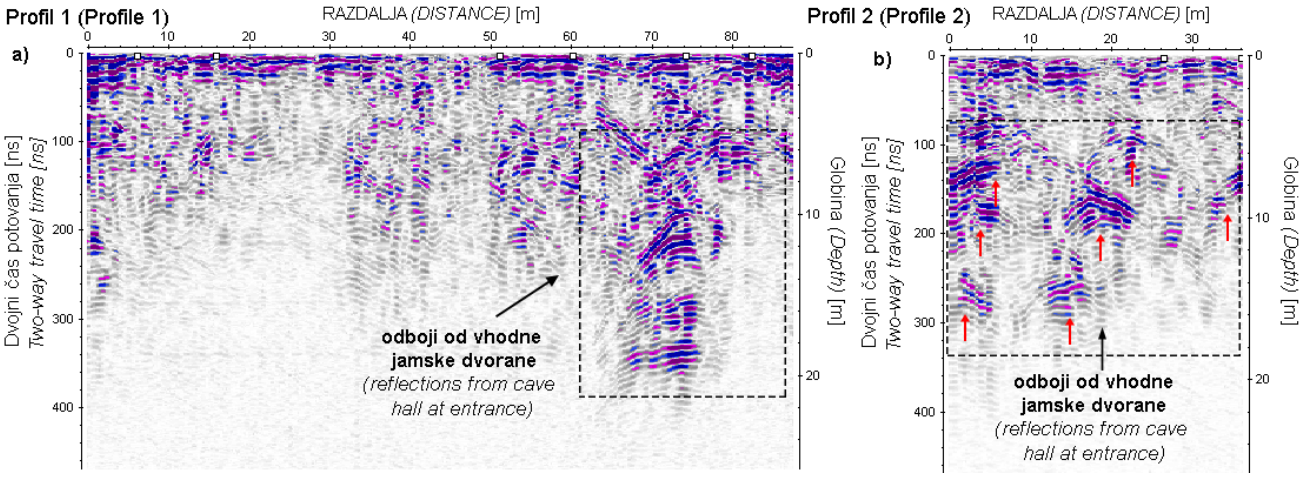

Sl. 10. Primer meritev nad Najdeno jamo, kjer je radargramski značaj na dveh profilih različen glede na obliko jame in smer profila. Zaradi kompleksne oblike jame se ta odraža zelo različno, kot nepopolna hiperbola (profil 1, pravokotno na smer razširjanja vhodne dvorane) in več manjših odbojev (profil 2, v smeri daljšega razširjanja vhodne dvorane).

Fig. 10. Example of measurements above Najdena cave, where the radargrams of two profiles are different depending on the cave shape and the direction of the profile. Due to the complex shape of the cave hall, it reflects very differently, for example as incomplete hyperbole (profile 1) and several smaller reflections (profile 2).

Omenila bi samo, da se izraz »*doline*« za vrtačo uporablja bolj v evropski literaturi, medtem ko se v Severni Ameriki ter v inženirsko-okoljskih raziskavah pogosteje uporablja izraz »*sinkhole*«, ki se nesistematično uporablja tako za vrtače kot tudi udornice, za udornice in območja pogrezanj pa tudi »*collapse sinkhole*« in redkeje »*collapse doline*« (Carbonel et al., 2015; Gutiérrez et al., 2014).

Na območjih, ki so podvržena procesom udiranja (ang. *collapse*) ali pogrezanja (ang. *subsidence*), je pomembno raziskati, kaj se dogaja v podpovršju, saj na površju pogosto ni vidnih znakov zakrasevanja. Ko se poruši ravnotežje, lahko pride do nenadnih udorov, ki lahko povzročijo ogromno škode. Večje območje takšnih pojavov predstavlja Florida in druga območja v ZDA kot so Teksas, Alabama in Pensilvanija. Drugi, počasnejši proces, pogrezanje oz. posedanje, pa prav tako povzroča nestabilnosti, ki vplivajo na infrastrukturo urbanih območij.

Poleg kraških pojavov v karbonatnih kamninah se podobni procesi odvijajo v evaporitnih kamninah kot je sadra, halit in anhidrit. Procesi zakrasevanja v evaporitnih kamninah so bistveno hitrejši od tistih v karbonatnih, zato so območja udorov in pogrezanj predmet številnih geofizikalnih raziskav. Procesi v evaporitnih kamninah se v marsikaterem pogledu precej razlikujejo od procesov v karbonatnih kamninah. Poleg hitrejšega raztapljanja so takšne kamnine tudi mehansko manj odporne in stabilne ter bolj duktilnega značaja. Georadarsko metodo so uporabili v številnih raziskavah vzdolž Mrtvega morja (Frumkin et al., 2011; Ezersky et al., 2017; Ronen et al., 2019). V zadnjih 30 letih je bilo evidentiranih na stotine udorov vzdolž Mrtvega morja tako v Izraelu kot v Jordaniji, pri čemer je prišlo do več nesreč na urbanih območjih (Frumkin et al., 2011). Jame oz. praznine na tem območju se pojavljajo večinoma na globini 20–70 m in pod nivojem slane podzemne vode, kar predstavlja glavni omejitveni dejavnik za georadarsko metodo, zato so bile za detekcijo globljih jam uporabljene tudi druge geofizikalne metode. Integracija geofizikalnih metod z ostalimi geološkimi metodami je bistveno izboljšala zaznavanje praznin in potencialnih območij za nastanek udora. Georadar se je izkazal za najboljšo izbiro pri zaznavanju praznin v plitvem podpovršju do globine 15 m. Na sliki 11 je predstavljen takšen primer georadarskih meritev, kjer so z meritvami določili mesta potencialnih udorov (Ronen et al., 2019). Samo nekaj mesecev po meritvah je prišlo do udora. Odboji od praznin so večinoma zelo kompleksni.

Procese zakrasevanja v neogenskih evaporitih intenzivno preučujejo tudi na območju Zaragoze v Španiji (Rodriguez et al., 2014; Carbonel et al., 2015; Sevil et al., 2017). V Španiji izdanki evaporitnih kamnin (sadra, anhidrit, halit) neogenske,

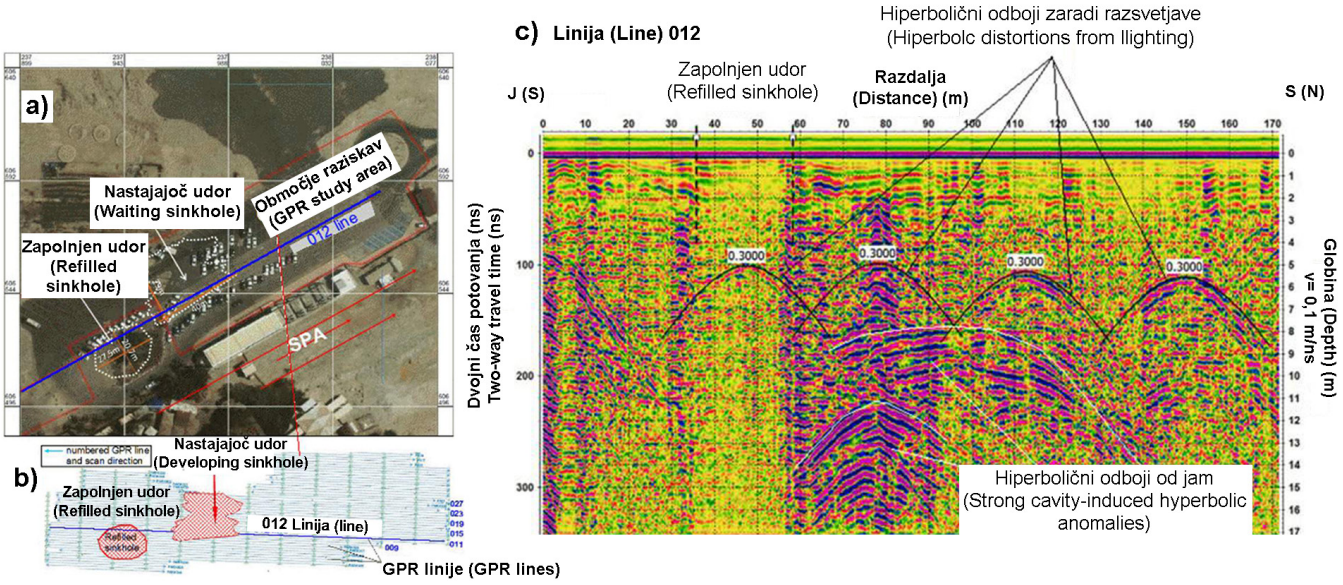

Sl. 11. Primer uporabe georadarja (ščitena 100 MHz antena) na območju udornic ob zahodni obali Mrtvega morja (iz Ronen et al., 2019 z dovoljenjem): a) zračni posnetek območja raziskav; b) shematski prikaz situacije trase profila 012; c) radargram linije 012, kjer območja močnih refleksov (hiperbol) pripadajo jamam na globini med 9–13 m.

Fig. 11. Example of the use of a georadar (shielded 100 MHz antenna) in the area of sinkholes along the western coast of the Dead Sea (from Ronen et al., 2019 with permission): a) an aerial view of the survey area; b) a schematic situation of the route of the profile 012; c) the radargram of line 012, where areas of strong reflections (hyperbola) belong to caves at depths between 9–13 m.

paleogenske in triasne starosti predstavljajo okoli 7 % površja (Gutiérrez et al., 2008). Zaradi hitrega raztapljanja prihaja do hitrih sprememb na površju, ki so odraz večinoma podzemnih procesov zakrasevanja. Zaradi varnosti in visokih stroškov sanacij so ta območja v zadnjih 20 letih vključena v številne raziskave, da bi bolje razumeli procese v evaporitnih kamninah, tok podzemne vode in nenazadnje, da bi preprečili tovrstne nesreče. V okviru geoloških, sedimentoloških in geomorfoloških raziskav sta bila georadar in električna upornostna tomografija velikokrat aplicirana. Rodriguez et al. (2014) so raziskali možnosti uporabe georadarja za karakterizacijo dveh depresij na pokritem krasu, ki sta nastali z različnima procesoma. Rezultati georadarskih meritev so tako omogočili zanesljivo določitev mej depresij, značilnosti njihove notranje geometrije z deformacijskimi značilnostmi. Na podlagi pridobljenih podpovršinskih podatkov so lahko sklepali na mehanizem pogrezanja in ocenili magnitudo le-tega. Metoda je imela tudi nekatere pomanjkljivosti. Zaradi prisotnosti glinenih in meljastih sedimentov znotraj vrtač je bil globinski doseg omejen, ponekod pa so nadpovršinski odboji (električna napeljava, zidovi, drevesa) povzročili motnje na radargramih. V raziskavi so uporabili neščiteni 100 MHz in 50 MHz anteni ter 180 MHz ščiteno anteno. Bistveno boljše rezultate so pridobili z neščiteno anteno. Na podlagi rezultatov neščitene antene so naredili celovito rekonstrukcijo območij pogrezanja in določili naklon plasti. Na radargramih ščitene antene so zaznali le meje depresij. V okviru interdisciplinarnih raziskav rezultate geofizikalnih metod dopolnjujejo tudi z razkopi (Carbonel et al., 2014; 2015; Sevil et al., 2017). Integracija georadarja in električne upornostne tomografije (ERT) z razkopi je prikazana na sliki 12.

V zadnjih 15 letih so tovrstne raziskave poleg zaznavanja jam, ki so lahko povezane tudi z mesti udorov, najbolj razširjena uporaba georadarske metode. Študije, ki obravnavajo to problematiko so številne (Delle Rose & Leucci, 2010; Gómez-Ortiz & Martín-Crespo, 2012; De Giorgi in Leucci, 2014; Bumpus in Kruse, 2014; Pueyo-Anchuela et al., 2015; Kaufmann et al., 2018), saj predvsem v urbanih območjih predstavljajo takšni pojavi eno

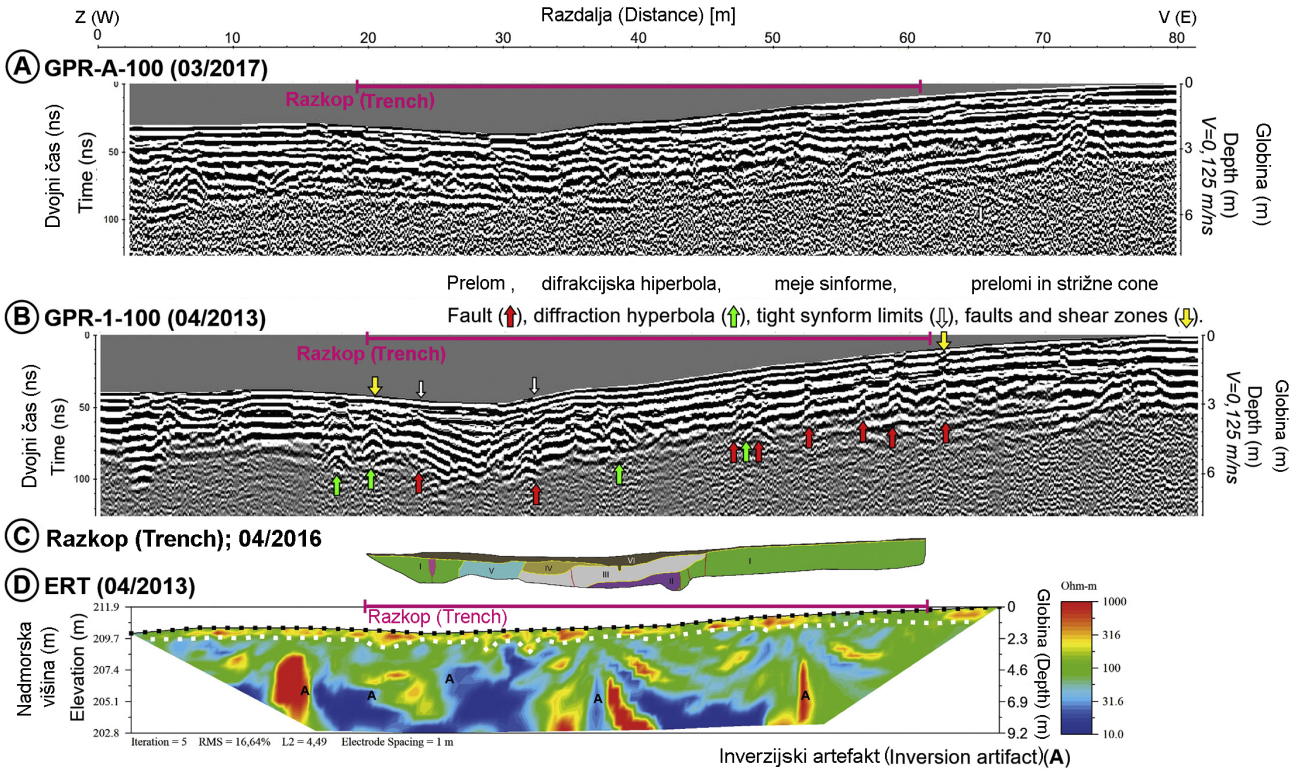

Sl. 12. Dopolnjevanje geofizikalnih metod z razkopi in geokronološkimi metodami (iz Sevil et al., 2017 z dovoljenjem): a) in b) depresija jasno vidna na radargramu slike 100 MHz antene. Profil iz leta 2013 je bistveno boljše kvalitete kot isti izmerjen leta 2017, kar je verjetno posledica večje vsebnosti vode v času meritev leta 2017; c) rezultati razkopa; d) rezultati ERT, kjer območje pogrezanja ni vidno, je pa viden stik z matično podlago.

Fig. 12: Integration of geophysical methods with excavations and geochronological methods (from Sevil et al., 2017 with permission): a) and b) the sinkhole is clearly visible on the radargram of the 100 MHz antenna image. The 2013 profile is of significantly better quality than the one measured in 2017, which is probably due to the higher water content at the time of the 2017 measurements; c) results of the excavation; d) ERT results where the subsidence area is not visible but contact with the bedrock is evident.

od najpogostejših oblik nevarnosti na kraškem površju zaradi česar so takšne raziskave velikokrat interdisciplinarne in jih dopolnjujejo nekatere tudi dražje metode. S tega vidika tovrstne raziskave prinašajo informacije, ki so preverjene z različnimi metodami, kar prispeva k boljšemu poznavanju georadarja v različnih terenskih pogojih, in imajo metodološki doprinos.

Epikras in kontakt tla/matična podlaga

Georadar se pri raziskavah tal največkrat uporablja za določevanje globine, lateralnega razširjanja in variabilnosti pedoloških horizontov, ki so značilni za posamezne skupine tal (Doolittle, 1987; Puckett et al., 1990; Stroh et al., 2001). Georadar lahko zazna mejne horizonte, ki se dovolj razlikujejo v pedološko-mineraloških lastnostih, da meje na radargramih predstavljajo prepoznaven reflektor. Z georadarjem načeloma ne moremo zaznati majhnih sprememb v značilnostih tal, kot so barva, struktura in poroznost ter prehodnih pedoloških horizontov (AB, AC, BC) in zveznih sprememb znotraj posameznih horizontov (Doolittle & Butnor, 2009).

Visoko amplitudne reflekse povzročajo nenadne spremembe na mejah med pedološkimi horizonti, ki jih povzročajo razlike v vsebnosti vlage, fizikalne razlike (spremembe v teksturi tal in gostoti) in/ali kemijske spremembe (prisotnost organskega materiala, kalcijevega karbonata in seskvioksidov). Eden izmed bolj značilnih horizontov je argilični horizont (Bt), ki vsebuje večji delež glinenih mineralov in ima tudi večjo gostoto (Collins & Doolittle, 1987). Prav tako je jasna meja v spodičnih horizontih (Bh, Bfe) zaradi prisotnosti humusa in seskvioksidov, ki se kopičijo iz višje ležečih horizontov.

Bt horizont smo zaznali na območju vrtač v konglomeratih, kjer so tla dobro razvita. Bt horizont je na območju pleistocenskih konglomeratov tudi precej debel. Na podlagi oblike Bt horizonta glede na današnjo morfologijo antropogeno spremenjenih vrtač smo z georadarskimi meritvami pridobili informacije o obliki in globini vrtač preden so bile te obdelane (Čeru et al., 2017).

Z georadarjem načeloma lahko zaznamo tudi mejo med sedimentom in matično podlago, če je meja nenadna in dovolj kontrastna. Navadno je ta meja prepoznavna kot visoko-amplitudni reflektor, ki je zvezen. Kljub vsemu pa velikokrat meja med nevezanim sedimentom in matično podlago ni jasna in je z georadarjem ne moremo zaznati, če prehod ni oster in raven, in če je zanj značilno, da se na meji pojavljajo večji kosi preperele matične podlage (Doolittle & Butnor, 2009). To je značilno za kraški sistem, kjer je meja med sedimentom in matično podlago neravna s pojavi kraških žepov in zveznim prehodom tal v preperelo matično podlago. V takšnih okoliščinah se je izkazalo, da meje med sedimentom in karbonatno podlago z georadarjem večinoma ne moremo zaznati.

V začetkih uporabe georadarja na krasu je bilo objavljenih nekaj raziskav, kjer so določevali mejo med tlemi in karbonatno podlago, medtem ko se je v zadnjih 20 letih število tovrstnih raziskav bistveno zmanjšalo. Doolittle & Collins (1998) sta uporabila EM indukcijo in georadar na krasu na dveh različnih lokacijah, Floridi in Pensilvaniji. Ugotovila sta, da imata obe metodi svoje pomanjkljivosti glede na lastnosti tal in specifike preučevanega terena. Interpretacija zaradi slabega globinskega dosega in ločljivosti ter premajhnega kontrasta v električnih lastnostih različnih materialov ni bila vedno jasna. Z uporabo 120 MHz antene so bile meritve na tleh v Pensilvaniji neuspešne, saj je bilo dušenje signala zaradi prisotnosti argiličnega horizonta preveliko, da bi lahko zaznali mejo med tlemi in karbonatno podlago. Metoda EM indukcije pa je v primeru bolj prevodnih tal dala boljše rezultate. Georadar je bil uspešnejši pri določevanju mej med peskom in apnencem ter med peskom, glino in zakraselim apnencem (Collins et al., 1990).

V Sloveniji karbonatne kamnine in depresije prekrivajo tla s precejšnjim deležem glinene komponente, zato je meja med tlemi in matično podlago težje določljiva. Prav tako tudi debeline in kontakta med zapolnitvijo in matično podlago v kraških depresijah na različnih območjih raziskav v Sloveniji večinoma nismo zaznali. Debelina sedimentov je bila prevelika oz. so lastnosti sedimentov onemogočale večji globinski doseg.

V primeru raziskav vrtač v konglomeratih smo kontakt določili posredno. Takšen primer raziskav je predstavljajo območje vrtač v najmlajšem konglomeratnem zasipu (Podbrezje), kjer smo kontakt določili na podlagi pojavljanja hiperbol, ki nakazujejo praznine oz. heterogenosti v konglomeratu. V dnu vrtače je na terenu vidna manjša poglobitev, kar se s pojavi večkratnih hiperboličnih odbojev (moder pravokotnik na sliki 13) odraža tudi na radargramu. Nekatere vrtače v konglomeratih so nastale s sufozijskimi procesi, pri katerih se nesprijet material spira skozi razpoke v spodaj ležeč zakrasel konglomerat, zato so na površju ponekod vidni grezi ali manjše poglobitve.

Poleg tipičnih kraških pojavov se je georadar izkazal kot primerna metoda tudi za karakterizacijo pokritega krasa in določitev meje med

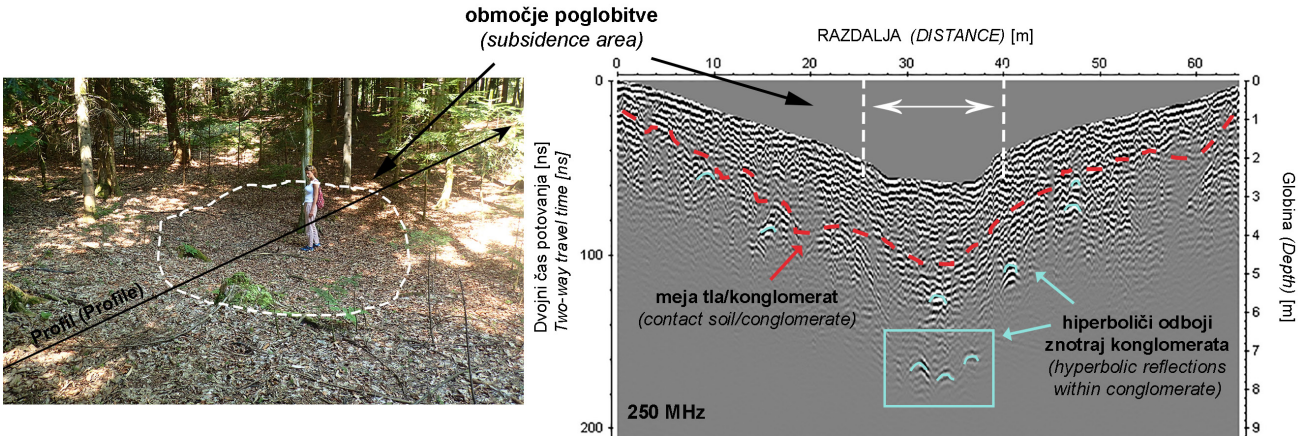

Sl. 13. Na podlagi pojavljanja hiperboličnih anomalij (modra barva) smo določili približno mejo med tlemi in konglomeratom (rdeča črtkana linija).

Fig. 13. The contact between soil and conglomerate bedrock (red dashed line) was defined by occurrences of hyperbolic diffractions (blue colour) related to the heterogeneities in conglomerate.

epikraško cono in kompaktnejšim apnencem pod njo (Tallini et al., 2006). V raziskavi so uporabili 40 MHz neščiteno in 100 MHz neščiteno anteno. Globinski doseg je v danih pogojih znašal 12 m (40 MHz) oz. 4 m (100 MHz), zato je bila večina meritev izvedenih s 40 MHz anteno. Tovrstne študije so zelo redke.

Kraški vodonosniki

Zelo pomembne so tudi raziskave kraških vodonosnikov, ki pogosto predstavljajo zelo ranljiva območja zajetij pitne vode. Georadar predstavlja komplementarno metodo za boljše razumevanje hidrodinamičnega mehanizma strukturno heterogenega kraškega hidrosistema, kjer na podlagi lociranja prelomov, kraških kanalov, votlin in ostalih kraških značilnosti lahko lažje karakteriziramo in konceptualiziramo strukturo vodonosnika. Pri raziskavah kraških vodonosnikov je navadno glavni cilj locirati razpoklinske cone in kanale, prelome in jame ter določiti geometrijo vseh teh elementov v prostoru in podatke iz vrtin dopolniti z georadarskimi rezultati (Al-Fares et al., 2002). Cunningham (2004) je na podlagi rezultatov študije ugotovil, da obstaja empirična povezava med izmerjenimi parametri iz vrtin (poroznost, hidravlična prevodnost) in poroznostjo pridobljeno iz slik karotažnih meritev v vrtinah ter amplitude signala georadarskih podatkov. Ugotovil je, da se amplituda radarskega signala zmanjšuje z večanjem poroznosti in hidravlične prevodnosti določene s podatki iz vrtin, kar omogoča kvalitativno ocenjevanje vertikalne in horizontalne porazdelitve poroznosti in hidravlične prevodnosti. Carrière et al. (2013) so kombinirali georadar in ERT za karakterizacijo kraških kamnin in z namenom bolje razumeti prenos vode znotraj nezasičene cone vodonosnika in skladiščenja vode. Z integracijo dopolnjujočih metod in poznavanjem geologije tega območja so uspeli podrobneje karakterizirati kamnine preučevanega območja (sl. 14). Kombinacijo ERT metode in georadarja so uporabili tudi v raziskavi vodonosnika v Kanadi (Martel et al., 2018). Izvedena je bila multidisciplinarna študija za boljše poznavanje podzemne dinamike toka in jamskih poti. Geofizikalne metode so dopolnilni s sledilnimi poskusi in vrtinami ter radarsko interferometrijo (InSAR) za detekcijo premikov na stavbah na območjih zapolnjene depresije.

Mount et al. (2014) so georadar uporabili za določitev porazdelitve poroznosti v vodonosniku in določitev lateralnega razširjanja kraških struktur. Na podlagi porazdelitve difrakcijskih hiperbol na radargramih so določili spremembe v hitrosti elektromagnetnega valovanja in iz tega je bila izračunana poroznost z uporabo petrofizikalnega modela CRIM (ang. *complex refractive index model*).

Iz opisanih in prikazanih primerov je za namen hidrogeoloških raziskav nujen multidisciplinaren pristop, ki poleg geofizikalnih metod zajema tudi hidrogeološke in druge metode.

Kamnolomi

V kamnolomih karbonatnih in evaporitnih kamnin procesi zakrasevanja, ki vodijo do nastanka jam, kraških kanalov in udorov, povzročajo številne težave pri eksploataciji mineralne surovine. Pogoji za georadarske meritve v odprtih površinskih kamnolomih so pogosto dobri, saj je površina ravna, preperinskega sloja, ki bi oviral prodiranje EM valovanja v globino ni. Poleg tega lahko rezultate georadarskih meritev vzporejamo z detajlnim geološko-strukturnim kartiranjem in ve-

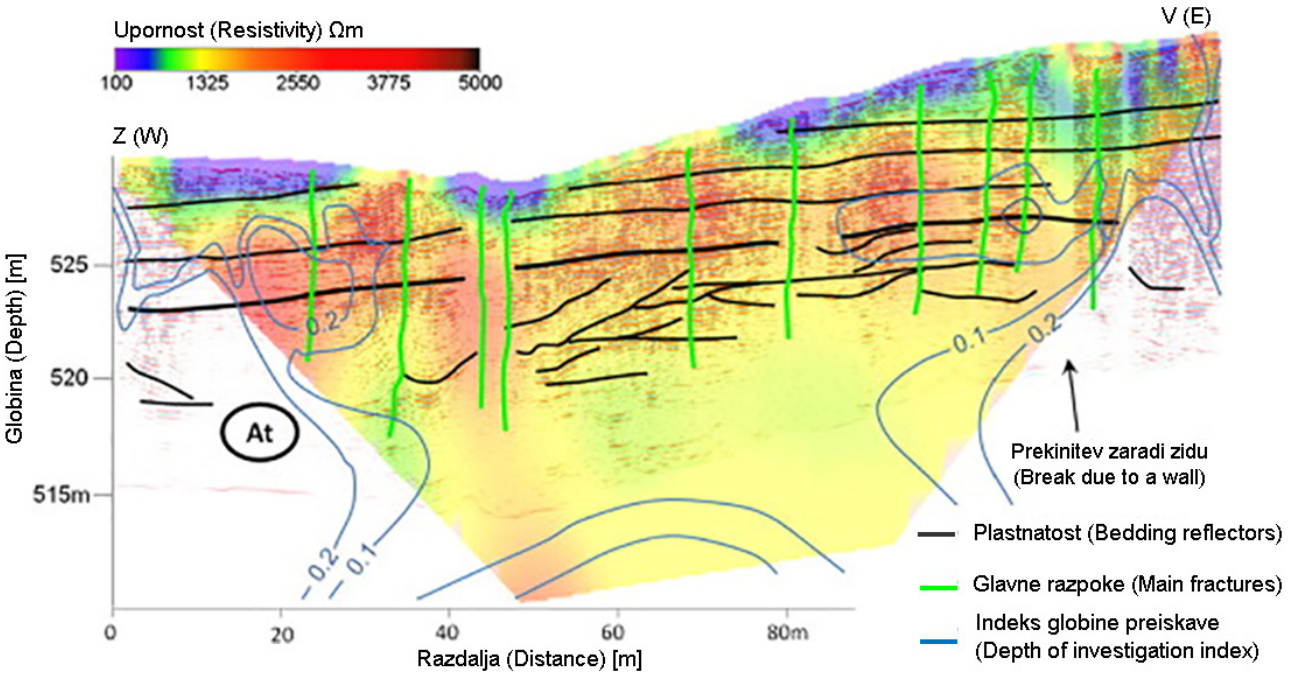

Sl. 14. Primer integracije rezultatov georadarja in električne upornostne tomografije (Carrière et al., 2013 z dovoljenjem). Podatki obeh metod so skladni, hkrati pa se dobro dopolnjujejo, pri čemer georadar poda podrobnejše informacije o strukturi plitvejšega podpovršja. Medtem ko je globinski doseg georadarja znašal do 12 m oz. na območjih, kjer je bil prisoten glinen material, celo samo dva metra, so rezultati ERT dopolnili podatke v globino.

Fig. 14. Integration of georadar and ERT results (Carrière et al., 2013 with permission). The data of both methods are consistent, but at the same time they complement each other well, with the georadar providing more detailed information on the structure of the shallower subsoil. While the depth of the georadar measurements was up to 12 m, or even just 2 metres in areas where clayey material was present, the ERT results completed the georadar data in greater depths.

likokrat tudi s podatki iz vrtin. Georadarska metoda se uporablja pri različnih fazah pridobivanja kamna. Lahko se uporablja v začetnih fazah pri splošni oceni kvalitete kamnoloma oz. bodočega nahajališča mineralnih surovin ali pri podrobnejših preiskavah, pri načrtovanju eksploatacijskega materiala, kjer je pomembno natančno določiti smeri prelomnih struktur, razpok in jam.

Za karakterizacijo strukturno-geoloških in hidrogeoloških značilnosti pri načrtovanju eksploatacijskih dejavnosti v kamnolomih se je georadar izkazal za zelo uporabno metodo v številnih študijah. Grandjean & Gourry (1996) sta uporabila georadar za zaznavanje in kartiranje razpok ter drugih kraških struktur v kamnolomu marmorja. Z uporabo 300 in 900 MHz antene so pridobili informacije do globine 15 oz. 8 m in naredili model razpok. Grasmueck et al. (2013) so uporabili 100 in 200 MHz anteni za raziskavo sub-vertikalnih razpok in jam v zapuščenem kamnolomu krednega apnenca. Z gosto mrežo vzporednih meritev in z ustreznimi naprednimi postopki obdelave (3D migracija podatkov) so naredili 3D model poteka vseh razpoklinskih con in določili glavne smeri prevladujočih razpok. V Sloveniji je bil georadar uporabljen v kamnolomu Rodež za zaznavanje kraških pojavov (Zajc et al., 2014).

V kamnolomih se lahko uporablja tako ščiten kot tudi neščiten sistem anten. Pri neščiteni anteni lahko prihaja do odboja od stene kamnoloma, zato meritve izvajamo po sredini etaže. Pri podzemnem pridobivanju kamna lahko težave povzročajo odboji od sten in stropa, seveda v odvisnosti od velikosti podzemnega pridobivalnega prostora. Meritve v Lipiškem kamnolomu so pokazale, da so nekateri radargrami zaradi nadpovršinskih odbojev popolnoma neuporabni, pri čemer se izkaže, da so ščitene antene primernejše (sl. 15). Na območjih, kjer so bile stene kamnoloma dovolj oddaljene, dobimo na radargramih le horizontalen odboj od stropa.

Brezstrope jame in jamski sedimenti

Poleg omenjenih aplikacij, ki so bolj ali manj uveljavljene v georadarski stroki, v tem poglavju podajam novo uporabo georadarja. Ker so brezstrope jame oz. posamezni segmenti brezstropih jam pomemben del današnje morfologije terena, je pomembno njihovo prepoznavanje na površju. Dokazi za obstoj brezstropih jam (jamska siga, jamski sedimenti…) velikokrat niso prisotni oz. so nerazpoznavni, zato je pomembno, da lahko z geofizikalnimi metodami dokažemo speleogenetski nastanek kraških oblik.

Območje obsežnejših študij brezstropih jam je bil otok Krk (Čeru et al., 2018a), jamskih sedimentov pa severni rob Planinskega polja (Čeru et al., 2018b). Območji sta bili izbrani zaradi za-

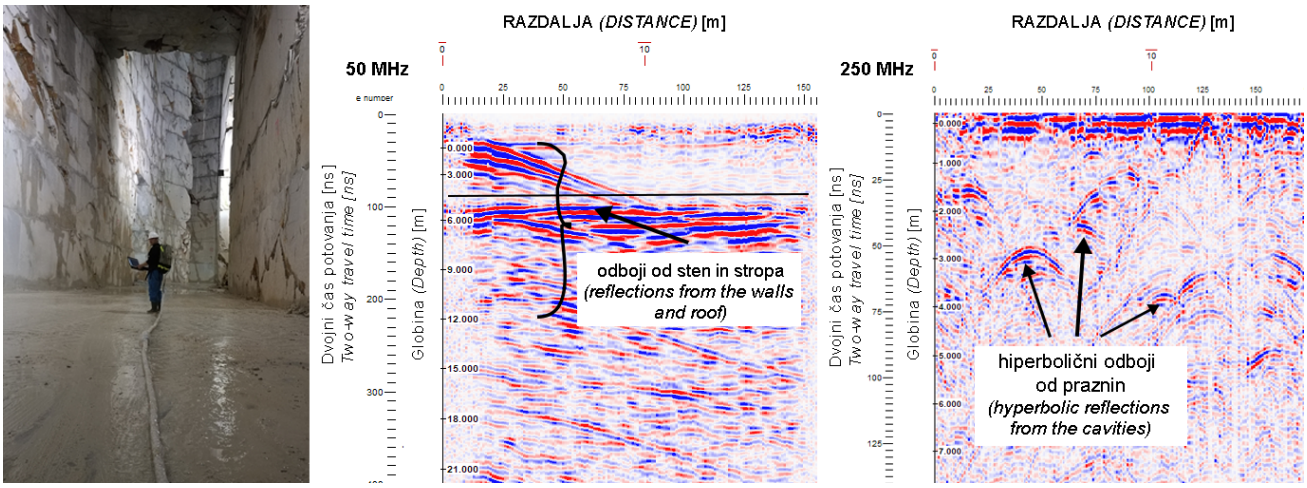

Sl. 15. Primer meritev v podzemnem pridobivalnem prostoru kamnoloma Lipica II. Pri 50 MHz neščiteni anteni nadpovršinski odboji od sten in stropa kamnoloma popolnoma prekrijejo odboje iz globine. Meritev s ščiteno 250 MHz anteno razkrije manjše praznine in diskontinuitete znotraj apnenca.

Fig. 15. Example of measurements in the underground Lipica II quarry. Surface reflections from the quarry walls and roof completely cover the GPR information with a 50 MHz unshielded antenna. Measurement with a 250 MHz shielded antenna reveals smaller voids and discontinuities within the limestone.

nimivega geološkega in geomorfološkega razvoja ter zaradi raznovrstnosti kraških oblik. Rezultati obeh študij predstavljajo novo uspešno uporabo georadarja v temeljni krasoslovni znanosti. Georadar se je izkazal za zelo uporabno metodo pri karakterizaciji brezstropih jam in pri prostorskih spremembah v značilnostih tal v primeru zaznavanja jamskih sedimentov. Čeprav se brezstrope jame na obeh območjih površinsko odražajo zelo različno, smo z različnim interdisciplinarnim pristopom, kjer je georadar predstavljal ključno metodo, uspeli pridobiti ustrezne podatke za njihovo lažjo rekonstrukcijo.

Na območju planote med Vrbnikom in Staro Baško smo z georadarskimi raziskavami določili mesta povezav med različnimi oblikami. Za ta je značilna večja debelina sedimentov, kar se na radargramih odraža z večjim dušenjem signala. Poleg tega smo našli več podzemnih nadaljevanj oz. podzemnih delov sicer večinoma denudiranega jamskega sistema. Definirali smo prehodno območje med površinskim in podpovršinskim delom brezstrope jame. Za ta območja so značilne manjše praznine, zato smo jih opredelili kot porušne oz. prehodne cone. S pomočjo georadarskih meritev in terenskega ter geomorfološkega pregleda na podlagi podatkov daljinskega zaznavanja smo opredelili 4 km dolg brezstrop jamski sistem.

Na območju severnega in vzhodnega obrobja Planinskega polja smo izvedli testne meritve za zaznavanje jamskih sedimentov. Želeli smo raziskati, kako zanesljivo lahko z georadarjem zaznamo jamske sedimente. Na območjih, kjer se jamski sedimenti pojavljajo skupaj z jamsko sigo, so meritve pokazale, da se ti jasno odražajo na radargramih z izrazitim dušenjem signala. Meritve smo nato izvedli tudi na širšem območju, kjer smo določili mesta jamskih sedimentov in njihovo razširjanje v prostoru (sl. 16). Da bi preverili zanesljivost metode in ugotovili, kateri dejavnik najbolj prispeva k dušenju signala, smo preučevali mineraloško-geokemične značilnosti jamskih sedimentov in tal. Raziskave so pokazale, da jamski sedimenti vsebujejo večji delež glinenih mineralov in Fe/Al oksidov in hidroksidov v primerjavi s tlemi na karbonatnih tleh. Na podlagi tega smo sklepali, da je poleg debeline sedimentov ključni dejavnik za povečano dušenje tudi drugačen delež posameznih mineralov. Poleg tega prisotnost Fe/Al oksidov in hidroksidov vpliva k večjemu zadrževanju vode, kar razloži tudi dejstvo, da se na območjih jamskih sedimentov voda zadržuje tudi čez daljša sušna obdobja.

Diskusija in zaključki

V prispevku smo podali pregled uporabe georadarja na krasu. Bistvena prednost georadarja je dobra ločljivost, ki omogoča natančen vpogled v podpovršje, zato predstavlja najbolj ustrezno geofizikalno metodo pri raziskavah, kjer nas zanimajo informacije do globine 30 m. Večina georadarskih raziskav krasa je osredotočenih na najbolj široko uveljavljene aplikacije kot je zaznavanje jam, raziskave kraških vodonosnikov in raziskave strukturnih lastnostih kamnin povezanih s procesi zakrasevanja. V zadnjih 20 letih so raziskave predvsem aplikativnega značaja in metoda se v integraciji z ostalimi uporablja pri

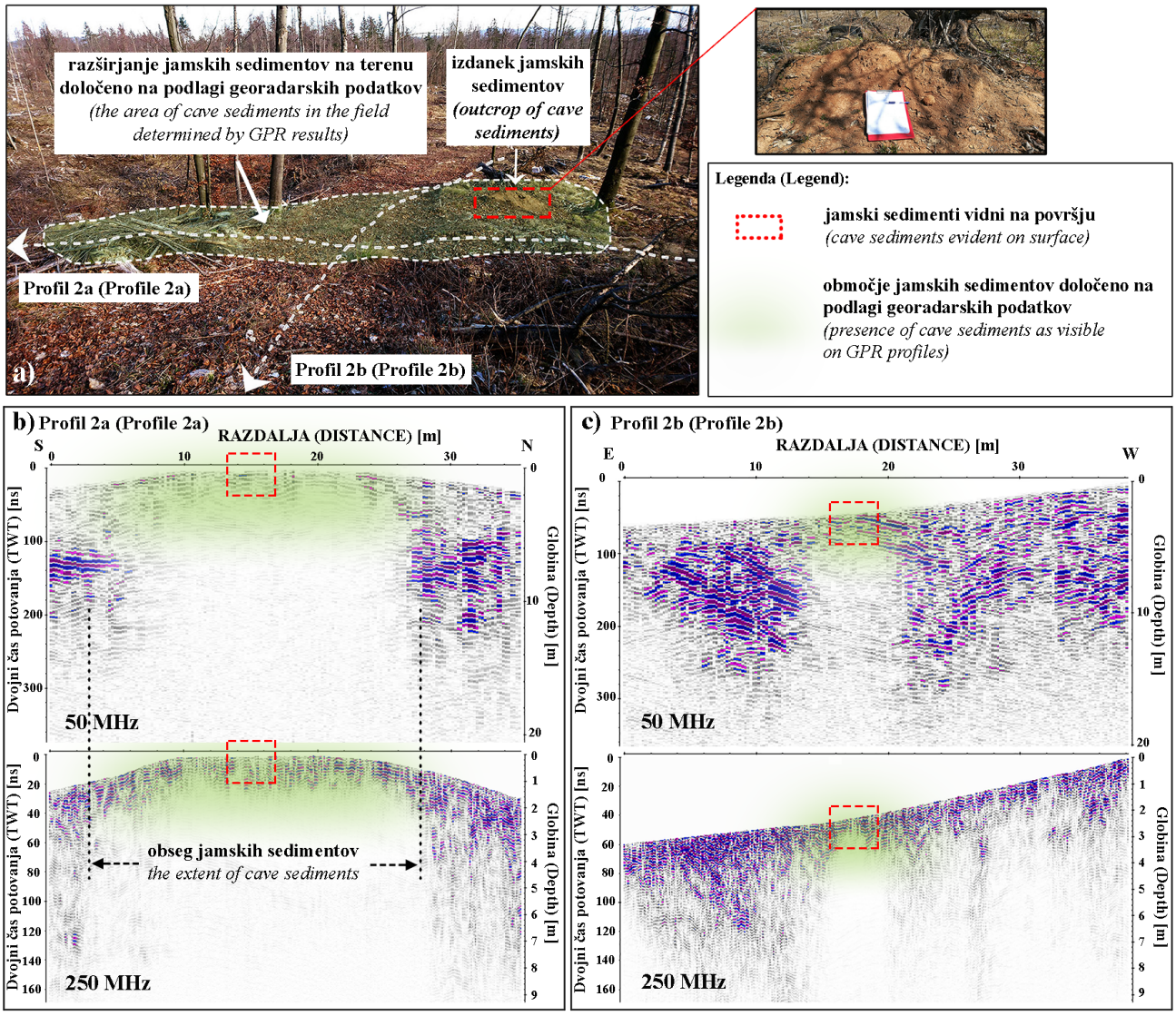

Sl. 16. Meritve jamskih sedimentov na območju severnega roba Planinskega polja z 50 in 250 MHz anteno (Čeru et al., 2018b): a) smer pravokotnih profilov 2a in 2b na območju jamskih sedimentov; b) na podlagi georadarskih rezultatov je bil določen obseg jamskih sedimentov tudi tam, kjer ti niso vidni na površju; c) območje jamskih sedimentov na radargramih sovpada z območjem na površju.

Fig. 16. Measurements of cave sediments in the northern part of Planinsko Polje with 50 and 250 MHz antennas (Čeru et al., 2018b): a) direction of perpendicular Profiles 2a and 2b in the area of the cave sediments outcrop; b) the extent of cave sediments was determined in Profile 2a even where they are not visible on the surface; c) boundaries of cave sediments detected by GPR are limited to the area of the outcrop visible on the surface.

preprečevanju nevarnosti pogojenih z zakrasevanjem. Zelo redke so temeljne raziskave, ki bi preučevale osnovna krasoslovna vprašanja. V članku smo predstavili pestrost uporabe metode in naredili kratek pregled po različnih aplikacijah, med katerimi smo izpostavili tudi nove aplikacije kot je zaznavanje brezstropih jam in jamskih sedimentov.

Kraško površje je večinoma težko prehodno in razgibano, kar predstavlja močno oviro za marsikatero geofizikalno metodo, a uporabljen sistem s 50 MHz RTA anteno omogoča meritve tudi na takšnih terenih. Omenjena antena se je izkazala za najbolj primerno za večino kraških aplikacij, pri čemer sta glavni prednosti primeren globinski doseg in lažje manevriranje z RTA anteno v primerjavi s ščiteno 250 MHz anteno.

Večina objavljenih raziskav je interdisciplinarnega značaja, kjer se rezultati geofizikalnih metod dopolnjujejo z geološkimi, hidrogeološkimi in geomorfološkimi metodami. Uporabnost metode je zelo odvisna od lastnosti terena in kraškega sistema. Enoznačna navodila za izvajanje georadarskih meritev na krasu niso smiselna, saj je uspešnost uporabe metode odvisna od številnih dejavnikov. Na območjih, kjer so prisotni sedimenti z večjih deležem glinenih mineralov, je dušenje signala močno, zato je globinski doseg lahko samo nekaj metrov ali manj. Po drugi strani, pa ravno ta lastnost metode omogoča, da

Tabela 4. Prednosti in nekatere omejitve georadarja pri različnih aplikacijah na krasu. (+ primerna, ± lahko pogojno uporabna z nekaterimi omejitvami, – ni primerna).

Table 4. Advantages and some limitations for different applications of GPR in karst. (+ appropriate, ± may be used, but not necessarily the most appropriate method, – not recommended).

Uporaba (*Application*)	**Možnost uporabe (*Possibility of use*)**	**Praktični nasveti, omejitve (*Practical guides, limitations*)**
Debelina kraških tal–stik z matično karbonatno podlago *Thickness of karst soil - contact with the carbonate bedrock*	–/ ±	- neenakomeren prehod med tlemi in matično podlago (neraven kontakt z vmesnimi žepi) - meja med tlemi in podlago večinoma ni nenadna, zato kontakt ne predstavlja dobrega reflektorja - rezultate priporočljivo korelirati z razkopi, cestnimi useki *- uneven transition between soils and bedrock (rough contact with cutters)* *- the boundary between the soil and the bedrock is rarely sudden, so the contact does not represent a good reflector* *- it is advisable to correlate the results with excavations, road cuts*
Debelina kraških tal–stik s konglomeratno podlago *Thickness of karst soil - contact with the conglomerate bedrock*	±	- meritve uspešne le v konglomeratnem zasipu najmlajše starosti, saj debelina tal ni prevelika - mejo med tlemi in konglomeratom smo določili na podlagi pojavljanja hiperbol zaradi nehomogenosti znotraj konglomerata *- measurements are only successful in the youngest conglomerate fill, since the soil is not too thick* *- the boundary between the soil and the conglomerate was determined based on the occurrence of hyperbolas as a result of inhomogeneity within the conglomerate*
Zaznavanje jam in praznin *Cave and cavity detection*	+	- metoda primerna ob uporabi primerne antene glede na globinski doseg in ločljivost metode - značaj anomalije v največji meri odvisen od oblike jame in smeri profila glede na geometrijo jame - odboji od kompleksnejših jam so lahko zelo »netipični« *- method appropriate when using the appropriate antenna with respect to the depth range and resolution of the method* *- the character of the anomaly depends largely on the shape of the cave and the direction of the profile with respect to the cave geometry* *- reflections from more complex caves can be very "atypical"*
Oblika dna vrtač in debelina sedimentov znotraj vrtač *The shape of the bottom of dolines and the thickness of sediments*	–/±	- močno dušenje signala zaradi prisotnosti sedimentov, ki vsebujejo precejšen delež glinene komponente *- strong attenuation of the signal due to the presence of sediments containing a significant proportion of a clay component*
Raziskave brezstropih jam *Unroofed cave research*	+	- primerna za zaznavanje povezav med denudiranimi deli brezstropih jam - primerna za zaznavanje podzemnega nadaljevanja brezstropih jam - možno raziskovanje prehodnega območja med denudiranim in podzemnim delom jamskega sistema *- suitable for finding links between segments of unroofed caves* *- suitable for detecting underground continuation of unroofed caves* *- it is possible to explore the transition of the transition area between the denuded and the underground parts of the cave system*
Jamski sedimenti *Cave sediments*	+	- metoda primerna, je pa potrebna pazljivost, da območij jamskih sedimentov ne zamenjamo z drugimi večjimi debelinami sedimentov – npr. zapolnjena brezna itd. *- the method is appropriate, but care must be taken not to confuse the cave sediment areas with other larger sediment thicknesses, e.g. filled shafts, etc.*
Pedološki horizonti *Pedological horizons*	+	- metoda primerna pri horizontih, ki se močno razlikujejo v dielektričnih lastnostih npr. Bt horizont - metoda primerna na tleh, kjer so horizonti dobro razviti (primer tal na karbonatnih konglomeratih) *- suitable for horizons that differ greatly in dielectric properties, e.g. Bt horizon* *- suitable in soils where horizons are well developed (for example soils on carbonate conglomerates)*
Jame in vrtače v konglomeratih *Caves and dolines in conglomerates*	±	- velika debelina razvitih tal na konglomeratnih terasah starejšega in srednjega zasipa lahko predstavlja omejitev - metoda primernejša na najmlajših konglomeratnih zasipih, kjer debelina tal ne presega 3 m *- excessive thickness of developed soil on the conglomerate terraces of the older and middle reaches* *- the method is more suitable on the youngest conglomerate backfill where the soil thickness does not exceed 3 m*

je primerna recimo za zaznavanje jamskih sedimentov, saj se ti na radargramih jasno odražajo kot območja večjega dušenja. Zaradi heterogenosti kraškega sistema so pogoji na terenu lahko zelo različni, zato v tabeli 4 podajam le nekatere usmeritve po aplikacijah. Podane so tudi nekatere aplikacije, ki v svetu še niso široko uveljavljene. Tekom raziskav se je izkazalo, da je georadar za nekatere aplikacije bolj za nekatere manj uporaben, zato podajamo tudi nekatere omejitve, na katere smo naleteli pri različnih raziskavah.

Z geofizikalnega vidika je kras s svojo heterogenostjo zelo kompleksen sistem, ki ima za uporabo georadarja določene omejitve, ki jih moramo upoštevati pri načrtovanju raziskav in interpretaciji podatkov. Zaradi heterogenosti sistema, v katerem se pojavljajo različne kraške oblike, kot so depresije in praznine, ki so lahko zapolnjene z zrakom ali/in sedimentom, lahko včasih le z rezultati različnih geofizikalnih metod pridobimo glavne informacije o strukturi podpovršja. Interdisciplinarnost raziskav je ključnega pomena, zato je za končno interpretacijo georadarske meritve potrebno dopolnjevati z geološkimi, hidrogeološkimi in geomorfološkimi metodami. Uporaba le ene geofizikalne metode lahko vodi do napačnih interpretacij, sploh v bolj kompleksnih sistemih, kjer lahko geofizikalnim podatkom ustreza več različnih modelov. Z razvojem tehnologije, boljšim poznavanjem teoretičnega ozadja metodologij in na podlagi praktičnih izkušenj raziskovalcev v zadnjih 15 letih, ima uporaba georadarja vse večji potencial pri različnih vprašanjih na krasu. Zaenkrat je večina georadarskih raziskav aplikativnega značaja, ki pa so velikokrat zasnovana tako, da je cilj študije tudi razumevanje kraških procesov, ki vodijo do nastanka različnih kraških oblik. Na ta način imamo čedalje več informacij in tudi znanja o kraškem podpovršju. Vse več se geofizikalne metode dopolnjujejo tudi z metodami daljinskega zaznavanja, kar kaže na to, da je prihodnost raziskav v interdisciplinarnem pristopu zelo različnih metod.

Zahvala

Raziskave v okviru doktorske disertacije, na katerem temelji tudi ta prispevek, so bile izvedene s podporo raziskovalnega programa P1-0011 in sklada za mlade raziskovalce 1000-15-0510, financirana s strani Javne agencije za raziskovalno dejavnost Republike Slovenije.

Literatura

Al-fares, W., Bakalowicz, M., Guérin, R. & Dukhan, M. 2002: Analysis of the karst aquifer structure of the Lamalou area (Hérault, France) with ground penetrating radar. Journal of Applied Geophysics, 51: 97–106. https://doi.org/10.1016/S0926-9851(02)00215-X

Andreo, B., Carrasco, F., Duran, J.J. & Lamoreaux, J.W. 2010: Advances in Research in Karst Media. Springer, Berlin: 429–434.

Andreo, B., Carrasco, F., Duran, J.J., Jimenez, P. & Lamoreaux, J.W. 2015: Hydrogeological and Environmental Investigations in Karst Systems. Springer, Berlin: 638 p.

Annan, A.P. 2009. Electromagnetic Principles of Ground Penetrating Radar. In: Jol, H.M. (ed.): Ground Penetrating Radar: Theory and Applications. Elsevier Science, Amsterdam, Netherlands: 3–37.

Beres, M., Luetscher, M. & Olivier, R. 2001: Integration of ground-penetrating radar and microgravimetric methods to map shallow caves. Journal of Applied Geophysics, 46: 249–262. https://doi.org/10.1016/S0926-9851(01)00042-8

Blindow, N. 2006: Ground Penetrating Radar. In: Kirsch, R. (ed.): Groundwater Geophysics. A Tool for Hidrogeology. Springer, Berlin: 227–252.

Blindow, N., Eisenburger, D., Illich, B., Petzold, H. & Richer, T. 2007: Ground Penetrating Radar. In: Knödel, K., Lange, G. & Voigt, H.J. (eds.): Environmental Geology. Handbook of Field Methods and Case Studies. Springer, Berlin: 283–335.

Brown, W.A., Stafford, K.W., Shaw-Faulkner, M. & Grubbs, A. 2011: A comparative integrated geophysical study of Horseshoe Chimney Cave, Colorado Bend State Park, Texas. International Journal of Speleology, 40: 9–16. http://dx.doi.org/10.5038/1827-806X.40.1.2

Bumpus, P.B. & Kruse, S.E. 2014: Self-potential monitoring for hydrologic investigations in urban covered-karst terrain. Geophysics, 79/6: B231–B242. https://doi.org/10.1190/geo2013-0354.1

Carbonel, D., Rodríguez, V., Gutiérrez, F., Mccalpin, J. P., Linares, R., Roqué, C., Zarroca, M., Guerrero, J. & Sasowsky, I. 2014: Evaluation of trenching, ground penetrating radar (GPR) and electrical resistivity tomography (ERT) for sinkhole characterization. Earth Surface Processes and Landforms, 39: 214–227. https://doi.org/10.1002/esp.3440

Carbonel, D., Rodríguez-Tribaldos, V., Gutiérrez, F., Galve, J.P., Guerrero, J., Zarroca, M., Roqué, C., Linares, R., McCalpin, J.P. & Acosta, E. 2015: Investigating a damaging buried sinkhole cluster in an urban area (Zaragoza city, NE Spain) integrating multiple techniques: Geomorphological surveys, DInSAR, DEMs, GPR, ERT, and trenching. Geomorphology, 229: 3–16. https://doi.org/10.1016/j.geomorph.2014.02.007

Cardarelli, E., Cercato, M., Cerreto, A. & Di Filippo, G. 2010: Electrical resistivity and seismic refraction tomography to detect buried cavities. Geophysical prospecting, 58: 685–695. https://doi.org/10.1111/j.1365-2478.2009.00854.x

Carrière, S.D., Chalikakis, K., Sénéchal, G., Danquigny, C. & Emblanch, C. 2013: Combining Electrical Resistivity Tomography and Ground Penetrating Radar to study geological structuring of karst Unsaturated Zone. Journal of Applied Geophysics, 94: 31–41. https://doi.org/10.1016/j.jappgeo.2013.03.014

Chalikakis, K., Plagnes, V., Guerin, R., Valois, R. & Bosch, F.P. 2011: Contribution of geophysical methods to karst-system exploration: An overview. Hydrogeology Journal, 19: 1169–1180. https://doi.org/10.1007/s10040-011-0746-x

Chamberlain, A.T., Sellers, W., Proctor, C. & Coard, R. 2000: Cave detection in limestone using ground penetrating radar. Journal of Archaeological Science, 27: 957–964. https://doi.org/10.1006/jasc.1999.0525

Collins, M.E. & Doolittle, J.A. 1987: Using ground-penetrating radar to study soil microvariability. Soil Science Society of America Journal, 51/2: 491–493. https://doi.org/10.1016/0016-7061(94)90008-6

Collins, M.E., Puckett, W.E., Schellentrager, G.W. & Yust, N.A. 1990: Using gpr for micro-analyses of soils and karst features on the chiefland limestone plain in florida. Geoderma, 47: 159–170. https://doi.org/10.1016/0016-7061(90)90053-C

Cunningham, K.J. 2004: Application of ground-penetrating radar, digital optical borehole images, and cores for characterization of porosity hydraulic conductivity and paleokarst in the Biscayne aquifer, southeastern Florida, USA. Journal of Applied Geophysics, 55: 61–76. https://doi.org/10.1016/j.jappgeo.2003.06.005

Čeru, T., Šegina, E. & Gosar, A. 2017: Geomorphological dating of Pleistocene conglomerates in central Slovenia based on spatial analyses of dolines using LiDAR and Ground Penetrating Radar. Remote Sensing, 9: 1213. https://doi.org/10.3390/rs9121213

Čeru, T., Šegina, E., Knez, M., Benac, Č. & Gosar, A. 2018a: Detecting and characterizing unroofed caves by ground penetrating radar. Geomorphology, 303: 524–539. https://doi.org/10.1016/j.geomorph.2017.11.004

Čeru, T., Dolenec, M. & Gosar, A. 2018b: Application of Ground Penetrating Radar Supported by Mineralogical-Geochemical Methods for Mapping Unroofed Cave Sediments. Remote Sensing, 10: 639. https://doi.org/10.3390/rs10040639

Čeru, T. 2019: Geofizikalne raziskave površinskih in podpovršinskih kraških oblik z metodo nizkofrekvenčnega georadarja s poudarkom na analizi jam in vrtač. Doktorska disertacija. Univerza v Ljubljani, Naravoslovnotehniška fakulteta, Ljubljana: 176 p.

Davis, J.L. & Annan, A.P. 1989: Ground-Penetrating radar for high-resolution mapping of soil and rock stratigraphy. Geophysical Prospecting, 37: 531–551. https://doi.org/10.1111/j.1365-2478.1989.tb02221.x

De Giorgi, L. & Leucci, G. 2014: Detection of Hazardous Cavities Below a Road Using Combined Geophysical Methods. Surveys in Geophysics, 35/4: 1003–1021. https://doi.org/10.1007/s10712-013-9277-4

Delle Rose, M. & Leucci, G. 2010: Towards an integrated approach for characterization of sinkhole hazards in urban environments: The unstable coastal site of Casalabate, Lecce, Italy. Journal of Geophysics and Engineering, 7: 143–154. https://doi.org/10.1088%2F1742-2132%2F7%2F2%2F004

Doolittle, J.A. 1987: Using ground-penetrating radar to increase the quality and efficiency of soil surveys. In: Reybold, W.U., Peterson, G.W. (eds.): Soil Survey Techniques. Madison, Wisconsin, USA, Soil Science Society of America, Special Publication, 20: 11–32.

Doolittle, J.A. & Collins, M.E. 1998: A comparison of EM induction and GPR methods in areas of karst. Geoderma, 85: 83–102. https://doi.org/10.1016/S0016-7061(98)00012-3

Doolittle, J.A. & Butnor, J.R. 2009: Soils, Peatlands, and Biomonitoring. In: Jol, H.M. (ed.): Ground Penetrating Radar: Theory and Applications. Elsevier Science, Amsterdam, Netherlands: 179–192.

El-Qady, G., Hafez, M., Abdalla, M.A. & Ushijima, K. 2005: Imaging subsurface cavities using geoelectric tomography and

ground-penetrating radar. Journal of Cave and Karst Studies, 67: 174–181.

Ezersky, M.G., Legchenko, A., Eppelbaum, L. & Al-Zoubi, A. 2017: Overview of the geophysical studies in the dead sea coastal area related to evaporite karst and recent sinkhole development. International Journal of Speleology, 46: 277–302. https://doi.org/10.5038/1827-806X.46.2.2087

Frumkin, A., Ezersky, M., Al-Zoubi, A., Akkawi, E. & Abueladas, A.R. 2011: The Dead Sea sinkhole hazard: Geophysical assessment of salt dissolution and collapse. Geomorphology, 134: 102–117. https://doi.org/10.1016/j.geomorph.2011.04.023

Gómez-Ortiz, D. & Martín-Crespo, T. 2012: Assessing the risk of subsidence of a sinkhole collapse using ground penetrating radar and electrical resistivity tomography. Engineering Geology, 149–150: 1–12. https://doi.org/10.1016/j.enggeo.2012.07.022

Grandjean, G. & Gourry, J.C. 1996: GPR data processing for 3D fracture mapping in a marble quarry (Thassos, Greece). Journal of Applied Geophysics, 36: 19–30. https://doi.org/10.1016/S0926-9851(96)00029-8

Grasmueck, M., Quintà, M.C., Pomar, K. & Eberli, G.P. 2013: Diffraction imaging of sub-vertical fractures and karst with full--resolution 3D Ground-Penetrating Radar. Geophysical Prospecting, 61: 907–918. https://doi.org/10.1111/1365-2478.12004

Gutiérrez, F., Calaforra, J.M., Cardona, F., Ortí, F., Durán, J.J. & Garay, P. 2008: Geological and environmental implications of the evaporite karst in Spain. Environmental Geology, 53: 951–965. https://doi.org/10.1007/s00254-007-0721-y

Gutiérrez, F., Parise, M., De Waele, J. & Jourde, H. 2014: A review on natural and human--induced geohazards and impacts in karst. Earth-Science Reviews, 138: 61–88. https://doi.org/10.1016/j.earscirev.2014.08.002

Kaufmann, G., Romanov, D., Tippelt, T., Vienken, T., Werban, U., Dietrich, P., Mai, F., Börner, F. 2018: Mapping and modelling of collapse sinkholes in soluble rock: The Münsterdorf site, northern Germany. Journal of Applied Geophysics, 154: 64–80. https://doi.org/10.1016/j.jappgeo.2018.04.021

Lazzari, M., Loperte, A. & Perrone, A. 2010: Near surface geophysics techniques and geomorphological approach to reconstruct the hazard cave map in historical and urban areas. Advances in Geoscience, 24: 35–44. https://doi.org/10.5194/adgeo-24-35-2010

Leucci, G. & De Giorgi, L. 2010: Microgravimetric and ground penetrating radar geophysical methods to map the shallow karstic cavities network in a coastal area (Marina Di Capilungo, Lecce, Italy). Exploration Geophysics, 41: 178–188. https://doi.org/10.1071/EG09029

Martel, R., Castellazzi, P., Gloaguen, E., Trépanier, L. & Garfias, J. 2018: ERT, GPR, InSAR, and tracer tests to characterize karst aquifer systems under urban areas: The case of Quebec City. Geomorphology, 310: 45–56. https://doi.org/10.1016/j.geomorph.2018.03.003

Martínez-Moreno, F.J., Pedrera, A., Ruano, P., Galindo-Zaldívar, J., Martos-Rosillo, S., González-Castillo, L., Sánchez-Úbeda, J.P. & Marín-Lechado C. 2013: Combined microgravity, electrical resistivity tomography and induced polarization to detect deeply buried caves: Algaidilla cave (Southern Spain). Engineering Geology, 162: 67–78. https://doi.org/10.1016/j.enggeo.2013.05.008

Martínez-Moreno, F.J., Galindo-Zaldívar, J., Pedrera, A., Teixido, T., Ruano, P., Peña, J.A., González-Castillo, L., Ruiz-Constán, A., López-Chicano, M. & Martín-Rosales, W. 2014: Integrated geophysical methods for studying the karst system of Gruta de las Maravillas (Aracena, Southwest Spain). Journal of Applied Geophysics, 107: 149–162. https://doi.org/10.1016/j.jappgeo.2014.05.021

Mochales, T., Casas, A.M., Pueyo, E.L., Pueyo, O., Román, M.T., Pocoví, A., Soriano, M.A. & Ansón, D. 2008: Detection of underground cavities by combining gravity, magnetic and ground penetrating radar surveys: a case study from Zaragoza area, NE Spain. Environmental Geology, 53/5: 1067–1077. https://doi.org/10.1007/s00254-007-0733-7

Mount, G.J., Comas, X. & Cunningham, K.J. 2014: Characterization of the porosity distribution in the upper part of the karst Biscayne aquifer using common offset ground penetrating radar, Everglades National Park, Florida. Journal of Hydrology, 515: 223–236. https://doi.org/10.1016/j.jhydrol.2014.04.048

Murphy, P., Westerman, A.R., Clark, R., Booth, A. & Parr, A. 2008: Enhancing understanding of breakdown and collapse in the Yorkshire Dales using ground penetrating radar on cave sediments. Engineering Geology, 99: 160–168. https://doi.org/10.1016/j.enggeo.2007.11.015

Neal, A. 2004: Ground-penetrating radar and its use in sedimentology: Principles, problems and progress. Earth-Science Reviews, 66: 261–330.

Puckett, W.E., Collins, M.E. & Schellentrager, G.W. 1990: Design of soil map units on a karst area in west central Florida. Soil Science Society of America Journal, 54: 1068–1073. https://doi.org/10.2136/sssaj1990.03615995005400040023x

Pueyo Anchuela, O., Casas Sainz, A.M., Pocoví Juan, A. & Gil Garbí, H. 2015: Assessing karst hazards in urbanized areas. Case study and methodological considerations in the mantle karst from Zaragoza city (NE Spain). Engineering Geology, 184: 29–42. https://doi.org/10.1016/j.enggeo.2014.10.025

Reynolds, J.M. 2011: An introduction to Applied and Environmental Geophysics. Wiley, New York: 712 p.

Rodriguez, V., Gutiérrez, F., Green, A.G., Carbonel, D., Horstmeyer, H. & Schmelzbach, C. 2014: Characterizing sagging and collapse sinkholes in a mantled karst by means of ground penetrating radar (GPR). Environmental and Engineering Geoscience, 20: 109–132. https://doi.org/10.2113/gseegeosci.20.2.109

Ronen, A., Ezersky, M., Beck, A., Gatenio, B., & Simhayov, R.B. 2019: Use of GPR method for prediction of sinkholes formation along the Dead Sea Shores, Israel. Geomorphology, 328: 28–43. https://doi.org/10.1016/j.geomorph.2018.11.030

Schrott, L. & Sass, O. 2008: Application of field geophysics in geomorphology: Advances and limitations exemplified by case studies. Geomorphology, 93: 55–73. https://doi.org/10.1016/j.geomorph.2006.12.024

Sevil, J., Gutiérrez, F., Zarroca, M., Desir, G., Carbonel, D., Guerrero, J., Linares, R., Roqué, C. & Fabregat, I. 2017: Sinkhole investigation in an urban area by trenching in combination with GPR, ERT and high-precision leveling. Mantled evaporite karst of Zaragoza city, NE Spain. Engineering Geology, 231: 9–20. https://doi.org/10.1016/j.enggeo.2017.10.009

Stroh, J.C., Archer, S., Doolittle, J.A. & Wilding, L. 2001: Detection of edaphic discontinuities with ground-penetrating radar and electromagnetic induction. Landscape Ecology, 16/5: 377–390. https://doi.org/10.1023/A:1017556712316

Tallini, M., Gasbarri, D., Ranalli, D. & Scozzafava, M. 2006: Investigating epikarst using low-frequency GPR: example from the Gran Sasso range Central Italy. Bulletin of Engineering Geology and the Environment, 65/4: 435–443. https://doi.org/10.1007/s10064-005-0017-y

Wai-Lok Lai, W., Dérobert, X. & Annan, P. 2018: A review of Ground Penetrating Radar application in civil engineering: A 30-year journey from Locating and Testing to Imaging and Diagnosis. NDT & E International, 96: 58–78. https://doi.org/10.1016/j.ndteint.2017.04.002

Waltham, T., Bell, F. & Culshaw, M. 2005: Sinkholes and Subsidence. Karst and Cavernous Rocks in Engineering and Construction. Springer, Berlin: 382 p.

Zajícová, K. & Chuman, T. 2019: Application of ground penetrating radar methods in soil studies: A review. Geoderma, 343: 116–129. https://doi.org/10.1016/j.geoderma.2019.02.024

Zajc, M., Pogačnik, Ž. & Gosar, A. 2014: Ground penetrating radar and structural geological mapping investigation of karst and tectonic features in flyschoid rocks as geological hazard for exploitation. International Journal of Rock Mechanics and Mining Science, 67: 78–87. https://doi.org/10.1016/j.ijrmms.2014.01.011

GEOLOGIJA *62/2*, 301–319, Ljubljana 2019
https://doi.org/10.5474/geologija.2019.015

Razširjenost pesticidov v vodonosniku Dravskega polja

Occurence of pesticides in Dravsko polje aquifer

Anja KOROŠA & Nina MALI

Geološki zavod Slovenije, Dimičeva ulica 14, SI – 1000 Ljubljana, Slovenija;
e-mail: anja.korosa@geo-zs.si; nina.mali@geo-zs.si

Prejeto / Received 16. 10. 2019; Sprejeto / Accepted 18. 12. 2019; Objavljeno na spletu / Published online 24. 12. 2019

Ključne besede: podzemna voda, vodonosnik Dravsko polje, pesticidi
Key words: groundwater, aquifer Dravsko polje, pesticides

Izvleček

V članku predstavljamo rezultate raziskave pojavnosti in koncentracij pesticidov v podzemni vodi Dravskega polja v obdobju 2013–2015. Na podlagi rezultatov smo ocenili prostorsko razširjenost pesticidov v podzemni vodi in jo povezali z rabo prostora. V obdobju dveh let smo odvzeli 76 vzorcev podzemne vode na 19 različnih lokacijah. V podzemni vodi smo določili 15 pesticidov z njihovimi metaboliti. Najpogosteje določen pesticid v podzemni vodi je še vedno atrazin in njegov razgradni produkt desetilatrazin. Sledijo mu metolaklor, terbutilazin in njegov razgradni produkt desetilterbutilazin. Pesticidi alaklor, dimetenamid, metazaklor in terbutrin niso bili določeni. Analiza zaznanih pesticidov z rabo prostora kaže na višje vrednosti na območjih z intenzivno kmetijsko dejavnostjo. V severnem delu Dravskega polja, južnem robu mesta Maribor, so koncentracije pesticidov manjše, povišane vrednosti pesticidov pa se pojavljajo v južnem delu Dravskega polja, kar sovpada tudi z intenzivnejšo kmetijsko rabo tal na tem območju. Z vrednotenjem razmerij med razgradnim produktom in primarnim pesticidom iz naslova atrazina in terbutilazina (DAR in DTA/TBA) smo ocenili »starosti« onesnaženja. Presenetljiva je visoka pojavnost atrazina, ki je lahko posledica starih bremen, počasne razgradnje in hidrogeoloških pogojev ali pa uporabe atrazina po uveljavitvi prepovedi uporabe.

Abstract

The article presents the results of a research on the occurrence and concentration of pesticides in the groundwater of the Dravsko polje aquifer in the period from 2013 to 2015. Based on the results, the evaluation of spatial distribution of pesticides in groundwater and the relation to land use was performed. In different hydrogeological periods, 76 groundwater samples were collected at 19 different locations. 15 pesticides with their metabolites in groundwater were identified. Despite the prohibition of use, atrazine and its degradation product desethylatrazine still remain the most commonly detected pesticides in groundwater. They are followed by metolachlor, desethylterbutylazine and terbutylazine. The pesticides alachlor, dimetamide, metazachlor and terbutrin were not detected. The analysis of detected pesticides by land use indicates higher values in areas with intensive agricultural activity. In the northern part of the Dravsko polje, where the city of Maribor is located, pesticide concentrations are lower. Increased pesticide values occur in the southern part of the Dravsko polje, which coincides with more intensive agricultural land use of the area. The coefficient of degradation product / primary pesticide ratio (DAR and DTA/TBA) was used to estimate the "age" of contamination from atrazine and terbutilazine. Surprising is the high incidence of atrazine, which may result from old burdens, slow decomposition and hydrogeological conditions, or the use of atrazine after the enactment of the ban.

Uvod

Pesticidi so snovi, ki se predvsem v kmetijstvu, pa tudi v gospodinjstvu, uporabljajo za zatiranje škodljivcev, plevelov in rastlinskih bolezni (Koroša & Mali, 2012). Uporabljajo jih tudi v gozdarstvu, lesarstvu, ladjedelništvu, itd. Po svojem nastanku so lahko naravne snovi, izolirane iz rastlin, ali sintetično pridobljene s sintezo. Po svoji naravi so te spojine biološko aktivne, nekatere so celo strupene. V podzemni vodi se pojavljajo tako primarne spojine, kot njihovi produkti razpadanja. Raziskave v Veliki Britaniji so pokazale, da so v podzemni vodi odkrili višje koncentracije produktov razgradnje (metabolitov) v primerjavi s koncentracijami matičnih spojin (Kolpin et al., 2004; Lapworth & Gooddy, 2006). V okolje najpogosteje pridejo zaradi uporabe v kmetijstvu.

Pesticide razdelimo na šest skupin: fungicide (kaptan, benomil, triadimefon, folpet, mankozeb), insekticide (DDT, metidation, metomil, lindan, heptaklor), herbicide (atrazin, alaklor, simazin, propazin, metolaklor, terbutilazin), akaricide (dikofol, propargit, klorfentazin), rodenticide (endrin, varfarin, cinkfosfid) in limacide (metaldehid, metiokarb) (Yadav & Devi, 2017).

Onesnaženje podzemne vode s pesticidi je svetovni problem. Ostanke pesticidov najdemo v vodonosnikih širom po svetu (Åkesson et al., 2013; Kolpin et al., 1998). Gre za kompleksno problematiko zaradi razširjene uporabe pesticidov pri predelavi hrane in zaradi njihove širitve in akumulacije v okolju (Tadeo, 2008). Globalna produkcija in uporaba pesticidov s časom narašča (Bernhardt et al., 2017; Sjerps et al., 2017). Pesticidni pripravki lahko vsebujejo eno ali več aktivnih snovi, ki lahko z izpiranjem iz kmetijskih površin prehaja v površinsko in podzemno vodo (González-Rodríguez et al., 2011; Heuvelink et al., 2010; van Eerdt et al., 2014). Te emisije lahko predstavljajo tveganje za ekosisteme ali zdravje ljudi (Kim et al., 2017; Munz et al., 2017; Nienstedt et al., 2012; Shelton et al., 2014; Stehle and Schulz, 2015).

Seznami dovoljenih aktivnih snovi za uporabo se spreminjajo. Na podlagi novih spoznanj je mogoče določene aktivne snovi prepovedati, lahko pa se prepoznajo nove, kot možne nadomestne snovi, ki so dovoljene (Sjerps et al., 2017). V Evropi so pesticidi regulirani in dovoljeni v skladu z Uredbo o fitofarmacevtskih sredstvih 1107/2009. Standard Evropske unije za pitno vodo iz Evropske direktive o pitni vodi (Uradni list EU, št. 98/83/ES) in standard kakovosti vode za telesa podzemne vode po direktivi o podzemni vodi (Direktiva 2006/118/ES) določata najvišjo koncentracijo posameznega pesticida na 0,1 µg/l in vsoto merjenih pesticidov na 0,5 µg/l. Za oceno stanja oz. obremenitev podzemne vode so pomembne tako primarne spojine, kot tudi njihovi razgradni produkti.

Poročanja o obsegu onesnaženja podzemne vode s pesticidi so v svetu zelo različna in so odvisna od osveščenosti ljudi, stopnje raziskanosti, kvalitete monitoringov ter načina in intenzivnosti uporabe pesticidov (McManus et al., 2017). Na območju Dravskega polja so že v osemdesetih letih prejšnjega stoletja zaznali zelo visoke vrednosti pesticidov v podzemni vodi. Študije v letih 1982-1989 so pokazale, da so bile razmere na Dravskem polju glede onesnaženosti s pesticidi izjemno slabe (Brumen et al., 1990). Zanemarjanje prvih signalov je ob specifičnih razmerah privedlo do izrazitega povišanja koncentracij pesticidov v podzemni vodi, predvsem zaradi gramoznic, kjer so bili odloženi tudi ostanki pesticidov (Brumen et al., 1990). Izredno povečanje koncentracije pesticidov na črpališčih v začetku poletja 1989 je pripeljalo do zaprtja treh večjih vodovodov. Sprejet je bil republiški interventni zakon za izvedbo oskrbe s kvalitetno pitno vodo in za sanacijo podzemne vode na Dravskem polju. Nekatere zasute gramoznice so bile tudi sanirane (Knez & Regent, 1993; Fliser et al., 1991).

Na območju Dravskega polja je uporaba pesticidov regulirana med drugim tudi z Uredbo o vodovarstvenem območju za vodno telo vodonosnikov Dravsko-ptujskega polja (Uradni list RS, 2007). Uredba prepoveduje uporabo fitofarmacevtskih sredstev za zatiranje škodljivih organizmov na kmetijskih zemljiščih na najožjih vodovarstvenih območjih. Kakovost podzemne vode na Dravskem polju se kontrolira v okviru državnega monitoringa voda. Kemijsko stanje vodonosnika glede na pesticide je bilo v l. 2000 slabo. V obdobju 1993-2000 so bile presežene mejne vrednosti (Uradni list RS, 2002) za metolaklor, atrazin, njegova razgradna produkta desetilatrazin in desizopropilatrazin, prometrin in vsota pesticidov, čeprav so bili že opazni trendi padanja koncentracij (ARSO, 2004). Tudi v obdobju 2012-2018 je bilo kemijsko stanje podzemne vode za telo podzemne vode Dravska kotlina, kateremu pripada vodonosnik Dravskega polja, prepoznano kot slabo. Čeprav nekatere vrednosti pesticidov presegajo standarde kakovosti, pa dolgoročno trendi vsebnosti pesticidov padajo, tudi najbolj kritičnih kot sta atrazin in desetilatrazin (ARSO, 2019).

Glede na pretekle velike obremenitve podzemne vode s pesticidi, je bil namen raziskave preveriti trenutno stanje prisotnosti pesticidov v podzemni vodi aluvialnega vodonosnika Dravskega polja. V članku predstavljamo rezultate raziskave v obdobju 2013-2015. Cilji raziskave so bili (1) ugotoviti stanje prisotnost izbranih pesticidov in njihove koncentracije, (2) oceniti njihovo prostorsko razširjenost ter (3) povezati rabo prostora z njihovo prisotnostjo v podzemni vodi.

Območje raziskav

Dravsko polje leži v severovzhodnem delu Slovenije in pripada telesu podzemne vode »Dravska kotlina (3012)« (Uradni list RS, 2005). Dravsko polje predstavlja ravnino med Slovenskimi goricami, Pohorjem, Dravinjskimi goricami in Halozami. Na vzhodu se nadaljuje v Ptujsko polje. Območje Dravskega polja pokriva 293,2 km^2. Hidrološka mreža je v osrednjem delu redka in ni razvejana, ob robu ravnine pa je gostejša (Urbanc et al., 2014). Najvišji predeli Dravskega polja ležijo ob vznožju Pohorja (290 m n.m.v), najnižji pa pri sotočju Drave in Dravinje v jugozahodnem delu (207 m n.m.v) (Petauer, 1980). Glavni vodotok je reka Drava, ki teče v smeri severozahod-jugovzhod. Manjši vodotoki in potoki so Dravinja, Polskava, Kameniščica, Reka, Trojšnica in Devina. Rečni režim Drave je izrazito fluvioglacialen, za katerega je značilno, da ima najvišje povprečne mesečne pretoke maja in junija, najnižje pa januarja in februarja. Ostali vodotoki tega območja imajo večinoma dežno-snežni rečni režim z najvišjimi povprečnimi pretoki marca in aprila ter najnižjimi avgusta. Območje pripada zmernemu celinskemu podnebju osrednje Slovenije za katerega je značilen celinski padavinski režim z povprečno letno količino padavin od 1200 do 1300 mm. Povprečna letna temperatura zraka je med 8 °C in 12 °C (ARSO, 2017). Potencialno evapotranspiracijo na Dravskem polju sta ocenila Kolbezen in Pristov (1998) po Penmanu med 650 in 700 mm/leto. Prestor in Janža (2006) sta po metodi Kennessya ocenila infiltracijo na obravnavanem območju Dravskega polja na od 300 do 400 mm/leto.

Na Dravskem polju imamo opraviti s tremi tipičnimi vodonosniki: prvi (aluvialni) vodonosnik (do 32 m globine), drugi (terciarni) vodonosnik (od 40 – 200 m globine) in tretji (termalni) vodonosnik (do 1000 m globine). Najbližje površju in najbolj ranljiv je aluvialni vodonosnik, kateri je bil predmet naših raziskav. Voda v njem se hitro obnavlja, in sicer pretežno iz padavin ter s ponikanjem površinskih vod. Drugi vodonosnik nima neposrednih povezav s površinskimi vodami in le na določenih mestih s prvim vodonosnikom, zato se količinsko obnavlja veliko počasneje (v 1.000 letih). Tretji termalni vodonosnik se nahaja v globljih terciarnih sedimentih in predterciarni podlagi (ARSO, 2009).

Prodni (aluvialni) zasip Dravskega polja predstavlja dobro prepusten odprt vodonosnik s koeficientom hidravlične prepustnosti od $5{\cdot}10^{-4}$ do $6{\cdot}10^{-3}$ m/s (Urbanc et al., 2014). Povprečna debelina vodonosnika je ocenjena na 20 m (Urbanc et al., 2014). Na podlagi suhe prostorninske teže materiala je ocenjena učinkovita poroznost vodonosnika približno 0,25, na podlagi prostorninske teže naravno vlažnega materiala pa na najmanj 0,15 (Žlebnik, 1982). Povprečna debelina nenasičene cone je ocenjena na podlagi izdelanega modela na 8,35 m (Urbanc et al., 2014, Mali & Koroša, 2016), povprečna debelina zasičene cone je 12,05 m (Urbanc et al., 2014), glede na podatke iz leta 1999 pa od 15 do 17 m (Žlebnik & Drobne, 1998). Podzemna voda se v kvartarnem vodonosniku Dravskega polja pretaka v generalni smeri od zahoda proti vzhodu. Gre za odprti vodonosnik, ki napaja z infiltracijo padavin in s ponikanjem pohorskih potokov na zahodnem delu Dravskega polja. Smer toka podzemne vode kaže lokalno manjša odstopanja od generalne smeri toka podzemne vode od zahoda proti vzhodu. Vodonosnik Dravsko polje je eden od glavnih virov pitne vode za občino Maribor in okoliške občine.

Glede na podatke državnega monitoringa podzemnih vod, je kemijsko stanje vodnega telesa Dravska kotlina slabo zaradi vsebnosti nitratov in pesticidov (ARSO, 2019). Vzroki so predvsem v intenzivnem kmetijstvu, ki je najbolj prisotno v južnem delu raziskovalnega prostora in manj v severnem delu, kjer leži mesto Maribor. Kmetijstvo je usmerjeno predvsem v živinorejo, med drugim tudi v vzrejo perutnine. Živinoreja je poleg dušika tudi vir za organska onesnaževala, na primer farmakološko aktivne snovi, ki se uporabljajo pri vzreji živali. Kmetijstvo je zato osnovni vir slabega stanja podzemne vode zaradi gnojenja poljedelskih površin in obdelave s pesticidnimi pripravki.

Poleg kmetijske rabe tal na okolje vplivajo urbana območja z urejeno oz. neurejeno kanalizacijsko infrastrukturo. Na območjih, kjer ni zgrajenih kanalizacijskih sistemov, gospodinjstva in stanovanjski objekti uporabljajo greznice. Glede na bazo podatkov Evidence hišnih številk (EHIŠ) lahko ocenimo, da je na celotnem Dravskem polju okoli 130.095 prebivalcev. Kanalizacijsko najbolj urejeno območje je severno območje, najslabše pa

osrednji del Dravskega polja. Na obravnavanem raziskovalnem območju je 7 čistilnih naprav. Eden od virov organskih onesnaževal v podzemni vodi so IED zavezanci (to so zavezanci, ki morajo pridobiti okoljevarstveno dovoljenje v skladu z Direktivo o industrijskih emisijah (Industry Emissions Directive), med katere spadajo industrijski obrati, bencinske črpalke, odlagališča, itd. Pri zavezancih IED poznamo različne tipe izpustov. To so komunalne odpadne vode, avtopralnice, hladilne vode, odpadne vode iz kemičnih čistilnic, tehnološke vode, odpadne vode iz kotlovnic, raznih pralnic, proizvodenj tekstila, kozmetike, itd. Območje Dravskega polja ima dobro razvito prometno infrastrukturo. Od avtocest, lokalnih cest, železnic pa tudi letališče. V kategorijo odlagališč na Dravskem polju spadajo komunalna odlagališča ter divja odlagališča, ki so nenadzorovana in še toliko bolj škodljiva za okolje. Na raziskovalnem območju Dravskega polja sta dve odlagališči komunalnih odpadkov. Začasno odlagališče Dogoše in odlagališče na območju mesta Maribor - Pobrežje. Obe odlagališči imata status zaprtih odlagališč. Na območju Kidričevega sta tudi dve industrijski odlagališči odpadkov, ki sta nastali pri proizvodnji glinice in aluminija. Za podatkovno bazo divjih odlagališč skrbi društvo Ekologi brez meja (2019). V bazi imajo fizične osebe in organizacije kot registrirani uporabniki omogočen pregled in vnos lokacij divjih odlagališč. Po razpoložljivih podatkih registra divjih odlagališč je na Dravskem polju še 416 različnih divjih odlagališč. Klasificirana so glede na tip odpadkov (organski, gradbeni, komunalni, kosovni, pnevmatike, motorna vozila, salonitne plošče, nevarni odpadki ter sodi z nevarnimi odpadki). Od teh je 268 odlagališč s komunalnimi odpadki, 202 odlagališči z gradbenimi odpadki, 160 odlagališč s kosovnimi odpadki, 136 odlagališč z biološkimi odpadki, 123 odlagališč z nevarnimi odpadki, 71 odlagališč, kjer je odložen salonit, 17 odlagališč s pnevmatikami in tri avtomobilska odlagališča.

Hidrogeološke razmere na Dravskem polju v času raziskav

Smer toka podzemne vode, na podlagi meritev gladin, kaže lokalno manjša odstopanja od generalne smeri toka podzemne vode od zahoda proti vzhodu (sl. 1). Najmanjša debelina nenasičene cone je v južnem delu vodonosnika na območju merilnih mest VP-4, OP-2 in V-25. Najdebelejša nenasičena cona se nahaja na območju merilnih mest PAC-5, PAC-2 in PCI-2 v severnem delu vodonosnika. Debelina nasičene plasti je najdebelejša v južnem, spodnjem, delu vodonosnika, medtem ko je nasičena plast najtanjša v severnem delu, ob pobočju Pohorja (Urbanc et al., 2014). Ne glede na vodno stanje smo meritve (vzorčenje) izvedli v oktobru (2013, 2014) in aprilu (2014, 2015). V obdobju meritev je bila na Dravskem polju zabeležena najnižja gladina podzemne vode v oktobru 2013 (224,13 m n.m.v.), oktobra 2014 pa je bila zabeležena najvišja gladina podzemne vode (256,93 m n.m.v.).

V sklopu opravljenih raziskav na Dravskem polju smo ob vsakem vzorčenju podzemne vode izmerili tudi nivo podzemne vode, T, pH, električno prevodnost (EC) ter oksidacijsko-redukcijski potencial (Eh). V času naših raziskav določanja prisotnosti pesticidov v podzemni vodi so bile določene vrednosti pH podzemne vode Dravskega polja od 6,64 do 7,82 ter EC med 483 in 1031 µS/cm. Vrednosti EC so v osrednjem in južnem delu Dravskega polja višje od 700 µS/cm. Na določenih mestih tako na južnem kot severnem delu dosegajo celo vrednosti višje od 900 µS/cm. Vrednosti oksidacijsko-redukcijskega potenciala (Eh) nihajo med 11 in 323 mV. Izmerjene vrednosti temperature (T) nihajo med 11,1 in 15,8 °C.

Izbor pesticidov in njihovo obnašanje

Transport pesticidov je odvisen od njihovih fizikalno-kemijskih lastnosti in lastnosti okolja, v katerem potujejo. Zadnja desetletja se je povečalo razumevanje vpliva lastnosti in procesov prisotnosti in razporejanja pesticidov v zemljinah in sedimentih z različnimi pedološkimi in geološkimi lastnostmi. Spoznanja temeljijo na podlagi laboratorijskih raziskav (Clausen et al., 2004), terenskih eksperimentov (Boesten and van der Pas, 2000; Funari et al., 1998), regionalnih in nacionalnih programov monitoringov ter študija značilnosti med stopnjo onesnaženja, različnimi hidrogeološkimi značilnostmi in rabo prostora v zaledju vodnih virov (Gaw et al., 2008; Steele et al., 2008; Worrall and Kolpin, 2004). Razgradnja pesticidov je odvisna od pogojev v okolju, predvsem vremenskih razmer (temperature, sončnega sevanja, količine padavin, drugo), lastnosti tal in sedimentov (aktivnost mikroorganizmov, pedoloških in geoloških značilnosti). Lastnosti pesticidov, zadrževalni časi podzemne vode, redoks pogoji in celotna obremenitev so faktorji, ki določajo transportne poti in dinamiko pesticidov v vodonosniku. Pesticidi, ki so bili odloženi na površje, migrirajo skozi tla (Oppel et al., 2004; Scheytt et al., 2004) in nenasičeno cono v nasičeno cono vodonosnika (Snyder, 2004; Zuehlke et al., 2004). Glavni procesi, ki kontrolirajo organ-

ska onesnaževala med transportom, so sorpcija, ionska izmenjava v vodonosniku in njihova mikrobiološka razgradnja (Lapworth et al., 2012). Migracija aktivnih snovi in njihovih razgradnih produktov je določena s topnostjo v vodi (Water solubility, Sw), hidrofobnostjo oz. hidrofilnostjo (izraženo s porazdelitvenim koeficientom, Kow oz. logKow), koeficientom odvisnim od pH (Dow), koeficientom adsorpcije/desorpcije (izražen kot Koc) ter kislostjo (izraženo s pKa) in hlapnostjo iz vode (izraženo s Henryjevo konstanto). Za boljšo oceno okoljskega tveganja zaradi uporabe pesticidov so se razvili različni indikatorji ocene tveganja (Gutsche & Rossberg, 1997; Padovani et al., 2004; Reus and Leendertse, 2000; Sorensen et al., 2015; van der Werf and Zimmer, 1998) in modeli obnašanja pesticidov v podzemni vodi (Carsel et al., 1985; Jarvis et al., 1991; Tiktak et al., 2004).

Za analizo pesticidov v podzemni vodi Dravskega polja smo izbrali 15 pesticidov in njihovih razgradnih produktov (2,6-diklorobenzamid, alaklor, atrazin, desetilatrazin, desizopropilatrazin, terbutilazin, desetilterbutilazin, dimetenamid, klorotoluron, metazaklor, metolaklor, prometrin, propazin, simazin in terbutrin) (Tabela 1).

V program preiskav je vključenih 15 spojin, od tega 11 matičnih spojin in štirje razgradni produkti. Le za šest spojin - terbutilazin, metolaklor, metazaklor, dimetenamid, klortoluron, je raba pesticidnih pripravkov dovoljena. Ostali so prepovedani oz. so se pa uporabljali v preteklosti.

Glede na Seznam registriranih fitofarmacevtskih sredstev na dan 25.9.2019 (MKGP, 2019) je terbutilazin selektivni herbicid in se skupaj z dimetenamidom uporablja za pridelavo koruze. Po prepovedi uporabe atrazina v EU je terbutilazin njegov nadomestek. Desetilterbutilazin je razgradni produkt terbutilazina. Najdemo ga lahko na kmetijskih obdelovalnih območjih, v sedimentih ter površinskih in podzemnih vodah. Metolaklor je prav tako herbicid, ki se uporablja za zatiranje nekaterih plevelov v kmetijstvu, ob cestah in pri vzgoji okrasnih rastlin. V zemlji se razgrajuje hitreje, v vodi počasneje. Klorotoluron se skupaj z ostalimi aktivnimi snovmi uporablja pri zatiranju plevelov ter drugih rastlin, ki motijo rast pšenice, rži ter ječmena (MKGP, 2019). Metazaklor se uporablja pri pridelavi brstičnega ohrovta, gorjušica, oljna ogrščica ter drugih podobnih ter okrasnih rastlin (MKGP, 2019). Med

Tabela 1. Pesticidi, ki so bili vključeni v analizo podzemne vode na Dravskem polju.
Table 1. Pesticides included in the analysis of groundwater in the Drava field.

	CAS št. / CAS no.	Uporaba / Use	Uporaba v letih 2013-2015/ Use in years 2015-2015
2,6-diklorobenzamid	2008-58-4	razgradni produkt herbicida diklobenila	Prepovedan
Alaklor	15972-60-8	herbicid	Prepovedan
Atrazin	1912-24-9	herbicid	Prepovedan
Desetilatrazin	6190-65-4	razgradni produkt herbicida atrazina	Prepovedan
Desetilterbutilazin	30125-63-4	razgradni produkt herbicida terbutilazina	Dovoljen
Desizopropilatrazin	1007-28-9	razgradni produkt herbicida atrazina	Prepovedan
Dimetenamid	87674-68-8	herbicid	Dovoljen
Klortoluron	15545-48-9	herbicid	Dovoljen
Metazaklor	67129-08-2	herbicid	Prepovedan
Metolaklor	51218-45-2	herbicid	Dovoljen
Prometrin	7287-19-6	herbicid	Prepovedan
Propazin	139-40-2	herbicid	Prepovedan
Simazin	122-34-9	herbicid	Prepovedan
Terbutilazin	5915-41-3	herbicid	Dovoljen
Terbutrin	886-50-0	herbicid	Prepovedan

*CAS št. / CAS no. - registrska številka CAS / CAS (Chemical Abstracts Service) Registry Number

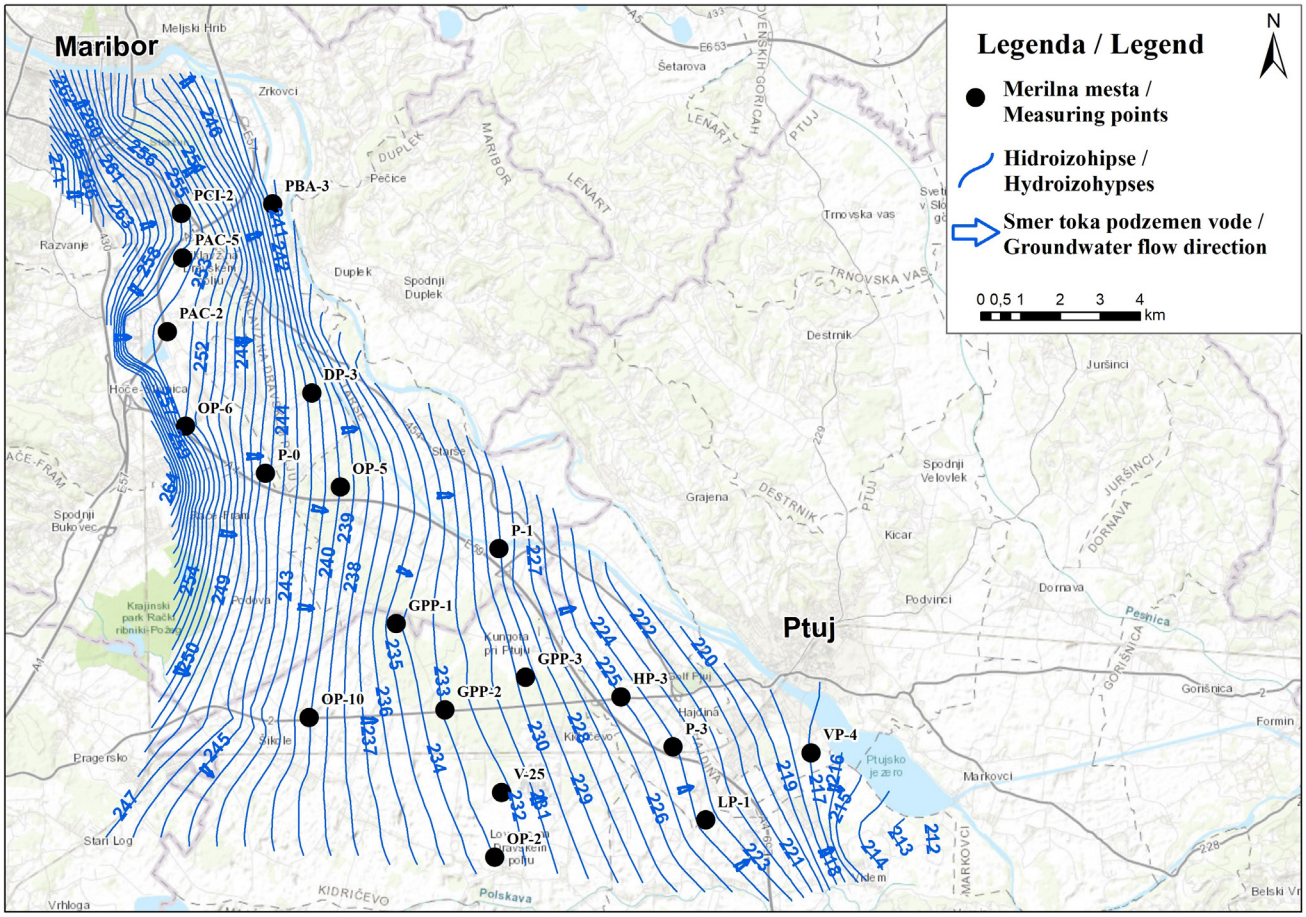

Sl. 1. Karta merilnih mest, hidroizohips in smeri toka podzemne vode na Dravskem polju (april 2014).
Fig. 1. Map of the measuring points, hydroisohips and groundwater flow direction in the Drava field (April 2014).

največkrat detektiranimi, tudi v najvišjih koncentracijah, še vedno najdemo atrazin ter njegove razgradne produkte. Atrazin je herbicid, ki se je uporabljal za zatiranje plevela. V Sloveniji je v celoti prepovedan od leta 2003. Razgradna produkta atrazina sta desetilatrazin in desizopropilatrazin. Zanju veljajo enaki toksikološki zaključki in enake zahteve, kot za atrazin. Med prepovedanimi sta tudi simazin in propazin. Simazin prištevamo med herbicide iz skupine triazinov. Uporabljal se je za odstranjevanje plevela, podobno kot atrazin je sedaj prepovedan v Evropski uniji Direktiva (91/414/EGS). Propazin je herbicid, ki se je uporabljal v obliki škropila, ob ali po sajenju raznih kultur. Stabilen je v nevtralnih rahlo kislih ali alkalnih medijih. Med prepovedanimi so še diklobenil, alaklor, prometrin in terbutrin. 2,6-diklorobenzamid je razgradni produkt diklobenila, ki se je uporabljal za zatiranje plevelov v sadovnjakih, vinogradih, nasadih okrasnega grmovja, itd., med drugim tudi ob železniških tirih in postajah.

Materiali in metode

Določitev merilnih mest

Ocena reprezentativnosti merilnih mest je narejena na osnovi navodil ISO standarda za vzorčenje podzemne vode (SIST ISO 5667-11:2010). Izbrana merilna mesta so piezometri s podobnimi lastnostmi, ki lahko vplivajo na ustreznost vzorčenja (globina objekta, vgrajeni materiali, dostopnost, itd.). Merilna mesta so bila določena na podlagi razpoložljivih podatkov arhiva Geološkega zavoda Slovenije o lokacijah, o litološki zgradbi, tehnični izvedbi vrtin (globina, premer, lokacija filtrov, itd.), meritvah gladin podzemne vode (GPV), črpalnih poskusih ter o kemijskih analizah vode.

V mrežo merilnih mest je bilo vključenih 19 merilnih mest, od tega tudi dve mesti, ki sta vključeni v državni program monitoringa kemijskega stanja podzemne vode (LP -1 in P-1). Lokacije merilnih mest so prikazane na sliki 1.

Analiza rabe tal

Klasifikacijo rabe prostora smo izvedli z uporabo podatkov CORINE 2012 (Corine land cover – CLC) za rabo zemljišč za Evropo (ARSO, 2016) za celotno območje Dravskega polja ter za vsako merilno mesto posebej. Na osnovi baze pokrovnosti tal CLC 2012 in prostorske analize smo določili deleže površine posamezne enote pokrovnosti tal. Razrede pokrovnosti tal smo združili v 4 večje enote: kmetijske površine (45,65 %), gozd (22,84 %), urbana območja (19,65 %) in industrijska območja (2,26 %), ostalo predstavljajo vodne površine (reke, jezera, itd.). Urbana območja predstavljajo naselja in zaselki ter vsa infrastruktura, ki služi opravljanju človekovih dejavnosti. V kategorijo »industrijskih površin« smo uvrstili industrijske obrate, cestno in železniško omrežje, letališče, kamnolome in odlagališča. V kategorijo kmetijskih zemljišč spadajo njivske površine ter mešane kmetijske površine. Enota gozd združuje vse vrste od listnatega, mešanega in iglastega gozda ter grmičasti gozd. Obdelavo podatkov in izračune smo izvedli z uporabo programske opreme Statistica (Stat Soft Inc., 2012), prostorsko analizo pa z uporabo ArcMap (ESRI Inc., 2004).

Napajalna zaledja merilnih mest

Karakteristike napajalnega zaledja vrtin smo določili za vsako vrtino glede na hidrogeološke značilnosti vodonosnika, izražene s hitrostjo in smerjo toka podzemne vode (Koroša, 2019). Pretok podzemne vode smo izračunali po Darcyjevi enačbi. Koeficient prepustnosti (K) smo za vsako vzorčno mesto ocenili na podlagi predhodnih raziskav črpalnih poskusov in drugih raziskav (Krivic et al., 2012; Brenčič & Ratej 2006; Urbanc et al., 2014; Brenčič, 1998; Brenčič, 2004). Gradient je bil določen na podlagi izrisanih hidroizohips. Razdaljo območja napajanja smo določili na podlagi izračuna hitrosti toka podzemne vode v smeri gorvodno v obdobju enega leta v pravokotni smeri na hidroizohipse. Ker ne gre za stalno črpanje vode iz vzorčevanih objektov, smo napajalno območje omejili na kot 30°, kot določa metodologija v Pravilniku o kriterijih za določitev vodovarstvenega območja (Uradni list RS, 2004b). Za vsako merilno mesto so bili določeni podatki o rabi tal ter potencialnih onesnaževalcih.

Vzorčenje

Za določitev pesticidov v podzemni vodi Dravskega polja smo izpeljali štiri vzorčenja v letih 2013-2015, in sicer v jesenskem (oktober 2013, 2014) in pomladnem (april 2014, 2015) obdobju. Na obravnavanem območju smo odvzeli vzorce podzemne vode za kvantitativno kemijsko analizo podzemne vode za pesticide in njihove razgradne produkte na devetnajstih merilnih mestih. Vzorčenje podzemne vode smo izvedli skladno z določili standarda SIST ISO 5667-11:2010. Z vzorci podzemne vode smo ravnali skladno z določili standarda SIST ISO 5667-3. Vzorčenje podzemne vode je potekalo s črpalko Grundfos MP-1TM, katere pretok je bil 0,2 l/s, na globini od 3 m do 16 m, glede na gladino podzemne vode v merilnem mestu. Za kvantitativno kemijsko analizo pesticidov smo odvzeli 1 l vode v rjavo steklenico z zamaški s PTFE linerjem. Pri vzorčenju smo uporabili zaščitne rokavice za enkratno uporabo, ki se po vsakem vzorčenju zavržejo. Vsi vzorci so bili dostavljeni v laboratorij v največ 6 urah, ter nadalje obdelani po postopkih določenih z merilno metodo. Skupno smo odvzeli 76 vzorcev vode.

Analizne metode

Kvantitativne kemijske analize pesticidov v podzemni vodi so bile izvedene v laboratoriju JP VO-KA d.o.o. Uporabljena je bila modificirana metoda EPA 525.2, ki temelji na ekstrakciji na trdno fazo (SPE) in uporabi metode sklopitve plinske kromatografije in masne spektrometrije (GC-MS). Podrobneje so metodo opisali Auersperger et al. (2005). Uporabljena merilna metoda je validirana.

Vrednotenje razmerij pesticidov in njihovih razgradnih produktov

Razmerje DAR, ki sta ga prvič predstavila Adams & Thurman (1991), pojasnjuje vsebnosti razgradnega produkta (desetilatrazin) in primarne spojine (atrazin). DAR je uporaben za namen določitve »starosti« onesnaženja. Z DAR smo izračunali razmerje med desetilatrazinom in atrazinom, za razdelitev točkovnih in razpršenih virov onesnaženja v podzemni vodi. Majhno razmerje DAR pomeni, da je prisotnega več atrazina v primerjavi z desetilatrazinom, kar nakazuje na »sveže« onesnaženje in je lahko tudi kazalnik točkovnega vira onesnaženja. Na osnovi rezultatov vsebnosti terbutilazina in desetilterbutilazina, lahko tako kot razmerje DAR, izračunamo tudi razmerje med desetilterbutilazinom in terbutilazinom (DTA/TBA). Milan et al. (2015) so razmerje DTA/TBA uporabili v podzemni vodi za analizo interakcije med herbicidom in tlemi. Razmerje, manjše od 1, kaže na točkovni vir onesnaženja, saj desetilterbutilazin počasneje izginja v nenasičeni coni kot terbutilazin.

Tabela 2. Statistična analiza meritev pesticidov v podzemni vodi Dravskega polja.
Table 2. Statistical analysis of pesticide measurements in the Drava field groundwater.

	LOD (µg/l)	LOQ (µg/l)	N	Povp.	Md	Min.	Max.	Std.Dev.
2,6-diklorobenzamid	0,002	0,0067	3	0,01	0,01	0,01	0,01	0
Alaklor	0,002	0,0067	–					
Atrazin	0,002	0,0067	76	0,07	0,05	0,01	0,23	0,06
Desetilatrazin	0,002	0,0067	76	0,08	0,06	0,01	0,21	0,06
Desetilterbutilazin	0,002	0,0067	34	0,01	0,01	0,01	0,03	0,01
Desizopropilatrazin	0,01	0,0033	1	0,04	0,04	0,04	0,04	-
Dimetenamid	0,002	0,0067	–					
Klortoluron	0,002	0,0067	3	0,01	0,01	0,01	0,01	0
Metazaklor	0,005	0,017	–					
Metolaklor	0,002	0,0067	40	0,02	0,01	0,01	0,07	0,02
Prometrin	0,002	0,0067	8	0,03	0,02	0,01	0,05	0,02
Propazin	0,002	0,0067	4	0,01	0,01	0,01	0,01	0
Simazin	0,002	0,0067	21	0,01	0,01	0,01	0,03	0,01
Terbutilazin	0,001	0,0033	24	0,01	0,01	0,01	0,05	0,01
Terbutrin	0,005	0,017	–					

*LOD - meja detekcije/Limit of detection; LOQ - meja določljivosti/Limit of quantification;
N – št. določenih vzorcev nad LOQ/No. of samples above the LOQ; Povp. - povprečna vrednost/Average value;
Md – mediana/Median; Min. – najmanjša vrednost/Minimum value; Max. – največja vrednost/Maximum value;
Std.Dev. – standardna deviacija/Standard deviation

Rezultati in diskusija

Prisotnost pesticidov v podzemni vodi

Rezultati prisotnosti in statistika meritev pesticidov v podzemni vodi Dravskega polja je prikazana v tabeli 2. Nekateri od preiskovanih pesticidov niso bili zaznani niti enkrat. Takšni pesticidi, ki niso bili določeni nad spodnjo mejo določljivosti (LOQ) ali mejo zaznavanja uporabljene merilne metode za posamezno spojino (LOD) so: alaklor, dimetenamid, metazaklor, terbutrin (Tabela 2).

Atrazin in njegov razgradni produkt desetilatrazin sta bila določena v vseh vzorcih (76) podzemne vode (sl. 2). Sledijo jima metolaklor (40), razgradni produkt desetilterbutilazin (34), terbutilazin (24), simazin (21), prometrin (8), propazin (4), razgradni produkt 2,6-diklorobenzamid in klorotoluron (3) ter razgradni produkt desizopropilatrazin (1). Izmerjena vsebnost navedenih spojin je bila nad LOQ. Izmerjena vsebnost ostalih spojin ne presega vrednosti LOQ za posamezno spojino (sl. 2).

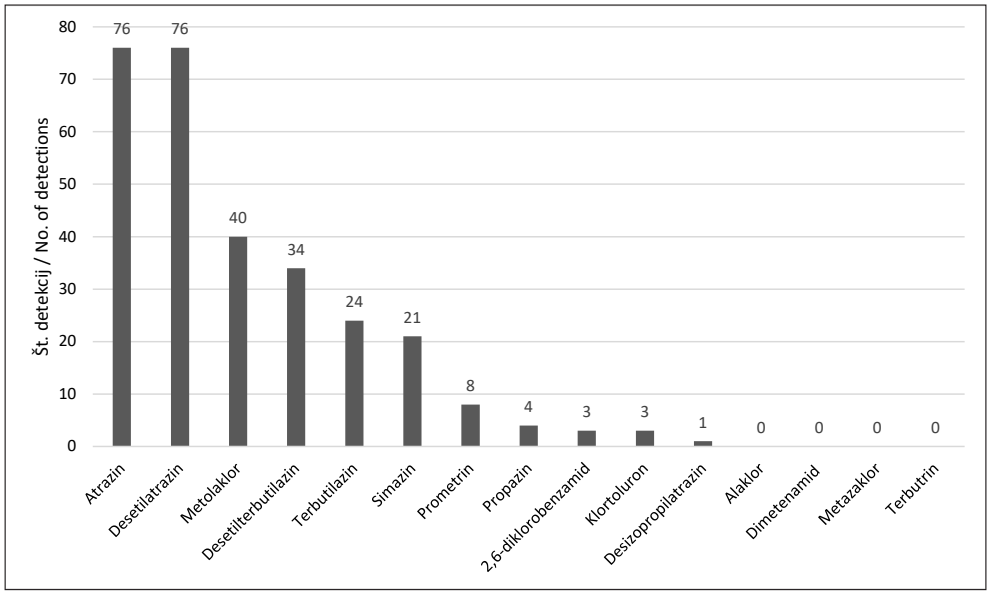

Sl. 2. Pogostost pojavljanja pesticidov v podzemni vodi Dravskega polja.

Fig. 2. Frequency of pesticide occurrence in Dravsko polje groundwater.

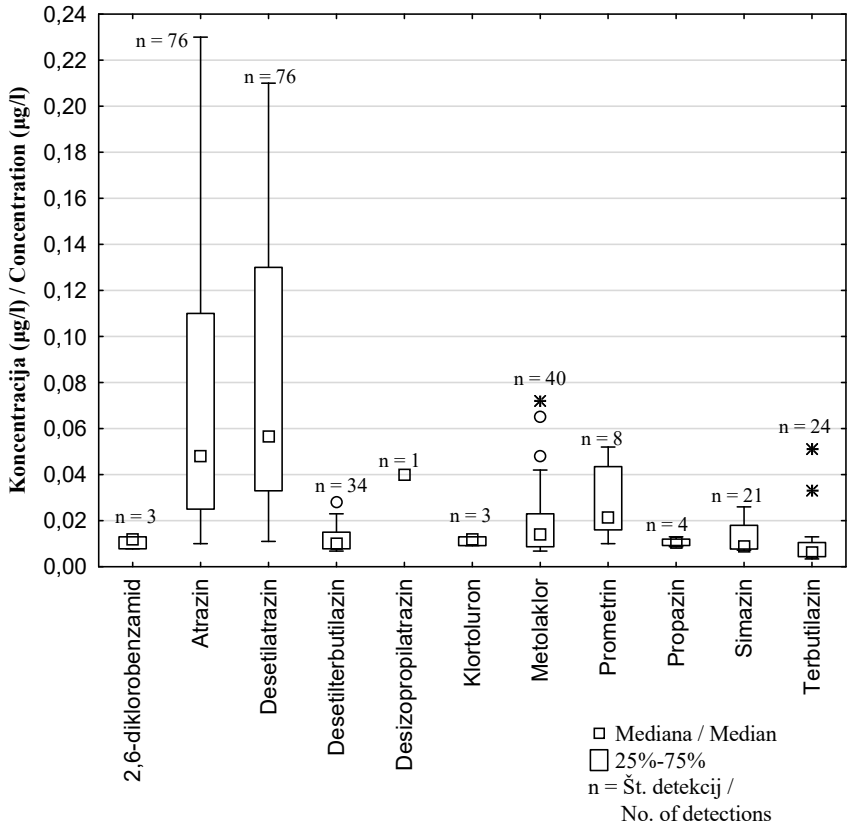

Sl. 3. Koncentracije izmerjenih pesticidov v podzemni vodi Dravskega polja.

Fig. 3. Concentrations of measured pesticides in Dravsko polje groundwater.

Na sliki 3 so predstavljene minimalne, povprečne in maksimalne vrednosti izbranih pesticidov v podzemni vodi Dravskega polja. Tisti, ki niso bili niti enkrat določeni nad mejo LOQ, niso prikazani. Visoke koncentracije dosegata pesticid atrazin (maks. 0,23 µg/l; min. 0,01 µg/l; povpr. 0,07 µg/l) in njegov razgradni produkt desetilatrazin (max. 0,21 µg/l; min. 0,01 µg/l; povpr. 0,08 µg/l), ki mestoma presegata mejno vrednost določeno s Uredbo o stanju podzemnih voda (Uradni list RS, 2009), 0,1 µg/l. Ostale preiskovane spojine niso bile zaznane v povišanih koncentracijah, nad mejno vrednostjo 0,1 µg/l (Tabela 2).

Nekateri pesticidi so se pojavili samo na enem merilnem mestu. Razgradni produkt 2,6-diklorobenzamid se je trikrat pojavil na merilnem mestu V-25. Pojav 2,6-diklorobenzamida na merilnem mestu V-25 je glede na zaledje najverjetneje kmetijskega izvora. Klorotoluron je bil zaznan trikrat samo na merilnem mestu GPP-3, ki ima v svojem širokem zaledju veliko kmetijskih površin, kljub temu, da je njegova lokacija v gozdu. Glede na to, da je zaznan samo na tem merilnem mestu, je možen izvor tudi v nelegalnih zasutih jamah in odloženih materialih v gozdu. Prepovedan pesticid propazin je bil zaznan v vseh štirih vzorčenjih samo na merilnem mestu HP-3. Tudi to merilno mesto, ni tipično kmetijsko, leži ob prometnici. V njegovem širšem zaledju pa najdemo tudi kmetijske površine (Tabela 3). Glede na to, da so bili ti trije pesticidi zaznani samo na teh merilnih mestih, lahko rečemo, da gre v teh primerih verjetno za točkovna onesnaženja.

Prostorska in časovna porazdelitev pesticidov v podzemni vodi glede na rabo prostora

Za namen prostorskega prikaza prisotnosti pesticidov v obdobju naših raziskav so na sliki 4 prikazane komulativne vrednosti (vsota) štirih vzorčenj izmerjenih vsebnostih šestih spojin, atrazina, desetilatrazina in simazina, (sl. 4a) ter terbutilazina, desetilterbutilazina, metolaklora, (sl. 4b), ki so bili največkrat zaznani v podzemni vodi Dravskega polja. Izmerjene vsebnosti pesticidov, ki so prepovedani za uporabo so prikazane na sliki 4a. Največje vrednosti atrazina in desetilatrazina so prisotne na območju južnega dela Dravskega polja, kjer je kmetijstvo sedaj in je bilo tudi v preteklosti najbolj intenzivno. Simazin se pojavlja le točkovno (sl. 4a). Vsote izmerjenih vsebnosti pesticidov, katerih raba je dovoljena, so prikazane na sliki 4b. Vsote izmerjenih vsebnosti terbutilazina, desetilterbutilazina in metolaklora kažejo drugačno razporeditev po vodonosniku. Terbutilazin in desetilterbutilazin se pojavljata po celem vodonosniku, izmerjene vsebnosti metolaklora so večje v zahodnem delu vodonosnika. Najvišje vrednosti metolaklora so se pojavile na merilnem mestu P-1 (0,072 µg/l).

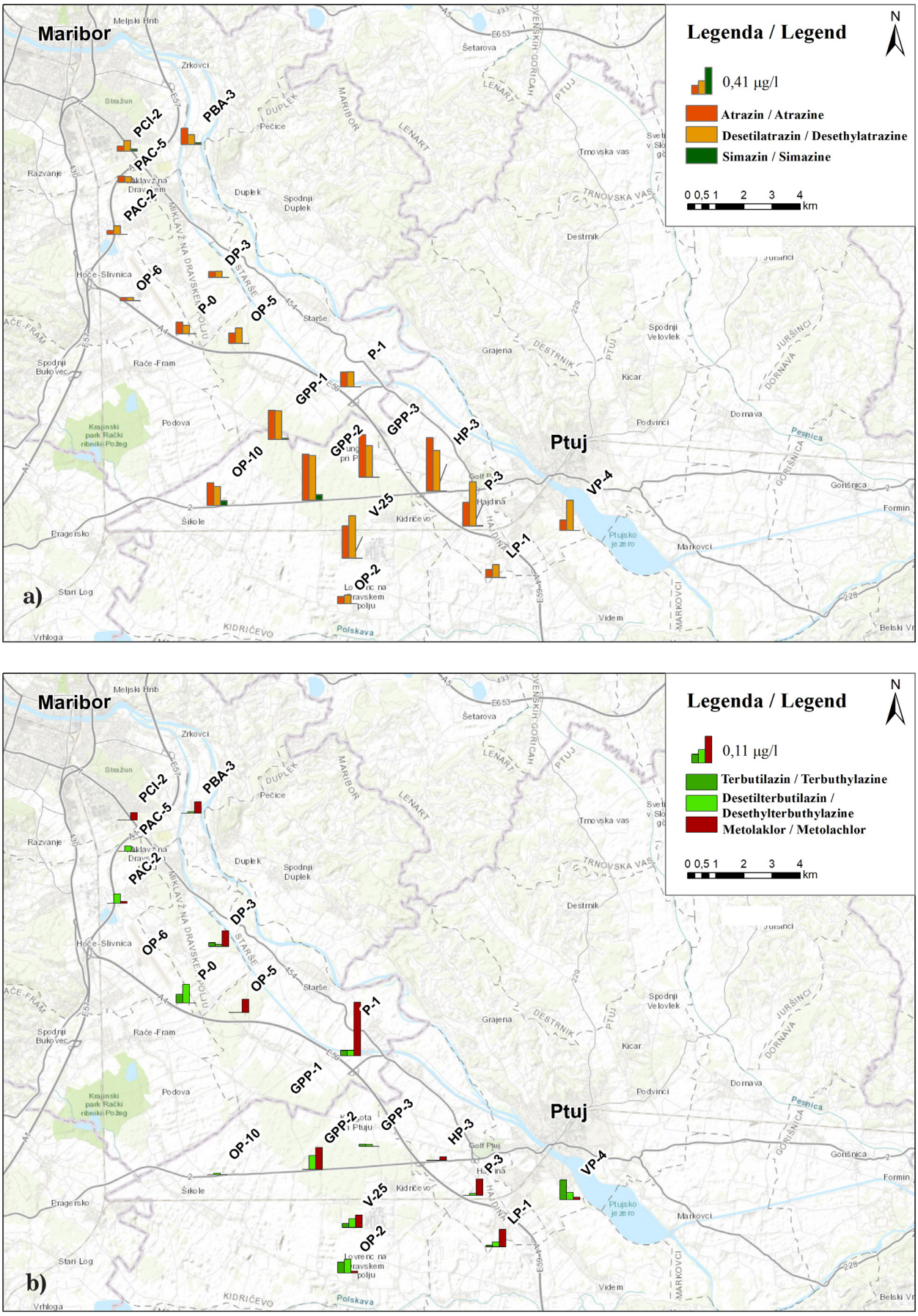

Sl. 4. Prostorski prikaz komulativnih vrednosti (vsota): a) atrazina, desetilatrazina in simazina; b) terbutilazina, desetilterbutilazina in metolaklora.

Fig. 4. Spatial representation of the cumulative values (sum) of: a) atrazine, desethylatrazine and simazine b) terbuthylazine, desethylterbuthylazine and metolachlor.

Tabela 3. Podatki o zaledju posamenega merilnega mesta na Dravskem polju.
Table 3. Background data of each measuring point in the Dravsko polje.

Merilno mesto / Measuring point	Ceste / Roads	Kanalizacija / Sewage system	Železnica / Railroad	Št. prebivalcev / No. Of population	Kmetijske površine / Agricultural land	Urbano / Urban	Industrijske površine / Industrial	Gozd / Forest	IED zavezanci / IEDs	Divja odlagališča / Wild landfills	I skupina (G+K) / I group (F + A)	II skupina (U+I) / II group (U + I)
	(m)	(m)	(m)		(%)	(%)	(%)	(%)				
DP-3	6656	5944	0	848	63,54	31,72	4,61	0,13	0	0	63,7	36,3
GPP-1	963	0	0	0	96,46	0	0	3,54	0	0	100,0	0,0
GPP-2	3144	0	0	0	99,25	0	0	0,75	0	0	100,0	0,0
GPP-3	1860	0	0	0	0	0	0	100	0	3	100,0	0,0
HP-3	8609	5791	8	1094	10,43	31,59	1,76	56,22	0	1	66,7	33,4
PAC-2	8375	9218	557	779	39,61	38,94	12,95	8,5	2	0	48,1	51,9
PAC-5	6011	12222	3821	28	77,2	0	22,79	0,01	2	0	77,2	22,8
PBA-3	8022	6839	0	100	14,07	11,87	6,02	68,04	4	9	82,1	17,9
PCI-2	7456	8307	2839	25	86,46	2,49	8,77	2,28	1	0	88,8	11,3
LP-1	1387	0	0	0	89,68	0	7,29	3,03	0	1	92,7	7,3
OP-10	3996	486	0	115	92,01	7,99	0	0	0	0	92,0	8,0
OP-2	1297	510	0	74	94,71	5,29	0	0	0	3	94,7	5,3
OP-5	6382	3399	0	159	58,59	12,75	0	28,66	0	0	87,3	12,8
OP-6	7597	3908	858	813	37,21	43,24	0	19,55	0	2	56,8	43,2
P-0	2363	686	0	131	96,6	3,4	0	0	0	1	96,6	3,4
P-1	4537	3821	0	466	89,2	3,74	0	7,06	0	0	96,3	3,7
P-3	3934	1891	467	74	29,92	0	22,28	47,8	0	4	77,7	22,3
V-25	2141	0	0	0	93,13	0,18	6,69	0	0	5	93,1	6,9
VP-4	10455	5520	0	858	54,67	40,07	0	5,26	0	1	59,9	40,1

Podatki za določitev prispevnega oz. napajalnega območja za posamezno merilno mesto so zbrani v tabeli 3. Na podlagi povprečnega koeficienta prepustnosti ($3{,}5 \cdot 10^{-3}$ m/s) in povprečnega gradienta (0,004), smo izračunali povprečno površino zaledja za posamezno merilno mesto za obdobje enega leta. Povprečna površina zaledja meri 1,14 km^2. Na osnovi baze pokrovnosti tal CLC 2012 in prostorske analize smo določili deleže posamezne enote pokrovnosti tal za zaledje vsakega merilnega mesta. Merilna mesta z izrazito kmetijskim zaledjem (nad 80 %) so GPP-1, GPP-2, PCI-2, LP-1, OP-10, OP-2, P-0, P-1 in V-25. Vrtina, pri kateri v zaledju prevladuje gozd (nad 80 %), je GPP-3. 52 % urbanega in industrijskega zaledja skupaj predstavlja zaledje pri vrtini PAC-2. Pri ostalih vrtinah je zaledje mešano (Tabela 3).

Za prikaz prisotnosti pesticidov v podzemni vodi na Dravskem polju smo uporabili vsote povprečnih vrednosti vseh pesticidov za merilno mesto. Prostorski prikaz vsote pesticidov s podatki o rabi tal v zaledju merilnih mest je prikazan na sliki 5. Podzemna voda Dravskega polja v delu južneje od merilnega mesta OP-5 kaže večjo obremenjenost s pesticidi, kot v severnem delu, kjer se nahajajo urbana območja in mesto Maribor. Vsota pesticidov na določenih mestih v južnem delu presega mejo dovoljenega glede na Pravilnik o pitni vodi (Uradni list RS, 2004a) Prostorska porazdeljenost vsote pesticidov sovpada z zaledjem vrtin. V južnem delu vodonosnika je intenzivnejša kmetijska raba prostora. To se odraža tudi v koncentracijah pesticidov v podzemni vodi (sl. 5).

Iz analize prostora zaledja merilnih mest je razvidno, da gre v veliki meri za mešano rabo prostora. Zaradi tega smo združili rabo prostora samo v dve kategoriji: v skupino I kmetijska območja in gozd ter v skupino II urbana in industrijska območja (Tabela 3). Iz diagrama rabe prostora in skupne vsote pesticidov (sl. 6) je razvidno, da v severnem delu Dravskega polja, kjer je v zaledju merilnih mest več ko 10 % urbanih površin, povprečne vrednosti skupnih pesticidov ne presegajo 0,15 µg/l. V osrednjem in južnem delu, kjer je zaledje merilnih mest 90 % kmetijskih površin, so povprečne vrednosti skupnih pesticidov do 0,45 ug/l. Na južnem delu Dravskega polja izstopajo merilna mesta VP-4, HP-3 in P-3, gre za

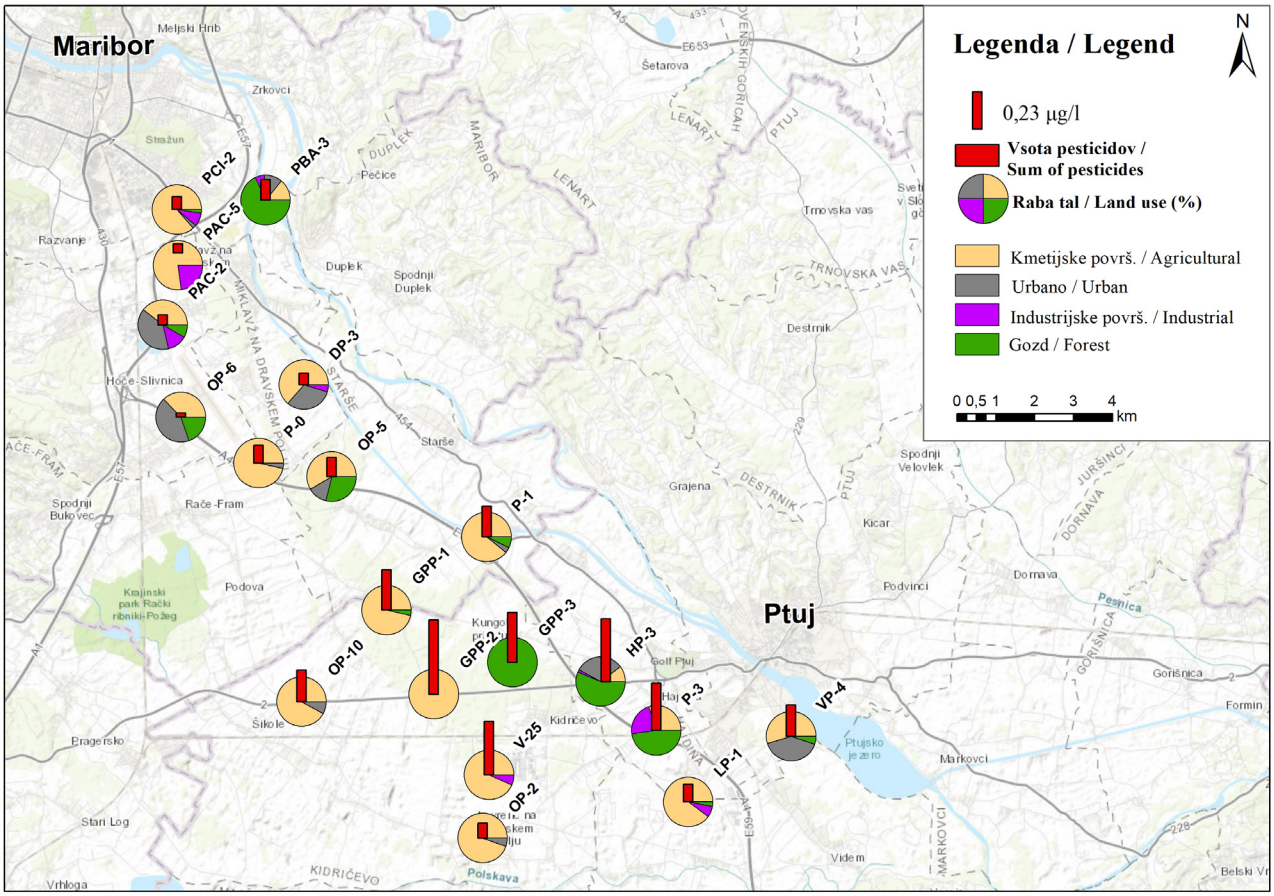

Sl. 5. Prostorska porazdelitev povprečne vsote pesticidov v podzemni vodi Dravskega polja.
Fig. 5. Spatial distribution of the sum of pesticides in Dravsko polje aquifer.

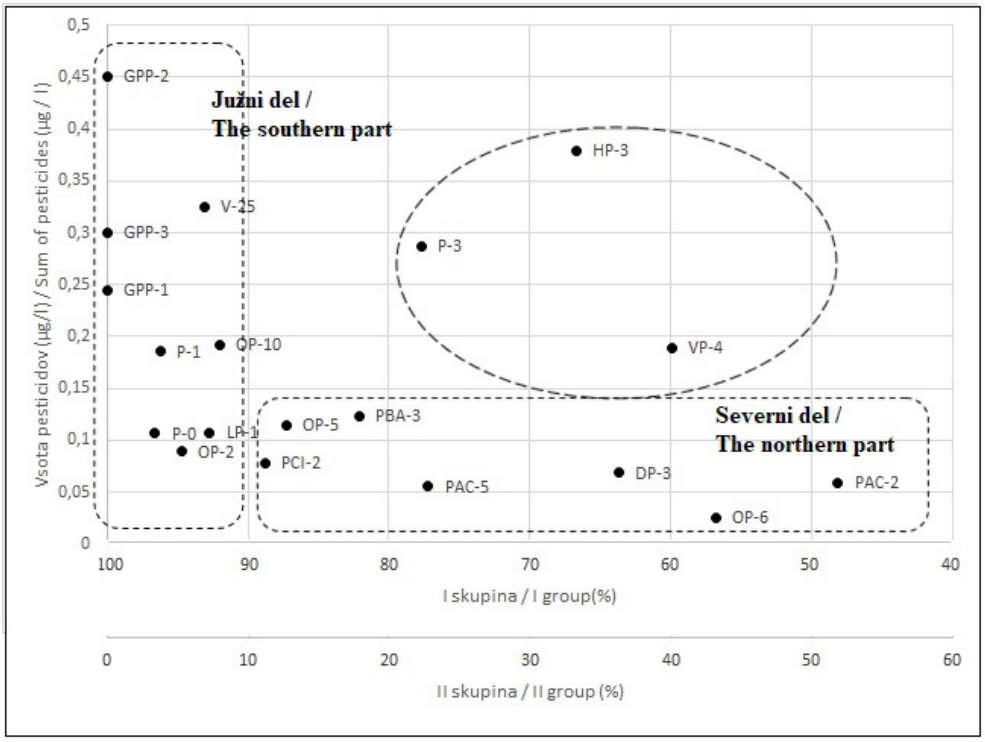

Sl. 6. Diagram rabe prostora in skupne vsote pesticidov za posamezno točko na Dravskem polju.

Fig. 6. Diagram of land use and total sum of pesticides for each point in the Dravsko polje.

merilna mesta, ki imajo v svojem ožjem zaledju večji delež urbane in industrijske rabe tal, širše gledano pa so na območju kmetijskih površin in gozda, ki jim pripisujemo vpliv na prisotnost pesticidov v vodi. Za vsa merilna mesta je značilna tudi neposredna bližina ceste, bodisi lokalne ceste ali avtoceste ter prisotnost divjih odlagališč v zaledju (Tabela 3).

Razmerje pesticidov in njihovih razgradnih produktov

V podzemni vodi Dravskega polja se pojavljata pesticida atrazin in terbutilazin in njuni razgradni produkti desetilatrazin, deizopropilatrazin in desetilterbutilazin. Prisotnost atrazina v povečanih koncentracijah v podzemni vodi na nekaterih mestih lahko razložimo kot rezultat njegove uporabe v preteklosti in njegove obstojnosti v okolju. Razmerje DAR smo uporabili pri določitvi »starosti« onesnaženja z atrazinom in njegovim razgradnim produktom desetilatrazinom. Majhno razmerje DAR kaže na »sveže« onesnaženje in je lahko kazalnik točkovnega vira onesnaženja. Pri vseh 76 vzorcih podzemne vode Dravskega polja smo izračunali koeficient DAR od 0,54 (P-0) do 3,18 (VP-4). Najmanjše vrednosti so bile določene v točki P-0 (0,54 – okt. 2013, 0,55 – apr. 2014). Povprečne vrednosti koeficient DAR so nizke v točkah PBA-3 (0,62), GPP-3 (0,75), HP-3 (0,76), OP-10 (0,81), PAC-5 (0,93), in GPP-2 (0,96). Na skoraj polovico merilnih mest so vrednosti DAR nižje od 1, kar je presenetljivo glede na to, da je prepoved uporabe atrazina v veljavi že dalj časa. Visoka pojavnost atrazina je lahko posledica starih bremen in zasutih gramoznic, zaradi počasne razgradnje in hidrogeoloških pogojev ali pa uporabe v kmetijstvu po uveljavitvi prepovedi.

Na osnovi rezultatov vsebnosti terbutilazina in desetilterbutilazina smo izračunali tudi razmerje med desetilterbutilazinom in terbutilazinom (DTA/TBA) (sl. 8). Razmerje, manjše od 1, kaže na točkovni vir onesnaženja, saj desetilterbutilazin počasneje izginja v nenasičeni coni kot terbutilazin. Razmerja DTA/TBA ni bilo možno izračunati za vsa merjenja na vseh merilnih mestih, saj so bile koncentracije terbutilazina in/ali desetilterbutilazina na nekaterih mestih pod LOD. V našem primeru smo lahko DTA/TBA izračunali na štirih različnih točkah (sl. 9). Najniže je bil izračunan na točki VP-4 (0,24 – apr. 2015), najviše pa v točki P-0 (2,97 – okt. 2014). Na merilnih mestih OP-2 in P-0 se terbutilazin in desetilterbutilazin skupaj pojavita v vseh štirih vzorčenjih. Na ostalih mestih se pojavita le v določenih serijah.

Glede na dejstvo, da je atrazin po prepovedi uporabe zamenjal terbutilazin, je na sliki 9 prikazano razmerje med vrednostmi DAR in vrednostmi DTA/TBA za merilna mesta P-0, V-25, OP-2 in VP-4. Iz grafa (sl. 9) vidimo, da je na merilnem mestu VP-4 DAR najvišji, medtem, ko je DTB/TBA najnižji. Obratno je na merilnem mestu P-0. Merilno mesto VP-4 spada med merilna mesta, ki imajo v svojem ožjem zaledju značilen delež urbane in industrijske rabe tal, kar

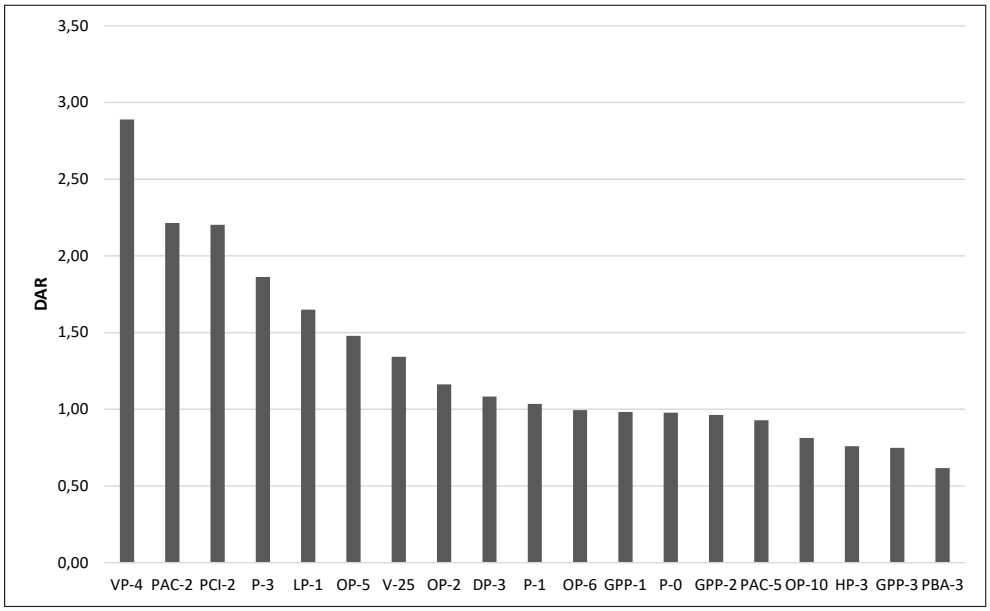

Sl. 7. Povprečno razmerje DAR.

Fig. 7. Average ratio DAR.

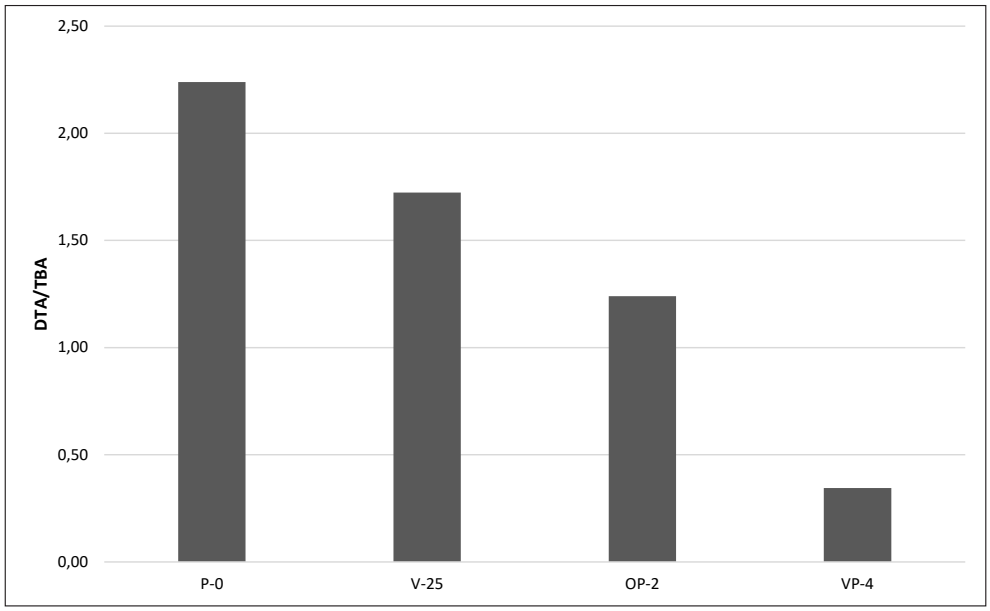

Sl. 8. Razmerje DTA/TBA po posameznih merilnih mestih.

Fig. 8. DTA/TBA ratio.

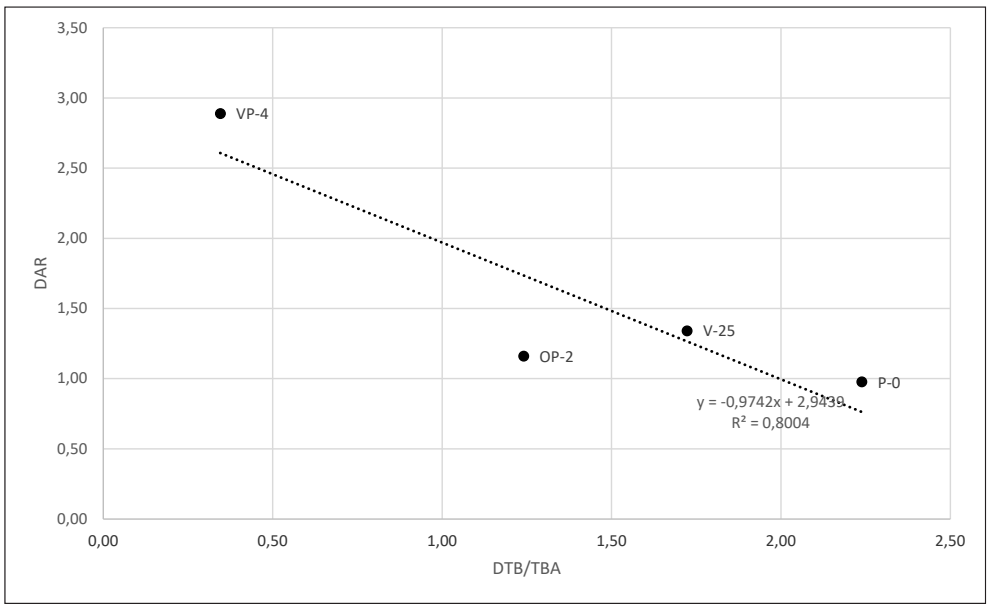

Sl. 9. Razmerje med vrednostmi DAR in vrednostmi DTA/TBA.

Fig. 9. Relationship between DAR values and DTA / TBA values.

lahko pojasni nizko razmerje med vrednostmi DAR in DTA/TBA in kaže na sveže onesnaženje z terbutilazinom. Vrednosti nakazujejo, da je na merilnem mestu, kjer je DAR visok, več razgradnega produkta desetilatrazina, kar pomeni, da atrazin ni bil v uporabi že nekaj časa, hkrati pa je na istem merilnem mestu, večja koncentracija terbutilazina v primerjavi z desetilterbutilazinom, kar nakazuje na uporabo le tega. Iz tega lahko sklepamo, da je bila uporaba atrazina že pred nekaj časa opuščena, ter nadomeščena z uporabo terbutilazina. Medtem, ko bi lahko na merilnih mestih z obratnimi vrednostmi sklepali nasprotno. Kljub temu, pa je pri takšni interpretaciji potrebno pogledati široko, ter upoštevati tudi različne hidrogeološke parametre, ki lahko vplivajo na koncentracijo pesticidov v podzemni vodi. Ena od teh je debelina nenasičene cone, ki je na merilnem mestu VP-4 manjša v primerjavi z drugimi. Glede na to, da so pa vrednosti DTB/TBA nižje od 1, lahko sklepamo tudi na točkovno onesnaženje.

Zaključki

Vodonosnik Dravskega polja je zaradi rabe prostora in dejavnosti podvržen različnim vplivom iz kmetijstva, urbanega okolja, industrije, itd. Največji delež rabe prostora predstavljajo kmetijske površine, ki so tudi glavni vir pesticidov v okolju in podzemni vodi. V naši raziskavi smo prišli do naslednjih zaključkov:

Po celotnem Dravskem polju smo potrdili pogosto pojavljanje pesticidov, kateri lahko dosežejo tudi koncentracije, ki lahko predstavljajo tudi tveganja za zdravje ljudi (WHO, 2017).

Atrazin in njegov metabolit desetilatrazin sta še vedno, kljub več desetletni prepovedi uporabe fitofarmacevtskih sredstev na osnovi atrazina, najpogosteje in v najvišjih koncentracijah zaznani spojini v podzemni vodi Dravskega polja.

2,6-diklorobenzamid (razgradni produkt diklobenila), klorotoluron, metolaklor, propazin, prometrin, simazin, terbutilazin in desetilterbutilazin (razgradni produkt terbutilazina), so bili določeni v vsebnostih, katere so pod mejo dovoljenega, glede na pravilnik o pitni vodi (Uradni list RS, 2004a).

Alaklor, dimetenamid, metazaklor in terbutrin niso bili zaznani v podzemni vodi Dravskega polja.

Pojav pesticidov klorotolurona, propazina in razgradnega produkta diklobenila 2,6- diklorobenzamida na posameznih merilnih mestih nakazuje na lokalno onesnaženje omejenega območja.

Rezultati potrjujejo, da je pojavnost pesticidov v podzemni vodi povezana z rabo prostora v zaledju. Povišane vrednosti pesticidov se pojavljajo v južnem delu Dravskega polja, kar sovpada z intenzivnejšo kmetijsko rabo tal na tem območju. V severnem delu, z večjim deležem urbanih in industrijskih površin (skupina II) so koncentracije pesticidov manjše.

Izmed vseh merilnih mest izstopajo tri (VP-4, HP-3 in P-3), ki imajo v svojem ožjem zaledju urbano in industrijsko rabo tal, širše gledano pa so na območju kmetijskih površin in gozda, kar verjetno vpliva na višje zaznane koncentracije pesticidov v podzemni vodi.

Metodologijo vrednotenja razmerij med razgradnim produktom in primarnim pesticidom (DAR in DTA/TBA) se je izkazala za uporabno pri določitvi »starosti« onesnaženja iz naslova atrazin in terbutilazina.

Na skoraj polovici merilnih mest so vrednosti DAR nižje od 1, kar je presenetljivo glede na to, da je prepoved uporabe atrazina v veljavi že dalj časa. Visoka pojavnost atrazina je lahko posledica starih bremen zaradi počasne razgradnje in hidrogeoloških pogojev ali pa uporabe po uveljavitvi prepovedi.

Pojav pesticidov z naslova prepovedanih fitofarmacevtskih pripravkov kaže na možnost prepovedane uporabe na kmetijskih površinah ali na vir »na črno« odloženih v zasutih gramoznicah. Te snovi se lahko tudi dalj časa akumulirajo (zadržujejo) v nenasičeni coni.

Zahvala

Raziskava je bila narejena v okviru Programa usposabljanja mladih raziskovalcev ter v okviru Raziskovalnega programa P1-0020, ki se izvajata na Geološkem zavodu Slovenije in ju financira Javna agencija za raziskovalno dejavnost. Raziskave so bile narejene tudi v okvirih projekta GeoERA (Hover), ki prejel sredstva raziskovalnega in inovacijskega programa Evropske unije Obzorje 2020 (v skladu s sporazumom št. 731166).

Literatura

Adams, C.D. & Thurman, E.M. 1991: Formation and transport of desethylatrazine in the soil and vadose zone. Journal of Environmental Quality, 20/3: 540–547. https://doi.org/10.2134/jeq1991.00472425002000030007x

Aelion, CM & Mathur, PP. 2001: Atrazine biodegradation to deisopropylatrazine and deethylatrazine in coastal sediments of different land uses. Environmental Toxicology

and Chemistry, 20/11: 2411-2419. https://doi.org/10.1002/etc.5620201103

Åkesson, M, Sparrenbom, CJ, Carlsson, C. & Kreuger, J. 2013: Statistical screening for descriptive parameters for pesticide occurrence in a shallow groundwater catchment. Journal of Hydrolog, 477: 165-174. https://doi.org/10.1016/j.jhydrol.2012.11.025

ARSO 2004: Poročilo o kakovosti podzemne vode aluvialnih vodonosnikov v letih 2001 in 2002. http://www.arso.gov.si/vode/podzemne%20vode/publikacije%20in%20poro%c4%8dila/Aluvijalni_2001in2002.pdf (10.10.2019).

ARSO 2016: Karta pokrovnosti tal po CORINE 2012 [digitalno kartografsko gradivo]. Ljubljana: Ministrstvo za kmetijstvo in okolje, Agencija Republike Slovenije za okolje. https://gis.arso.gov.si/wfs_web/faces/WFSLayersList.jspx (16.5.2017).

ARSO 2017: Podnebne razmere v Sloveniji (obdobje 1971-2000): 1-27. http://meteo.arso.gov.si/ (16.12.2017.)

ARSO 2018: Ocena kemijskega stanja podzemen vode. Obdobje 2006-2018. Dostopno na: https://www.arso.gov.si/vode/podzemne%20vode/.

ARSO 2019: Kemijsko stanje podzemen vode v Sloveniji, Poročilo za leto 2018. Dostopno na: https://www.arso.gov.si/novice/datoteke/041039-2203_kemijsko%20stanje%20voda%202018_fin.pdf (16.9.2019).

Auersperger, P., Lah, K., Kus, J. & Marsel, J. 2005: High precision procedure for determination of selected herbicides and their degradation products in drinking water by solid-phase extraction and gas chromatography–mass spectrometry. Journal of Chromatography A, 1088/1-2: 234-241. https://doi.org/10.1016/j.chroma.2005.04.100

Bedding, N.D., McIntyre, A.E., Perry, R. & Lester, J.N. 1982: Organic contaminants in the aquatic environment I. Sources and occurrence. Science of the Total Environment, 25: 143-167.

Bernhardt, E.S., Rosi, E.J. & Gessner, M.O. 2017: Synthetic chemicals as agents of global change. Frontiers in Ecology and the Environment, 15/2: 84-90. https://doi.org/10.1002/fee.1450

Boesten, J.J.T.I. & van der Pas L.J.T. 2000: Movement of water, bromide and the pesticides ethoprophos and bentazone in a sandy soil: the Vredepeel data set. Agricultural Water Management, 44: 21-42. https://doi.org/10.1016/S0378-3774(99)00082-7

Brenčič, M. 1998: Poročilo o hidrogeoloških delih vzdolž AC Slivnica Pesnica na področju severnega dela Dravskega polja. Geološki zavod Slovenije. Ljubljana: 24 p.

Brenčič, M. 2004. Hidrogeološko poročilo za potrebe izdelave idejnega projekta avtoceste Slivnica Draženci. Geološki zavod Slovenije, Ljubljana: 36 p.

Brenčič, M. & Ratej, J. 2006: Hidrogeološko poročilo za potrebe izdelave obratovalnega monitoringa na odlagališču baliranih odpadkov Dogoše. Geološki zavod Slovenije, Ljubljana:18 p.

Brumen, S., Medved, M. & Žerjal, E. 1990: Pesticidi v pitni vodi – Dravsko polje 1989. Ujma, 4: 104-107.

Carsel, R.F., Mulkey, L.A., Lorber, M.N. & Baskin, L.B. 1985: The Pesticide Root Zone Model (PRZM): A procedure for evaluating pesticide leaching threats to groundwater. Ecological Modelling, 30: 49-69. https://doi.org/10.1016/0304-3800(85)90036-5

Clausen, L., Larsen, F. & Albrechtsen, H-J. 2004: Sorption of the Herbicide Dichlobenil and the Metabolite 2,6-Dichlorobenzamide on Soils and Aquifer Sediments. Environmental Science & Technology, 38: 4510-4518. https://doi.org/10.1021/es035263i

Direktiva 91/414/EGS: Direktiva Sveta z dne 15. julija 1991 o dajanju fitofarmacevtskih sredstev v promet.

Direktiva 98/83/ES: Direktiva Evropska parlamenta in Sveta 1998: z dne 3. novembra 1998 o kakovosti vode, namenjene za prehrano ljudi. UL L 330, 5. 12. 1998, str. 32–54.

Direktiva 2006/118/ES: Direktiva Evropskega parlamenta in Sveta z dne 12. decembra 2006 o varstvu podzemne vode pred onesnaževanjem in poslabšanjem.

Ekologi brez meja. 2019. Register divjih odlagališč. http://register.ocistimo.si/RegisterDivjihOdlagalisc/ (Pridobljeno: 12.5.2019).

ESRI Inc. 2004: ArcINFO ver 9, Software. Environmental Research Institute. (http://www.esri.com/).

Fliser, B., Žerjal, E. & Veronek, M. 1991: Ekološka sanacija jame pri Križu na Dravskem polju. Gradbeni vestnik, 1,2: 36-37.

Funari, E., Barbieri, L., Bottoni, P., Del Carlo, G., Forti, S., Giuliano, G. Marinelli, A., Santini, C. & Zavatti, A. 1998: Comparison of the leaching properties of alachlor, metolachlor, triazines and some of their metabolites in an experimental field. Chemosphere; 36: 1759-1773. https://doi.org/10.1016/S0045-6535(97)10070-4

Gaw, S, Close, M.E. & Flintoft, M.J. 2008: Fifth national survey of pesticides in groundwater in New Zealand. New Zealand Journal of Marine and Freshwater Research, 42: 397-407.

González-Rodríguez, R.M., Rial-Otero, R., Cancho-Grande, B., Gonzalez-Barreiro, C. & Simal-Gándara, J. A 2011: Review on the Fate of Pesticides during the Processes within the Food-Production Chain. Critical Reviews in Food Science and Nutrition, 51: 99-114. https://doi.org/10.1080/10408390903432625

Gutsche, V. & Rossberg, D. 1997: SYNOPS 1.1: a model to assess and to compare the environmental risk potential of active ingredients in plant protection products. Agriculture, Ecosystems & Environment, 64: 181-188.

Heuvelink, G.B.M., Burgers, S.L.G.E., Tiktak, A. & Van Den Berg, F.V. 2010: Uncertainty and stochastic sensitivity analysis of the GeoPEARL pesticide leaching model. Geoderma, 155: 186-192. https://doi.org/10.1016/j.geoderma.2009.07.004

Jarvis, N.J., Jansson, P.E., Dik, P.E. & Messing, I. 1991: Modelling water and solute transport in macroporous soil. I. Model description and sensitivity analysis. Journal of Soil Science, 42/1: 59-70. https://doi.org/10.1111/j.1365-2389.1991.tb00091.x

Kim, K-H, Kabir, E. & Jahan, SA. 2017: Exposure to pesticides and the associated human health effects. Science of the Total Environment, 575: 525-535. https://doi.org/10.1016/j.scitotenv.2016.09.009

Knez, M. & Regent, T. 1993: Sanacija opuščenih gramoznic na Dravskem polju. Dostopno na: http://mvd20.com/LETO1993/R23.pdf (16.11.2019).

Kolbezen, M. & Pristov, J. 1998: Površinski vodotoki in vodna bilanca Slovenije. Ljubljana: Ministrstvo za okolje in prostor: Hidrometeorološki zavod Republike Slovenije.

Kolpin, D.W., Barbash, J.E. & Gilliom, R.J. 1998: Occurrence of Pesticides in Shallow Groundwater of the United States: Initial Results from the National Water-Quality Assessment Program. Environmental Science & Technology, 32: 558-566. https://doi.org/10.1021/es970412g

Kolpin, D.W., Schnoebelen, D.J. & Thurman, E.M. 2004: Degradates Provide Insight to Spatial and Temporal Trends of Herbicides in Ground Water. Ground Water, 42: 601-608. https://doi.org/10.1111/j.1745-6584.2004.tb02628.x

Koroša, A. & Mali, N. 2012:. Pregled novih organskih onesnaževal v podzemni vodi v Sloveniji. Geologija, 55/2: 243–262. https://doi.org/10.5474/geologija.2012.015

Koroša, A, Auersperger, P. & Mali, N. 2016: Determination of micro-organic contaminants in groundwater (Maribor, Slovenia). Science of the Total Environment; 571: 1419-1431. https://doi.org/10.1016/j.scitotenv.2016.06.103

Koroša, A. 2019: Izvor in transport organskih onesnaževal v medzrnskih vodonosnikih. Doktorska disertacija. Univerza v Ljubljani, Naravoslovnotehniška fakulteta Ljubljana: 207 p.

Krivic, J. 2012: Hidrogeološke raziskave dinamike podzemne vode v okolici črpališča Dobrovce. Geološki zavod Slovenije, Ljubljana: 13 p.

Lapworth, D.J., Baran, N., Stuart, M.E., Manamsa, K. & Talbot, J. 2015: Persistent and emerging micro-organic contaminants in Chalk groundwater of England and France. Environmental Pollution, 203: 214-225. https://doi.org/10.1016/j.envpol.2015.02.030

Lapworth, D.J., Baran, N., Stuart, M.E. & Ward, R.S. 2012: Emerging organic contaminants in groundwater: A review of sources, fate and occurrence. Environmental Pollution, 163: 287-303. https://doi.org/10.1016/j.envpol.2011.12.034

Lapworth, D.J. & Gooddym, D.C. 2006: Source and persistence of pesticides in a semi-confined chalk aquifer of southeast England. Environmental Pollution, 144: 1031-1044.

Mali, N. & Koroša, A. 2015. Assessment of nitrate transport in the unsaturated (coarse gravel) zone by means of tracing experiment (Selniška dobrava, Slovenia). Geologija, 58/2: 183–194. https://doi.org/10.5474/geologija.2015.014

McManus, S.L., Coxon, C.E., Mellander, P.E., Danaher, M. & Richards, K.G. 2017: Hydrogeological characteristics influencing the occurrence of pesticides and pesticide metabolites in groundwater across the Republic of Ireland. Science of the Total Environment, 601-602: 594-602. https://doi.org/10.1016/j.scitotenv.2017.05.082

Milan, M., Ferrero, A., Fogliatto, S., Piano, S. & Vidotto, F. 2015. Leaching of S-metolachlor, terbuthylazine, desethyl-terbuthylazine, mesotrione, flufenacet, isoxaflutole, and diketonitrile in field lysimeters as affected by the time elapsed between spraying and first leaching event. Journal of Environmental Science and Health Part B 50, 12: 851–861. https://doi.org/10.1080/03601234.2015.1062650

MKGP, Ministrstvo za kmetijstvo, gozdarstvo in prehrano. http://spletni2.furs.gov.si/FFS/REGSR/index.htm (Pridobljeno 7.7. 2018.)

Munz, N.A., Burdon, F.J., de Zwart, D., Junghans, M., Melo, L., Reyes, M. et al. 2017: Pesticides drive risk of micropollutants in wastewater-impacted streams during low flow conditions. Water Research, 110: 366-377. https://doi.org/10.1016/j.watres.2016.11.001

Nienstedt, K.M., Brock, T.C.M., van Wensem, J., Montforts, M., Hart, A., Aagaard. A., et al. 2012: Development of a framework based on an ecosystem services approach for deriving specific protection goals for environmental risk assessment of pesticides. Science of the Total Environment; 415: 31-38. https://doi.org/10.1016/j.scitotenv.2011.05.057

Oppel, J., Broll, G., Löffler, D., Meller, M., Römbke, J. & Ternes, T. 2004: Leaching behaviour of pharmaceuticals in soil-testing-systems: a part of an environmental risk assessment for groundwater protection. Science of the Total Environment, 328: 265-273. https://doi.org/10.1016/j.scitotenv.2004.02.004

Padovani, L., Trevisan, M. & Capri, E. 2004: A calculation procedure to assess potential environmental risk of pesticides at the farm level. Ecological Indicators, 4: 111-123. https://doi.org/10.1016/j.ecolind.2004.01.002

Petauer, D. 1980: Hidrogeologija Dravskega polja. Diplomsko delo. Naravoslovnotehniška fakulteta, Ljubljana: 39 p.

Prestor, J. & Janža, M. 2006: Ocena višine infiltracije (po metodi Kennessy) in ranljivosti podzemne vode na območju Slovenije. Geološkega zavoda Slovenije.

Reus, J.A.W.A. & Leendertse, P.C. 2000: The environmental yardstick for pesticides: a practical indicator used in the Netherlands. Crop Protection, 19: 637-641.

Ritter, L., Solomon, K., Sibley, P., Hall, K., Keen, P., Mattu, G. & Linton, B. 2002: Sources, pathways, and relative risks of contaminants in surface water and groundwater: a perspective prepared for the Walkerton inquiry. Journal of Toxicology and Environmental Health Part A, 65: 1-142. https://doi.org/10.1080/152873902753338572

Scheytt, T., Mersmann, P., Leidig, M., Pekdeger, A. & Heberer, T. 2004: Transport of Pharmaceutically Active Compounds in Saturated Laboratory Columns. Ground Water, 42: 767-773.

Sedlak, D. & Pinkston, K. 2001: Factors affecting the concentrations of pharmaceuticals released to the aquatic environment. Water Resour Update 2001, 120:56–64

Shelton, J.F., Geraghty, E.M., Tancredi, D.J., Delwiche, L.D., Schmidt, R.J., Ritz, B., Hansen, R.L. & Hertz-Picciotto, I. 2014: Neurodevelopmental Disorders and Prenatal Residential Proximity to Agricultural Pesticides: The Charge Study. Environmental Health Perspectives, 122: 1103-1109. https://doi.org/10.1289/ehp.1307044

SIST ISO 5667-11, 2010: Kakovost vode, vzorčenje – 11. del: Navodilo za vzorčenje podzemne vode, 1-10.

SIST EN ISO 5667-03, 2012: Kakovost vode, vzorčenje – 3. del: Navodilo za hranjenje in ravnanje z vzorci.

Sjerps, R.M.A., ter Laak, T.L. & Zwolsman, G.J.J.G. 2017: Projected impact of climate change and chemical emissions on the water quality of the European rivers Rhine and Meuse: A drinking water perspective. Science of the Total Environment, 601-602: 1682-1694. https://doi.org/10.1016/j.scitotenv.2017.05.250

Snyder, S.A. 2004: Biological and physical attenuation of endocrine disruptors and pharmaceuticals: implications for water reuse. Ground Water Monitoring & Remediation, 24/2. 108-118. https://doi.org/10.1111/j.1745-6592.2004.tb00719.x

Sorensen, J.P.R., Lapworth, D.J, Nkhuwa, D.C.W., Stuart, M.E., Gooddy, D.C., Bell, R.A., Chirwa, M., Kabika, J., Liemisa, M., Chibesa, M. & Pedleyd, S. 2015: Emerging contaminants in urban groundwater sources in Africa. Water Research, 72: 51-63. https://doi.org/10.1016/j.watres.2014.08.002

Stat Soft Inc., 2012: STATISTICA (Data Analysis Software System), Version 11 – Software. Stat Soft Inc.(www.statsoft.com).

Steele, G.V., Johnson, H.M., Sandstrom, M.W., Capel, P.D., Barbash, J.E. 2008: Occurrence and Fate of Pesticides in Four Contrasting Agricultural Settings in the United States. Journal of environmental quality, 37: 1116-1132. https://doi.org/10.2134/jeq2007.0166

Stehle, S. & Schulz, R. 2015: Agricultural insecticides threaten surface waters at the global scale. Proceedings of the National Academy of Sciences, 112: 5750-5755. https://doi.org/10.1073/pnas.1500232112

Stuart, M., Lapworth, D., Crane, E. & Hart, A. 2012: Review of risk from potential emerging contaminants in UK groundwater. Science of the Total Environment, 416: 1-21. https://doi.org/10.1016/j.scitotenv.2011.11.072

Tadeo, J.L. 2008: Analysis of Pesticides in Food and Environmental Samples. CRC Press, Boca Raton, Florida: 384 p.

Tiktak, A., de Nie, D.S., Piñeros Garcet, J.D., Jones, A. & Vanclooster, M. 2004: Assessment of the pesticide leaching risk at the Pan-European level. The EuroPEARL approach. Journal of Hydrology, 289: 222-238. https://doi.org/10.1016/j.jhydrol.2003.11.030

TOXNET. Toxicology data network. http://toxnet.nlm.nih.gov/cgi-bin/sis/search2/r?dbs+hsdb:@term+@DOCNO+113 (Pridobljeno 30.9. 2019).

Uradni list RS 2002: Uredba o kakovosti podzemne vode. Uradni list RS, št. 11/02, 41/04 – ZVO-1 in 100/05.

Uradni list RS 2004a: Pravilnik o pitni vodi. Uradni list RS, št. 19/04, 35/04, 26/06, 92/06, 25/09, 74/2015 in 51/2017.

Uradni list RS 2004b: Pravilnik o kriterijih za določitev vodovarstvenega območja. Uradni list RS, št. 64/04, 5/06, 58/11 in 15/16.

Uradni list RS 2005: Pravilnik o določitvi vodnih teles podzemnih vod. Uradni list RS, št. 63/05 in 8/18.

Uradni list RS 2007: Uredba o vodovarstvenem območju za vodno telo vodonosnikov Dravsko-ptujskega polja. Uradni list RS, št. 59/07, 32/11, 24/13 in 79/15.

Uradni list RS 2009: Uredbo o stanju podzemnih voda. Uradni list RS št. 25/2009, 08/2012 in 66/2016.

Urbanc, J., Krivic, J., Mali, N., Ferjan Stanič, T., Koroša, A., Šram, D., Mezga, K., Bizjak, M., Medić, M., Bole, Z., Lojen, S., Pintar, M., Udovč, A., Glavan, M., Kacjan-Maršić, N., Jamšek, A., Valentar, V., Zadravec, D., Pušenjak, M. & Klemenčič Kosi, S. 2014: Možnosti kmetovanja na vodovarstvenih območjih: zaključno poročilo projekta. Geološki zavod Slovenije, Ljubljana: 154 p.

van der Werf, H.M.G. & Zimmer, C. 1998: An indicator of pesticide environmental impact based on a fuzzy expert system. Chemosphere, 36: 2225-2249. https://doi.org/10.1016/S0045-6535(97)10194-1

van Eerdt, M.M., Spruijt, J., van der Wal, E., van Zeijts, H. & Tiktak, A. 2014: Costs and effectiveness of on-farm measures to reduce aquatic risks from pesticides in the Netherlands. Pest management science, 70: 1840-1849. https://doi.org/10.1002/ps.3729

WHO, World Health Organization 2017: SZO - Guidelines for Drinking – water Quality. https://apps.who.int/iris/bitstream/handle/10665/254637/9789241549950-eng.pdf;jsessionid=3D049E809F7CD80889A-604FA649BE1CD?sequence=1 (17.12.2019)

Worrall, F., Kolpin, D.W. 2004: Aquifer vulnerability to pesticide pollution–combining soil, land-use and aquifer properties with molecular descriptors. Journal of Hydrology, 293: 191-204. https://doi.org/10.1016/j.jhydrol.2004.01.013

Zuehlke, S., Duennbier, U., Heberer, T. & Fritz, B. 2004: Analysis of Endocrine Disrupting Steroids: Investigation of Their Release into the Environment and Their Behavior During Bank Filtration. Ground Water Monitoring & Remediation; 24: 78-85. https://doi.org/10.1111/j.1745-6592.2004.tb00715.x

Žlebnik, L. 1982. Hidrogeološke razmere na Dravskem polju. Geologija, 25/1: 151–164. https://doi.org/10.5474/geologija.1991.008

Žlebnik, L. & Drobne, F. 1998. Pliocenski vodonosniki – pomemben vir neoporečne pitne vode za ptujsko – ormoško regijo. Geologija, 41: 339–354. https://doi.org/10.5474/geologija.1998.017

Yadav, I.C. & Devi NL 2017: Pesticides classification and its impact on human and environment. Environmental Science and Engineering, 140 –158.

Navodila avtorjem

GEOLOGIJA objavlja znanstvene in strokovne članke s področja geologije in sorodnih ved. Revija izhaja dvakrat letno. Članke recenzirajo domači in tuji strokovnjaki z obravnavanega področja. Ob oddaji člankov avtorji predlagajo **tri recenzente**, uredništvo si pridržuje pravico do izbire recenzentov po lastni presoji. Avtorji morajo članek popraviti v skladu z recenzentskimi pripombami ali utemeljiti zakaj se z njimi ne strinjajo.

Avtorstvo: Za izvirnost podatkov, predvsem pa mnenj, idej, sklepov in citirano literaturo so odgovorni avtorji. Z objavo v GEOLOGIJI se tudi obvežejo, da ne bodo drugje objavili prispevka z isto vsebino.

Avtorji z objavo prispevka v GEOLOGIJI potrjujejo, da se strinjajo, da je njihov prispevek odprto dostopen z izbrano licenco CC-BY.

Jezik: Članki naj bodo napisani v angleškem, izjemoma v slovenskem jeziku, vsi pa morajo imeti slovenski in angleški izvleček. Za prevod poskrbijo avtorji prispevkov sami.

Vrste prispevkov:

Izvirni znanstveni članek
Izvirni znanstveni članek je prva objava originalnih raziskovalnih rezultatov v takšni obliki, da se raziskava lahko ponovi, ugotovitve pa preverijo. Praviloma je organiziran po shemi IMRAD (**I**ntroduction, **M**ethods, **R**esults, **A**nd **D**iscussion).

Pregledni znanstveni članek
Pregledni znanstveni članek je pregled najnovejših del o določenem predmetnem področju, del posameznega raziskovalca ali skupine raziskovalcev z namenom povzemati, analizirati, evalvirati ali sintetizirati informacije, ki so že bile publicirane. Prinaša nove sinteze, ki vključujejo tudi rezultate lastnega raziskovanja avtorja.

Strokovni članek
Strokovni članek je predstavitev že znanega, s poudarkom na uporabnosti rezultatov izvirnih raziskav in širjenju znanja.

Diskusija in polemika
Prispevek, v katerem avtor ocenjuje ali komentira neko delo, objavljeno v GEOLOGIJI, ali z avtorjem strokovno polemizira.

Recenzija, prikaz knjige
Prispevek, v katerem avtor predstavlja vsebino nove knjige.

Oblika prispevka: Besedilo pripravite v urejevalniku Microsoft Word. Prispevki naj praviloma ne bodo daljši od 20 strani formata A4, v kar so vštete tudi slike, tabele in table. Le v izjemnih primerih je možno, ob predhodnem dogovoru z uredništvom, tiskati tudi daljše prispevke.

Članek oddajte uredništvu vključno z vsemi slikami, tabelami in tablami v elektronski obliki po naslednjem sistemu:
- *Naslov članka (do 12 besed)*
- *Avtorji (ime in priimek, poštni in elektronski naslov)*
- *Ključne besede (do 7 besed)*
- *Izvleček (do 300 besed)*
- *Besedilo*
- *Literatura*
- *Podnaslovi slik in tabel*
- *Tabele, Slike, Table*

Citiranje: V literaturi naj avtorji prispevkov praviloma upoštevajo le objavljene vire. Poročila in rokopise naj navajajo le v izjemnih primerih, z navedbo kje so shranjeni. V seznamu literature naj bodo navedena samo v članku omenjena dela. Citirana dela, ki imajo DOI identifikator (angl. Digital Object Identifier), morajo imeti ta identifikator izpisan na koncu citata. Za citiranje revije uporabljamo standardno okrajšavo naslova revije. Med besedilom prispevka citirajte samo avtorjev priimek, v oklepaju pa navajajte letnico izida navedenega dela in po potrebi tudi stran. Če navajate delo dveh avtorjev, izpišite med tekstom prispevka oba priimka (npr. Pleničar & Buser, 1967), pri treh ali več avtorjih pa napišite samo prvo ime in dodajte et al. z letnico (npr. Mlakar et al., 1992). Citiranje virov z medmrežja v primeru, kjer avtor ni poznan, zapišemo (Internet 1). V seznamu literaturo navajajte po abecednem redu avtorjev.

Imena fosilov (rod in vrsta) naj bodo napisana poševno, imena višjih taksonomskih enot (družina, razred, itn.) pa normalno. Imena avtorjev taksonov naj bodo prav tako napisana normalno, npr. *Clypeaster pyramidalis* Michelin, *Galeanella tollmanni* (Kristan), Echinoidea.

Primeri citiranja članka:

Mali, N., Urbanc, J. & Leis, A. 2007: Tracing of water movement through the unsaturated zone of a coarse gravel aquifer by means of dye and deuterated water. Environ. geol., 51/8: 1401–1412. https://doi.org/10.1007/s00254-006-0437-4

Pleničar, M. 1993: *Apricardia pachiniana* Sirna from lower part of Liburnian beds at Divača (Triest-Komen Plateau). Geologija, 35: 65–68

Primer citirane knjige:

Flügel, E. 2004: Mikrofacies of Carbonate Rocks. Springer Verlag, Berlin: 976 p.

Jurkovšek, B., Toman, M., Ogorelec, B., Šribar, L., Drobne, K., Poljak, M. & Šribar, Lj. 1996: Formacijska geološka karta južnega dela Tržaško-komenske planote – Kredne in paleogenske kamnine 1: 50.000 = Geological map of the southern part of the Trieste-Komen plateau – Cretaceous and Paleogene carbonate rocks. Geološki zavod Slovenije, Ljubljana: 143 p., incl. Pls. 23, 1 geol. map.

Primer citiranja poglavja iz knjige:

Turnšek, D. & Drobne, K. 1998: Paleocene corals from the northern Adriatic platform. In: Hottinger, L. & Drobne, K. (eds.): Paleogene Shallow Benthos of the Tethys. Dela SAZU, IV. Razreda, 34/2: 129–154, incl. 10 Pls.

Primer citiranja virov z medmrežja:

Če sta znana avtor in naslov citirane enote zapišemo:
Čarman, M. 2009: Priporočila lastnikom objektov, zgrajenih na nestabilnih območjih. Internet: http://www.geo-zs.si/UserFiles/1/File/Nasveti_lastnikom_objektov_na_nestabilnih_tleh.pdf (17. 1. 2010)

Če avtor ni poznan zapišemo tako:
Internet: http://www.geo-zs.si/ (22. 10. 2009)

Če se navaja več enot z medmrežja, jim dodamo še številko:
Internet 1: http://www.geo-zs.si/ (15. 11. 2000)
Internet 2: http://www.geo-zs.si/ (10. 12. 2009)

Slike, tabele in table: Slike (ilustracije in fotografije), tabele in table morajo biti zaporedno oštevilčene in označene kot sl. 1, sl. 2 itn., oddane v formatu TIFF, JPG, EPS ali PDF z ločljivostjo 300 dpi. Le izjemoma je možno objaviti tudi barvne slike, vendar samo po predhodnem dogovoru z uredništvom. Če avtorji oddajo barvne slike bodo te v barvah objavljene samo v spletni različici članka. Pazite, da bo tudi slika tiskana v sivi tehniki berljiva. Grafični materiali naj bodo usklajeni z zrcalom revije, kar pomeni, da so široki največ 172 mm (ena stran) ali 83 mm (pol strani, en stolpec) in visoki največ 235 mm. Večjih formatov od omenjenega zrcala GEOLOGIJE ne tiskamo na zgib, je pa možno, da večje oziroma daljše slike natisnemo na dveh straneh (skupaj na levi in desni strani) z vmesnim "rezom". V besedilu prispevka morate omeniti vsako sliko po številčnem vrstnem redu. Dovoljenja za objavo slikovnega gradiva iz drugih revij, publikacij in knjig, si pridobijo avtorji sami.

Če je članek napisan v slovenskem jeziku, mora imeti celotno besedilo, ki je na slikah in tabelah tudi v angleškem jeziku. Podnaslovi naj bodo čim krajši.

Korekture: Avtorji prejmejo po elektronski pošti članek v avtorski pregled. Popravijo lahko samo tiskarske napake. Krajši dodatki ali spremembe pri korekturah so možne samo na avtorjeve stroške.

Prispevki so prosto dostopni na spletnem mestu: http://www.geologija-revija.si/

Oddaja prispevkov:

Avtorje prosimo, da prispevke oddajo v elektronski obliki na naslov uredništva:

GEOLOGIJA
Geološki zavod Slovenije
Dimičeva ulica 14, SI-1000 Ljubljana
bernarda.bole@geo-zs.si ali urednik@geologija-revija.si

Uredništvo Geologije

Instructions for authors

Scope of the journal: GEOLOGIJA publishes scientific papers which contribute to understanding of the geology of Slovenia or to general understanding of all fields of geology. Some shorter contributions on technical or conceptual issues are also welcome. Occasionally, a collection of symposia papers is also published.
All submitted manuscripts are peer-reviewed. When submitting paper, authors should recommend at least **three reviewers**. Note that the editorial office retains the sole right to decide whether or not the suggested reviewers are used. Authors should correct their papers according to the instructions given by the reviewers. Should you disagree with any part of the reviews, please explain why. Revised manuscript will be reconsidered for publication.

Author's declaration: Submission of a paper for publication in GEOLOGIJA implies that the work described has not been published previously, that it is not under consideration for publication elsewhere and that, if accepted, it will not be published elsewhere.
Authors agree that their contributions published in GEOLOGIJA are open access under the licence CC-BY.

Language: Papers should be written in English or Slovene, and should have both English and Slovene abstracts.

Types of papers:

Original scientific paper
In an original scientific paper, original research results are published for the first time and in such a form that the research can be repeated and the results checked. It should be organised according to the IMRAD scheme (**I**ntroduction, **M**ethods, **R**esults, **A**nd **D**iscussion).

Review scientific paper
In a review scientific paper the newest published works on specific research field or works of a single researcher or a group of researchers are presented in order to summarise, analyse, evaluate or synthesise previously published information. However, it should contain new information and/or new interpretations.

Professional paper
Technical papers give information on research results that have already been published and emphasise their applicability.

Discussion paper
A discussion gives an evaluation of another paper, or parts of it, published in GEOLOGIJA or discusses its ideas.

Book review
This is a contribution that presents a content of a new book in the field of geology.

Style guide:
Submitted manuscripts should not exceed 20 pages of A4 format including figures, tables and plates. Only exceptionally and in agreement with the editorial board longer contributions can also be accepted.
Manuscripts submitted to the editorial office should include figures, tables and plates in electronic format organized according to the following scheme:
- *Title (maximum 12 words)*
- *Authors (full name and family name, postal address and e-mail address)*
- *Key words (maximum 7 words)*
- *Abstract (maximum 300 words)*
- *Text*
- *References*
- *Figure and Table Captions*
- *Tables, Figures, Plates*

References: References should be cited in the text as follows: (Flügel, 2004) for a single author, (Pleničar & Buser, 1967) for two authors and (Mlakar et al., 1992) for multiple authors. Pages and figures should be cited as follows: (Pleničar, 1993, p. 67) and (Pleničar, 1993, fig. 1). Anonymous internet resources should be cited as (Internet 1). Only published references should be cited. Manuscripts should be cited only in some special cases in which it also has to be stated where they are kept. Cited reference list should include only publications that are mentioned in the paper. Authors should be listed alphabetically. Journal titles should be given in a standard abbreviated form. A DOI identifier, if there is any, should be placed at the end as shown in the first case below.

Taxonomic names should be in italics, while names of the authors of taxonomic names should be in normal, such as *Clypeaster pyramidalis* Michelin, *Galeanella tollmanni* (Kristan), Echinoidea.

Articles should be listed as follows:
Mali, N., Urbanc, J. & Leis, A. 2007: Tracing of water movement through the unsaturated zone of a coarse gravel aquifer by means of dye and deuterated water. Environ. geol., 51/8: 1401–1412. https://doi.org/10.1007/s00254-006-0437-4
Pleničar, M. 1993: *Apricardia pachiniana* Sirna from lower part of Liburnian beds at Divača (Triest-Komen Plateau). Geologija, 35: 65–68.

Books should be listed as follows:
Flügel, E. 2004: Mikrofacies of Carbonate Rocks. Springer Verlag, Berlin: 976 p.
Jurkovšek, B., Toman, M., Ogorelec, B., Šribar, L., Drobne, K., Poljak, M. & Šribar, Lj. 1996: Formacijska geološka karta južnega dela Tržaško-komenske planote – Kredne in paleogenske kamnine 1: 50.000 = Geological map of the southern part of the Trieste-Komen plateau – Cretaceous and Paleogene carbonate rocks. Geološki zavod Slovenije, Ljubljana: 143 p., incl. Pls. 23, 1 geol. map.

Book chapters should be listed as follows:
Turnšek, D. & Drobne, K. 1998: Paleocene corals from the northern Adriatic platform. In: Hottinger, L. & Drobne, K. (eds.): Paleogene Shallow Benthos of the Tethys. Dela SAZU, IV. Razreda, 34/2: 129–154, incl. 10 Pls.

Internet sources should be listed as follows:
Known author and title:
Čarman, M. 2009: Priporočila lastnikom objektov, zgrajenih na nestabilnih območjih. Internet: http://www.geo-zs.si/UserFiles/1/File/Nasveti_lastnikom_objektov_na_nestabilnih_tleh.pdf (17. 1. 2010)
Unknown authors and title:
Internet: http://www.geo-zs.si/ (22.10.2009)

When more than one unit from the internet are cited they should be numbered:
Internet 1: http://www.geo-zs.si/ (15.11. 2000)
Internet 2: http://www.geo-zs.si/ (10.12. 2009)

Figures, tables and plates: Figures (illustrations and photographs), tables and plates should be numbered consecutively and marked as Fig. 1, Fig. 2 etc., and saved as TIFF, JPG, EPS or PDF files and submitted at 300 dpi. Colour pictures will be published only on the basis of previous agreement with the editorial office. If, together with the article, you submit colour figures then these figures will appear in colour only in the Website version of the article. Be careful that the grey scale printed version is also readable. Graphic materials should be adapted to the journal's format. They should be up to 172 mm (one page) or 83 mm wide (half page, one column), and up to 235 mm high. Larger formats can only be printed as a double-sided illustration (left and right) with a cut in the middle. All graphic materials should be referred to in the text and numbered in the sequence in which they are cited. The approval for using illustrations previously published in other journals or books should be obtained by each author.
When a paper is written in Slovene it has to have the entire text which accompanies illustrations and tables written both in Slovene and English. Figure and table captions should be kept as short as possible.

Proofs: Proofs (in pdf format) will be sent by e-mail to the corresponding author. Corrections are made by the authors. They should correct only typographical errors. Short additions and changes are possible, but they will be charged to the authors.

GEOLOGIJA is an open access journal; all pdfs can be downloaded from the website: http://www.geologija-revija.si/en/

Submission: Authors should submit their papers in electronic form to the address of the GEOLOGIJA editorial office:

GEOLOGIJA
Geological Survey of Slovenia
Dimičeva ulica 14, SI-1000 Ljubljana, Slovenia
bernarda.bole@geo-zs.si or urednik@geologija-revija.si

The Editorial Office

GEOLOGIJA

št.: 62/2, 2019

www.geologija-revija.si

ISSN 0016-7789

GeoZS
Geološki zavod Slovenije